Synthesis and evaluation of dopaminergic prodrugs designed for transdermal iontophoretic drug delivery

Graan, Jeroen de

Synthesis and evaluation of dopaminergic prodrugs designed for transdermal iontophoretic drug delivery

Highly water-soluble amino acid ester prodrugs applicable for the treatment of Parkinson's disease

Jeroen de Graan

Synthesis and evaluation of dopaminergic prodrugs designed for transdermal iontophoretic drug delivery

Highly water-soluble amino acid ester prodrugs applicable for the treatment of Parkinson's disease

Proefschrift

ter verkrijging van het doctoraat in de
Wiskunde en Natuurwetenschappen
aan de Rijksuniversiteit Groningen
op gezag van de
Rector Magnificus, dr. E. Sterken,
in het openbaar te verdedigen op
maandag 21 mei 2012
om 14.30 uur

door

Jeroen de Graan

geboren op 15 februari 1980

te Lima, Peru

To my grandparents,
parents and sister

Table of contents

1

Introduction

1.1 DOPAMINE AND ITS FUNCTION IN THE CENTRAL NERVOUS SYSTEM

The nervous system is divided into the central nervous system (CNS) and the peripheral nervous system. Neurotransmission between nerve cells is realized by generation of action potentials. This generally results in a release of a chemical neurotransmitter which stimulates or inhibits another cell. An example of such a chemical neurotransmitter is dopamine (DA).[1] DA (2-(3,4-dihydroxyphenyl)ethylamine) is a catecholamine neurotransmitter found in neurons of both the CNS and peripheral nervous system. Although DAergic neurons correspond to less than 1% of the total number of brain neurons, they play a significant role in brain functions, such as motivation, working memory and motor behavior. A high concentration of the DA is found in the striatum, which forms an important part of the extrapyramidal system and is known to control motor activity.[2, 3] The DA neurons in this pathway play an important role in the pathophysiology and treatment of Parkinson's disease.

DA is formed from its precursor L-DOPA (3,4-dihydroxy-L-phenylalanine) by aromatic-L-amino-acid decarboxylase (AAAD) (Scheme 1.1). The clearance of DA occurs by re-uptake into the presynaptic neuron, or by metabolic inactivation by monoamine oxidase B (MAO-B) as well as catechol-O-methyltransferase (COMT).[4] Homovanillic acid (HVA, 4-hydroxy-3-methoxyphenylacetic acid) is the final and main metabolic break-down product of DA in the human brain. Most of the brain DA is first attacked by MAO-B to give 3,4-dihydroxyphenylacetic acid (DOPAC) and subsequently attacked by COMT to form HVA. Another route occurs via initial O-methylation by COMT to give 3-methoxytyramine (3-MT) followed by oxidative deamination by MAO-B to give HVA.[5]
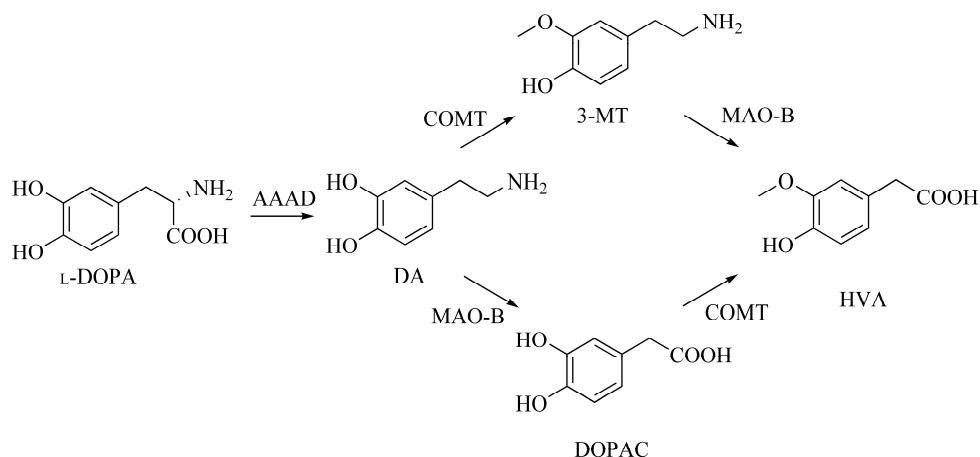
Scheme 1.1 Main pathway of biosynthesis and catabolism of DA in the mammalian organism.[5]

1.2 ANATOMY OF THE DOPAMINE SYSTEM

Techniques to detect DA neurons and localize DA receptors have identified distinct DA pathways in the brain of which the nigrostriatal, mesolimbic, mesocortical and tuberoinfundibular are the major pathways (Figure 1.1).[4, 6]

The highly organized nigrostriatal pathway is the major DA pathway of the brain and originates from the substantia nigra pars compacta (SNc) projecting to the corpus striatum of the basal nuclei, whose function is to produce a smooth coordination in movement. A second prominent DA pathway is the mesolimbic pathway, which has cell bodies in the ventral tegmental area and sends axons to the limbic system, whose primary responsibility is the regulation of reward and related emotion-based behaviour.[1, 3, 6, 7] The mesocortical pathway has DAergic projections to the prefrontal cortex and modulates cognitive behaviour[7], learning and memory.[8] The tuberoinfundibular pathway has its cell bodies in the hypothalamus and projects toward the pituitary gland.[9]
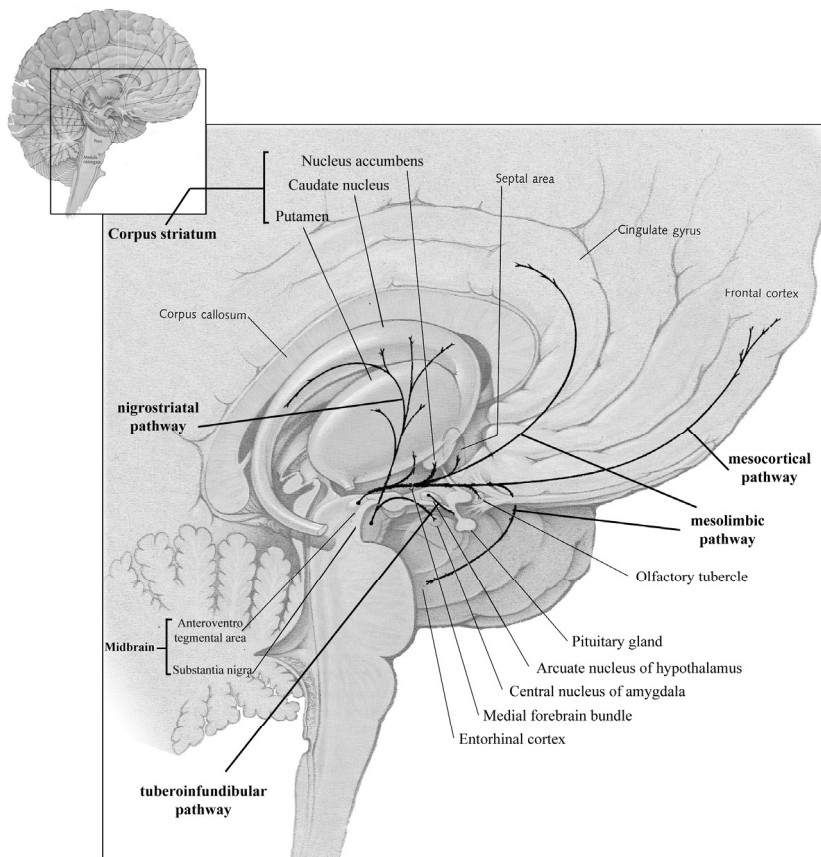
Figure 1.1 Nigrostriatal, mesolimbic, mesocortical and tuberoinfundibular DAergic pathways.[4, 9]

1.3 DOPAMINE RECEPTORS

DA exerts its action by binding to specific membrane DA receptors. Five distinct DA receptors have been subdivided into two subfamilies, D_1- and D_2-like, on the basis of their biochemical and pharmacological properties.[8] The D_1 and D_5 receptors are classified as "D_1-like" and the D_2, D_3 and D_4 receptors are considered to be "D_2-like".[10]

1.3.1 G protein-coupled receptor structure

The DA receptor subtypes belong to the large G protein-coupled receptor (GPCR) family. The receptors are characterized structurally by the presence of 7 transmembrane domains which form the DA binding site.[4, 10] Members of the same DA subfamily share considerable homology in their transmembrane domains (Figure 1.2).[11]
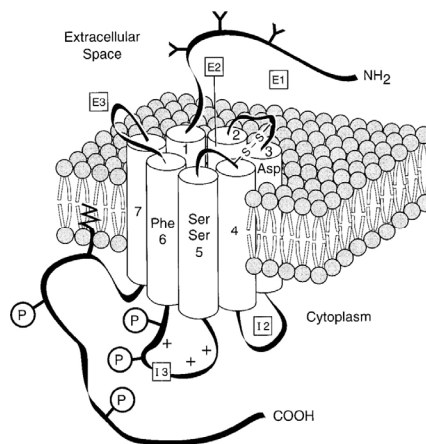
Figure 1.2 DA receptor structure.[11]

1.3.2 Second messenger pathways

The best-described effects mediated by DA are the activation or inhibition of the cyclic adenosine monophosphate (cAMP) pathway via adenylate cyclase (AC), and modulation of Ca^{2+} signalling.[8] Two distinct guanosine triphosphate(GTP)-binding proteins regulate cAMP formation: one is specific for stimulation of AC (G_s), and the other is specific for its inhibition (G_i).[1, 4, 8, 9, 12] All D_1-like receptors stimulate cAMP accumulation[10] and the D_2-like receptors inhibit the activity of AC.[8, 10, 11, 13, 14]

1.3.3 Distribution of the dopamine receptor families in the brain

D_1- and D_2-like receptors have similar regional distributions in rat, monkey, and human brain, with the highest concentrations in striatum, olfactory bulb, and substantia nigra (SN). The DA receptor subtypes appear to be expressed by distinct populations of GABAergic

(GABA, γ-aminobutyric acid) neurons: the DA D_1 receptors are located in striatonigral neurons coexpressing substance P and dynorphin, and the DA D_2 receptors are located in striatopallidal neurons coexpressing enkephalin.[13] The relative abundance of the DA receptors in the rat CNS would be $D_1>D_2>D_3>D_5>D_4$.[10] Both rat D_1 and D_2 mRNA (messenger ribonucleic acid) are each found in about 45% of striatal neurons.[13] The D_3 receptor mRNA is mainly detected in telencephalic areas receiving DAergic inputs from the A10 cell group[15], the D_4 receptor mRNA appears to have a cortical, limbic and hypothalamic distribution, and D_5 mRNA was localized in the hippocampus and in the parafascicular nucleus of the thalamus.[16]

1.3.4 Pharmacology

Although DA antagonism plays an important role in treating diseases of the CNS, the scope of this thesis mainly concern DA D_1 and DA D_2 agonism and its clinical applications. Therefore, DA antagonists will not be discussed. The interest we have in DA D_1 and DA D_2 receptor agonists is related to the function of these receptors in the brain and their involvement in Parkinson's disease.

LS-186899 (dihydrexidine) and its polycyclic analogues A-86929, DAR 201 (dinapsoline), dinoxyline and doxanthrine are examples of selective DA D_1 receptor agonists.[17] The di-*N*-substituted phenethylamines RU 24926 and RU 24213, the di-*N*-substituted 5-hydroxy-2-aminotetralins N-0434 and N-0437, and the partial ergoline LY 171555 (Quinpirole), selectively stimulate the DA D_2 receptor.[13] A classical DA agonist such as apomorphine is considered to be a mixed agonist at the D_1 and D_2 receptor (Figure 1.3).[8]
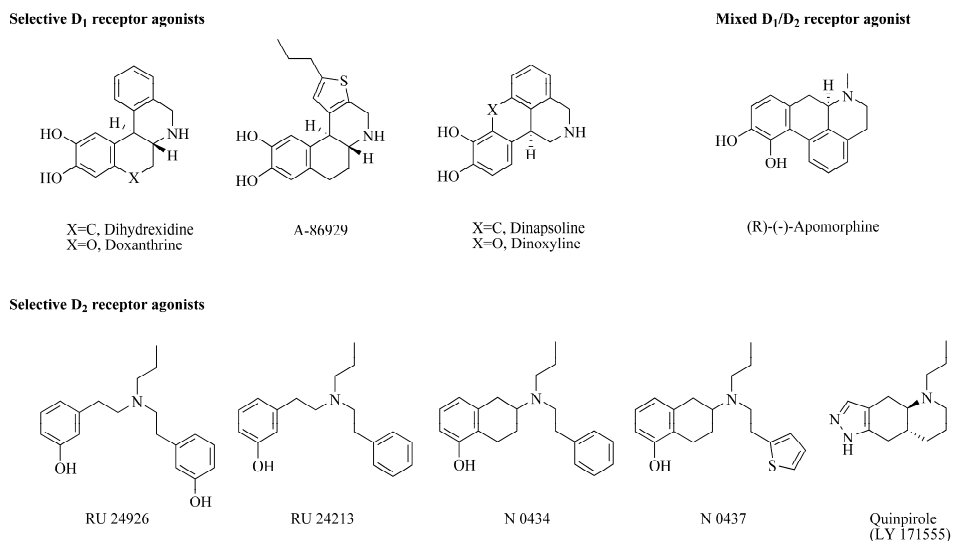
Figure 1.3 Selective DA D_1 and D_2 receptor agonists and the mixed DA D_1/D_2 receptor agonist apomorphine.[8, 13, 17, 18]

1.3.5 Dopamine autoreceptor

DA autoreceptors located on nerve endings and somatodendritic sites of nigrostriatal DAergic neurons can modulate the synthesis and release of DA. Stimulation of these autoreceptors depresses spontaneous electrical activity and inhibits the synthesis and release of DA.[13] Although these DA autoreceptors appear to be very similar to the post-synaptic D_2 receptor, many agonists display substantially greater affinity at the former site.[15, 19, 20] This could be explained by a large receptor reserve of the DA autoreceptor.[21]

1.3.6 Interaction between dopamine D_1 and D_2 receptors

The different effects of DA on the neurons of the two major output systems of the striatum to the SN and the globus pallidus (GP) are mediated by their specific expression of D_1 and D_2 DA receptor subtypes, respectively. Moreover, simultaneously administered D_1 and D_2 agonists suggest a synergistic interaction between D_1 and D_2 DA receptors.[22] Several lines of evidence have led to the conceptualization of D_1/D_2 interaction[15, 22-24] and to the hypothesis that concurrent DA D_1 and D_2 receptor stimulation is necessary for the full expression of postsynaptic receptor-mediated effects of DA and DA agonists in the basal ganglia.[24, 25] Murray et al. suggested that there may be at least two forms of functional interaction between D_1 and D_2 systems: one co-operative and the other oppositional.[26] Moreover, behavioral and biochemical effects of selective receptor blockade are significantly altered by concurrent stimulation or inhibition of the complementary receptor subtype.[27]

1.4 PARKINSON'S DISEASE

Parkinson's disease was first described by James Parkinson in 1817.[28] Parkinson's disease is classically defined as a progressive, idiopathic, neurodegenerative disease associated with four fundamental motoric signs: akinesia/bradykinesia, rest tremor, cogwheel rigidity and postural instability. A resting tremor is the first symptom in 70% of Parkinson's disease patients.[29-31]

The prevalence of Parkinson's disease in industrialised countries is estimated at 0.3% of the general population and about 1.8% of the population older than age 65 years.[32, 33] People of all ethnic origins are affected, and men are slightly more prone to the disorder.[34, 35] Young-onset Parkinson's disease affects 5-10% of patients.[36]

Parkinson's disease is probably a result of multiple factors acting together, including ageing, genetic susceptibility, and environmental exposures. 1-Methyl-4-phenyl-1,2,3,6-tetrahydropyridine (MPTP) is the only toxic agent that has been directly linked to development of parkinsonism. Pesticide exposure, living in rural areas (in industrialised countries), and drinking well water have all been linked to Parkinson's disease. Conversely, certain environmental exposures seem to lessen the risk of Parkinson's disease, like

cigarette smoking and the intake of caffeine.[31] Five genes have been identified that are important in autosomal dominant and autosomal recessive forms of Parkinson's disease.[37]

1.4.1 Neuropathology

Most striatal neurons are GABAergic neurons that receive glutamatergic inputs from terminals that originate in the cortex and thalamus. A common feature of cortical-subcortical loops is their projection from the motor cortices to the basal ganglia with entry via striatal areas and outflow through the internal globus pallidus (GPi) or the SNr. Each loop contains 'direct' and 'indirect' pathways, the former projecting directly from striatum to GPi/SNr and the latter through the external globus pallidus (GPe) and the subthalamic nucleus (STN) to reach GPi/SNr (Figure 1.4). SNc DA neurons differentially influence the striatopallidal neuronal activity. DA facilitates activity in D_1-bearing neurons, which have an inhibitory effect on the GPi (direct pathway). DA inhibits activity in D_2-bearing neurons, which lead to excitation of the GPe (indirect pathway). Outflow from both pathways rejoin and then project directly back to the originating cortical structure via the thalamus. Movement facilitation is associated with increased activity in the direct pathway and reduced activity in the indirect pathway.[29, 30, 38, 39]
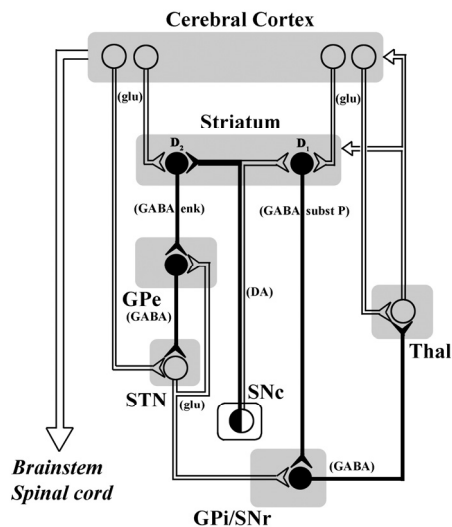
Figure 1.4 Simplified diagram of the circuitry and neurotransmitters of the basal ganglia-thalamocortical circuitry, indicating the parallel 'direct' and 'indirect' pathways from the striatum to the basal ganglia output nuclei in a normal situation. Inhibitory neurons are shown as filled symbols, excitatory neurons are open symbols. Abbreviations: DA, dopamine; D_1, dopamine D_1 receptor; D_2, dopamine D_2 receptor; enk, enkephalin; GABA, γ-aminobutyric acid; GPe, external segment of globus pallidus; GPi, internal segment of globus pallidus; glu, glutamate; SNc, substantia nigra pars compacta; SNr, substantia nigra pars reticulata; subst P, substance P, STN, subthalamic nucleus; Thal, thalamus.[40-42]

The loss of neurons in the nigrostriatal DA-containing pathway is a principal feature of Parkinson's disease, and may initially be compensated for by downregulation of the DA transporter, heightened postsynaptic receptor sensitivity, and changes in STN and GPi firing. However, compensatory mechanisms eventually fail and D_2-bearing neurons become overactive whereas D_1-bearing neurons become hypoactive. These changes eventually lead to an excessive inhibition of thalamocortical and brainstem motor neurons, and the development of parkinsonian features.[29, 30, 38, 39, 43] Although striatal deficiency constitutes the bulk of parkinsonian abnormalities, other neuronal systems are also affected.[30, 44, 45]

DAergic neurons continue to be lost throughout the course of Parkinson's disease. Regression analysis indicates that parkinsonian symptoms are seen only after DAergic neuronal loss has reached a certain threshold.[44] Neurodegeneration could be related to mitochondrial dysfunction, oxidative stress, apoptosis, misfolding and aggregation of proteins, excitotoxicity, and inflammation. The presence of Lewy bodies in addition to loss of pigmented neurons in the SN, is accepted as neuropathological confirmation of the diagnosis Parkinson's disease.[30, 31, 38, 44, 46, 47]

1.4.2 Animal models used to study dopamine receptor ligands

One of the Parkinson's disease models results from the administration of the neurotoxic MPTP to primates (including humans) which causes irreversible and severe parkinsonian symptoms and includes degeneration of nigral DA neurons.[48] After systemic administration MPTP crosses the blood-brain barrier (BBB), and once in the brain MPTP is metabolized to MPP^+ (1-methyl-4-phenylpyridinium) by MAO-B which is taken up into DA neurons and subsequently blocks complex I within mitochondria (Figure 1.5).[46]

MPTP MPP^+
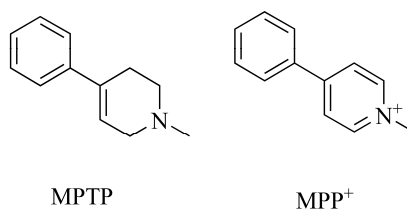
Figure 1.5 Structures of MPTP and MPP^+.[46]

6-Hydroxydopamine (6-OH-DA) is a commonly used neurotoxin to create Parkinson's disease models of hemiparkinsonian rats.[49] A particular model results from the 6-OH-DA-induced destruction of the DAergic nigrostriatal pathway but sparing of the DAergic mesolimbic pathway, which parallels the MPTP-induced hemiparkinsonian model in primates.[50] An alternative 6-OH-DA model causes slow partial lesion of DAergic neurons and has been used to mimic the slow progression of Parkinson's disease.[48]

16

1.4.3 Microdialysis
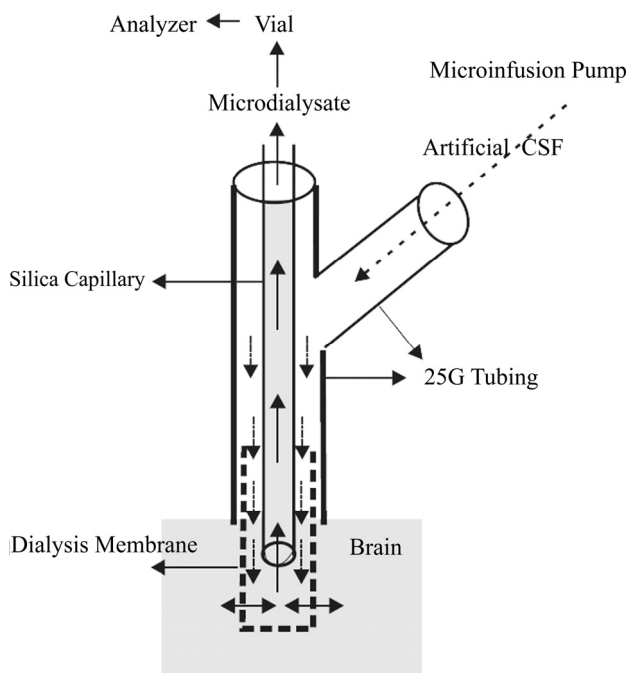
Figure 1.6 Schematic representation of a microdialysis probe. The dialysis membrane is constantly perfused with artificial cerebrospinal fluid (CSF) by a microinfusion pump and molecules are exchanged with the brain extracellular fluid (ECF) by diffusion in both directions. After transportation of the microdialysate through the silica capilary outlet tube, it is collected and the neurotransmitter or drug of interest could be subjected to analysis.[51, 52]

In this thesis the microdialysis technique was used to monitor DA release in the extracellular fluid of the anesthetized rat. This method is based on the dialysis principle in which a membrane, permeable to water and small molecules, separates two fluid compartments. A schematic representation of a microdialysis probe is shown in Figure 1.6. Advantages of brain solute extraction by microdialysis are:[52-55]

1 Microdialysis can be performed in living, awake and freely moving animals and a significant amount of data can be obtained from each animal experiment.
2 Microdialysis detects the free drug and/or neurotransmitter at a specific region within the brain.
3 Microdialysis offers the advantage of protein-free sample fluids that can directly be analyzed by high-performance liquid chromatography (HPLC) or liquid chromatography–mass spectrometry (HPLC-MS).
4 In the freely moving "conscious" animal central neurochemical activity can be monitored in close relation to sensory, motor, or cognitive processes.

5   Microdialysis during anesthesia is easier to use than microdialysis in the freely moving animal, and anesthesia eliminates sensory or behavioural influences on the neurotransmitter systems of interest.

6   Microdialysis can both introduce and remove molecules into and from the brain, respectively.

1.4.4 Treatment of Parkinson's disease

The current treatment for Parkinson's disease is largely symptomatic rather than preventive. Pharmacological treatment is based on restoring the DA deficiency and may be classified into two main categories. The first category is a strategy that uses drugs to increase DA concentrations at the synaptic junction. The second approach is the use of drugs that mimic the action of DA (Figure 1.7).[56]
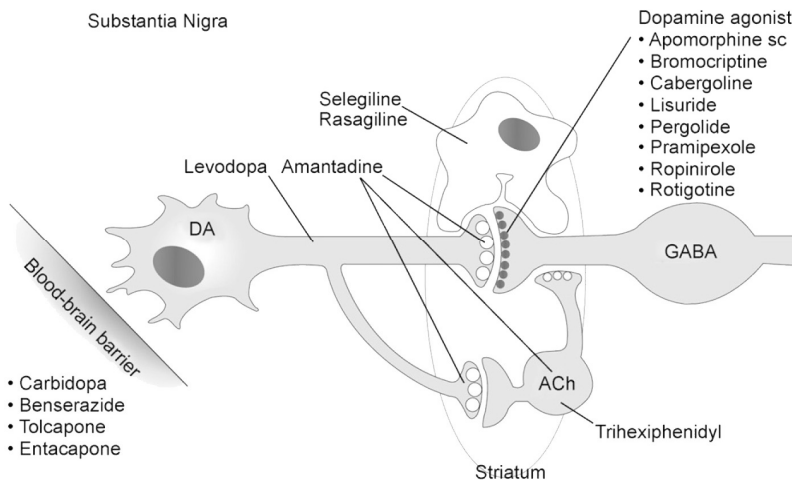
Figure 1.7 Sites of action of Parkinson's disease drugs.[56]

1.4.4.1 *L*-dopa and drugs that increase dopamine concentrations

The most effective pharmacologic treatment for Parkinson's disease is *L*-DOPA.[31] In contrast to DA which is unable to cross the BBB, the precursor *L*-DOPA is transported actively into the brain where it is converted to DA. Initially, all motoric features of Parkinson's disease have benefit from this pharmacologic treatment.[30] *L*-DOPA acts on both DA D_1 and D_2 receptor families[57] and since there are equal numbers of these receptors in the human striatum, simultaneous activation may be one of the explanations for the superior effects of *L*-DOPA.[58]

L-DOPA is combined with carbidopa or benserazide, which are AAAD inhibitors, to prevent systemic adverse effects related to the peripheral metabolism of *L*-DOPA.[59] *L*-DOPA is degraded by COMT in several organs, notably the gut, the liver, and the brain[60],

18

and therefore COMT inhibitors, e.g. entacapone and tolcapone, are given to extend the half-life of *L*-DOPA.[61] Selegiline and rasagiline which are MAO-B inhibitors selectively reduce the metabolism of *L*-DOPA and DA in the brain (Figure 1.8).[59, 62]

Side-effects of DA receptor stimulation are nausea, vomiting, dyskinesias, hallucinations, delusions, and sexual function enhancement.[63]
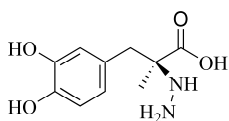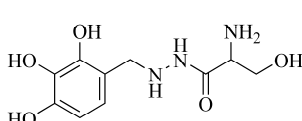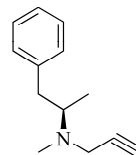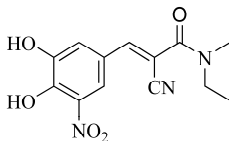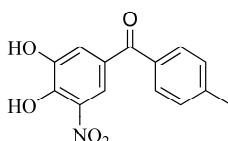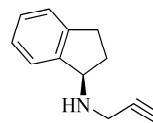
Figure 1.8 Drugs that increase DA concentrations.[61]

1.4.4.2 Motor complications involved with long–term *L*-DOPA treatment: motor fluctuations and dyskinesia

Long-term *L*-DOPA treatment is an important risk factor for the development of motor complications, i.e. motor fluctuations and dyskinesia.[64] The motor complications could be related to abnormal intermittent or pulsatile stimulation of DA receptors, dysregulation of downstream genes and proteins, and the induction of abnormal neuronal firing patterns in basal ganglia output neurons.[65] With advancing disease, there is a progressive loss of striatal DAergic terminals and a reduction in their buffering capacity. Consequently, striatal DA becomes totally dependent on peripheral *L*-DOPA availability and striatal DA receptors are exposed to alternating high and low levels of DA with the risk of ensuing motor complications.[60, 64] The motor fluctuations may be predictable, termed wearing-off or end-of-dose fluctuations, but they can become unpredictable, referred to as on-off phenomena. About a quarter to half of patients taking *L*-DOPA develop motor fluctuations after 5 years.[31, 66]

1.4.4.3 Delay or prevention of motor complications by continuous dopaminergic stimulation

In practice the early use of continuous release *L*-DOPA formulations induced the same rate of motor complications as the standard *L*-DOPA therapy. Because motor complications are clearly related to *L*-DOPA, DA agonists could be interesting drugs to use for continuous DAergic stimulation (CDS).[67-70] DA agonists are however less well tolerated than *L*-DOPA in early Parkinson's disease[71], and the antiparkinsonian benefits of DA agonists are less than that of *L*-DOPA.[72] Nevertheless, evidence shows that motor complications might be prevented, delayed or even reversed by delivering DAergic therapy by CDS.[38, 60]

1.4.4.4 Treatment of motor fluctuations

A large body of scientific and clinical information supports the idea that discontinuous or pulsatile stimulation of striatal DA receptors contributes to the development of *L*-DOPA - induced motor complications and favours the use of CDS-based therapies.[39] Therefore, treatment of motor fluctuations focuses on improvement of *L*-DOPA absorption and alteration in timing of doses. The addition of DA agonists to pharmacotherapy is also considered to reduce motor fluctuations.[31, 65, 67] The application of *L*-DOPA/carbidopa-gel suspension directly in the duodenum (Duodopa®) permits a continuous delivery by a portable pump, resulting in less variability in *L*-DOPA concentrations, and thereby in less motor fluctuations compared to oral *L*-DOPA administration.[73]

1.4.4.5 Treatment of dyskinesias

The first strategy for reducing dyskinesia is to reduce antiparkinsonian medications that are adjunctive therapy and may contribute to dyskinesia, e.g. selegiline, *L*-DOPA controlled release preparations, and DA agonists. Although the latter rarely cause dyskinesias by themselves, when added to *L*-DOPA they may augment dyskinesia. Low-dose L-DOPA treatment appears to have a slightly lower incidence of drug-induced dyskinesias[74] and therefore also L-DOPA itself may be reduced. A second strategy is to add drugs. Amantadine (Figure 1.9) may have antidyskinetic effects perhaps through antagonism of the *N*-methyl-*D*-aspartate (NMDA) glutamate receptor[31], and addition of DA agonists in combination with a reduced dosis or stop of *L*-DOPA may be very effective.[67, 75]
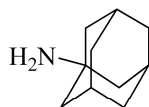
Amantadine

Figure 1.9 Amantadine.

CDS via subcutaneous DA agonist infusions may eventually control dyskinesias[75], and Duodopa® treatment resulted in reduced time and intensity of dyskinesia.[73] A third strategy, for severe, disabling dyskinesia is through brain surgery, e.g. by pallidotomy[67], which is gradually being replaced by deep brain stimulation.[76]

1.4.4.6 Dopamine agonists

DA agonist monotherapy is usually sufficient to control parkinsonism for the first couple of years, and DA agonists are also prescribed as adjuncts to *L*-DOPA to improve response and reduce motor complications.[31, 66, 77] The effect of DA agonists on non-motor domains like mood or cognition is now acknowledged as a key factor in fully addressing patients' needs.[77, 78] Furthermore, DA receptor agonists have been shown to produce neuroprotective activities in experimental models, although no drug has been unequivocally proven to be neuroprotective in the parkinsonian patient.[79]

Bromocriptine   Pergolide   Lisuride   Pramipexole

Ropinirole   Cabergoline   Rotigotine (N-0923)   (R)-(-)-Apomorphine
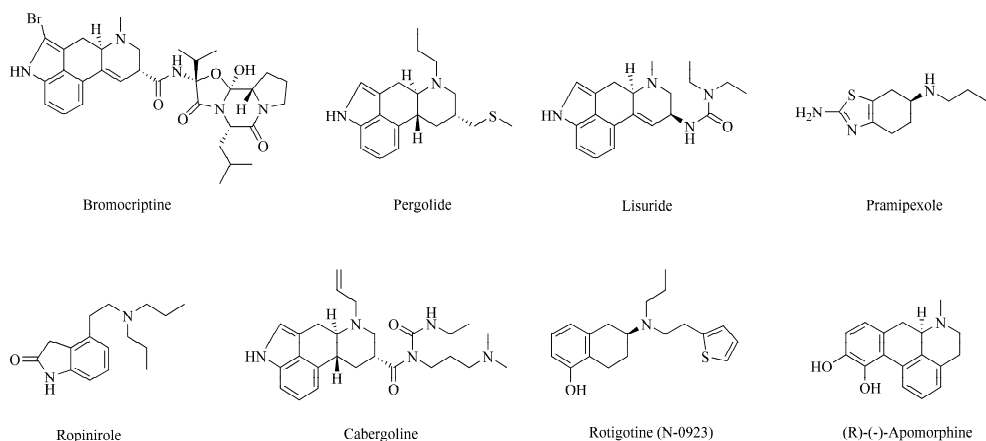
Figure 1.10 DA receptor agonists.[80]

The older, "first generation" agonists are ergot-containing drugs including bromocriptine (Parlodel®), pergolide (Permax®) and lisuride.[59] Two of the "second generation" most commonly prescribed DA agonists are the non-ergoline drugs pramipexole (Mirapex®) and ropinirole (Requip®).[59, 80, 81] Pramipexole is currently also being investigated for its potential to modify disease progression by neuroprotection[82] and its action on mood in Parkinson's disease.[83, 84] Ropinirole, cabergoline and rotigotine (N-0923) are DA receptor agonists which have been approved for the treatment of Parkinson's disease[66, 80], and the latter is used for continuous transdermal administration (Neupro®).[59, 60] At present, intermittent subcutaneous apomorphine is the only acute treatment for "off" episodes in Parkinson's disease.[85] Apomorphine is a short-acting DA D_1/D_2 receptor agonist[62] and the oral administration is limited by high hepatic first pass metabolism and adverse side effects.[80]

1.4.4.7 Anticholinergics and amantadine

Anticholinergics are benztropine, biperiden, orphenadrine, procyclidine, and trihexyphenidyl and can be used in young patients in whom tremor is the major symptom.[31, 59, 68] Elderly patients seem to be more susceptible to the peripheral (e.g. urinary retention, blurred vision, constipation, tachycardia) and centrally-mediated (e.g. mental confusion) adverse effects of anticholinergic agents, which limit their usefulness in older patients.[86] Amantadine, which has weak antiparkinson actions, is sometimes used for initial therapy (Figure 1.9).[31]

1.4.4.8 Surgery

There has been resurgence in the use of surgical techniques for the treatment of Parkinson's disease such as pallidotomy, thalamotomy, and more specifically deep brain stimulation (DBS),[47] where electrodes are placed in the brain which stimulate the GPi, STN or thalamus. DBS causes less irreversible brain trauma than ablative surgery. Furthermore, the functional lesion induced by high frequency stimulation can be easily adjusted.[87-89] Nevertheless, akinesia can not be alleviated, mechanical defects and infection are a risk, DBS can not slow down disease progression, it's is expensive, and expertise in several fields is required. All these factors limit the widespread applicability of DBS.[90]

1.5 MEDICINAL CHEMISTRY OF CENTRALLY ACTING DOPAMINE D_2 AND D_1/D_2 RECEPTOR AGONISTS

1.5.1 Structure-activity relationships of dopamine receptor agonists: rotameric conformation

Giesecke showed by X-ray diffractometric analysis that the trans conformation of DA hydrochloride is favoured as compared to the cis conformation (Figure 1.11).[91] Cannon defined α- and β-rotamers of the trans conformation of DA, in which the catechol ring is coplanar with the plane of the ethylamine side chain, and proposed that these are significant in agonist-receptor interactions.[92]

cis conformation   *trans* conformation   *trans* conformation
                                   α-rotamer   β-rotamer
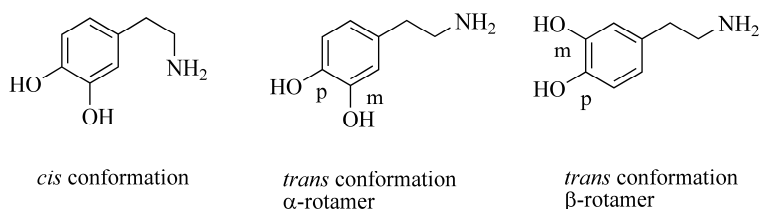
Figure 1.11 *Cis* and *trans* conformations and α- and β-rotamers of DA.[92]

McDermed et al. observed that for DA agonists which are α-rotamers, the S-enantiomer is more active, while for compounds which are β-rotamers the R-enantiomer is the more active form. If the structure of (S)-5-Hydroxy-2-(*N,N*-di-*n*-propylamino)tetralin ((S)-5-OH-DPAT) is rotated and is superimposed over the structure of (R)-7-Hydroxy-2-(*N,N*,-di-*n*-propylamino)tetralin ((R)-7-OH-DPAT) to obtain a similar orientation of the amino group and the meta alcohol groups, the amine moieties are pointing in the same direction (Figure 1.12).[93, 94]

(S)-5-OH-DPAT   (R)-7-OH-DPAT   Superimposition
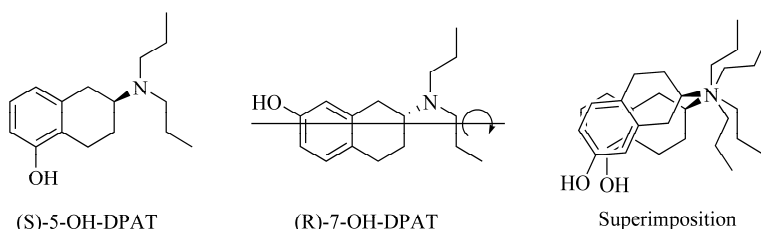
Figure 1.12 Superimposition of (S)-5-OH-DPAT and (R)-7-OH-DPAT.[93, 94]

In an extended model by Wikström et al. using monohydroxylated 3-phenylpiperidines and octahydrobenzo[f]quinolines a relationship was found between the absolute configuration, the ring position of the alcohol group and the size of the *N*-alkyl substituents, named "upwards" and "downwards".[95, 96] α- and β-rotamers of benzo[*f*]quinolines and benzo[*g*]quinolines have been investigated and all α-rotameric conformations appeared to be more potent than the β-conformations.[97, 98] Nevertheless, it is not yet clear which of the two rotamers the DA receptor actually prefers.[98-100]

1.5.2 5-OH-DPAT and N-0437

5-Hydroxy-2-(*N,N*-di-*n*-propylamino)tetralin (5-OH-DPAT) is a DA receptor agonist with a higher selectivity for D_2- over D_1-receptors and the agonist potency resides in the (S)-enantiomer (Figure 1.13).[101, 102] A derivative, 5-hydroxy-2-(*N*-propyl-*N*-2-thienylethylamino)tetralin (N-0437) was found to be an even more potent DA agonist than (S)-5-OH-DPAT[102], and showed a long duration of action.[103] The differential actions of (R)- and (S)-N-0437 gave rise to mutual antagonism, thus providing a strong argument for using the enantiomers instead of the racemate in clinical situations.[18, 104]

Structure-activity studies with series of tetralins showed the effect of chemical differences on the biological activity. 5-OH-DPAT is more potent than its 6- and 7-hydroxy analogs and apomorphine, but less so than its 5,6-dihydroxy analog.[93] 6-Hydroxy-2-(*N,N*-di-*n*-propylamino)tetralin (6-OH-DPAT) lost most of the DAergic potency whereas 7-OH-DPAT is also a potent DA receptor ligand. In contrast, 8-OH-DPAT is a potent and selective serotonergic 5-HT$_{1A}$-receptor agonist.[101, 102] Hacksell et al. investigated an extensive series of *N*-alkylated 2-aminotetralins and concluded that an *n*-propyl group on the nitrogen is optimal for activity.[109] The (S)-enantiomers of the *N*-nitrilepropyl and

(methylthio)propyl derivatives of 5-hydroxy-2-aminotetralins also showed high DAergic activities.[110]
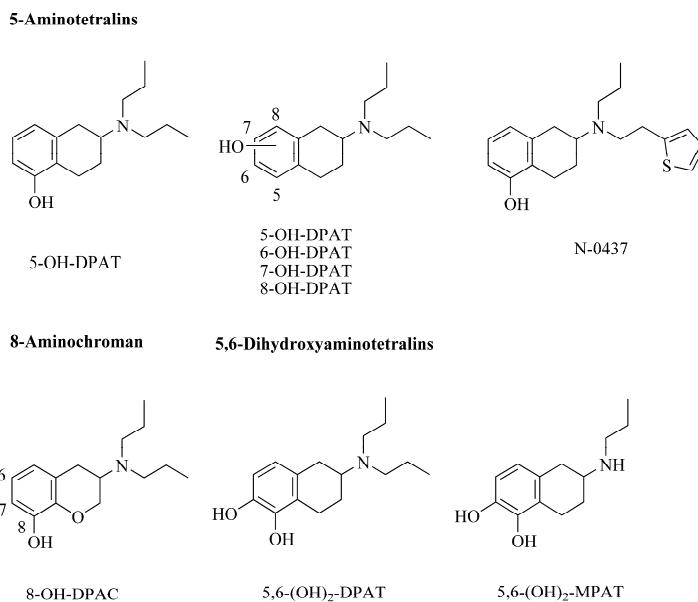
Figure 1.13 5-OH-DPAT and derivatives, N-0437, 8-OH-DPAC, 5,6-(OH)$_2$-DPAT and 5,6-(OH)$_2$-MPAT.[93, 102, 102, 105-108]

1.5.3 8-OH-DPAC

8-Hydroxy-3,4-dihydro-3-(*N,N*-di-*n*-propylamino)-*2H*-1-benzopyran (8-OH-DPAC) has been shown to be a potent, centrally acting agonist at DA D$_2$ receptors.[18, 111] In fact, it shows enhanced selectivity for the presynaptic DA D$_2$ receptors. 8-OH-DPAC was found to be a more potent DA agonist than apomorphine and its carbon analogue 5-OH-DPAT *in vitro*, and the (-)-enantiomer shows higher affinity and selectivity for DA D$_2$ receptors than the (+)-enantiomer (the absolute stereochemistry of the enantiomers of 8-OH-DPAC has not been found in literature).[105, 112-114] Then again, 8-OH-DPAC was shown to be less potent than 5-OH-DPAT *in vivo*[112], which is probably due to rapid metabolic degradation.[113]

1.5.4 5,6-(OH)$_2$-DPAT

Potent central DAergic-like activity can also be found in molecules where a free catechol group resides in the proper spatial relationship to the nitrogen atom, as in apomorphine.[115] The catechol 5,6-dihydroxy-2-(*N,N*-di-*n*-propylamino)tetralin (5,6-(OH)$_2$-DPAT) was found to be a potent mixed DA D$_1$/D$_2$ receptor agonist.[97, 116, 117] Experiments showed a higher DAergic binding and *in vivo* effect for the (-)-enantiomer.[118] Moreover, 5,6-(OH)$_2$-DPAT and its analogue 5,6-dihydroxy-2-(*N-n*-propylamino)tetralin (5,6-(OH)$_2$-MPAT)

showed low ED_{50} values for inhibition of locomotion and induction of stereotypy[119], and were more potent than apomorphine as an emetic.[116]

1.5.5 Metabolism of monophenolic and catecholic dopamine agonists

Due to the fact that most of the potent DA receptor agonists contain aromatic hydroxyl functionalities, they have poor pharmacokinetic properties. Although both monophenolic and catecholic aromatic compounds are metabolically labile, the first are chemically and metabolically more stable than the latter.[109] Phenols and catechols are likely to be conjugated on their first passage through the liver after p.o. or i.p. administration, the so-called first-pass metabolism. Therefore, the central activity of catecholic drugs was mostly studied by using the peripheral subcutaneous route of administration.[106, 116, 120] In addition, an electronically activated aromatic nucleus such as a phenol is susceptible to aromatic hydroxylation by the cytochrome P-450 enzyme system and catechols are degraded by the enzyme COMT.[18, 121]

1.6 BLOOD BRAIN BARRIER

The brain is separated from direct contact with blood by the presence of two barriers: the BBB and the blood-cerebrospinal fluid barrier (BCSFB). The first and largest barrier is the BBB, which contains tight junctions between the cells, restricting the passage of mainly hydrophilic drugs. The second barrier is the BCSFB. Its barrier function is provided by tight junctions between cells which contact the cerebrospinal fluid. The tight junctions are slightly more permeable than those of the BBB.

Molecules can cross the BBB both by passive and active transport. Passive transport (diffusion) depends on size, charge and lipid solubility of the drug. Lipophilic, small, and non-charged drugs diffuse transcellularly easier than do hydrophilic, large and charged drugs. The capillaries of the BBB express proteins involved in active transport, i.e. uptake and excretion (e.g. P-glycoprotein). These proteins are also responsible for the degradation of proteins, peptides, neurotransmitters and drugs, forming a significant metabolic barrier. As the "gatekeeper" to the brain, the BBB determines the ability of drugs to gain entrance to brain extracellular fluid and reach therapeutic concentrations within the CNS.[53, 55, 122] Overall, more than 98% of all small-molecule drugs and approximately 100% of large-molecule drugs do not cross the BBB.[123]

1.7 PRODRUGS

1.7.1 General

Major barriers could exist in the pharmacokinetic phase of a drug which may limit its usefulness, i.e. incomplete absorption, incomplete systemic bioavailability due to first-pass metabolism, too rapid absorption or excretion, toxicity problems, and poor site-specificity of the drug.[101] In order to circumvent these barriers a drug might be converted to a prodrug with improved delivery properties over the parent drug molecule. A prodrug is a pharmacologically inactive derivative of a parent drug molecule that requires chemical or enzymatic biotransformation in order to release the active drug, i.e bioactivation (Figure 1.14).[124]
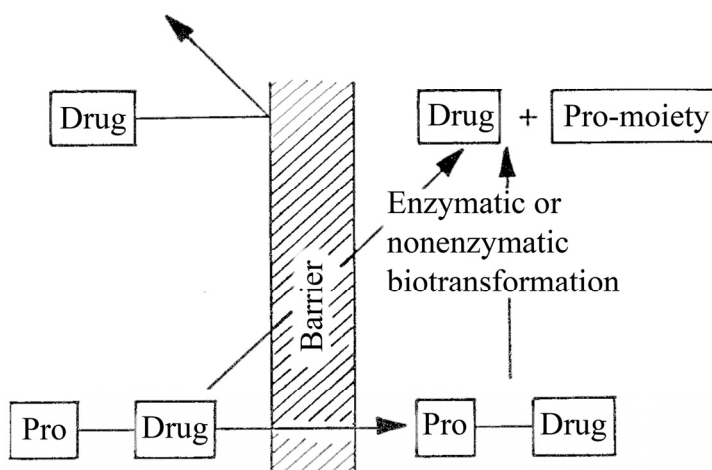
Figure 1.14 Schematic illustration of the prodrug concept.[101, 124]

Several criteria should be considered in the design of a prodrug[101]:
1 The functional groups on the parent drug molecule which are amenable to chemical derivatization.
2 The mechanisms and systems available in the organism for the required bioactivation.
3 Synthesis and purification of the prodrug should be relatively simple.
4 The prodrug should be chemically stable in bulk form.

Examples of noteworthy blockbuster prodrugs are omeprazole, simvastatin, enalapril, and acyclovir (Figure 1.15).[125]

From toxicological view, prodrugs must be considered new drugs[126] and preferably pro-moieties that are known to be nontoxic should be used.[125] Many drugs contain hydroxyl or carboxyl functional groups and the popularity of using esters as a prodrug type for these drugs stems primarily from the fact that the organism is rich in enzymes capable of

hydrolyzing esters. In addition, by appropriate esterification it is possible to obtain derivatives with almost any desirable hydrophilicity or lipophilicity as well as *in vivo* lability.[124] Other examples of functional groups which could be utilized in prodrugs are ethers, carbonates, phosphates and amides.
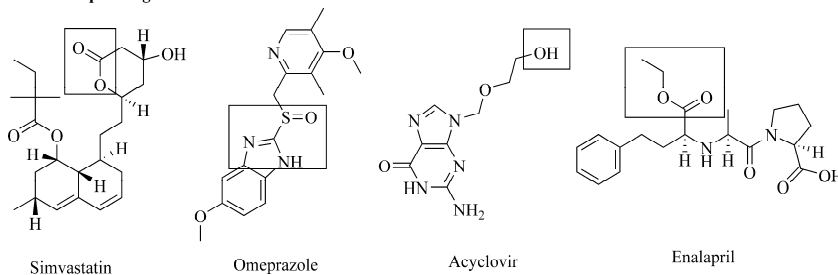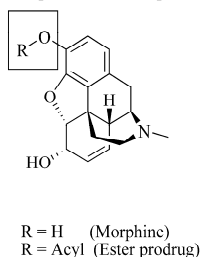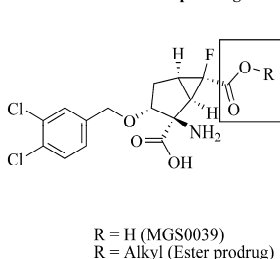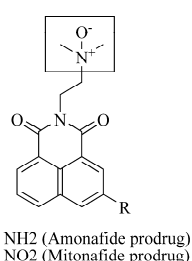
Figure 1.15 Structures of noteworthy blockbuster prodrugs, the ester prodrug of morphine, the prodrug of MGS0039, and amonafide and mitonafide *N*-oxide prodrugs. The prodrug moieties of the drugs are indicated by a box.[125, 127-129]

Common prodrug strategies are: prolongated drug delivery, improved cell permeation, carrier-mediated transport, site-directed drug delivery, site-specific drug release, and antibody-directed enzyme prodrug therapy (ADEPT).

Prolonging the duration of action of a drug can be accomplished by the prodrug approach in two principal ways[101]:
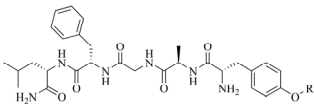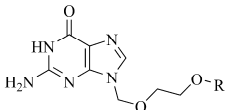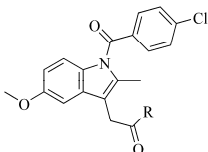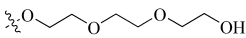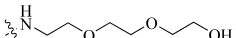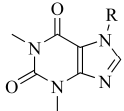
1   through sustained delivery of the prodrug form to the systemic circulation, e.g. lipid emulsions of morphine and its ester prodrugs (Figure 1.15)[130],

2   through design of prodrugs possessing a slow conversion to the parent drug in the organism, e.g. phosphoramidate monoesters of zidovudine (AZT)[131, 132], and polymeric prodrugs of ketoprofen and naproxen.[128]

Drugs that are too hydrophilic frequently have low bioavailabilities. The absorption could be improved by derivatization with a more lipophilic moiety.[101, 125] Eligible drugs for this strategy are e.g. amino alcoholic β-blocking agents[133], drugs with an ionic phosphate moiety[124], and carboxylic acids such as the active acid of enalapril and MGS0039 (Figure 1.15).[127] Carrier-mediated transport could also actively enhance intestinal absorption, e.g.

by usage of intestinal peptide transporters.[125] Site-directed drug delivery is a strategy that affords increased or selective transport of the parent drug to the site of action, e.g. simvastatin which undergoes predominant uptake by the liver. A drug that is released site-specifically can be distributed everywhere but is activated at a specific site, e.g. acyclovir, omeprazole[101], prophalan[134], and the *N*-oxide amonafide and mitonafide prodrugs (Figure 1.15).[129] In ADEPT monoclonal antibody-enzyme conjugates are targeted to antigens present on tumor cell surfaces where they could activate anticancer prodrugs site-selectively.[135]

In the following paragraphs we will discuss several topics in regard of prodrug design. Because the prodrugs in this thesis are based on phenolic DA agonists, i.e. 5-OH-DPAT and 8-OH-DPAC, we will mainly focus on the derivatization of alcoholic drugs.

Table 1.1 Prodrugs of Leu-enkephalin, acyclovir, indomethacin, and theophylline.

Name parent drug	Structure	R group	Half-life (hours)
Leu-enkephalin[136]			68 (pH 7.4, 37 ºC)
			15 (pH 7.4, 37 ºC)
			No degradation after 30 hours (pH 7.4, 37 ºC)
Acyclovir[137]			>300 (pH 6, 40 ºC)
			70 (pH 6, 40 ºC)
Indomethacin[138]			5 (pH 5, 37 ºC)
			15 (pH 5, 37 ºC)
Theophylline[139]			0.01 (pH 7, 20 ºC)
			0.03 (pH 9, 32 ºC)

1.7.2 Chemical stability

The stability of a prodrug plays an important role in drug bioavailability, formulation and storage. Ideal water soluble prodrug design requires an *in vitro*/*in vivo* stability ratio of nearly 106 and this may be readily achievable if the bioactivation is enzyme dependent. Besides usage of the various enzyme systems of the body to carry out the necessary activation of prodrugs, the buffered and relatively constant value of the physiological pH (7.4) may be useful in triggering the release of a drug from a prodrug.[124, 126] When purely chemical prodrug activation is chosen, interspecies variability, genetic polymorphisms, and drug-drug interaction problems are no concern.[125]

1.7.2.1 Alkyl ester prodrugs

Since chemical ester hydrolysis is both specific acid and base catalyzed, ester hydrolysis rates are pH-dependent. Since the hydroxide ion catalyzed rate constant, kOH- is generally much larger than the hydronium-catalyzed rate constant, k_{H+}, the pH of optimum stability of most alkyl esters is typically between 3.5 and 5.[126] Examples of alkyl esters are the acetyl, propionyl and pivaloyl ester prodrugs of a leu-enkephalin analogue (Table 1.1).[136]

1.7.2.2 Amino acid ester prodrugs

The diverse properties of the various amino acid residues, combined with the fact that usually they are nontoxic, give esterification with these moieties wide applicability in prodrug design. Especially to increase solubility and bioavailability, e.g. the *L*-valine ester of acyclovir (Table 1.1).[124] However, the introduction of ionizable functionalities, i.e. an amino or carboxylic acid group, is often associated with decreased stability.[140] The major reason for the low stability of α-amino and short-chained aliphatic amino acid esters in aqueous solution at pH values affording their favourable water-solubility (i.e. pH 3-5) is due to the strongly electron-withdrawing effect of the protonated amino group which activates the ester linkage toward hydroxide ion attack. Another reason for the facilitated ester hydrolysis is intramolecular catalysis or assistance by the neighbouring amino group. The mechanisms involved include intramolecular nucleophilic catalysis, intramolecular general-base catalysis or general-acid specicific base catalysis as depicted in Figure 1.17.[101] Relatively stable amino acid esters under both acid- and base-catalyzed hydrolytic conditions are esters of cyclopropane amino acids as seen with acyclovir prodrugs (Table 1.1).[137]

1.7.2.2 Prodrugs with other pro-moieties

Amide prodrugs, e.g. the prodrug of indomethacin, are in general more chemically stable than the ester prodrugs.[138] The hydrolysis rates of *N*-alkyloxycarbonyl prodrugs, e.g. of the

prodrugs of theophylline, are relatively considerably slower than the rates of the *N*-alkylcarbonyl prodrugs (Table 1.1).[139]
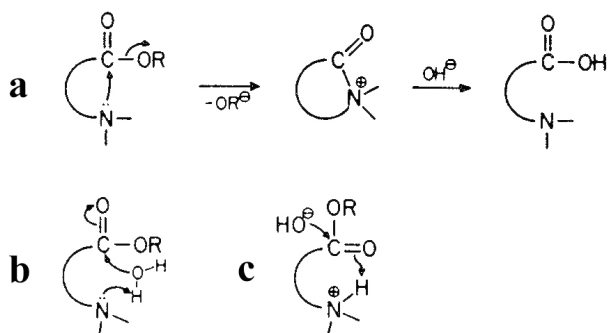
Figure 1.17. Mechanisms of amino acid ester hydrolysis: (a) intramolecular nucleophilic catalysis, (b) intramolecular general-base catalysis or (c) general-acid specicific base catalysis.[101]

1.7.3 Enzymatic stability

Enzymes are classified according to function into six major groups: oxidoreductases, transferases, hydrolases, lyases, isomerases, and ligases.[124] While prodrug activation through bioconversion as a time- and tissue-controlled process has a clear benefit, the inter- and intraspecies variability, genetic polymorphism, and the potential for drug-drug interactions pose significant challenges for such a prodrug strategy.[125] In this thesis we describe the synthesis and study of ester prodrugs and we will therefore focus on esterases, a subgroup of the hydrolases. Esterases hydrolyze ester functional groups and are distributed widely in vertebrate tissues and blood.[124]
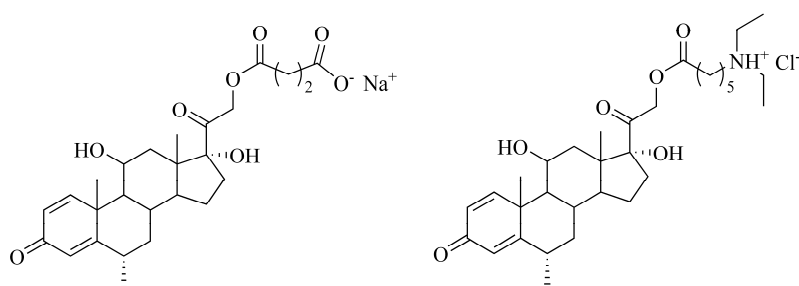
Methylprednisolone prodrugs

Figure 1.18 An anionic and a cationic example of methylprednisolone prodrugs.[141]

1.7.3.1 The influence of amino acids on enzymatic stability

As discussed in Section 1.7.2.2, amino acid prodrugs have wide applicability in prodrug design. The susceptibility of amino acid esters to undergo enzymatic hydrolysis could be affected by the structure of the amino functionality and size of the acyl moiety.[142] Enzymatic hydrolysis studies with prodrug esters of methylprednisolone suggest that derivatives having an anionic moiety are not hydrolyzed in serum, while compounds having a cationic moiety are hyrolyzed rapidly by serum esterases (Figure 1.18).[141]

1.7.3.2 Protection against first-pass metabolism

Drugs containing phenolic groups, e.g. 5-OH-DPAT and N-0437, undergo extensive first-pass metabolism (Section 1.5.5). Nonetheless, several prodrug approaches are available to prevent this:[101]

1   Mask the metabolizable moiety, e.g. derivatization with an acid to yield an ester prodrug;
2   Design of an ester with a built-in esterase inhibiting function, e.g. bambuterol which exhibits esterase-inhibiting properties;
3   To derivatize the susceptible drug molecule at some other position in the molecule so that the prodrug obtained is no longer a substrate for the presystemic metabolizing enzyme.
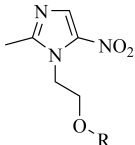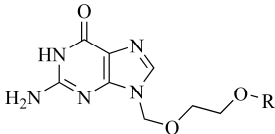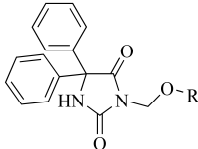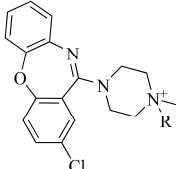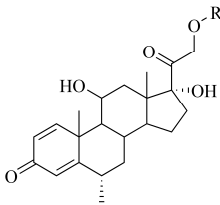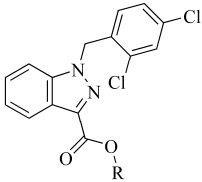
1.7.4 Increased solubility of prodrugs

Two physico-chemical strategies can be employed to increase the aqueous solubility of a drug: (i) derivatization of the drug in order to decrease the melting point and (ii) introduction of an ionic or ionisable group by a pro-moiety. The most commonly used esters for increasing aqueous solubility of alcoholic drugs are amino acid esters[142-152], dicarboxylic acid esters[144, 147], phosphates[150, 153-155], sulphates[144] and polyols[156] (Table 1.2). For a drug or prodrug having ionizable functional groups, salt formation can also be a powerful tool in improving the formulation properties. The salt form of a drug is known to influence a number of physicochemical properties of the parent compound, including solubility and dissolution rate, stability and hygroscopicity.[124, 126]

Another strategy to increase water solubility is the use of micellar prodrugs, as was shown in a series of PEG-paclitaxel conjugate prodrugs.[157] Besides being highly water soluble, micelles have additional advantages: they solubilize poorly soluble degradation products which may otherwise precipitate and they are self-stabilizing due to protection of the hydrolytically labile prodrug linkage within the micelle interior.[158]

Table 1.2 Examples of water-soluble prodrugs.

Name parent drug	Prodrug structure	R group
Metronidazole[145, 149]		Amino acid ester
Acyclovir[147]		Amino acid ester, dicarboxylic acid ester
3-(Hydroxymethyl)-phenytoin[150]		Amino acid ester, phosphate
Loxapine[153-155]		Methylene phosphate
Methylprednisolone[144]		Amino acid ester, dicarboxylic acid ester, or carboxy alkane sulphate
Lonidamine[156]		Polyhydric alcohol

1.7.5 Prodrugs aimed at oligopeptide and glucose transporters

The oral bioavailability of poorly absorbed drugs can be enhanced by targeting them to oligopeptide transporters[159, 160] such as the peptide transporter 1 (PEPT1) which actively transports small peptides.[161] Oligopeptide transporters are highly expressed in the intestine and are also enriched in some cancer epithelial cells and can be used for delivery of peptidomimetic anticancer agents.[162, 163]

Table 1.3 Structures of amino acid ester prodrugs aimed at oligopeptide transporters.

Name parent drug	Prodrug structure[a]	R group
Floxuridine[164-166]		Val, Phe, Pro, Asp, Lys, Leu, Ile, or Gly
BDCRB[167, 168]		Val, Phe, Pro, Asp, Lys, or Ile
PMEA[169]		Val, Phe, Ile, Gly, or Ala
Zidovudine[170]		Phe, Lys, Ile, Tyr, or Gln

[a] $n = 1$ or 2, $X = O$ or S.
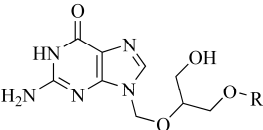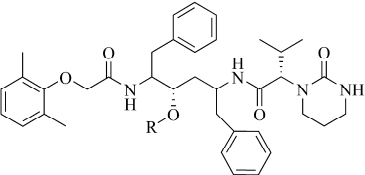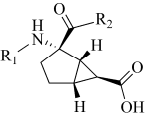
In this section several examples of amino acid ester prodrugs of antiviral and antitumor agents are presented (Table 1.3). Floxuridine prodrug strategies offer great potential, not only for increased drug absorption by targeting the PEPT1 transporter, but as well for improved tumor selectivity and drug efficacy.[164, 166, 171, 172] Amino acid prodrugs of gemcitabine[173], 2-bromo-5,6-dichloro-1-(β-*D*-ribofuranosyl)benzimidazole (BDCRB)[167, 168], 9-[2-(phosphonomethoxy)-ethyl] adenine (PMEA)[169] also exhibited enhanced transport or affinity for PEPT1. Additionally, amino acid prodrugs could increase drug activity, evasion of metabolizing enzymes, bioavailability, and reduce toxicity. The enhanced uptake by HIV-1 infected cells of amino acid prodrugs of AZT[170] and the increased nasal uptake of amino acid prodrugs of acyclovir[174] probably also involves an active transport system.

In addition to targeting an active amino acid transport system, incorporation of glycosyl or polyhydric pro-moieties could increase the affinity for sugar active transport systems in order to increase absorption, e.g. a lonidamine prodrug which targets the glucose transporter GLUT-1 (Table 1.2).[156]

1.7.6 Dipeptide ester prodrugs

The dipeptide prodrug strategy can be applied to increase solubility, optimize chemical and enzymatic stability, improve active transport by membrane peptide transporters, increase bioavailability, enhance pharmacological activity, and decrease toxicity. Examples are dipeptide ester prodrugs of ganciclovir[175], lopinavir[176], LY354740[177] (Table 1.4), acyclovir[178, 179], and floxuridine[172]. According to Nashed and Mitra both geometrical isomerism and hydrogen bonding of dipeptide ester prodrugs might enhance the stability compared to the mono amino acid ester prodrugs.[180] The stabilizing effect of the substituents of alkyl dipeptides has the following order: isobutyl ≥ isopropyl > ethyl > methyl > H, which indicates that steric hindrance influences the chemical stability.[181] This stability relationship was also found for dipeptide ester prodrugs. A valine residue linked to the parent drug in dipeptide prodrugs is of outmost importance to improve chemical stability, while the *N*-terminal residue can be used for further fine tuning of the prodrug's properties.[182] Moreover, incorporation of *D*-valine in a dipeptide did not abolish its affinity towards peptide transporters, though it enhanced the enzymatic stability of the prodrug to a certain extent.[183]

Table 1.4 Structures of dipeptide ester prodrugs.

Name parent drug	Prodrug structure	R group
Ganciclovir[175]		Val-Val-, Gly-Val-, Tyr-Val-, Val-Gly-, Tyr-Gly-, Val-Tyr-, or Gly-Tyr-
Lopinavir[176]		Gly-Val-, or Val-Val
LY354740[177]		R1 or R2 = Ala, Leu, Phe, Val, Gly, Met, Pro, Ile, Tyr, Lys, or Ser

Besides basic hydrolysis of the ester bond, the chemical release of the parent drug of dipeptide esters can also follow another pathway, i.e. cyclization-activation. In this pathway dipeptide esters are degraded to the parent drug and corresponding 2,5-diketopiperazines by intramolecular activation (Figure 1.19).[184, 185] The development of prodrugs that can regenerate the parent drug through non-enzymatic pathways has emerged as an alternative approach in which prodrug activation is not influenced by inter- and intraindividual

variability that affects enzymatic activity. Furthermore, intramolecular pathways have a key role in a more refined two-step prodrug activation, where an initial enzymatic cleavage step is followed by a cyclization-elimination reaction that releases the active drug.[186, 187]
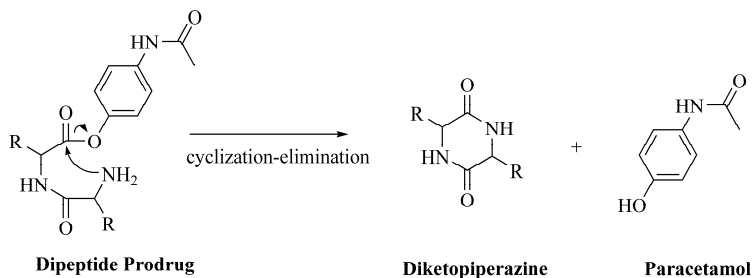
Figure 1.19 Formation of diketopiperazines from a dipeptide prodrug of paracetamol.[184]

1.7.7 Prodrugs for delivery to the central nervous system

The major neurological diseases affecting the brain may be categorized as neurodegenerative, cerebrovascular, inflammatory (infectious and autoimmune) and cancerous.[188] The vascular route would be very promising in drug delivery for targeting the brain, if the BBB could be passed. In general, polar hydrophilic drugs are not easily transported across the BBB (Section 1.6). Fortunately, lipidization through prodrugs offers a possibility for an efficient CNS delivery of polar drugs.[189, 190] Although the brain tissue activity of non specific esterases is unfavourable for utility of esterase activated prodrugs, a variety of oxidative enzymes could be utilized as biotransformation system in the conversion of drugs unable to cross BBB.[188]

In the absence of lipid-mediated mechanisms, circulating molecules can penetrate into the CNS by interaction with endogenous transport systems.[188] Several carriers are targets for this approach, e.g. the *L*-amino acid transporter LAT1 and the glucose transporter GLUT1.[191] The use of *L*-DOPA for the brain targeting of DA which does not cross the BBB, is a classical example of modification of the drug structure, with the aim of obtaining a prodrug as a "pseudonutrient" substrate for LAT1.[188] The crucial role played by glutathione in the pathogenesis of Parkinson's disease and the presence of its influx transporters at the basolateral membrane of the BBB served as the basis for an anti-Parkinson glutathione-based prodrug design.[192]
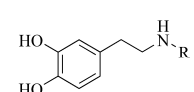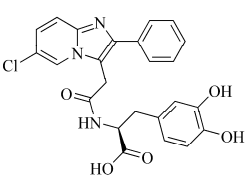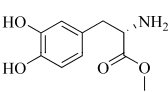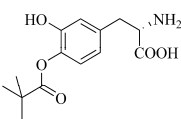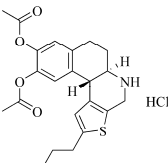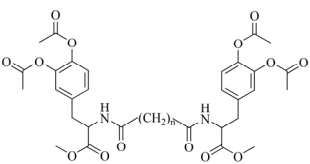
1.7.8 Dopaminergic prodrugs

Several strategies are available to increase the brain uptake, absorption and bioavailability of DA and DAergic compounds. Glycosyl prodrugs of DA have been developed to increase brain uptake by targeting the GLUT1 transporter.[193] Also the lipophilic phenyl-imidazopyridine moiety in dopimid prodrugs can increase the brain uptake of DA. Another

advantage of this strategy is that upon delivery into the brain dopimid prodrugs are cleaved to the active *L*-DOPA (or DA) and phenyl-imidazopyridine moieties, of which the latter could improve the antiparkinsonian therapeutic effect.[194] Improvement of solubility offers potential for more rapid and consistent absorption, and a higher bioavailability as seen with the *L*-DOPA methyl ester.[195-198]

Because phenolic and catecholic functional groups are sensitive to oxidation, these groups can be protected against first-pass metabolism by esterification, e.g. the *L*-DOPA pivaloyl ester prodrug NB-355[199], apomorphine diester produgs[200-203], and ABT-431 which is the diester prodrug of the potent and selective DA D$_1$ receptor agonist A-86929.[204] Furthermore, dimeric prodrugs of *L*-DOPA were synthesized to protect multiple functional groups against metabolism and to improve physicochemical properties (Table 1.5).[205, 206]

Table 1.5 DAergic prodrugs.

Prodrug	Structure	Advantage over parent drug
Glycosyl DA derivatives[193]	R = glucose coupled via linker	Interaction with GLUT1 carrier in the BBB
Dopimid compounds[194]		Phenyl-imidazopyridine: 1) serves as a lipophilic carrier for DA and *L*-DOPA to penetrate the BBB 2) influences DAergic neurons through the GABA-benzodiazepine receptor complex
L-DOPA methyl ester[195-198]		Increased solubility
NB-355[199]		Protection of the catechol against first-pass metabolism by mono-esterification.
ABT-431[204]		Protection of the catechol against first-pass metabolism by di-esterification.
Diamides of (O,O-diacetyl)- *L*-DOPA-methyl ester[205, 206]		1) Protection of multiple functional groups against enzymatic degradation 2) Improved physicochemical properties

(S)-PD148903 is an orally active prodrug with enone structure which is converted by an oxidative bioactivation mechanism to the corresponding catechol and is delivered enantioselectively into the CNS.[207, 208] Though less potent than the parent drug, the oxime derivative of PD148903 was also orally active.[209] With a potency comparable to that of apomorphine, the enone prodrug GMC-6650 can potentially compete with *L*-DOPA and apomorphine in the treatment of Parkinson's disease.[210] TL-334, the active form of GMC-6650 showed an extremely potent DAergic activity, however, the bioavailability was low due to rapid metabolization of the catechol moiety (Figure 1.20).[211]

In vivo bioactivation

GMC-6650   TL-334   PD148903
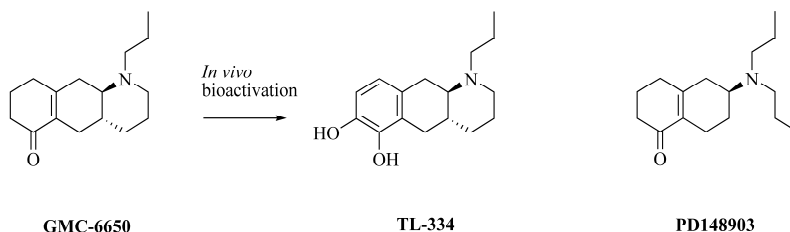
Figure 1.20 Structure of PD148903 and the *in vivo* bioactivation of GMC-6650 into TL-334.[210, 211]

1.8 TRANSDERMAL DRUG DELIVERY

1.8.1 Skin and routes of skin penetration

The skin's barrier function is accomplished by the stratum corneum (SC) which prevents the flux of toxins into the body and minimizes water loss.[212, 213] The SC is an extremely thin layer that is formed by a laminate of compressed keratin-filled corneocytes anchored in a lipophilic matrix.[214, 215] The next consecutive layers are the epidermis and the dermis. At epidermal-dermal junction exists an efficient blood supply which provides a mechanism for eliminating drugs from the local area.[124, 216] A skin penetrant has three potential pathways to the viable tissue, i.e. via sweat ducts, across the SC between the appendages, or through hair follicles with associated sebaceous glands (Figure 1.21).[217]

1.8.2 Passive transdermal drug delivery

The transdermal mode offers several advantages: (1) the skin presents a relatively large surface area for absorption; (2) the application is a non-invasive procedure; (3) the potential for sustained release and (4) controlled input kinetics[218]; (5) circumvention of the first-pass effect; (6) potential for self-administration; and (7) the production of the systems is generally inexpensive.[219] Ideally, a transdermal drug must possess both good lipoidal and aqueous solubilities.[218] All drugs presently administered across skin have an adequate high lipophilicity and low molecular mass (<500 Da).[212] Other factors that influence the passive transdermal delivery are the molecular shape, polarity, charge[220], chirality and melting

point.[221] Presently available transdermal patches for passive delivery can be classified into two categories on the basis of their design: reservoir-type patches and matrix-type patches.[212] The worldwide transdermal market consists of eight FDA-approved active agents: scopolamine, nitroglycerin, clonidine, oestradiol, fentanyl, nicotine, testosterone and norethisterone.[218] In addition, rotigotine (N-0437) is available formulated in a patch against symptoms of Parkinson's disease and restless legs syndrome.[222, 223]
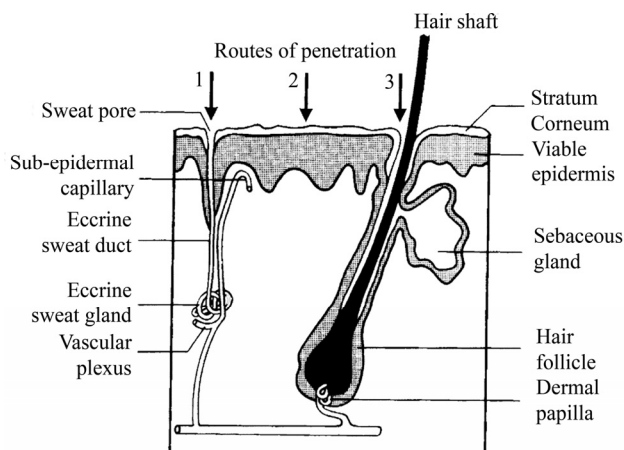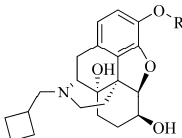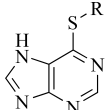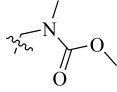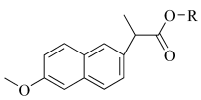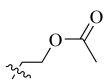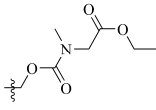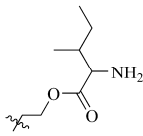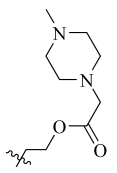
Figure 1.21 Simplified diagram of skin structure and possible routes for drug penetration: (1) via the sweat ducts; (2) across the stratum corneum or (3) through the hair follicles with their associated sebaceous glands.[217]

1.8.3 Prodrugs for passive transdermal drug delivery

Prodrugs which enhance the passive transdermal delivery are presented in Table 1.6 The blood circulation contains many enzymes which are capable of releasing a drug from the prodrug after transdermal delivery. Also the epidermis contains many non-specific enzymes capable of metabolizing prodrugs[224], and because of stereoselective enzymatic degradation chiral prodrugs may be transported stereoselective through the skin.[225] For these reasons the transdermal delivery of prodrugs has considerable potency for therapeutic applications.[124]

Both good aqueous and lipid solubility is an important factor for the passive transdermal flux[139], and several pro-moieties are available to achieve this good biphasic solubility. Increase of lipophilicity by alkylcarbonate formation[219] or esterification with an alkylgroup improves penetration through the skin and displays profound therapeutic effects as observed for prodrugs of nalbuphine, temozolomide, and captopril.[226, 232, 233] Other pro-moieties that were developed to improve the passive transdermal flux are *N*-alkyl-*N*-alkyloxycarbonylaminomethyl groups[227], acyloxyalkyl esters[231], aminocarbonyloxymethyl esters[228], aminoacyloxyalkyl esters[230] and methylpiperazinylacyloxyalkyl ester[229] (Table 1.6), some of which showed satisfactory aqueous solubility and improved topical delivery.

Table 1.6 Structures of prodrugs suitable for passive transdermal delivery and their passive transdermal flux *in vitro*.

Name parent drug	Structure	R group	Type of pro-moiety	Flux (nmol/cm^2/h)
Nalbuphine[226]			Alkyl ester	3 (human skin)
6-Mercaptopurine[227]			*N*-Alkyl-*N*-alkyloxycarbonyl-aminomethyl	15 (hairless mouse skin)
Naproxen[228-231]			Acyloxyalkyl ester	0.44 (human skin)
			Aminocarbonyloxy-methyl ester	0.06 (human skin)
			Aminoacyloxyalkyl ester	5.1 (human skin)
			Methylpiperazinyl-acyloxyalkyl ester	25 (human skin)

1.8.4 Iontophoresis

The essential components of an iontophoresis system are the current source, the anode reservoir system and the cathode reservoir system. The principle of iontophoresis is to transport the drug out of the reservoir into or through the skin, with eventual absorption of the drug by the vasculature for distribution throughout the body (Figure 1.22).[234] Ions prefer skin entry via the pores, such as hair follicles and sweat ducts[235], but ions can also be delivered via the intercellular route.[236] Binding within the skin may form a barrier for drug absorption.[237]

Three main mechanisms enhance molecular transport in iontophoresis: (a) charged species are driven primarily by electro-repulsion from the driving electrode; (b) the flow of electric current may increase the permeability of skin; and (c) electro-osmosis may affect

uncharged molecules and large polar peptides.[217] The electro-repulsive effect produces the largest enhancement to the flux of small lipophilic cations[238], and the fraction of current carried by each type of ion is called the transference number.[239] A linear relationship has been observed between the apparent flux and the applied current for several compounds.[240] Enhancement by electro-osmosis involves the delivery of molecules that are dragged by electrically induced solvent flow[212], and its impact increases with the size of the ion.[235] At the physiological pH of 7.4 the transport of positively charged solutes by iontophoresis is facilitated by the negatively charged proteins in the SC.[241]
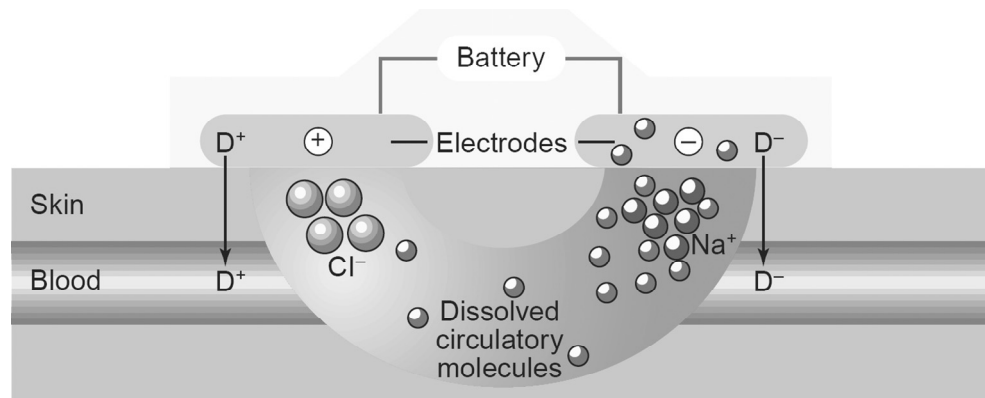
Figure 1.22 Schematic of an iontophoretic device. D^+ is a cationic drug, D^- is an anionic drug.[218]

Many factors have been shown to affect the results of iontophoresis. These include the current strength, physicochemical properties of the compound, drug formulation, equipment used, biological variations, skin temperature and duration of iontophoresis.[235] Drug concentration and drug charge are important factors affecting the iontophoretic process. An increase in concentration increases flux upto a point, after which the flux becomes independent of the donor concentration.[240] Although the drug charge is an important physicochemical property which governs iontophoretic transport, the influence of drug charge on iontophoresis is not yet unambiguously clarified.[212, 234, 235] The optimal application sites of an iontophoretic device are the upper outer arm or chest. Bodyweight and race do not affect the pharmacokinetics.[242] Examples of iontophoretic delivery systems are the fentanyl HCl iontophoresis transdermal system (fentanyl ITS; IONSYS™, Ortho-McNeil, Inc, Raritan, NJ)[243], Lidosite®, Iomed Phoresor® II, and Ocuphor™.[240]

1.8.4.1 Advantages and limitations of iontophoresis

Transdermal iontophoresis not only provides the usual benefits of transdermal drug delivery (Section 1.8.2) but it has several additional advantages:

1   Iontophoresis can be used for programmed and controlled delivery by adjusting the current to the patient's needs, as the transdermal flux of the drug is proportional to the applied electrical current.[240]

2   Iontophoresis can be used for constant drug delivery. The peaks and valleys of blood concentration that are inherent for oral and systemic administration can be avoided simply by maintaining the current at a level known to provide the desired serum level.[234] Electronic controllers are used to keep the current output constant resulting in a constant drug delivery rate.[244]

3   Iontophoresis may provide overall improved drug delivery when the currently available dosage form provides very limited bioavailability.[234]

The main limitations of iontophoresis are:

1   The impossibility to achieve a high transference number with some drugs.[234]

2   If the molecule cannot be formulated as an ion, the prospects of its moving through the skin in sufficient quantity in order to be therapeutically effective are poor. Furthermore, it must exist in ionic form over the variable pH range of the skin of about 4.0 to 7.3.[234]

3   Iontophoresis does not affect the delivery of macromolecules or vaccines, unless used in combination with other methods that increase skin permeability.[219]

4   The vulnerability of the skin limits the amount of current that can safely pass through the skin.[234]

1.8.4.2 Drugs suitable for iontophoretic drug delivery

Iontophoresis was used clinically to rapidly deliver lidocaine for local anesthesia.[219, 245] Pilocarpine can be adminstered by transdermal iontophoresis to induce sweating as part of a cystic fibrosis diagnostic test.[219] The fentanyl ITS was approved as a iontophoretic patch which enables patients to periodically activate the patch by administering a bolus of fentanyl based on their need for pain relief.[243, 246] Also glipizide[247] and venlafaxine hydrochloride are considered promising candidates for transdermal iontophoretic delivery (Figure 1.25).[248]
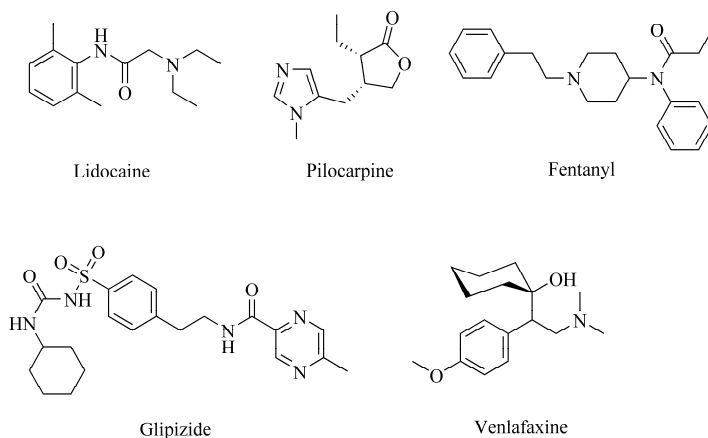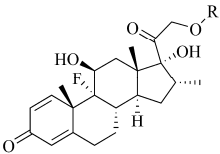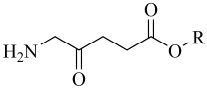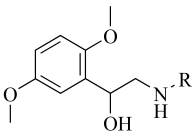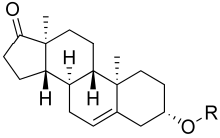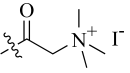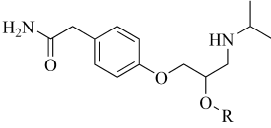
Figure 1.23 Drugs which are suitable for transdermal iontophoretic delivery.

1.8.4.3 Prodrugs suitable for iontophoretic drug delivery

Prodrug design based upon a charged precursor of an active drug to be delivered by iontophoresis is a promising strategy to deliver drugs transdermally. The different enzymes present in the skin may be utilized by the prodrugs to regenerate the active parent drug.[220] Examples of prodrugs which were investigated for transdermal iontophoretic delivery are prodrugs of dexamethasone[249], 5-aminolevulinic acid[250-252], desglymidodrine[253], acyclovir[254], dehydroepiandrosterone[255], nalbuphine[226], and atenolol[256] (Table 1.1, Table 1.6 and Table 1.7).

Table 1.7 Structures of prodrugs suitable for transdermal iontophoretic delivery and their transdermal iontophoretic flux *in vitro*. Also the skin type, electrical current strength and the drug concentration in the donor phase are presented.

Name parent drug	Structure	R group	Flux (nmol/cm^2/h)
Dexamethasone[249]			83 (dermatomed porcine skin, 0.38 mA/cm^2, 4.25 mM)
5-Aminolevulinic acid[250-252]		$-CH_3$	4300 (dermatomed porcine skin, 0.5 mA/cm^2, 15 mM)
Desglymidodrine[253]			922 (dermatomed human skin, 0.1 mA/cm^2, 34 mM)
Dehydroepiandrosterone[255]			71 (rabbit ear skin, 0.5 mA/cm^2, 1.6 mM)
Atenolol[256]			1150 (dermatomed porcine skin, 0.5 mA/cm^2, 20 mM

1.8.5 Other methods for transdermal drug delivery

Besides iontophoresis several other penetration enhancing techniques are available. The most extensively investigated methods involve the use of chemicals that can reversibly

diminish the skin's barrier. Also ultrasound or skin electroporation are techniques to temporarily decrease the skin's barrier function.[217, 218] Needles of micron dimensions can pierce into the skin surface to create holes large enough for molecules to enter[212] and because the SC usually provides the permeation barrier, ablation may also be considered.[217] Furthermore, combinations of penetration enhancers are often more effective and reduce the required 'dose' of each enhancer.[212] Examples are the combination of gel with iontophoresis for the delivery of triamcinolone acetonide acetate[257] and the combination of iontophoresis with microneedles in the case of methotrexate (Figure 1.26).[258]

Triamcinolone acetonide acetate   **Methotrexate**
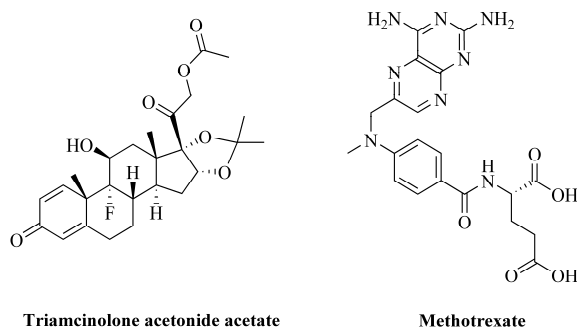
Figure 1.24 Structures of triamcinolone acetonide acetate and methotrexate.
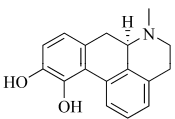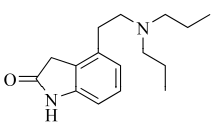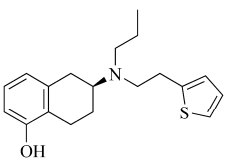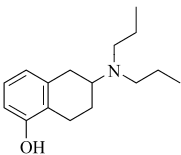
1.8.6 Transdermal drug delivery, iontophoresis and Parkinson's disease

In addition to investigation of the passive transdermal drug delivery of potent DAergic drugs such as (-)-N-0437[259, 260] and (+)-PHNO[261, 262], also the iontophoretic transdermal drug delivery has been explored in the field of antiparkinsonian drugs (Table 1.8). The iontophoretic delivery of apomorphine can be controlled and manipulated accurately by the applied current[263, 264] and may be an attractive tool in future clinical pharmacological investigations in patients with Parkinson's disease (Table 1.8).[265] Besides the current, also secondary effects such as convective flow and electro-osmosis may contribute to the delivery of apomorphine.[266] A chip-controlled iontophoretic system, which is able to directly measure a patient's physical symptoms of Parkinson's disease and accordingly regulate the drug input, seems to be a promising technique.[267]

Iontophoretic delivery of ropinirole was not proportional to drug concentration in vitro[268], nevertheless iontophoresis was able to deliver therapeutic amounts of ropinirole hydrochloride *in vivo*.[271] For the iontophoretic delivery of rotigotine the electro-repulsion was the main mechanism of the iontophoretic transport and crucial factors were: pH and NaCl concentration of the donor phase[272], drug concentration, current density, and skin thickness.[269] The iontophoretic transport of 5-OH-DPAT *in vitro* was found to increase linearly with concentration and current density, providing a convenient way to manage dose titration for Parkinson's disease therapy.[270] Moreover, 5-OH-DPAT showed a considerable

DAergic effect *in vivo*, indicating that therapeutically effective concentrations were achieved.[273]

Table 1.8 Structures of DA agonists suitable for transdermal iontophoretic delivery and their transdermal iontophoretic flux in vitro. Also the skin type, electrical current strength and the drug concentration in the donor phase are presented.

Name parent drug	Structure	Flux (nmol/cm^2/h)
(R)-Apomorphine[263]		140 (dermatomed human skin, 0.5 mA/cm^2, 15 mM)
Ropinirole[268]		43 (full-thickness porcine skin, 0.32 mA/cm^2, 2.5 mM)
Rotigotine (N-0437)[269]		38 (dermatomed human skin, 0.5 mA/cm^2, 4 mM)
5-OH-DPAT[270]		266 (dermatomed human skin, 0.5 mA/cm^2, 7 mM)

1.9 AIM OF THIS THESIS

Nugroho had determined the optimal conditions for the iontophoretic transport of 5-OH-DPAT across human skin *in vitro*.[270] Moreover, he investigated the iontophoretic delivery of 5-OH-DPAT *in vivo* and concluded that the DA agonist was successfully delivered in sufficients amounts into the striatum to achieve a strong DAergic effect.[274] In succession of Nugroho's research, the iontophoretic delivery of 5-OH-DPAT needs further investigation in order to obtain a drug or prodrug which is applicable for administration to patients with Parkinson's disease. The main aim of this study is the development of prodrugs and derivatives of 5-OH-DPAT with optimized physicochemical properties for transdermal delivery by iontophoresis. The main challenges to overcome were the limited solubility of the hydrobromide salt of 5-OH-DPAT, and the stability issues that appear when a prodrug strategy is applied, especially when amino acids are used as pro-moieties.

To achieve an improved iontophoretic profile of newly designed prodrugs or derivatives of 5-OH-DPAT, *in vitro* and *in vivo* studies are necessary. The results of the iontophoretic *in vitro* studies may lead to the selection of the optimal candidate for *in vivo* experiments which include: 1) the validation of a rat model for the iontophoretic delivery of 5-OH-DPAT in combination with microdialysis using an alternative anaesthetic method compared to the one used by Nugroho; and 2) the investigation of the iontophoretic transdermal delivery of a prodrug or derivative of 5-OH-DPAT with enhanced physico-chemical properties.

In this thesis we studied amino acid ester prodrugs of 5-OH-DPAT, dipeptide ester prodrugs of 5-OH-DPAT, and amino acid ester prodrugs of 8-OH-DPAC.

1.10 REFERENCES

1. Fox, S. I. *Human physiology;* WCB McGraw Hill: Boston etc., 1999; , pp xx, 731.
2. Carlsson, A. The occurrence, distribution and physiological role of catecholamines in the nervous system. *Pharmacol. Rev.* **1959**, *11,* 490-3.
3. Chinta, S. J.; Andersen, J. K. Dopaminergic neurons. *Int. J. Biochem. Cell. Biol.* **2005**, *37,* 942-6.
4. Crocker, A. D. Dopamine - Mechanisms of action. *Aust. Prescr.* **1994**, *17,* 17-21.
5. Hornykiewicz, O. Dopamine (3-hydroxytyramine) and brain function. *Pharmacol. Rev.* **1966**, *18,* 925-64.
6. Moore, R. Y.; Bloom, F. E. Central catecholamine neuron systems: anatomy and physiology of the dopamine systems. *Annu. Rev. Neurosci.* **1978**, *1,* 129-69.
7. Iversen, S. D.; Iversen, L. L. Dopamine: 50 years in perspective. *Trends Neurosci.* **2007**, *30,* 188-93.
8. Vallone, D.; Picetti, R.; Borrelli, E. Structure and function of dopamine receptors. *Neurosci. Biobehav. Rev.* **2000**, *24,* 125-32.
9. Snyder, S. H. *Drugs and the brain;* Scientific American Books : Distributed by W.H. Freeman: New York, 1986; , pp 228 p.
10. Jaber, M.; Robinson, S. W.; Missale, C.; Caron, M. G. Dopamine receptors and brain function. *Neuropharmacology* **1996**, *35,* 1503-19.
11. Missale, C.; Nash, S. R.; Robinson, S. W.; Jaber, M.; Caron, M. G. Dopamine receptors: from structure to function. *Physiol. Rev.* **1998**, *78,* 189-225.
12. Pivonello, R.; Ferone, D.; Lombardi, G.; Colao, A.; Lamberts, S. W.; Hofland, L. J. Novel insights in dopamine receptor physiology. *Eur. J. Endocrinol.* **2007**, *156 Suppl 1,* S13-21.
13. Stoof, J. C.; Kebabian, J. W. Two dopamine receptors: biochemistry, physiology and pharmacology. *Life Sci.* **1984**, *35,* 2281-96.
14. De Keyser, J. Subtypes and localization of dopamine receptors in human brain. *Neurochem. Int.* **1993**, *22,* 83-93.
15. White, F. J. D-1 dopamine receptor stimulation enables the inhibition of nucleus accumbens neurons by a D-2 receptor agonist. *Eur. J. Pharmacol.* **1987**, *135,* 101-5.
16. Meador-Woodruff, J. H.; Mansour, A.; Grandy, D. K.; Damask, S. P.; Civelli, O.; J., W. S.,Jr Distribution of D5 dopamine receptor mRNA in rat brain. *Neurosci. Lett.* **1992**, *145,* 209-12.
17. Zhang, J.; Xiong, B.; Zhen, X.; Zhang, A. Dopamine D1 receptor ligands: where are we now and where are we going. *Med. Res. Rev.* **2009**, *29,* 272-94.
18. Wikstrom, H. Centrally acting dopamine D2 receptor ligands: agonists. *Progr. Med. Chem.* **1992**, *29,* 185-216.
19. Vives, F.; Mogenson, G. J. Electrophysiological study of the effects of D1 and D2 dopamine antagonists on the interaction of converging inputs from the sensory-motor cortex and substantia nigra neurons in the rat. *Neuroscience* **1986**, *17,* 349-59.

20.   Yokoo, H.; Goldstein, M.; Meller, E. Receptor reserve at striatal dopamine receptors modulating the release of [3H]dopamine. *Eur. J. Pharmacol.* **1988**, *155,* 323-7.

21.   Meller, E.; Helmer-Matyjek, E.; Bohmaker, K.; Adler, C. H.; Friedhoff, A. J.; Goldstein, M. Receptor reserve at striatal dopamine autoreceptors: implications for selectivity of dopamine agonists. *Eur. J. Pharmacol.* **1986**, *123,* 311-4.

22.   Robertson, G. S.; Robertson, H. A. Synergistic effects of D1 and D2 dopamine agonists on turning behaviour in rats. *Brain Res.* **1986**, *384,* 387-90.

23.   Gerfen, C. R.; Keefe, K. A.; Gauda, E. B. D1 and D2 dopamine receptor function in the striatum: coactivation of D1- and D2-dopamine receptors on separate populations of neurons results in potentiated immediate early gene response in D1-containing neurons. *J. Neurosci.* **1995**, *15,* 8167-76.

24.   Sonsalla, P. K.; Manzino, L.; Heikkila, R. E. Interactions of D1 and D2 dopamine receptors on the ipsilateral vs. contralateral side in rats with unilateral lesions of the dopaminergic nigrostriatal pathway. *J. Pharmacol. Exp. Ther* **1988**, *247,* 180-5.

25.   Carlson, J. H.; Bergstrom, D. A.; Walters, J. R. Stimulation of both D1 and D2 dopamine receptors appears necessary for full expression of postsynaptic effects of dopamine agonists: a neurophysiological study. *Brain Res.* **1987**, *400,* 205-18.

26.   Murray, A. M.; Waddington, J. L. The induction of grooming and vacuous chewing by a series of selective D-1 dopamine receptor agonists: two directions of D-1:D-2 interaction. *Eur. J. Pharmacol.* **1989**, *160,* 377-84.

27.   Braun, A. R.; Laruelle, M.; Mouradian, M. M. Interactions between D1 and D2 dopamine receptor family agonists and antagonists: the effects of chronic exposure on behavior and receptor binding in rats and their clinical implications. *J. Neural Transm.* **1997**, *104,* 341-62.

28.   Parkinson, J. An essay on the shaking palsy (Reprinted). *J. Neuropsychiatry Clin. Neurosci.* **2002**, *14,* 223-236.

29.   Albin, R. L.; Young, A. B.; Penney, J. B. The functional anatomy of basal ganglia disorders. *Trends Neurosci.* **1989**, *12,* 366-75.

30.   Mandir, A. S.; Vaughan, C. Pathophysiology of Parkinson's disease. *Int. Rev. Psychiatr.* **2000**, *12,* 270-280.

31.   Samii, A.; Nutt, J. G.; Ransom, B. R. Parkinson's disease. *Lancet* **2004**, *363,* 1783-1793.

32.   Rajput, A. H. Frequency and Cause of Parkinsons-Disease. *Canadian Journal of Neurological Sciences* **1992**, *19,* 103-107.

33.   de Rijk, M. C.; Launer, L. J.; Berger, K.; Breteler, M. M.; Dartigues, J. F.; Baldereschi, M.; Fratiglioni, L.; Lobo, A.; Martinez-Lage, J.; Trenkwalder, C.; Hofman, A. Prevalence of Parkinson's disease in Europe: A collaborative study of population-based cohorts. Neurologic Diseases in the Elderly Research Group. *Neurology* **2000**, *54,* S21-3.

34.   Baldereschi, M.; Di Carlo, A.; Rocca, W. A.; Vanni, P.; Maggi, S.; Perissinotto, E.; Grigoletto, F.; Amaducci, L.; Inzitari, D. Parkinson's disease and parkinsonism in a longitudinal study: two-fold higher incidence in men. ILSA Working Group. Italian Longitudinal Study on Aging. *Neurology* **2000**, *55,* 1358-63.

35.   Lai, B. C.; Schulzer, M.; Marion, S.; Teschke, K.; Tsui, J. K. The prevalence of Parkinson's disease in British Columbia, Canada, estimated by using drug tracer methodology. *Parkinsonism Rel. Disord.* **2003**, *9,* 233-8.

36.   Muthane, U. B.; Swamy, H. S.; Satishchandra, P.; Subhash, M. N.; Rao, S.; Subbakrishna, D. Early onset Parkinson's disease: are juvenile- and young-onset different? *Mov. Disorders* **1994**, *9,* 539-44.

37.   Pankratz, N.; Foroud, T. Genetics of Parkinson disease. *Genet. Med.* **2007**, *9,* 801-11.

38.   Olanow, C. W. The scientific basis for the current treatment of Parkinson's disease. *Annu. Rev. Med.* **2004**, *55,* 41-60.

39.   Olanow, C. W.; Obeso, J. A.; Stocchi, F. Continuous dopamine-receptor treatment of Parkinson's disease: scientific rationale and clinical implications. *Lancet Neurol.* **2006**, *5,* 677-87.

40.   Gerfen, C. R.; Engber, T. M.; Mahan, L. C.; Susel, Z.; Chase, T. N.; J., M. F.,Jr; Sibley, D. R. D1 and D2 dopamine receptor-regulated gene expression of striatonigral and striatopallidal neurons. *Science* **1990**, *250,* 1429-32.

41.   Alexander, G. E.; Crutcher, M. D. Functional architecture of basal ganglia circuits: neural substrates of parallel processing. *Trends Neurosci.* **1990**, *13,* 266-71.

42.   DeLong, M. R. Primate models of movement disorders of basal ganglia origin. *Trends Neurosci.* **1990**, *13,* 281-5.

43.   Chesselet, M. F.; Delfs, J. M. Basal ganglia and movement disorders: an update. *Trends Neurosci.* **1996**, *19,* 417-22.

44.   Agid, Y. Parkinsons-Disease - Pathophysiology. *Lancet* **1991**, *337,* 1321-1324.

45.   Carey, R. J.; DePalma, G.; Damianopoulos, E.; Hopkins, A.; Shanahan, A.; Muller, C. P.; Huston, J. P. Dopaminergic and serotonergic autoreceptor stimulation effects are equivalent and additive in the suppression of spontaneous and cocaine induced locomotor activity. *Brain Res.* **2004**, *1019,* 134-43.

46.   Dauer, W.; Przedborski, S. Parkinson's disease: mechanisms and models. *Neuron* **2003**, *39,* 889-909.

47.   Schapira, A. H. Science, medicine, and the future: Parkinson's disease. *BMJ* **1999**, *318,* 311-4.

48.   Shimohama, S.; Sawada, H.; Kitamura, Y.; Taniguchi, T. Disease model: Parkinson's disease. *Trends Mol. Med.* **2003**, *9,* 360-5.

49.   Herrera-Marschitz, M.; Ungerstedt, U. Evidence that striatal efferents relate to different dopamine receptors. *Brain Res.* **1984**, *323,* 269-78.

50.   Perese, D. A.; Ulman, J.; Viola, J.; Ewing, S. E.; Bankiewicz, K. S. A 6-hydroxydopamine-induced selective parkinsonian rat model. *Brain Res.* **1989**, *494,* 285-93.

51.   Ribeiro, E. B. Studying the central control of food intake and obesity in rats. *Rev. Nutr.* **2009**, *22,* 163-171.

52.   Westerink, B. H. C. Monitoring Molecules in the Conscious Brain by Microdialysis. *Trends Anal. Chem.* **1992**, *11,* 176-182.

53.   de Lange, E. C.; Danhof, M. Considerations in the use of cerebrospinal fluid pharmacokinetics to predict brain target concentrations in the clinical setting: implications of the barriers between blood and brain. *Clin. Pharmacokinet.* **2002**, *41,* 691-703.

54.   de Souza Silva, M. A.; Müller, C. P.; Huston, J. P. Microdialysis in the brain of anesthetized vs. freely moving animals. In *Handbook of Behavioral Neuroscience;* Westerink, B. H. C., Cremers, T. I. F. H., Eds.; Elsevier: 2007; Vol. 16, pp 71-91; 1.5.

55.   Smith, Q. R. A review of blood-brain barrier transport techniques. *Meth. Mol. Med.* **2003**, *89,* 193-208.

56.   Stacy, M. Pharmacotherapy for advanced Parkinson's disease. *Pharmacotherapy* **2000**, *20,* 8S-16S.

57.   Schapira, A. H.; Bezard, E.; Brotchie, J.; Calon, F.; Collingridge, G. L.; Ferger, B.; Hengerer, B.; Hirsch, E.; Jenner, P.; Le Novere, N.; Obeso, J. A.; Schwarzschild, M. A.; Spampinato, U.; Davidai, G. Novel pharmacological targets for the treatment of Parkinson's disease. *Nat. Rev. Drug Discov.* **2006**, *5,* 845-54.

58.   Vermeulen, R. J.; Jongenelen, C. A.; Langeveld, C. H.; Wolters, E. C.; Stoof, J. C.; Drukarch, B. Dopamine D1 receptor agonists display a different intrinsic activity in rat, monkey and human astrocytes. *Eur. J. Pharmacol.* **1994**, *269,* 121-5.

59.   Rezak, M. Current pharmacotherapeutic treatment options in Parkinson's disease. *Disease-a-Month* **2007**, *53,* 214-22.

60.   Chase, T. N. Levodopa therapy: consequences of the nonphysiologic replacement of dopamine. *Neurology* **1998**, *50,* S17-25.

61.   Kurth, M. C.; Adler, C. H. COMT inhibition: a new treatment strategy for Parkinson's disease. *Neurology* **1998**, *50,* S3-14.

62.   Fung, V. S. C.; Hely, M. A.; De Moore, G.; Morris, J. G. L. Drugs for Parkinson's disease. *Aust. Prescr.* **2001**, *24,* 92-95.

63.   Keltner, N. L.; Hogan, B.; Guy, D. M. Dopaminergic and serotonergic receptor function in the CNS. *Perspect. Psychiatr. Care* **2001**, *37,* 65-8.

64.   Olanow, C. W.; Schapira, A. H. V.; Rascol, O. Continuous dopamine-receptor stimulation in early Parkinson's disease. *Trends Neurosci.* **2000**, *23,* S117-S126.

65.   Rascol, O.; Brooks, D. J.; Korczyn, A. D.; De Deyn, P. P.; Clarke, C. E.; Lang, A. E. A five-year study of the incidence of dyskinesia in patients with early Parkinson's disease who were treated with ropinirole or levodopa. 056 Study Group. *N. Engl. J. Med.* **2000**, *342,* 1484-91.

66.   Hagan, J. J.; Middlemiss, D. N.; Sharpe, P. C.; Poste, G. H. Parkinson's disease: Prospects for improved drug therapy. *Trends Pharmacol. Sci.* **1997**, *18,* 156-163.

67.   Nutt, J. G. Motor fluctuations and dyskinesia in Parkinson's disease. *Parkinsonism Rel. Disord.* **2001**, *8,* 101-8.

68.   Rascol, O.; Goetz, C.; Koller, W.; Poewe, W.; Sampaio, C. Treatment interventions for Parkinson's disease: an evidence based assessment. *Lancet* **2002**, *359,* 1589-98.

69.   Scheller, D.; Durmuller, N.; Moser, P.; Porsolt, R. D. Continuous stimulation of dopaminergic receptors by rotigotine does not interfere with the sleep-wake cycle in the rat. *Eur. J. Pharmacol.* **2008**, *584,* 111-7.

70.   Stocchi, F.; Vacca, L.; De Pandis, M. F.; Barbato, L.; Valente, M.; Ruggieri, S. Subcutaneous continuous apomorphine infusion in fluctuating patients with Parkinson's disease: long-term results. *J. Neurol. Sci.* **2001**, *22,* 93-4.

71.   Inzelberg, R.; Schechtman, E.; Nisipeanu, P. Cabergoline, pramipexole and ropinirole used as monotherapy in early Parkinson's disease: an evidence-based comparison. *Drugs Aging* **2003**, *20,* 847-55.

72.   Stacy, M.; Galbreath, A. Optimizing long-term therapy for Parkinson disease: levodopa, dopamine agonists, and treatment-associated dyskinesia. *Clin. Neuropharmacol.* **2008**, *31,* 51-6.

73.   Odin, P.; Wolters, E.; Antonini, A. Continuous dopaminergic stimulation achieved by duodenal levodopa infusion. *J. Neurol. Sci.* **2008**, *29 Suppl 5,* S387-8.

74.   Poewe, W. H.; Lees, A. J.; Stern, G. M. Low-dose L-dopa therapy in Parkinson's disease: a 6-year follow-up study. *Neurology* **1986**, *36,* 1528-30.

75.   Poewe, W. Adjuncts to levodopa therapy: dopamine agonists. *Neurology* **1998**, *50,* S23-6; discussion S44-8.

76.   Merola, A.; Zibetti, M.; Angrisano, S.; Rizzi, L.; Lanotte, M.; Lopiano, L. Comparison of subthalamic nucleus deep brain stimulation and Duodopa in the treatment of advanced Parkinson's disease. *Mov. Disorders* **2011**, *26,* 664-70.

77.   Antonini, A.; Barone, P. Dopamine agonist-based strategies in the treatment of Parkinson's disease. *J. Neurol. Sci.* **2008**, *29 Suppl 5,* S371-4.

78.   Mehta, M. A.; Riedel, W. J. Dopaminergic enhancement of cognitive function. *Curr. Pharm. Des.* **2006**, *12,* 2487-500.

79.   Radad, K.; Gille, G.; Rausch, W. D. Short review on dopamine agonists: insight into clinical and research studies relevant to Parkinson's disease. *Pharmacol. Rep.* **2005**, *57,* 701-12.

80.   Sit, S. Y. Dopamine agonists in the treatment of Parkinson's disease - Past, present and future. *Curr. Pharm. Des.* **2000**, *6,* 1211-1248.

81.   Schrag, A. E.; Brooks, D. J.; Brunt, E.; Fuell, D.; Korczyn, A.; Poewe, W.; Quinn, N. P.; Rascol, O.; Stocchi, F. The safety of ropinirole, a selective nonergoline dopamine agonist, in patients with Parkinson's disease. *Clin. Neuropharmacol.* **1998**, *21,* 169-75.

82.   Schapira, A. H.; Albrecht, S.; Barone, P.; Comella, C. L.; McDermott, M. P.; Mizuno, Y.; Poewe, W.; Rascol, O.; Marek, K. Rationale for delayed-start study of pramipexole in Parkinson's disease: the PROUD study. *Mov. Disorders* **2010**, *25,* 1627-32.

83.   Lemke, M. R.; Brecht, H. M.; Koester, J.; Reichmann, H. Effects of the dopamine agonist pramipexole on depression, anhedonia and motor functioning in Parkinson's disease. *J. Neurol. Sci.* **2006**, *248,* 266-70.

84.   Barone, P.; Scarzella, L.; Marconi, R.; Antonini, A.; Morgante, L.; Bracco, F.; Zappia, M.; Musch, B. Pramipexole versus sertraline in the treatment of depression in Parkinson's disease: a national multicenter parallel-group randomized study. *J. Neurol.* **2006**, *253,* 601-7.

85.   Stacy, M.; Silver, D. Apomorphine for the acute treatment of "off" episodes in Parkinson's disease. *Parkinsonism Rel. Disord.* **2008**, *14,* 85-92.

86.   Brocks, D. R. Anticholinergic drugs used in Parkinson's disease: An overlooked class of drugs from a pharmacokinetic perspective. *J. Pharm. Pharmaceut. Sci.* **1999**, *2,* 39-46.

87. AnonymousDeep-brain stimulation of the subthalamic nucleus or the pars interna of the globus pallidus in Parkinson's disease. *N. Engl. J. Med.* **2001**, *345,* 956-63.

88. Lozano, A. M. Surgery for Parkinson's disease, the five W's: why, who, what, where, and when. *Adv. Neurol.* **2003**, *91,* 303-7.

89. Walker, R. H.; Koch, R. J.; Sweeney, J. E.; Moore, C.; Meshul, C. K. Effects of subthalamic nucleus lesions and stimulation upon glutamate levels in the dopamine-depleted rat striatum. *Neuroreport* **2009**, *20,* 770-5.

90. Yuan, H.; Zhang, Z. W.; Liang, L. W.; Shen, Q.; Wang, X. D.; Ren, S. M.; Ma, H. J.; Jiao, S. J.; Liu, P. Treatment strategies for Parkinson's disease. *Neuroscience Bulletin* **2010**, *26,* 66-76.

91. Giesecke, J. Refinement of the structure of dopamine hydrochloride. *Acta Crystallogr. , Sect. B* **1980**, *36,* 178-181.

92. Cannon, J. G. Structure-activity relationships of dopamine agonists. *Annu. Rev. Pharmacol. Toxicol.* **1983**, *23,* 103-29.

93. McDermed, J. D.; McKenzie, G. M.; Freeman, H. S. Synthesis and Dopaminergic Activity of (+/-)-1,2,3,4-Tetrahydronaphthalene, (+)-1,2,3,4-Tetrahydronaphthalene, and (-)-2-Dipropylamino-5-Hydroxy-1,2,3,4-Tetrahydronaphthalene. *J. Med. Chem.* **1976**, *19,* 547-549.

94. McDermed, J. D.; Freeman, H. S.; Ferris, R. M. Enantioselectivity in the binding of (+)- and (-)-2-amino-6,7-dihydroxy-1,2,3,4-tetrahydronaphthalene and related agonists to dopamine receptors (Abstr). In *Catecholamines, basic and clinical frontiers;* Udsin, E., Kopin, I. J. and Barchas, J., Eds.; Pergamon Press New York: 1979; pp 568-570.

95. Liljefors, T.; Wikstrom, H. A molecular mechanics approach to the understanding of presynaptic selectivity for centrally acting dopamine receptor agonists of the phenylpiperidine series. *J. Med. Chem.* **1986**, *29,* 1896-904.

96. Wikstrom, H.; Andersson, B.; Sanchez, D.; Lindberg, P.; Arvidsson, L. E.; Johansson, A. M.; Nilsson, J. L. G.; Svensson, K.; Hjorth, S.; Carlsson, A. Resolved Monophenolic 2-Aminotetralins and 1,2,3,4,4A,5,6,10B-Octahydrobenzo[F]Quinolines - Structural and Stereochemical Considerations for Centrally Acting Presynaptic and Postsynaptic Dopamine-Receptor Agonists. *J. Med. Chem.* **1985**, *28,* 215-225.

97. Bhatnagar, R. K.; Arneric, S. P.; Cannon, J. G.; Flynn, J.; Long, J. P. Structure activity relationships of presynaptic dopamine receptor agonists. *Pharmacol. Biochem. Behav.* **1982**, *17 Suppl 1,* 11-9.

98. Costall, B.; Lim, S. K.; Naylor, R. J.; Cannon, J. G. On the preferred rotameric conformation for dopamine agonist action: an illusory quest. *J. Pharm. Pharmacol.* **1982**, *34,* 246-54.

99. Horn, A. S.; Rodgers, J. R. 2-amino-6,7-dihydroxytetrahydronaphthalene and the receptor-site preferred conformation of dopamine--a commentary. *J. Pharm. Pharmacol.* **1980**, *32,* 521-4.

100. Woodruff, G. N.; Watling, K. J.; Andrews, C. D.; Poat, J. A.; McDermed, J. D. Dopamine receptors in rat striatum and nucleus accumbens; conformational studies using rigid analogues of dopamine. *J. Pharm. Pharmacol.* **1977**, *29,* 422-7.

101. Krogsgaard-Larsen, P.; Bundgaard, H. *A Textbook of Drug Design and Development;* Harwood Academic Publishers: 1991; .

102. vanVliet, L. A.; Tepper, P. G.; Dijkstra, D.; Damsma, G.; Wikstrom, H.; Pugsley, T. A.; Akunne, H. C.; Heffner, T. G.; Glase, S. A.; Wise, L. D. Affinity for dopamine D-2, D-3, and D-4 receptors of 2-aminotetralins. Relevance of D-2 agonist binding for determination of receptor subtype selectivity. *J. Med. Chem.* **1996**, *39,* 4233-4237.

103. Van der Weide, J.; De Vries, J. B.; Tepper, P. G.; Horn, A. S. Pharmacological profiles of three new, potent and selective dopamine receptor agonists: N-0434, N-0437 and N-0734. *Eur. J. Pharmacol.* **1986**, *125,* 273-82.

104. Timmerman, W.; Dubocovich, M. L.; Westerink, B. H.; De Vries, J. B.; Tepper, P. G.; Horn, A. S. The enantiomers of the dopamine agonist N-0437: in vivo and in vitro effects on the release of striatal dopamine. *Eur. J. Pharmacol.* **1989**, *166,* 1-11.

105. Alneirabeyeh, M.; Reynaud, D.; Podona, T.; Ou, L.; Perdicakis, C.; Coudert, G.; Guillaumet, G.; Pichat, L.; Gharib, A.; Sarda, N. Methoxy and Hydroxy Derivatives of 3,4-Dihydro-3-(Di-Normal-Propylamino)-2H-1-Benzopyrans - New Synthesis and Dopaminergic Activity. *Eur. J. Med. Chem.* **1991**, *26,* 497-504.

106.   Cannon, J. G.; Lee, T.; Goldman, H. D.; Costall, B.; Naylor, R. J. Cerebral Dopamine Agonist Properties of Some 2-Aminotetralin Derivatives After Peripheral and Intracerebral Administration. *J. Med. Chem.* **1977**, *20,* 1111-1116.

107.   Copinga, S.; Dijkstra, D.; Devries, J. B.; Grol, C. J.; Horn, A. S. Synthesis and Pharmacological Evaluation of 5,6,7,8-Tetrahydro-6-[Propyl[2-(2-Thienyl)Ethyl]Amino]-1,2-Naphthalenediol - A Novel Nonselective Dopamine-Receptor Agonist. *Recl. Trav. Chim. Pays-Bas* **1993**, *112,* 137-142.

108.   Dijkstra, D.; Mulder, T. B.; Rollema, H.; Tepper, P. G.; Van der Weide, J.; Horn, A. S. Synthesis and pharmacology of trans-4-n-propyl-3,4,4a,10b-tetrahydro-2H,5H-1-benzopyrano[4,3-b]-1,4-oxazin-7- and -9-ols: the significance of nitrogen pKa values for central dopamine receptor activation. *J. Med. Chem.* **1988**, *31,* 2178-82.

109.   Hacksell, U.; Svensson, U.; Nilsson, J. L. G.; Hjorth, S.; Carlsson, A.; Wikstrom, H.; Lindberg, P.; Sanchez, D. N-Alkylated 2-Aminotetralins - Central Dopamine-Receptor Stimulating Activity. *J. Med. Chem.* **1979**, *22,* 1469-1475.

110.   Seiler, M. P.; Stoll, A. P.; Closse, A.; Frick, W.; Jaton, A.; Vigouret, J. M. Structure-Activity-Relationships of Dopaminergic 5-Hydroxy-2-Aminotetralin Derivatives with Functionalized N-Alkyl Substituents. *J. Med. Chem.* **1986**, *29,* 912-917.

111.   Boye, S.; Pfeiffer, B.; Renard, P.; Rettori, M. C.; Guillaumet, G.; Viaud, M. C. N,N-disubstituted aminomethyl benzofuran derivatives: synthesis and preliminary binding evaluation. *Bioorg. Med. Chem.* **1999**, *7,* 335-41.

112.   Horn, A. S.; Kaptein, B.; Vermue, N. A.; Devries, J. B.; Mulder, T. B. A. Synthesis and Dopaminergic Activity of a New Oxygen Isostere of the 2-Aminotetralins - N,N-Dipropyl-8-Hydroxy-3-Chromanamine. *Eur. J. Med. Chem.* **1988**, *23,* 325-328.

113.   Vermue, N. A.; Kaptein, B.; Tepper, P. G.; de Vries, J. B.; Horn, A. S. Pharmacological profile of N,N dipropyl-8-hydroxy-3-chromanamine, an oxygen isostere of the dopamine agonist N,N dipropyl-5-hydroxy-2-aminotetralin with enhanced presynaptic selectivity. *Arch. Int. Pharmacodyn. Ther.* **1988**, *293,* 37-56.

114.   Wise, L. D.; Dewald, H. A.; Hawkins, E. S.; Reynolds, D. M.; Heffner, T. G.; Meltzer, L. T.; Pugsley, T. A. 6-Hydroxy-3,4-Dihydro-3-(Dipropylamino)-2H-1-Benzopyrans and 8-Hydroxy-3,4-Dihydro-3-(Dipropylamino)-2H-1-Benzopyrans - Dopamine Agonists with Autoreceptor Selectivity. *J. Med. Chem.* **1988**, *31,* 688-691.

115.   Saari, W. S.; King, S. W.; Lotti, V. J.; Scriabin.A Synthesis and Biological-Activity of Some Aporphine Derivatives Related to Apomorphine. *J. Med. Chem.* **1974**, *17,* 1086-1090.

116.   McDermed, J. D.; McKenzie, G. M.; Phillips, A. P. Synthesis and Pharmacology of Some 2-Aminotetralins - Dopamine Receptor Agonists. *J. Med. Chem.* **1975**, *18,* 362-367.

117.   Rollema, H.; Feenstra, M. G.; Grol, C. J.; Lewis, M. H.; Staples, L.; Mailman, R. B. S(-)DP-5,6-ADTN as an in vivo dopamine receptor ligand: relation between displacement by dopamine agonists and their pharmacological effects. *Naunyn-Schmiedeberg's Arch. Pharmacol.* **1986**, *332,* 338-45.

118.   Grol, C. J.; Jansen, L. J.; Rollema, H. Resolution of 5,6-Dihydroxy-2-(N,N-Di-Normal-Propylamino)Tetralin in Relation to the Structural and Stereochemical Requirements for Centrally Acting Dopamine Agonists. *J. Med. Chem.* **1985**, *28,* 679-683.

119.   Bradbury, A. J.; Cannon, J. G.; Costall, B.; Naylor, R. J. A comparison of dopamine agonist action to inhibit locomotor activity and to induce stereotyped behaviour in the mouse. *Eur. J. Pharmacol.* **1984**, *105,* 33-47.

120.   Horn, A. S.; Grol, C. J.; Dijkstra, D.; Mulder, A. H. Facile Syntheses of Potent Dopaminergic Agonists and Their Effects on Neurotransmitter Release. *J. Med. Chem.* **1978**, *21,* 825-828.

121.   Wikstrom, H.; Elebring, T.; Hallnemo, G.; Andersson, B.; Svensson, K.; Carlsson, A.; Rollema, H. Occurrence and Pharmacological Significance of Metabolic Ortho-Hydroxylation of 5-Hydroxy-2-(Di-Normal-Propylamino)Tetralin and 8-Hydroxy-2-(Di-Normal-Propylamino)Tetralin. *J. Med. Chem.* **1988**, *31,* 1080-1084.

122.   Bickel, U. How to measure drug transport across the blood-brain barrier. *Neurorx* **2005**, *2,* 15-26.

123.   Pardridge, W. M. The blood-brain barrier and neurotherapeutics. *Neurorx* **2005**, *2,* 1-2.

124.   Bundgaard, H. *Design of prodrugs;* Elsevier: Amsterdam etc., 1985; , pp VII, 360.
125.   Ettmayer, P.; Amidon, G. L.; Clement, B.; Testa, B. Lessons learned from marketed and investigational prodrugs. *J. Med. Chem.* **2004**, *47,* 2393-404.
126.   Roche, E. B. *Bioreversible carriers in drug design : theory and applications;* Pergamon Press: New York etc., 1987; , pp VIII, 292.
127.   Nakamura, M.; Kawakita, Y.; Yasuhara, A.; Fukasawa, Y.; Yoshida, K.; Sakagami, K.; Nakazato, A. In vitro and in vivo evaluation of the metabolism and bioavailability of ester prodrugs of MGS0039 (3-(3,4-dichlorobenzyloxy)-2-amino-6-fluorobicyclo[3.1.0] hexane-2,6-dicarboxylic acid), a potent metabotropic glutamate receptor antagonist. *Drug Metab. Dispos.* **2006**, *34,* 369-374.
128.   Wang, L. F.; Chiang, H. N.; Wu, P. C. Kinetics and hydrolysis mechanism of polymeric prodrugs containing ibuprofen, ketoprofen, and naproxen as pendent agents. *J. Biomater. Sci. , Polym. Ed.* **2002**, *13,* 287-299.
129.   Yin, H.; Xu, Y.; Qian, X.; Li, Y.; Liu, J. Novel N-oxide of naphthalimides as prodrug leads against hypoxic solid tumor: synthesis and biological evaluation. *Bioorg. Med. Chem. Lett.* **2007**, *17,* 2166-70.
130.   Wang, J. J.; Sung, K. C.; Yeh, C. H.; Fang, J. Y. The delivery and antinociceptive effects of morphine and its ester prodrugs from lipid emulsions. *Int. J. Pharm.* **2008**, *353,* 95-104.
131.   Song, H.; Griesgraber, G. W.; Wagner, C. R.; Zimmerman, C. L. Pharmacokinetics of amino acid phosphoramidate monoesters of zidovudine in rats. *Antimicrob. Agents Chemother.* **2002**, *46,* 1357-1363.
132.   Wagner, C. R.; Chang, S. L.; Griesgraber, G. W.; Song, H.; McIntee, E. J.; Zimmerman, C. L. Antiviral nucleoside drug delivery via amino acid phosphoramidates. *Nucleos. Nucleot.* **1999**, *18,* 913-9.
133.   Hovgaard, L.; Brondsted, H.; Buur, A.; Bundgaard, H. Drug delivery studies in Caco-2 monolayers. Synthesis, hydrolysis, and transport of O-cyclopropane carboxylic acid ester prodrugs of various beta-blocking agents. *Pharm. Res.* **1995**, *12,* 387-92.
134.   Mittal, S.; Song, X. Q.; Vig, B. S.; Amidon, G. L. Proline prodrug of melphalan targeted to prolidase, a prodrug activating enzyme overexpressed in melanoma. *Pharm. Res.* **2007**, *24,* 1290-1298.
135.   Vrudhula, V. M.; Svensson, H. P.; Kennedy, K. A.; Senter, P. D.; Wallace, P. M. Antitumor activities of a cephalosporin prodrug in combination with monoclonal antibody-beta-lactamase conjugates. *Bioconjugate Chem.* **1993**, *4,* 334-40.
136.   Fredholt, K.; Adrian, C.; Just, L.; Larsen, D. H.; Weng, S. S.; Moss, B.; Friis, G. J. Chemical and enzymatic stability as well as transport properties of a Leu-enkephalin analogue and ester prodrugs thereof. *J. Controlled Release* **2000**, *63,* 261-273.
137.   Bender, D. M.; Peterson, J. A.; McCarthy, J. R.; Gunaydin, H.; Takano, Y.; Houk, K. N. Cyclopropanecarboxylic acid esters as potential prodrugs with enhanced hydrolytic stability. *Org. Lett.* **2008**, *10,* 509-511.
138.   Chandrasekaran, S.; Al-Ghananeem, A. M.; Riggs, R. M.; Crooks, P. A. Synthesis and stability of two indomethacin prodrugs. *Bioorg. Med. Chem. Lett.* **2006**, *16,* 1874-1879.
139.   Sloan, K. B.; DellaVecchia, S. A.; Estes, J. V.; Roberts, W. J. 7-alkylcarbonyl and 7-alkyloxycarbonyl prodrugs of theophylline. *Int. J. Pharm.* **2000**, *205,* 53-63.
140.   Robinson, R. P.; Reiter, L. A.; Barth, W. E.; Campeta, A. M.; Cooper, K.; Cronin, B. J.; Destito, R.; Donahue, K. M.; Falkner, F. C.; Fiese, E. F.; Johnson, D. L.; Kuperman, A. V.; Liston, T. E.; Malloy, D.; Martin, J. J.; Mitchell, D. Y.; Rusek, F. W.; Shamblin, S. L.; Wright, C. F. Discovery of the hemifumarate and (alpha-L-alanyloxy)methyl ether as prodrugs of an antirheumatic oxindole: Prodrugs for the enolic OH group. *J. Med. Chem.* **1996**, *39,* 10-18.
141.   Anderson, B. D.; Conradi, R. A.; Spilman, C. H.; Forbes, A. D. Strategies in the design of solution-stable, water-soluble prodrugs III: influence of the pro-moiety on the bioconversion of 21-esters of corticosteroids. *J. Pharm. Sci.* **1985**, *74,* 382-7.
142.   Takata, J.; Karube, Y.; Nagata, Y.; Matsushima, Y. Prodrugs of Vitamin-e .1. Preparation and Enzymatic-Hydrolysis of Aminoalkanecarboxylic Acid-Esters of D-Alpha-Tocopherol. *J. Pharm. Sci.* **1995**, *84,* 96-100.

143.   Altomare, C.; Trapani, G.; Latrofa, A.; Serra, M.; Sanna, E.; Biggio, G.; Liso, G. Highly water-soluble derivatives of the anesthetic agent propofol: in vitro and in vivo evaluation of cyclic amino acid esters. *Eur. J. Pharm. Sci.* **2003**, *20,* 17-26.

144.   Anderson, B. D.; Conradi, R. A.; Knuth, K. E. Strategies in the design of solution-stable, water-soluble prodrugs I: a physical-organic approach to pro-moiety selection for 21-esters of corticosteroids. *J. Pharm. Sci.* **1985**, *74,* 365-74.

145.   Bundgaard, H.; Larsen, C.; Arnold, E. Prodrugs as Drug Delivery Systems .27. Chemical-Stability and Bioavailability of a Water-Soluble Prodrug of Metronidazole for Parenteral Administration. *Int. J. Pharm.* **1984**, *18,* 79-87.

146.   Bundgaard, H.; Larsen, C.; Thorbek, P. Prodrugs as Drug Delivery Systems .26. Preparation and Enzymatic-Hydrolysis of Various Water-Soluble Amino-Acid Esters of Metronidazole. *Int. J. Pharm.* **1984**, *18,* 67-77.

147.   Colla, L.; De Clercq, E.; Busson, R.; Vanderhaeghe, H. Synthesis and antiviral activity of water-soluble esters of acyclovir [9-[(2-hydroxyethoxy)methyl]guanine]. *J. Med. Chem.* **1983**, *26,* 602-4.

148.   Hewawasam, P.; Ding, M.; Chen, N.; King, D.; Knipe, J.; Pajor, L.; Ortiz, A.; Gribkoff, V. K.; Starrett, J. Synthesis of water-soluble prodrugs of BMS-191011: a maxi-K channel opener targeted for post-stroke neuroprotection. *Bioorg. Med. Chem. Lett.* **2003**, *13,* 1695-8.

149.   Mahfouz, N. M.; Hassan, M. A. Synthesis, chemical and enzymatic hydrolysis, and bioavailability evaluation in rabbits of metronidazole amino acid ester prodrugs with enhanced water solubility. *J. Pharm. Pharmacol.* **2001**, *53,* 841-848.

150.   Varia, S. A.; Schuller, S.; Stella, V. J. Phenytoin prodrugs IV: Hydrolysis of various 3-(hydroxymethyl)phenytoin esters. *J. Pharm. Sci.* **1984**, *73,* 1074-80.

151.   Vollmann, K.; Qurishi, R.; Hockemeyer, J.; Muller, C. E. Synthesis and properties of a new water-soluble prodrug of the adenosine A 2A receptor antagonist MSX-2. *Molecules* **2008**, *13,* 348-59.

152.   Xiao, Z.; Vance, J. R.; Bastow, K. F.; Brossi, A.; Wang, H. K.; Lee, K. H. Antitumor agents. Part 235: Novel 4'-ester etoposide analogues as potent DNA topoisomerase II inhibitors with improved therapeutic potential. *Bioorg. Med. Chem.* **2004**, *12,* 3363-9.

153.   Krise, J. P.; Charman, W. N.; Charman, S. A.; Stella, V. J. A novel prodrug approach for tertiary amines. 3. In vivo evaluation of two N-phosphonooxymethyl prodrugs in rats and dogs. *J. Pharm. Sci.* **1999**, *88,* 928-932.

154.   Krise, J. P.; Narisawa, S.; Stella, V. J. A novel prodrug approach for tertiary amines. 2. Physicochemical and in vitro enzymatic evaluation of selected N-phosphonooxymethyl prodrugs. *J. Pharm. Sci.* **1999**, *88,* 922-927.

155.   Krise, J. P.; Zygmunt, J.; Georg, G. I.; Stella, V. J. Novel prodrug approach for tertiary amines: Synthesis and preliminary evaluation of N-phosphonooxymethyl prodrugs. *J. Med. Chem.* **1999**, *42,* 3094-3100.

156.   Giorgioni, G.; Ruggieri, S.; Di Stefano, A.; Sozio, P.; Cinque, B.; Di Marzio, L.; Santoni, G.; Claudi, F. Glycosyl and polyalcoholic prodrugs of lonidamine. *Bioorg. Med. Chem. Lett.* **2008**, *18,* 2445-50.

157.   Ryu, B. Y.; Sohn, J. S.; Hess, M.; Choi, S. K.; Choi, J. K.; Jo, B. W. Synthesis and anti-cancer efficacy of rapid hydrolysed water-soluble paclitaxel pro-drugs. *J. Biomater. Sci. , Polym. Ed.* **2008**, *19,* 311-24.

158.   Anderson, B. D.; Conradi, R. A.; Knuth, K. E.; Nail, S. L. Strategies in the design of solution-stable, water-soluble prodrugs II: properties of micellar prodrugs of methylprednisolone. *J. Pharm. Sci.* **1985**, *74,* 375-81.

159.   Oh, D. M.; Han, H. K.; Amidon, G. L. Drug transport and targeting. Intestinal transport. *Pharm. Biotechnol.* **1999**, *12,* 59-88.

160.   Rubio-Aliaga, I.; Daniel, H. Mammalian peptide transporters as targets for drug delivery. *Trends Pharmacol. Sci.* **2002**, *23,* 434-40.

161.   Meredith, D.; Boyd, C. A. Oligopeptide transport by epithelial cells. *J. Membr. Biol.* **1995**, *145,* 1-12.

162.   Gonzalez, D. E.; Covitz, K. M.; Sadee, W.; Mrsny, R. J. An oligopeptide transporter is expressed at high levels in the pancreatic carcinoma cell lines AsPc-1 and Capan-2. *Cancer Res.* **1998**, *58,* 519-25.

163.   Nakanishi, T.; Tamai, I.; Takaki, A.; Tsuji, A. Cancer cell-targeted drug delivery utilizing oligopeptide transport activity. *Int. J. Cancer* **2000**, *88,* 274-80.

164.   Landowski, C. P.; Vig, B. S.; Song, X.; Amidon, G. L. Targeted delivery to PEPT1-overexpressing cells: acidic, basic, and secondary floxuridine amino acid ester prodrugs. *Mol. Cancer Ther.* **2005**, *4,* 659-67.

165.   Tsume, Y.; Vig, B. S.; Sun, J.; Landowski, C. P.; Hilfinger, J. M.; Ramachandran, C.; Amidon, G. L. Enhanced absorption and growth inhibition with amino acid monoester prodrugs of floxuridine by targeting hPEPT1 transporters. *Molecules* **2008**, *13,* 1441-54.

166.   Vig, B. S.; Lorenzi, P. J.; Mittal, S.; Landowski, C. P.; Shin, H. C.; Mosberg, H. I.; Hilfinger, J. M.; Amidon, G. L. Amino acid ester prodrugs of floxuridine: Synthesis and effects of structure, stereochemistry, and site of esterification on the rate of hydrolysis. *Pharm. Res.* **2003**, *20,* 1381-1388.

167.   Lorenzi, P. L.; Landowski, C. P.; Song, X. Q.; Borysko, K. Z.; Breitenbach, J. M.; Kim, J. S.; Hilfinger, J. M.; Townsend, L. B.; Drach, J. C.; Amidon, G. L. Amino acid ester prodrugs of 2-bromo-5,6-dichloro-1-(beta-D-ribofuranosyl) benzimidazole enhance metabolic stability in vitro and in vivo. *J. Pharmacol. Exp. Ther* **2005**, *314,* 883-890.

168.   Song, X.; Vig, B. S.; Lorenzi, P. L.; Drach, J. C.; Townsend, L. B.; Amidon, G. L. Amino acid ester prodrugs of the antiviral agent 2-bromo-5,6-dichloro-1-(beta-D-ribofuranosyl)benzimidazole as potential substrates of hPEPT1 transporter. *J. Med. Chem.* **2005**, *48,* 1274-7.

169.   Fu, X.; Jiang, S.; Li, C.; Xin, J.; Yang, Y.; Ji, R. Design and synthesis of novel bis(L-amino acid) ester prodrugs of 9-[2-(phosphonomethoxy)ethyl]adenine (PMEA) with improved anti-HBV activity. *Bioorg. Med. Chem. Lett.* **2007**, *17,* 465-70.

170.   Aggarwal, S. K.; Gogu, S. R.; Rangan, S. R. S.; Agrawal, K. C. Synthesis and Biological Evaluation of Prodrugs of Zidovudine. *J. Med. Chem.* **1990**, *33,* 1505-1510.

171.   Landowski, C. P.; Song, X. Q.; Lorenzi, P. L.; Hilfinger, J. M.; Amidon, G. L. Floxuridine amino acid ester prodrugs: Enhancing Caco-2 permeability and resistance to glycosidic bond metabolism. *Pharm. Res.* **2005**, *22,* 1510-1518.

172.   Tsume, Y.; Hilfinger, J. M.; Amidon, G. L. Enhanced cancer cell growth inhibition by dipeptide prodrugs of floxuridine: increased transporter affinity and metabolic stability. *Mol. Pharmaceutics* **2008**, *5,* 717-27.

173.   Song, X.; Lorenzi, P. L.; Landowski, C. P.; Vig, B. S.; Hilfinger, J. M.; Amidon, G. L. Amino acid ester prodrugs of the anticancer agent gemcitabine: synthesis, bioconversion, metabolic bioevasion, and hPEPT1-mediated transport. *Mol. Pharmaceutics* **2005**, *2,* 157-167.

174.   Yang, C.; Gao, H.; Mitra, A. K. Chemical stability, enzymatic hydrolysis, and nasal uptake of amino acid ester prodrugs of acyclovir. *J. Pharm. Sci.* **2001**, *90,* 617-24.

175.   Majumdar, S.; Nashed, Y. E.; Patel, K.; Jain, R.; Itahashi, M.; Neumann, D. M.; Hill, J. M.; Mitra, A. K. Dipeptide monoester ganciclovir prodrugs for treating HSV-1-induced corneal epithelial and stromal keratitis: in vitro and in vivo evaluations. *J. Ocul. Pharmacol. Therapeut.* **2005**, *21,* 463-74.

176.   Agarwal, S.; Boddu, S. H.; Jain, R.; Samanta, S.; Pal, D.; Mitra, A. K. Peptide prodrugs: improved oral absorption of lopinavir, a HIV protease inhibitor. *Int. J. Pharm.* **2008**, *359,* 7-14.

177.   Bueno, A. B.; Collado, I.; de Dios, A.; Dominguez, C.; Martin, J. A.; Martin, L. M.; Martinez-Grau, M. A.; Montero, C.; Pedregal, C.; Catlow, J.; Coffey, D. S.; Clay, M. P.; Dantzig, A. H.; Lindstrom, T.; Monn, J. A.; Jiang, H.; Schoepp, D. D.; Stratford, R. E.; Tabas, L. B.; Tizzano, J. P.; Wright, R. A.; Herin, M. F. Dipeptides as effective prodrugs of the unnatural amino acid (+)-2-aminobicyclo[3.1.0]hexane-2,6-dicarboxylic acid (LY354740), a selective group II metabotropic glutamate receptor agonist. *J. Med. Chem.* **2005**, *48,* 5305-20.

178.   Anand, B. S.; Katragadda, S.; Mitra, A. K. Pharmacokinetics of novel dipeptide ester prodrugs of acyclovir after oral administration: intestinal absorption and liver metabolism. *J. Pharmacol. Exp. Ther* **2004**, *311,* 659-67.

179.   Anand, B.; Nashed, Y.; Mitra, A. Novel dipeptide prodrugs of acyclovir for ocular herpes infections: Bioreversion, antiviral activity and transport across rabbit cornea. *Curr. Eye Res.* **2003**, *26,* 151-63.

180.   Nashed, Y. E.; Mitra, A. K. Synthesis and characterization of novel dipeptide ester prodrugs of acyclovir. *Spectrochim. Acta, Part A* **2003**, *59,* 2033-9.

181.   Jarboe, C. J.; Noll, B. W.; Hass, L. F. The influence of various alpha-alkyl and alpha-hydroxyalkyl substituents on the stability of dipeptides in dilute alkali. *Biochem. Biophys. Res. Commun.* **1971**, *43,* 1029-34.

182.   Santos, C. R.; Capela, R.; Pereira, C. S.; Valente, E.; Gouveia, L.; Pannecouque, C.; De Clercq, E.; Moreira, R.; Gomes, P. Structure-activity relationships for dipeptide prodrugs of acyclovir: Implications for prodrug design. *Eur. J. Med. Chem.* **2008**, .

183.   Talluri, R. S.; Samanta, S. K.; Gaudana, R.; Mitra, A. K. Synthesis, metabolism and cellular permeability of enzymatically stable dipeptide prodrugs of acyclovir. *Int. J. Pharm.* **2008**, *361,* 118-24.

184.   Santos, C.; Mateus, M. L.; dos Santos, A. P.; Moreira, R.; de Oliveira, E.; Gomes, P. Cyclization-activated prodrugs. Synthesis, reactivity and toxicity of dipeptide esters of paracetamol. *Bioorg. Med. Chem. Lett.* **2005**, *15,* 1595-1598.

185.   Santos, C.; Morais, J.; Gouveia, L.; de Clercq, E.; Pannecouque, C.; Nielsen, C. U.; Steffansen, B.; Moreira, R.; Gomes, P. Dipeptide derivatives of AZT: synthesis, chemical stability, activation in human plasma, hPEPT1 affinity, and antiviral activity. *ChemMedChem* **2008**, *3,* 970-8.

186.   Gomes, P.; Vale, N.; Moreira, R. Cyclization-activated prodrugs. *Molecules* **2007**, *12,* 2484-2506.

187.   Kohchi, Y.; Hattori, K.; Oikawa, N.; Mizuguchi, E.; Isshiki, Y.; Aso, K.; Yoshinari, K.; Shirai, H.; Miwa, M.; Inagaki, Y.; Ura, M.; Ogawa, K.; Okabe, H.; Ishitsuka, H.; Shimma, N. Design and synthesis of novel prodrugs of 2'-deoxy-2'-methylidenecytidine activated by membrane dipeptidase overexpressed in tumor tissues. *Bioorg. Med. Chem. Lett.* **2007**, *17,* 2241-5.

188.   Pavan, B.; Dalpiaz, A.; Ciliberti, N.; Biondi, C.; Manfredini, S.; Vertuani, S. Progress in drug delivery to the central nervous system by the prodrug approach. *Molecules* **2008**, *13,* 1035-65.

189.   Greene, D. L.; Hau, V. S.; Abbruscato, T. J.; Bartosz, H.; Misicka, A.; Lipkowski, A. W.; Hom, S.; Gillespie, T. J.; Hruby, V. J.; Davis, T. P. Enkephalin analog prodrugs: Assessment of in vitro conversion, enzyme cleavage characterization and blood-brain barrier permeability. *J. Pharmacol. Exp. Ther* **1996**, *277,* 1366-1375.

190.   Rautio, J.; Laine, K.; Gynther, M.; Savolainen, J. Prodrug approaches for CNS delivery. *AAPS Journal* **2008**, *10,* 92-102.

191.   Gynther, M.; Laine, K.; Ropponen, J.; Leppanen, J.; Mannila, A.; Nevalainen, T.; Savolainen, J.; Jarvinen, T.; Rautio, J. Large Neutral Amino Acid Transporter Enables Brain Drug Delivery via Prodrugs. *J. Med. Chem.* **2008**, *51,* 932-6.

192.   More, S. S.; Vince, R. Design, synthesis and biological evaluation of glutathione peptidomimetics as components of anti-Parkinson prodrugs. *J. Med. Chem.* **2008**, *51,* 4581-8.

193.   Fernandez, C.; Nieto, O.; Fontenla, J. A.; Rivas, E.; de Ceballos, M. L.; Fernandez-Mayoralas, A. Synthesis of glycosyl derivatives as dopamine prodrugs: interaction with glucose carrier GLUT-1. *Org. Biomol. Chem* **2003**, *1,* 767-71.

194.   Denora, N.; Laquintana, V.; Lopedota, A.; Serra, M.; Dazzi, L.; Biggio, G.; Pal, D.; Mitra, A. K.; Latrofa, A.; Trapani, G.; Liso, G. Novel L-dopa and dopamine prodrugs containing a 2-phenyl-imidazopyridine moiety. *Pharm. Res.* **2007**, *24,* 1309-1324.

195.   Di Stefano, A.; Sozio, P.; Cerasa, L. S. Antiparkinson Prodrugs. *Molecules* **2008**, *13,* 46-68.

196.   Itoh, S.; Oo, C. A feasibility study of differential delivery of levodopa ester and benserazide using site-specific intestinal loops in rats. *J. Pharm. Sci.* **2010**, *99,* 227-33.

197.   Stocchi, F.; Marconi, S. Factors associated with motor fluctuations and dyskinesia in Parkinson Disease: potential role of a new melevodopa plus carbidopa formulation (Sirio). *Clin. Neuropharmacol.* **2010**, *33,* 198-203.

198.   Zangaglia, R.; Stocchi, F.; Sciarretta, M.; Antonini, A.; Mancini, F.; Guidi, M.; Martignoni, E.; Pacchetti, C. Clinical experiences with levodopa methylester (melevodopa) in patients with

Parkinson disease experiencing motor fluctuations: an open-label observational study. *Clin. Neuropharmacol.* **2010**, *33,* 61-6.

199.   Ihara, M.; Tsuchiya, Y.; Sawasaki, Y.; Hisaka, A.; Takehana, H.; Tomimoto, K.; Yano, M. A new potential prodrug to improve the duration of L-dopa: L-3-(3-hydroxy-4-pivaloyloxyphenyl)alanine. *J. Pharm. Sci.* **1989**, *78,* 525-9.

200.   Baldessarini, R. J.; Kula, N. S.; Walton, K. G.; Borgman, R. J. Hydrolysis of Diester Prodrugs of Apomorphine. *Biochem. Pharmacol.* **1977**, *26,* 1749-1756.

201.   Baldessarini, R. J.; Walton, K. G.; Borgman, R. J. Esters of apomorphine and N,N-dimethyldopamine as agonists of dopamine receptors in the rat brain in vivo. *Neuropharmacology* **1975**, *14,* 725-31.

202.   Borgman, R. J. Prolonged apomorphine-like behavioural effects of apomorphine esters. *Neuropharmacology* **1976**, *15,* 471-8.

203.   Borgman, R. J.; Baldessarini, R. J.; Walton, K. G. Diester Derivatives As Apomorphine Prodrugs. *J. Med. Chem.* **1976**, *19,* 717-719.

204.   Shiosaki, K.; Jenner, P.; Asin, K. E.; Britton, D. R.; Lin, C. W.; Michaelides, M.; Smith, L.; Bianchi, B.; Didomenico, S.; Hodges, L.; Hong, Y. F.; Mahan, L.; Mikusa, J.; Miller, T.; Nikkel, A.; Stashko, M.; Witte, D.; Williams, M. ABT-431: The diacetyl prodrug of A-86929, a potent and selective dopamine D-1 receptor agonist: In vitro characterization and effects in animal models of Parkinson's disease. *J. Pharmacol. Exp. Ther* **1996**, *276,* 150-160.

205.   Di Stefano, A.; Carafa, M.; Sozio, P.; Pinnen, F.; Braghiroli, D.; Orlando, G.; Cannazza, G.; Ricciutelli, M.; Marianecci, C.; Santucci, E. Evaluation of rat striatal L-dopa and DA concentration after intraperitoneal administration of L-dopa prodrugs in liposomal formulations. *J. Controlled Release* **2004**, *99,* 293-300.

206.   Di Stefano, A.; Mosciatti, B.; Cingolani, G. M.; Giorgioni, G.; Ricciutelli, M.; Cacciatore, I.; Sozio, P.; Claudi, F. Dimeric L-dopa derivatives as potential prodrugs. *Bioorg. Med. Chem. Lett.* **2001**, *11,* 1085-8.

207.   Venhuis, B. J.; Dijkstra, D.; Wustrow, D. J.; Meltzer, L. T.; Wise, L. D.; Johnson, S. J.; Heffner, T. G.; Wikstrom, H. V. Orally active analogues of the dopaminergic prodrug 6-(N,N-di-n-propylamino)-3,4,5,6,7,8-hexahydro-2H-naphthalen-1-one: synthesis and pharmacological activity. *J. Med. Chem.* **2003**, *46,* 584-90.

208.   Venhuis, B. J.; Rodenhuis, N.; Wikstrom, H. V.; Wustrow, D.; Meltzer, L. T.; Wise, L. D.; Johnson, S. J.; Pugsley, T. A.; Sundell, S.; Dijkstra, D. A new type of prodrug of catecholamines: an opportunity to improve the treatment of Parkinson's disease. *J. Med. Chem.* **2002**, *45,* 2349-51.

209.   Venhuis, B. J.; Dijkstra, D.; Wustrow, D.; Meltzer, L. T.; Wise, L. D.; Johnson, S. J.; Wikstrom, H. V. Orally active oxime derivatives of the dopaminergic prodrug 6-(N,N-di-n-propylamino)-3,4,5,6,7,8-hexahydro-2H-naphthalen-1-one. Synthesis and pharmacological activity. *J. Med. Chem.* **2003**, *46,* 4136-40.

210.   Liu, D.; Wikstrom, H. V.; Dijkstra, D.; de Vries, J. B.; Venhuis, B. J. Extremely potent orally active benzo[g]quinoline analogue of the dopaminergic prodrug: 1-propyl-trans-2,3,4,4a,5,7,8,9,10,10a-decahydro-1H-benzo-[g]quinolin-6-on e [corrected]. *J. Med. Chem.* **2006**, *49,* 1494-8.

211.   Liu, D.; Dijkstra, D.; de Vries, J. B.; Wikstrom, H. V. A novel synthesis and pharmacological evaluation of a potential dopamine D1/D2 agonist: 1-propyl-1,2,3,4,4a,5,10,10a-octahydrobenzo[g]quinoline-6,7-diol. *Bioorg. Med. Chem.* **2008**, *16,* 3438-44.

212.   Prausnitz, M. R.; Mitragotri, S.; Langer, R. Current status and future potential of transdermal drug delivery. *Nat. Rev. Drug Discov.* **2004**, *3,* 115-124.

213.   Scheuplein, R. J.; Blank, I. H. Permeability of the skin. *Physiol. Rev.* **1971**, *51,* 702-47.

214.   Christophers, E. Cellular architecture of the stratum corneum. *J. Invest. Dermatol.* **1971**, *56,* 165-9.

215.   Elias, P. M. Lipids and the epidermal permeability barrier. *Arch. Dermatol. Forsch.* **1981**, *270,* 95-117.

216.   Boehnlein, J.; Sakr, A.; Lichtin, J. L.; Bronaugh, R. L. Characterization of esterase and alcohol dehydrogenase activity in skin. Metabolism of retinyl palmitate to retinol (vitamin A) during percutaneous absorption. *Pharm. Res.* **1994**, *11,* 1155-9.

217.   Barry, B. W. Novel mechanisms and devices to enable successful transdermal drug delivery. *Eur. J. Pharm. Sci.* **2001**, *14,* 101-14.

218.   Naik, A.; Kalia, Y. N.; Guy, R. H. Transdermal drug delivery: overcoming the skin's barrier function. *Pharm. Sci. Technol. Today* **2000**, *3,* 318-326.

219.   Prausnitz, M. R.; Langer, R. Transdermal drug delivery. *Nat. Biotechnol.* **2008**, *26,* 1261-8.

220.   Anroop, B.; Ghosh, B. Prodrugs for transdermal drug delivery. *Pharmaceu. Rev.* **2007**, *5,* .

221.   Touitou, E.; Chow, D. D.; Lawter, J. R. Chiral Beta-Blockers for Transdermal Delivery. *Int. J. Pharm.* **1994**, *104,* 19-28.

222.   Reichmann, H. Transdermal delivery of dopamine receptor agonists. *Parkinsonism Rel. Disord.* **2009**, *15 Suppl 4,* S93-6.

223.   Sixel-Doring, F.; Trenkwalder, C. Rotigotine transdermal delivery for the treatment of restless legs syndrome. *Expert Opin. Pharmacother.* **2010**, *11,* 649-56.

224.   Pillai, O.; Hamad, M. O.; Crooks, P. A.; Stinchcomb, A. L. Physicochemical evaluation, in vitro human skin diffusion, and concurrent biotransformation of 3-O-alkyl carbonate prodrugs of naltrexone. *Pharm. Res.* **2004**, *21,* 1146-1152.

225.   Ahmed, S.; Imai, T.; Otagiri, M. Evaluation of stereoselective transdermal transport and concurrent cutaneous hydrolysis of several ester prodrugs of propranolol: Mechanism of stereoselective permeation. *Pharm. Res.* **1996**, *13,* 1524-1529.

226.   Sung, K. C.; Fang, J. Y.; Hu, O. Y. P. Delivery of nalbuphine and its prodrugs across skin by passive diffusion and iontophoresis. *J. Controlled Release* **2000**, *67,* 1-8.

227.   Majumdar, S.; Sloan, K. B. Synthesis, hydrolyses and dermal delivery of N-alkyl-N-alkyloxycarbonylaminomethyl (NANAOCAM) derivatives of phenol, imide and thiol containing drugs. *Bioorg. Med. Chem. Lett.* **2006**, *16,* 3590-3594.

228.   Mendes, E.; Furtado, T.; Neres, J.; Iley, J.; Jarvinen, T.; Rautio, J.; Moreira, R. Synthesis, stability and in vitro dermal evaluation of aminocarbonyloxymethyl esters as prodrugs of carboxylic acid agents. *Bioorg. Med. Chem.* **2002**, *10,* 809-816.

229.   Rautio, J.; Nevalainen, T.; Taipale, H.; Vepsalainen, J.; Gynther, J.; Laine, K.; Jarvinen, T. Synthesis and in vitro evaluation of novel morpholinyl- and methylpiperazinylacyloxyalkyl prodrugs of 2-(6-methoxy-2-naphthyl)propionic acid (Naproxen) for topical drug delivery. *J. Med. Chem.* **2000**, *43,* 1489-94.

230.   Rautio, J.; Nevalainen, T.; Taipale, H.; Vepsalainen, J.; Gynther, J.; Pedersen, T.; Jarvinen, T. Synthesis and in vitro evaluation of aminoacyloxyalkyl esters of 2-(6-methoxy-2-naphthyl)propionic acid as novel naproxen prodrugs for dermal drug delivery. *Pharm. Res.* **1999**, *16,* 1172-1178.

231.   Rautio, J.; Taipale, H.; Gynther, J.; Vepsalainen, J.; Nevalainen, T.; Jarvinen, T. In vitro evaluation of acyloxyalkyl esters as dermal prodrugs of ketoprofen and naproxen. *J. Pharm. Sci.* **1998**, *87,* 1622-8.

232.   Moss, G. P.; Gullick, D. R.; Cox, P. A.; Alexander, C.; Ingram, M. J.; Smart, J. D.; Pugh, W. J. Design, synthesis and characterization of captopril prodrugs for enhanced percutaneous absorption. *J. Pharm. Pharmacol.* **2006**, *58,* 167-177.

233.   Suppasansatorn, P.; Wang, G.; Conway, B. R.; Wang, W.; Wang, Y. Skin delivery potency and antitumor activities of temozolomide ester prodrugs. *Cancer Lett.* **2006**, *244,* 42-52.

234.   Sage, B. H. Iontophoresis. In *Percutaneous Penetration Enhancers;* Smith, E. W., Maibach, H. I., Eds.; CRC Press.Inc.: 1995; pp 351-368.

235.   Rawat, S.; Vengurlekar, S.; Rakesh, B.; Jain, S.; Srikarti, G. Transdermal Delivery by Iontophoresis. *Indian J. Pharm. Sci.* **2008**, *70,* 5-10; 5.

236.   Viscusi, E. R.; Witkowski, T. A. Iontophoresis: the process behind noninvasive drug delivery. *Regional Anesthesia and Pain Medicine* **2005**, *30,* 292-4.

237.   Cullander, C. What are the pathways of iontophoretic current flow through mammalian skin? *Adv. Drug Delivery Rev.* **1992**, *9,* 119-135; 119.

238.   Marro, D.; Kalia, Y. N.; Delgado-Charro, M. B.; Guy, R. H. Contributions of electromigration and electroosmosis to iontophoretic drug delivery. *Pharm. Res.* **2001**, *18,* 1701-8.

239.   Phipps, J. B.; Gyory, J. R. Transdermal ion migration. *Adv. Drug Delivery Rev.* **1992**, *9,* 137-176; 137.

240.   Dixit, N.; Bali, V.; Baboota, S.; Ahuja, A.; Ali, J. Iontophoresis - an approach for controlled drug delivery: a review. *Curr. Drug Deliv.* **2007**, *4,* 1-10.

241.   Yoshida, N. H.; Roberts, M. S. Structure Transport Relationships in Transdermal Iontophoresis. *Adv. Drug Delivery Rev.* **1992**, *9,* 239-264.

242.   Gupta, S. K.; Hwang, S.; Southam, M.; Sathyan, G. Effects of application site and subject demographics on the pharmacokinetics of fentanyl HCl patient-controlled transdermal system (PCTS). *Clin. Pharmacokinet.* **2005**, *44 Suppl 1,* 25-32.

243.   Heitz, J. W.; Witkowski, T. A.; Viscusi, E. R. New and emerging analgesics and analgesic technologies for acute pain management. *Curr. Opin. Anaesthesiol.* **2009**, *22,* 608-17.

244.   Subramony, J. A.; Sharma, A.; Phipps, J. B. Microprocessor controlled transdermal drug delivery. *Int. J. Pharm.* **2006**, *317,* 1-6.

245.   Holovics, H. J.; Anderson, C. R.; Levine, B. S.; Hui, H. W.; Lunte, C. E. Investigation of Drug Delivery by Iontophoresis in a Surgical Wound Utilizing Microdialysis. *Pharm. Res.* **2007**, .

246.   Viscusi, E. R.; Reynolds, L.; Chung, F.; Atkinson, L. E.; Khanna, S. Patient-controlled transdermal fentanyl hydrochloride vs intravenous morphine pump for postoperative pain: a randomized controlled trial. *JAMA* **2004**, *291,* 1333-41.

247.   Jain, A.; Ghosh, B.; Rajgor, N.; Desai, B. G. Passive and iontophoretic permeation of glipizide. *Eur. J. Pharm. Biopharm.* **2008**, *69,* 958-63.

248.   Singh, G.; Ghosh, B.; Kaushalkumar, D.; Somsekhar, V. Screening of venlafaxine hydrochloride for transdermal delivery: passive diffusion and iontophoresis. *AAPS PharmSciTech* **2008**, *9,* 791-7.

249.   Sylvestre, J. P.; Diaz-Marin, C.; Delgado-Charro, M. B.; Guy, R. H. Iontophoresis of dexamethasone phosphate: competition with chloride ions. *J. Controlled Release* **2008**, *131,* 41-6.

250.   Lopez, R. F. V.; Bentley, M. V. L. B.; gado-Charro, M. B.; Salomon, D.; van den Bergh, H.; Lange, N.; Guy, R. H. Enhanced delivery of 5-aminolevulinic acid esters by iontophoresis in vitro. *Photochem. Photobiol.* **2003**, *77,* 304-308.

251.   Merclin, N.; Bender, J.; Sparr, E.; Guy, R. H.; Ehrsson, H.; Engstrom, S. Transdermal delivery from a lipid sponge phase-iontophoretic and passive transport in vitro of 5-aminolevulinic acid and its methyl ester. *J. Controlled Release* **2004**, *100,* 191-198.

252.   Merclin, N.; Bramer, T.; Edsman, K. Iontophoretic delivery of 5-aminolevulinic acid and its methyl ester using a carbopol gel as vehicle. *J. Controlled Release* **2004**, *98,* 57-65.

253.   Wang, Y. P.; Fan, Q. X.; Song, Y. F.; Michniak, B. Effects of fatty acids and iontophoresis on the delivery of midodrine hydrochloride and the structure of human skin. *Pharm. Res.* **2003**, *20,* 1612-1618.

254.   Abla, N.; Naik, A.; Guy, R. H.; Kalia, Y. N. Topical iontophoresis of valaciclovir hydrochloride improves cutaneous aciclovir delivery. *Pharm. Res.* **2006**, *23,* 1842-1849.

255.   Laneri, S.; Sacchi, A.; di Frassello, E. A.; Luraschi, E.; Colombo, P.; Santi, P. Ionized prodrugs of dehydroepiandrosterone for transdermal iontophoretic delivery. *Pharm. Res.* **1999**, *16,* 1818-1824.

256.   Anroop, B.; Ghosh, B.; Parcha, V.; Khanam, J. Transdermal delivery of atenolol: effect of prodrugs and iontophoresis. *Curr. Drug Deliv.* **2009**, *6,* 280-90.

257.   Liu, W.; Hu, M.; Xue, C.; Xu, H.; Yang, X. Investigation of the carbopol gel of solid lipid nanoparticles for the transdermal iontophoretic delivery of triamcinolone acetonide acetate. *Int. J. Pharm.* **2008**, *364,* 135-41.

258.   Vemulapalli, V.; Yang, Y.; Friden, P. M.; Banga, A. K. Synergistic effect of iontophoresis and soluble microneedles for transdermal delivery of methotrexate. *J. Pharm. Pharmacol.* **2008**, *60,* 27-33.

259.   Timmerman, W.; Westerink, B. H.; De Vries, J. B.; Tepper, P. G.; Horn, A. S. Microdialysis and striatal dopamine release: stereoselective actions of the enantiomers of N-0437. *Eur. J. Pharmacol.* **1989**, *162,* 143-50.

260.   Loschmann, P. A.; Chong, P. N.; Nomoto, M.; Tepper, P. G.; Horn, A. S.; Jenner, P.; Marsden, C. D. Stereoselective reversal of MPTP-induced parkinsonism in the marmoset after dermal application of N-0437. *Eur. J. Pharmacol.* **1989**, *166,* 373-80.

261.   Coleman, R. J.; Lange, K. W.; Quinn, N. P.; Loper, A. E.; Bondi, J. V.; Hichens, M.; Stahl, S. M.; Marsden, C. D. The antiparkinsonian actions and pharmacokinetics of transdermal (+)-4-propyl-9-hydroxynaphthoxazine (+PHNO): preliminary results. *Mov. Disorders* **1989**, *4,* 129-38.

262.   Rupniak, N. M.; Tye, S. J.; Jennings, C. A.; Loper, A. E.; Bondi, J. V.; Hichens, M.; Hand, E.; Iversen, S. D.; Stahl, S. M. Antiparkinsonian efficacy of a novel transdermal delivery system for (+)-PHNO in MPTP-treated squirrel monkeys. *Neurology* **1989**, *39,* 329-35.

263.   van der Geest, R.; Danhof, M.; Bodde, H. E. Iontophoretic delivery of apomorphine I: In vitro optimization and validation. *Pharm. Res.* **1997**, *14,* 1798-1803.

264.   van der Geest, R.; van Laar, T.; Gubbens-Stibbe, J. M.; Bodde, H. E.; Danhof, M. Iontophoretic delivery of apomorphine II: An in vivo study in patients with Parkinson's disease. *Pharm. Res.* **1997**, *14,* 1804-1810.

265.   Danhof, M.; Van der Geest, R.; Van Laar, T.; Bodde, H. E. An integrated pharmacokinetic-pharmacodynamic approach to optimization of R-apomorphine delivery in Parkinson's disease. *Adv. Drug Delivery Rev.* **1998**, *33,* 253-263.

266.   Li, G. L.; Danhof, M.; Bouwstra, J. A. Lontophoretic delivery of apomorphine in vitro: physicochemic considerations. *Pharm. Res.* **2001**, *18,* 1509-13.

267.   Junginger, H. E. Iontophoretic delivery of apomorphine: from in-vitro modelling to the Parkinson patient. *Adv. Drug Delivery Rev.* **2002**, *54,* S57-S75.

268.   Luzardo-Alvarez, A.; Delgado-Charro, M. B.; Blanco-Mendez, J. Iontophoretic delivery of ropinirole hydrochloride: effect of current density and vehicle formulation. *Pharm. Res.* **2001**, *18,* 1714-20.

269.   Nugroho, A. K.; Li, G. L.; Grossklaus, A.; Danhof, M.; Bouwstra, J. A. Transdermal iontophoresis of rotigotine: influence of concentration, temperature and current density in human skin in vitro. *J. Controlled Release* **2004**, *96,* 159-167.

270.   Nugroho, A. K.; Li, L.; Dijkstra, D.; Wikstrom, H.; Danhof, M.; Bouwstra, J. A. Transdermal iontophoresis of the dopamine agonist 5-OH-DPAT in human skin in vitro. *J. Controlled Release* **2005**, *103,* 393-403.

271.   Luzardo-Alvarez, A.; Delgado-Charro, M. B.; Blanco-Mendez, J. In vivo iontophoretic administration of ropinirole hydrochloride. *J. Pharm. Sci.* **2003**, *92,* 2441-8.

272.   Nugroho, A. K.; Li, G. L.; Danhof, M.; Bouwstra, J. A. Transdermal iontophoresis of rotigotine across human stratum corneum in vitro: Influence of pH and NaCl concentration. *Pharm. Res.* **2004**, *21,* 844-850.

273.   Nugroho, A. K.; Romeijn, S. G.; Zwier, R.; De Vries, J. B.; Dijkstra, D.; Wikstrom, H.; la-Pasqua, O.; Danhof, M.; Bouwstra, J. A. Pharmacokinetics and pharmacodynamics analysis of transdermal iontophoresis of 5-OH-DPAT in rats: In vitro-in vivo correlation. *J. Pharm. Sci.* **2006**, *95,* 1570-1585.

274.   Nugroho, A. K. Transdermal iontophoretic delivery of dopamine agonists: *in vitro - in vivo* correlation based on novel compartmental modeling, Leiden University, The Netherlands, Leiden, 2005.

2

Synthesis of a series of prodrugs of the potent dopamine (DA) D$_2$ agonist 5-hydroxy-2-(*N,N,*-di-*n*-propylamino)tetralin (5-OH-DPAT), compounds designed for iontophoretic transdermal delivery

Abstract

The administration of 5-OH-DPAT by transdermal iontophoretic transdermal delivery is promising, but further optimization for human administration is necessary. A prodrug strategy with amino acid pro-moieties would be ideal to improve the physicochemical properties of 5-OH-DPAT for iontophoresis as well as for its formulation. By tailoring the pro-moieties we aimed to improve the chemical stability while maintaining high enzymatic instability for blood and skin esterases. In conclusion, a series of amino acid ester prodrugs of 5-OH-DPAT was synthesized ready to be examined in stability and iontophoretic experiments in vitro and in vivo.

2.1 INTRODUCTION

5-Hydroxy-2-(*N,N*-di-*n*-propylamino)tetralin (5-OH-DPAT, **2.12**, Figure 2.1) is a potent DA D_2 receptor agonist and a potential candidate for iontophoretic delivery in the treatment of patients with Parkinson's disease.[1-4] The *in vitro* and *in vivo* iontophoretic administration of 5-OH-DPAT and other dopamine (DA) agonists has been thoroughly investigated.[5-12] These studies show that the administration of DA agonists is promising, but further optimization for human administration is necessary. A prodrug strategy would be ideal to improve the physicochemical properties of 5-OH-DPAT for iontophoresis and its formulation.

2.12
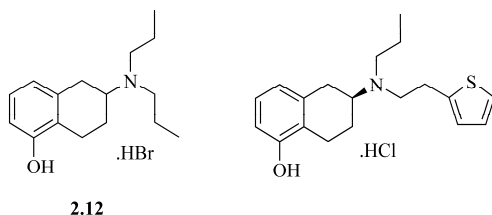
Figure 2.1 Structures of 5-OH-DPAT.HBr and rotigotine.HCl.

First, higher hydrophilicity proved beneficial for the iontophoretic flux.[13] Second, for 5-OH-DPAT and rotigotine (Figure 2.1) it has been demonstrated that the drug concentration is positively correlated to the transdermal flux.[7, 9] Third, iontophoretic flux is negatively correlated to the molecular weight.[14] It would therefore be convenient to improve the hydrophilicity and aqueous solubility of 5-OH-DPAT by introduction of a small hydrophilic functional group, e.g. an amino or alcoholic group, preferably in a water soluble salt form. An amino acid, a widely used pro-moiety, especially for carrier-mediated absorption, would be suitable for this purpose.[15] The application for transdermal iontophoresis of cationic amino acid ester prodrugs of several non-ionic drugs has been investigated before. Valacyclovir hydrochloride (Figure 2.2), the L-valine ester prodrug of

acyclovir, showed superior iontophoresis over the parent molecule.[16] Also the amino acid ester prodrugs of dehydroepiandrosteron (DHEA) resulted in an improved iontophoretic flux, together with a decreased drug lipophilicity and an increased aqueous solubility.[17] In the case of the cationic molecule 5-OH-DPAT hydrobromide, a second chargeable group may be beneficial for the iontophoretic flux and aqueous solubility.[18] In addition, an increase in flux would also allow a reduction of the electrical current strength, which may lessen skin irritation.[19] And the increased solubility could result in a patient-friendly advantage, i.e. minimization of the patch size.

R = H   (Acyclovir)   R = H   (DHEA)
R = L-Valine.HCl   (Valacyclovir)   R = Glycine.HCl or Trimethylglycine iodide (Prodrug)
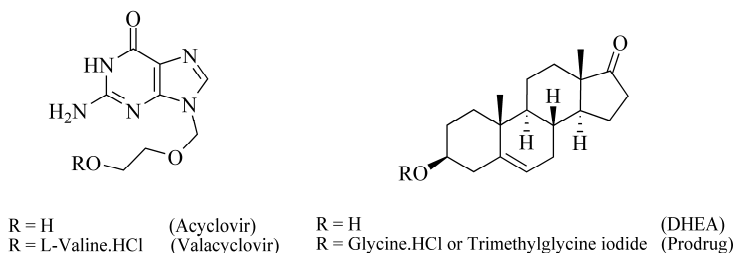
Figure 2.2 Structures of the parent drugs and amino acid ester prodrugs of acyclovir and dehydroepiandrosterone (DHEA).

Several studies have been performed concerning the synthesis of prodrugs of DAergic agonists. These phenolic or catecholic DA receptor agonists were esterified into mono- or diesters.[20] The chemical and enzymatic stability are important properties of a prodrug, and the finding of a good ratio between these properties could pose a challenge.[21, 22] Previous investigations show that this can also be achieved when amino acid ester prodrugs are utilized. Various water-soluble amino acid ester prodrugs of aliphatic alcohols have been synthesized of which the *L*-valine, *L*-isoleucine, 1-aminocyclopropane carboxylic acid and the β-amino acids ester prodrugs were chemically the most stable, while they showed sufficient enzymatic lability.[23-30] In general, the chemical and enzymatic stability of amino acid ester prodrugs of aromatic alcohols e.g. 5-OH-DPAT, are expected to be lower in comparison to amino acid esters of aliphatic alcohols.[31-33] Although some non-endogenous bulky *N*-alkylated amino acid ester prodrugs showed high chemical stability and solubility, natural amino acids are preferred.[34]

In this chapter the synthesis of a series of amino acid ester prodrugs of the phenolic 5-OH-DPAT is described. With several analogous prodrug series in hands we can roughly explore the influence of alcoholic, basic and bulky side chains, alkylation of the amino group, and chain elongation on the chemical stability of the phenolic ester. By tailoring the amino acid pro-moieties we aim to improve the chemical stability of the prodrug while maintaining high enzymatic lability for blood and skin esterases. These prodrugs and the results of the stability tests could be a useful tool for the development of prodrugs of other phenolic drugs which need higher aqueous solubility, an amino acid moiety for peptide carrier-mediated transport, and/or a positively chargeable amino group. The prodrugs with optimal stability

and physico-chemical properties for transdermal iontophoresis will be used for further investigation.

2.2 CHEMISTRY

2.2.1 Synthesis of (S) and (R)-5-hydroxy-2-(*N*,*N*-di-*n*-propyl-amino)tetralin ((S)-2.12) and (R)-2.12)

1,6-Dimethoxynaphthalene (**2.7**) was prepared by methylation of 1,6-dihydroxynaphthalene with dimethyl sulfate under basic aqueous conditions with a yield of 83%. Subsequently, the naphthalene ether **2.7** was reduced to the enol ether intermediate followed by acid hydrolysis to 5-methoxy-tetralone **2.8** with a yield of 89%.[35] After the condensation with benzylamine, subsequent catalytic hydrogenation of the imine and treatment with hydrogen chloride, 2-(benzylamino)-5-methoxytetralin was obtained as the hydrochloride salt with a yield of 56%. Our initial attempt of resolution by fractional recrystallization of the mandelates of **2.9** from ether yielded no crystals, but instead an oily precipitation.[2] Eventually, the (S)- and (R)-enantiomers of **2.9** were resolved in moderate yields by a more convenient fractional recrystallization of the diastereomeric (-)- and (+)-di-*p*-toluoyltartrates, respectively, from 96% ethanol (Scheme 2.1).[36]
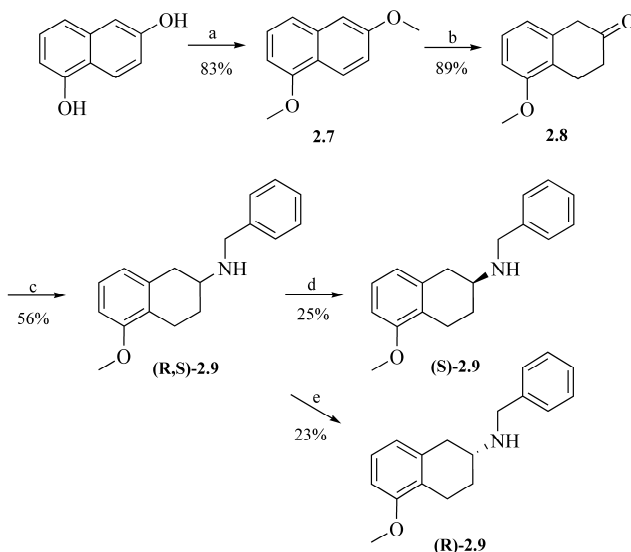
Scheme 2.1 Synthesis and resolution of (±)-2-(benzylamino)-5-methoxytetralin (**2.9**). Reagents and conditions: a) (CH$_3$)$_2$SO$_4$, 2N NaOH, reflux; b) Na, EtOH; 2N HCl (aq), reflux; c) benzylamine, *p*-toluenesulfonic acid, 3.5 bar H$_2$, PtO$_2$ in EtOH, RT, overnight; d) fractional recrystallization with (-)-di-*p*-toluoyl-*L*-tartaric acid in 96% EtOH; e) fractional recrystallization with (+)-di-*p*-toluoyl-*D*-tartaric acid in 96% EtOH.

The enantiomers **(S)-2.9** and **(R)-2.9** were debenzylated by hydrogenolysis with 10% palladium on carbon to give amines **(S)-2.10** and **(R)-2.10** with yields of 94% and 80%, respectively. These primary amines were propylated with 4 equivalents of 1-iodopropane to the tertiary amines **(S)-2.11** and **(R)-2.11**, with yields of 64% and 54%, respectively. Finally, the phenolic enantiomers of 5-OH-DPAT (**(S)-2.12** and **(R)-2.12**) were obtained after demethylation by refluxing in 48% hydrobromic acid (Scheme 2.2).[1, 2, 36]
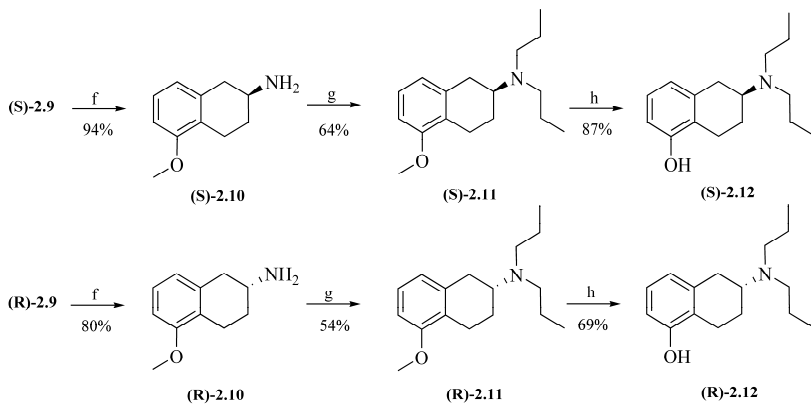
Scheme 2.2 Synthesis of (S)-5-OH-DPAT (**(S)-2.12**) and (R)-5-OH-DPAT (**(R)-2.12**). Reagents and conditions: f) 3.5 bar H_2, 10% Pd/C in EtOH, 40 °C; g) 1-iodopropane (4 eq), K_2CO_3 in acetonitrile, reflux; h) 48% HBr, reflux.

During the synthesis of **(S)-2.11** a side-product was observed with a yield of 19% when 8 equivalents of 1-iodopropane were used instead of 4 equivalents. This side product was the propylated quaternary amine, which could be removed from **(S)-2.11** by column chromatography (Scheme 2.3).
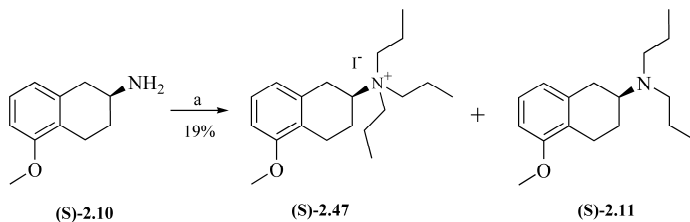
Scheme 2.3 Synthesis of (S)-5-hydroxy-2-(*N,N,N*-tri-*n*-propyl-ammonium)tetralin iodide-salt. Reagents and conditions: a) 1-iodopropane (8 eq), K_2CO_3 in acetonitrile, reflux.

2.2.2 Protection of amino acids

The *N-tert*-butoxycarbonyl(Boc)-protected *L*-alanine (**2.1**), *L*-proline (**2.2**), *N*-methylglycine (**2.3**), γ-aminobutyric acid (**2.4**) and 5-aminovaleric acid (**2.5**) were successfully prepared from their respective amino acids and di-*tert*-butyl dicarbonate in yields between 34% and 77% (Scheme 2.4). The other *N*-protected amino acids were purchased from commercial suppliers.
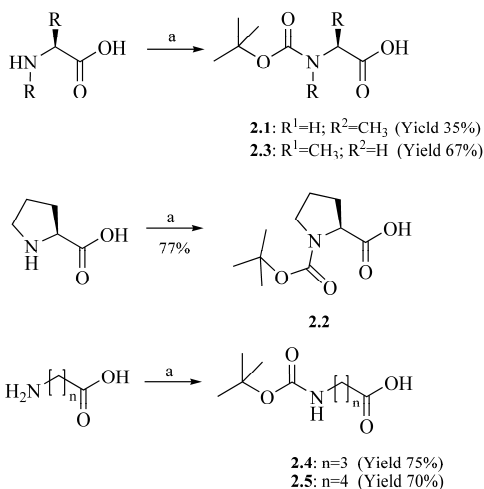
Scheme 2.4 *N*-Boc-protection of *L*-alanine, *N*-methylglycine, *L*-proline, γ-aminobutyric acid and 5-aminovaleric acid. Reagents and conditions: a) Boc$_2$O, NaHCO$_3$, H$_2$O/THF (1:1), RT.

2.2.3 Preparation of amino acid esters of 5-OH–DPAT

The hydroxy moiety of (S)-5-OH-DPAT (**(S)-2.12**) was esterified with the *N*-protected amino acids according to Scheme 2.5 and Scheme 2.6. As coupling reagent *N*-(3-dimethylaminopropyl)-*N'*-ethylcarbodiimide (EDC) was used. To suppress racemization and catalyze the coupling 1-hydroxybenzotriazole (HOBt) was added. According to this method, the *N*-Boc-protected esters of (S)-5-OH-DPAT with glycine (**2.13**), *L*-alanine (**2.14**), 1-amino-cyclopropanecarboxylic acid (**2.15**), *L*-valine (**2.16**), *D*-valine, (**2.17**) *L*-isoleucine (**2.18**), *L*-phenylalanine (**2.20**), *L*-lysine (**2.21**) and *L*-proline (**2.23**) were synthesized with yields between 49% and 77%.
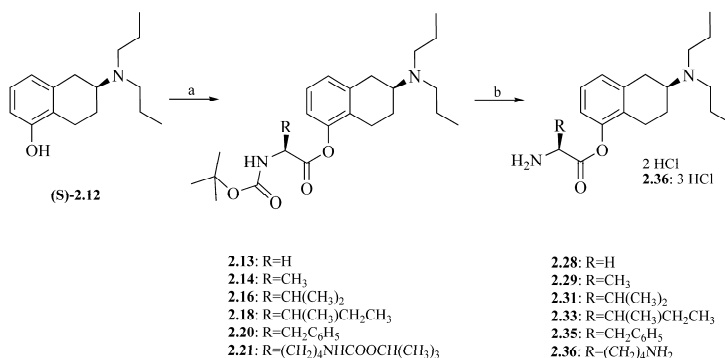
Scheme 2.5 Synthesis of glycine (**2.28**), *L*-alanine (**2.29**), *L*-valine (**2.31**), *L*-isoleucine (**2.33**), *L*-phenylalanine (**2.35**) and *L*-lysine (**2.36**) (S)-2-(di-*n*-propyl-amino)tetralin-5-yl esters as 2HCl salts (**2.36**=3HCl salt). Reagents and conditions: a) EDC, *N*-*tert*-Boc-amino acid, HOBt hydrate, 0 °C-RT; b) 4N HCl in dioxane, RT.

The deprotection of the Boc-protected compounds **2.13-2.18**, **2.20, 2.21** and **2.23** was carried out with a solution of hydrogen chloride in dioxane.[37] After reaction completion, decantation of the solvent and drying *in vacuo*, the solid hygroscopic foams were reprecipitated from dry methanol with dry ether to remove excess dioxane. The hydrochloride salts **2.28-2.33**, **2.35-2.37** were obtained with yields between 80% and 100%. Only the *D*-valine (**2.32**) and *L*-lysine (**2.36**) (S)-5-OH-DPAT esters gave lower yields, 32% and 10%, respectively.
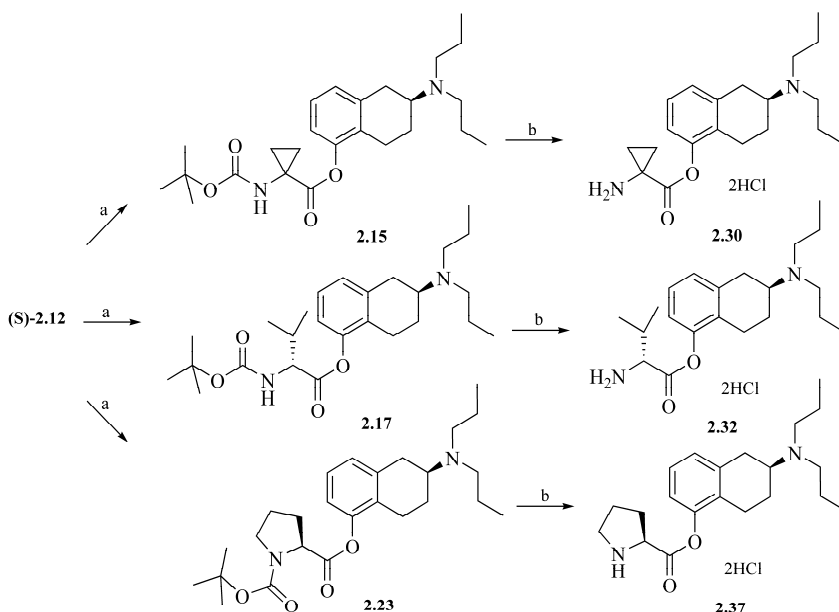
Scheme 2.6 Synthesis of 1-aminocyclopropane-1-carboxylic acid (**2.30**), *D*-valine (**2.32**), *L*-proline (**2.37**) (S)-2-(di-*n*-propyl-amino)tetralin-5-yl esters as 2HCl salts. Reagents and conditions: a) EDC, *N-tert*-Boc-amino acid, HOBt hydrate, 0 °C-RT; b) 4N HCl in dioxane, RT.

The esterification of (R)-5-OH-DPAT (**(R)-2.12**) with di-protected *N-tert*-Boc-O-benzyl-*L*-serine was also established by carbodiimide coupling, and yielded the *L*-serine ester of (R)-5-OH-DPAT (**2.19**). The debenzylation of compound **2.19** was performed by hydrogenolysis in ethanol at 45°C and 3 bar hydrogen atmosphere to obtain compound **2.42** with a yield of 47%. Subsequently, the deprotected alcohol **2.42** was treated with hydrogen chloride in dioxane to remove the Boc group. The product **2.34** was reprecipitated from dry methanol with dry ether to obtain the hygroscopic dihydrochloride salt with a yield of 26% (Scheme 2.7).
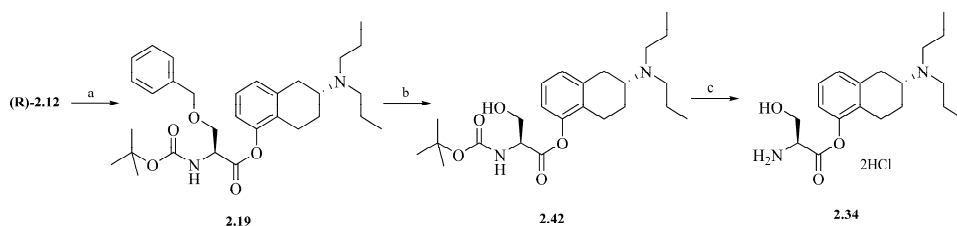
Scheme 2.7 Synthesis of *L*-serine (R)-2-(di-*n*-propyl-amino)tetralin-5-yl ester 2HCl salt (**2.34**). Reagents and conditions: a) EDC, *N-tert*-Boc-O-benzyl-*L*-serine, HOBt hydrate, 0 °C-RT; b) ~3 bar H$_2$, 10% Pd/C in EtOH, 45 °C; c) 4N HCl in dioxane, RT.

A special case was the synthesis of the *L*-arginine ester of (S)-5-OH-DPAT (Scheme 2.8). First, *L*-arginine was protected with three carbobenzyloxy groups (Cbz) by a one-pot synthetic method as described by Jetten *et al.*[38] Although the *N*-urethane formation was facilitated by prior silylation of the amine groups, a reasonable amount (>50%) of the di-Cbz-*L*-arginine side-product was found after mass spectrometry analysis, but could be removed by column chromatography followed by recrystallization. The overall yield of the synthesis of N$^\alpha$, N$^\delta$, N$^\omega$-tri-Cbz-*L*-arginine (**2.6**) was 36%. The N$^\alpha$, N$^\delta$, N$^\omega$-tri-Cbz-*L*-arginine (S)-5-OH-DPAT ester (**2.22**) was formed by the same coupling method as described before and was subsequently debenzylated by hydrogenolysis with 10% palladium on carbon as catalyst in a solution of hydrogen chloride in dry methanol. The *L*-arginine (S)-5-OH-DPAT ester (**2.43**) was precipitated with dry ether and was obtained as the tetra-hydrochloride salt with a yield of 79%.
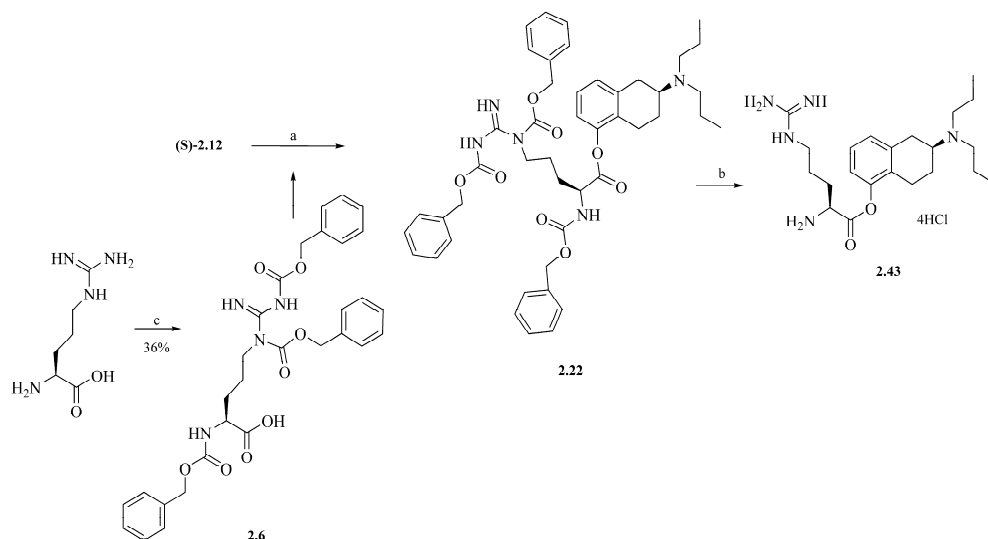
Scheme 2.8 Synthesis of *L*-arginine (S)-2-(di-*n*-propyl-amino)tetralin-5-yl ester 4HCl salt (**2.43**). Reagents and conditions: a) EDC, HOBt hydrate, 0 °C-RT; b) ~1 bar H$_2$, 10% Pd/C, 0.3N HCl in MeOH, RT; c) i) TMS-Cl, DIPEA, 45°C in 1,2-dichloroethane, ii) benzylchloroformate, 0 °C-RT.

The *N*-Boc-*N*-methylglycine (S)-5-OH-DPAT ester (**2.24**) and the dimethylglycine (R)-5-OH-DPAT ester (**2.44**) were synthesized by the coupling of *N-tert*-Boc-*N*-methylglycine and *N,N*-dimethylglycine respectively to the corresponding enantiomers of 5-OH-DPAT. Compound **2.44** was converted to the dihydrochloride salt with hydrogen chloride in methanol and the yields for **2.24** and **2.44** were 45% and 57%, respectively. Finally, compound **2.24** was deprotected with hydrogen chloride in dioxane to give the dihydrochloride salt of **2.38** with a yield of 92% (Scheme 2.9).
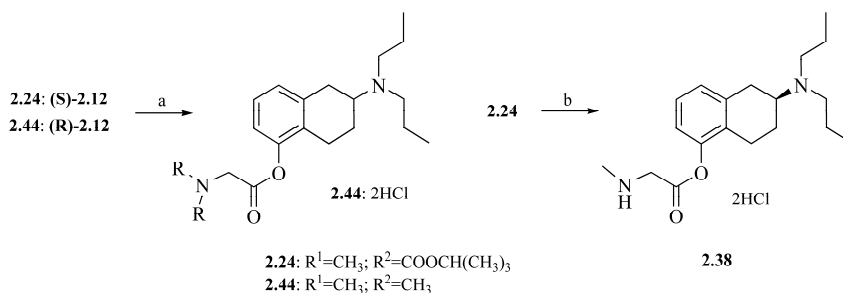
Scheme 2.9 Synthesis of *N,N*-dimethylglycine (R)-2-(di-*n*-propyl-amino)tetralin-5-yl ester 2HCl salt (**2.44**) and *N*-methylglycine (S)-2-(di-*n*-propyl-amino)tetralin-5-yl ester 2HCl salt (**2.38**). Reagents and conditions: a) EDC, *N-tert*-Boc-N-methylglycine (**2.24**) / *N,N*-dimethylglycine (**2.44**), HOBt hydrate, 0 °C-RT; b) 4N HCl in dioxane, RT.

After the formation of the acid chloride of *N,N,N*-trimethylglycine with thionyl chloride at reflux temperature, the *N,N,N*-trimethylglycine (R)-5-OH-DPAT ester (**2.46**) was synthesized by nucleophilic substitution of the acid chloride with (R)-5-OH-DPAT (Scheme 2.10).[39]
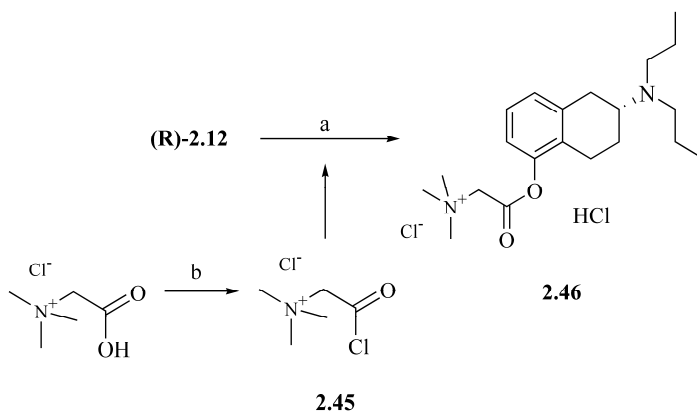
Scheme 2.10 Synthesis of *N,N,N*-trimethylglycine (R)-2-(di-*n*-propyl-amino)tetralin-5-yl ester Cl.HCl salt (**2.46**). Reagents and conditions: a) pyridine, CH$_2$Cl$_2$, 0 °C; b) SOCl$_2$, 70 °C.

The *N*-Boc-β-alanine (**2.25**), *N*-Boc-γ-aminobutyric acid (**2.26**) and *N*-Boc-5-aminovaleric acid (**2.27**) esters of 5-OH-DPAT were synthesized from the corresponding *N*-Boc protected amino acids and 5-OH-DPAT. The reaction was again established by the coupling

reagent EDC and HOBt, of which the latter is added to catalyze the coupling reaction. The final compounds **2.39-2.41** were obtained as dihydrochloride salts after Boc-deprotection with hydrogen chloride in dioxane with yields between 85% and 89% (Scheme 2.11).
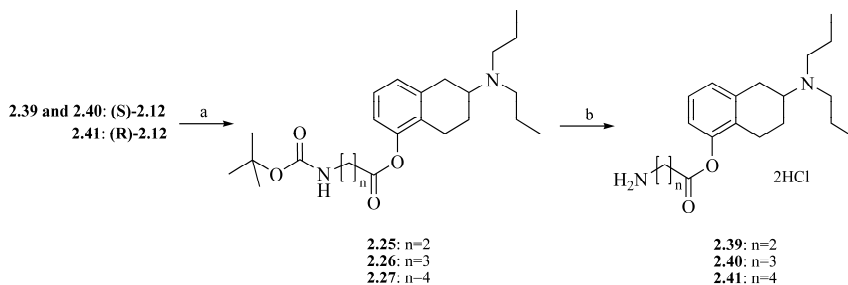
Scheme 2.11 Synthesis of β-alanine (**2.39**), γ-aminobutyric acid (**2.40**), 5-aminovaleric acid (**2.41**) 5-OH-DPAT esters as 2HCl salts. Reagents and conditions: a) EDC, *N-tert*-Boc-amino acid, HOBt hydrate, 0 °C-RT; b) 4N HCl in dioxane, RT.

2.3 DISCUSSION

The enantiomers of intermediate **2.9** were successfully resolved by fractional recrystallization with the corresponding enantiomers of di-*p*-toluoyltartaric acid. The oil precipitation instead of crystal formation that was observed during resolution with mandelic acid may have been caused by the presence of impurities which interfered with this particular recrystallization method. The synthesized enantiomerically pure enantiomers of **2.12** were used in the follow-up synthesis of the amino acid ester prodrugs. *In vivo* data of **(S)-2.12** are presented in Chapter 5.

Initial use of the carbodiimide coupling reagent *N,N'*-dicyclohexylcarbodiimide (DCC) for the synthesis of the amino acid 5-OH-DPAT ester prodrugs gave fair yields, but the ureas which were generated during the reaction were difficult to remove. The side-product ureas of reaction with EDC were water soluble and easily removed from the organic layer by washing with water.[40] EDC was used for all couplings and gave yields between 38% and 90%.

Unfortunately, in contrast to the serine analog **2.19**, the N-*tert*-Boc-O-benzyl-*L*-threonine ester could not be debenzylated by catalytic hydrogenolysis and for this reason the synthesis of the L-threonine ester of 5-OH-DPAT was abandoned. *N*-Boc deprotection for the synthesis of amino acid ester prodrugs is typically carried out in a mixture of trifluoroacetic acid and dichloromethane.[17, 23, 26, 27, 29]

Although the deprotection with trifluoroacetic acid was feasible, in our case the reaction with hydrogen chloride in dioxane and the resulting products as hydrochloride salts offered some advantages:

- The product precipitated as an oil which indicated reaction progress.

- The precipitated product could be readily isolated from the solvent by decantation, thereby circumventing the needs for evaporation *in vacuo* which would lead to major hydrolysis.
- The acidic environment protected the ester against hydrolysis.
- Chloride atoms are necessary for the electrochemical process of iontophoresis at the anode.
- Addition of extra sodium chloride in the iontophoretic donor compartment could be minimized and thus less sodium cations would be present to compete with the cationic drug molecules during iontophoretic transport.

Deprotection with hydrogen chloride in methanol or tetrahydrofuran also gave good yields, but lacked the reaction progress indication and facile isolation, because the product did not precipitate. A disadvantage of the hydrochloride salt form of the prodrugs was hygroscopicity, which impeded easy handling and storage. Alternative salt forms were considered. It has been reported that different salt forms have different specific conductivities and that conductivity experiments will provide information concerning the general suitability of a drug for iontophoresis.[41] Salt combinations with monocarboxylic acids are less soluble in water, while those of dicarboxylic acids confer water solubility if one carboxylic acid is left free.[42] If stability is a problem, and the salt is hygroscopic it would seem more reasonable to select a less polar acid, e.g. carboxylic.[43] Based on these arguments it would be interesting to convert the hygroscopic hydrochloride salts to dicarboxylic acid salts (e.g. maleate or fumarate) and determine the conductivities and aqueous solubility in future experiments.

To form alternative salts, the hydrochloride salts should be converted to the free amine. The following conversion methods were performed with the glycine analog **2.28**: 1) washing a solution of the prodrug in an organic solvent with an aqueous basic solution; 2) reaction of the prodrug with solid inorganic base (NaHCO$_3$, Na$_2$CO$_3$) in dry organic solvent; 3) reaction of the prodrug with 1 equivalent of triethylamine to precipitate the triethylamine hydrochloride salt from the solution. None of these methods prevented the hydrolysis of the glycine prodrug during conversion to the free amine or during the evaporation of the prodrug solution. Interestingly, in contrast to the other synthesized 5-OH-DPAT esters, the *N,N*-dimethylglycine prodrug **2.44** (free amine) and the *N,N,N*-trimethylglycine prodrug **2.46** (chloride salt) could be purified by column chromatography without occurrence of hydrolysis. Prodrug **2.44** which appeared to be stable in its free amine form could be a candidate for an alternative salt form. Nevertheless, the suitability of **2.44** for iontophoresis should first be examined in chemical stability studies.

Conformational isomers were observed for the *N*-Boc-*N*-methylglycine compounds in both proton and carbon NMR spectra. This may be explained by different isomers of the amide bond.[44] In the carbon NMR (nuclear magnetic resonance) spectra of some of the prodrugs

we also found chemical shifts for two conformational isomers, which may also be explained by isomerism of the amide bond.

Table 2.1 Overall yields and purities (HPLC) of the synthesis of 5-OH-DPAT (**2.12**) from 1,6-dihydroxynaphthalene, and the synthesis of prodrugs **2.28-2.41, 2.43, 2.44** and **2.46** from 5-OH-DPAT.

Compound	Prodrug Moiety	Yield (%)	Purity (%)
(S)-2.12	-	11	100[a]
(R)-2.12	-	6	99[a]
2.28	Glycine	50	98
2.29	*L*-Alanine	47	100
2.30	1-Aminocyclopropane-1-carboxylic acid	40	100
2.31	*L*-Valine	60	96
2.32	*D*-Valine	19	100
2.33	*L*-Isoleucine	69	100
2.34	*L*-Serine	5	98
2.35	*L*-Phenylalanine	52	100
2.36	*L*-Lysine	6	99
2.43	*L*-Arginine	47	99
2.37	*L*-Proline	42	100
2.38	*N*-Methylglycine	41	98
2.44	*N,N*-Dimethylglycine	57	100
2.46	*N,N,N*-Trimethylglycine	74	100
2.39	β-Alanine	77	99
2.40	γ-Aminobutyric acid	59	>95
2.41	5-Aminovaleric acid	32	96

[a] Purity determined on gas chromatography–mass spectrometry (GCMS)

The influence on iontophoretic flux of additional charges could be negative or positive, which depends on the interaction of the molecules with charged sites in the stratum corneum, the hydrated molecular volume of the ions and the charge/molecular weight ratio.[45-47] The novelty of this series of prodrugs is that they contain at least two chargeable amino groups which may lead to increased iontophoretic transport. Additionally, prodrugs **2.28-2.33**, **2.35** and **2.37** contain sterically hindered groups which could increase stability against chemical and enzymatic hydrolysis. Prodrugs **2.34**, **2.36** and **2.43** have polar side chain groups, i.e. alcohol and amino groups, which may increase aqueous solubility. In addition, prodrugs **2.36** and **2.43** could change iontophoretic flux by introduction of a third chargeable group in the molecule. Compounds **2.37**, **2.38**, **2.44** and **2.46** vary in degree of alkylation of the α-amino group, and therefore also vary in degree of protonation. Prodrug **2.46** is even permanently protonated and is independent to pH changes in the skin during transport, as long as the prodrug remains intact. Prodrugs **2.39-2.41** differ in the number of methylene groups between the amino and carboxylic acid functional group.

In conclusion, amino acid ester prodrugs of 5-OH-DPAT were synthesized (Table 2.1) with structural differences in order to control chemical and enzymatic stability, increase aqueous solubility and improve iontophoretic transport. The chemical and enzymatic stability should be determined in order to select candidates for *in vitro* and *in vivo* experiments.

2.4. EXPERIMENTAL

2.4.1 General

Thin-layer chromatography (TLC) was performed on aluminium sheets of silica gel 60 F_{254} or aluminium oxide F_{254} neutral, the spots were observed under ultraviolet light (254 nm) or visualized with I_2 vapour or $KMnO_4$ solution. The chemical purity of the final compounds **2.29**, **2.35**, **2.37**, **2.38**, **2.40**, **2.43** and **2.44** were analyzed isocratically on HPLC system (**A**), which consisted of an ISCO Model 2360 Gradient Programmer, a Waters 510 HPLC Pump, a Waters 486 Tunable Absorbance Detector and a HP 3396 Series II Integrator. Prodrugs **2.28**, **2.30**, **2.31**, **2.32**, **2.33**, **2.34**, **2.36**, **2.39**, **2.41** and **2.46** were analyzed isocratically on a Hewlett Packard Series 1100 HPLC system (**B**) connected to a Tray-Cooling Marathon Basic+ Autosampler and a Hewlett Packard HP3395 Integrator. All samples were injected onto a Supelco Discovery C18 reversed-phase column (5 μm, 250 x 4.6 mm I.D.). The mobile phase consisted of a mixture of 23% acetonitrile and 77% water with 0.1% trifluoroacetic acid added. The flow rate was set at 1.0 mL/min and the analysis was performed at room temperature. The compounds were detected by UV at $\lambda = 217$ nm. The e.e. of compound **(S)-2.9** was determined with HPLC system **A** at $\lambda = 254$ nm on a Chiralpak AD column (250 x 10 mm) with an eluent mixture of 96% hexane and 4% isopropanol with 0.1% triethylamine added and at a flow rate of 4.0 ml/min**.** The e.e. of compounds **(S)-2.12** and **(R)-2.12** was determined with HPLC system **A** at $\lambda = 275$ nm on a Chiralcel OD column (250 x 10 mm) with an eluent mixture of 98.4% hexane and 1.6% isopropanol with 0.1% triethylamine added and at a flow rate of 4.0 ml/min. IR spectra were obtained on a ATI Mattson Genesis series FTIR™. Optical rotations were determined on a Perkin-Elmer polarimeter 241 (Na, 589 nm). Chromatography was performed using MP Ecochrom silica gel 32-63, 60 Å. Electron ionization (EI) mass spectra were obtained on a Shimadzu GCMS-QP5000 fitted with a CP-Sil 5 CB Lowbleed/MS column (15 m, 0.25mm, filmthickness 0.10μm). Electrospray ionization (ESI) mass spectra were recorded by the Mass Spectrometry Core Facility unit of the University of Groningen on a SCIEX API3000 triple quadrupole mass spectrometer (Applied Biosystems/MDS SCIEX) equipped with a Turbo Ion Spray interface and operated in the positive ion mode. High-resolution mass spectrometry (HR-MS) was performed by the mass spectrometry unit of the University of Groningen using a flow injection method on a LTQ-Orbitrap XL mass spectrometer (Thermo Electron, Bremen, Germany) operating in positive ion mode with a resolution of 60000 at m/z 400. ^{1}H NMR spectra were recorded on a Varian Gemini 200 (at 200 MHz), a Varian VXR 300 (at 300 MHz) and a Varian Mercuri Plus 400 (at 400 MHz) spectrometer. ^{13}C NMR spectra were recorded at 50.3 MHz on a Varian Gemini 200 spectrometer. The chemical shifts are reported as part per million (δ). The splitting patterns are designated as follows: s (singlet), br s (broad singlet), d (doublet), dd (double doublet), br d (broad doublet), t (triplet), q (quartet), m (multiplet). The coupling constants (J) are reported in hertz (Hz). In case of two isomers, the chemical shift of only one of the isomers was notated in the list of chemical shifts. Elemental analysis was performed by the microanalytical department of the University of Groningen on a Euro EA 3000

elemental analyzer (Eurovector) for C,H,N, on a CHN-O-Rapid (Heraeus) for O, and Cl was determined potentiometrically with the use of a 665 Dosimat and a 713 pH meter. The measured values were within 0.4% of the theoretical values, except where noted. All reagents were commercially available from Sigma Aldrich and Acros Organics and were used without purification. CH_2Cl_2 was dried by Al_2O_3/molecular sieves 4Å, Et_2O was dried with Na wire, and MeOH was distilled from Mg/I_2 and dried over molecular sieves 3Å.

2.4.2 General procedure for the protection of amino acids 2.1-2.5

Di-*tert*-butyl-dicarbonate (38.5 mmol) was added to a suspension of the amino acid (35.0 mmol) and $NaHCO_3$ (175 mmol) in 85 mL H_2O/THF (1:1). The reaction mixture was stirred overnight. The organic solvent was removed under reduced pressure and the remaining suspension was acidified with 4N HCl (aq, 40 mL) while cooled in ice. The aqueous mixture was extracted with EtOAc (2x150 mL) and the combined organic layers were washed with brine, dried on $MgSO_4$ and evaporated *in vacuo*. After recrystallization from EtOAc/Hexane, the Boc-protected amino acid was obtained as white needles.

N-*tert*-Boc-*L*-alanine (2.1). Yield: 35%; IR (KBr, cm^{-1}) ν_{max} 3383, 2987, 1739, 1691; ^{1}H NMR (200 MHz, CD_3OD): δ 4.10 (q, *J*=7 Hz, 1H, CH), 1.43 (s, 9H, $OC(CH_3)_3$), 1.34 (d, *J*=7.4 hz, 3H, CH_3); ^{13}C NMR (50 MHz, CD_3OD): δ 175.6, 79.2, 49.2, 27.5, 16.7.
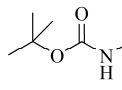
N-*tert*-Boc-*L*-proline (2.2). Yield: 77%; IR (KBr, cm^{-1}) ν_{max} 2967, 1739.
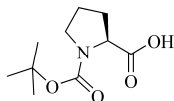
N-*tert*-Boc-*N*-methylglycine (2.3). Yield: 67%; IR (KBr, cm^{-1}) ν_{max} 2976, 1693; ^{1}H NMR (200 MHz, $CDCl_3$) of rotamer A δ 4.00 (s, 2H, CH_2), 2.91 (s, 3H, CH_3), 1.44 (s, 9H, $OC(CH_3)_3$), rotamer B δ 3.91 (s, 2H, CH_2), 2.91 (s, 3H, CH_3), 1.40 (s, 9H, $OC(CH_3)_3$); ^{13}C NMR (50 MHz, $CDCl_3$) of rotamer A δ 175.3, 156.6, 80.9, 50.9, 35.8, 28.5, rotamer B δ 175.3, 155.8, 80.9, 50.3, 35.7, 28.4.
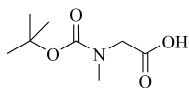
N-*tert*-Boc-γ-aminobutyric acid (2.4). Yield: 75%; IR (NaCl, cm^{-1}) ν_{max} 3344 (br), 2977, 1712, 1527.
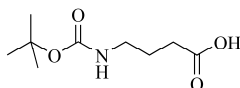
N-*tert*-Boc-5-aminovaleric acid (2.5). Yield: 70%; IR (KBr, cm^{-1}) ν_{max} 3373, 2984, 1713, 1685, 1523; ^{1}H NMR (200 MHz, CD_3OD): δ 3.04 (t, *J*=6.6 Hz, 2H, δ-CH_2), 2.30 (t, *J*=7.1 Hz, 2H, α-CH_2), 1.73-1.38 (m, 4H, β-CH_2 γ-CH_2), 1.43 (s, 9H, $OC(CH_3)_3$); ^{13}C NMR (50 MHz, CD_3OD): δ 176.2, 135.7, 78.7, 39.8, 33.3, 29.3, 27.6, 22.1.
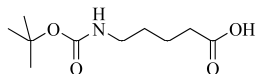
2.4.3 N^α, N^δ, N^ω-tri-benzyloxycarbonyl-*L*-arginine (2.6).[38]

Suspend *L*-arginine (5.0 g, 28.7 mmol) in a mixture of dry 1,2-dichloroethane (50 mL) and DIPEA (38 mL, 229 mmol) under nitrogen atmosphere. Slowly TMS-Cl (29 mL, 227 mmol) was added and the reaction mixture was heated at 45 °C for 2 hours. The mixture was cooled down to 5 °C and another portion of DIPEA (19 mL, 115 mmol) was added. Benzylchloroformate (16 mL, 113 mmol) was added to the ice-cooled suspension and the mixture was allowed to attain room temperature. After addition of another portion of 1,2-dichloroethane (50 mL) the reaction mixture was stirred for 1 hour. 1N HCl (aq, 34 mL) was added, the reaction mixture was partitioned between H_2O (50 mL) and CH_2Cl_2 (50 mL), and extracted with

CH$_2$Cl$_2$ (2x100 mL). The combined organic layers were evaporated *in vacuo* and the orange oil was purified by column chromatography (SiO$_2$, CH$_2$Cl$_2$/MeOH) and recrystallized from MeOH/H$_2$O (4:1) to yield **2.6** as white crystals (6.0 g, 36%). IR (KBr, cm^{-1}) v_{max} 3384, 1721, 1688; ^{1}H NMR (200 MHz, CDCl$_3$): δ 7.47-7.21 (m, 15H, CH$_2$*C$_6$H$_5$*), 5.76 (br d, *J*=7.9 Hz, 1H, NH), 5.20 (s, 2H, O*CH$_2$*C$_6$H$_5$), 5.09 (s, 2H, O*CH$_2$*C$_6$H$_5$), 5.05 (s, 2H, O*CH$_2$*C$_6$H$_5$), 4.43-4.25 (m, 1H, α-CH), 4.06-3.83 (m, 2H, δ-CH$_2$), 1.90-1.42 (m, 4H, β-CH$_2$, γ-CH$_2$); ^{13}C NMR (50 MHz, CDCl$_3$): δ 176.0, 163.8, 160.7, 156.6, 156.0, 137.0, 136.4, 134.8, 129.1, 129.0, 128.7, 128.6, 128.5, 128.4, 128.3, 128.1, 69.2, 67.3, 67.2, 54.0, 44.4, 29.0, 25.0; ESI-MS *m/z* 577.2 (M+H)$^+$.

2.4.4 Synthesis of (S)– and (R)-5-hydroxy-2-(di-*n*-propyl-amino)tetralin

**1,6-dimethoxynaphthalene (2.7).**[35] 1,6-dihydroxynaphthalene (150 g, 0.94 mol) was dissolved in 2N NaOH (800 mL) and dimethyl sulphate (250 mL, 2.6 mol) was added while stirring vigorously. The temperature of the reaction mixture increased to 62 ^{o}C and the solution became acidic (pH 2). A second portion of 2N NaOH (500 mL) and dimethyl sulphate (50 mL, 0.52 mol) was added respectively and the warm solution was stirred vigorously for 1 hour. 4N NaOH (100 mL) was added and the reaction mixture was refluxed for 4 hours. After attaining r.t. the H$_2$O layer was extracted with CH$_2$Cl$_2$ (3 x 250 mL), washed with 2N NaOH (3 x 350 mL) and brine (400 mL), and dried on Na$_2$SO$_4$. After filtration and evaporation *in vacuo* the obtained brown oil was purified by column chromatography (Al$_2$O$_3$, CH$_2$Cl$_2$) resulting in compound **2.1** as a light yellow oil which solidified on standing (146 g, 83%). Purity: 100% (GCMS); IR (KBr, cm^{-1}) v_{max} 2965, 1627, 1581, 1450, 1370, 1222; ^{1}H NMR (200 MHz, CDCl$_3$): δ 8.26-8.10 (m, 1H, ArH), 7.42-7.28 (m, 2H, ArH), 7.18-7.05 (m, 2H, ArH, 6.78-6.63 (m, 1H, ArH), 3.99 (s, 3H, OCH3), 3.93 (s, 3H, OCH$_3$); ^{13}C NMR (50 MHz, CDCl$_3$): δ 158.4, 155.9, 136.2, 126.9, 124.0, 121.0, 119.5, 117.8, 106.0, 102.3, 55.7, 55.5; EI-MS *m/z* 188 (M)$^+$.

5-methoxy-2-tetralone (2.8).[35] A solution of 1,6-dimethoxynaphthalene (63.77 g, 0.339 mol) in absolute EtOH (585 mL) was heated to reflux. Sodium (40.2 g, 1.75 mol) cut in small pieces was added to the nitrogen-flushed reaction mixture as rapidly as possible. Another portion of absolute EtOH (160 mL) was added and the reaction mixture was refluxed for 1.5 hours until all sodium had reacted. After cooling down in ice the mixture was acidified with aqueous 1N HCl (850 mL) and subsequently with aqueous 4N HCl (570 mL) to pH 2.5 and the colour changed from white to yellow. After refluxing for 1 hour, yellow oil precipitated, was collected separately from the reaction mixture. The EtOH was evaporated *in vacuo* from the H$_2$O/EtOH layer, until mostly H$_2$O was left. The H$_2$O layer was extracted with Et$_2$O (3 x 500 mL). The separately collected yellow oil was added to the extractions and the Et$_2$O layer was washed with brine, dried on Na$_2$SO$_4$, filtrated and evaporated *in vacuo* to afford the crude product as an orange oil (59 g). The oil was purified by vacuum distillation to yield compound **2.2** as a light yellow oil which solidified on standing (53 g, 89%). Bp 94-98 ^{o}C (0.13 mbar); Purity: 98% (GCMS); IR (NaCl, cm^{-1}) v_{max} 2937, 1717, 1587; ^{1}H NMR (200 MHz, CDCl$_3$): δ 7,19 (m, 1H, ArH), 6,76 (m, 2H, ArH), 3,86 (s, 3H, OCH$_3$), 3,57 (s, 2H, ArCH$_2$CO), 3.09 (t, *J* = 7 Hz, 2H, ArCH$_2$), 2.53 (t, *J* = 7 Hz, 2H, CH2CO); ^{13}C NMR (50 MHz, CDCl$_3$): δ 209.4, 154.7, 133.5, 126.0, 123.5, 118.9, 106.9, 53.9, 43.2, 36.4, 19.4; EI-MS *m/z* 176 (M)$^+$.

(±)-2-(benzylamino)-5-methoxytetralin HCl-salt ((±)-2.9).[2] Benzylamine (94 mL, 0.86 mol) and *p*-toluenesulfonic acid monohydrate (4 g, 0.02 mol) were added to a solution of 5-methoxy-2-tetralone (120 g, 0.68 mol) in toluene (500 mL) under nitrogen atmosphere. The reaction mixture was refluxed for 2 hours with continuous removal of water via a Dean-Stark water trap. After completion of the reaction, the solvent was evaporated *in vacuo*, absolute EtOH (150 mL) was added and the solution was transferred to a Parr flask. After addition of PtO$_2$ (1.18 g), the reaction mixture was hydrogenated under a pressure of 3.5 bar H$_2$ overnight. The
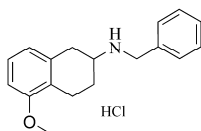
suspension was filtrated, evaporated *in vacuo* and the crude product was obtained as a brown oil (183 g). The free amine was converted to the HCl salt and recrystallized from MeOH/EtOAc which yielded compound **2.3** as pink crystals (116 g, 56%). Purity: 97.8%; IR (KBr, cm^{-1}) ν_{max} 2932, 2768, 2640, 1585; ^{1}H NMR (200 MHz, d_6-DMSO): δ 9.78 (br s, 1H, NH), 7.78-7.60 (m, 2H, ArH), 7.49-7.31 (m, 3H, ArH), 7.10 (t, *J*=7.93 Hz, 1H, ArH), 6.76 Hz (d, *J*=7.93 Hz, 1H, ArH), 6.69 (d, *J*=7.34 Hz, 1H, ArH), 4.23 (s, 2H, CH$_2$C$_6$H$_5$), 3.73 (s, 3H, OCH$_3$), 3.48-3.02 (m, 3H, H$_{1ax}$, H$_{1eq}$, H$_{2ax}$), 2.96-2.76 (m, 1H, H$_{4eq}$), 2.55-2.30 (m, 2H, H$_{3eq}$, H$_{4ax}$), 1.99-1.71 (m, 1H, H$_{3ax}$); ^{13}C NMR (50 MHz, d_6-DMSO): δ 157.4, 134.6, 133.0, 130.9, 129.4, 129.2, 127.4, 124.0, 121.7, 108.5, 55.9, 53.7, 47.9, 31.9, 25.3, 22.3; EI-MS *m/z* 267 (M)$^+$.

(S)-2-(benzylamino)-5-methoxytetralin HCl-salt ((S)-2.9).[36] (-)-Di-*p*-toluoyl-*L*-tartaric acid (131.0 g, 0.34 mol) and racemic 2-(benzylamino)-5-methoxytetralin (90.6 g, 0.34 mol) were added together and were recrystallized 3 times from 96% EtOH (7.9 L, 5.8 L, 4.8 L). The tartrate-salt was converted to HCl-salt and recrystallized from MeOH-Et$_2$O and yielded **(S)-2.3** as white solid crystals (25.9 g, 25%). Purity: 100% (GCMS); $[\alpha]_D^{21} -64.0°$ (c 0.27, MeOH); e.e.>98% (HPLC); ^{1}H NMR (200 MHz, DMSO): δ 7.70-7.55 (m, 2H, ArH), 7.46-7.29 (m, 3H, ArH), 7.10 (t, *J*=7.94 Hz, 1H, ArH), 6.75 Hz (d, *J*=7.93 Hz, 1H, ArH), 6.69 (d, *J*=7.64 Hz, 1H, ArH), 4.18 (s, 2H, CH$_2$C$_6$H$_5$), 3.73 (s, 3H, OCH$_3$), 3.34-2.97 (m, 3H, H$_{1ax}$, H$_{1eq}$, H$_{2ax}$), 2.96-2.73 (m, 1H, H$_{4eq}$), 2.58-2.26 (m, 2H, H$_{3eq}$, H$_{4ax}$), 1.95-1.67 (m, 1H, H$_{3ax}$); ^{13}C NMR (50 MHz, DMSO): δ 157.4, 134.9, 133.8, 130.7, 129.2, 127.4, 124.1, 121.7, 108.4, 55.9, 53.6, 48.1, 32.3, 25.7, 22.3; EI-MS *m/z* 267 (M)$^+$.
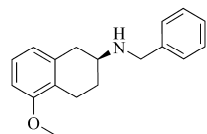
(R)-2-(benzylamino)-5-methoxytetralin HCl-salt ((R)-2.9).[36] The motherliquors of the recrystallizations of compound **(S)-2.3** were collected, evaporated *in vacuo* and converted to the free amine. (+)-Di-*p*-toluoyl-*D*-tartaric acid (80.4 g, 0.21 mol) was added to the resultant oil (55.7 g, 0.21 mol) and the mixture was recrystallized 3 times from 96% EtOH (4.9 L, 4.5 L, 3.9 L). The tartrate-salt was converted to HCl-salt and recrystallized from MeOH-Et$_2$O and yielded **(R)-2.3** as white solid crystals (23.7 g, 23%).
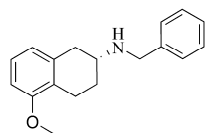
(S)-2-amino-5-methoxytetralin ((S)-2.10).[36] The HCl-salt of **(S)-2.9** was converted to the free amine (21.8 g, 0.08 mol), dissolved in EtOH 100% (300 mL) and Pd/C 10% (15 g) was added under nitrogen atmosphere. The solution was transferred to a Parr flask and hydrogenolyzed at 40 °C under 3.5 bar H$_2$ atmosphere. After completion of the reaction the mixture was filtrated and evaporated *in vacuo* to yield the free amine of **(S)-2.10** as an oil (14.0 g, 94%). IR (KBr, cm^{-1}) ν_{max} 2953, 2629, 1587.
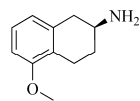
(R)-2-amino-5-methoxytetralin ((R)-2.10).[36] Similar to the procedure described for the synthesis of **(S)-2.10**. Compound **(R)-2.10** was obtained as an oil (10.8 g, 80%).
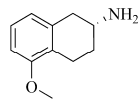
(S)-5-methoxy-2-(N,N-di-n-propylamino)-tetralin ((S)-2.11).[2] A solution of 1-iodopropane (30 mL, 0.31 mol) and **(S)-2.10** (13.9 g, 0.079 mol) in acetonitrile (200 mL) was refluxed with 100 mL of K$_2$CO$_3$ (aq, sat) for 2.5 hours. After separation of the organic layer, evaporation *in vacuo* and purification on column chromatography (SiO$_2$, EtOAc/Hexane=1:4) compound **(S)-2.11** was yielded as a yellow oil (13.2 g, 64%). Purity: 100% (GCMS); ^{1}H NMR (300 MHz, CDCl$_3$): δ 7.10 (t, *J*=7.9 Hz, 1H, ArH), 6.73 (d, *J*=7.6 Hz, 1H, ArH), 6.66 (d, *J*=7.9 Hz, 1H, ArH), 3.82 (s, 3H, OCH$_3$), 3.11-2.64 (m, 4H, H$_{1ax}$, H$_{1eq}$, H$_{2ax}$, H$_{4eq}$), 2.63-2.40 (m, 5H, H$_{4ax}$, N(CH$_2$CH$_2$CH$_3$)$_2$), 2.16-2.00 (m, 1H, H$_{3eq}$), 1.70-1.39 (m, 5H, H$_{3ax}$, N(CH$_2$CH$_2$CH$_3$)$_2$), 0.91 (t, *J*=7.3 Hz, 6H, N(CH$_2$CH$_2$CH$_3$)$_2$); ^{13}C NMR (50 MHz, CDCl$_3$): δ 157.4, 138.5, 126.3, 125.6, 121.9, 107.0, 56.7, 55.4, 52.9, 32.5, 25.9, 24.2, 22.4, 12.2; EI-MS *m/z* 261 (M)$^+$.

(R)-5-methoxy-2-(*N,N*-di-*n*-propylamino)-tetralin ((R)-2.11).[2] Similar to the procedure described for the synthesis of **(S)-2.11**. Compound **(R)-2.11** was obtained as a yellow oil (8.6 g, 54%). Purity: 100% (GCMS); IR (NaCl, cm^{-1}) ν_{max} 2953, 1585, 1468, 1259, 1095; ^{1}H NMR (200 MHz, CDCl$_3$): δ 7.12 (t, *J*=7.9 Hz, 1H, ArH), 6.76 (d, *J*=7.6 Hz, 1H, ArH), 6.68 (d, *J*=8.2 Hz, 1H, ArH), 3.84 (s, 3H, OCH$_3$), 3.14-2.73 (m, 4H, H$_{1ax}$, H$_{1eq}$, H$_{2ax}$, H$_{4eq}$), 2.71-2.40 (m, 5H, H$_{4ax}$, N(*CH$_2$*CH$_2$CH$_3$)$_2$), 2.18-2.02 (m, 1H, H$_{3eq}$), 1.72-1.49 (m, 1H, H$_{3ax}$), 1.48-1.39 (m, 4H, N(CH$_2$*CH$_2$*CH$_3$)$_2$), 0.94 (t, *J*=7.4 Hz, 6H, N(CH$_2$CH$_2$*CH$_3$)$_2$); ^{13}C NMR (50 MHz, CDCl$_3$): δ 157.5, 138.5, 126.3, 125.6, 121.9, 107.0, 56.7, 55.4, 52.9, 32.5, 25.9, 24.2, 22.5, 12.2; EI-MS *m/z* 261 (M)$^+$.
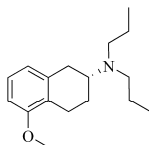
(S)-5-hydroxy-2-(*N,N*-di-*n*-propyl-amino)tetralin HBr-salt((S)-2.12).[1] A mixture of freshly distilled 48% HBr (40 mL) and **(S)-2.11** (13.2 g, 0.05 mol) was refluxed for 1.5 hours under nitrogen atmosphere. After cooling down, the reaction mixture was evaporated *in vacuo* and the resultant pink solid material was recrystallized from 100% EtOH to afford **(S)-2.12** as white crystals (14.5 g, 87%). Purity: 100% (GCMS); $[\alpha]_D^{23}-66.7°\,(c\,1.00, MeOH)$; e.e.=100% (HPLC); IR (KBr, cm^{-1}) ν_{max} 3243, 2931, 2690,2639, 2515, 1590,1465. 1276; ^{1}H NMR (200 MHz, CD$_3$OD): δ 6.96 (t, *J*=7.8 Hz, 1H, ArH), 6.64 (d, *J*=7.6 Hz, 1H, ArH), 6.63 (d, *J*=8.2 Hz, 1H, ArH), 3.78-3.55 (m, 1H, H$_{2ax}$), 3.40-2.94 (m, 7H, H$_{1ax}$, H$_{1eq}$, N(*CH$_2$*CH$_2$CH$_3$)$_2$, H$_{4eq}$), 2.78-2.49 (m, 1H, H$_{4ax}$), 2.44-2.26 (m, 1H, H$_{3eq}$), 2.02-1.69 (m, 5H, H$_{3ax}$, N(CH$_2$*CH$_2$*CH$_3$)$_2$), 1.05 (t, *J*=7.3 Hz, 6H, N(CH$_2$CH$_2$*CH$_3$)$_2$); ^{13}C NMR (50 MHz, CD$_3$OD): δ 154.9, 133.7, 126.8, 121.9, 120.1, 112.3, 60.6, 52.5, 29.6, 23.7, 22.5, 18.7, 10.2; ESI-MS *m/z* 248.1 (M+H)$^+$.
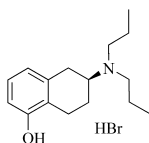
(R)-5-hydroxy-2-(*N,N*-di-*n*-propyl-amino)tetralin HBr-salt ((R)-2.12).[1] A mixture of freshly distilled 48% HBr (25 mL) and **(R)-2.11** (8.6 g, 0.03 mol) was refluxed for 4 hours under nitrogen atmosphere. After cooling down, the reaction mixture was evaporated *in vacuo* and the resultant pink solid material was recrystallized from 100% EtOH to afford **(R)-2.12** as white crystals (7.4 g, 69%). Purity: 99% (GCMS); $[\alpha]_D^{20}+65.3°\,(c\,1.00, MeOH)$; e.e.>99% (HPLC); IR (KBr, cm^{-1}) ν_{max} 3243, 2933, 2690, 2652,1590, 1465, 1277; ^{1}H NMR (200 MHz, CD$_3$OD): δ 6.96 (t, *J*=7.8 Hz, 1H, ArH), 6.64 (d, *J*=7.6 Hz, 1H, ArH), 6.63 (d, *J*=7.9 Hz, 1H, ArH), 3.83-3.58 (m, 1H, H$_{2ax}$), 3.39-2.97 (m, 7H, H$_{1ax}$, H$_{1eq}$, N(*CH$_2$*CH$_2$CH$_3$)$_2$, H$_{4eq}$), 2.75-2.52 (m, 1H, H$_{4ax}$), 2.44-2.27 (m, 1H, H$_{3eq}$), 2.01-1.68 (m, 5H, H$_{3ax}$, N(CH$_2$*CH$_2$*CH$_3$)$_2$), 1.05 (t, *J*=7.2 Hz, 6H, N(CH$_2$CH$_2$*CH$_3$)$_2$); ^{13}C NMR (50 MHz, CD$_3$OD): δ 154.9, 133.7, 126.8, 121.9, 120.1, 112.3, 60.6, 52.5, 29.6, 23.7, 22.5, 18.7, 10.2; EI-MS *m/z* 247 (M)$^+$.
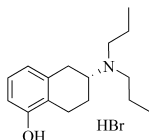
(S)-5-hydroxy-2-(*N,N,N*-tri-*n*-propyl-ammonium)tetralin iodide salt ((S)-2.47). A solution of 1-iodopropane (81 mL, 0.83 mol) and **(S)-2.10** (18.4 g, 0.10 mol) in acetonitrile (450 mL) was refluxed with 150 mL of K$_2$CO$_3$ (aq, sat) overnight. After separation of the organic layer, evaporation *in vacuo* and purification on column chromatography (SiO$_2$, CH$_2$Cl$_2$) the iodide salt of compound **(S)-2.47** was yielded as a white solid (8 g, 19%). ^{1}H NMR (300 MHz, CDCl$_3$): δ 7.12 (t, *J*=7.9 Hz, 1H, ArH), 6.80 (d, *J*=7.6 Hz, 1H, ArH), 6.68 (d, *J*=8.2 Hz, 1H, ArH), 3.81 (s, 3H, OCH$_3$), 3.82-3.64 (m, 1H, H$_2$), 3.63-3.37 (m, 6H, (*CH$_2$*CH$_2$CH$_3$)$_3$), 3.36-3.02 (m, 3H, H$_1$, H$_4$), 2.77-2.50 (m, 2H, H$_3$, H$_4$), 2.03-1.67 (m, 7H, H$_3$, N(CH$_2$*CH$_2$*CH$_3$)$_3$), 1.08 (t, *J*=7.6 Hz, 6H, CH$_3$); ^{13}C NMR (50 MHz, CDCl$_3$): δ 157.3, 133.2, 127.6, 123.3, 121.6, 108.3, 69.5, 61.0, 55.6, 30.9, 24.6, 24.2, 17.8, 11.6.

2.4.5 General procedure for preparation of protected amino acid (S)-2-(*N,N*-di-*n*-propyl-amino)tetralin-5-yl esters 2.13-2.18 and 2.20-2.26, *N-tert*-Boc-*O*-benzyl-*L*-serine (R)-2-(*N,N*-di-*n*-propyl-amino)tetralin-5-yl ester (2.19) and *N-tert*-Boc-5-aminovaleric acid (R)-2-(*N,N*-di-*n*-propyl-amino)tetralin-5-yl ester (2.27).

The protected amino acid (0.88 mmol) and HOBt hydrate (0.96 mmol) were suspended in 5 mL anhydrous CH$_2$Cl$_2$ under nitrogen atmosphere and cooled to 0 °C. EDC (0.96 mmol) was added and

the reaction mixture was stirred for 15 minutes. After all solid material dissolved, the free amine of 5-OH-DPAT (0.80 mmol) in 1 mL anhydrous CH_2Cl_2 was slowly added to the yellow suspension. The solution was allowed to attain room temperature and was stirred for 2 hours until the reaction was complete. CH_2Cl_2 (100 mL) was added and the reaction mixture was washed with aqueous 0.1 N HCl (10 mL), 1.0 N NaOH (20 mL) and brine (10 mL). The organic layer was dried over $MgSO_4$ and evaporated *in vacuo*; the resultant yellow oil was purified by column chromatography (CH_2Cl_2/MeOH = 20:1) to afford the pure compounds **2.13-2.27** as colourless oils.

***N*-*tert*-Boc-glycine (S)-2-(*N,N*-di-*n*-propyl-amino)tetralin-5-yl ester (2.13).** Yield: 59%; IR (KBr, cm^{-1}) ν_{max} 3381 (br), 2957, 1773, 1716, 1514; ^{1}H NMR (200 MHz, CDCl$_3$): δ 7.12 (t, *J*=7.6 Hz, 1H, ArH), 6.99 (d, *J*=7.3 Hz, 1H, ArH), 6.84 (d, *J*=7.3 Hz, 1H, ArH), 5.09 (br s, 1H, NH), 4.17 (d, *J*=5.6 Hz, 2H, α-CH$_2$), 3.06-2.63 (m, 4H, H$_{1ax}$, H$_{1eq}$, H$_{2ax}$, H$_{4eq}$), 2.61-2.24 (m, 5H, H$_{4ax}$, N(*CH$_2$*CH$_2$CH$_3$)$_2$), 2.13-1.94 (m, 1H, H$_{3eq}$), 1.68-1.28 (m, 5H, H$_{3ax}$, N(CH$_2$*CH$_2$*CH$_3$)$_2$), 1.47 (s, 9H, OC(CH$_3$)$_3$), 0.88 (t, *J*=7.4 Hz, 6H, CH$_3$); ^{13}C NMR (50 MHz, CDCl$_3$): δ 167.1, 154.1, 147.0, 137.7, 127.3, 126.0, 124.8, 117.2, 78.7, 54.7, 51.1, 40.9, 30.6, 26.8, 23.6, 22.5, 20.5, 10.4; HR-MS *m/z* Calcd. for C$_{23}$H$_{37}$N$_2$O$_4$ 405.2747 (M+1)$^+$, found 405.2767 (M+1)$^+$.
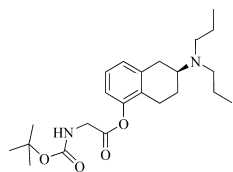
***N*-*tert*-Boc-*L*-alanine (S)-2-(*N,N*-di-*n*-propyl-amino)tetralin-5-yl ester (2.14).** Yield: 56%; IR (KBr, cm^{-1}) ν_{max} 3357, 2975, 1746, 1706, 1525; ^{1}H NMR (200 MHz, CDCl$_3$): δ 7.12 (t, *J*=8 Hz, 1H, ArH), 6.99 (d, *J*=7 Hz, 1H, ArH), 6.83 (d, *J*=8 Hz, 1H, ArH), 5.10 (br d, *J*=7.1 Hz, 1H, NH), 4.69-4.36 (m, 1H, α-CH), 3.04-2.61 (m, 4H, H$_{1ax}$, H$_{1eq}$, H$_{2ax}$, H$_{4eq}$), 2.60-2.27 (m, 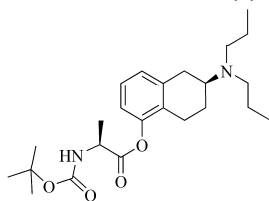5H, H$_{4ax}$, N(*CH$_2$*CH$_2$CH$_3$)$_2$), 2.11-1.90 (m, 1H, H$_{3eq}$), 1.83-1.32 (m, 5H, H$_{3ax}$, N(CH$_2$*CH$_2$*CH$_3$)$_2$), 1.56 (d, *J*=7.3 Hz, 3H, β-CH$_3$), 1.46 (s, 9H, OC(CH$_3$)$_3$), 0.88 (t, *J*=7.4 Hz, 6H, CH$_3$); ^{13}C NMR (50 MHz, CDCl3): δ 170.2, 153.5, 147.0, 137.6, 127.3, 126.0, 124.8, 117.2, 78.5, 54.6, 51.1, 47.9, 30.7, 26.8, 23.6, 22.5, 20.6, 17.2, 10.4; HR-MS *m/z* Calcd. for C$_{24}$H$_{39}$N$_2$O$_4$ 419.2904 (M+1)$^+$, found 419.2913 (M+1)$^+$.

***N*-*tert*-Boc-1-aminocyclopropane-1-carboxylic acid (S)-2-(*N,N*-di-*n*-propyl-amino)tetralin-5-yl ester (2.15).** Yield: 49%; IR (NaCl, cm^{-1}) ν_{max} 3377 (br), 2957, 1746, 1729, 1713, 1503, 1461, 1366, 1247, 1169, 1140; ^{1}H NMR (300 MHz, CDCl$_3$): δ 7.10 (t, *J*=7.9 Hz, 1H, ArH), 6.97 (d, *J*=7.3 Hz, 1H, ArH), 6.82 (d, *J*=7.7 Hz, 1H, ArH), 5.12 (br s, 1H, NH), 3.03-2.67 (m, 4H, H$_{1ax}$, H$_{1eq}$, H$_{2ax}$, H$_{4eq}$), 2.61-2.39 (m, 1H, H$_{4ax}$), 2.47 (t, *J*=7.5 Hz, 4H, N(*CH$_2$*CH$_2$CH$_3$)$_2$), 2.10-1.94 (m, 1H, H$_{3eq}$), 1.76-1.64 (m, 2H, β-CH$_2$), 1.46 (s, 9H, OC(CH$_3$)$_3$), 1.63-1.37 (m, 5H, H$_{3ax}$, N(CH$_2$*CH$_2$*CH$_3$)$_2$), 1.36-1.20 (m, 2H, β-CH$_2$), 0.88 (t, *J*=7.3 Hz, 6H, CH$_3$); ^{13}C NMR (50 MHz, CDCl$_3$): δ 171.8, 156.1, 149.1, 139.1, 129.1, 127.5, 126.5, 119.1, 56.5, 52.8, 32.3, 28.5, 25.3, 24.2, 22.1, 18.6, 12.1; HR-MS *m/z* Calcd. for C$_{25}$H$_{39}$N$_2$O$_4$ 431.29043 (M+H)$^+$, found 431.28940 (M+H)$^+$.
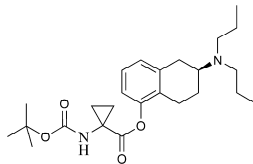
***N*-*tert*-Boc-L-valine (S)-2-(*N,N*-di-*n*-propyl-amino)tetralin-5-yl ester (2.16).** Yield: 66%; IR (KBr, cm^{-1}) ν_{max} 3363, 2956, 1738, 1706, 1521; ^{1}H NMR (200 MHz, CDCl$_3$): δ 7.11 (t, *J*=8 Hz, 1H, ArH), 6.99 (d, *J*=7 Hz, 1H, ArH), 6.82 (d, *J*=8 Hz, 1H, ArH), 5.06 (br d, *J*=9.1 Hz, 1H, NH), 4.47 (dd, *J*=9 Hz, 4 Hz, 1H, α-CH), 3.04-2.62 (m, 4H, H$_{1ax}$, H$_{1eq}$, H$_{2ax}$, H$_{4eq}$), 2.61-2.20 (m, 6H, H$_{4ax}$, N(*CH$_2$*CH$_2$CH$_3$)$_2$, β-CH), 2.10-1.93 (m, 1H, H$_{3eq}$), 1.68-1.31 (m, 5H, H$_{3ax}$, N(CH$_2$*CH$_2$*CH$_3$)$_2$), 1.47 (s, 9H, OC(CH$_3$)$_3$), 1.09 (d, *J*=6.8 Hz, 3H, γ-CH$_3$), 1.02 (d, *J*=7.0 Hz, 3H, γ-CH$_3$), 0.88 (t, *J*=7 Hz, 6H, CH$_3$); ^{13}C NMR (50 MHz, CDCl$_3$): δ 169.3, 154.2, 147.1, 137.7, 127.3, 125.9, 124.7, 117.3, 78.4, 57.2, 54.6, 51.1, 30.7, 29.7, 26.8, 23.6, 22.7, 20.6, 17.9, 16.0, 10.4; HR-MS *m/z* Calcd. for C$_{26}$H$_{43}$N$_2$O$_4$ 447.3217 (M+1)$^+$, found 447.3197 (M+1)$^+$.

***N-tert*-Boc-*D*-valine (S)-2-(*N,N*-di-*n*-propyl-amino)tetralin-5-yl ester (2.17).** Yield: 60%; IR (NaCl, cm^{-1}) ν_{max} 3365 (br), 2959, 1759, 1715, 1499; ^{1}H NMR (200 MHz, CDCl$_3$): δ 7.12 (t, *J*=7.8 Hz, 1H, ArH), 6.99 (d, *J*=7.3 Hz, 1H, ArH), 6.81 (d, *J*=7.4 Hz, 1H, ArH), 5.06 (br d, *J*=9.1 Hz, 1H, NH), 4.46 (dd, *J*=9.4 Hz, 4.7 Hz, 1H, α-CH), 3.05-2.63 (m, 4H, H$_{1ax}$, H$_{1eq}$, H$_{2ax}$, H$_{4eq}$), 2.62-2.18 (m, 6H, H$_{4ax}$, N(CH_2CH$_2$CH$_3$)$_2$, β-CH), 2.13-1.90 (m, 1H, H$_{3eq}$), 1.70-1.30 (m, 5H, H$_{3ax}$, N(CH$_2$CH_2CH$_3$)$_2$), 1.47 (s, 9H, OC(CH$_3$)$_3$), 1.09 (d, *J*=6.8 Hz, 3H, γ-CH$_3$), 1.02 (d, *J*=7.1 Hz, 3H, γ-CH$_3$), 0.88 (t, *J*=7.3 Hz, 6H, CH$_3$); ^{13}C NMR (50 MHz, CDCl$_3$): δ 171.2, 156.0, 148.9, 139.1, 129.1, 127.7, 126.5, 119.0, 80.2, 58.9, 56.5, 52.8, 32.2, 31.5, 28.6, 25.3, 24.4, 22.2, 19.5, 17.8, 12.1; EI-MS *m/z* 446 (M+H)$^+$.
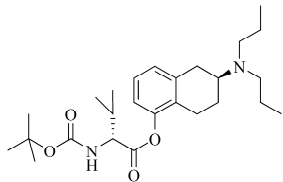
***N-tert*-Boc-*L*-isoleucine (S)-2-(*N,N*-di-*n*-propyl-amino)tetralin-5-yl ester (2.18).** Yield: 77%; IR (NaCl, cm^{-1}) ν_{max} 3342 (br), 2960, 1759, 1715, 1503; ^{1}H NMR (200 MHz, CDCl$_3$): δ 7.12 (t, *J*=8 Hz, 1H, ArH), 6.99 (d, *J*=7 Hz, 1H, ArH), 6.82 (d, *J*=8 Hz, 1H, ArH), 5.07 (br d, *J*=8.8 Hz, 1H, NH), 4.51 (dd, *J*=9.2 Hz, 4.5 Hz, 1H, α-CH), 3.06-2.65 (m, 4H, H$_{1ax}$, H$_{1eq}$, H$_{2ax}$, H$_{4eq}$), 2.64-2.30 (m, 5H, H$_{4ax}$, N(CH_2CH$_2$CH$_3$)$_2$), 2.15-1.90 (m, 2H, H$_{3eq}$, β-CH), 1.70-1.12 (m, 7H, H$_{3ax}$, N(CH$_2$CH_2CH$_3$)$_2$, γ-CH$_2$), 1.46 (s, 9H, OC(CH$_3$)$_3$), 1.07 (d, *J*=6.8 Hz, 3H, β^1-CH$_3$), 0.98 (t, *J*=7.4 Hz, 3H, δ-CH$_3$), 0.88 (t, *J*=7.4 Hz, 6H, CH$_3$); ^{13}C NMR (50 MHz, CDCl$_3$): δ 171.2, 155.9, 148.8, 128.9, 127.7, 126.6, 119.1, 105.0, 80.2, 58.5, 56.5, 52.8, 38.2, 32.2, 28.6, 25.3, 25.2, 24.4, 22.1, 16.1, 12.1, 11.9; HR-MS *m/z* Calcd. for C$_{27}$H$_{45}$N$_2$O$_4$ 461.3373 (M+1)$^+$, found 461.3388 (M+1)$^+$.
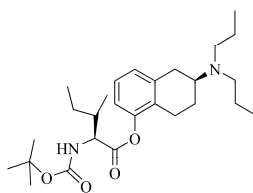
***N-tert*-Boc-O-benzyl-*L*-serine (R)-2-(*N,N*-di-*n*-propyl-amino)tetralin-5-yl ester (2.19).** Yield: 43%; IR (NaCl, cm^{-1}) ν_{max} 3453, 2956, 1767, 1720, 1501; ^{1}H NMR (400 MHz, CDCl$_3$): δ 7.40-7.22 (m, 5H, ArH), 7.10 (t, *J*=7.9 Hz, 1H, ArH), 6.98 (d, *J*=7.3 Hz, 1H, ArH), 6.80 (d, *J*=7.7 Hz, 1H, ArH), 5.51 (d, *J*=8.8 Hz, 1H, NH), 4.70 (d, *J*=8.8 Hz, 1H, α-CH), 4.60 and 4.57 (AB-system, *J*$_{AB}$=11.7 Hz, 2H, ArCH$_2$), 3.82 and 4.11 (dd, *J*=9.3 Hz, *J*=2.9 Hz, 2H, CH$_2$O), 3.01-2.67 (m, 4H, H$_{1ax}$, H$_{1eq}$, H$_{2ax}$, H$_{4eq}$), 2.55-2.34 (m, 5H, H$_{4ax}$, N(CH_2CH$_2$CH$_3$)$_2$), 1.96-1.83 (m, 1H, H$_{3eq}$), 1.57-1.33 (m, 5H, H$_{3ax}$, N(CH$_2$CH_2CH$_3$)$_2$), 1.47 (s, 9H, OC(CH$_3$)$_3$), 0.89 (t, *J*=7.3 Hz, 6H, CH$_3$); 13C NMR (50 MHz, CDCl3): δ 169.5, 155.7, 148.9, 139.1, 137.6, 120.1, 128.7, 128.1, 127.9, 127.7, 126.5, 119.1, 80.4, 73.8, 70.6, 56.6, 54.5, 52.8, 32.2, 28.6, 25.2, 24.1, 22.0, 12.1; HR-MS *m/z* Calcd. for C$_{31}$H$_{45}$N$_2$O$_5$ 525.3323 (M+H)$^+$, found 525.33179 (M+H)$^+$.

***N-tert*-Boc-*L*-phenylalanine (S)-2-(*N,N*-di-*n*-propyl-amino)tetralin-5-yl ester (2.20).** Yield: 67%; IR (NaCl, cm^{-1}) ν_{max} 3401 (br), 2958, 1762, 1715, 1495; ^{1}H NMR (200 MHz, CDCl$_3$): δ 7.45-7.12 (m, 5H, ArH), 7.10 (t, *J*=7.6 Hz, 1H, ArH), 6.98 (d, *J*=7.3 Hz, 1H, ArH), 6.73 (d, *J*=7.6 Hz, 1H, ArH), 5.13-4.96 (m, 2H, NH), 4.91-4.71 (m, 1H, α-CH), 3.40-3.08 (m, 2H, CHCH_2C$_6$H$_5$), 3.03-2.55 (m, 4H, H$_{1ax}$, H$_{1eq}$, H$_{2ax}$, H$_{4eq}$), 2.54-2.28 (m, 5H, H$_{4ax}$, N(CH_2CH$_2$CH$_3$)$_2$), 2.07-1.89 (m, 1H, H$_{3eq}$), 1.65-1.27 (m, 5H, H$_{3ax}$, N(CH$_2$CH_2CH$_3$)$_2$), 1.43 (s, 9H, OC(CH$_3$)$_3$), 0.88 (t, *J*=7 Hz, 6H, CH$_3$); ^{13}C NMR (50 MHz, CDCl$_3$): δ 167.0, 153.6, 147.0, 137.7, 134.3, 128.0, 127.2, 125.9, 124.7, 117.2, 78.6, 54.7, 53.1, 51.1, 36.8, 30.6, 26.8, 23.6, 22.5, 20.6, 10.4; HR-MS *m/z* Calcd. for C$_{30}$H$_{43}$N$_2$O$_4$ 495.3217 (M+1)$^+$, found 495.3232 (M+1)$^+$.

***N*α,*N*ε-di-*tert*-Boc-*L*-lysine (S)-2-(*N,N*-di-*n*-propyl-amino)tetralin-5-yl ester (2.21).** Yield: 57%; IR (NaCl, cm^{-1}) ν_{max} 3353 (br), 2956, 1761, 1712, 1695, 1515; ^{1}H NMR (200 MHz, CDCl$_3$): δ 7.12 (t, *J*=7.8 Hz, 1H, ArH), 6.99 (d, *J*=7.1 Hz, 1H, ArH), 6.81 (d, *J*=7.4 Hz, 1H, ArH), 5.18 (br d, *J*=7.3 Hz, 1H, NH), 4.62 (br s, 1H, NH), 4.56-4.42 (m, 1H, α-CH), 3.25-3.07 (m, 2H, ε-CH$_2$), 3.06-2.63 (m, 4H,
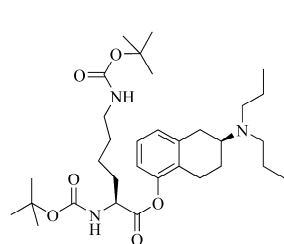
H$_{1ax}$, H$_{1eq}$, H$_{2ax}$, H$_{4eq}$), 2.61-2.37 (m, 5H, H$_{4ax}$, N(*CH$_2$*CH$_2$CH$_3$)$_2$), 2.14-1.68 (m, 3H, H$_{3eq}$, β-CH$_2$), 1.67-1.34 (m, 9H, H$_{3ax}$, N(CH$_2$*CH$_2$*CH$_3$)$_2$, γ-CH$_2$, δ-CH$_2$), 1.46 (s, 9H, OC(CH$_3$)$_3$), 1.44 (s, 9H, OC(CH$_3$)$_3$) 0.88 (t, *J*=7.4 Hz, 6H, CH$_3$); ^{13}C NMR (50 MHz, CDCl3): δ 171.6, 155.8, 148.8, 139.1, 128.9, 127.7, 126.6, 119.1, 80.3, 56.5, 53.8, 52.7, 40.2, 32.4, 32.2, 29.9, 28.7, 28.6, 25.2, 24.3, 22.9, 22.1, 12.1.

Nα, Nδ, Nω-tri-benzyloxycarbonyl-*L*-arginine (S)-2-(*N,N*-di-*n*-propyl-amino)tetralin-5-yl ester (2.22). Yield: 60%; IR (KBr, cm^{-1}) ν$_{max}$ 3388, 2957, 1760, 1720, 1691, 1608, 1509; ^{1}H NMR (200 MHz, CDCl$_3$): δ 9.46 (br s, 1H, NH), 9.28 (br s, 1H, NH), 7.47-7.20 (m, 15H, CH2*C$_6$H$_5$*), 7.09 (t, *J*=8 Hz, 1H, ArH), 6.98 (d, *J*=7 Hz, 1H, ArH), 6.77 (d, *J*=8 Hz, 1H, ArH), 5.74 (br d, *J*=8.5 Hz, 1H, NH), 5.23 (s, 2H, O*CH$_2$*C$_6$H$_5$), 5.09 (s, 4H, O*CH$_2$*C$_6$H$_5$), 4.74-4.54 (m, 1H, α-CH), 4.19-3.88 (m, 2H, δ-CH$_2$), 3.04-2.63 (m, 4H, H$_{1ax}$, H$_{1eq}$, H$_{2ax}$, H$_{4eq}$), 2.58-2.19 (m, 5H, H$_{4ax}$, N(*CH$_2$*CH$_2$CH$_3$)$_2$), 2.08-1.67 (m, 5H, H$_{3eq}$, β-CH$_2$, γ-CH$_2$), 1.66-1.34 (m, 5H, H$_{3ax}$, N(CH$_2$*CH$_2$*CH$_3$)$_2$), 0.89 (t, *J*=7.3 Hz, 6H, CH$_3$); ^{13}C NMR (50 MHz, CDCl$_3$): δ 171.0, 164.0, 160.8, 156.4, 156.0, 148.7, 137.1, 136.5, 134.8, 129.14, 129.07, 128.82, 128.75, 128.59, 128.56, 128.4, 128.3, 128.0, 127.8, 126.6, 119.0, 69.2, 67.2, 56.5, 54.2, 52.7, 44.3, 32.3, 29.2, 25.3, 24.2, 22.1, 12.1; HR-MS *m/z* Calcd. for C$_{46}$H$_{56}$N$_5$O$_8$ 806.4123 (M+1)$^+$, found 806.4139 (M+1)$^+$.
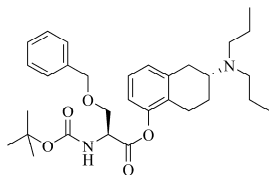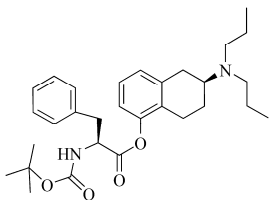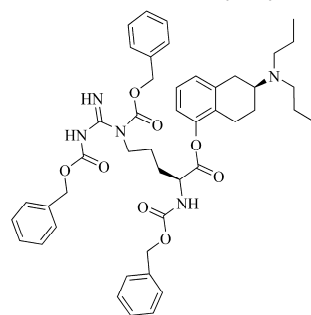
N-tert-Boc-*L*-proline (S)-2-(*N,N*-di-*n*-propyl-amino)tetralin-5-yl ester (2.23). Yield: 51%; IR (NaCl, cm^{-1}) ν$_{max}$ 2959, 1767, 1706; ^{1}H NMR (200 MHz, CDCl$_3$): δ 7.20-7.03 (m, 1H, ArH), 7.02-6.91 (m, 1H, ArH), 6.90-6.75 (m, 1H, ArH), 4.62-4.43 (m, 1H, α-CH), 3.72-3.34 (m, 2H, δ-CH$_2$), 3.03-2.64 (m, 4H, H$_{1ax}$, H$_{1eq}$, H$_{2ax}$, H$_{4eq}$), 2.63-1.87 (m, 10H, H$_{4ax}$, N(*CH$_2$*CH$_2$CH$_3$)$_2$, β-CH$_2$, γ-CH$_2$, H$_{3eq}$), 1.68-1.30 (m, 5H, H$_{3ax}$, N(CH$_2$*CH$_2$*CH$_3$)$_2$), 1.47 (s, 9H, OC(CH$_3$)$_3$), 0.88 (t, *J*=7.4 Hz, 6H, CH$_3$); ^{13}C NMR (50 MHz, CDCl$_3$): δ 169.5, 152.1, 137.6, 131.6, 127.1, 125.7, 124.7, 117.0, 78.4, 57.5, 54.6, 51.0, 44.9, 30.5, 29.7, 28.6, 26.9, 23.7, 22.6, 22.1, 20.6, 10.4; HR-MS *m/z* Calcd. for C$_{26}$H$_{41}$N$_2$O$_4$ 445.3060 (M+1)$^+$, found 445.3055 (M+1)$^+$.
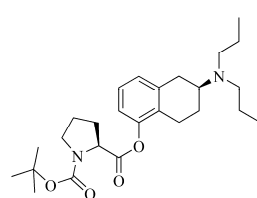
N-tert-Boc-sarcosine (S)-2-(*N,N*-di-*n*-propyl-amino)tetralin-5-yl ester (2.24). Yield: 45%; IR (NaCl, cm^{-1}) ν$_{max}$ 2959, 1770, 1703; ^{1}H NMR (200 MHz, CDCl$_3$): δ 7.12 (t, *J*=8 Hz, 1H, ArH), 6.99 (d, *J*=8 Hz, 1H, ArH), 6.84 (d, *J*=6 Hz, 1H, ArH), 4.20 (d, *J*=12.6, 2H, α-CH$_2$), 3.01 (d, *J*=4.4 Hz, 3H, NCH$_3$), 2.97-2.64 (m, 4H, H$_{1ax}$, H$_{1eq}$, H$_{2ax}$, H$_{4eq}$), 2.63-2.35 (m, 5H, H$_{4ax}$, N(*CH$_2$*CH$_2$CH$_3$)$_2$), 2.11-1.93 (m, 1H, H$_{3eq}$), 1.68-1.31 (m, 5H, H$_{3ax}$, N(CH$_2$*CH$_2$*CH$_3$)$_2$), 1.47 (s, 9H, OC(CH$_3$)$_3$), 0.88 (t, *J*=7.3 Hz, 6H, CH$_3$); ^{13}C NMR (50 MHz, CDCl$_3$): δ 166.7, 147.0, 137.6, 127.2, 126.0, 125.8, 124.8, 117.4, 117.1, 78.9, 54.7, 51.1, 49.4, 48.9, 34.2, 30.6, 30.4, 26.8, 23.7, 22.7, 20.6, 10.4; HR-MS *m/z* Calcd. for C$_{24}$H$_{39}$N$_2$O$_4$ 419.2904 (M+1)$^+$, found 419.2906 (M+1)$^+$.
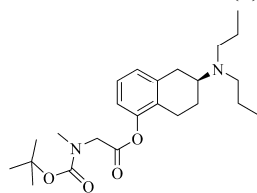
N-tert-Boc-β-alanine (S)-2-(*N,N*-di-*n*-propyl-amino)tetralin-5-yl ester (2.25). Yield: 90%; IR (NaCl, cm^{-1}) ν$_{max}$ 3367 (br), 2954, 1754, 1715, 1504; ^{1}H NMR (200 MHz, CDCl$_3$): δ 7.12 (t, *J*=7.6 Hz, 1H, ArH), 6.99 (d, *J*=7.3 Hz, 1H, ArH), 6.82 (d, *J*=7.9 Hz, 1H, ArH), 5.04 (br s, 1H, NH), 3.50 (q, *J*=6.2 Hz, 2H, β-CH$_2$), 3.05-2.67 (m, 4H, H$_{1ax}$, H$_{1eq}$, H$_{2ax}$, H$_{4eq}$), 2.80 (t, *J*=6.2 Hz, 2H, α-CH$_2$), 2.63-2.17 (m, 5H, H$_{4ax}$, N(*CH$_2$*CH$_2$CH$_3$)$_2$), 2.12-1.95 (m, 1H, H$_{3eq}$), 1.70-1.33 (m, 5H, H$_{3ax}$, N(CH$_2$*CH$_2$*CH$_3$)$_2$),
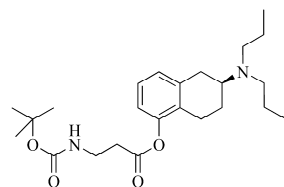
1.45 (s, 9H, OC(CH$_3$)$_3$), 0.88 (t, *J*=7.3 Hz, 6H, CH$_3$); ^{13}C NMR (50 MHz, CDCl$_3$): δ 169.3, 154.3, 147.1, 137.7, 127.2, 125.9, 124.8, 117.4, 78.0, 54.6, 51.1, 34.7, 33.0, 30.6, 26.9, 23.7, 22.6, 20.6, 10.4; HR-MS *m/z* Calcd. for C$_{24}$H$_{39}$N$_2$O$_4$ 419.2904 (M+1)$^+$, found 419.2912 (M+1)$^+$.

N-tert-Boc-γ-aminobutyric acid (S)-2-(*N,N*-di-*n*-propyl-amino)tetralin-5-yl ester (2.26). Yield: 66%; IR (NaCl, cm^{-1}) ν$_{max}$ 3388 (br), 2962, 1758, 1714, 1515; ^{1}H NMR (200 MHz, CDCl$_3$): δ 7.11 (t, *J*=7.6 Hz, 1H, ArH), 6.98 (d, *J*=7.3 Hz, 1H, ArH), 6.82 (d, *J*=7.6 Hz, 1H, ArH), 4.67 (br s, 1H, NH), 3.25 (q, *J*=6.5, 2H, γ-CH$_2$), 3.04-2.69 (m, 4H, H$_{1ax}$, H$_{1eq}$, H$_{2ax}$, H$_{4eq}$), 2.61 (t, *J*=7.3 Hz, 2H, α-CH$_2$), 2.51-2.38 (m, 5H, H$_{4ax}$, N(*CH$_2$*CH$_2$CH$_3$)$_2$), 2.11-1.71 (m, 1H, H$_{3eq}$), 1.94 (quintet, *J*=7.1 Hz, 2H, β-CH$_2$), 1.70-1.31 (m, 5H, H$_{3ax}$, N(CH$_2$*CH$_2$*CH$_3$)$_2$), 1.45 (s, 9H, OC(CH$_3$)$_3$), 0.88 (t, *J*=7 Hz, 6H, CH$_3$); ^{13}C NMR (50 MHz, CDCl$_3$): δ 170.1, 154.5, 147.3, 137.6, 127.3, 125.8, 124.7, 117.4, 54.7, 51.1, 38.4, 30.6, 30.0, 26.9, 23.9, 23.7, 22.6, 20.6, 10.4; HR-MS *m/z* Calcd. for C$_{25}$H$_{41}$N$_2$O$_4$ 433.3060 (M+1)$^+$, found 433.3054 (M+1)$^+$.
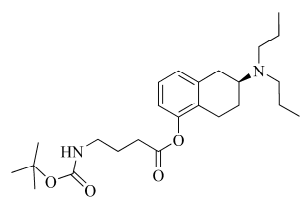
N-tert-Boc-5-aminovaleric acid (R)-2-(*N,N*-di-n-propyl-amino)tetralin-5-yl ester (2.27). Yield: 38%; IR (NaCl, cm^{-1}) ν$_{max}$ 3362 (br), 2956, 1757, 1713, 1517, 1461, 1365, 1247, 1172; ^{1}H NMR (200 MHz, CDCl$_3$): δ 7.12 (t, *J*=7.6 Hz, 1H, ArH), 6.98 (d, *J*=7.6 Hz, 1H, ArH), 6.80 (d, *J*=7.6 Hz, 1H, ArH), 4.60 (br s, 1H, NH), 3.17 (q, *J*=6.5, 2H, δ-CH$_2$), 3.05-2.65 (m, 4H, H$_{1ax}$, H$_{1eq}$, H$_{2ax}$, H$_{4eq}$), 2.59 (t, *J*=7.2 Hz, 2H, α-CH$_2$), 2.53-2.37 (m, 5H, H$_{4ax}$, N(*CH$_2$*CH$_2$CH$_3$)$_2$), 2.14-1.97 (m, 1H, H$_{3eq}$), 1.88-1.68 (m, 2H, γ-CH$_2$), 1.67-1.54 (m, 2H, β-CH$_2$), 1.53-1.33 (m, 5H, H$_{3ax}$, N(CH$_2$*CH$_2$*CH$_3$)$_2$), 1.44 (s, 9H, OC(CH$_3$)$_3$), 0.88 (t, *J*=7.3 Hz, 6H, CH$_3$); ^{13}C NMR (50 MHz, CDCl$_3$): δ 172.0, 156.2, 149.0, 139.0, 129.9, 127.5, 126.6, 119.3, 79.4, 56.5, 52.8, 40.3, 33.9, 32.2, 29.8, 28.6, 25.3, 24.3, 22.3, 22.1, 12.1; HR-MS *m/z* Calcd. for C$_{26}$H$_{43}$N$_2$O$_4$ 447.32173 (M+H)$^+$, found 447.32062 (M+H)$^+$.
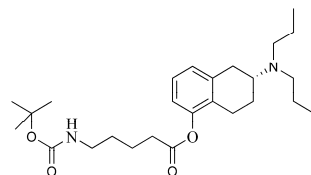
2.4.6 General deprotection procedure for the preparation of the amino acid (S)-2-(*N,N*-di-*n*-propyl-amino)tetralin-5-yl ester hydrochlorides 2.28-2.33 and 2.35-2.41 and *L*-Serine (R)-2-(*N,N*-di-*n*-propyl-amino)tetralin-5-yl ester 2HCl salt (2.34)

The *N*-tert-Boc-amino acid 2-(di-*n*-propyl-amino)tetralin-5-yl ester (0.40 mmol) was dissolved in 4 N HCl in dioxane (5 mL) under nitrogen atmosphere. The solution was stirred for 15 minutes at r.t. until a colourless oil precipitated. The solvent was carefully removed, the remaining oil was triturated with dry Et$_2$O and the solvent was evaporated *in vacuo* to afford a white solid foam. The solid material was dissolved in dry MeOH (2 mL) under N$_2$ atmosphere. After the solution was cooled in ice, the product was precipitated with dry Et$_2$O (50 mL) to afford an oil. The solvent was removed, the remaining oil was evaporated *in vacuo* and dried on the oil pump overnight to afford the hydrochloric acid salts of **2.28-2.41** as hygroscopic white solid foams.

Glycine (S)-2-(*N,N*-di-*n*-propyl-amino)tetralin-5-yl ester 2HCl salt (2.28). Yield: 85%; Purity: 98% (HPLC); IR (KBr, cm^{-1}) ν$_{max}$ 3413 (br), 2952, 2623, 1772; ^{1}H NMR (400 MHz, CD$_3$OD):δ 7.25 (t, *J*=7.7 Hz, 1H, ArH), 7.18 (d, *J*=7.3 Hz, 1H, ArH), 7.04 (d, *J*=7.7 Hz, 1H, ArH), 4.22 (s, 2H, α-CH$_2$), 3.81-3.76 (m, 1H, H$_{2ax}$), 3.37-3.08 (m, 6H, H$_{1ax}$, H$_{1eq}$, N(*CH$_2$*CH$_2$CH$_3$)$_2$), 3.07-2.95 (m, 1H, H$_{4eq}$), 2.79-2.64 (m, 1H, H$_{4ax}$), 2.45-2.33 (m, 1H, H$_{3eq}$), 2.03-1.89 (m, 1H, H$_{3ax}$), 1.88-1.74 (m, 4H, N(CH$_2$*CH$_2$*CH$_3$)$_2$), 1.05 (t, *J*=7.3 Hz, 6H, N(CH$_2$CH$_2$*CH$_3$*)$_2$); ^{13}C NMR (50 MHz, CD$_3$OD): δ 166.1, 148.3, 135.1, 127.7, 127.5, 127.2, 119.9, 59.9, 52.6, 40.0, 29.2, 23.2, 22.7, 18.5, 10.2; HR-MS *m/z* Calcd. for C$_{18}$H$_{29}$N$_2$O$_2$ 305.22235 (M)$^+$, found 305.22238 (M)$^+$.
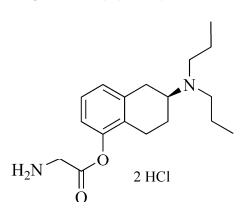
L-Alanine (S)-2-(*N,N*-di-*n*-propyl-amino)tetralin-5-yl ester 2HCl salt (2.29). Yield: 84%; Purity: 100% (HPLC); IR (KBr, cm^{-1}) ν$_{max}$ 3436 (br), 2967, 2644, 1768; ^{1}H NMR (400 MHz, CD$_3$OD):δ 7.26 (t, *J*=8 Hz, 1H, ArH), 7.18 (d, *J*=7.3 Hz, 1H, ArH), 7.02 (d, *J*=7.7 Hz, 1H, ArH), 4.47 (q, *J*=7.3 Hz, 1H, α-CH), 3.84-3.70 (m, 1H, H$_{2ax}$), 3.39-3.06 (m, 6H, H$_{1ax}$, H$_{1eq}$, N(*CH$_2$*CH$_2$CH$_3$)$_2$), 3.05-2.95 (m,
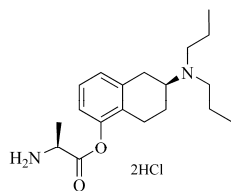
1H, H$_{4eq}$), 2.76-2.64 (m, 1H, H$_{4ax}$), 2.44-2.34 (m, 1H, H$_{3eq}$), 2.05-1.90 (m, 1H, H$_{3ax}$), 1.89-1.77 (m, 4H, N(CH$_2$CH_2CH$_3$)$_2$), 1.75 (d, J=7.3 Hz, 3H, CHCH_3) 1.05 (t, J=7.3 Hz, 6H, N(CH$_2$CH$_2$CH_3)$_2$); ^{13}C NMR (50 MHz, CD$_3$OD): δ 168.6, 148.3, 135.1, 127.8, 127.4, 127.2, 119.8, 59.8, 52.5, 29.2, 27.5, 23.2, 22.7, 18.6, 15.2, 10.2; HR-MS m/z Calcd. for C$_{19}$H$_{31}$N$_2$O$_2$ 319.23801 (M+H)$^+$, found 319.23792 (M+H)$^+$.

1-Aminocyclopropane-1-carboxylic acid (S)-2-(*N,N*-di-*n*-propyl-amino)tetralin-5-yl ester 2HCl salt (2.30). Yield: 81%; Purity: 100% (HPLC); IR (KBr, cm^{-1}) ν$_{max}$ 3431 (br), 2969, 2659, 1753, 1460, 1173; ^{1}H NMR (400 MHz, CD$_3$OD): δ 7.25 (t, J=7.7 Hz, 1H, ArH), 7.18 (d, J=7.7 Hz, 1H, ArH), 7.01 (d, J=7.7 Hz, 1H, ArH), 3.83-3.70 (m, 1H, H$_{2ax}$), 3.38-3.08 (m, 6H, H$_{1ax}$, H$_{1eq}$, N(CH_2CH$_2$CH$_3$)$_2$), 2.97 (dd, J=7.2 Hz, 3.3 Hz, 1H, H$_{4eq}$), 2.78-2.64 (m, 1H, H$_{4ax}$), 2.47-2.36 (m, 1H, H$_{3eq}$), 2.02-1.74 (m, 7H, H$_{3ax}$, β-CH$_2$), N(CH$_2$CH_2CH$_3$)$_2$), 1.68-1.58 (m, 2H, β-CH$_2$), 1.05 (t, J=7.3 Hz, 6H, CH$_3$); ^{13}C NMR (50 MHz, CDCl$_3$): δ 168.2, 148.3, 135.2, 127.8, 127.6, 127.2, 119.8, 59.8, 52.5, 34.3, 29.2, 23.2, 22.7, 18.5, 13.9, 10.2; HR-MS m/z Calcd. for C$_{20}$H$_{31}$N$_2$O$_2$ 331.23801 (M+H)$^+$, found 331.23816 (M+H)$^+$.

***L*-Valine (S)-2-(*N,N*-di-*n*-propyl-amino)tetralin-5-yl ester 2HCl salt (2.31).** Yield: 90%; Purity: 96% (HPLC); IR (KBr, cm^{-1}) ν$_{max}$ 3416 (br), 2969, 2622, 1762; ^{1}H NMR (200 MHz, CD$_3$OD): δ 7.28 (t, J=7.8 Hz, 1H, ArH), 7.20 (d, J=6.6 Hz, 1H, ArH), 7.02 (d, J=7.6 Hz, 1H, ArH), 4.33 (d, J=4.1 Hz, 1H, α-CH), 3.88-3.68 (m, 1H, H$_{2ax}$), 3.39-2.93 (m, 7H, H$_{1ax}$, H$_{1eq}$, N(CH_2CH$_2$CH$_3$)$_2$, H$_{4eq}$), 2.85-2.67 (m, 1H, H$_{4ax}$), 2.62-2.45 (m, 1H, β-CH), 2.45-2.29 (m, 1H, H$_{3eq}$), 2.06-1.70 (m, 5H, H$_{3ax}$, N(CH$_2$CH_2CH$_3$)$_2$), 1.22 (dd, J=7.1 Hz, J=3.5 Hz, 6H, γ-CH$_3$), 1.05 (t, J=7.3 Hz, 6H, N(CH$_2$CH$_2$CH_3)$_2$); ^{13}C NMR (50 MHz, CD$_3$OD): δ 167.6, 148.4, 135.3, 127.8, 127.4, 127.2, 119.8, 59.8, 58.4, 52.5, 29.9, 29.3, 23.2, 23.0, 18.5, 17.5, 17.2, 10.2; HR-MS m/z Calcd. for C$_{21}$H$_{35}$N$_2$O$_2$ 347.26931 (M+H)$^+$, found 347.26828 (M+H)$^+$.
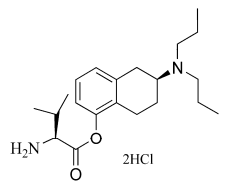
***D*-valine (S)-2-(*N,N*-di-*n*-propyl-amino)tetralin-5-yl ester 2HCl salt (2.32).** Yield: 32%. Purity: 100% (HPLC); IR (KBr, cm^{-1}) ν$_{max}$ 3418 (br), 2966, 2637, 1763, 1462, 1186; ^{1}H NMR (400 MHz, CD$_3$OD): δ 7.27 (t, J=7.9 Hz, 1H, ArH), 7.19 (d, J=7.3 Hz, 1H, ArH), 7.02 (d, J=7.7 Hz, 1H, ArH), 4.34 (d, J=4.4 Hz, 1H, α-CH), 3.84-3.71 (m, 1H, H$_{2ax}$), 3.42-2.95 (m, 7H, H$_{1ax}$, H$_{1eq}$, N(CH_2CH$_2$CH$_3$)$_2$, H$_{4eq}$), 2.82-2.67 (m, 1H, H$_{4ax}$), 2.60-2.48 (m, 1H, β-CH), 2.47-2.35 (m, 1H, H$_{3eq}$), 2.04-1.75 (m, 5H, H$_{3ax}$, N(CH$_2$CH_2CH$_3$)$_2$), 1.22 (dd, J=7.0 Hz, J=1.8 Hz, 6H, γ-CH$_3$), 1.05 (t, J=7.3 Hz, 6H, N(CH$_2$CH$_2$CH_3)$_2$); ^{13}C NMR (50 MHz, CD$_3$OD): δ 167.5, 148.4, 135.3, 127.9, 127.5, 127.2, 119.7, 59.8, 58.3, 52.6, 29.9, 29.2, 23.2, 23.0, 18.5, 17.4, 17.3, 10.2; HR-MS m/z Calcd. for C$_{21}$H$_{35}$N$_2$O$_2$ 347.26931 (M+H)$^+$, found 347.2692 (M+H)$^+$.

***L*-Isoleucine (S)-2-(*N,N*-di-*n*-propyl-amino)tetralin-5-yl ester 2HCl salt (2.33).** Yield: 89%; Purity: 100% (HPLC); IR (KBr, cm^{-1}) ν$_{max}$ 3451 {br), 2967, 2641, 1763; ^{1}H NMR (400 MHz, CD$_3$OD): δ 7.26 (t, J=7.9 Hz, 1H, ArH), 7.19 (d, J=7.3 Hz, 1H, ArH), 7.02 (d, J=7.7 Hz, 1H, ArH), 4.41 (d, J=3.7 Hz, 1H, α-CH), 3.85-3.73 (m, 1H, H$_{2ax}$), 3.42-2.96 (m, 7H, H$_{1ax}$, H$_{1eq}$, N(CH_2CH$_2$CH$_3$)$_2$, H$_{4eq}$), 2.84-2.67 (m, 1H, H$_{4ax}$), 2.48-2.38 (m, 1H, H$_{3eq}$), 2.29-2.16 (m, 1H, β-CH), 2.05-1.77 (m, 5H, H$_{3ax}$, N(CH$_2$CH_2CH$_3$)$_2$), 1.76-1.63 (m, 1H, γ-CH$_2$), 1.59-1.43 (m, 1H, γ-CH$_2$) 1.20 (d, J=7.0 Hz, 3H, β-CHCH_3), 1.09 (t, J=7.3 Hz, 3H, δ-CH$_3$), 1.05 (t, J=7.3 Hz, 6H, N(CH$_2$CH$_2$CH_3)$_2$); ^{13}C NMR (50 MHz, CD$_3$OD): δ 167.5, 147.8, 135.3, 127.9, 127.4, 127.2, 119.8, 59.8, 57.4, 52.5, 36.7, 29.2, 25.6, 23.2, 23.1, 18.4, 14.1, 11.0, 10.2; HR-MS m/z Calcd. for C$_{22}$H$_{37}$N$_2$O$_2$ 361.28496 (M+H)$^+$, found 361.28506 (M+H)$^+$.

L-Serine (R)-2-(*N,N*-di-*n*-propyl-amino)tetralin-5-yl ester 2HCl salt (2.34). Yield: 26%; Purity: 98%; ^{1}H NMR (200 MHz, CD$_3$OD): δ 7.32-7.09 (m, 2H, ArH), 7.04 (d, *J*=7.1 Hz, 1H, ArH), 4.53 (s, 1H, α-CH), 4.04 and 4.35 (AB-system, *J*$_{AB}$=9.4 Hz, 2H, CH$_2$OH), 3.87-3.68 (m, 1H, H$_{2ax}$), 3.39-2.92 (m, 7H, H$_{1ax}$, H$_{1eq}$, N(*CH$_2$*CH$_2$CH$_3$)$_2$, H$_{4eq}$), 2.87-2.58 (m, 1H, H$_{4ax}$), 2.51-2.29 (m, 1H, H$_{3eq}$), 2.07-1.68 (m, 5H, H$_{3ax}$, N(CH$_2$*CH$_2$*CH$_3$)$_2$), 1.05 (t, *J*=7.1 Hz, 6H, N(CH$_2$CH$_2$*CH$_3$)$_2$); ^{13}C NMR (50 MHz, CD$_3$OD): δ 166.6, 148.4, 135.5, 127.8, 127.6, 127.2, 119.9, 67.0, 59.9, 55.0, 53.0, 29.2, 23.2, 22.7, 18.6, 10.2.

L-Phenylalanine (S)-2-(*N,N*-di-*n*-propyl-amino)tetralin-5-yl ester 2HCl salt (2.35). Yield: 78%; Purity: 100% (HPLC); IR (KBr, cm^{-1}) ν$_{max}$ 3415 (br), 2967, 2641, 1763; ^{1}H NMR (400 MHz, CD$_3$OD):δ 7.52-7.31 (m, 5H, C$_6$H$_5$), 7.23 (t, *J*=8 Hz, 1H, ArH), 7.16 (d, *J*=7.7 Hz, 1H, ArH), 6.93 (d, *J*=7.7 Hz, 1H, ArH), 4.72 (t, *J*=7 Hz, 1H, α-CH), 3.83-3.68 (m, 1H, H$_{2ax}$), 3.55-3.34 (m, 2H, β-CH$_2$), 3.33-3.05 (m, 6H, H$_{1ax}$, H$_{1eq}$, N(*CH$_2$*CH$_2$CH$_3$)$_2$), 2.89-2.73 (m, 1H, H$_{4eq}$), 2.63-2.48 (m, 1H, H$_{4ax}$), 2.39-2.28 (m, 1H, H$_{3eq}$), 1.97-1.73 (m, 5H, H$_{3ax}$, N(CH$_2$*CH$_2$*CH$_3$)$_2$), 1.05 (t, *J*=7.3 Hz, 6H, N(CH$_2$CH$_2$*CH$_3$)$_2$); ^{13}C NMR (50 MHz, CD$_3$OD): δ 167.7, 148.3, 135.1, 134.1, 129.5, 129.1, 128.0, 127.8, 127.3, 127.1, 119.7, 59.8, 54.0, 52.5, 36.5, 29.1, 23.1, 22.6, 18.6, 10.1; HR-MS *m/z* Calcd. for C$_{25}$H$_{35}$N$_2$O$_2$ 395.26931 (M+H)$^+$, found 395.2688 (M+H)$^+$.
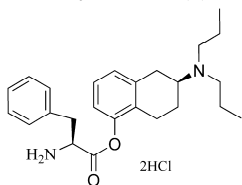
L-Lysine (S)-2-(*N,N*-di-*n*-propyl-amino)tetralin-5-yl ester 3HCl salt (2.36). Yield: 10%; Purity: 99% (HPLC); IR (KBr, cm^{-1}) ν$_{max}$ 3398 (br), 2968, 2660, 1765, 1461, 1200, 1182; ^{1}H NMR (200 MHz, CD$_3$OD):δ 7.33-7.15 (m, 2H, ArH), 7.10-6.98 (m, 1H, ArH), 4.46 (t, *J*=6.4 Hz, 1H, α-CH), 3.88-3.64 (m, 1H, H$_{2ax}$), 3.40-2.90 (m, 9H, H$_{1ax}$, H$_{1eq}$, H$_{4eq}$, ε-CH$_2$, N(*CH$_2$*CH$_2$CH$_3$)$_2$), 2.85-2.61 (m, 1H, H$_{4ax}$), 2.53-2.37 (m, 1H, H$_{3eq}$), 2.36-2.02 (m, 2H, β-CH$_2$), 2.01-1.51 (m, 9H, H$_{3ax}$, γ-CH$_2$, δ-CH$_2$, N(CH$_2$*CH$_2$*CH$_3$)$_2$), 1.05 (t, *J*=7.3 Hz, 6H, N(CH$_2$CH$_2$*CH$_3$)$_2$); ^{13}C NMR (50 MHz, CD$_3$OD): δ 148.3, 135.2, 127.8, 127.4, 127.2, 59.9, 52.9, 52.7, 52.5, 49.1, 39.1, 29.9, 26.9, 23.2, 22.9, 18.6, 10.2; HR-MS *m/z* Calcd. for C$_{22}$H$_{38}$N$_3$O$_2$ 376.2959 (M+H)$^+$, found 376.2959 (M+H)$^+$.
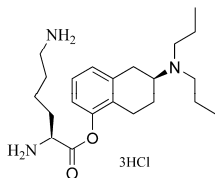
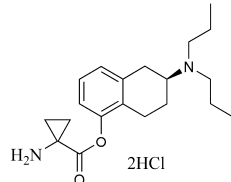**L-Proline (S)-2-(*N,N*-di-*n*-propyl-amino)tetralin-5-yl ester 2HCl salt (2.37).** Yield: 82%; Purity: 100% (HPLC); IR (KBr, cm^{-1}) ν$_{max}$ 3441 (br), 2966, 2637, 1762; ^{1}H NMR (400 MHz, CD$_3$OD): δ 7.26 (t, *J*=8 Hz, 1H, ArH), 7.19 (d, *J*=7.7 Hz, 1H, ArH), 7.07 (d, *J*=7.7 Hz, 1H, ArH), 4.80 (t, *J*=8 Hz, 1H, α-CH), 3.82-3.70 (m, 1H, H$_{2ax}$), 3.54-3.42 (m, 2H, δ-CH$_2$), 3.36-3.09 (m, 6H, H$_{1ax}$, H$_{1eq}$, N(*CH$_2$*CH$_2$CH$_3$)$_2$), 3.08-2.98 (m, 1H, H$_{4eq}$), 2.78-2.57 (m, 2H, H$_{β-CH2}$, H$_{4ax}$), 2.45-2.33 (m, 2H, H$_{\mathbf{β-CH2}}$, H$_{3eq}$), 2.24-2.12 (m, 2H, γ-CH$_2$), 2.04-1.84 (m, 1H, H$_{3ax}$), 1.83-1.75 (m, 4H, N(CH$_2$*CH$_2$*CH$_3$)$_2$), 1.05 (t, *J*=7.3 Hz, 6H, N(CH$_2$CH$_2$*CH$_3$)$_2$); ^{13}C NMR (50 MHz, CD$_3$OD): δ 167.6, 148.3, 135.1, 127.9, 127.4, 127.2, 119.8, 59.8, 59.7, 52.5, 46.1, 29.2, 28.5, 23.5, 23.1, 22.7, 18.6, 10.1; HR-MS *m/z* Calcd. for C$_{21}$H$_{33}$N$_2$O$_2$ 345.25366 (M+H)$^+$, found 345.25357 (M+H)$^+$.
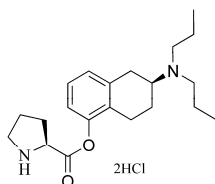
N-Methylglycine (S)-2-(*N,N*-di-*n*-propyl-amino)tetralin-5-yl ester 2HCl salt (2.38). Yield: 92%; Purity: 98% (HPLC); IR (KBr, cm^{-1}) ν$_{max}$ 3442 (br), 2951, 2649, 1771; ^{1}H NMR (400 MHz, CD$_3$OD):δ 7.25 (t, *J*=7.9 Hz 1H, ArH), 7.18 (d, *J*=7.3 Hz, 1H, ArH), 7.05 (d, *J*=7.3 Hz, 1H, ArH), 4.87 (s, 2H, α-CH$_2$), 3.83-3.70 (m, 1H, H2$_{ax}$), 3.38-2.95 (m, 7H, H$_{1ax}$, H$_{1eq}$, H$_{4eq}$, N(*CH$_2$*CH$_2$CH$_3$)$_2$), 2.84 (s, 3H, NCH$_3$), 2.78-2.63 (m, 1H, H$_{4ax}$), 2.47-2.34 (m, 1H, H$_{3eq}$), 2.03-1.74 (m, 5H, H$_{3ax}$, N(CH$_2$*CH$_2$*CH$_3$)$_2$), 1.05 (t, *J*=7.1 Hz, 6H, CH$_3$) ; ^{13}C NMR (50 MHz, CD$_3$OD): δ 165.3, 152.1, 135.2, 127.8, 127.2, 127.1, 119.9, 59.9, 52.9, 52.5, 32.5, 23.2, 22.7, 18.6, 18.4, 10.2; HR-MS *m/z* Calcd. for C$_{19}$H$_{31}$N$_2$O$_2$ 319.23801 (M+H)$^+$, found 319.23782 (M+H)$^+$.

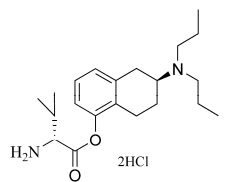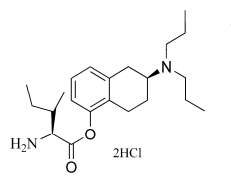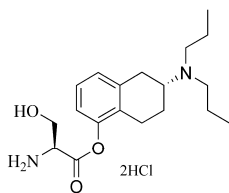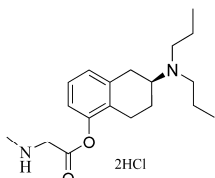**β-Alanine (S)-2-(*N,N*-di-*n*-propyl-amino)tetralin-5-yl ester 2HCl salt (2.39).** Yield: 86%; Purity: 99% (HPLC); IR (KBr, cm^{-1}) ν_{max} 3399 (br), 2968, 2653, 1753; ^{1}H NMR (400 MHz, CD$_3$OD):δ 7.23 (t, *J*=8 Hz, 1H, ArH), 7.14 (d, *J*=7.7 Hz, 1H, ArH), 7.00 (d, *J*=8.1 Hz, 1H, ArH), 3.83-3.68 (m, 1H, H$_{2ax}$), 3.38-3.11 (m, 8H, H$_{1ax}$, H$_{1eq}$, β-CH$_2$, N(CH$_2$CH$_2$CH$_3$)$_2$), 3.09 (t, *J*=6.6 Hz, 2H, α-CH$_2$), 3.05-2.91 (m, 1H, H$_{4eq}$), 2.77-2.64 (m, 1H, H$_{4ax}$), 2.44-2.31 (m, 1H, H$_{3eq}$), 2.04-1.90 (m, 1H, H$_{3ax}$), 1.89-1.70 (m, 4H, N(CH$_2$CH$_2$CH$_3$)$_2$), 1.05 (t, *J*=7.3 Hz, 6H, N(CH$_2$CH$_2$CH$_3$)$_2$); ^{13}C NMR (50 MHz, CD$_3$OD): δ 169.4, 148.8, 134.8, 127.6, 127.3, 127.0, 120.1, 59.9, 35.0, 31.0, 29.2, 23.2, 22.7, 18.6, 10.1; HR-MS *m/z* Calcd. for C$_{19}$H$_{31}$N$_2$O$_2$ 319.23801 (M+H)$^+$, found 319.23788 (M+H)$^+$.
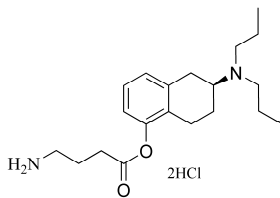
γ-Aminobutyric acid (S)-2-(*N,N*-di-*n*-propyl-amino)tetralin-5-yl ester 2HCl salt (2.40). Yield: 89%; Purity: >95% (HPLC); IR (KBr, cm^{-1}) ν_{max} 3430 (br), 2959, 2641, 1752; ^{1}H NMR (400 MHz, CD$_3$OD):δ 7.22 (t, *J*=7.7 Hz, 1H, ArH), 7.13 (d, *J*=7.7 Hz, 1H, ArH), 6.95 (d, *J*=7.7 Hz, 1H, ArH), 3.83-3.69 (m, 1H, H$_{2ax}$), 3.37-3.09 (m, 6H, H$_{1ax}$, H$_{1eq}$, N(CH$_2$CH$_2$CH$_3$)$_2$), 3.07 (t, *J*=7.7 Hz, 2H, γ-CH$_2$), 3.02-2.91 (m, 1H, H$_{4eq}$), 2.81 (t, *J*=7 Hz, 2H, α-CH$_2$), 2.74-2.60 (m, 1H, H$_{4ax}$), 2.43-2.33 (m, 1H, H$_{3eq}$), 2.07 (p, *J*=7.5 Hz, 2H, β-CH$_2$), 2.00-1.89 (m, 1H, H$_{3ax}$), 1.88-1.73 (m, 4H, N(CH$_2$CH$_2$CH$_3$)$_2$), 1.05 (t, *J*=7 Hz, 6H, N(CH$_2$CH$_2$CH$_3$)$_2$); ^{13}C NMR (50 MHz, CD$_3$OD): δ 171.2, 149.0, 134.7, 127.6, 127.1, 127.0, 120.2, 59.9, 52.5, 38.8, 30.3, 29.2, 23.3, 22.8, 22.6, 18.6, 10.1; HR-MS *m/z* Calcd. for C$_{20}$H$_{33}$N$_2$O$_2$ 333.25366 (M+H)$^+$, found 333.25357 (M+H)$^+$.
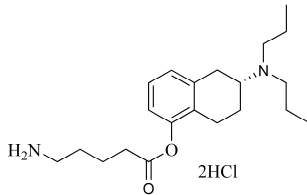
5-Aminovaleric acid (R)-2-(*N,N*-di-*n*-propyl-amino)tetralin-5-yl ester 2HCl salt (2.41). Yield: 85%; Purity: 96% (HPLC); IR (KBr, cm^{-1}) ν_{max} 3428 (br), 2929, 2634, 1751, 1463, 1137; ^{1}H NMR (400 MHz, CD$_3$OD):δ 7.21 (t, *J*=7.7 Hz, 1H, ArH), 7.12 (d, *J*=7.3 Hz, 1H, ArH), 6.93 (d, *J*=7.7 Hz, 1H, ArH), 3.80-3.68 (m, 1H, H$_{2ax}$), 3.37-3.05 (m, 6H, H$_{1ax}$, H$_{1eq}$, N(CH$_2$CH$_2$CH$_3$)$_2$), 3.04-2.87 (m, 3H, H$_{4eq}$, δ-CH$_2$), 2.78-2.60 (m, 3H, H$_{4ax}$, α-CH$_2$), 2.44-2.32 (m, 1H, H$_{3eq}$), 2.00-1.70 (m, 9H, H$_{3ax}$, β-CH$_2$, γ-CH$_2$, N(CH$_2$CH$_2$CH$_3$)$_2$), 1.05 (t, *J*=7.1 Hz, 6H, N(CH$_2$CH$_2$CH$_3$)$_2$); ^{13}C NMR (50 MHz, CD$_3$OD): δ 171.8, 149.1, 134.7, 127.6, 127.0, 120.2, 60.0, 39.3, 32.9, 29.2, 26.8, 23.3, 22.8, 21.6, 18.6, 18.4, 10.2; HR-MS *m/z* Calcd. for C$_{21}$H$_{35}$N$_2$O$_2$ 347.26931 (M+H)$^+$, found 347.26932 (M+H)$^+$.

2.4.7 *N-tert*-Boc-*L*-serine (R)-2-(*N,N*-di-*n*-propyl-amino)tetralin-5-yl ester (2.42). To a solution of **2.19** (75 mg, 0.14 mmol) in 7 mL absolute EtOH was added Pd-C 10% (30 mg). The suspension was shaken under H$_2$ (3 bar) atmosphere at 45 ^{o}C for 4 hours. The black suspension was filtered and evaporated *in vacuo*. The resultant light yellow oil was purified by column chromatography (CH$_2$Cl$_2$/MeOH = 20 : 1) to afford **2.42** (29 mg, 47%) as a colourless oil. IR (KBr, cm^{-1}) ν_{max} 3348 (br), 2973, 2640, 1772, 1709, 1459, 1154; HR-MS *m/z* Calcd. for C$_{39}$H$_{24}$N$_2$O$_5$ 435.2854 (M+H)$^+$, found 435.2851 (M+H)$^+$.
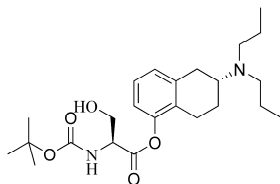
2.4.8 *L*-Arginine (S)-2-(*N,N*-di-*n*-propyl-amino)tetralin-5-yl ester 4HCl salt (2.43). The *N*-benzyloxy protected *L*-arginine ester **2.22** (0.23 g, 0.28 mmol) was dissolved in a mixture of dry MeOH (30 mL) and 2N HCl in dry MeOH (5 mL) under N$_2$ atmosphere. Pd-C 10% (50 mg) was added and the mixture was stirred vigorously for 1.5 hours under H$_2$ (1 bar) atmosphere at r.t. until gas formation ceased. The black suspension was filtered and the colourless solution was cooled to 0 ^{o}C in ice and precipitated with dry Et$_2$O to obtain white solid material. The solvent
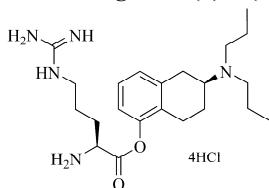
was removed and the white solid material was dried *in vacuo* to afford the tetrahydrochloric acid salt of compound **2.43** (0.12 g, 79%) as a hygroscopic white powder. Purity: 99% (HPLC); IR (KBr, cm^{-1}) ν_{max} 3411, 3171, 2951, 1762, 1667; ^{1}H NMR (300 MHz, CD$_3$OD): δ 7.34-7.11 (m, 2H, ArH), 7.06 (d, *J*=7.3 Hz, 1H, ArH), 4.55-4.42 (m, 1H, α-CH), 3.89-3.67 (m, 1H, H$_{2ax}$), 3.44-2.91 (m, 9H, H$_{1ax}$, H$_{1eq}$, δ-CH$_2$, N(*CH$_2$*CH$_2$CH$_3$)$_2$), H$_{4eq}$), 2.87-2.63 (m, 1H, H$_{4ax}$), 2.54-2.37 (m, 1H, β-CH), 2.36-2.08 (m, 2H, H$_{3eq}$, β-CH), 2.07-2.65 (m, 7H, H$_{3ax}$, N(CH$_2$*CH$_2$*CH$_3$)$_2$), γ-CH$_2$), 1.05 (t, *J*=6.4 Hz, 6H, N(CH$_2$CH$_2$*CH$_3$)$_2$); ^{13}C NMR (50 MHz, CD$_3$OD): δ 172.8, 157.5, 136.5, 135.2, 127.9, 127.3, 127.2, 119.9, 59.9, 52.6, 50.3, 47.5, 40.6, 23.3, 23.0, 18.7, 18.5, 10.2; HR-MS *m/z* Calcd. for C$_{22}$H$_{38}$N$_5$O$_2$ 404.302 (M+H)$^+$, found 404.30206 (M+H)$^+$; Anal. Calcd for C$_{22}$H$_{41}$N$_5$O$_2$Cl$_4$: C, 48.10; H, 7.52; N, 12.75. Found: C, 48.37; H, 7.72; N, 12.91.

2.4.9 *N,N*-Dimethylglycine (R)-2-(*N,N*-di-*n*-propyl-amino)tetralin-5-yl ester 2HCl salt (2.44).
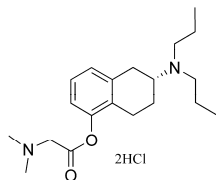
Dimethylglycine.HCl (0.63 g, 4.5 mmol) and DMAP (1.08 g, 8.9 mmol) were suspended in 10 mL anhydrous CH$_2$Cl$_2$ under nitrogen atmosphere and cooled to 0 ^{o}C. EDC (0.86 mL, 4.9 mmol) was added and the reaction mixture was stirred for 15 minutes. 5-OH-DPAT (1.0 g, 4.0 mmol) in 3 mL anhydrous CH$_2$Cl$_2$ was slowly added to the cloudy suspension. The clear light orange solution was allowed to attain room temperature and was stirred for 2 hours until the reaction was complete. CH$_2$Cl$_2$ (50 mL) was added and the reaction mixture was washed with H$_2$O (3 x 10 mL) and brine (10 mL).
The organic layer was dried over Na$_2$SO$_4$ and evaporated *in vacuo*; the resultant light pink-orange solid material was purified by column chromatography (CH$_2$Cl$_2$/MeOH = 10:1) to afford the free amine of compound **2.44** as a colourless oil (0.97 g). The free amine was dissolved in 3 mL 2N HCl in dry MeOH and cooled to 0 ^{o}C in ice under N$_2$. The hydrochloride salt was precipitated as white solid material with dry Et$_2$O. The solvent was removed and the salt was reprecipitated from dry MeOH with dry Et$_2$O. The solvent was removed and the precipitate was evaporated *in vacuo* to afford **3m** as a hygroscopic white powder (0.14 g, 57%). Purity: 100% (HPLC); IR (KBr, cm^{-1}) ν_{max} 3424 (br), 2935, 2482, 2368, 1768, 1461, 1365, 1205; ^{1}H NMR (200 MHz, CD$_3$OD):δ 7.26 (t, *J*=7.6 Hz 1H, ArH), 7.19 (d, *J*=6.5 Hz, 1H, ArH), 7.09 (d, *J*=7.4 Hz, 1H, ArH), 4.57 (s, 2H, α-CH$_2$), 3.86-3.67 (m, 1H, H2$_{ax}$), 3.39-2.95 (m, 7H, H$_{1ax}$, H$_{1eq}$, H$_{4eq}$, N(*CH$_2$*CH$_2$CH$_3$)$_2$), 3.06 (s, 6H, N(CH$_3$)$_2$), 2.83-2.63 (m, 1H, H$_{4ax}$), 2.51-2.34 (m, 1H, H$_{3eq}$), 2.03-1.74 (m, 5H, H$_{3ax}$, N(CH$_2$*CH$_2$*CH$_3$)$_2$), 1.05 (t, *J*=7.2 Hz, 6H, CH$_3$); ^{13}C NMR (50 MHz, CD$_3$OD): δ 164.9, 148.2, 135.2, 127.9, 127.5, 127.2, 119.9, 59.9, 56.7, 52.7, 43.5, 29.2, 23.2, 22.8, 18.5, 10.2; HR-MS *m/z* Calcd. for C$_{20}$H$_{33}$N$_2$O$_2$ 333.25366 (M+1)$^+$, found 333.25345 (M+1)$^+$..

2.4.10 *N*-2-Chlorocarbonylmethyl-*N,N,N*-trimethylammoniumchloride (2.45).
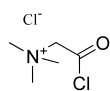
Oven-dried *N,N,N*-trimethylglycine.HCl (6.2 g, 40 mmol) was suspended in SOCl$_2$ (7.9 mL, 109 mmol) under nitrogen atmosphere. The suspension was stirred vigorously and heated at 70 ^{o}C for 2 hours until gas formation ceased. The yellow solution was evaporated *in vacuo* and the resultant yellow-white solid material was washed with dry CH$_2$Cl$_2$. After filtration and drying *in vacuo*, compound **2.45** was afforded as a white solid material (5.8 g, 82%). IR (KBr, cm^{-1}) ν_{max} 2830, 2480, 1742, 1179. ^{1}H NMR (400 MHz, *d$_6$*-DMSO): δ 4.47 (s, 2H, α-CH$_2$), 3.26 (s, 9H, N(CH$_3$)$_3$$^+$).

2.4.11 *N,N,N*-Trimethylglycine (R)-2-(*N,N*-di-*n*-propyl-amino)tetralin-5-yl ester Cl.HCl salt (2.46).

(R)-5-OH-DPAT (135 mg, 0.54 mmol) was dissolved in 1 mL dry CH$_2$Cl$_2$ under a nitrogen atmosphere. The solution was cooled in ice to 0 ^{o}C and pyridine (176 μL, 2.2 mmol) was added. A suspension of the betaïne acid chloride **2.45** (476 mg, 2.7 mmol) in 1.5 mL dry CH$_2$Cl$_2$ was dropwise added and the reaction mixture was stirred for 30 minutes. After filtration the solution was evaporated *in vacuo* and gave an orange-brown oil. The crude product was purified by column chromatography (CH$_2$Cl$_2$/MeOH, gradient = 4:1 to 2:1) to afford the chloride-hydrochloride salt **2.46** as a white hygroscopic powder (169 mg, 74%). Purity: 100% (HPLC); IR (KBr, cm^{-1}) ν_{max} 3436 (br), 2967, 2640, 1764, 1460, 1179; ^{1}H NMR (400 MHz, CD$_3$OD):δ 7.26 (t, *J*=7.7 Hz, 1H, ArH), 7.20 (d, *J*=7.7 Hz, 1H, ArH), 7.11 (d, *J*=7.7 Hz, 1H, ArH), 4.92 (d, *J*=1.8 Hz,

2H, α-CH$_2$), 3.82-3.70 (m, 1H, H$_{2ax}$), 3.45 (s, 9H, N(CH$_3$)$_3$$^+$), 3.40-3.10 (m, 6H, H$_{1ax}$, H$_{1eq}$, N(*CH$_2$*CH$_2CH_3$)$_2$), 3.09-2.98 (m, 1H, H$_{4eq}$), 2.80-2.67 (m, 1H, H$_{4ax}$), 2.49-2.37 (m, 1H, H$_{3eq}$), 2.04-1.92 (m, 1H, H$_{3ax}$), 1.91-1.75 (m, 4H, N(CH$_2$*CH$_2$*CH$_3$)$_2$), 1.05 (t, *J*=7.3 Hz, 6H, N(CH$_2$CH$_2$*CH$_3$*)$_2$); ^{13}C NMR (50 MHz, CD$_3$OD): δ 163.6, 147.9, 135.3, 127.9, 127.5, 127.2, 119.9, 62.8, 59.8, 53.5, 52.5, 29.2, 23.1, 22.8, 18.4, 10.2; HR-MS *m/z* Calcd. for C$_{21}$H$_{35}$N$_2$O$_2$ 347.2693 (M)$^+$, found 347.2692 (M)$^+$.
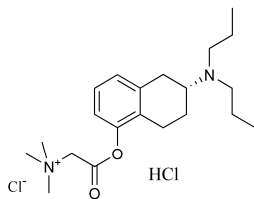
2.5 ACKNOWLEDGMENTS.

2.6 REFERENCES

1.   Hacksell, U.; Svensson, U.; Nilsson, J. L. G.; Hjorth, S.; Carlsson, A.; Wikstrom, H.; Lindberg, P.; Sanchez, D. N-Alkylated 2-Aminotetralins - Central Dopamine-Receptor Stimulating Activity. *J. Med. Chem.* **1979**, *22,* 1469-1475.

2.   McDermed, J. D.; McKenzie, G. M.; Freeman, H. S. Synthesis and Dopaminergic Activity of (+/-)-1,2,3,4-Tetrahydronaphthalene, (+)-1,2,3,4-Tetrahydronaphthalene, and (-)-2-Dipropylamino-5-Hydroxy-1,2,3,4-Tetrahydronaphthalene. *J. Med. Chem.* **1976**, *19,* 547-549.

3.   vanVliet, L. A.; Tepper, P. G.; Dijkstra, D.; Damsma, G.; Wikstrom, H.; Pugsley, T. A.; Akunne, H. C.; Heffner, T. G.; Glase, S. A.; Wise, L. D. Affinity for dopamine D-2, D-3, and D-4 receptors of 2-aminotetralins. Relevance of D-2 agonist binding for determination of receptor subtype selectivity. *J. Med. Chem.* **1996**, *39,* 4233-4237.

4.   Wikstrom, H.; Andersson, B.; Sanchez, D.; Lindberg, P.; Arvidsson, L. E.; Johansson, A. M.; Nilsson, J. L. G.; Svensson, K.; Hjorth, S.; Carlsson, A. Resolved Monophenolic 2-Aminotetralins and 1,2,3,4,4A,5,6,10B-Octahydrobenzo[F]Quinolines - Structural and Stereochemical Considerations for Centrally Acting Presynaptic and Postsynaptic Dopamine-Receptor Agonists. *J. Med. Chem.* **1985**, *28,* 215-225.

5.   van der Geest, R.; Danhof, M.; Bodde, H. E. Iontophoretic delivery of apomorphine I: In vitro optimization and validation. *Pharm. Res.* **1997**, *14,* 1798-1803.

6.   Luzardo-Alvarez, A.; Delgado-Charro, M. B.; Blanco-Mendez, J. Iontophoretic delivery of ropinirole hydrochloride: effect of current density and vehicle formulation. *Pharm. Res.* **2001**, *18,* 1714-20.

7.   Nugroho, A. K.; Li, G. L.; Grossklaus, A.; Danhof, M.; Bouwstra, J. A. Transdermal iontophoresis of rotigotine: influence of concentration, temperature and current density in human skin in vitro. *J. Controlled Release* **2004**, *96,* 159-167.

8.   Nugroho, A. K.; Li, G. L.; Danhof, M.; Bouwstra, J. A. Transdermal iontophoresis of rotigotine across human stratum corneum in vitro: Influence of pH and NaCl concentration. *Pharm. Res.* **2004**, *21,* 844-850.

9.   Nugroho, A. K.; Li, L.; Dijkstra, D.; Wikstrom, H.; Danhof, M.; Bouwstra, J. A. Transdermal iontophoresis of the dopamine agonist 5-OH-DPAT in human skin in vitro. *J. Controlled Release* **2005**, *103,* 393-403.

10.   Nugroho, A. K.; Romeijn, S. G.; Zwier, R.; De Vries, J. B.; Dijkstra, D.; Wikstrom, H.; la-Pasqua, O.; Danhof, M.; Bouwstra, J. A. Pharmacokinetics and pharmacodynamics analysis of transdermal iontophoresis of 5-OH-DPAT in rats: In vitro-in vivo correlation. *J. Pharm. Sci.* **2006**, *95,* 1570-1585.

11.   Luzardo-Alvarez, A.; Delgado-Charro, M. B.; Blanco-Mendez, J. In vivo iontophoretic administration of ropinirole hydrochloride. *J. Pharm. Sci.* **2003**, *92,* 2441-8.

12. van der Geest, R.; van Laar, T.; Gubbens-Stibbe, J. M.; Bodde, H. E.; Danhof, M. Iontophoretic delivery of apomorphine II: An in vivo study in patients with Parkinson's disease. *Pharm. Res.* **1997**, *14,* 1804-1810.

13. Sung, K. C.; Fang, J. Y.; Hu, O. Y. P. Delivery of nalbuphine and its prodrugs across skin by passive diffusion and iontophoresis. *J. Controlled Release* **2000**, *67,* 1-8.

14. Yoshida, N. H.; Roberts, M. S. Structure Transport Relationships in Transdermal Iontophoresis. *Adv. Drug Delivery Rev.* **1992**, *9,* 239-264.

15. Rautio, J.; Kumpulainen, H.; Heimbach, T.; Oliyai, R.; Oh, D.; Jarvinen, T.; Savolainen, J. Prodrugs: design and clinical applications. *Nat. Rev. Drug Discov.* **2008**, *7,* 255-70.

16. Abla, N.; Naik, A.; Guy, R. H.; Kalia, Y. N. Topical iontophoresis of valaciclovir hydrochloride improves cutaneous aciclovir delivery. *Pharm. Res.* **2006**, *23,* 1842-1849.

17. Laneri, S.; Sacchi, A.; di Frassello, E. A.; Luraschi, E.; Colombo, P.; Santi, P. Ionized prodrugs of dehydroepiandrosterone for transdermal iontophoretic delivery. *Pharm. Res.* **1999**, *16,* 1818-1824.

18. Prausnitz, M. R.; Mitragotri, S.; Langer, R. Current status and future potential of transdermal drug delivery. *Nat. Rev. Drug Discov.* **2004**, *3,* 115-124.

19. Anigbogu, A.; Patil, S.; Singh, P.; Liu, P.; Dinh, S.; Maibach, H. An in vivo investigation of the rabbit skin responses to transdermal iontophoresis. *Int. J. Pharm.* **2000**, *200,* 195-206.

20. Di Stefano, A.; Sozio, P.; Cerasa, L. S. Antiparkinson Prodrugs. *Molecules* **2008**, *13,* 46-68.

21. Bundgaard, H. *Design of prodrugs;* Elsevier: Amsterdam etc., 1985; , pp VII, 360.

22. Roche, E. B. *Bioreversible carriers in drug design : theory and applications;* Pergamon Press: New York etc., 1987; , pp VIII, 292.

23. Aggarwal, S. K.; Gogu, S. R.; Rangan, S. R. S.; Agrawal, K. C. Synthesis and Biological Evaluation of Prodrugs of Zidovudine. *J. Med. Chem.* **1990**, *33,* 1505-1510.

24. Bender, D. M.; Peterson, J. A.; McCarthy, J. R.; Gunaydin, H.; Takano, Y.; Houk, K. N. Cyclopropanecarboxylic acid esters as potential prodrugs with enhanced hydrolytic stability. *Org. Lett.* **2008**, *10,* 509-511.

25. Bundgaard, H.; Larsen, C.; Thorbek, P. Prodrugs as Drug Delivery Systems .26. Preparation and Enzymatic-Hydrolysis of Various Water-Soluble Amino-Acid Esters of Metronidazole. *Int. J. Pharm.* **1984**, *18,* 67-77.

26. Landowski, C. P.; Song, X. Q.; Lorenzi, P. L.; Hilfinger, J. M.; Amidon, G. L. Floxuridine amino acid ester prodrugs: Enhancing Caco-2 permeability and resistance to glycosidic bond metabolism. *Pharm. Res.* **2005**, *22,* 1510-1518.

27. Song, X.; Lorenzi, P. L.; Landowski, C. P.; Vig, B. S.; Hilfinger, J. M.; Amidon, G. L. Amino acid ester prodrugs of the anticancer agent gemcitabine: synthesis, bioconversion, metabolic bioevasion, and hPEPT1-mediated transport. *Mol. Pharmaceutics* **2005**, *2,* 157-167.

28. Takata, J.; Karube, Y.; Nagata, Y.; Matsushima, Y. Prodrugs of Vitamin-e .1. Preparation and Enzymatic-Hydrolysis of Aminoalkanecarboxylic Acid-Esters of D-Alpha-Tocopherol. *J. Pharm. Sci.* **1995**, *84,* 96-100.

29. Vig, B. S.; Lorenzi, P. J.; Mittal, S.; Landowski, C. P.; Shin, H. C.; Mosberg, H. I.; Hilfinger, J. M.; Amidon, G. L. Amino acid ester prodrugs of floxuridine: Synthesis and effects of structure, stereochemistry, and site of esterification on the rate of hydrolysis. *Pharm. Res.* **2003**, *20,* 1381-1388.

30. Colla, L.; De Clercq, E.; Busson, R.; Vanderhaeghe, H. Synthesis and antiviral activity of water-soluble esters of acyclovir [9-[(2-hydroxyethoxy)methyl]guanine]. *J. Med. Chem.* **1983**, *26,* 602-4.

31. Altomare, C.; Trapani, G.; Latrofa, A.; Serra, M.; Sanna, E.; Biggio, G.; Liso, G. Highly water-soluble derivatives of the anesthetic agent propofol: in vitro and in vivo evaluation of cyclic amino acid esters. *Eur. J. Pharm. Sci.* **2003**, *20,* 17-26.

32. Anderson, A.; Belelli, D.; Bennett, D. J.; Buchanan, K. I.; Casula, A.; Cooke, A.; Feilden, H.; Gemmell, D. K.; Hamilton, N. M.; Hutchinson, E. J.; Lambert, J. J.; Maidment, M. S.; McGuire, R.; McPhail, P.; Miller, S.; Muntoni, A.; Peters, J. A.; Sansbury, F. H.; Stevenson, D.; Sundaram, H. Alpha-amino acid phenolic ester derivatives: novel water-soluble general anesthetic agents which allosterically modulate GABA(A) receptors. *J. Med. Chem.* **2001**, *44,* 3582-91.

33.   Kovach, I. M.; Pitman, I. H.; Higuchi, T. Amino acid esters of phenols as prodrugs: synthesis and stability of glycine, beta-aspartic acid, and alpha-aspartic acid esters of p-acetamidophenol. *J. Pharm. Sci.* **1981**, *70,* 881-5.

34.   Mahfouz, N. M.; Hassan, M. A. Synthesis, chemical and enzymatic hydrolysis, and bioavailability evaluation in rabbits of metronidazole amino acid ester prodrugs with enhanced water solubility. *J. Pharm. Pharmacol.* **2001**, *53,* 841-848.

35.   Copinga, S.; Tepper, P. G.; Grol, C. J.; Horn, A. S.; Dubocovich, M. L. 2-Amido-8-Methoxytetralins - A Series of Nonindolic Melatonin-Like Agents. *J. Med. Chem.* **1993**, *36,* 2891-2898.

36.   Karlsson, A.; Bjork, L.; Pettersson, C.; Anden, N. E.; Hacksell, U. (R)-5-Hydroxy-2-(Dipropylamino)Tetralin and (S)-5-Hydroxy-2-(Dipropylamino)Tetralin (5-Oh Dpat) - Assessment of Optical Purities and Dopaminergic Activities. *Chirality* **1990**, *2,* 90-95.

37.   Matta, M. S.; Andracki, M. E. Rate-Controlling Step of Oxazolinone Formation - Secondary and Solvent Kinetic Isotope Effects. *J. Am. Chem. Soc.* **1985**, *107,* 6036-6039.

38.   Jetten, M.; Peters, C. A. M.; Vannispen, J. W. F. M.; Ottenheijm, H. C. J. A One-Pot N-Protection of L-Arginine. *Tetrahedron Lett.* **1991**, *32,* 6025-6028.

39.   Linch, A. L. US2359863, 1944.

40.   Marder, O.; Albericio, F. Industrial application of coupling reagents in peptides. *Chim. Oggi* **2003**, *21,* 35-40.

41.   Gangarosa, L. P.; Park, N. H.; Fong, B. C.; Scott, D. F.; Hill, J. M. Conductivity of drugs used for iontophoresis. *J. Pharm. Sci.* **1978**, *67,* 1439-43.

42.   Berge, S. M.; Bighley, L. D.; Monkhouse, D. C. Pharmaceutical Salts. *J. Pharm. Sci.* **1977**, *66,* 1-19.

43.   Gould, P. L. Salt Selection for Basic Drugs. *Int. J. Pharm.* **1986**, *33,* 201-217.

44.   Quintanilla-Licea, R.; Colunga-Valladares, J. F.; Caballero-Quintero, A.; Rodríguez-Padilla, C.; Tamez-Guerra, R.; Gómez-Flores, R.; Waksman, N. NMR Detection of Isomers Arising from Restricted Rotation of the C-N Amide Bond of N-Formyl-o-toluidine and N,N'-bis-Formyl-o-tolidine. *Molecules* **2002**, *7,* 662-673; 662.

45.   Lai, P. M.; Roberts, M. S. An analysis of solute structure-human epidermal transport relationships in epidermal iontophoresis using the ionic mobility: pore model. *J. Controlled Release* **1999**, *58,* 323-33.

46.   Abla, N.; Naik, A.; Guy, R. H.; Kalia, Y. N. Effect of charge and molecular weight on transdermal peptide delivery by iontophoresis. *Pharm. Res.* **2005**, *22,* 2069-78.

47.   Phipps, J. B.; Padmanabhan, R. V.; Lattin, G. A. Iontophoretic delivery of model inorganic and drug ions. *J. Pharm. Sci.* **1989**, *78,* 365-9.

3

Chemical stability and enzymatic hydrolysis of a series of amino acid ester prodrugs of the dopamine D_2 agonist 5-OH-DPAT

Abstract

The ratio between chemical (in vitro) and enzymatic (in vivo) stability determines the suitability of prodrugs for iontophoresis and other routes of administration. To select 5-OH-DPAT prodrugs for transdermal iontophoretic delivery based on optimal in vitro/in vivo ratios, the hydrolysis rates were determined in the donor phase of the iontophoretic device and in human blood plasma. Chemical stability studies in citrate buffer at pH 5 indicated that the L-valine and β-alanine prodrugs of (S)-5-OH-DPAT showed sufficient stability in vitro. Enzymatic stability studies in 80% human blood plasma indicated that these prodrugs are rapidly converted to the parent drug in vivo. In conlusion, L-valine and β-alanine prodrugs of 5-OH-DPAT may meet the requisites for improved transport across the skin by iontophoresis.

3.1. INTRODUCTION

Iontophoretic delivery has attracted attention because it represents a localized, non-invasive, convenient and rapid method to deliver water soluble, ionized medication into the skin. Iontophoretic drug delivery avoids the hepatic first-pass metabolism. In addition, it also reduces the chance of fluctuating plasma levels by providing programmed delivery of the drug. It also provides a rapid way to terminate the delivery by turning off the current.[1] Because of the many advantages there is growing interest in iontophoretic drug delivery.

Besides the applied electrical current strength, drug concentration is one of the most important factors affecting the iontophoretic process. High aqueous solubility of drugs or prodrugs is therefore favourable for iontophoresis. Effects of concentration have been studied for a number of drugs e.g. metoprolol and the dopamine (DA) agonists 5-OH DPAT and rotigotine.[2-4] All these drugs showed with an increase in concentration a proportional increase in flux. The pH of the donor compartment is also an important factor in iontophoretic drug delivery. The optimum pH for iontophoretic delivery of a compound is one where it exist predominantly in its ionized form.[5] However, the pH and more specifically the ion competition between the hydrogen ion and the drug ion to carry the current, also influences the iontophoretic flux. The optimum acidity in the donor phase for the transdermal iontophoretic delivery of 5-OH-DPAT was determined pH 5.[3]

Hydroxylated 2-aminotetralins exhibited low oral bioavailability in rats and humans. One of the primary reasons for this low bioavailability is probably an extensive first-pass metabolism. Various prodrug strategies have been employed to improve the oral absorption or passive transdermal administration of hydroxylated 2-aminotetralins by esterification with aliphatic and aromatic moieties.[6, 7] To overcome absorption barriers, prodrugs can also be designed by coupling e.g. amino acids to the phenol moiety. Because of the presence of high esterase activity these ester prodrugs will be cleaved to regenerate the parent

compound in the blood.[8] Amino acid prodrugs offer an additional advantage by producing non-toxic by-products *in vivo* during their bioactivation.[9]

Esterases, hydrolases which split ester bonds, hydrolyse a number of compounds used as drugs in humans and are important for the bioactivation of prodrugs. Cholinesterases are primarily involved in drug hydrolysis in plasma, and arylesterases in the plasma and red blood cells.[10] The low barrier H-bond between the amino acids Glu_{336} and His_{450} facilitates nucleophilic attack by the β-OH group of Ser_{203} on the carbonyl group of the substrate by carboxylesterases.[11] Apart from the blood, prodrugs can also be activated by esterases present within the skin.[12]

Human serum albumin (HSA) is an abundant plasma protein with ascribed ligand-binding and transport properties, and enzymatic activities. These enzymatic properties could benefit the release of parent drugs from its prodrug form. Although the enzymatic activity of a single HSA molecule is low, the concentration of this protein in the circulation is very high. Therefore this kind of prodrug activation is believed to be clinically relevant.[13] The activity of HSA on ester hydrolysis depends on the substrate, e.g. the prodrug isosorbide diaspirinate is hydrolyzed relatively slow by HSA compared to hydrolysis in human blood plasma (HBP).[14] Hydrolysis of a substrate by HSA occurs probably by acylation due to nucleophilic attack by Tyr_{411} or Lys_{199}, followed by hydrolysis.[15, 16] It is of interest to examine the contribution of HSA to enzymatic hydrolysis of 5-OH-DPAT prodrugs in HBP.

The ratio between chemical and enzymatic stability, i.e. the *in vitro*/*in vivo* stability ratio of prodrugs, determines their suitability for administration and is preferably around 10^6.[17] In this chapter the chemical and enzymatic stabilities of a series of amino acid ester prodrugs introduced in chapter 2 are evaluated. The chemical stability was tested under the same conditions used for *in vitro* and *in vivo* studies.[3, 18] That is, the chemical hydrolysis of the prodrugs was followed in citrate buffer pH 5 which is the acidity of the donor phase of the utilized iontophoretic system. To guarantee the rapid hydrolysis of 5-OH-DPAT ester prodrugs in blood after skin absorption, the enzymatic stability was determined in human blood plasma.

3.2 RESULTS

3.2.1 Influence of the prodrug concentration on hydrolysis half-life

The chemical hydrolysis of the 5-OH-DPAT prodrugs was studied in citrate buffer pH 5 (5mM) at 32 °C, representing the mean skin temperature. This particular buffer was chosen because of its optimal properties for iontophoretic experiments with 5-OH-DPAT *in vitro* as well as *in vivo*.[3, 18] At appropriate intervals samples were withdrawn and the observed first-order hydrolysis rate constants of the 5-OH-DPAT prodrugs were determined by

plotting the logarithm of the remaining prodrug concentration as a function of time. The first experiments with the newly synthesized prodrugs were conducted at a prodrug concentration of 0.31 mM (compounds **2.29**, **2.35**, **2.37**, **2.38**, **2.40**, **2.43** and **2.44**). Because of limited availability of the parent drug 5-OH-DPAT, we determined the optimal prodrug concentration. The glycine prodrug **2.28**, as representative for all 5-OH-DPAT prodrugs described in this chapter, was studied at concentrations of 0.05, 0.25 and 0.31 mM (Table 3.1). The estimated half-life of **2.28** at all three prodrug concentrations was around 20 hours and statistically not different. Similar results were shown for experiments with the *L*-valine prodrug **2.31** (data not shown). Based on these results the next stability experiments were conducted at a concentration of 0.05 mM (compounds **2.30-2.34**, **2.36**, **2.39**, **2.41** and **2.46**).

Table 3.1 Effect of concentration (n=3) on mean half-lives (± SEM) during hydrolysis of the glycine ester of 5-OH-DPAT (2.28) in 0.005 M citrate buffer (pH 5)

Prodrug Concentration (mM)	Estimated $t_{1/2}$ ± SEM (hours)
0.05	20.3±0.13
0.25	20.9±0.72
0.31	20.9±0.37

3.2.2 Non-enzymatic hydrolysis in citrate buffer

We have divided the prodrugs in five groups based on the side chain of the pro-moieties: prodrugs with bulky side chains, prodrugs with weakly basic side chains, prodrugs with alkylated α-amino groups, a homologous series and prodrugs with an alcoholic or aromatic side chain. The hydrolysis profiles of the 5-OH-DPAT prodrugs in citrate buffer pH 5 are plotted in Figure 3.1 and are based on the estimated half-lives presented in Table 3.2. The decrease in 5-OH-DPAT ester concentration was quantitatively accompanied by corresponding increase in 5-OH-DPAT concentration (data not shown).

A) Influence of bulky side chains on the chemical hydrolysis of 5-OH-DPAT prodrugs. The pseudo first-order hydrolysis rate plots for the chemical hydrolysis of prodrugs **2.28**-**2.33** are shown in Figure 3.1 A. This group of prodrugs consists of esterified amino acids which contain closely related aliphatic substituents in the side chain. The 1-aminocyclopropanecarboxylic acid prodrug **2.30** was chemically the most stable prodrug with a half-life of 150 hours. The glycine (**2.28**) and *L*-alanine (**2.29**) esters of 5-OH-DPAT were the least stable with half-lives of 21 and 16 hours, respectively. The *L*- and *D*-valine prodrugs **2.31** and **2.32** with comparable half-lives of 53 en 49 hours, respectively, were more stable than prodrug **2.28**. The *L*-isoleucine 5-OH-DPAT ester (**2.33**) was fairly stable with a half-life of 73 hours. Pairwise multiple comparisons of the half-lives of compounds **2.28-2.33** showed that the mean half-lives differed significantly ($p < 0.005$). Two exceptional cases were the glycine prodrug **2.28** versus the *L*-alanine prodrug **2.29** and the

diasteromeric pair: the *L*-valine prodrug **2.31** versus the *D*-valine prodrug **2.32**. The half-lives of these pairs did not differ significantly and thus showed similar chemical stability under the slight acidic conditions.
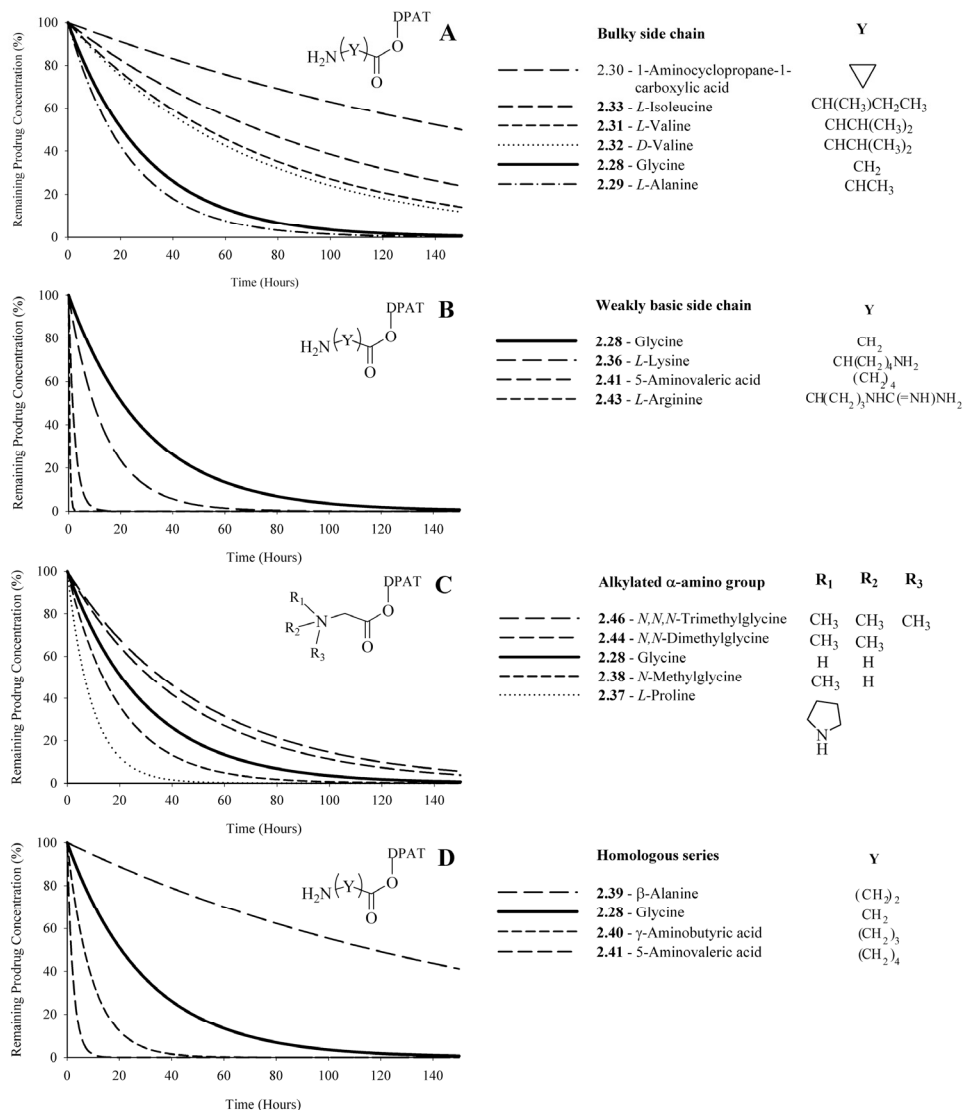
Figure 3.1 Pseudo first-order hydrolysis rate plots of 5-OH-DPAT prodrugs in citrate buffer pH 5 at 32°C, based on the estimated half-lives presented in Table 3.2. The prodrugs are listed per group in sequence of descending half-life. A) prodrugs with a bulky side chain; B) prodrugs with a weakly basic side chain; C) prodrugs with an alkylated α-amino group; D) homologous series.

B) Influence of a weakly basic side chain on the chemical hydrolysis of 5-OH-DPAT prodrugs. Figure 3.1 B shows the pseudo first-order hydrolysis rate plots of the glycine

(**2.28**), *L*-lysine (**2.36**), *L*-arginine (**2.43**) and 5-aminovaleric acid (**2.41**) prodrugs. This group of prodrugs contains weakly basic amino groups in the side chain. The half-lives of **2.36**, **2.41** and **2.43** were compared pairwise to each other and showed statistical significant differences ($p < 0.05$). The half-lives found for the prodrugs **2.36** and **2.43** were 10 and 0.3 hours, respectively, and prodrug **2.41** exhibited a half-life of 1.6 hours.

Table 3.2 Estimated half-lives (t1/2) of prodrugs 2.28-2.41, 2.43, 2.44 and 2.46 during hydrolysis in 5 mM citrate buffer, pH 5 at 32 ºC (n=3, exceptions are 2.28 (n=9), 2.30-2.33 and 2.39 (n=6).

Compound	5-OH-DPAT ester	Estimated $t_{1/2} \pm$ SEM (Hours) 5 mM Citrate Buffer (pH 5)	$t_{1/2}$ ratio prodrug compared to prodrug 2.28
A	**Bulky Side Chain**		
2.28	Glycine	20.7±0.3[a]	1
2.29	*L*-Alanine	16.2±0.3[a]	0.8
2.30	1-Aminocyclopropane-1-carboxylic acid	149.7±3.2	7.7
2.31	*L*-Valine	53.1±1.6[b]	2.6
2.32	*D*-Valine	48.7±6.9[b]	2.4
2.33	*L*-Isoleucine	72.7±2.8	3.5
B	**Basic Side Chain**		
2.36	*L*-Lysine	9.6±0.2	0.5
2.43	*L*-Arginine	0.3±0.004	0.01
C	**Alkylated α-amino group**		
2.37	*L*-Proline	6.6±0.2	0.3
2.38	*N*-Methylglycine	13.7±0.6	0.7
2.44	*N,N*-Dimethylglycine	31.8±0.1	1.5
2.46	*N,N,N*-Trimethylglycine	36.0±0.5	1.7
D	**Homologous Series**		
2.39	β-Alanine	117.0±5.3	5.7
2.40	γ-Aminobutyric acid	6.6±0.1	0.3
2.41	5-Aminovaleric acid	1.6±0.01	0.08
E	**Alcoholic and Aromatic Side Chain**		
2.34	*L*-Serine	18.6±0.5	0.9
2.35	*L*-Phenylalanine	17.1±0.3	0.8

[a, b]: Statistically no difference in mean $t_{1/2}$ after pairwise one-way ANOVA with post-hoc Tukey's test within the group of compounds **2.28-2.33** ($p < 0.05$).

C) Influence of alkylation of the α-amino group on the chemical hydrolysis of 5-OH-DPAT prodrugs. The pseudo first-order hydrolysis rate plots of the glycine (**2.28**), *L*-proline (**2.37**), *N*-methylglycine (**2.38**), *N,N*-dimethylglycine (**2.44**) and *N,N,N*-trimethylglycine (**2.46**) 5-OH-DPAT prodrugs are presented in Figure 3.1 C. The half-lives were evaluated pairwise against each other and were shown to differ significantly (*p* <

0.001). This group includes a series of prodrugs with primary, secondary, tertiary and quaternary alkylated amine groups of the pro-moiety. The half-lives of **2.37**, **2.38**, **2.44**, **2.46** were 7, 14, 32, 36 hours, respectively.

D) Influence of increasing chain length on the chemical hydrolysis of 5-OH-DPAT prodrugs. In Figure 3.1 D the pseudo first-order hydrolysis rate plots are shown of glycine (**2.28**), β-alanine (**2.39**), γ-aminobutyric acid (**2.40**) and 5-aminovaleric acid (**2.41**) 5-OH-DPAT ester prodrugs. The half-life values of compounds **2.28** and **2.39**-**2.41** were evaluated pairwise versus each other and were shown to differ significantly ($p < 0.001$). This group of prodrugs is characterized by a variable chain length between the ester and amino group, i.e. a homologous series. This range varies between one and four methylene groups. The half-lives of the prodrugs **2.39**, **2.40** and **2.41** are 117, 7 and 1.6 hours, respectively.

E) Influence of alcoholic and aromatic side chains on the chemical hydrolysis of 5-OH-DPAT prodrugs. In contrast to the prodrugs with *L*-serine (**2.34**) and *L*-phenylalanine (**2.35**) pro-moieties, the glycine prodrug contains no alcoholic or phenylic amino acid side chain. Although comparison of the half-lives of compounds **2.34** and **2.35** versus **2.28** showed significant differences ($p < 0.05$), the half-lives differed only 2 and 4 hours from the half-life of **2.28**, respectively. Therefore, the hydrolysis rate plots of **2.34** and **2.35** 5-OH-DPAT prodrugs were omitted from Figure 3.1.

3.2.3 Non–enzymatic hydrolysis in phosphate buffered saline

The 1-aminocyclopropanecarboxylic acid (**2.30**), *L*-valine (**2.31**), *D*-valine (**2.32**), *L*-isoleucine (**2.33**) and β-alanine (**2.39**) esters of 5-OH-DPAT were shown to be the most chemically stable prodrugs in citrate buffer pH 5 (Section 3.2.2). To further investigate the applicability of these prodrugs for iontophoretic delivery, the hydrolysis in human blood plasma was determined. First, the non-enzymatic hydrolysis of these prodrugs and compound **2.28** was determined at pH 7.4. The hydrolysis rate constants (k_{obs}) and half-lives ($t_{1/2}$) were obtained by measuring the initial rate of 5-OH-DPAT formation in triplicate during hydrolysis experiments in 9.5 mM phosphate buffered saline (PBS), pH 7.4. The hydrolysis rate plots of these experiments are presented in Figure 3.2 and are based on the estimated half-lives presented in Table 3.3.
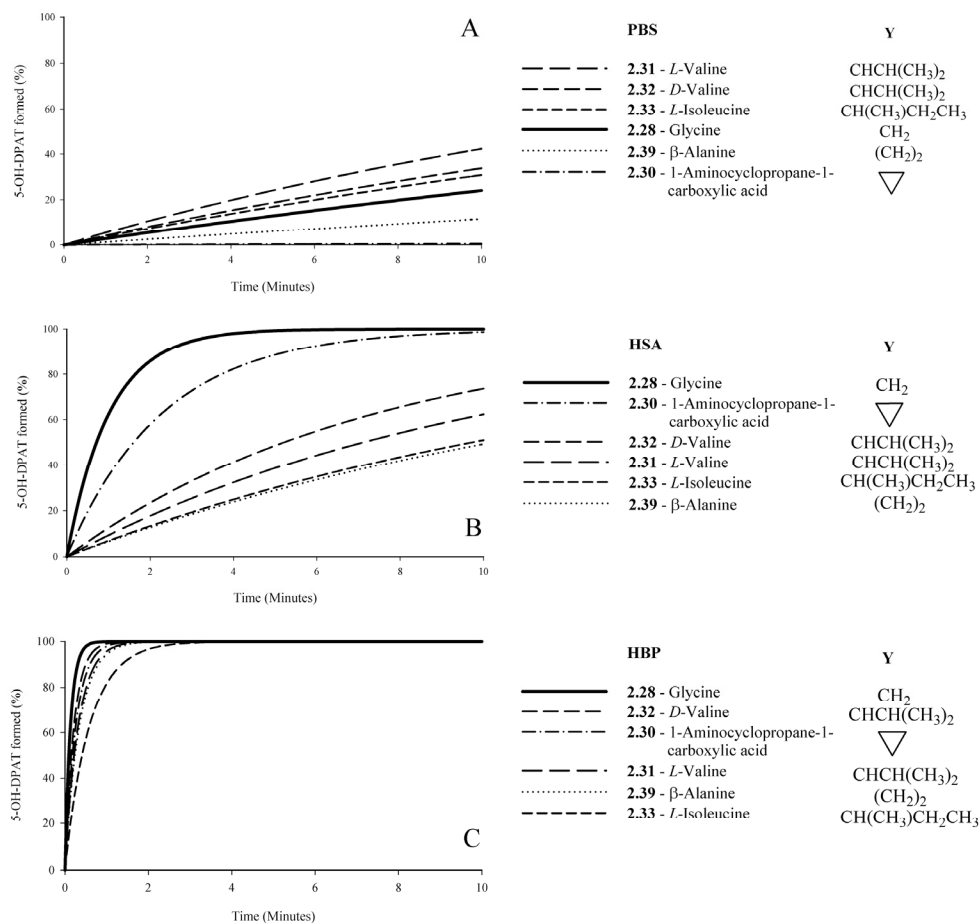
Figure 3.2 Pseudo first-order rate plots of 5-OH-DPAT formation during prodrug hydrolysis of prodrugs 2.28, 2.30-2.33 and 2.39 at 37 °C with an initial concentration of 100 µM in: A) 9.5 mM phosphate buffered saline (PBS) pH 7.4; B) 4% w/v human serum albumin (HSA) in PBS; C) 80% v/v human blood plasma (HBP) in PBS. The plots are based on the estimated half-lives presented in Table 3.3 and the prodrugs are listed per group in sequence of ascending half-life.

The 1-aminocyclopropane-1-carboxylic acid prodrug **2.30** was very stable compared to the other tested prodrugs, and we found a half-life of 1438 minutes (24 hours) ($p < 0.025$). This finding resembled relatively the highest chemical stability determined from hydrolysis experiments in citrate buffer pH 5. The half-lives of the other prodrugs were ranked in the following order: β-alanine (**2.39**, 57 min) > glycine (**2.28**, 25 min) > L-isoleucine (**2.33**, 19 min) ≥ D-valine (**2.32**, 17 min) ≥ L-valine (**2.31**, 13 min) ($p < 0.025$).

3.2.4 Enzymatic hydrolysis in human serum albumin and human blood plasma

According to the similar method described in section 3.2.3, the half-lives of compounds **2.28**, **2.30**-**2.33** and **2.39** were estimated when hydrolyzed in human serum albumin (HSA, 4% w/v) and human blood plasma (HBP, 80% v/v). The plots for the enzymatic hydrolysis rates for these compounds are presented in Figure 3.2 and are based on the estimated half-lives presented in Table 3.3.

A concentration of 4% HSA per 100 mL PBS at pH 7.4 resembles an 80% dilution of the mean normal albumin concentration of the general population (4.5±1.0 g /100 mL).[19] Table 3.3 shows the following stability trend under influence of HSA: β-alanine (**2.39**, 10 min) ≈ *L*-isoleucine (**2.33**, 10 min) > *L*-valine (**2.31**, 7 min) ≈ *D*-valine (**2.32**, 5 min) > 1-aminocyclopropane-1-carboxylic acid (**2.30**, 1.6 min) ≈ glycine (**2.28**, 0.7 min). The highest enzymatic stability in 4% HSA was found for prodrugs **2.33** and **2.39**. The half-lives of compounds **2.31** and **2.32** were not significantly different. Compared to the half-lives determined from hydrolysis experiments in PBS (Section 3.2.3), the half-lives of **2.31** and **2.32** decreased by a factor 1.8 and 3.2, respectively. The half-lives of prodrugs **2.28** and **2.30** were considerably decreased, namely with a factor 35 and 899, respectively.

Table 3.3 Estimated half-lives (t1/2) of the hydrolysis of prodrugs 2.28-2.41, 2.43, 2.44 and 2.46 at 37 °C (n=3) with an initial concentration of 100 μM in PBS, HSA and HBP.

Comp.	5-OH-DPAT ester	Estimated $t_{1/2}$ ± SEM (Minutes)					
		9.5 mM PBS (pH 7.4)	Human Serum Albumin (4%)	$t_{1/2}$ ratio HSA vs PBS	Human blood plasma (80%)	$t_{1/2}$ ratio HBP vs PBS	$t_{1/2}$ ratio HBP vs HSA
2.28	Glycine	25.2±1.5	0.71±0.04[c]	0.03	0.091±0.005[f]	0.004	0.13
2.30	1-Amino-cyclopropane-1-carboxylic acid	1438.3±52	1.6±0.1[c]	0.001	0.18±0.007[g, h]	0.0001	0.11
2.31	L-Valine	12.6±1.2[a]	7.1±0.01[d]	0.6	0.22±0.02[g, i]	0.02	0.03
2.32	D-Valine	16.8±0.2[a, b]	5.2±0.8[d]	0.3	0.15±0.01[f, g]	0.009	0.03
2.33	L-Isoleucine	18.8±0.9[b]	9.7±0.6[e]	0.5	0.41±0.02	0.02	0.04
2.39	β-Alanine	56.7±6.0	10.2±0.1[e]	0.2	0.24±0.01[h, i]	0.004	0.02

[a-i]: Statistically no difference in mean $t_{1/2}$ after pairwise one-way ANOVA with post-hoc Tukey's test within the group of compounds tested in PBS, HSA and HBP ($p < 0.025$).

Table 3.3 shows the following enzymatic stability trend in HBP (80%): *L*-isoleucine (**2.33**, 0.41 min) > β-alanine (**2.39**, 0.24 min) ≈ *L*-valine (**2.31**, 0.22 min) ≈ 1-aminocyclopropane-1-carboxylic acid (**2.30**, 0.18 min) ≈ *D*-valine (**2.32**, 0.15 min) ≈ glycine (**2.28**, 0.09 min). Prodrug **2.33** with the *L*-isoleucine pro-moiety is enzymatically the most stable prodrug, while the glycine prodrug **2.28** is the most labile prodrug. The *L*-valine and *D*-valine prodrugs are not significant different ($p < 0.025$) and together with compounds **2.30** and

2.39 show moderate half-lives between 0.15 and 0.24 minutes. Although small differences are observed between the half-lives of the prodrugs during hydrolysis in HBP, in general all prodrugs are enzymatically highly instable compared to their chemical stability.

3.3 DISCUSSION

Based on previous investigations on hydrolysis rates of several amino acid esters at various pH values and corrected for hydrolysis by the buffer concentration, the following general equation was formulated for the observed hydrolysis rate constant k_{obs} [20-22]

$$k_{obs} = k_0 \frac{a_H}{a_H + K_a} + k_{OH} a_{OH} \frac{a_H}{a_H + K_a} + k'_{OH} a_{OH} \frac{K_a}{a_H + K_a}$$ (Equation 3.1)

where the rate constant k_0 refers to the pH-independent hydrolysis of the protonated form of the ester prodrug. k_{OH} and k'_{OH} represent the second-order rate constants for the attack of the hydroxide ion on the protonated and unprotonated forms of the esters, respectively. These rate constants are based on several mechanisms of intramolecular catalysis, namely (a) intramolecular nucleophilic catalysis, (b) intramolecular general-base catalysis, (c) intramolecular general-acid specific base catalysis, and (d) electrostatic facilitation (Figure 3.3).[23] The factors $a_H/(a_H + K_a)$ and $K_a/(a_H + K_a)$ represent the fractions of the protonated and unprotonated forms of the total ester prodrug concentration, respectively. a_H and a_{OH} refer to the hydrogen ion and hydroxide ion activity and K_a is the ionization constant of the amino group in the amino acid ester prodrug.
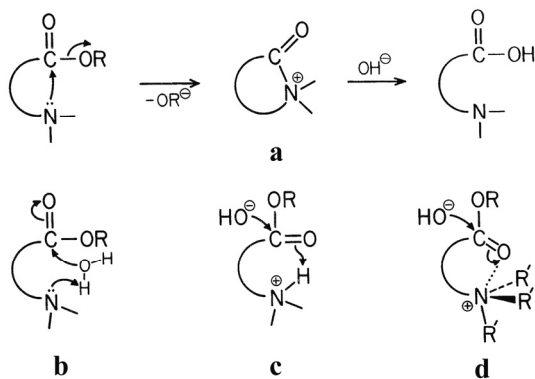
Figure 3.3 Mechanisms available to the neighbouring amino group for facilitation of ester hydrolysis.

We hypothesize that the pH-hydrolysis rate profile of the series of 5-OH-DPAT ester prodrugs follows equation 3.1. Most of the α-amino acid ester prodrugs that were investigated have calculated pK_a values of about 8, and at pH 5 the α-amino functional groups will be largely protonated.[24] Therefore the α-amino group is strongly electron-withdrawing and activates the ester function to hydrolysis. The mechanisms of the

hydrolysis of amino acid esters depend mainly on the pH range in which the hydrolysis takes place:

1   At pH values < 4, the primary reaction, k0, involves water attack on the protonated amino acid ester.

2   At pH values between pH 5 and the pKa value, the primary reaction is probably hydroxide ion attack on the protonated amino acid ester or attack of water on the unprotonated amino acid ester.

3   At pH > pKa, the major reaction is probably hydroxide attack on the unprotonated amino acid ester.[22]

Thus, at low pH the observed hydrolysis rate will be solely dependent on k_0 and the hydrolysis rate will be low. Therefore we use acidification with TFA to stop the hydrolysis in our experiments. Because a low buffer concentration was used consistently for all experiments, its intermolecular catalytic influence may be negligible.[22] Differences in k_{obs} are assumed to arise only from differences in pH (or a_{OH}), pK_a (or K_a) and intramolecular catalysis of the amino group of the pro-moiety defined as the rate constants k_0, k_{OH} and k'_{OH}. Equation 3.1 and the mechanisms shown in Figure 3.3 will be used for the explanation of the differences in chemical hydrolysis found for the amino acid ester prodrugs of 5-OH-DPAT.

3.3.1 Influence of the prodrug concentration on hydrolysis half-life

We found no differences in hydrolysis rate for the experiments with different initial prodrug concentrations. The intermolecular catalysis of the prodrugs and thus the influence of the prodrug concentrations on the hydrolysis half-life appears to be negligible in our experiments. Therefore, the chemical hydrolysis rate constants of all prodrugs were determined at initial concentrations of 0.05 or 0.31 mM and were statistically compared among each other in groups of analogous series.

3.3.2 Non-enzymatic hydrolysis in citrate buffer

A) Influence of bulky groups on the chemical hydrolysis of 5-OH-DPAT prodrugs.
The increasing steric hindrance from the glycine (**2.28**) and *L*-alanine (**2.29**) to the *L*-valine (**2.31**) and *D*-valine (**2.32**) to ultimately the *L*-isoleucine (**2.33**) 5-OH-DPAT esters was reflected in the increased chemical stability. Although the half-life of the *L*-alanine prodrug **2.29** according to the increased steric effect was expected to be higher than the half-life of the glycine prodrug **2.28**, it did not differ significantly. The experimental pK_a value of the amino functional group of *L*-alanine is 9.69, while this pK_a value for glycine is 9.60.[25, 26] If the negative effect on the hydrolysis rate by the increased steric hindrance of the methyl group side chain of **2.29** is balanced by the positive effect by the increased pK_a, this could be a reason for similar stability found for the *L*-alanine and glycine ester prodrugs. Although the 1-aminocyclopropanecarboxylic acid prodrug **2.30** was not sterically hindered

to the extent of prodrugs **2.31**, **2.32** and **2.33**, it was chemically the most stable prodrug in this series. Bender *et al* hypothesized that this increased chemical stability is caused by hyperconjugative stabilization of the carbonyl group by the cyclopropane ring.[27]

B) Influence of a weakly basic side chain on the chemical hydrolysis of 5-OH-DPAT prodrugs. Reference glycine ester prodrug **2.28** has an α-amino group with a calculated pK_a of 8.0.[24] In addition to an α-amino group with a pK_a of 8.1, *L*-lysine ester prodrug **2.36** has an extra amino group on the ε–position (pK_a 10) and *L*-arginine ester prodrug **2.43** has a guanidino group on the δ-position (pK_a 14). The amino group of 5-aminovaleric acid ester prodrug **2.41** is located on the δ-position of the amino acid and has a calculated pK_a of 10. The decreased chemical stability of this group of prodrugs may be explained by the introduction of an (additional) amino group with a higher pK_a value. Therefore these prodrugs have an increased intramolecular catalysis of hydrolysis. The lengthy chains of this group of prodrugs may cause various spatial conformations during intramolecular catalysis (Figure 3.3) which consist of 7 to 9-membered rings.

C) Influence of alkylation of the α-amino group on the chemical hydrolysis of 5-OH-DPAT prodrugs. The *L*-proline (**2.37**, pK_a 8.5) and *N*-methylglycine (**2.38**, pK_a 8.3) prodrugs are hydrolyzed faster than the reference glycine prodrug (**2.28**, pK_a 8.0). The positive effect on the hydrolysis of the greater pK_a values of prodrugs **2.37** and **2.38** compared to prodrug **2.28** may be explained by the corresponding greater fraction of protonated amino acid ester. This larger protonation gives a stimulation of intramolecular catalysis and an increased electron-withdrawing effect of the protonated amine on the carbonyl group making it more sensitive for hydrolysis. The *N,N*-dimethylglycine (**2.44**) and *N,N,N*-trimethylglycine (**2.46**) prodrugs are hydrolyzed slower than prodrug **2.28**. The higher half-lives compared to prodrug **2.28** can be explained by the lower calculated pK_a value of prodrug **2.44** (pK_a 7.0) and the absence of a pK_a value for the quaternary prodrug **2.46**. The hydrolysis of prodrug **2.46** is probably catalyzed by electrostatic facilitation (Figure 3.3).

D) Influence of increasing chain length on the chemical hydrolysis of 5-OH-DPAT prodrugs. The β-alanine (**2.39**, pK_a 8.8), γ-aminobutyric acid (**2.40**, pK_a 9.8), and 5-aminovaleric acid (**2.41**, pK_a 10.2) prodrugs all have higher calculated pK_a values than reference prodrug **2.28** (pK_a 8.0). With the exception of the β-alanine prodrug, the higher pK_a values of the prodrugs with an increased chain length gave shorter half-lives as expected from equation 3.1. Although the electron-withdrawing effect will decline with increasing chain length between the amino group and the carbonyl, the intramolecular catalytic influence of the amino group will remain pronounced. Interestingly, the β-alanine **2.39** is extremely stable in contrast to the chemically unstable prodrugs **2.40** and **2.41**. The stabilizing effect of β-alanine on chemical hydrolysis has previously been determined for metronidazole and *d*-α-tocopherol prodrugs.[28, 29] Moreover, Nam *et al.* found that folding effects of the terminal amino group might play an important role towards the amide

hydrolysis of prodrugs. The formation of the more stable five-membered ring intermediate during the amino mediated intramolecular cyclative cleavage of the γ-amino butyric acid prodrug was more favourable, compared to the constrained four-membered ring intermediate of the β-alanine prodrug.[30] The same reason could explain the chemical stability of the β-alanine ester prodrug of 5-OH-DPAT compared to the γ-aminobutyric acid and 5-aminovaleric acid ester prodrugs of 5-OH-DPAT.

E) Influence of alcoholic and aromatic side chains on the chemical hydrolysis of 5-OH-DPAT prodrugs. On the one hand, the calculated pK_a values of the *L*-serine prodrug **2.34** (pK_a 7.3) and the *L*-phenylalanine prodrug **2.35** (pK_a 7.74) are lower than the pK_a value of the glycine prodrug **2.28** (pK_a 8.08). As described in equation 3.1, a smaller pK_a results in a smaller protonated fraction of the amino functional groups. Thus both the electron-withdrawing effect and the intramolecular catalysis are decreased and consequently the ester is stabilized. Also the steric hindrance of prodrugs **2.34** and **2.35** is greater than the steric hindrance of **2.28**, which causes a stabilization of the ester group against hydrolysis. On the other hand, the predominant electron-withdrawing properties of the alcoholic and aromatic groups, could make the ester more susceptible to hydrolysis.[31] The corresponding half-lives found in this group of prodrugs may thus be explained by opposing effects of pK_a, steric hindrance and electron-withdrawing properties.

3.3.3 Non-enzymatic hydrolysis in phosphate buffered saline

Compounds **2.30**, **2.31**, **2.32**, **2.33** and **2.39** were selected as suitable candidates for further development because of their sufficient stability in citrate buffer. In general, the half-lives of the hydrolysis in PBS at pH 7.4 were considerably lower than the half-lives found for the hydrolysis in citrate buffer at pH 5. Thus, a higher pH has a destabilizing influence on the chemical hydrolysis of the 5-OH-DPAT prodrugs. This can be explained from equation 3.1, because a higher pH gives an increase of a_{OH} and therefore a higher hydrolysis rate. In contrast to the hydrolysis experiments performed in citrate buffer pH 5 at 32 °C, the glycine ester of 5-OH-DPAT **2.28** was chemically slightly more stable than the more bulky compounds **2.31**-**2.33** when hydrolyzed at pH 7.4 in PBS at 37 °C. Apparently, the role of steric hindrance on chemical stability at pH 7 has become smaller compared to its role on stability at pH 5. Both prodrugs **2.39** and **2.30** were the most stable prodrugs in PBS and these results resembled our previous data obtained from the chemical hydrolysis in citrate buffer.

3.3.4 Enzymatic hydrolysis in human serum albumin

L-isoleucine (**2.33**) and β-alanine (**2.39**) esters were showing the highest enzymatic stability in 4% HSA. The presence of HSA decreased the half-lives by a factor varying between 2 for the *L*-valine (**2.31**) and 1000 for the 1-aminocyclopropanecarboxylic acid (**2.30**) prodrugs compared to non-enzymatic hydrolysis in PBS pH 7.4 (Table 3.3). The influence

of HSA on hydrolysis was less pronounced for the steric hindered *L*-valine (**2.31**, factor 2), *D*-valine (**2.32**, factor 3) and *L*-isoleucine (**2.33**, factor 2) prodrugs, but was more distinct for the glycine (**2.28**, factor 33) and 1-aminocyclopropane-1-carboxylic acid (**2.30**, factor 1000) prodrugs which lacked branched aliphatic side chains. Thus, for the examined 5-OH-DPAT prodrugs the influence of HSA on the hydrolysis depended mostly on the substrate structure, especially steric hindrance played a crucial role in this. Even though, a contamination by a genuine hydrolase (mainly pseudo-cholinesterase) cannot be excluded.[32, 33]

Moreover, HSA is able to bind stereoselective a great number of various endogenous and exogenous compounds.[34] The catalytic activity of HSA on the *L*-alanine ester of *p*-nitrophenol was twice as high as the activity of HSA on the *D*-alanine ester. In contrast, the enzymatic activity on the *L*- and *D*-phenylalanine esters of *p*-nitrophenol was similar.[35] Reversible binding of prodrugs to HSA in combination with regeneration of parent drug by the esterase-like properties of HSA could lead to sustained release.[36] However, in our case the sustained release factor is already covered by controlled iontophoresis. Moreover, our studies showed that the prodrugs were hydrolyzed rapidly in HBP, which prevents sustained release in the blood stream. Based on the similar half-lives found for *L*- and *D*-valine (S)-5-OH-DPAT in 4% HSA we can conclude that HSA does not catalyse the hydrolysis of these prodrugs diastereoselectively.

3.3.5 Enzymatic hydrolysis in human blood plasma

Many examples have shown very rapid biotransformation rates for prodrugs in rodents, which could lead to an underestimation of the stability of the prodrugs in humans.[8] Therefore, we have chosen to determine the enzymatic hydrolysis of the 5-OH-DPAT prodrugs in HBP. The observed half-lives in HBP of all investigated prodrugs were less than 1 minute (Table 3.3). The ratios comparing the hydrolysis rates in HBP to HSA showed that influence of other hydrolyzing components found in HBP, like esterases, was more pronounced for the *L*-valine (**2.31**, factor 33), *D*-valine (**2.32**, factor 33) and *L*-isoleucine (**2.33**, factor 25) prodrugs with steric hindering side chains than for the glycine (**2.28**, factor 8) and 1-aminocyclopropane-1-carboxylic acid (**2.30**, factor 9) prodrugs. This observation was *vice versa* to the influence of HSA on the hydrolysis rate (*vide supra*). An exception was the β-alanine prodrug **2.39**, which was moderately affected by the HSA enzymatic acitivity, but was extremely labile to other hydrolyzing components in HBP, i.e. esterases. In addition to e.g. cholinesterase and arylesterase, human valacyclovirase could be responsible for the increased hydrolysis in HBP. Human valacyclovirase has a unique binding mode and specificity for amino acid esters.[37] In general, the amino acid prodrugs of 5-OH-DPAT are immediately hydrolysed in HBP pH 7.4 at 37 °C.

The hydrolysis of butyryl propranolol was non-stereoselective in plasma.[38] In addition, Udata *et al.* found that the disappearance of four diastereomeric phenylbutyryl propranolol

ester prodrugs in rat plasma was stereoselective.[39] Since esterase recognition typically favors *L*-amino acids over *D*-amino acids, the presence of *L*-amino acid residues makes the peptides better substrates for these enzymes.[8] With the aim to manipulate the enzymatic hydrolysis rate in HBP diastereomeric esters of *L*- and *D*-valine with (S)-5-OH-DPAT were synthesized and tested. Unfortunately, their half-lives showed no significant difference for hydrolysis in HBP. Thus, HBP does not catalyse the hydrolysis of the *L*- and *D*-valine (S)-5-OH-DPAT prodrugs diastereoselectively.

3.3.6 Selection of Prodrugs for further investigation

The 1-aminocyclopropane-1-carboxylic acid (**2.30**), *L*-valine (**2.31**), *D*-valine (**2.32**), *L*-isoleucine (**2.33**) and β-alanine (**2.39**) prodrugs are chemically stable at pH 5 which is the acidity in the donor compartment of iontophoretic experiments with 5-OH-DPAT. Moreover, these prodrugs will be rapidly hydrolyzed on arrival in the blood stream after transdermal delivery by iontophoresis. Because the valine prodrugs **2.31** and **2.32** show similar stabilities in HBP, the natural amino acid *L*-valine is preferred over the non-physiological amino acid *D*-valine. The *L*-isoleucine ester of 5-OH-DPAT (**2.33**) has a high lipophilicity which may have an adverse effect on transdermal iontophoretic delivery.[40] Therefore, the 1-aminocyclopropane-1-carboxylic acid (**2.30**), *L*-valine (**2.31**) and β-alanine (**2.39**) 5-OH-DPAT esters are promising candidates for further experiments. Nevertheless, the non-proteinogenic amino acids of compounds **2.30** and **2.39** have biological activities of their own. 1-Aminocyclopropane-1-carboxylic acid is a non-physiological partial agonist on the glycine modulatory site of the NDMA receptor.[41] And β-alanine occurs naturally in the CNS and has several recognized receptor sites, namely at the NDMA, glycine and GABA receptors.[42] Thus, in principle both amino acids could lead to side effects. Nevertheless, the β-alanine prodrug **2.39** is preferred because it has been used orally and topically, and is tolerated fairly well.[42]

In conclusion, in a series of novel amino acid ester prodrugs of 5-OH-DPAT we have identified some promising candidates for iontophoretic delivery. The stability is highly dependent on the side chain, and the prodrugs were completely hydrolysed instantaneously in 80% HBP at 37 °C. The *L*-valine (**2.31**)and β-alanine (**2.39**) prodrugs were acceptably stable in the iontophoresis donor phase at pH 5, and showed a 4-fold and 14-fold increase in solubility compared to 5-OH-DPAT itself (Chapter 5).[43] These prodrugs are suitable candidates for further *in vitro* and *in vivo* iontophoretic experiments.

3.4 EXPERIMENTAL SECTION

3.4.1 Materials

Trifluoroacetic acid (Fluka), citric acid trisodium salt (anhydrous, Sigma), citric acid (Aldrich), sodium phosphate dibasic anhydrous (Aldrich), potassium phosphate monobasic (Aldrich), human

serum albumin (96%-99% agarose gel electrophoresis, Sigma), screw top 2 mL amber vials (Supelco), black top closures with silicone septa (Supelco), inserts for 2 mL standard opening vial with 4.6 mm I.D. (Supelco) were purchased from Sigma-Aldrich. Sodium chloride (Merck) and potassium chloride (Merck) were purchased from VWR International (Amsterdam, The Netherlands). Pooled human plasma with lithium heparin as anticoagulant (6 individual mixed gender donors) was purchased from Sera Laboratories International (Bolney, United Kingdom). Acetonitrile HPLC-S (gradient grade) was obtained from Biosolve (Valkenswaard, The Netherlands). Ultrapure water was obtained after purification with an Arium 611 VF system fitted with a Sartopore 2 150 filter with a resistivity of 18.2 MΩ (Sartorius Stedim Biotech S.A., Aubagne, France). The handling of the hygroscopic prodrugs was performed in an Aldrich AtmosBag (Aldrich) under nitrogen atmosphere. The 70 mM NaCl 5mM citrate buffer was prepared by dissolving 0.818 gram citric acid trisodium salt, 0.352 gram citric acid and 4.091 gram sodium chloride in 1.0 L ultrapure water and adjusting the pH to 5.00 with 0.1 N sodium hydroxide or 0.1 N hydrochloric acid if necessary. The phosphate buffered saline 0.0095 M was prepared by dissolving 1.135 gram sodium phosphate dibasic anhydrous, 0.200 gram potassium phosphate monobasic, 8.125 gram sodium chloride and 0.1875 gram potassium chloride in 1.0 L ultrapure water and adjusting the pH to 7.4 with 0.1 M phosphoric acid or 0.1 N sodium hydroxide if necessary. The 4% (w/v) solution of human serum albumin was prepared by dissolving 5.0 grams human serum albumin in 125 mL phosphate buffered saline and adjusting the pH to 7.4 with 0.1 N NaOH. 80% (v/v) human blood plasma was prepared by diluting 39 mL human blood plasma to a total volume of 48.75 mL with phosphate buffered saline pH 7.4.

3.4.2 Hydrolysis of prodrugs in citrate buffer pH 5

The initial concentration used for compounds **2.29**, **2.35**, **2.37**, **2.38**, **2.40**, **2.43** and **2.44** was 0.31 mM. Prodrugs **2.30-2.34**, **2.36**, **2.39**, **2.41** and **2.46** were tested at initial prodrug concentrations of 0.05 mM.

The initial rates of hydrolysis were used to obtain the observed first-order rate constants (k_{obs}) and to calculate the half-lives ($t_{1/2}$). Least-square equations, derived by correlating areas in HPLC chromatograms to known concentrations of prodrug were used for calculation of the residual prodrug concentration in the studied samples. The correlation coefficients of the standard curves were 0.99. The observed first-order hydrolysis rate constants of the 5-OH-DPAT prodrugs were determined by plotting the logarithm of the remaining prodrug concentration as a function of time. The linear regression slopes of these plots ($r^2 \geq 0.95$) are related to the observed rate constant, k_{obs}, and are given

by: $k_{obs} = \dfrac{1}{\log e} \times slope\,(\log C \,vs\, time)$. The hydrolysis half-lives were then estimated by the

equation: $t_{1/2} = \dfrac{\ln 2}{k_{obs}}$. In order to study the relationship between the chemical stabilities, the results

were grouped in four series of related compounds and are presented in separate pseudo first-order rate plots in Figure 3.1 A-D. The half-lives are presented in Table 3.1. Statistical significance was evaluated with SigmaPlot for Windows v. 10 by performing one-way ANOVA with post-hoc Tukey's test to compare means within each separate group (n=3-9).

For the experiments with prodrugs **2.28**, **2.29**, **2.35**, **2.37**, **2.38**, **2.40**, **2.43** and **2.44** the chemical hydrolysis was initiated by adding 20 µl of a 62.5 mM stock solution in eluent to 3.98 mL 5 mM citrate buffer (pH 5) preheated at 32 °C. The final concentration of the resulting solutions was about

313 μM. The test solutions of the compounds were vortexed and maintained in a Lab-Line Orbit Shaker (model 310, J-KEM scientific, J-KEM 3300) at a constant temperature of 32±0.2 °C. At appropriate intervals samples of 20 μL were withdrawn and in order to inhibit further hydrolysis were diluted with 230 μL eluent giving a concentration of 25 μM. The samples were stored in the freezer until they were analyzed by HPLC. For the experiments with prodrugs **2.28**, **2.31**, **2.39** the chemical hydrolysis was initiated by adding 20 μl of a 25 mM stock solution in 5 mM citrate buffer (pH 5) to 1.98 mL 5 mM citrate buffer (pH 5) preheated at 32 °C. The final concentration of the resulting solutions was about 250 μM. The test solutions of the compounds were vortexed and maintained in a Lab-Line Orbit Shaker at a constant temperature of 32±0.2 °C. At appropriate intervals samples of 100 μL were withdrawn and diluted with 900 μL H_2O/ACN/TFA (2.9/1/0.004) giving a concentration of 25 μM. The samples were stored in the freezer until they were analyzed by HPLC. For the experiments with prodrugs **2.28**, **2.30**, **2.31**, **2.32**, **2.33**, **2.34**, **2.36**, **2.39**, **2.41** and **2.46** the chemical hydrolysis was initiated by adding 6 μl of a 25 mM stock solution in 5 mM citrate buffer (pH 5) to 2.994 mL 5 mM citrate buffer (pH 5) preheated at 32 °C. The final concentration of the resulting solutions was about 50 μM. The test solutions of the compounds were vortexed and maintained in a Lab-Line Orbit Shaker at a constant temperature of 32±0.2 °C. At appropriate intervals samples of 100 μL were withdrawn and diluted with 100 μL H_2O/ACN/TFA (1.2/1/0.004) giving a concentration of 25 μM. The samples were stored in the freezer until they were analyzed by HPLC. The compounds were estimated by measuring the peak areas or peak heights in relation to those of standards which were prepared by serial dilution of known concentrations (0.5, 5, 10 and 25 μM) and chromatographed under the same conditions.

3.4.3 Hydrolysis of prodrugs in phosphate buffered saline pH 7.4

The formation of 5-OH-DPAT during prodrug hydrolysis followed pseudo-first-order kinetics and is described by: $[5\text{-}OH\text{-}DPAT]_{formed} = [5\text{-}OH\text{-}DPAT]_{max}(1 - e^{-kt})$. The observed first-order hydrolysis rate constants of the 5-OH-DPAT formation from the selected prodrugs were determined by plotting the logarithm $(1 - \frac{[5\text{-}OH\text{-}DPAT]_{formed}}{[5\text{-}OH\text{-}DPAT]_{max}})$ as a function of time. The linear regression slopes of these plots ($r^2 \geq 0.95$) are related to the observed rate constant, k_{obs}, and are given by: $k_{obs} = \frac{1}{\log e} \times slope\,(\log C\,vs\,time)$. The half-lives ($t_{1/2}$) can be estimated by the equation: $t_{1/2} = \frac{\ln 2}{k}$.

For the experiments with prodrugs **2.28**, **2.30**, **2.31**, **2.32**, **2.33** and **2.39** the chemical hydrolysis was initiated by adding 8 μl of a 25 mM stock solution in citrate buffer (pH 5) to 1.992 mL phosphate buffered saline (pH 7.4) preheated at 37 °C. The final concentration of the resulting solutions was about 100 μM. The test solutions of the compounds were vortexed and maintained in a Lab-Line Orbit Shaker at a constant temperature of 37±0.2 °C. At appropriate intervals samples of 100 μL were withdrawn and diluted with 100 μL H_2O/ACN/TFA (1.2/1/0.004) giving a concentration of 50 μM. 100 μL of the samples was further diluted with 100 μL eluent to give a concentration of 25 μM. The samples were stored in the freezer until they were analyzed by HPLC. The compounds were estimated by measuring the peak areas or peak heights in relation to those of standards which were prepared by serial dilution of known concentrations (0.5, 5, 10 and 25 μM) and chromatographed under the same conditions.

3.4.4 Hydrolysis of prodrugs in human blood plasma (80% v/v)

The rates of enzymatic hydrolysis for prodrugs **2.28**, **2.30**, **2.31**, **2.32**, **2.33** and **2.39** were studied in human blood plasma (80% (v/v) in phosphate buffered saline of pH 7.4) at 37°C. The formation of 5-OH-DPAT which was measured during prodrug hydrolysis followed pseudo-first-order kinetics as described in **3.4.3** and the recovery of 5-OH-DPAT was 61%. The incubations were initiated by adding 8 μl of a 25 mM stock solution in citrate buffer (pH 5) to 1.992 mL human blood plasma (80%) preheated at 37 °C. The final concentration of the resulting solutions was about 100 μM. The test solutions of the compounds were vortexed and maintained in a Lab-Line Orbit Shaker at a constant temperature of 37±0.2 °C. At appropriate intervals samples of 100 μL were withdrawn and added to 100 μL cold 10% TFA in order to precipitate protein from the blood plasma. The samples were centrifuged for 10 minutes at 14,000 rpm and 100 μL of the resultant supernatant was then diluted with 100 μL H_2O/ACN (1.2/1). The samples were stored in the freezer until they were analyzed by HPLC. The compounds were estimated by measuring the peak areas or peak heights in relation to those of standards which were prepared by serial dilution of known concentrations (0.5, 5, 10 and 25 μM) and chromatographed under the same conditions.

3.4.5 Hydrolysis of prodrugs in a 4% (w/v) solution of human serum albumin in phosphate buffered saline pH 7.4

The rates of enzymatic hydrolysis for prodrugs **2.28**, **2.30**, **2.31**, **2.32**, **2.33** and **2.39** were studied in a solution of human serum albumin (4% (w/v) in phosphate buffered saline of pH 7.4) at 37°C. The formation of 5-OH-DPAT which was measured during prodrug hydrolysis followed pseudo-first-order kinetics as described in **3.4.3** and the recovery of 5-OH-DPAT was 66%. The method was similar to the procedure described for the enzymatic hydrolysis experiments in section 3.6.4.

3.4.6 HPLC analysis

Chemical Stability: samples of prodrugs **2.29**, **2.35**, **2.37**, **2.38**, **2.40**, **2.43** and **2.44** were analyzed isocratically on a HPLC system which consisted of an ISCO Model 2360 Gradient Programmer, a Waters 510 HPLC Pump, a Waters 486 Tunable Absorbance Detector and a HP 3396 Series II Integrator. Prodrugs **2.28**, **2.30**, **2.31**, **2.32**, **2.33**, **2.34**, **2.36**, **2.39**, **2.41** and **2.46** were analyzed isocratically on a Hewlett Packard Series 1100 HPLC system connected to a Tray-Cooling Marathon Basic+ Autosampler and a Hewlett Packard HP3395 Integrator. The samples were injected onto a Supelco Discovery C18 reversed-phase column (5 μm, 250 x 4.6 mm I.D.). The mobile phase consisted of a mixture of 23% acetonitrile and 77% water with 0.1% trifluoroacetic acid added. The flow was set at 1.0 mL/min and the analysis was performed at room temperature. The injection volume was 20 μL and the compounds were detected by UV at 217 nm. The run time was 12 minutes, except for compound **2.35** which had a run time of 20 minutes. The retention times of 5-OH-DPAT and the amino acid 5-OH-DPAT esters were: 9.57 min (**2.12**), 4.70 min (**2.28**), 4.85 min (**2.29**), 5.26 min (**2.30**), 7.31 min (**2.31**), 7.70 min (**2.32**), 10.92 min (**2.33**), 4.58 min (**2.34**), 15.34 min (**2.35**), 3.96 min (**2.36**), 5.25 min (**2.37**), 4.79 min (**2.38**), 5.14 min (**2.39**), 6.02 min (**2.40**), 6.68 min (**2.41**), 4.09 min (**2.43**), 4.97 min (**2.44**), 5.46 min (**2.46**).

Enzymatic Stability: samples of the prodrugs were analyzed according to a similar method described for the chemical stability on the Hewlett Packard Series 1100 HPLC system. The mobile phase consisted of a mixture of 21% acetonitrile and 79% water with 0.1% trifluoroacetic acid added. The

run time for the 80% (v/v) human blood plasma and 4% (w/v) human serum albumin experiments was 18 minutes and the retention time of 5-OH-DPAT was 11.65 minutes. The run time for the phosphate buffered saline pH 7.4 experiments was 14 minutes and the retention time of 5-OH-DPAT was 9.50 minutes.

3.4.7 Data analysis

All hydrolysis experiments were carried out in triplicate. The pseudo-first-order chemical hydrolysis rate constants (k) from the experiments conducted in citrate buffer were calculated from the linear slopes of plots of the logarithm of the remaining prodrug concentration against time (t). The pseudo-first-order enzymatic hydrolysis rate constants and the pseudo-first-order chemical hydrolysis rate constants from experiments conducted in phosphate buffered saline were calculated from the linear slopes of plots of the logarithm of the formed 5-OH-DPAT concentration against time. The slopes of these plots are related to the rate constant, k, and given by k = 2.303 x slope (log C vs time).   On the one hand the hydrolysis of the prodrug follows pseudo-first-order kinetics described by the formula: $[\text{Prodrug}] = [\text{Prodrug}]_0 \, e^{-kt}$. On the other hand, the formation of 5-OH-DPAT during prodrug hydrolysis also follow pseudo-first-order kinetics, but is described by another formula, i.e.: $[5\text{-OH-DPAT}] = [5\text{-OH-DPAT}]_{max} (1 - e^{-kt})$. The half-lives ($t_{1/2}$) can be estimated by the equation: $t_{1/2} = \dfrac{\ln 2}{k}$.

Statistical significance was evaluated with SigmaPlot for Windows Version 11.0 by performing one-way analysis of variance with post-hoc Tukey's test to compare means.

3.4.8 pK$_a$ calculation

The pK$_a$ values of the amino acid ester prodrugs were calculated with Pallas 1.2 of CompuDrug Chemistry Ltd.Copyright©1994.

3.5 ACKNOWLEDGMENTS

3.6 REFERENCES

1.   Dixit, N.; Bali, V.; Baboota, S.; Ahuja, A.; Ali, J. Iontophoresis - an approach for controlled drug delivery: a review. *Curr. Drug Deliv.* **2007**, *4,* 1-10.
2.   Nugroho, A. K.; Li, G. L.; Grossklaus, A.; Danhof, M.; Bouwstra, J. A. Transdermal iontophoresis of rotigotine: influence of concentration, temperature and current density in human skin in vitro. *J. Controlled Release* **2004**, *96,* 159-167.
3.   Nugroho, A. K.; Li, L.; Dijkstra, D.; Wikstrom, H.; Danhof, M.; Bouwstra, J. A. Transdermal iontophoresis of the dopamine agonist 5-OH-DPAT in human skin in vitro. *J. Controlled Release* **2005**, *103,* 393-403.

4.   Thysman, S.; Preat, V.; Roland, M. Factors affecting iontophoretic mobility of metoprolol. *J. Pharm. Sci.* **1992**, *81,* 670-5.

5.   Siddiqui, O.; Roberts, M. S.; Polack, A. E. The effect of iontophoresis and vehicle pH on the in-vitro permeation of lignocaine through human stratum corneum. *J. Pharm. Pharmacol.* **1985**, *37,* 732-5.

6.   den Daas, I.; Tepper, P. G.; Horn, A. S. Improvement of the oral bioavailability of the selective dopamine agonist N-0437 in rats: the in vitro and in vivo activity of eight ester prodrugs. *Naunyn-Schmiedeberg's Arch. Pharmacol.* **1990**, *341,* 186-91.

7.   den Daas, I.; Tepper, P. G.; Rollema, H.; Horn, A. S. Transdermal administration of the dopamine agonist N-0437 and seven ester prodrugs: comparison with oral administration in the 6-OHDA turning model. *Naunyn-Schmiedeberg's Arch. Pharmacol.* **1990**, *342,* 655-9.

8.   Liederer, B. M.; Borchardt, R. T. Enzymes involved in the bioconversion of ester-based prodrugs. *J. Pharm. Sci.* **2006**, *95,* 1177-95.

9.   Kovach, I. M.; Pitman, I. H.; Higuchi, T. Amino acid esters of phenols as prodrugs: synthesis and stability of glycine, beta-aspartic acid, and alpha-aspartic acid esters of p-acetamidophenol. *J. Pharm. Sci.* **1981**, *70,* 881-5.

10.   Williams, F. M. Clinical significance of esterases in man. *Clin. Pharmacokinet.* **1985**, *10,* 392-403.

11.   Hosokawa, M. Structure and catalytic properties of carboxylesterase isozymes involved in metabolic activation of prodrugs. *Molecules* **2008**, *13,* 412-31.

12.   Jewell, C.; Prusakiewicz, J. J.; Ackermann, C.; Payne, N. A.; Fate, G.; Williams, F. M. The distribution of esterases in the skin of the minipig. *Toxicol. Lett.* **2007**, *173,* 118-23.

13.   Varshney, A.; Sen, P.; Ahmad, E.; Rehan, M.; Subbarao, N.; Khan, R. H. Ligand binding strategies of human serum albumin: How can the cargo be utilized? *Chirality* **2009**, .

14.   Gilmer, J. F.; Moriarty, L. M.; Lally, M. N.; Clancy, J. M. Isosorbide-based aspirin prodrugs. II. Hydrolysis kinetics of isosorbide diaspirinate. *Eur. J. Pharm. Sci.* **2002**, *16,* 297-304.

15.   Sakurai, Y.; Ma, S. F.; Watanabe, H.; Yamaotsu, N.; Hirono, S.; Kurono, Y.; Kragh-Hansen, U.; Otagiri, M. Esterase-like activity of serum albumin: characterization of its structural chemistry using p-nitrophenyl esters as substrates. *Pharm. Res.* **2004**, *21,* 285-92.

16.   Yang, F.; Bian, C.; Zhu, L.; Zhao, G.; Huang, Z.; Huang, M. Effect of human serum albumin on drug metabolism: structural evidence of esterase activity of human serum albumin. *J. Struct. Biol.* **2007**, *157,* 348-55.

17.   Bundgaard, H. *Design of prodrugs;* Elsevier: Amsterdam etc., 1985; , pp VII, 360.

18.   Nugroho, A. K.; Romeijn, S. G.; Zwier, R.; De Vries, J. B.; Dijkstra, D.; Wikstrom, H.; la-Pasqua, O.; Danhof, M.; Bouwstra, J. A. Pharmacokinetics and pharmacodynamics analysis of transdermal iontophoresis of 5-OH-DPAT in rats: In vitro-in vivo correlation. *J. Pharm. Sci.* **2006**, *95,* 1570-1585.

19.   Dugdale, D. C.; Zieve, D. *Albumin - serum;* 2009; .

20.   Bundgaard, H.; Larsen, C.; Arnold, E. Prodrugs as Drug Delivery Systems .27. Chemical-Stability and Bioavailability of a Water-Soluble Prodrug of Metronidazole for Parenteral Administration. *Int. J. Pharm.* **1984**, *18,* 79-87.

21.   Wolfenden, R. Mechanism of Hydrolysis of Amino Acyl Rna. *Biochemistry* **1963**, *2,* 1090-&.

22.   Varia, S. A.; Schuller, S.; Stella, V. J. Phenytoin prodrugs IV: Hydrolysis of various 3-(hydroxymethyl)phenytoin esters. *J. Pharm. Sci.* **1984**, *73,* 1074-80.

23.   Bruice, T. C.; Benkovic, S. J. *Bioorganic mechanisms;* W. A. Benjamin: New York, 1966; , pp v.

24.   AnonymousPallas 1.2. **1994**, .

25.   Dawson, R. M. C.; Elliott, D. C.; Elliott, W. H.; Jones, K. M. *Data for Biochemical Research;* Clarendon Press: Oxford, 1959; .

26.   Williams, R.; Jencks, W. P.; Westheimer, F. H. *pKa Data Compiled by R. Williams;* .

27.   Bender, D. M.; Peterson, J. A.; McCarthy, J. R.; Gunaydin, H.; Takano, Y.; Houk, K. N. Cyclopropanecarboxylic acid esters as potential prodrugs with enhanced hydrolytic stability. *Org. Lett.* **2008**, *10,* 509-511.

28.   Bundgaard, H.; Larsen, C.; Thorbek, P. Prodrugs as Drug Delivery Systems .26. Preparation and Enzymatic-Hydrolysis of Various Water-Soluble Amino-Acid Esters of Metronidazole. *Int. J. Pharm.* **1984**, *18,* 67-77.

29.   Takata, J.; Karube, Y.; Nagata, Y.; Matsushima, Y. Prodrugs of Vitamin-e .1. Preparation and Enzymatic-Hydrolysis of Aminoalkanecarboxylic Acid-Esters of D-Alpha-Tocopherol. *J. Pharm. Sci.* **1995**, *84,* 96-100.

30.   Nam, N. H.; Kim, Y.; You, Y. J.; Hong, D. H.; Kim, H. M.; Ahn, B. Z. Water soluble prodrugs of the antitumor agent 3-[(3-amino-4-methoxy)phenyl]-2-(3,4,5-trimethoxyphenyl)cyclopent-2-ene-1-one. *Bioorg. Med. Chem.* **2003**, *11,* 1021-9.

31.   Taft, R. W. Separation of Polar, Steric, and Resonance Effects in Reactivity. In *Steric Effects in Organic Chemistry;* Newman, M. S., Ed.; John Wiley & Sons, Inc.: 1956; .

32.   Salvi, A.; Carrupt, P. A.; Mayer, J. M.; Testa, B. Esterase-like activity of human serum albumin toward prodrug esters of nicotinic acid. *Drug Metab. Dispos.* **1997**, *25,* 395-398.

33.   Chapuis, N.; Bruhlmann, C.; Reist, M.; Carrupt, P. A.; Mayer, J. M.; Testa, B. The esterase-like activity of serum albumin may be due to cholinesterase contamination. *Pharm. Res.* **2001**, *18,* 1435-9.

34.   Chuang, V. T.; Otagiri, M. Stereoselective binding of human serum albumin. *Chirality* **2006**, *18,* 159-66.

35.   Kurono, Y.; Kushida, I.; Tanaka, H.; Ikeda, K. Esterase-like activity of human serum albumin. VIII. Reaction with amino acid p-nitrophenyl esters. *Chem. Pharm. Bull.* **1992**, *40,* 2169-72.

36.   Ostergaard, J.; Larsen, C. Bioreversible derivatives of phenol. 1. The role of human serum albumin as related to the stability and binding properties of carbonate esters with fatty acid-like structures in aqueous solution and biological media. *Molecules* **2007**, *12,* 2380-95.

37.   Lai, L.; Xu, Z.; Zhou, J.; Lee, K. D.; Amidon, G. L. Molecular basis of prodrug activation by human valacyclovirase, an alpha-amino acid ester hydrolase. *J. Biol. Chem.* **2008**, *283,* 9318-27.

38.   Yoshigae, Y.; Imai, T.; Taketani, M.; Otagiri, M. Characterization of esterases involved in the stereoselective hydrolysis of ester-type prodrugs of propranolol in rat liver and plasma. *Chirality* **1999**, *11,* 10-13.

39.   Udata, C.; Tirucherai, G.; Mitra, A. K. Synthesis, stereoselective enzymatic hydrolysis, and skin permeation of diastereomeric propranolol ester prodrugs. *J. Pharm. Sci.* **1999**, *88,* 544-50.

40.   Sung, K. C.; Fang, J. Y.; Hu, O. Y. P. Delivery of nalbuphine and its prodrugs across skin by passive diffusion and iontophoresis. *J. Controlled Release* **2000**, *67,* 1-8.

41.   Brackmann, F.; de Meijere, A. Natural occurrence, syntheses, and applications of cyclopropyl-group-containing alpha-amino acids. 1. 1-aminocyclopropanecarboxylic acid and other 2,3-methanoamino acids. *Chem. Rev.* **2007**, *107,* 4493-537.

42.   Tiedje, K. E.; Stevens, K.; Barnes, S.; Weaver, D. F. beta-Alanine as a small molecule neurotransmitter. *Neurochem. Int.* **2010**, .

43.   Ackaert, O. W.; De Graan, J.; Capancioni, R.; Della Pasqua, O. E.; Dijkstra, D.; Westerink, B. H.; Danhof, M.; Bouwstra, J. A. The in vitro and in vivo evaluation of new synthesized prodrugs of 5-OH-DPAT for iontophoretic delivery. *J. Controlled Release* **2010**, *144,* 296-305.

4

The pharmacokinetics and pharmacological effect of (S)-5-OH-DPAT following controlled delivery with transdermal iontophoresis

[a]Department of Medicinal Chemistry, University Center of Pharmacy, University of Groningen, The Netherlands
[b]Division of Drug Delivery Technology, Leiden/Amsterdam Center for Drug Research, Leiden, The Netherlands
[c]Division of Pharmacology, Leiden/Amsterdam Center for Drug Research, Leiden, The Netherlands
[d]Division of Analytical Biosciences, Leiden/Amsterdam Center for Drug Research, Leiden, The Netherlands
[e]Department of Biomonitoring and Sensoring, University Center of Pharmacy, University of Groningen, The Netherlands
[f]Clinical Pharmacology and Discovery Medicine, GlaxoSmithKline, Greenford, United Kingdom
[*]Contributed equally as first author

Abstract

The pharmacokinetic (PK) and pharmacodynamic (PD) properties of the active (S)-enantiomer of the potent dopamine (DA) agonist 5-OH-DPAT were investigated in a novel anesthetized animal model. First, the relationship between current density, in vivo transport and plasma profile was characterized. Second, the effect of the anesthetic mixture, transdermal iontophoresis and blood sampling on the striatal DA release (PD endpoint) was investigated. Third, the PK-PD relationship following transdermal iontophoresis was investigated during a controlled and reversible pharmacological response. Given that the striatal DA levels are unaltered during experimental procedures, this rat model can be used to investigate the PK-PD relationship. The in vivo flux was found to be linearly correlated with the current density. Following both transdermal iontophoresis and IV infusion, a strong and reversible PD effect was observed. Compartmental modeling showed that the relationship between drug plasma concentration and biomarker response can be best characterized by an effect compartment, rather than an indirect response model. In addition, covariate analysis suggested that the delivery rate can affect the pharmacodynamic efficiency. Finally, simultaneous PK-PD analysis revealed that steady delivery rates are translated into continuous DAergic stimulation. This can be of great benefit for reducing side effects in the symptomatic treatment of Parkinson's disease with 5-OH-DPAT.

4.1 INTRODUCTION

Transdermal iontophoresis is a well established physical method to facilitate the percutaneous penetration of molecules.[1] By application of a small electrical current across the skin iontophoresis enhances the transdermal delivery of therapeutic agents. An important advantage of transdermal delivery is the circumvention of the hepatic first-pass metabolism, making it an interesting non-invasive alternative for oral drug delivery. A particular advantage of iontophoresis is the possibility to tailor the delivery to the patient's needs by adjusting the current density. This may allow for better therapeutic efficacy and reduction in overdosing and subsequent side effects. These properties make iontophoresis an excellent method for the transdermal delivery of drug molecules for the symptomatic treatment of Parkinson's disease.

Parkinson's disease is a neurodegenerative disorder, which is characterized by tremor, akinesia, rigidity and postural instability.[2] Up to today orally dosed levodopa is still the most effective symptomatic treatment, but chronic use eventually leads to severe long-term side-effects, i.e. dyskinesia and the *on-off* phenomenon.[3, 4] Current strategy to prevent or delay the onset of these side-effects is to administer therapeutics in a constant and controlled manner.[5] Therefore, the transdermal iontophoretic delivery of the DAergic

agonists (R)-apomorphine, ropinirole and 5-OH-DPAT were investigated *in vivo* for their application in symptomatic treatment of Parkinson's disease.[6-9]

Besides a constant and controlled delivery, another attractive property of iontophoresis is the possibility to develop a feedback system. In this approach, the concentration of a relevant biomarker, extracted for instance with reverse iontophoresis, can be used to titrate the transdermal iontophoretic delivery of the drug molecule. Preferably, a pharmacodynamic endpoint instead of the drug plasma concentration should be chosen to monitor the drug effect. Under experimental conditions, striatal DA concentration, measured by microdialysis, has been shown to be a biomarker for DAergic activity.[10, 11]

In the current investigation, we have therefore characterized pharmacokinetic-pharmacodynamic (PK-PD) relationships of the DA agonist following transdermal iontophoresis using DA as a measure of the pharmacological effect. In order to optimize the feedback system, we have also performed an integrated evaluation of relationship between the pharmacodynamics, pharmacokinetics and the delivery rates of the compound. In a previous study, the PK-PD of 5-OH-DPAT as assessed, however a ceiling effect was observed, with DAergic levels not altering throughout the time frame of the experiments.[7]

The aims of this study were three-fold. First, to examine the relationship between the current density, the *in vivo* iontophoretic transport and the (S)-5-OH-DPAT plasma profile. Given the requirement for the use of anaesthesia to conduct transdermal iontophoresis, second, to examine the effect of the anesthetic mixture, transdermal iontophoresis and blood sampling on the striatal DA release. Third, to assess the PK-PD relationship following transdermal iontophoresis of (S)-5-OH-DPAT, ensuring the induction of a controlled and reversible effect.[7]

(S)-5-OH-DPAT   (R)-d$_2$-5-OH-DPAT
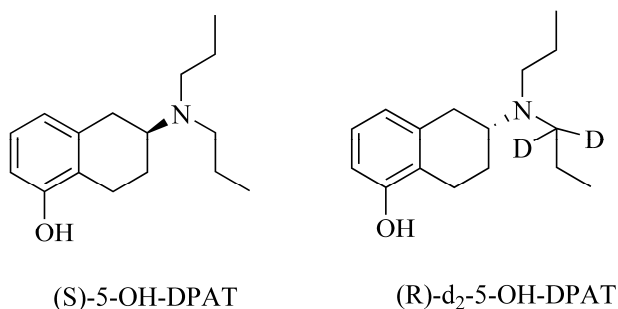
Figure 4.1 The molecular structures of (S)-5-hydroxy-2-(N,N-di-n-propylamino-tetralin ((S)-5-OH-DPAT) and (R)-5-hydroxy-2-(N-n-propyl-N-α,α-dideutero-propylamino)-tetralin ((R)-d2-5-OH-DPAT)

A comprehensive approach based on non-linear mixed effects modeling was used that allows us to characterize and predict the time course of drug action. Furthermore this approach enables to combine data from different experiments to obtain individual and population PK-PD parameter estimates.[12] Extensive PK-PD modeling is further applied to

characterize the pharmacodynamic effect. The PK model to describe the plasma concentration was adapted from literature.[7] Given that a delay is observed between plasma concentrations and the onset of the pharmacological response, two PD models are compared to describe the DA release: the effect compartment model[13] *vs* the indirect response type I model[14]. The results of this comparison add value to the efforts in the optimization of drug delivery. We ultimately illustrate how PK-PD relationships can be used to design a delivery system for symptomatic treatment of Parkinson's disease.

4.2 CHEMISTRY

For the analysis of the *in vivo* samples an internal standard was required. We have synthesized the deuterated form of 5-OH-DPAT. The first applied route (Scheme 4.1) to obtain deuterated compound **4.3** was deuteration of 5-methoxy-2-(*N,N*-diallylamino)tetralin (**4.1**) with deuterium gas and a catalyst. However, 5-methoxy-2-(*N,N*-di-(β,γ-dideutero)propylamino)-tetralin (**4.2**) was not the only deuterated product obtained. Due to hydrogen-deuterium scrambling, compound **4.2** was not only exclusively deuterated on the allyl bond but also on other positions in the molecule.[15, 16] Lower deuterium pressure or alternative catalysts may reduce this phenomenon. We obtained a series of related deuterated products with molecular weights of 263, 267 and 269 m/z, meaning that up to eight positions were deuterated.
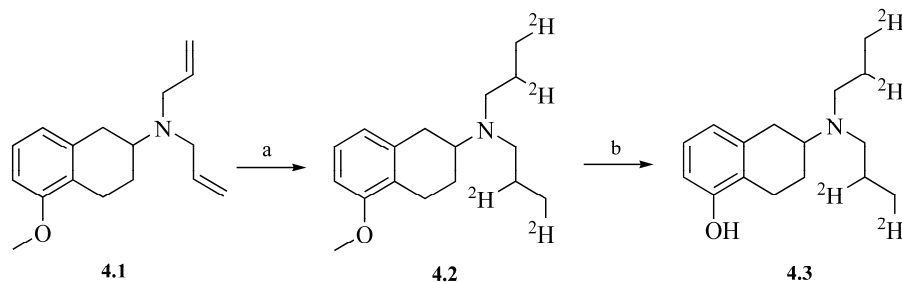
Scheme 4.1 Synthesis of 5-methoxy-2-(*N,N*-di-(β,γ-dideutero)propylamino)tetralin (4.3). Conditions and reagents: a) 1 bar D_2, PtO_2 or PdO in CD_3OD, RT, 30 min; b) 48% HBr, reflux.

An alternative deuteration strategy was employed (Scheme 4.2). (R)-5-Methoxy-2-(*N-n*-propylamino)tetralin (**(R)-4.4**) was converted to the propionamide **(R)-4.5**. Subsequently, **(R)-4.5** was reduced to compound **(R)-4.6** with lithium aluminium deuteride and only the amide moiety was deuterated. After demethylation with 48% hydrobromic acid, the final compound (R)-5-hydroxy-2-(*N*-propyl-*N*-α,α-dideutero-propylamino)tetralin (**(R)-4.7**) was obtained with an overall yield of 13%.
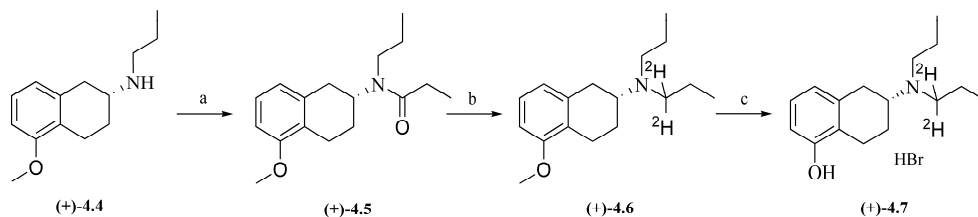
Scheme 4.2 Synthesis of (R)-5-hydroxy-2-(*N-n*-propyl-*N*-α,α-dideutero-propylamino)-tetralin HBr salt ((R)-4.7). Reagents and conditions: a) 1.25 M NaOH, propionylchloride, CH$_2$Cl$_2$, RT; b) LiAlD$_4$, THF, RT; c) 48% HBr, reflux.

4.3 EXPERIMENTAL

4.3.1 Chemistry

4.3.1.1 General

The materials and analysis methods for the chemistry are described in section 2.4.1

4.3.1.2 Preparation of (*R*)-5-hydroxy-2-(*N-n*-propyl-*N*-α,α-dideuterio-propylamino)-tetralin HBr salt (Internal Standard)

(R)-5-methoxy-2-(*N*-propylpropionamido)-tetralin ((R)-4.5).[17] (R)-5-Methoxy-2-(*N*-n-propyl-amino)-tetralin (prepared from **(R)-2.9** according to similar procedures as for the synthesis of **8.14**, 1.0 g, 4.6 mmol) was dissolved in a mixture of CH$_2$Cl$_2$ (50 mL) and 1.25 M NaOH (50 mL). Slowly propionylchloride (1.0 mL, 11.5 mmol) was added and the reaction mixture was stirred for 20 minutes at r.t. CH$_2$Cl$_2$ (100 mL) was added and the organic layer was separated, dried on Na$_2$SO$_4$, filtrated and evaporated *in vacuo* to afford crude **(R)-4.5** as an oil (1.0 g, 79%). Purity: 96% (GCMS); EI-MS *m/z* 275 (M)$^+$.
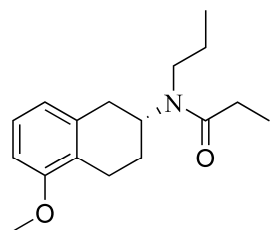
(R)-5-methoxy-2-(*N*-propyl-*N*-(α,α-dideuterio-propyl)amino)-tetralin ((R)-4.6). Under nitrogen atmosphere a solution of **(R)-4.5** (0.84 g, 3.1 mmol) in dry THF (10 mL) was added to a suspension of LiAlD$_4$ (0.19 g, 4.5 mmol) in dry THF (20 mL) and the mixture was stirred for 30 minutes at r.t. After addition of EtOAc (10 mL), diluted H$_2$SO$_4$ (2 mL) was added until precipitation at pH 4. The mixture was filtrated, basified with 2N NaOH (2 mL) and extracted with EtOAc (2x100 mL). The combined organic layers were washed with brine, dried on Na$_2$SO$_4$, evaporated *in vacuo* and purified on column chromatography (SiO$_2$ (NH$_3$), Hexane/EtOAc=8:1) to yield **(R)-4.6** as an oil (0.80 g, 77%).
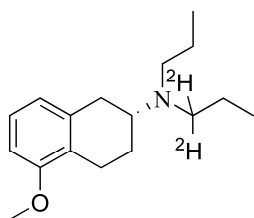
(R)-5-hydroxy-2-(*N*-propyl-*N*-α,α-dideuterio-propylamino)-tetralin HBr salt ((R)-4.7). A mixture of freshly distilled 48% HBr (10 mL) and **(R)-4.6** (0.41 g, 1.6 mmol) was refluxed for 2 hours under nitrogen atmosphere. After cooling down, the formed crystals were filtrated and
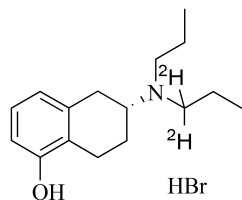
recrystallized from MeOH/EtOAc to afford the HBr-salt of **(R)-4.7** as white crystals (0.11 g, 21%). Purity>95% (GCMS); ^{1}H NMR (200 MHz, CD$_3$OD):δ 6.97 (t, J=7.6 Hz 1H, ArH), 6.75-6.55 (m, 2H, ArH), 3.82-3.77 (m, 1H, H2$_{ax}$), 3.43-2.88 (m, 5H, H$_{1ax}$, H$_{1eq}$, H$_{4eq}$, N(CH_2CH$_2$CH$_3$)), 2.78-2.50 (m, 1H, H$_{4ax}$), 2.46-2.23 (m, 1H, H$_{3eq}$), 2.03-1.63 (m, 5H, H$_{3ax}$, N(CH$_2$CH_2CH$_3$)$_2$), 1.05 (t, J=7.3 Hz, 6H, CH$_3$) ; ^{13}C NMR (50 MHz, CD$_3$OD): δ 154.9, 133.7, 126.8, 121.9, 120.1, 112.3, 60.6, 52.7, 29.6, 23.7, 22.5, 18.6, 10.2; EI-MS m/z 249 (M)$^+$.

4.3.2 Materials

Silver and silver chloride (puritiy >99.99%) were obtained from Sigma-Aldrich (Zwijndrecht, the Netherlands). Acetonitrile (LC-MS grade), ammonium acetate (LC-MS grade), acetic acid (LC-MS grade) and methanol (LC-MS grade) were purchased from Biosolve (Valkenswaard, the Netherlands). Ammonium hydroxide (25% w/v; analytical grade) was obtained from Baker (Deventer, the Netherlands). NaCl 0.9% was purchased from the hospital pharmacy of LUMC (Leiden, the Netherlands). EDTA was obtained from Merck (Merck KGaA, Darmstadt, Germany). All solutions were prepared in Millipore water with a resistivity of more than 18 MΩ.cm.

4.3.3 Iontophoresis patches

A detailed description of the iontophoresis patches, used for the transdermal iontophoresis studies can be found elsewhere.[7] Briefly, the iontophoresis patches were prepared by the Fine Mechanical Department of Leiden University from elastic silicon materials (silicon: Smooth-Sil 920; Smooth-on Inc., Easton, PA, USA). The volume of the patches was 2.3 ml and the active area was 2.5 cm². The patch was fixed on wound dressing film (Opsite Flexigrid, Smith&Nephew, Hoofdorp, The Netherlands), which can be attached to the skin during the experiment. Ag/AgCl was used as driver electrode pair.

4.3.4 Animals

Animal procedures were conducted in accordance with guidelines published in the NIH guide for the care and use of laboratory animals and all protocols were approved by the Institutional Animal Care and Use Committee of the University of Groningen and Leiden University. The pharmacokinetic (PK) and the pharmacokinetic-pharmacodynamic (PK-PD) studies were performed in albino male Wistar rats (280-340 g) obtained from Charles River (Maastricht, the Netherlands) and Harlan (Horst, the Netherlands), respectively. Prior to surgery the animals were housed at least 1 week in Plexiglas cages, maximum 6 animals per cage with free access to water and standard laboratory chow. The cages were placed in a room with a controlled temperature at 21 °C and controlled humidity between 60-65% and a light-dark cycle of 12 h.

4.3.5 Pharmacokinetic (PK) studies

In these studies the relationship between the current density and the plasma concentration profile of (S)-5-OH-DPAT following transdermal iontophoresis was investigated. (S)-5-OH-DPAT was administered by transdermal iontophoresis and intravenous (IV) infusion to the same animals with a

one week interval between treatments. The use of both routes of administration allowed improved pharmacokinetic parameter estimation. A detailed description of the experiments is given below.

4.3.5.1 Surgical procedures

Prior to surgery the animals were anaesthetized with a combination of Dormicum® (midazolam, 5 mg.ml^{-1}, Roche Nederland, Mijdrecht, the Netherlands) and Hypnorm® (fentanyl citrate 0.315 mg.ml^{-1} + fluanizone 10 mg.ml-1, Janssen Pharmaceutica, Beerse, Belgium) at a dose of 0.5 mL.kg^{-1} rat weight. The permanent cannulation was performed using Polethene tubings (Rubler BV, Hilversum, the Netherlands) with the diameter of 0.58 mm (I.D.) – 0.96 mm (O.D.) and 0.28 mm (I.D.) – 0.61 mm (O.D.), respectively for femoral vein and artery cannulation. After surgery the animals were housed individually and were allowed to recover during one week.

4.3.5.2 Experimental procedures

In the first part of the study (S)-5-OH-DPAT was administered by transdermal iontophoresis. First, the animals were anesthetized with Hypnorm® and Dormicum® (0.5 mL.kg^{-1}) and the hair of the back was removed using an electrical clipper and a scalpel. A pair of patches was attached to the skin surface. After 15 min the patches were filled with (S)-5-OH-DPAT (3.9 mM) at pH 5 (citric buffer, 5 mM) and with PBS pH 7.4 (NaCl: 8 g.L-1, Na_2HPO_4: 2.86 g.L-1, KH_2PO_4: 0.2 g.L-1, KCl: 0.19 g.L-1) at the anodal and the cathodal side, respectively. The following protocol was used for the iontophoresis studies: 15 min passive diffusion + 120 min 75 μA.cm-2 + 120 min 150 μA.cm-2. At time=255 min, the patches were removed and the skin was wiped using a tissue paper. Blood samples were taken at regular time intervals during the current application and after removal of the patch: 0, 15, 45, 75, 105, 135, 165, 195, 225, 255, 270, 285, 315, 345, 390, 435 min. Blood samples (0.2 ml) were collected using lithium-heparin containing tubes (Microvette® 200 Plasma/Lithium Heparin, Sarsted BV, Etten-Leur, the Netherlands). Plasma was then separated by centrifugation at a speed of 6000 rpm during 10 min. The samples were kept at -20 °C prior to analysis with LC-MS-MS.

After 1 week of recovery in individualized housing, animals received a total dose of 29 nmol (S)-5-OH-DPAT, dissolved in 0.9% NaCl, during 15-min IV infusion. At regular time intervals blood samples were taken from the femoral artery cannula: 0, 15, 20, 30, 45, 60, 75, 90, 105, 120, 150, 180 min. The samples were prepared in the same way as described above following iontophoretic delivery (see above). In all experiments the animals were kept in an anaesthetized condition during the experiment using Hypnorm® and Dormicum®.

4.3.6 On-line microdialysis studies (PK-PD studies)

This series of experiments consisted of three parts. First, the influence of anesthesia and iontophoresis on the striatal DA release (PD end point) was determined with on-line microdialysis. Second, the pharmacokinetic (PK) and pharmacodynamic (PD) properties following transdermal iontophoretic delivery were examined. Third, to explore the implications of differences in delivery rate on the PK and PD parameters, (S)-5-OH-DPAT was administered with IV infusion. In all experiments the striatal DA level and the striatal 5-OH-DPAT concentration were monitored by microdialysis with simultaneous blood sampling for the analysis of (S)-5-OH-DPAT plasma concentrations. A detailed description of the experiments is given below.

4.3.6.1 Surgical procedures

Prior to surgery the rats were anaesthetized with Isofluran 2% in N_2O/O_2 (2/1). The permanent cannulations were performed using silicone catheters (inner diameter (I.D.): 0.5 mm; outer diameter (O.D.): 0.9 mm) (UNO BV, Zevenaar, The Netherlands). The catheters were inserted approximately 2 cm inside the vessels. The catheters were tunneled subcutaneously, externalized at the back of the head. After the cannulation the rats were kept under anaesthetized condition and mounted into a stereotaxic frame for the implementation of microdialysis probes in left and right striatum according to a method described previously.[10, 11] After exposing and anesthetizing the skull with 0.5% marcaine-adrenaline, the holes for probe insertion were drilled. A Y-shaped dialysis probe was used for the experiments, with an exposed tip length of 3 mm. The dialysis canulla (I.D.: 0.24 mm; O.D.: 0.34 mm) was prepared from polyacrylonitrile/sodium methallyl sulfonate copolymer (AN 69, Hospal, Bologna, Italy). The microdialysis canulla was implanted in the striatum. The following coordinates were used according to the atlas of Paxinos and Watson[18]: AP +0.9, LM ± 3.0 relative to bregma, and Vd – 6.0 below dura. Before insertion into the brain, the dialysis probe was perfused successively with 70% ethanol, ultrapure water and Ringer solution (140 mM NaCl, 3.0 mM KCl, 1.2 mM $CaCl_2$, 1.0 mM $MgCl_2$). The dialysis probe was positioned in the burr hole under stereotaxic guidance. The probe was cemented in this position with dental cement. Thereafter the rats were housed solitary.

4.3.6.2 Experimental procedures

The PK-PD experiments were performed 15-20 h after cannulation and implementation of the probes. The rats were anaesthetized prior to and kept under anesthetized condition during the experiment with Hypnorm® and Dormicum® at a starting dose of 0.5 mL.kg^{-1} and subsequently with hourly doses of 0.17 mL.kg^{-1}.

First, to dismiss the potential confounding effects of anaesthesia, an iontophoretic control experiment was conducted administering only citric buffer (pH 5.0, 5 mM), as this is the donor phase used for transdermal iontophoresis, without (S)-5-OH-DPAT. Before the start of the experiment, the hair of the back of the anesthetized rat was removed with an electrical clipper and scalpel. 15 min after attaching the patches to the skin surface, the cathodal patch was filled with PBS pH 7.4 and the anodal patch was filled with donor solution. The protocol for iontophoresis was: 15 min passive diffusion + 90 min current application (250 µA.cm-2). The patch was removed and the skin was wiped using tissue paper. To include the influence of blood sampling on the DA level, blood samples were taken at regular time intervals: 0, 15, 30, 45, 60, 75, 90, 105, 120, 135, 165, 195, 225, 255, and 285. Blood sampling and subsequent preparation of the samples were identical to the procedures used for the PK studies following transdermal iontophoresis (cf. supra).

Second, a PK-PD microdialysis study following transdermal iontophoretic delivery of (S)-5-OH-DPAT was performed. The donor solution consisted of (S)-5-OH-DPAT (3.9 mM), buffered with a citric buffer (pH 5, 5 mM). All the experimental procedures were identical to the control experiment, as described in the previous paragraph. Third, a PK-PD microdialysis study was performed with a total dose of 113 nmol 5-OH-DPAT, dissolved in NaCl 0.9%, administered as a 10-min IV infusion. Blood sampling and subsequent preparation of the samples were identical to the procedures used for the PK studies following IV infusion (*cf.* supra).

In all the PK-PD studies the DA level and the 5-OH-DPAT concentration were monitored in the left and right striatum, respectively, with microdialysis. The microdialysis probes in the striata were

perfused with Ringer solution at a flow of 2 μL.min-1 (CMA/102 Microdialysis Pump, Sweden). Every 15 min a sample was collected for analysis with a total volume of 30 μl. The analysis of the microdialysate samples is described below (Section 4.3.7.2).

4.3.7 Sample analysis

4.3.7.1 Blood samples of (S)–5-OH-DPAT

The blood samples of 5-OH-DPAT were analyzed with an on-line solid-phase extraction-liquid-chromatography-mass spectrometry/mass spectrometry (SPE-LC-MS/MS) method. 5 μl of the internal standard (d_2-5-OH-DPAT; 5 ng.ml-1) was added to 35 μl of the collected plasma and 350 μl acetonitrile was added to precipitate the proteins. The mixture was vortexed and centrifuged at a speed of 8000 rpm during 10 min at 10 °C. The supernatant was dried and redissolved in 50 μl MilliQ and 3 μl was injected on to the SPE cartridge. An external binary HPLC pump (Gynkotek, Munich, Germany) and an external Agilent 1200, 2/6 switch valve (Agilent Technology, Santa Clara. CA, USA) were used for the SPE sample trapping. The samples were trapped in a Hysphere Resin C8, endcapped, 10 x 4 mm, 10 μm SPE cartridge (Spark Holland B.V, The Netherland). Prior to injection, the SPE cartridge was conditioned with 50mM ammonium acetate buffer pH 9, after the injection the sample was trapped with 10mM ammonium acetate buffer pH 9/ACN (4:1 v/v) during 1 min with a flow of 0.4 ml.min-1. Subsequently, the valve was switched placing the SPE cartridge in-line with the LC system for elution onto the analytical column. Elution of 5-OH-DPAT and its internal standard was accomplished by flushing the SPE column with H_2O/ACN (1:9 v/v) during 4 min with a flow of 0.05 ml.min-1 and 1 min with 1 ml.min-1. Finally, the cartridge was switched off-line again and re-conditioned using a 50mM ammonium acetate buffer at pH 9 during 2 min with a flow of 1 ml.min-1. To analyze the extracted sample an Agilent 1200 HPLC system with autosampler (Agilent Technology, Santa Clara. CA, USA) was coupled online with an Agilent 6460 Triple Quadrupole mass spectrometer (Agilent Technology, Santa Clara. CA, USA). The samples were analyzed by μPLC-MS/MS using an Altima HP C18 column (150X 1.0 mm; 5 μm) (Grace Davison Discovery Sciences, Lokeren, Belgium). The mobile phase consisted of 10 mM ammonium acetate buffer pH 3.7: Acetonitril (2.3:1 v/v) was used. The total analysis time was 11 min, the flow-rate was 100 μl.min-1, the temperature of the autosample tray was set to 4 ºC and the column temperature was set to room temperature. The detection was performed with a triple quadrupole mass spectrometer in the positive-ion electrospray mode and all analytes were monitored with Multiple Reaction Monitoring (MRM). 5-OH-DPAT and the internal standard d_2-5-OH-DPAT were ionized to produce the protonated molecules at m/z 248 and m/z 250, respectively. Upon collision (collision energy 15 eV; fragmentor enenergy 120 V) the pre-cursor ions of both 5-OH-DPAT and d_2-5-OH-DPAT produced the same product-ion at m/z 147, corresponding to 5-hydroxy-aminotetraline. System operation and handling the acquired data was performed using Agilent MassHunter data acquisition software (version, B.02.00; Agilent). Calibration curves showed a linear response when using concentrations of compounds between 0.2 and 50 ng.mL-1 (R^2>0.999). The recovery, limit of detection (LOD) and limit of quantification (LOQ) were experimentally determined at 93.9 ± 2.9 %, 0.07 and 0.2 ng.ml-1, respectively.

4.3.7.2 Microdialysate samples of (S)-5-OH-DPAT

To analyze the striatal 5-OH-DPAT concentration the dialysate from the probe in the right striatum was collected every 15 min, resulting in a total volume of 30 μL per sample. Subsequently, 70 μL of a 7.15 nM solution of (R)- d_2-5-OH-DPAT as internal standard was added to yield final concentrations of 5 nM internal standard in a 100 μL mixture of water + 0.1% formic acid and Ringer (1:1). The solution was analyzed using LC-MS/MS. The HPLC system consisted of a Shimadzu LC 20 AD binary system with a Shimadzu SIL 20AC autosampler. The samples were injected on a Grace Alltech Alltima HP C18 EPS reverse-phased column (3 μm, length 150 x 2.1 mm I.D.) (Grace Alltech, Lokeren, Belgium). The mobile phase consisted of a mixture of 0.1% formic acid in water (solvent A) and 0.1% formic acid in acetonitrile (solvent B). The gradient was programmed as follows: 1 minute isocratically at 15% B, increase in 7.5 min to 95% B, 2.5 min isocratically at 95% B, decrease in 1 minute to 15% B and isocratically for 5 min at 15% B. The total runtime was 17 min. The flow was set at 0.4 mL.min-1 and the analysis was performed at room temperature. The injection volume was 20 μL (partial loop fill) and the compounds were detected on a SCIEX API3000 triple quadrupole mass spectrometer (Applied Biosystems/MDS SCIEX, Foster City, CA, USA) equipped with a Turbo Ion Spray interface. The mass spectrometer was operated in the positive ion mode with MRM, quantifying transition pairs of m/z 248.2/147.1 and 250.2/147.1 for 5-OH-DPAT and d_2-5-OH-DPAT, respectively. Instrument parameters were as follows: Ion spray voltage 5000 V, nebulizer gas 13, curtain gas 13, TIST (Turbo Ion Spray Temperature) 500 °C, CAD gas 4, declustering potential (DP)=35 V, focusing potential (FP)=130 V, entrance potential (EP)=10 V. The detection limit of 5-OH-DPAT was 1 fmol which is 0.25 pg (5×10^{-11} M, 20 μL injection volume).

4.3.7.3 Striatal concentration of dopamine and metabolites

The dialysate contents of DA and its metabolites were quantified from the probe implanted at the left striatum by an on-line HPLC with electrochemical detection with the detection limit of 1 fmol/sample. A HPLC pump (LC-10AD vp, Shimadzu, Japan) was used in conjunction with an analytical cell (5011A, ESA, Chelmsford, MA, USA) and a electrochemical detector (Coulochem II, ESA, Chelmsford, MA, USA) working at +300 mV for DOPAC and HIAA and -300 mV for DA. The analytical column was a Supelco Supelcosil™ LC-18-DB column (150 mm x 4.6 mm, 3 μm) (Sigma-Aldrich Chemie B.V., Zwijndrecht, The Netherlands). The mobile phase consisted of a mixture of 4.1 g.L^{-1} sodium acetate (Merck), 215 mg.L^{-1} octane sulphonic acid, 186 mg.L^{-1} EDTA, 7% methanol and ultrapure water (pH=4.2 with glacial acetic acid). Data were converted into percentage of basal levels. The basal levels were determined from four consecutive samples (less than 20% variation), and set to 100%. After the experiments the rats were sacrificed and the brains were removed. The removed brains were kept in 4% paraformaldehyde solution until they were sectioned to control the location of the dialysis probes.

4.3.8 Data Analysis

A non-linear mixed effects modeling approach was used to describe the pharmacokinetics of (S)-5-OH-DPAT in plasma and the DA levels (PD end-point) in the striatum. The *in vivo* data following transdermal and IV infusion were combined for analysis.

4.3.8.1 PK model

A detailed description of the pharmacokinetic model for (S)-5-OH-DPAT has been reported elsewhere.[7] Briefly, the PK model is based on compartmental mass transfer to describe the iontophoretic transport *in vivo*. Data fitting was performed according to the ordinary differential equations 1, 2 and 3 for transdermal iontophoretic delivery:

$$\frac{dX_1(t)}{dt} = I_0.N - K_R.X_1(t) \tag{1}$$

$$\frac{dX_2(t)}{dt} = K_R.X_1(t) - k.X_2(t) - k_{23}.X_2(t) + k_{32}.X_3(t) \tag{2}$$

$$\frac{dX_3(t)}{dt} = k_{23}.X_2(t) - k_{32}.X_3(t) \tag{3}$$

With $\frac{dX_i(t)}{dt}$ as the rate of change in the amount of the drug in compartment i, X_i as the amount of the drug in compartment i, which refers to the skin compartment (i=1), the plasma compartment (i=2) and the peripheral compartment (i=3). I_0 is defined as the zero order mass input during iontophoresis, K_R as the first order release rate constant from skin to plasma, k as the first order elimination rate constant, k_{23} and k_{32} as the first order distribution rate constants from plasma to tissue and tissue to plasma, respectively. N is a flag in the model to indicate that the input rate I_0 is only valid during the iontophoresis period.

Following intravenous administration, data was modeled using equation 4, which describes the rate of change in amount of the drug in the plasma compartment:

$$\frac{dX_2(t)}{dt} = Rate.M - k.X_2(t) - k_{23}.X_2(t) + k_{32}.X_3(t) \tag{4}$$

With *Rate* as the zero order intravenous infusion rate and *M* as a flag to indicate that the *Rate* only applies during the duration of the infusion. Equation 3 was used to describe the rate of change in the peripheral compartment.

4.3.8.2 PD model

Two PD models were compared to fit the data of the DA release in the striatum during and after transdermal iontophoresis and intravenous infusion. The first model was the indirect response (IDR) type I model in analogy to the model proposed by Nugroho *et al.*[7] The levels of 5-OH-DPAT in the plasma (Cp) were directly linked to the DAergic effect. The equations of the model to describe the rate of change in the DA concentration $\frac{dC_{DA}(t)}{dt}$ in the striatum:

$$\frac{dC_{DA}(t)}{dt} = k_{in}^0 \cdot \left(1 - \frac{I_{max}.C_p(t)^H}{IC_{50} + C_p(t)^H} \right) - k_{out}.C_{DA}(t) \tag{5}$$

$$k_{in}^0 = k_{out}.C_{DA}(0) \tag{6}$$

With I_{max} as the maximum inhibition of the DA production, IC_{50} is the plasma concentration of 5-OH-DPAT at which 50% of maximum inhibition is observed, H is the slope of the curve (Hill coefficient),

k^0_{in} is the zero order rate constant for the production of response, k_{out} is the first order rate constant for the loss of response, $C_{DA}(0)$ is the baseline values of DA (i.e., DA concentration prior to the inhibiting effect of 5-OH-DPAT).

In the second model, an extra hypothetic compartment was introduced to account for the delay between plasma concentration and the response, i.e. the effect compartment. The rate of change of drug concentration $\dfrac{dC_e(t)}{dt}$ in the effect compartment can be described as follows:

$$\frac{dC_e(t)}{dt} = k_{e0}.\left(C_2(t) - C_e(t)\right) \tag{7}$$

With k_{e0} as the first order distribution rate constant from plasma to effect compartment and the elimination rate constant from the effect compartment. The effect is described by the sigmoid I_{max} model using the following equation:

$$C_{DA} = C_{DA}(0).\left(1 - \frac{I_{max}.C_e(t)^H}{IC_{50}{}^H + C_e(t)^H}\right) \tag{8}$$

With C_e as the drug concentration in the effect compartment.

4.3.8.3 Model parameters

A detailed description of the PK and PD modeling steps is presented elsewhere.[7] In short, the data analysis was performed using NONMEM version VI (NONMEM project group, University of California, San Francisco, USA) with ADVAN6 TRANS1 TOL=5 from PREDPP as subroutines. The fixed effect parameters (θ) included: I_0, K_R, clearance (CL), inter compartmental clearance (Q), volume of central compartment (V_2), volume of peripheral compartment (V_3), k_{out}, I_{max}, and IC_{50} and k_{e0}. Variability in pharmacokinetic parameters was assumed to be log-normally distributed in the population. Inter-individual variability was modeled by an exponential error model as written in Equation 9:

$$P_i = \theta.\exp(\eta_i) \tag{9}$$

in which θ is the population value for the fixed effect parameter P, P_i is the individual estimate and η_i is the normally distributed interindividual random variable with mean zero and variance ω^2. The coefficient of variation (CV %) of the structural model parameters is expressed as percentage of the root mean square of the interindividual variability term. The residual error was modeled by a proportional error model as written in Equation 10:

$$C_{ob,ij} = C_{pred,ij}.(1 + \varepsilon_{ij,1}) \tag{10}$$

where $C_{obs,ij}$ is the jth observed concentration in the ith individual, $C_{pred,ij}$ is the predicted concentration, and ε_{ij} is the normally distributed residual random variable with mean zero and variance σ^2.

The estimation of the final population parameters was performed using the conventional first order estimation method (FOCE). The PK model parameters were estimated independently and subsequently used as input for the PD analysis. During model building, goodness-of-fit was based on

statistical and graphical diagnostic data. Model selection and identification was based on the likelihood ratio test, coefficient of variation of parameter estimates, parameter correlations and goodness-of-fit plots. For the likelihood ratio test, the significance level for the inclusion of one parameter was set at $p<0.05$, which corresponds with a decrease of 3.84 points in the minimum value of the objective function (MVOF) under the assumption that the difference in MVOF between two nested models is χ^2 distributed. Non-nested models are evaluated using the Aikaike Information Criterion (AIC), which is the MVOF plus two times the number of parameters. The following goodness-of-fit plots were subjected to visual inspection to detect systemic deviations from the model fits: individual observed versus population and individual predicted values. Finally, the performance of the population PK and PK-PD models were assessed by simulating 100 data sets with the final model parameter estimates. The evaluation of model performance also included visual predictive check (VPC), as implemented in Xpose 4 (R version 2.7.0, R-foundation).[19]

4.4 RESULTS

Three series of *in vivo* experiments were conducted to investigate the controllability of transdermal iontophoresis and to explore the potential impact of delivery rate on the PK-PD relationship of (S)-5-OH-DPAT. In the first study, the influence of the current density on drug pharmacokinetics in plasma profile was assessed. Two current densities were applied consecutively for 2h (75 and 150 $\mu A.cm^{-2}$). In addition, (S)-5-OH-DPAT was administered as an IV infusion to the same animals to discriminate delivery-related properties from intrinsic pharmacokinetic properties. The crossover design also allowed higher precision of the parameter estimates. In the second study, the influence of the anesthetics, iontophoresis and blood sampling on the striatal DA level (PD endpoint) was investigated as a validation procedure for this experimental model. In the third study, the PK-PD relationship was investigated across a range of exposures, with maximum effects being attained for a short period followed by return of DA levels back to baseline conditions. For this reason, transdermal iontophoresis (250 $\mu A.cm^{-2}$) was applied up to 1.5h. In analogy to the first study presented above, (S)-5-OH-DPAT was also administered with IV infusion to enable separation of delivery-related properties from intrinsic pharmacokinetic properties.

4.4.1 PK properties following iontophoresis and IV infusion

In these studies two different current densities (75 and 150 $\mu A.cm^{-2}$) were applied consecutively during 2 h to investigate the impact of flux on plasma profiles. Moreover it was of interest to determine the time to reach steady state conditions. The results of the pharmacokinetic studies are depicted in Figure 4.2. After 15 min of passive diffusion prior to iontophoresis no detectable amount was transported into the plasma (data not shown). In contrast, drug plasma level increase immediately when switching on the current. In almost all the animals steady state plasma levels were achieved after 2 h of 75 $\mu A.cm^{-2}$ current application, with an average plasma concentration (C_p) of 4.1 ± 1.9 $ng.ml^{-1}$. By further increasing the current density to 150 $\mu A.cm^{-2}$, C_p increased to 9.4 ± 4.8 $ng.ml^{-1}$ after 2 h

approximately. In parallel, following IV infusion, C_p reached a maximum of 5.3 ± 0.5 ng.ml^{-1} after 15 min (data not shown). After the discontinuation of infusion or upon termination of the current application, the C_p declined according to a 2-compartment disposition model.
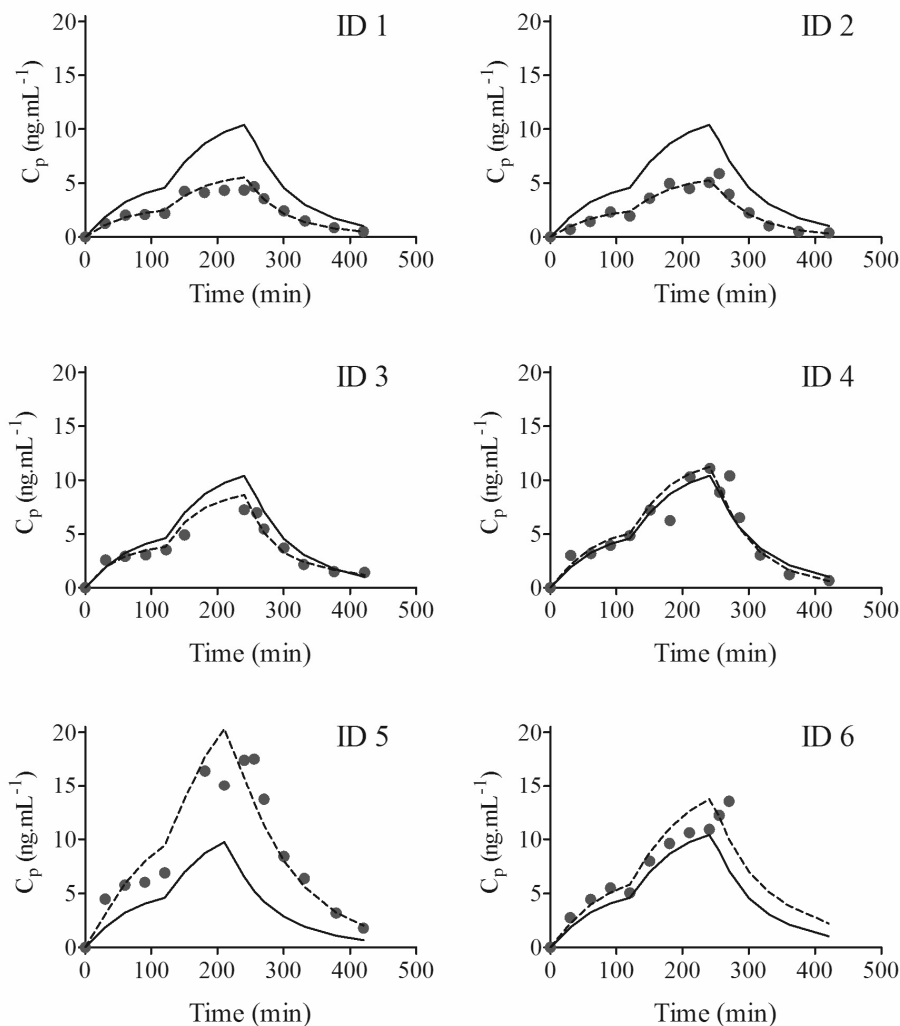
Figure 4.2 The observed data (filled circles) of the plasma concentration (Cp) of the individual rats during and after transdermal iontophoretic delivery of (S)-5-OH-DPAT (3.9 mM) together with the population model prediction (solid line) and the individual model prediction (dashed line). The following protocol was used: 120 min current density of 75 µA.cm^{-2}+120 min current density of 150 µA.cm-2. The patch was removed after 240 minutes.
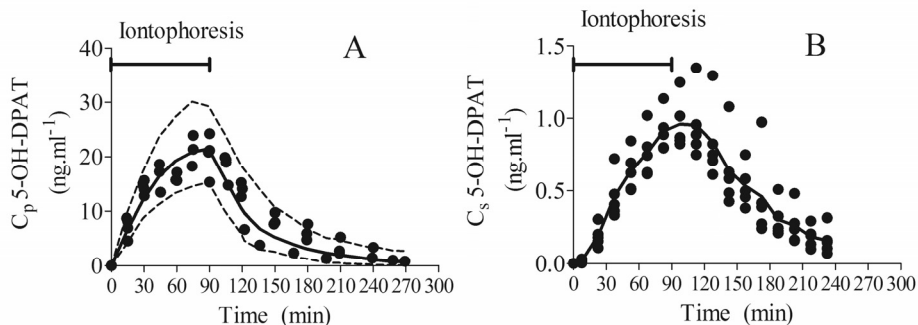
Figure 4.3 A: (S)-5-OH-DPAT concentration-time profiles in blood plasma following transdermal iontophoresis of (S)-5-OH-DPAT (3.9 mM). Depicted are the observed data (filled circles) together with simulated median (50%, solid line) and the upper and lower limit of the model-simulated interquantile concentration range (97.5%-5%, dashed lines).

B: (S)-5-OH-DPAT concentration-time profiles in striatum following transdermal iontophoresis of (S)-5-OH-DPAT (3.9 mM). Depicted are the observed data together with the mean.

4.4.2 Validation of the rat model to investigate the PD effect

The potential effects of anaesthesia (fentanyl+fluanisone and midazolam), of blood sampling and of transdermal iontophoresis on the striatal levels of DA (PD end-point) were investigated. The results of this control experiment are presented in Figure 4.4A. DA levels remained stable in the period immediately before attaching the patch (-60 to -15 min) and in the 15 minute period of passive diffusion before iontophoresis (-15 to 0 min). The DA levels, which were set to 100% showed a non-significant small increase from $97 \pm 3\%$ to $100 \pm 4\%$ during iontophoresis, followed by a stronger increase to $114 \pm 6\%$ during 115 min after the end of iontophoresis. These results indicate the suitability of the anesthetized rat model for monitoring of DA levels to evaluate the properties of transdermal iontophoretic delivery or IV infusion of (S)-5-OH-DPAT.

4.4.3 PK-PD relationships following iontophoresis and IV infusion

The pharmacokinetics and pharmacodynamics of (S)-5-OH-DPAT were assessed following transdermal iontophoresis and IV infusion. With regard to the PK, no detectable plasma concentration could be observed after 15 min passive diffusion (data not shown). When starting the current application (250 μA.cm^{-2}) the plasma concentration increased immediately and tended towards steady state after 90 min of current application (Fig.4.3A). The average concentration after 90 min of iontophoresis was 20.4 ± 3.7 ng.ml^{-1}. Following IV infusion, C_p reached a maximum of 29.9 ± 2.4 ng.ml^{-1} after 10 min (data not shown). The decline in plasma concentration post (S)-5-OH-DPAT administration was best described by a 2-compartment disposition model. Following transdermal iontophoresis the (S)-5-OH-DPAT concentrations in the striatum were also monitored. As shown in Figure

4.3B, 5-OH-DPAT concentrations increased to 0.96 ± 0.18 ng.ml^{-1} during current application, but this effect occured after a small delay (between 7.5 and 22.5 min) in relation to the beginning of iontophoresis. The concentrations decreased again with the same delay upon discontinuation of the iontophoretic current.
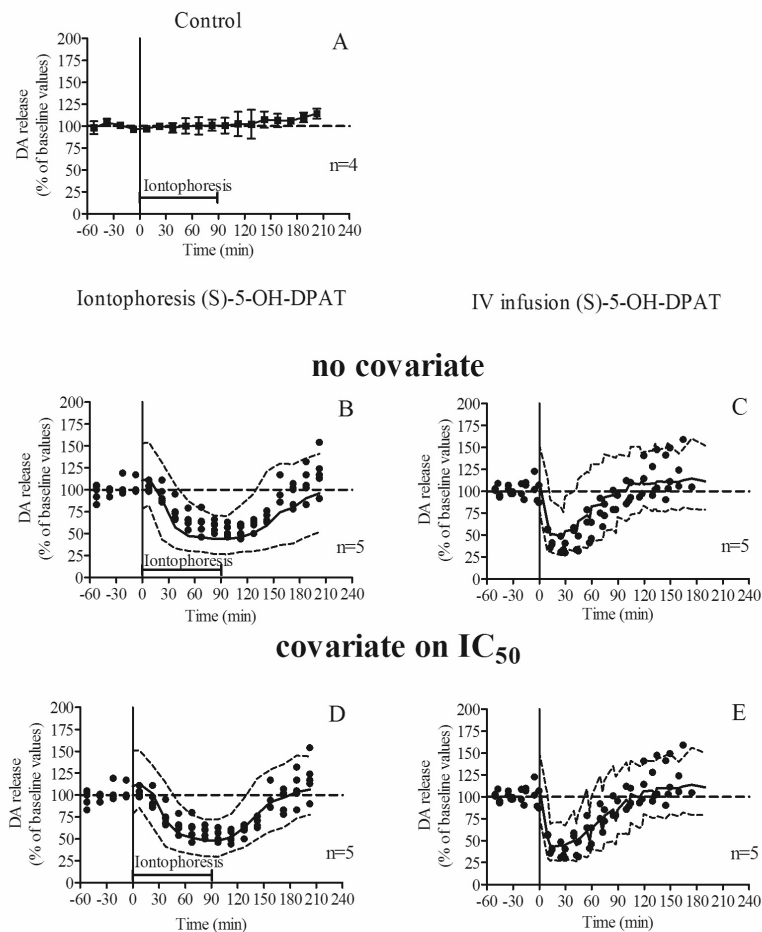
Figure 4.4 The DA release, expressed as % of baseline *vs* time: **A**: transdermal iontophoresis of only buffer (control experiment) **B, D**: transdermal iontophoresis of (S)-5-OH-DPAT (3.9 mM). **C,E**: IV infusion of (S)-5-OH-DPAT (113 µM).
A: depicted is the mean ± S.D. **B-E**: depicted are the observations (filled circles) together with the model simulated interquantile DA% range (2.5 %-97.5%, dashed lines) and the simulated median (50%, solid line). A number of 100 samples were simulated based on the final parameter estimates.
B,C: the visual predictive check without including a covariate of route of administration on IC$_{50}$. **D,E**: the visual predictive check including a covariate of route of administration on IC$_{50}$. In all panels the average DA release of 4 consecutive points prior to administration (time=-60 to -15 min) was set to 100%.

4.4.4 PK-PD analysis following transdermal iontophoretic delivery and IV infusion

The striatal DA release (PD endpoint) was monitored on-line simultaneously with plasma and striatal concentration of (S)-5-OH-DPAT. These results are presented in Figure 4.4. Firstly, the pharmacodynamic effect was monitored following iontophoresis (15 min passive diffusion + 90 min of iontophoresis 250 μA.cm^{-2}) (Fig. 4.4B). During passive diffusion (-15 to 0 min) no change in DA levels were observed. Subsequently, DA levels gradually decreased to a minimum of 48.8 $\pm$ 5.1% of basal values within 94.5 $\pm$ 16.4 min after the start of the iontophoresis. DA levels returned to baseline values 79.4 $\pm$ 11.3 min after the end of iontophoresis. In contrast, IV infusion of (S)-5-OH-DPAT resulted in an immediate decrease in the DA level. Maximum inhibition of 38.3 $\pm$ 8.4 % relative to baseline values was achieved after 42.1 $\pm$ 2.5 min (t_{max}) after start of IV infusion (Fig. 4.4C). DA levels returned to baseline values within 120.4 $\pm$ 20.5 min after the end of infusion. A slight rebound effect was observed at the end of the experiment. DA level further increased to 119 $\pm$ 22 and 120 $\pm$ 23% relative to baseline after transdermal delivery and IV infusion, respectively.

The pharmacokinetic data following transdermal iontophoresis analyzed simultaneously with the PK data following intravenous infusion. The objective of the integrated analysis was to facilitate discrimination between delivery-specific parameters (I_0, K_R) and drug-specific parameters (V_2, V_3, CL, Q). The larger sample size also allowed for more precise estimation of model parameters. The resulting parameters are provided in Table 4.1. The low relative standard error (RSE) for all the fixed effect parameters (RSE $\leq$ 30%) indicates high precision of estimates. Moreover, as observed in Figure 4.2 and in Figure 4.5A, the model accurately describes the time course of plasma concentration during and after current application.

An integrated approach was also applied to the PK-PD experiments. The analysis of the PK-PD data following IV administration and iontophoresis was performed simultaneously. In analogy to the PK study, the plasma concentration profile could be described by the proposed compartment model. In Figure 4.3A, the VPC depicts the goodness of fit, with observed data randomly distributed within the 95% confidence interval (C.I.). In addition, the diagnostic plots (Figure 4.5B) show a good correlation between the observed and predicted C_p.
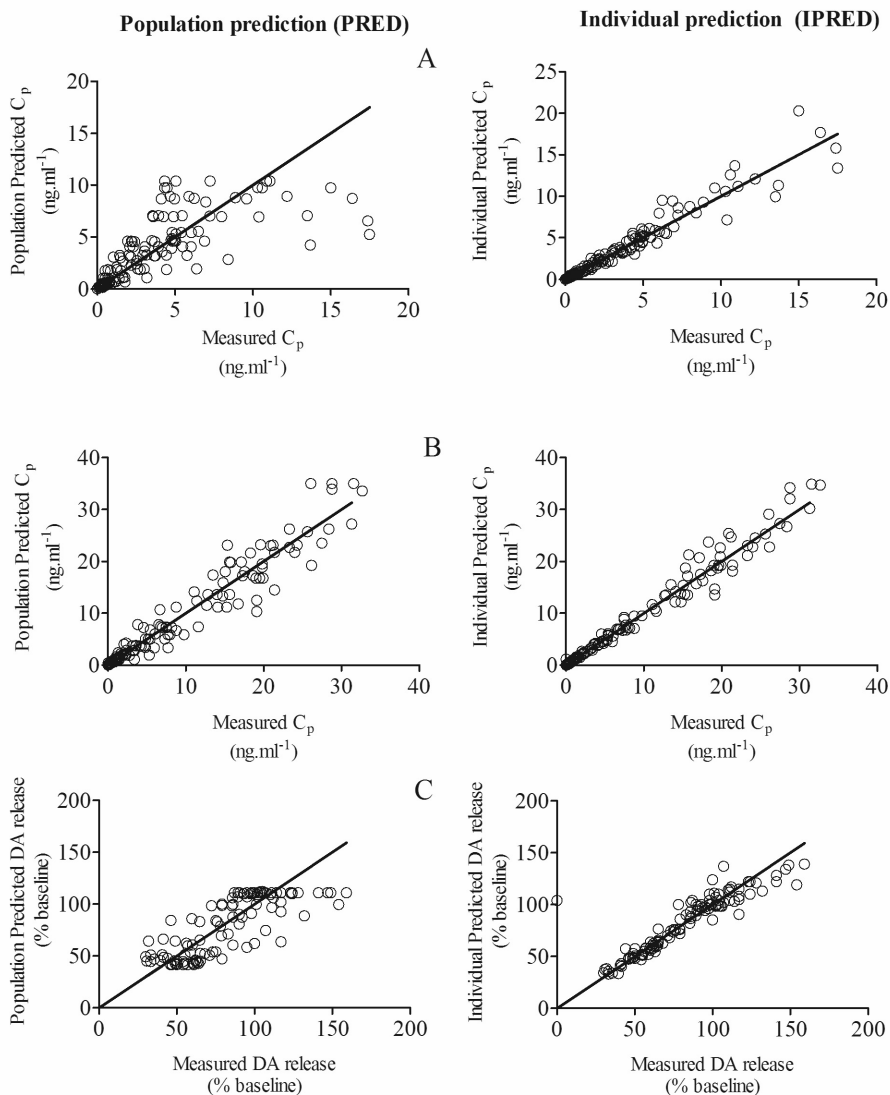
Figure 4.5 Diagnostic plots of the plasma and striatum analysis using the integrated PK-PD model. A: Analysis of plasma concentration (Cp) of (S)-5-OH-DPAT following IV infusion and iontophoresis during the PK study. B: Analysis of plasma concentration (Cp) of (S)-5-OH-DPAT following IV infusion and iontophoresis during the microdialysis study. C: Analysis of DA release in striatum, expressed as % of baseline values, following IV infusion and iontophoresis. In every panel the population prediction (left graph) and individual prediction (right graph) vs the measured value is displayed.

Table 4.1 The population estimates obtained from fitting the plasma profile and/or the pharmacological response following transdermal iontophoresis. During the PK study, two different current densities (75 and 150 µA.cm-2) were applied consecutively for 2h. During the PK-PD study, a current density of 250 µA.cm-2 was applied for 1.5h.

parameter	unit	PK study Estimate		PK study Between animal variabity		PK-PD study Estimate		PK-PD study Between animal variabity	
		mean	RSE %	mean	RSE %	mean	RSE %	mean	RSE %
V_2	L	0.5	6			0.5	18	0.100	71
V_3	L	1.7	16	0.189	46	0.7	16	0.109	42
CL	L.h^{-1}	2.6	13	0.194	45	2.0	6	0.027	29
Q	L.h^{-1}	2.5	9			1.9	23	0.218	44
J_{ss} 75	nmol.cm^{-2}.h^{-1}	24.7	29						
J_{ss} 150	nmol.cm^{-2}.h^{-1}	51.3	30						
J_{ss} 250	nmol.cm^{-2}.h^{-1}					87.3	8	0.000	/
K_R	h^{-1}	2.2	21			5.5	26	0.000	/
k_{e0}	h^{-1}					3.9	10	0.192	77
IC_{50} IONTO	ng.ml^{-1}					4.4	13	0.162	50
IC_{50} IV	ng.ml^{-1}					1.9	11		
N						3.2	10	0.000	/
I_{MAX}	DA%					41.6	8	0.045	36
Sigma PK		0.037	12			0.0246	20		
Sigma PD						0.0120	22		

The effect of (S)-5-OH-DPAT (striatal DA release) was assessed by two pharmacodynamic models. The first model consisted of a turnover model, i.e. with indirect response type I[14], and the second model consisted of an effect compartment and a sigmoid I_{max} model.[13] The AIC of the effect compartment was lower than the turnover model. In addition, an improved distribution of the observations in the 95% C.I. of the VPC and a lower residual standard error (RSE) of the parameter estimates were observed when fitting the data with the effect compartment model (comparison not shown). Therefore the effect compartment model was selected for further evaluation of the PK-PD relationship of (S)-5-OH-DPAT. Given the small bias observed in the simulated median profiles of DA (Figure 4.4B and 4.4C), a covariate analysis was performed, which revealed differences in IC_{50} depending upon the administration route. Incorporation of the route of administration as covariate into the model improved the VPC (Figure 4.4D and 4.4E) and the objective function decreased significantly (χ^2-test; p<0.05). The resulting parameters are summarized in Table 4.1. PK

and PD parameters were estimated with good precision, as indicated by a relatively low RSE of the parameters ($\leq 26\%$).

Figure 4.4D and 4.4E depict the 95 C.I. together with the simulated median response when including route of administration as covariate in the model. It can be observed that the model slightly under- and overpredicts the median of the DA release following transdermal iontophoresis and IV infusion, respectively. Nonetheless, 95% of the observations can be found within the boundaries of the confidence interval. Finally, goodness-of-fit plots for the DA release (Figure 4.5C) show that the model accurately predicts the observed DA release for both administration routes.

4.5 DISCUSSION

The present study provides novel information on the pharmacokinetic and pharmacodynamic properties of the active enantiomer of the potent DA agonist (S)-5-OH-DPAT. Specifically, the present investigation focused on the controllability of the transdermal iontophoretic delivery of this compound with regard to the plasma concentration and the DAergic activity in the striatum.

4.5.1 Relationship between current density and plasma profile

With regard to the controllability of the plasma concentration, the relationship between the applied current density and the corresponding plasma profile was investigated. Three different current densities (75, 150 and 250 μA.cm^{-2}) were applied in 2 different studies. A comparison of the pharmacokinetic parameters however of the PK-study (using two current densities 75, 150 μA.cm^{-2}) and the PK-PD study (applying 250 μA.cm^{-2}) revealed a difference in peripheral volume of distribution (V_3), central (Cl) and peripheral clearance (Q). The difference in these pharmacokinetic parameters can be attributed to the difference in recovery period after surgery of the animals in the two studies, rather than due to differences in transport/delivery. For the PK-studies, the animals were allowed to recover for at least 1 week, whereas the PK-PD studies were executed 15-20h post surgery. Similar results were found by Torres-Molina and co-workers, who demonstrated that the placement of a permanent cannula in the jugular vein influences the PK parameters of amoxycilin and antipyrin in rats. The PK parameters depended on the time of execution of the experiment after placement of the cannula.[20] This should be taken into account when designing new experiments, especially with a cross-over design.

Despite the difference in PK parameters between the two studies, a clear linear dependency ($R^2=0.999$) was observed (Figure 4.6) between the applied current density and the *in vivo* steady state flux, calculated from the zero order mass input using the following equation[21]:

$$\text{Flux}_{SS} = \frac{I_0}{S} \tag{11}$$

In literature similar results were reported for the iontophoretic delivery *in vivo* of hydromorphone and ropinirole.[6, 22] Moreover, Patel *et al.* recently demonstrated the controllability of the plasma concentration profiles by the current density for zolmitriptan.[23] These results show that, despite differences in PK properties, the drug input into the skin can be controlled very carefully by adjusting the current density. This can be very useful in initiating therapeutic treatment with DA agonist, adjusting the dose to the demand of the individual patient.

Based on this relationship between the *in vivo* flux and the current density, the *in vivo* flux, applying a current density of 500 µA.cm^{-2}, was estimated at 174.9 nmol.cm^{-2}.h^{-1}. Despite the interspecies differences, this value differs only 21% from the *in vitro* flux across human stratum corneum (211.9±11.1 nmol.cm^{-2}.h^{-1}), when applying a current density of 500 µA.cm^{-2}.[24] This indicates that *in vitro* transport parameters can be used to predict drug delivery properties *in vivo*, even across species. Regarding the rat skin, iontophoretic transport is frequently comparable with human skin, in which iontophoresis may diminish interspecies variations in *in vitro* skin permeation studies.[25, 26]

Our findings suggest the possibility of further refinement of future experiments for the evaluation of drug delivery by iontophoresis. In fact, a model-based approach can be used to provide guidance for optimal sampling and dose selection as well as by allowing a more quantitative assessment of safety margins. This is one of the reasons why PK-PD modeling is gaining a more prominent place in the different stages of drug development.[27]

4.5.2 PK-PD relationship

Next to a controlled plasma concentration the second aim of our investigation was to characterize the PK-PD relationship of (S)-5-OH-DPAT. A previous study showed that 5-OH-DPAT, administered with transdermal iontophoresis can cause a very strong pharmacodynamic effect. However it was observed that even after 3 h post-iontophoresis the DA level (PD end-point) did not recover to its initial state.[7] In addition, during these studies choral hydrate was used as anesthetic.[7] Chloral hydrate is not considered the optimal choice for anesthesia of small animals, like rodents. Moreover several studies showed that choral hydrate influences the striatal DA turnover[28-30] and enhances the suppressive effects of several DA agonists.[31] Therefore our studies were performed following IV infusion and iontophoresis to explore the implications and validate the use of new anesthetic procedures in conjunction with on-line brain microdialysis.[10, 11] In addition, we assessed the PK-PD relationship under a wider range of exposures, ensuring reversibility of the PD effect.
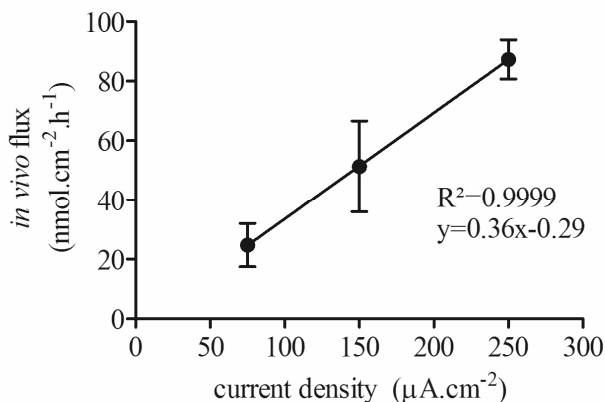
Figure 4.6 In vivo flux vs current density. Each data point presents the parameter estimate, determined with compartmental modeling, with the standard error of the parameter estimate. In each experiment 4-6 rats were used.

A mixture of fentanyl, fluanisone and midazolam was chosen to anesthetize the animals. However, it has been reported in literature that these anesthetics individually also can affect the striatal DA metabolism. Fentanyl and fluanisone can increase the DA turnover in the striatum[32-34], while midazolam has been reported to decrease the DA levels in a dose dependent manner.[35] Besides the effect of the combination of anesthetics, the effect of iontophoresis and blood sampling on the DA level was also investigated. As shown in Figure 4.4A, the stimulating effect of fentanyl and fluanisone and the inhibiting effect of midazolam on the DA release were balanced during iontophoresis. After iontophoresis the DA release increased slightly, which could indicate a dominating effect of fentanyl. Nonetheless a rat model was established with stable DA release levels during anesthesia, which enables us to investigate the DAergic effect of (S)-5-OH-DPAT following intravenous infusion and transdermal iontophoresis.

For both administration routes a decrease in striatal DA level can be observed which returns to baseline within 2 h after ending the administration. This demonstrates that a controlled reversible effect can be obtained. Moreover, DA levels seem to reach steady state following transdermal iontophoresis, in parallel to time course of concentrations in plasma. These results suggest that steady state concentrations of (S)-5-OH-DPAT translate into a steady state decrease of the DA level. Given that DA synthesis is indirectly controlled by presynaptic DA receptors, these findings suggest a continuous stimulation of the DA receptors.[36, 37] Likewise, it has been shown that stable plasma levels of rotigotine, another potent 2-aminotetralin, also result into continuous DAergic stimulation.[38] This could be of great benefit for symptomatic treatment of Parkinson's disease. It is generally believed that continuous DAergic stimulation is currently the best strategy to reduce motor complications after long-term use of DAergic agents.[5] However, further investigations are required

applying current for a longer time period with different doses to confirm the applicability of transdermal iontophoresis of DA agonists like (S)-5-OH-DPAT.

4.5.3 PK-PD modeling

The plasma profile and the DA release following IV infusion and transdermal iontophoresis were analyzed using compartmental modeling. Plotting the DA release *vs* the plasma concentration showed a counter clock-wise hysteresis (data not shown). This indicates a time delay between the plasma concentration and the pharmacological response. To account for this delay an effect compartment model was compared with an indirect response model type I.[14] In the present study, it is shown that the DA release is best described by an effect compartment in conjunction with the sigmoidal I_{max} model. This suggests that the delay between plasma concentration and pharmacological response is attributed to the distribution from plasma to site of action, rather than because of a slow onset of the effect. This is further supported by the delayed increase in striatal 5-OH-DPAT concentration following transdermal iontophoresis in Figure 4.3B. These findings shed light into the mechanisms underlying delay reported by Nugroho *et al.*, who described the DA release, following transdermal iontophoresis of 5-OH-DPAT with an indirect response model type I.[7]

As observed in Table 4.1, the IC_{50} is approximately 2.3 times lower when administering (S)-5-OH-DPAT with IV infusion compared to the IC_{50} with transdermal administration. This raises an important question regarding the role of the delivery rate: Do differences in delivery rate alter the response profiles of (S)-5-OH-DPAT? This question can be addressed by estimating the pharmacodynamic efficiency (EFF), defined as the pharmacological response per unit of concentration, as shown in the following equation:

$$EFF = \frac{AAEC}{AUC} \tag{12}$$

Where AUC (ng.ml^{-1}.min) is the area under the plasma 5-OH-DPAT concentration curve and AAEC (DA%.min) is the area above the effect curve (normalized for baseline DA levels). For the IV infusion EFF was 9.2 ± 2.3 ml.ng^{-1}, which is approximately 1.9 ± 0.8 times higher than the EFF following transdermal iontophoresis, estimated at 4.8 ± 1.7 ml.ng^{-1}. Given that the delivery rate during IV infusion was approximately 3.5 times higher than during transdermal iontophoresis, these observations suggest that a high delivery rate may improve the pharmacodynamic efficiency. In this respect, transdermal iontophoresis can be a suitable delivery technique, since the delivery rate can easily be adjusted using different current densities (Figure 4.6). For instance a loading dose, by applying a higher current density at the start of the iontophoretic delivery, can be combined with a maintenance dose, by gradually decreasing the current density to a certain level. Follow-up studies based on drug administration with different delivery rates should be performed to confirm these findings.

The use of an integrated PK-PD approach, simultaneously monitoring drug concentrations in plasma and pharmacodynamic effects, has several benefits over experimental designs in which C_p or the PD effect are evaluated independently. First, it was shown that a steady state plasma concentration may result in a continuous stimulation of the DA receptor. Second, PK-PD modeling contributes to further understanding of the mechanisms and time course of drug action. Third, PK-PD model parameters can be used to support the design of future experiments. Furthermore, the assessment of PK-PD relationships enables discrimination between delivery-specific and drug-specific parameters. This distinction is critical in drug delivery research, in that it warrants the identification of the factors which may ultimately determine treatment response *in vivo*.

In conclusion, these studies demonstrate that transdermal iontophoresis can be an excellent delivery route for continuous controlled administration of (S)-5-OH-DPAT and other potent DA agonists for the symptomatic treatment of Parkinson's disease. PK-PD modeling suggests that target distribution causes the delay between plasma concentration and drug effect. In addition, modulation of the delivery rate seems to have a direct impact on the pharmacodynamics. These results are very important for understanding of the mechanisms underlying drug transport and disposition following transdermal iontophoresis. This information will be crucial for designing a self-controlled delivery device, guided by a feedback system.

4.6 ACKNOWLEDGMENTS.

4.7 REFERENCES

1. Dixit, N.; Bali, V.; Baboota, S.; Ahuja, A.; Ali, J. Iontophoresis - an approach for controlled drug delivery: a review. *Curr. Drug Deliv.* **2007**, *4,* 1-10.
2. Tugwell, C. *Parkinson's disease in focus;* Pharmaceutical Press: London, 2008; , pp 237.
3. Rajput, A. H.; Fenton, M. E.; Birdi, S.; Macaulay, R.; George, D.; Rozdilsky, B.; Ang, L. C.; Senthilselvan, A.; Hornykiewicz, O. Clinical-pathological study of levodopa complications. *Mov. Disorders* **2002**, *17,* 289-96.
4. Syed, N.; Murphy, J.; T., Z.,Jr; Mark, M. H.; Sage, J. I. Ten years' experience with enteral levodopa infusions for motor fluctuations in Parkinson's disease. *Mov. Disorders* **1998**, *13,* 336-8.
5. Steiger, M. Constant dopaminergic stimulation by transdermal delivery of dopaminergic drugs: a new treatment paradigm in Parkinson's disease. *Eur. J. Neurol.* **2008**, *15,* 6-15.

6.   Luzardo-Alvarez, A.; Delgado-Charro, M. B.; Blanco-Mendez, J. In vivo iontophoretic administration of ropinirole hydrochloride. *J. Pharm. Sci.* **2003**, *92,* 2441-8.

7.   Nugroho, A. K.; Romeijn, S. G.; Zwier, R.; De Vries, J. B.; Dijkstra, D.; Wikstrom, H.; la-Pasqua, O.; Danhof, M.; Bouwstra, J. A. Pharmacokinetics and pharmacodynamics analysis of transdermal iontophoresis of 5-OH-DPAT in rats: In vitro-in vivo correlation. *J. Pharm. Sci.* **2006**, *95,* 1570-1585.

8.   van der Geest, R.; Danhof, M.; Bodde, H. E. Iontophoretic delivery of apomorphine I: In vitro optimization and validation. *Pharm. Res.* **1997**, *14,* 1798-1803.

9.   van der Geest, R.; van Laar, T.; Gubbens-Stibbe, J. M.; Bodde, H. E.; Danhof, M. Iontophoretic delivery of apomorphine II: An in vivo study in patients with Parkinson's disease. *Pharm. Res.* **1997**, *14,* 1804-1810.

10.   Imperato, A.; Dichiara, G. Trans-Striatal Dialysis Coupled to Reverse Phase High-Performance Liquid-Chromatography with Electrochemical Detection - a New Method for the Study of the Invivo Release of Endogenous Dopamine and Metabolites. *J. Neurosci.* **1984**, *4,* 966-977.

11.   Westerink, B. H. C. Monitoring Molecules in the Conscious Brain by Microdialysis. *Trends Anal. Chem.* **1992**, *11,* 176-182.

12.   Wright, P. M. Population based pharmacokinetic analysis: why do we need it; what is it; and what has it told us about anaesthetics? *Br. J. Anaesth.* **1998**, *80,* 488-501.

13.   Holford, N. H.; Sheiner, L. B. Understanding the dose-effect relationship: clinical application of pharmacokinetic-pharmacodynamic models. *Clin. Pharmacokinet.* **1981**, *6,* 429-53.

14.   Sharma, A.; Jusko, W. J. Characterization of four basic models of indirect pharmacodynamic responses. *J. Pharmacokinet. Biopharm.* **1996**, *24,* 611-35.

15.   Bond, G. C. Platinum Metals as Hydrogenation Catalysts. *Platinum Met. Rev.* **1957**, *1,* 87-93; 87.

16.   Oba, M.; Ohkuma, K.; Hitokawa, H.; Shirai, A.; Nishiyama, K. Convenient synthesis of deuterated glutamic acid, proline and leucine via catalytic deuteration of unsaturated pyroglutamate derivatives. *Journal of Labelled Compounds & Radiopharmaceuticals* **2006**, *49,* 229-235.

17.   Wikstrom, H.; Andersson, B.; Sanchez, D.; Lindberg, P.; Arvidsson, L. E.; Johansson, A. M.; Nilsson, J. L. G.; Svensson, K.; Hjorth, S.; Carlsson, A. Resolved Monophenolic 2-Aminotetralins and 1,2,3,4,4A,5,6,10B-Octahydrobenzo[F]Quinolines - Structural and Stereochemical Considerations for Centrally Acting Presynaptic and Postsynaptic Dopamine-Receptor Agonists. *J. Med. Chem.* **1985**, *28,* 215-225.

18.   Paxinos, G.; Watson, C. *The rat brain in stereotaxic coordinates;* Academic Press: Sydney etc., 1982; , pp gepag. VII, 12. ill. 33 cm.

19.   Holford, N. *The Visual Predictive Check-Superiority to Standard Diagnostic (Rorschach) Plots;* 2005; .

20.   Torres-Molina, F.; Aristorena, J. C.; Garcia-Carbonell, C.; Granero, L.; Chesa-Jimenez, J.; Pla-Delfina, J.; Peris-Ribera, J. E. Influence of permanent cannulation of the jugular vein on pharmacokinetics of amoxycillin and antipyrine in the rat. *Pharm. Res.* **1992**, *9,* 1587-91.

21.   Nugroho, A. K.; Della-Pasqua, O.; Danhof, M.; Bouwstra, J. A. Compartmental modeling of transdermal iontophoretic transport II: in vivo model derivation and application. *Pharm. Res.* **2005**, *22,* 335-46.

22.   Padmanabhan, R. In vitro and in vivo evaluation of transdermal iontophoretic delivery of hydromorphone. *J. Controlled Release* **1990**, *11,* 335-346.

23.   Patel, S. R.; Zhong, H.; Sharma, A.; Kalia, Y. N. Controlled non-invasive transdermal iontophoretic delivery of zolmitriptan hydrochloride in vitro and in vivo. *Eur. J. Pharm. Biopharm.* **2009**, *72,* 304-9.

24.   Ackaert, O. W.; Van Smeden, J.; De Graan, J.; Dijkstra, D.; Danhof, M.; Bouwstra, J. A. Mechanistic studies of the transdermal iontophoretic delivery of 5-OH-DPAT in vitro. *J. Pharm. Sci.* **2010**, *99,* 275-85.

25.   Godin, B.; Touitou, E. Transdermal skin delivery: predictions for humans from in vivo, ex vivo and animal models. *Adv. Drug Delivery Rev.* **2007**, *59,* 1152-61.

26.   Kanikkannan, N.; Singh, J.; Ramarao, P. In vitro transdermal iontophoretic transport of timolol maleate: effect of age and species. *J. Controlled Release* **2001**, *71,* 99-105.

27.   Rajman, I. PK/PD modelling and simulations: utility in drug development. *Drug Discovery Today* **2008**, *13,* 341-6.

28.   Ford, A. P.; Marsden, C. A. Influence of anaesthetics on rat striatal dopamine metabolism in vivo. *Brain Res.* **1986**, *379,* 162-6.

29.   Westerink, B. H.; Korf, J. Comparison of effects of drugs on dopamine metabolism in the substantia nigra and the corpus striatum of rat brain. *Eur. J. Pharmacol.* **1976**, *40,* 131-6.

30.   Zhang, W.; Tilson, H.; Stachowiak, M. K.; Hong, J. S. Repeated haloperidol administration changes basal release of striatal dopamine and subsequent response to haloperidol challenge. *Brain Res.* **1989**, *484,* 389-92.

31.   Kelland, M. D.; Freeman, A. S.; Chiodo, L. A. Chloral hydrate anesthesia alters the responsiveness of identified midbrain dopamine neurons to dopamine agonist administration. *Synapse* **1989**, *3,* 30-7.

32.   Fregnan, G. B.; Porta, R. A comparison between some biochemical and behavioural effects produced by neuroleptics. *Arzneim. -Forsch.* **1981**, *31,* 70-4.

33.   Freye, E.; Kuschinsky, K. Effects of fentanyl and droperidol on the dopamine metabolism of the rat striatum. *Pharmacology* **1976**, *14,* 1-7.

34.   Milne, B.; Quintin, L.; Pujol, J. F. Fentanyl increases catecholamine oxidation current measured by in vivo voltammetry in the rat striatum. *Can. J. Anaesth.* **1989**, *36,* 155-9.

35.   Takada, K.; Murai, T.; Kanayama, T.; Koshikawa, N. Effects of midazolam and flunitrazepam on the release of dopamine from rat striatum measured by in vivo microdialysis. *Br. J. Anaesth.* **1993**, *70,* 181-5.

36.   Roth, R. H.; Nowycky, M. C. Nonstriatal dopaminergic neurons: role of presynaptic receptors in the modulation of transmitter synthesis. *Adv. Biochem. Psychopharmacol.* **1977**, *16,* 465-70.

37.   Westfall, T. C.; Besson, M. J.; Giorguieff, M. F.; Glowinski, J. The role of presynaptic receptors in the release and synthesis of 3H-dopamine by slices of rat striatum. *Naunyn-Schmiedeberg's Arch. Pharmacol.* **1976**, *292,* 279-87.

38.   Kehr, J.; Hu, X. J.; Goiny, M.; Scheller, D. K. Continuous delivery of rotigotine decreases extracellular dopamine suggesting continuous receptor stimulation. *J. Neural Transm.* **2007**, *114,* 1027-31.

5

The *in vitro* and *in vivo* evaluation of new synthesized prodrugs of 5-OH-DPAT for iontophoretic delivery

[a]Department of Medicinal Chemistry, University Center of Pharmacy, University of Groningen, The Netherlands
[b]Division of Pharmacology, Leiden/Amsterdam Center for Drug Research, Leiden, The Netherlands
[c]Division of Drug Delivery Technology, Leiden/Amsterdam Center for Drug Research, Leiden, The Netherlands
[d]Department of Biomonitoring and Sensing, University Center of Pharmacy, University of Groningen, The Netherlands
[e]Clinical Pharmacology and Discovery Medicine, GlaxoSmithKline, Greenford, United Kingdom
[*]Contributed equally as first author

Abstract

The feasibility of transdermal iontophoretic transport of 4 novel ester prodrugs of 5-OH-DPAT (glycine-, proline-, valine- and β-alanine-5-OH-DPAT) was investigated in vitro and in vivo. Based on the chemical stability of the prodrugs, the best candidates were selected for in vitro transport studies across human skin. The pharmacokinetics and pharmacodynamic effect of the prodrug with highest transport efficiency, was investigated in a rat model. The in vitro transport, plasma profile and pharmacological response were analyzed with compartmental modeling. Valine- and β-alanine-5-OH-DPAT were acceptably stable in the donor phase and showed a 4-fold and 14-fold increase in solubility compared to 5-OH-DPAT. Compared to 5-OH-DPAT, valine- and β-alanine-5-OH-DPAT were transported less and more efficiently across human skin, respectively. Despite a higher in vitro transport, lower plasma concentrations were observed following 1.5 h current application (250 µA.cm^{-2}) of β-alanine-(S)-5-OH-DPAT in comparison to (S)-5-OH-DPAT. However the prodrug showed higher plasma concentrations post-iontophoresis, explained by a delayed release due to hydrolysis and skin depot formation. This resulted in a pharmacological effect with the same maximum as 5-OH-DPAT, but the effect lasted for a longer time. The current findings suggest that β-alanine-5-OH-DPAT is a promising prodrug, with a good balance between stability, transport efficiency and enzymatic conversion.

5.1 INTRODUCTION

Transdermal delivery has been explored thoroughly as an alternative for oral delivery and injections. However, the main hurdle for transdermal delivery is the barrier function of the skin located in the outermost layer of the skin, the stratum corneum. An attractive approach to overcome this main barrier for drug delivery is iontophoresis. By applying a small current across the skin it is possible to enhance the transport of low molecular weight molecules across the skin. One of the interesting properties of this technique is the possibility to modulate the transport rate into and through the skin. This is an important advantage for drugs with a narrow therapeutic window, such as dopamine (DA) agonists (e.g. rotigotine, apomorphine, pergolide, 5-OH-DPAT). Most of the DA agonists are considered moderate lipophillic and have a relative low solubility in aqueous solutions.[1-3] For this reason, besides a low efficiency in iontophoretic transport, the low solubility of DA agonists can be a limitation for application with transdermal iontophoresis. Increasing the maximum solubility in the donor phase can be achieved by adjusting the donor phase (co-solvent, surfactant, source of Cl$^-$-ions) or by changing the salt form. Another approach is the use of prodrugs with the desired physicochemical properties to overcome the problem of solubility and increase the efficiency in iontophoretic transport.[4] The principle goal of synthesizing prodrugs is to chemically modify an existing pharmacologically active drug in a form that can be reversed to the parent drug *in vivo*, with the aim to change the

physicochemical and/or pharmacokinetic properties. Moreover for transdermal delivery a prodrug should be enzymatically metabolized in a controllable and predictable manner once it has penetrated the main barrier, the stratum corneum.[5-7]
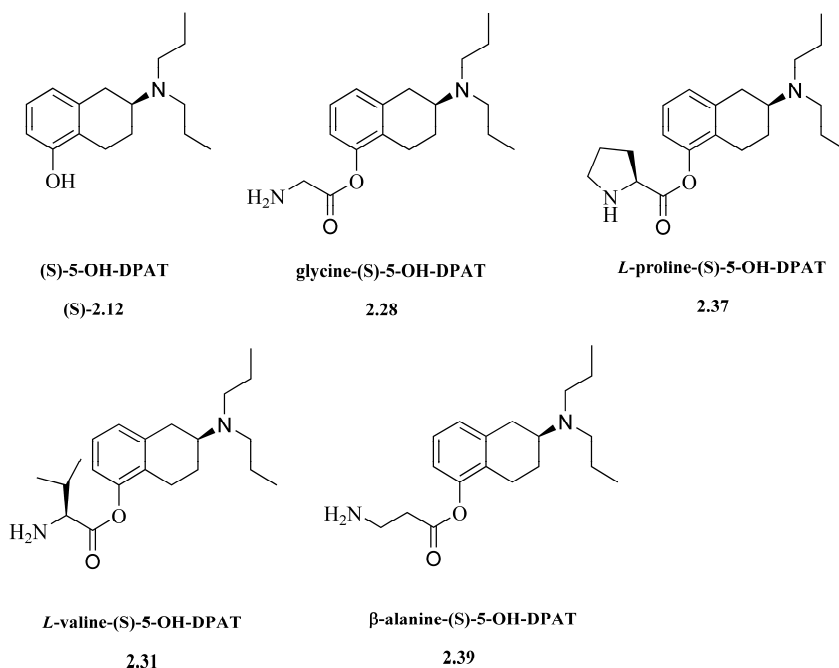
Figure 5.1 Molecular structures of (S)-5-OH-DPAT ((S)-2.12) and the 4 synthesized prodrugs, glycine-(S)-5-OH-DPAT (2.28), L-proline-(S)-5-OH-DPAT (2.37), L-valine-(S)-5-OH-DPAT (2.31) and β-alanine-S-5-OHDPAT (2.39).

The main focus of the present study is to identify a prodrug that is transported efficiently with transdermal iontophoresis and is hydrolyzed during transport through the skin. This implies a good balance between the transport rate and the rate of enzymatic conversion of the prodrug. Previous studies showed that transdermal iontophoretic delivery of 5-OH-DPAT resulted in a strong pharmacological response, which is believed to meet the requirements for symptomatic therapy with a reasonable patch size and acceptable current density. However, further improving the iontophoretic delivery could merely enhance the clinical applicability of this DA agonist by reduction of the patch size and more importantly minimization of the current density. Therefore 5-OH-DPAT, a DA agonist with limited aqueous solubility, was esterified with 4 different natural occurring amino acids (Figure 5.1). These amino acids contain an extra chargeable aminogroup, providing the possibility to investigate the influence of an additional charge on the iontophoretic delivery of 5-OH-DPAT. The stability of these 4 prodrugs is investigated and the most stable compounds are selected for transdermal iontophoretic transport. Depending on the iontophoretic transport efficiency of the selected prodrugs *in vitro* across human stratum corneum and dermatomed human skin, the *in vivo* transport of the most promising candidate is further investigated.

The plasma profile and the pharmacodynamic effect are monitored simultaneously in an animal model under anaesthetized conditions. Both *in vitro* and *in vivo* transport profiles are analyzed using compartmental modeling. Taking the hydrolysis of the prodrug into account, an adaptation to existing kinetic models is made to describe the transdermal iontophoretic delivery *in vivo*.[8, 9]

5.2 MATERIALS AND METHODS

5.2.1 General synthesis of the glycine, L-proline, β-alanine and L-valine esters of 5-OH-DPAT

The full description of the synthesis of the 4 prodrugs of 5-OH-DPAT is described in Chapter 2.[10] Briefly 5-OH-DPAT was esterified to the N-protected amino acid with the carbodiimide coupling reagent N-(3-dimethylaminopropyl)-N'-ethylcarbodiimide (EDC). 1-Hydroxybenzotriazole (HOBt) was added to suppress racemisation. The deprotection of the Boc-protected compound was carried out in 4N HCl in dioxane. After removal of the solvent and evaporation *in vacuo*, the solid hygroscopic foams were reprecipitated from dry methanol with dry ether to remove excess dioxane. The prodrugs were obtained as white hygroscopic di-HCl salts with a purity of >95% (HPLC).

5.2.2 Materials

5-OH-DPAT and 5-hydroxy-2-(N-n-propyl-N-α,α-dideutero-propylamino)-tetralin (d_2-5-OH-DPAT) (HBr salts, purity > 8%) were synthesized at the Department of Medicinal Chemistry of the University of Groningen, Groningen, the Netherlands. Silver, silver chloride (purity >99.99%), trypsin (Type III from bovine pancreas) and trypsin inhibitor (Type II-S from soybean) were obtained from Sigma-Aldrich (Zwijndrecht, The Netherlands). Acetaminophen was purchased from Brocacef BV (Maarssen, the Netherlands) and D-Mannitol was obtained from BDH Laboratory supplies (Poole, UK). Spectra/Por® RC dialysis membrane disks (cut off value of 6000-8000 Da) were purchased from Spectrum laboratories, Inc (Rancho Dominquez, Ca, USA). Tetrahydrofuran (THF, stabilized, purity >99.8%) was obtained from Biosolve (Valkenswaard, the Netherlands). Triethylamine (TEA, purity >99%) was obtained from Acros Organics (Geel, Belgium). All other chemicals and solvents were of analytical grade. All solutions were prepared in Millipore water with a resistance of more than 18 MΩ.cm.

5.2.3 Stability of glycine-, proline-, valine- and β-alanine-5-OH-DPAT

The stability of the prodrugs was investigated under various conditions. At the starting point 1 mg.ml^{-1} of proline- and glycine-5-OH-DPAT and 0.02 mg.ml^{-1} of valine- and β-alanine-5-OH-DPAT were dissolved in the buffer solution. The buffer solution was citric buffer (5 mM, pH 5.0 + 4 g.L^{-1} NaCl+ 23.1 g.L^{-1} D-mannitol), PBS pH 6.2 (NaCl: 8 g.l^{-1}, KCl: 0.19 g.l^{-1}, Na$_2$HPO$_4$.2H$_2$O: 0.43 g.l^{-1}, KH$_2$PO$_4$: 0.97 g.l^{-1}) or PBS pH 7.4 (NaCl: 8 g.l^{-1}, Na$_2$HPO$_4$: 2.86 g.l^{-1}, KH$_2$PO$_4$: 0.2 g.l^{-1}, KCl:0.19 g.l^{-1}). The solutions were continuously stirred and kept constant at the desired temperature, using a thermostat controlled water bath. If required a circular sheet of human stratum corneum (HSC) (ø=18 mm) was added to the solution and a current of 320 μA was applied. At regular time intervals samples

were taken from the solution and diluted in Millipore water, containing 0.1% trifluoroacetic acid to stop the degradation. Both the amount of remaining prodrug and the parent drug 5-OH-DPAT were quantified by RP-HPLC. The amount of remaining prodrug was plotted as a function of time to calculate the first order rate constant, k and the corresponding half life.

5.2.4 Maximum solubility of valine–5-OH-DPAT and β–alanine-5-OH-DPAT

The solubility studies of the different compounds were carried out as described elsewhere.[2] Briefly, each compound was solubilized in citric buffer 5 mM, pH 5 + 4 g.L^{-1} NaCl + 23.1 g.L^{-1} D-mannitol. Subsequently the pH in each test tube was adjusted to pH 5.0 with 1M NaOH or 1M HCl under continuous shaking. Each solution was shaken for 48 h, after which the solution was centrifuged and filtered. The concentration in each solution was determined with HPLC. Due to the limited availability of the compound and the relative high solubility, this assay was performed in monoplicate (n=1).

5.2.5 in vitro transport studies

The preparation of dermatomed human skin (DHS) and human stratum corneum was performed according to the method described previously.[11] All transport experiments were carried out as described elsewhere.[11] The donor formulation (citric buffer 5 mM, pH 5.0, NaCl: 4 g.L^{-1}, D-mannitol: 23.1 g.L^{-1}), containing the solute, was added to the anodal chamber. The cathodal chamber was filled with PBS pH 7.4. Unless described differently, the acceptor phase, maintained at 32°C, was continuously perfused with PBS pH 7.4 at a flow rate of 7.0 ml.h^{-1}. The following protocol was used: 6 h passive diffusion + 9 h iontophoresis (500 μA.cm^{-2}) + 5 h passive diffusion. Samples were collected every hour with an automatic fraction collector (ISCO Retriever IV, Beun De Ronde BV, Abcoude, The Netherlands). To stop the hydrolysis after transport through the skin and before analysis TFA (0.1% v/v) was added to each sample. The specific conditions of the individual transport studies are described below.

5.2.5.1 Iontophoretic delivery of valine-OH-DPAT and β-alanine-5-OH-DPAT

The iontophoretic delivery of valine-5-OH-DPAT across HSC and DHS was studied at a concentration of 3.9 mM.

Iontophoretic delivery of β-alanine-5-OH-DPAT across HSC was studied at 3 different concentrations (1.5 mM, 3.9 mM or 7.0 mM). For the transport study with 1.5 mM as donor phase the current was only applied for 7 h, after which the experiment was stopped. Transport studies across DHS were performed with a donor concentration of 3.9 mM. For all experiments PBS pH 7.4 was used as acceptor phase.

5.2.5.2 Electroosmotic flux across HSC

The electroosmotic flux across HSC was investigated during iontophoretic transport of valine- and β-alanine-5-OH-DPAT (3.9 mM), buffered at pH 5.0. Acetaminophen (15 mM) was added to the donor phase as a marker for the electroosmosis. PBS pH 7.4 was used as acceptor phase.

5.2.6 Hydrolysis after transport across HSC and DHS

The prodrugs valine-5-OH-DPAT and β-alanine-5-OH-DPAT are expected to hydrolyze during transdermal transport. Although stratum corneum is considered as the main barrier of the skin, the majority of the enzymes, such as esterases can be found in the epidermis.[12] Therefore the hydrolysis of the prodrugs (donor conc: 3.9 mM) was determined during iontophoresis across HSC and DHS. In case of valine-5-OH-DPAT, PBS pH 6.2 was used as acceptor phase and for β-alanine-5-OH-DPAT PBS pH 7.4 was used. The remaining prodrug was determined in the acceptor phase every hour after transport, taking the degradation in the donor phase and acceptor phase into account.

5.2.7 PK-PD studies

In the following studies the pharmacokinetic (PK) and pharmacodynamic (PD) properties of ß-ala-(S)-5-OH-DPAT following transdermal iontophoretic delivery were determined simultaneously by taking blood samples (PK) and using on-line microdialysis (PD). For these studies, the active enantiomer (S)-5-OH-DPAT, was esterified with ß-alanine. Animal procedures were conducted in accordance with guidelines published in the NIH guide for the care and use of laboratory animals and all protocols were approved by the Institutional Animal Care and Use Committee of the University of Groningen. The surgical, experimental and analytical procedures were identical to the methods used for PK-PD studies performed with the parent drug (S)-5-OH-DPAT.[9] A brief description is outlined below.

5.2.7.1 Animals

The pharmacokinetic-pharmacodynamic (PK-PD) studies were performed in albino male wistar rats (280-340 g) obtained from Harlan (Horst, the Netherlands). Prior to surgery the animals were housed at least 1 week in plexiglas cages, maximum 6 animals per cage with free access to water and standard laboratory chow. The cages were placed in a room with a controlled temperature at 21 °C and controlled humidity between 60-65% and a light-dark cycle of 12h.

5.2.7.2 Surgical procedures

Prior to surgery the rats were anaesthetized with Isofluran 2% in N_2O/O_2 (2/1). The permanent cannulations in the femoral vein and femoral artery were performed using silicone catheters (inner diameter (ID): 0.5 mm; outer diameter (OD): 0.9 mm) (UNO BV, Zevenaar, The Netherlands). After the cannulation the rats were kept under anaesthetized condition and mounted into a sterotaxic frame for the implementation of the microdialysis probes. A Y-shaped dialysis probe was used for the experiments, with an exposed tip length of 3 mm. The dialysis canulla (ID: 0.24 mm; OD: 0.34 mm) was prepared from polyacrylonitrile/sodium methallyl sulfonate copolymer (AN 69, Hospal, Bologna, Italy). The microdialysis canulla was implanted in the striatum. The following coordinates were used according to the atlas of Paxinos and Watson[13]: AP +0.9, LM ± 3.0 relative to bregma, and Vd – 6.0 below dura. The dialysis probe, filled with Ringer solution (140 mM NaCl, 3.0 mM KCl, 1.2 mM $CaCl_2$, 1.0 mM $MgCl_2$), was positioned and fixed in the burr hole under stereotaxic guidance. Thereafter the rats were housed solitary.

5.2.7.3 Experimental procedures

The PK-PD studies were performed 15-20 h after permanent cannulation and implementation of the probes. The rats were anaesthetized prior to and kept under anesthetized condition during the experiment with Hypnorm® and Dormicum® at a starting dose of 0.5 mL.kg⁻¹ and subsequent 1h doses of 0.17 mL.kg⁻¹.

The donor solution consisted of ß-ala-(S)-5-OH-DPAT (3.9 mM), buffered in citric buffer 5 mM at pH 5. Before the start of the experiment, the hair of the back of the anesthetized rat was removed with an electrical clipper and scalpel. 15 minutes after attaching the patches to the skin surface, the cathodal patch was filled with PBS pH 7.4 and the anodal patch was filled with donor solution. The volume of the patches was 2.3 ml and the active area was 2.5 cm^2. The protocol for the transdermal iontophoretic PK-PD studies was: 15 min passive diffusion + 90 min current application (250 µA.cm⁻²). The patch was removed and the skin was wiped using tissue paper. Blood samples were taken at regular time intervals: 0, 15, 30, 45, 60, 75, 90, 105, 120, 135, 165, 195, 225, 255, 285 min. The blood samples (0.2 ml) were collected using lithium-heparin containing tubes (Microvette® 200 Plasma/Lithium Heparin, Sarsted BV, Etten-Leur, the Netherlands) and subsequently the plasma samples were separated from the blood cells by centrifugation. The samples were kept at -20 °C prior to analysis with LC-MS/MS. The microdialysis probes in the striata were perfused with Ringer solution at a flow of 2 µL.min⁻¹ (CMA/102 Microdialysis Pump, Sweden). The analysis of the microdialysate samples are described below.

5.2.8 Analytical method

5.2.8.1 in vitro samples

Different HPLC methods were developed, in order to analyze simultaneously the respective prodrug, the parent drug 5-OH-DPAT and, if required, acetaminophen by RP-HPLC using a Superspher® 60 RP-select B, 75 mm-4 mm column (Merck KGaA, Darmstadt, Germany). The prodrugs of 5-OH-DPAT and acetaminophen were detected using a UV detector (Dual λ Absorbance Detector 2487, Waters, Milford, USA). The absorption wavelengths for the prodrugs and acetaminophen were 220 nm and 243 nm respectively. 5-OH-DPAT was detected using a scanning fluorescence detector (Waters™ 474, Millipore, Milford, MA, USA) with excitation wavelength and emission wavelength of 276 nm and 302 nm, respectively. The composition of the mobile phase for analyzing the respective prodrug together with 5-OH-DPAT is presented in table 1. The flow rate was set to 1.5 ml.min-1 and the volume of injection was 200 µl. Calibration curves showed a linear response when using concentrations of compounds between 0.1 and 40 µg.ml⁻¹ (R^2>0.999). The limit of detection (LOD) and limit of quantification (LOQ) for these HPLC methods can also be found in table 5.1.

5.2.8.2 Blood samples of (S)–5-OH-DPAT

Since the hydrolysis of ß-ala-(S)-5-OH-DPAT to (S)-5-OH-DPAT is occurring very rapidly in human blood plasma ($t_{1/2}$=0.24 min in 80% human blood plasma), only (S)-5-OH-DPAT was analyzed in plasma.[10] Blood samples of 5-OH-DPAT were analyzed with an on-line solid-phase-extraction-liquid-chromatography-mass spectrometry/mass spectrometry (SPE-LC-MS/MS) method, described elsewhere.[8] Briefly, after addition of the internal standard (d_2-5-OH-DPAT; 5 ng.ml⁻¹) to the collected

plasma, acetonitrile was added to precipitate the proteins. The mixture was vortexed, centrifuged, after which the supernatant was dried and redissolved in MilliQ and injected on the SPE cartridge (Hysphere Resin C8, endcapped, 10 x 4 mm (ID), 10μm SPE cartridge (Spark Holland B.V, The Netherland)). An external binary HPLC pump (Gynkotek, Germany) and an external Agilent 1200, 2/6 switch valve (Agilent Technology, USA) were used for the SPE sample trapping.

Table 5.1 Physicochemical properties of the different molecules investigated (Mw, charge/Mw ratio and cLogP) and the composition of the mobile phase with the corresponding limit of detection (LOD) and limit of quantification (LOQ).

Compound	Mw	Charge/ Mw (x10^3)	clogP[a]	Mobile phase Composition (v/v)	TEA (mM)	LOD (μg.ml^{-1})	LOQ (μg.ml^{-1})
	(g.mol^{-1})	(mol.g^{-1})					
gly-5-OH-DPAT	304.4	6.6	3.6	Ace 50 mM/ACN 85/15	0	n.d	n.d
pro-5-OH-DPAT	344.5	5.8	4.1	Ace 50 mM /ACN 74/26	0	n.d	n.d
val-5-OH-DPAT	346.5	5.8	4.8	Ace 100 mM /THF 95/5	30	0.25	0.41
β-ala-5-OHDPAT	318.4	6.3	3.8	Ace 100 mM/THF 97.5/2.5	30	1.6	2.7
5-OH-DPAT	247.4	4.0	4.3	*		1.4.10^{-3}	2.4.10^{-3}
acetaminophen	151.2	0.0	n.d	*		0.9.10^{-3}	1.4.10^{-3}

Ace: acetatebuffer pH 3.6; nd: not determined; * :mobile phase is dependent on the prodrug investigated
[a]cLogP was calculated using ACD/Chemsketch[14-16]; n.d.:not determined

First the SPE cartridge was conditioned, then the injected sample was trapped, consequently the valve was switched to the analysis column after which the SPE cartridge was cleaned. Finally the cartridge was conditioned again. To analyze the extracted sample an Agilent 1200 HPLC system with autosampler (Agilent Technology, USA) was coupled online with an Agilent 6460 Triple Quadrupole mass spectrometer (Agilent Technology, USA). The samples were analyzed by μPLC-MS/MS using an Altima HP C18 column (150X 1.0 mm; 5 μm) (Grace Davison Discovery Sciences, Belgium). The detection was performed with a triple quadrupole mass spectrometer in the positive-ion electrospray mode and all analytes were monitored with Multiple Reaction Monitoring (MRM). System operation and handling the acquired data was performed using Agilent MassHunter data acquisition software (version, B.02.00; Agilent). Calibration curves showed a linear response when using concentrations of compounds between 0.2 and 50 ng.ml^{-1} (r^2>0.999). The recovery, limit of detection (LOD) and limit of quantification (LOQ) were experimentally determined at 93.9 ± 2.9 %, 0.07 and 0.2 ng.ml^{-1}, respectively.

5.2.8.3 Microdialysate samples

To analyze the striatal 5-OH-DPAT concentration the dialysate from the probe in the right striatum was collected every 15 min resulting a total volume of 30 μL per sample. The solution was analyzed using LC-MS/MS method, described elsewhere.[8] Briefly, d_2-5-OH-DPAT.HBr was added as internal standard to a 100 μL mixture of water + 0.1% formic acid and Ringer (1:1). The HPLC system consisted of a Shimadzu LC 20 AD binary system with a Shimadzu SIL 20AC autosampler. The

samples were injected on a Grace Alltech Alltima HP C18 EPS reverse-phased column (150 x 2.1 mm (ID), 3 μm). The compounds were detected on a SCIEX API3000 triple quadrupole mass spectrometer (Applied Biosystems/MDS SCIEX) equipped with a Turbo Ion Spray interface. The mass spectrometer was operated in the positive ion mode with MRM. The detection limit of 5-OH-DPAT was 12.5 pg.ml^{-1}.

The dialysate contents of DA and its metabolites were quantified from the probe implanted at the right striatum by an on-line HPLC with electrochemical detection with the detection limit of 1 fMol per sample. An HPLC pump (LC-10AD vp, Shimadzu, Japan) was used in conjunction with an analytical cell (5011A, ESA, Chelmsford, MA, USA) and an electrochemical detector (Coulochem II, ESA) working at +300 mV for DOPAC and HIAA and -300 mV for DA. The analytical column was a Supelco Supelcosil™ LC-18-DB column (150 mm x 4.6 mm (ID), 3μm). Data were converted into percentage of basal levels. The basal levels were determined from four consecutive samples (less than 20% variation), and set at 100%. After the experiments the rats were sacrificed and the brains were removed. After removal the brains were kept in 4% paraformaldehyde solution until they were sectioned to control the location of the dialysis probes.

5.2.9 Data modeling

The data of the *in vitro* transport of valine-, β-alanine-5-OH-DPAT and 5-OH-DPAT and the PK-PD data following transdermal iontophoresis of β-alanine-(S)-5-OH-DPAT was analyzed using non-linear mixed effects modeling.

in vitro model

Previous studies suggested that two transport routes are involved in the iontophoretic delivery, linked in parallel.[17] Therefore to describe the iontophoretic transport across the skin, one zero order mass input I_0 from donor compartment into the skin during current application and two first order release constants K_{R1} and K_{R2} from skin to acceptor are used (Figure 5.2). The iontophoretic flux *in vitro* during iontophoresis can be described with the following equations:

$$J(t) = \frac{I_0}{S}(1 - e^{-K_{R1}.(t-t_L)}) + \frac{I_0}{S}(1 - e^{-K_{R2}.(t-t_L)}) \tag{1}$$

$$J_{SS} = 2.\frac{I_0}{S} \tag{2}$$

where $J(t)$ is the flux at time t and S is the diffusion area and t_L is the kinetic lag time parameter, introduced to address the time required for drug molecules to enter the skin compartment and J_{ss} as the flux at steady state.

During the post iontophoresis period only one release constant is sufficient to describe the passive flux, resulting in the following equation:

$$J(t) = \frac{P_{PI}}{S}(1 - e^{-K_{R2}.(t-T)}) + \left(\frac{I_0}{S}(1 - e^{-K_{R1}.(T-t_L)}) + \frac{I_0}{S}(1 - e^{-K_{R2}.(T-t_L)})\right).e^{-K_{R2}(t-T)} \tag{3}$$

where T is time of current application and P_{PI} is the zero order drug input due to the passive driving force in the post iontophoretic period.
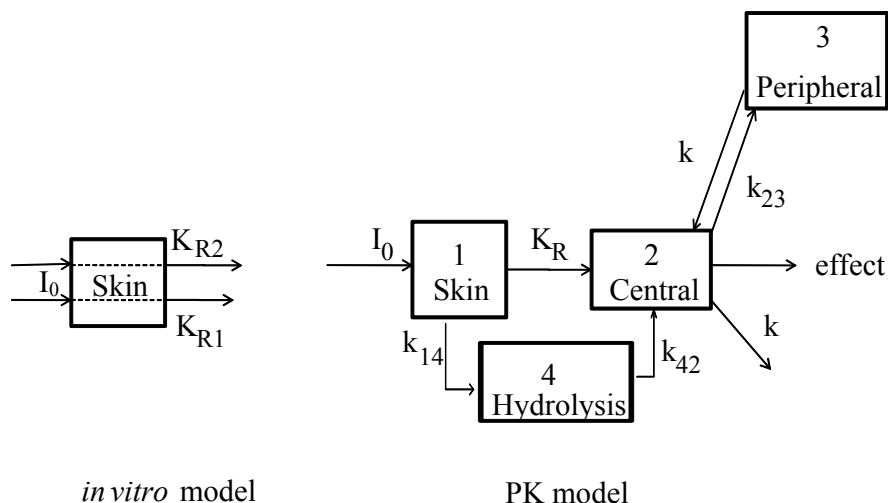
Figure 5.2 Overview of the compartmental models, used to fit the *in vitro* iontophoretic flux profiles during the iontophoresis period (*in vitro* model) and the model, used to fit the plasma profile during the iontophoretic period (PK model).

I_0: the zero order input during the time of current application

K_{R1} and K_{R2}: first order release constants from the skin to the acceptor phase (*in vitro*)

K_R: the first order release constants from the skin to the plasma (*in vivo*)

k: the elimination rate constant

k_{14}: the first order skin-hydrolysis compartment distribution rate constant

k_{42}: the first order hydrolysis compartment-plasma distribution rate constant

k_{23}: the first order plasma-peripheral distribution rate constant

k_{32}: the first order peripheral-plasma distribution rate constant

PK model

Since the hydrolysis of β-ala-(S)-5-OH-DPAT to (S)-5-OH-DPAT is occurring very rapidly in the blood, only the plasma concentration of the parent drug (S)-5-OH-DPAT was monitored. To account for the hydrolysis of β-ala-(S)-5-OH-DPAT to (S)-5-OH-DPAT during transport, an adaptation was made to the basic PK model, developed by Nugroho *et al.* to describe the plasma concentration following transdermal iontophoresis.[18] It is believed that during transport of the prodrug into and through the skin 2 effects occur: hydrolysis and depot formation. The resulting effect of both mechanisms is described with the addition of a extra compartment, as illustrated in Figure 5.2. The differential equations to describe the plasma concentration of (S)-5-OH-DPAT following transdermal iontophoretic delivery of β-ala-(S)-5-OH-DPAT are:

$$\frac{dX_1(t)}{dt} = I_0.N - K_R.X_1(t) - k_{14}.X_1(t) \tag{4}$$

$$\frac{dX_2(t)}{dt} = K_R.X_1(t) + k_{32}.X_3(t) + k_{42}.X_4(t) - k_{23}.X_2(t) - k.X_2(t) \tag{5}$$

$$\frac{dX_3(t)}{dt} = k_{23}.X_2(t) - k_{32}.X_3(t) \tag{6}$$

$$\frac{dX_4(t)}{dt} = k_{14}.X_1(t) - k_{42}.X_4(t) \tag{7}$$

With $\dfrac{dX_1(t)}{dt}$ as the rate of change in the amount of the drug in compartment i, X_i as the amount of the drug in compartment i, which refers to the skin compartment (i=1), the plasma compartment (i=2), the peripheral compartment (i=3) and the hydrolysis compartment (i=4). I_0 is defined as the zero order mass input, K_R as the first order release rate constant from skin to plasma, k as the first order elimination rate constant, k_{23} and k_{32} as the first order distribution rate constants from plasma to tissue and tissue to plasma, respectively. k_{14} and k_{42} are the rate constants for the mass transfer from the skin to hydrolysis compartment and from the hydrolysis compartment to the systemic circulation. N is a flag in the model to indicate that the input rate I_0 is only valid during the iontophoresis period.

PD model

An effect compartment model was used to describe the DA release following transdermal iontophoresis of β-ala-(S)-5-OH-DPAT. The rate of change of drug concentration $\dfrac{dC_e(t)}{dt}$ in the effect compartment can be described as follows:

$$\frac{dC_e(t)}{dt} = k_{eo}.(C_2(t) - C_e(t)) \tag{8}$$

With k_{e0} as the rate constant from plasma to the effect compartment and the elimination rate constant from the effect compartment. The striatal DA release C_{DA}, which is the pharmacodynamic end-point, is described by the sigmoid I_{max} model using the following equation:

$$C_{DA} = C_{DA}(0).\left(1 - \frac{I_{max}.C_e(t)^H}{IC_{50}{}^H + C_e(t)^H}\right) \tag{9}$$

Where I_{max} is the maximum inhibition of the DA production, IC_{50} is the plasma concentration of 5-OH-DPAT to produce 50% of I_{max}, H is the Hill-slope coefficient, $C_{DA}(0)$ is the baseline values of DA (i.e., DA concentration prior to the inhibiting effect of 5-OH-DPAT).

PK–PD data following IV infusion and transdermal delivery of (S)-5-OH-DPAT, obtained from literature, were included in the data set to obtain more reliable parameter estimates.[8] In analogy to the PK–PD model of (S)-5-OH-DPAT a covariate of route of administration for IC_{50} was added.[8] The fixed effect parameters (θ) included: I_0, K_R, clearance (CL), inter compartmental clearance (Q), volume of the central compartment (V_2), volume of the peripheral compartment (V_3), k_{e0}, I_{max} and IC_{50}. Variability in pharmacokinetic parameters was assumed to be log-normally distributed in the population. Inter-individual variability was modeled by an exponential error model as written in Equation 10:

$$P_i = \theta.\exp(\eta_i) \tag{10}$$

in which θ is the population value for the fixed effect parameter P, P_i is the individual estimate and η_i is the normally distributed interindividual random variable with mean zero and variance ω^2. The coefficient of variation (CV%) of the structural model parameters is expressed as percentage of the root mean square of the interindividual variability term. The residual error was modeled by a proportional error model as written in Equation 11:

$$C_{obs,ij} = C_{pred,ij}.(1 + \varepsilon_{ij,1}) + \varepsilon_{ij,2} \tag{11}$$

where $C_{obs,ij}$ is the jth observed concentration in the ith individual, $C_{pred,ij}$ is the predicted concentration, and ε_{ij} is the normally distributed residual random variable with mean zero and variance σ^2. The estimation of the final population parameters was performed using the conventional first order estimation method (FOCE). The PK model parameters were estimated independently and subsequently used as input for the PD analysis. During model building, goodness-of-fit was based on statistical and graphical diagnostic criteria. Model selection and identification was based on likelihood ratio test, coefficient of variation of parameter estimates, parameter correlations and goodness-of-fit plots. For the likelihood ratio test, the significance level for the inclusion of one parameter was set at p<0.05, which corresponds with a decrease of 3.84 points, in the minimum valua of the objective function (MVOF) under the assumption that the difference in MVOF between two nested models is χ^2 distributed. The following goodness-of-fit plots were subjected to visual inspection to detect systemic deviations from the model fits: individual observed versus population and individual predicted values. Finally, the performance of the population PK and PK-PD models were assessed by simulating 100 data sets with the final model parameter estimates. The evaluation of model performance also included visual predictive check (VPC), as implemented in Xpose 4 (R version 2.7.0, R-foundation).[19]

5.2.10 Data analysis

All data are presented as mean ± standard deviation (SD). When a statistical analysis was performed comparing only 2 groups, a Students t-test was used. When 3 or more groups were compared, a 1-way ANOVA statistical analysis was executed. Comparing effect of two factors simultaneously was performed using 2-way ANOVA. If the overall p-value was less than 0.05, a bonferonni post-test was applied to compare different groups. For all statistical analysis a significance level of p<0.05 was used.

5.3 RESULTS

5.3.1 Stability of prodrugs of 5-OH-DPAT in different conditions

A series of prodrugs of 5-OH-DPAT were synthesized by esterification of 5-OH-DPAT with different amino acids.[10] Because ester bounds are known to be susceptible to hydrolysis, the chemical stability of prodrugs was investigated. The various conditions were selected to mimic the conditions in the different compartments during iontophoretic transport. Apparent first order rate constants for hydrolysis were determined from the slopes of various plots of percent remaining prodrug *vs* time. The corresponding half lives are presented in Figure 5.3. Glycine-5-OH-DPAT and proline-5-OH-DPAT show a limited chemical stability in a citric buffer pH 5.0 at room temperature with a half life of 9.6 and 7.5 h, respectively. Valine-5-OH-DPAT and β-alanine-5-OH-DPAT are stable under this condition with a half life of 318 and 692h, respectively. However increasing the pH from 5.0 to 6.2 at room temperature (RT) decreases the half life of both valine- and β-alanine-5-OH-DPAT to 7.6 h and to 64.2h, respectively. Further increasing the pH to 7.4 decreases the half life of the prodrugs to 0.7 and 4.5h for valine- and β-alanine-5-OH-DPAT,

respectively. Increasing the temperature from RT to 32 °C, the skin temperature, decreased the stability of glycine-, valine- and β-alanine-5-OH-DPAT. For instance the half life of valine-5-OH-DPAT at pH 6.2 decreases from 7.6 to 5.1h when increasing the temperature. Current application and the presence of HSC however do not affect the stability of the prodrugs. Since valine- and β-alanine-5-OH-DPAT are the most stable prodrugs, these 2 compounds were selected for further investigations, concerning solubility and transdermal transport.
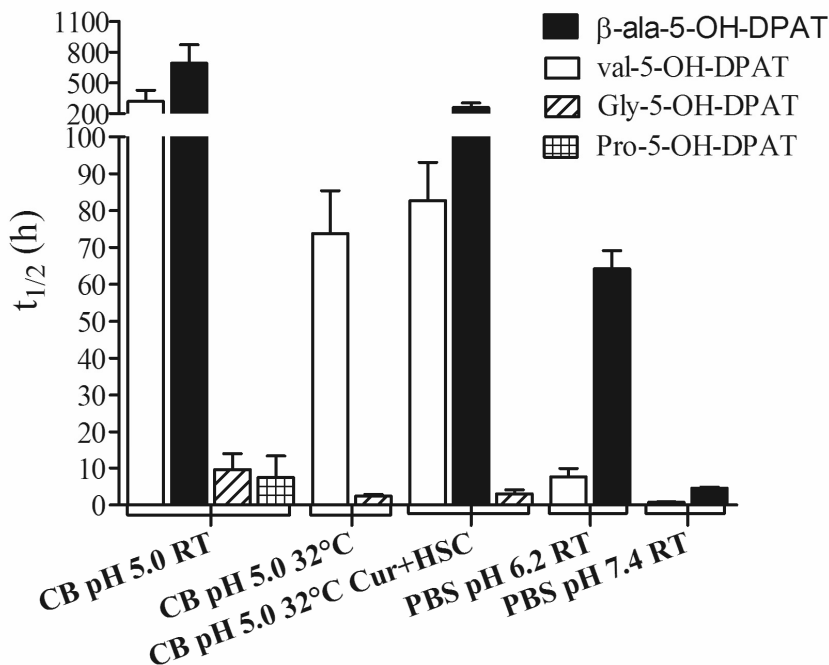
Figure 5.3 The half life (t1/2) of the hydrolysis of the prodrugs glycine-5-OH-DPAT (striped bar), proline-5-OH-DPAT (blocked bar), valine-5-OH-DPAT (white bar) and β-alanine-5-OH-DPAT (black bar) under various conditions. The data are presented as estimate + the upper limit of the estimate. CB: citric buffer 5 mM; RT: room temperature; HSC: human stratum corneum; Cur: current 320 µA.

5.3.2 Solubility of valine- and β-alanine-5-OH-DPAT

The maximum solubility was determined in citric buffer 5.0 mM pH 5 as this is the donor solution, used for transport studies. The maximum solubility of valine-5-OH-DPAT is 232.2 mM. With respect to β-alanine-5-OH-DPAT the maximum solubility is expected to be higher than 832.2 mM. At this concentration the maximum solubility of β-alanine-5-OH-DPAT is not yet reached. However, the study was discontinued due to the limited availability of the compound.
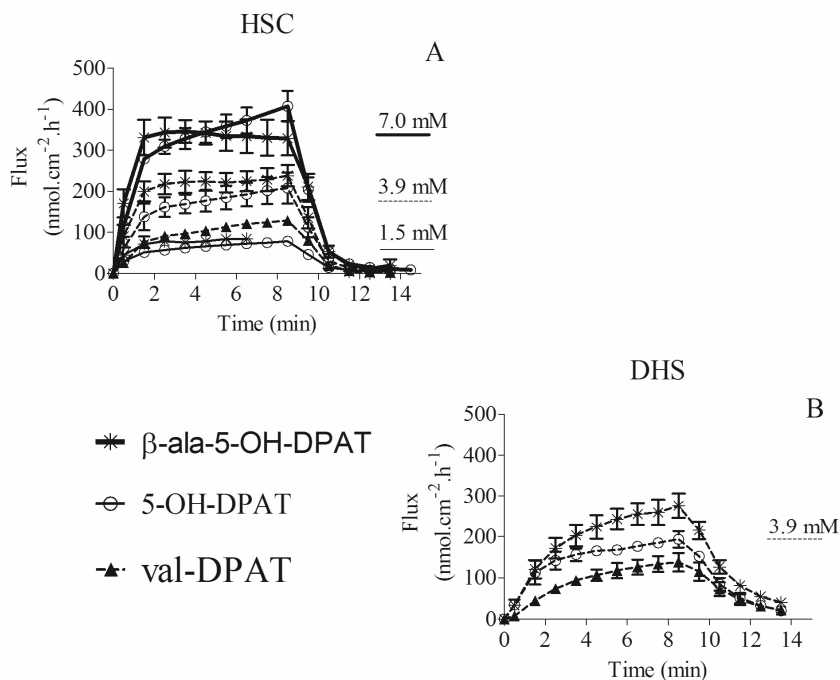
Figure 5.4 *In vitro* flux profiles of valine-5-OH-DPAT (closed triangle), β-ala-5-OH-DPAT (star) and 5-OH-DPAT (open circle). **A:** Iontophoresis of valine-5-OH-DPAT (only 3.9 mM (intermittent line)) and β-ala-5-OH-DPAT and 5-OH-DPAT at 3 different concentrations (1.5 (solid line), 3.9 (intermittent line), 7.0 mM (thick solid line)) across stratum corneum. **B:** Iontophoresis of 3.9 mM valine-5-OH-DPAT, β-ala-5-OH-DPAT and 5-OH-DPAT across dermatomed human skin. PBS pH 7.4 was used in all experiments as acceptor phase.

5.3.3 In vitro iontophoresis of the two prodrugs in comparison to 5-OH-DPAT

Figure 5.4 illustrates the iontophoretic flux profiles of the prodrugs at different concentrations under various conditions. The flux profiles of the parent drug, adapted from literature, were added to the graphs for comparison.[20] In case of the prodrugs the non-hydrolyzed and the hydrolyzed fraction of the prodrug are added and the resulting total flux is displayed in figure 5.4. The iontophoretic transport of across HSC of the two prodrugs was evaluated in comparison to each other and their parent drug 5-OH-DPAT, using PBS pH 7.4 as acceptor phase (Figure 5.4A). The flux after 9h current application of β-alanine-5-OH-DPAT (238.0 ± 26.1 and 329.6 ± 41.9 nmol.cm^{-2}.h^{-1}) across HSC is not significantly different from the flux of the parent drug 5-OH-DPAT (207.7 ± 38.0 and 407.7 ± 37.0 nmol.cm^{-2}.h^{-1}) at 3.9 and 7.0 mM donor concentrations ($p>0.05$; 2-way ANOVA). Since the assay of iontophoretic delivery of 1.5 mM β-alanine-5-OH-DPAT was stopped after 7h of current application this time point was chosen to compare the flux of prodrug and parent

drug. A similar flux was observed for β-alanine-5-OH-DPAT (84.1 ± 5.6 nmol.cm^{-2}.h^{-1}), compared to 1.5 mM 5-OH-DPAT (78.2 ± 6.2 nmol.cm^{-2}.h^{-1}) ($p < 0.05$; t-test).

The results of the transport studies across DHS, with PBS pH 7.4 as acceptor phase, are depicted in Fig. 5.4B. 2-way ANOVA was performed to analyze the Flux after 9h of current application (Flux$_{9h}$) across HSC and DHS for all the compounds at 3.9 mM. An overall significant difference could be observed between the Flux$_{9h}$ of the different compounds, which was due to compound variation and not due to the use of the different skin types ($p < 0.05$). Bonferonni's post-test demonstrated that the Flux$_{9h}$ of the prodrug β-alanine-5-OH-DPAT is significantly higher compared to the Flux$_{9h}$ of valine-5-OH-DPAT across DHS and HSC. In addition only across DHS the Flux$_{9h}$ of β-alanine-5-OH-DPAT is significantly higher than the Flux$_{9h}$ of the parent drug, 5-OH-DPAT. Furthermore the Flux$_{9h}$ of valine-5-OH-DPAT was significantly lower compared to the Flux$_{9h}$ of the parent drug across HSC and DHS.

Acetaminophen (15 mM) as electroosmotic marker was added to the donor concentration to quantify the electroosmotic flux. 1-way ANOVA, with a bonferonni post test showed that the electroosmotic flux during transport of valine-5-OH-DPAT (7.8 ± 1.9 nmol.cm^{-2}.h^{-1}) is significantly lower than the electroosmotic flux of 5-OH-DPAT (13.7 ± 3.4 nmol.cm^{-2}.h^{-1}) ($p < 0.05$), however not significantly different from β-alanine-5-OH-DPAT (11.7 ± 4.2 nmol.cm^{-2}.h^{-1}) ($p > 0.05$). Also the electroosmotic flux of 5-OH-DPAT and β-alanine-5-OH-DPAT are not significantly different ($p > 0.05$).

The iontophoretic transport profile across HSC and DHS of 3.9 mM β-alanine-5-OH-DPAT was modeled using Equations 1 and 3. The resulting parameters are displayed in Table 5.2. The estimated steady state flux, calculated with Equation 2, is higher for DHS, compared to HSC. The lag time (T_{lag}) and passive driving force post iontophoresis (Pass=P_{PI}/S) are also higher for DHS, whereas the release constants K_{R1} and K_{R2} are lower compared to HSC.

5.3.4 Hydrolysis during transport through HSC and DHS

Approximately $19.8 \pm 2.6\%$ and $55.4 \pm 15.1\%$ of β-alanine-5-OH-DPAT is hydrolyzed in 5-OH-DPAT when transported across HSC and DHS, respectively, using PBS pH 7.4 as acceptor phase. A similar observation is found for val-5-OH-DPAT, using PBS pH 6.2 as acceptor phase: $26.8 \pm 5.4\%$ and 100% valine-5-OH-DPAT is converted into 5-OH-DPAT when transported through HSC and DHS, respectively.

5.3.5 In vivo iontophoretic delivery of ß-ala-(S)-5-OH-DPAT

The PK and PD of the active S-enantiomer of the most promising prodrug ß-ala-(S)-5-OH-DPAT following transdermal delivery were investigated simultaneously. For comparison the plasma-, striatum profile and the DA release following transdermal iontophoresis of the

parent drug (S)-5-OH-DPAT, adapted from literature, are added to the resulting graphs (Figure 5.5B-D).[8]
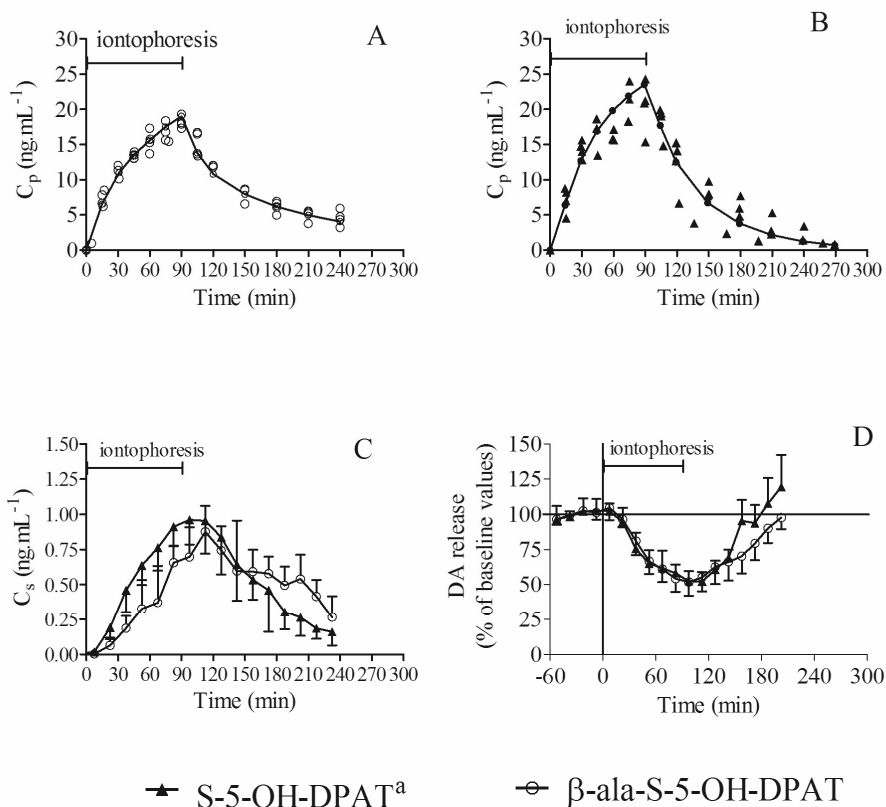
Figure 5.5 Resulting graphs of the PK-PD study with β-ala-(S)-5-OH-DPAT (open circle) together the results of (S)-5-OH-DPAT (closed triangle), adapted from literature. The observed plasma concentration (C_p) of (S)-5-OH-DPAT, following transdermal iontophoresis of β-ala-(S)-5-OH-DPAT **(A)** and (S)-5-OH-DPAT **(B)** are presented together with the population prediction (PRED)(full line). **C:** The striatal concentration of (S)-5-OH-DPAT (C_s), presented as mean ± SD, following iontophoretic delivery of β-ala-(S)-5-OH-DPAT and (S)-5-OH-DPAT. **D:** The DA release in the striatum, as % baseline, presented as mean ± SD, following iontophoretic delivery of β-ala-(S)-5-OH-DPAT and (S)-5-OH-DPAT. [a]adapted from literature[8]

5.3.5.1 Plasma profile

The prodrug is rapidly hydrolyzed to (S)-5-OH-DPAT in blood plasma, since the half life is 0.24 min in 80% human blood plasma.[10] Therefore the plasma concentration of the parent drug (S)-5-OH-DPAT was monitored during the PK-PD study. No detectible amount of (S)-5-OH-DPAT was observed after 15 min of passive diffusion (data not shown). Current

application starts at t=0 min, as depicted in Figure 5.5A. As can be observed current application results in immediate increase in plasma concentration. After 90 min of current application, the plasma profile tends towards a steady state situation. The resulting plasma concentration at time=90 min is 18.2±0.8 ng.ml^{-1}. After current application is discontinued and the patch is removed, the profile shows a decline in plasma concentration, which is best described with a 2-compartmental model.

5.3.5.2 Striatum profile

The 5-OH-DPAT concentration of the microdialysate samples of the left striatum was analyzed following transdermal iontophoresis of ß-ala-(S)-5-OH-DPAT. With a delay of approximately 7.5 min, the striatal 5-OH-DPAT concentration (C_s) increased when starting iontophoresis to a maximum level of 0.88±0.18 ng.ml^{-1}. This maximum was reached 22.5 min after switching off the current (t=112.5 min). After this time point C_s declines again.

5.3.5.3 Pharmacodynamic effect

With on-line microdialysis the DA concentration (the pharmacodynamic end-point) in the right striatum was monitored. The resulting DA release profile (mean ± SD) is depicted in Figure 5.5D. Prior to iontophoresis the DA level was monitored and the average DA level from 4 consecutive points was set to 100%. As can be observed, when starting iontophoresis the DA level decreases with a lag time between 7.5 and 22.5 min. The DA level decreases to near steady state level of 48.6±8.2% baseline, 94.5 min after the start of iontophoresis. After removal of the patch, the DA level recovers again to its initial state (DA release=100%) at time=189.2±12.1 min following prodrug iontophoresis.

5.3.6 Non-linear mixed effects modeling: model evaluation

The *in vitro* transport flux profiles, the plasma profile and the pharmacodynamic effect are modeled with non linear mixed effects modeling, using compartmental models. The resulting parameter estimates are depicted in Table 5.2. A relatively low Residual Standard Error (RSE%) for the fixed *in vitro* (≤ 35%) and *in vivo* parameters estimates (≤ 23%) indicates a reliable prediction of the estimates. Moreover Figure 5.6A and B, displaying the visual predictive check (VPC), demonstrates that the *in vivo* observations are well distributed between the 2.5th and the 97.5th percentiles. This indicates that the variability, predicted by the PK/PD model, corresponds with the observed variability. In addition the diagnostic plots of the PK and PD profile, shown in figure 5.6C-F, indicate that the proposed PK-PD model adequately describes the plasma profile and pharmacodynamic effect.

Table 5.2 The resulting population estimates of simultaneous modeling the plasma concentration and DA release following transdermal iontophoresis of β-ala-(S)-5-OH-DPAT (3.9 mM) in male wistar rats. The resulting parameters of fitting the in vitro transdermal iontophoretic transport of β-ala-5-OH-DPAT (3.9 mM) across human stratum corneum (HSC) and dermatomed human skin (DHS) is depicted. PBS pH 7.4 was used as acceptor phase for the in vitro experiments.

		Estimate		Between animal variability				Estimate		Between subject variability	
Para-meter	unit	mean	RSE %	mean	RSE %	Para-meter	unit	mean	RSE %	mean	RSE %
PK-PD						**HSC (*in vitro*)**					
V_2	L	0.46	18	0.13	97	J_{ss} 500	*	272.5	4		
V_3	L	0.78	16	0.07	52	K_{R1}	h^{-1}	0.278	28	0.516	82
CL	$L.h^{-1}$	2	6	0.02	38	K_{R2}	h^{-1}	1.69	8	0.035	23
Q	$L.h^{-1}$	1.96	21	0.16	73	T_{lag}	h	0.005			
J_{ss} 250	*	110.6	8			Pass	*	n.d.			
K_R	h^{-1}	0.31	23								
k_{14}	h^{-1}	5.06	23			Sigma 1		0.019	17		
k_{42}	h^{-1}	4.79	21			Sigma 2		1.93	36		
k_{eo}	h^{-1}	3.79	12	0.19	48						
IC_{50}	$ng.ml^{-1}$	4.50	12	0.07	35						
N		3.12	9			**DHS (*in vitro*)**					
I_{max}		40.9	7	0.03	39	J_{ss} 500	*	381.3	7		
						K_{R1}	h^{-1}	0.069	35	0.212	23
						K_{R2}	h^{-1}	0.588	5	0.3	51
						T_{lag}	h	0.22	10		
						Pass	*	29.1	14	0.045	33
Sigma 1	PK	0.02	24			Sigma 1		0.002	67		
Sigma 1	PD	0.01	20			Sigma 2		18.4	59		

*: unit of J_{ss} and Pass is: $nmol.cm^{-2}.h^{-1}$

Sigma 1: proportional error; Sigma 2: additive error

n.d.: not determined because the parameter value was constrained to 0

5.4 DISCUSSION

The general aim of the present study is to evaluate different prodrugs and select the best candidate(s) for transdermal iontophoretic delivery. The presence of enzymes in the skin, such as esterases and amidases, makes the use of prodrugs an interesting approach for transdermal delivery. The prodrugs can be tailored to improve drug delivery and during transport across the skin, the enzymes hydrolyze the prodrugs to their active parent drug.[7]

5.4.1 Chemical stability and solubility

Ester prodrugs, as presented in this paper, are not only susceptible to enzymatic, but also to chemical hydrolysis. The stability of the prodrugs in different aqueous solutions is highly dependent on the side chain, esterified with 5-OH-DPAT (stability: glycine < proline < valine < β-alanine). Based on these results valine- and β-alanine-5-OH-DPAT were selected for further investigating the transdermal iontophoretic transport across human skin.

Esterification of 5-OH-DPAT with valine and β-alanine improved its solubility tremendously. The solubility of valine- and β-alanine-5-OH-DPAT was respectively 4 and more than 14 times higher, compared to its parent drug 5-OH-DPAT.[20] A higher solubility enables reduction of the patch volume, while keeping sufficient amount of drug in the patch. Presumably addition of an extra chargeable amine group contributes substantially to the solubility of the prodrugs.
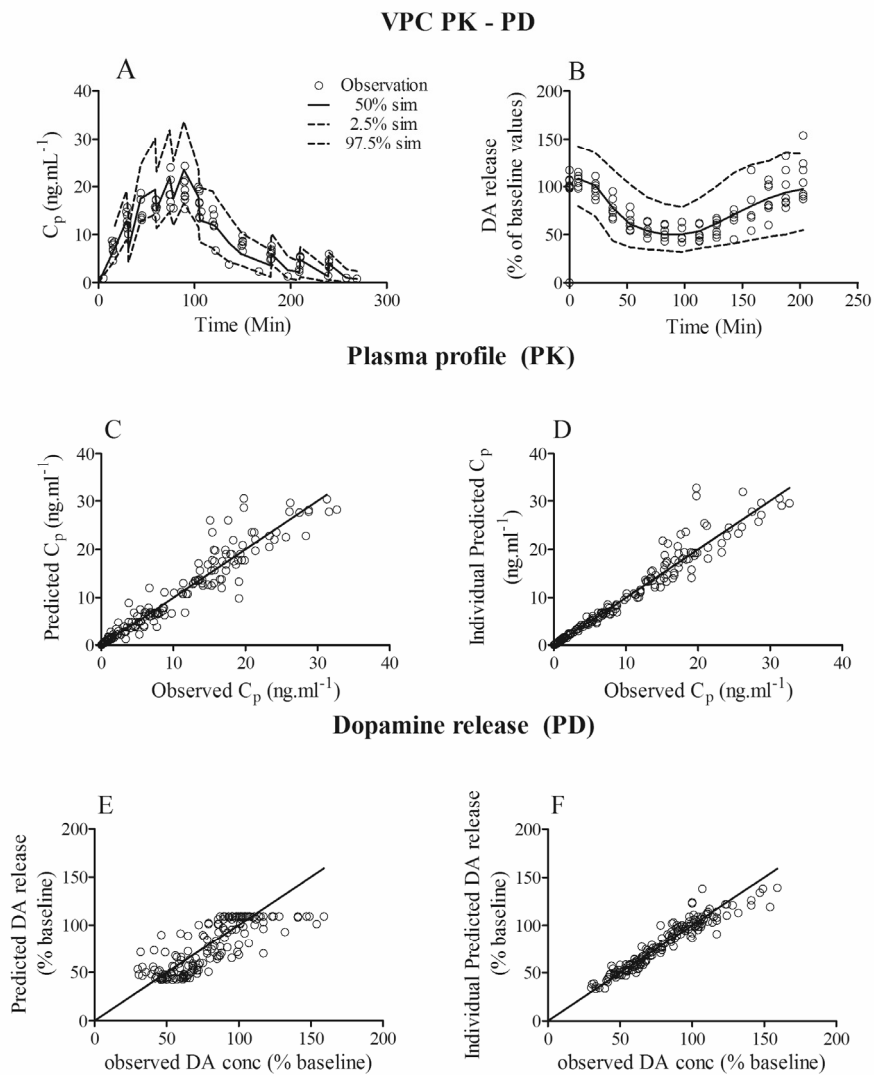
5.4.2 Transdermal iontophoresis in vitro

At pH 5.0 both prodrugs have an additional charge compared to 5-OH-DPAT. When increasing the charge from monovalent to bivalent, this affects in several ways the transport: (i) bivalent ions have a larger hydrated volume, as suggested by Lai and Roberts, which can result in a reduced flux[21], (ii) bivalent ions interact more with charged sites in SC, which according to Phipps *et al.* will result in a reduced flux[22] and (iii) an increase in the charge/molecular weight ratio results in an equivalent higher electromigrative flux.[23] It is suggested that the lipophilicity, indicated by the cLogP (Table 5.1), of the prodrugs influences the balance between these three factors and therefore affects the transport efficiency.[14-16] Only for the more hydrophilic prodrug β-alanine-5-OH-DPAT with a charge/Mw ratio which is 1.5 times higher compared to 5-OH-DPAT, resulted in almost in an equivalent increase (1.4 times) in the total flux after 9h of current application across DHS. The flux of β-alanine-5-OH-DPAT is less affected by the increased hydrated volume and the skin interaction. In contrast valine-5-OH-DPAT with a hydrophobic prodrug moiety is retained more by the skin and shows a decreased flux compared to 5-OH-DPAT. This hypothesis is strengthened by the decreased electroosmotic flux during transport of valine-5-OH-DPAT. Valine-5-OH-DPAT is retained more strongly and the two positive charges cause a neutralization of the skin negative charges, resulting in a reduced electroosmotic flux. Furthermore, the transport of valine-5-OH-DPAT is less affected by the charge/molecular weight ratio. These results are in agreement with the computational studies performed by Schuetz *et al.*, who predicted with a 3D quantitative structure-permeation relationship that iontophoresis was favored by peptide hydrophilicity and hindered by voluminous localized hydrophobicity.[24]

Besides the transport efficiency it is also important to determine the rate of hydrolysis during iontophoretic transport across human skin in order to be able to predict the amount of prodrug and parent drug that will taken up by the blood stream. In analogy to the chemical stability, β-alanine-5-OH-DPAT is the more stable prodrug. For both prodrugs an increased hydrolysis is observed when transported across DHS. This increased hydrolysis rate is the result of 2 mechanisms. First, the presence of enzymes, such as esterases, is more abundant in the epidermis. Second, the increased migration time through DHS and the slower release from the DHS, reflected by K_{R1} and K_{R2} (Table 5.2), results in a possibly longer interaction of enzymes with the prodrugs augmenting the hydrolysis rate. The remaining prodrug that is not hydrolyzed during transdermal transport is expected to be

hydrolyzed rapidly when taken up by the blood stream, since the enzymatic half life of valine- and β-alanine-5-OH-DPAT in 80% human blood plasma was 0.22 and 0.24 min, respectively.[10]

VPC PK - PD

Plasma profile (PK)

Dopamine release (PD)

Figure 5.6. Diagnostic plots of simultaneous fitting the plasma concentration (**A, C, D**) and the DA release (**B, E, F**) following the transdermal iontophoresis of β-ala-(S)-5-OH-DPAT. Depicted are the observations (open circles) together with the interquantile concentration range (2.5%-97.5%, intermittent line) and the median (50%, solid line) of the plasma profile (**A**) and the DA release profile (**B**). A number of 100 samples were simulated based on the final parameter estimates. **C,E:** population predicted vs the observed data. **D,F:** individual prediction vs the observed data.

160

5.4.3 PK-PD properties

The pharmacokinetic and pharmacodynamic properties of β-alanine-(S)-5-OH-DPAT, the more stable and soluble prodrug with improved *in vitro* transport efficiency, were investigated in an animal model. Under anesthetized conditions blood samples were taken and the DA level in the striatum (pharmacodynamic end-point) was monitored on-line with microdialysis. This animal model is identical to the animal model used to investigate the PK-PD properties of (S)-5-OH-DPAT, which enables us to compare the prodrug to its parent drug.[8] The plasma concentration profile of (S)-5-OH-DPAT (C_p) following transdermal iontophoresis of the prodrug differs on 3 aspects from the profile following (S)-5-OH-DPAT administration, as can be observed in Figure 5.5A-B. (i) The increase in plasma concentration during current application is slower for the prodrug than for the parent drug. This is reflected by a decreased skin release constant K_R for the prodrug (Table 5.2).[8] (ii) After 90 min of current application the population predicted C_p is lower for β-ala-(S)-5-OH-DPAT (19 ng.ml^{-1}) than for (S)-5-OH-DPAT (23.5 ng.ml^{-1}). (iii) During the elimination phase the C_p profile is different following administration of prodrug *vs* parent drug. It is hypothesized that these 3 differences can be partially attributed to the hydrolysis of the prodrug during transdermal transport, assuming the hydrolysis in blood plasma is occurring instantaneously. Furthermore it is believed that after penetration through the stratum corneum depot formation of the prodrug in the viable epidermis also delays the release to the systemic circulation. The resulting effect was included in the PK-model by adding an extra compartment between the skin and the central compartment (Figure 5.2). This model adequately described the plasma profile following transdermal administration of the prodrug (Figure 5.6).

In addition the resulting parameter estimates corresponded very well with the parameters of (S)-5-OH-DPAT obtained for the PK-PD study.[8] It can be observed in Figure 5.5C that in analogy to C_p the increase in C_s during the absorption phase is faster and that the striatal clearance is going more rapidly following iontophoresis of the parent drug (S)-5-OH-DPAT. Finally the difference in C_p and C_s profile following prodrug *vs* parent drug administration resulted also in a different striatal DA release profile (Figure 5.5D). During the iontophoretic period no difference was observed in DA release with the same maximum. This suggests that despite a lower steady state plasma concentration the same maximum effect can be achieved. Post-iontophoresis however the time for the DA release to recover to baseline values post-iontophoresis was significantly longer for the prodrug (99.2±12.1 min) compared to (S)-5-OH-DPAT (79.4±1.3 min) (t-test; p<0.05). This can be attributed to higher C_p values after removal of the patch due to delayed skin release. On the one hand, this prolonged effect can be a drawback to initiate therapy to treat Parkinson's disease, since rapid changes in delivery schemes may be required. On the other hand, the prolonged effect of the prodrug can be beneficial for patients who suffer from nocturnal disturbances. Nocturnal disturbances are one of the most common non-motor complications

in patients with Parkinson's disease.[25] It is believed that continuous stimulation of the DA receptor during the night can reduce the occurrence of nocturnal disturbances.[26]

5.4.4 *in vitro-in vivo* correlation

Fitting *in vitro* and *in vivo* transport using compartmental modeling allowed us to compare both iontophoretic transports. Different kinetic models were used to describe the *in vitro* and *in vivo* transport of the prodrug β-alanine-(S)-5-OH-DPAT. This suggests that different transport mechanisms can be involved *in vitro* and *in vivo*. These differences can at least partially be attributed to 3 factors. First, the structure of human skin differs from the structure of rats. Mainly the thickness of the different skin layers, the stratum corneum lipid composition and the density of hair follicles will contribute to the difference.[27] But previous studies showed that iontophoresis under constant current conditions diminishes the interspecies variations[28] and that rat skin has comparable permeation kinetic parameters with human skin.[27] Second, the clearance of the penetrant by the acceptor flow may be different from the clearance *in vivo* by the microcirculation in the skin.[27] Third, the activity of the esterase *in vivo* may be different from the esterase activity in freshly excised skin. Despite these differences a good correlation was observed between the steady state flux *in vitro* and *in vivo*. Assuming that there is a linear correlation *in vivo* between the flux and the current density[8], applying a current density of 500 µA.cm^{-2} would result in an *in vivo* steady state flux ($J_{ss}=I_0/S$) of 221.2 nmol.cm^{-2}.h^{-1}. This flux corresponded best with the *in vitro* J_{ss} across HSC (272.5 nmol.cm^{-2}.h^{-1}) compared to the J_{ss} across DHS (381.3 nmol.cm^{-2}.h^{-1}). This suggests that transport across HSC can provide valuable information for prediction towards the *in vivo* situation for this particular compound. Whether this is also the case for other drugs, remains to be established.

In conclusion this study demonstrates the potential of improving solubility, iontophoretic transport and changing the plasma profile and the PD effect of the promising DA agonist 5-OH-DPAT with the use of prodrugs. A good balance was found between an efficient transport rate and enzymatic conversion to the parent drug during transdermal transport. Of the synthesized prodrugs, presented in this research, β-alanine-5-OH-DPAT is the most promising prodrug and is a potential candidate for further investigation. This sufficiently stable prodrug shows a tremendous increase in solubility, which can be beneficial for manufacturing and practical use. The increased *in vitro* flux of β-alanine-5-OH-DPAT across human skin did not result in higher steady state plasma concentrations, but in a prolonged effect which reached the same maximum level as was observed with the parent drug.

5.5 ACKNOWLEDGEMENTS

Department of biomonitoring and sensing (University Center of Pharmacy, University of Groningen, the Netherlands) for his support with the animal studies.

5.6 REFERENCES

1.   Coldwell, M. C.; Boyfield, I.; Brown, T.; Hagan, J. J.; Middlemiss, D. N. Comparison of the functional potencies of ropinirole and other dopamine receptor agonists at human D2(long), D3 and D4.4 receptors expressed in Chinese hamster ovary cells. *Br. J. Pharmacol.* **1999**, *127,* 1696-702.

2.   Nugroho, A. K.; Li, G. L.; Danhof, M.; Bouwstra, J. A. Transdermal iontophoresis of rotigotine across human stratum corneum in vitro: Influence of pH and NaCl concentration. *Pharm. Res.* **2004**, *21,* 844-850.

3.   van der Geest, R.; Danhof, M.; Bodde, H. E. Iontophoretic delivery of apomorphine I: In vitro optimization and validation. *Pharm. Res.* **1997**, *14,* 1798-1803.

4.   Abla, N.; Naik, A.; Guy, R. H.; Kalia, Y. N. Topical iontophoresis of valaciclovir hydrochloride improves cutaneous aciclovir delivery. *Pharm. Res.* **2006**, *23,* 1842-1849.

5.   Laneri, S.; Sacchi, A.; di Frassello, E. A.; Luraschi, E.; Colombo, P.; Santi, P. Ionized prodrugs of dehydroepiandrosterone for transdermal iontophoretic delivery. *Pharm. Res.* **1999**, *16,* 1818-1824.

6.   Wang, J. J.; Sung, K. C.; Huang, J. F.; Yeh, C. H.; Fang, J. Y. Ester prodrugs of morphine improve transdermal drug delivery: a mechanistic study. *J. Pharm. Pharmacol.* **2007**, *59,* 917-25.

7.   Guy, R. H.; Hadgraft, J.; Bucks, D. A. Transdermal drug delivery and cutaneous metabolism. *Xenobiotica* **1987**, *17,* 325-43.

8.   Ackaert, O. W.; De Graan, J.; Shi, S.; Vreeken, R.; Pasqua, O. E.; Dijkstra, D.; Westerink, B. H.; Danhof, M.; Bouwstra, J. A. The pharmacokinetics and pharmacological effect of (S)-5-OH-DPAT following controlled delivery with transdermal iontophoresis. *J. Pharm. Sci.* **2011**, *100,* 2996-3009.

9.   Nugroho, A. K.; Romeijn, S. G.; Zwier, R.; De Vries, J. B.; Dijkstra, D.; Wikstrom, H.; la-Pasqua, O.; Danhof, M.; Bouwstra, J. A. Pharmacokinetics and pharmacodynamics analysis of transdermal iontophoresis of 5-OH-DPAT in rats: In vitro-in vivo correlation. *J. Pharm. Sci.* **2006**, *95,* 1570-1585.

10.   De Graan, J.; Ackaert, O. W.; al., E. Synthesis and evaluation of the chemical and enzymatic stability of a series of novel amino acid prodrugs of the potent dopamine D2 agonist (S)-5-OH-DPAT developed for transdermal iontophoresis. *In preparation* **2011**, .

11.   Nugroho, A. K.; Li, L.; Dijkstra, D.; Wikstrom, H.; Danhof, M.; Bouwstra, J. A. Transdermal iontophoresis of the dopamine agonist 5-OH-DPAT in human skin in vitro. *J. Controlled Release* **2005**, *103,* 393-403.

12.   Prusakiewicz, J. J.; Ackermann, C.; Voorman, R. Comparison of skin esterase activities from different species. *Pharm. Res.* **2006**, *23,* 1517-24.

13.   Paxinos, G.; Watson, C. *The rat brain in stereotaxic coordinates;* Academic Press: Sydney etc., 1982; , , pp gepag. VII, 12. ill. 33 cm.

14.   Tetko, I. V.; Gasteiger, J.; Todeschini, R.; Mauri, A.; Livingstone, D.; Ertl, P.; Palyulin, V. A.; Radchenko, E. V.; Zefirov, N. S.; Makarenko, A. S.; Tanchuk, V. Y.; Prokopenko, V. V. Virtual computational chemistry laboratory - design and description. *J. Comput. -Aided Mol. Des.* **2005**, *19,* 453-463; 453.

15.   Tetko, I. V.; Bruneau, P. Application of ALOGPS to predict 1-octanol/water distribution coefficients, logP, and logD, of AstraZeneca in-house database. *J. Pharm. Sci.* **2004**, *93,* 3103-10.

16.   Anonymous *VCCLAB, Virtual Computational Chemistry Laboratory;* 2005; .

17.   Ackaert, O. W.; De Graan, J.; Capancioni, R.; Dijkstra, D.; Danhof, M.; Bouwstra, J. A. Transdermal iontophoretic delivery of a novel series of dopamine agonists in vitro: physicochemical considerations. *J. Pharm. Pharmacol.* **2010**, *62,* 709-20.

18.   Nugroho, A. K.; Della-Pasqua, O.; Danhof, M.; Bouwstra, J. A. Compartmental modeling of transdermal iontophoretic transport II: in vivo model derivation and application. *Pharm. Res.* **2005**, *22,* 335-46.

19.   Holford, N. *The Visual Predictive Check-Superiority to Standard Diagnostic (Rorschach) Plots;* 2005; .

20.   Ackaert, O. W.; Van Smeden, J.; De Graan, J.; Dijkstra, D.; Danhof, M.; Bouwstra, J. A. Mechanistic studies of the transdermal iontophoretic delivery of 5-OH-DPAT in vitro. *J. Pharm. Sci.* **2010**, *99, 275-85*.

21.   Lai, P. M.; Roberts, M. S. An analysis of solute structure-human epidermal transport relationships in epidermal iontophoresis using the ionic mobility: pore model. *J. Controlled Release* **1999**, *58,* 323-33.

22.   Phipps, J. B.; Padmanabhan, R. V.; Lattin, G. A. Iontophoretic delivery of model inorganic and drug ions. *J. Pharm. Sci.* **1989**, *78,* 365-9.

23.   Abla, N.; Naik, A.; Guy, R. H.; Kalia, Y. N. Effect of charge and molecular weight on transdermal peptide delivery by iontophoresis. *Pharm. Res.* **2005**, *22,* 2069-78.

24.   Schuetz, Y. B.; Carrupt, P. A.; Naik, A.; Guy, R. H.; Kalia, Y. N. Structure-permeation relationships for the non-invasive transdermal delivery of cationic peptides by iontophoresis. *Eur. J. Pharm. Sci.* **2006**, *29,* 53-9.

25.   Comella, C. L. Sleep disorders in Parkinson's disease: an overview. *Mov. Disorders* **2007**, *22 Suppl 17,* S367-73.

26.   Steiger, M. Constant dopaminergic stimulation by transdermal delivery of dopaminergic drugs: a new treatment paradigm in Parkinson's disease. *Eur. J. Neurol.* **2008**, *15,* 6-15.

27.   Godin, B.; Touitou, E. Transdermal skin delivery: predictions for humans from in vivo, ex vivo and animal models. *Adv. Drug Delivery Rev.* **2007**, *59,* 1152-61.

28.   Kanikkannan, N.; Singh, J.; Ramarao, P. In vitro transdermal iontophoretic transport of timolol maleate: effect of age and species. *J. Controlled Release* **2001**, *71,* 99-105.

6

Synthesis and chemical stability studies of dipeptide ester prodrugs of (S)-5-OH-DPAT

Abstract

Mono amino acid ester prodrugs of 5-OH-DPAT showed a good in vitro/in vivo stability ratio, but an improved chemical stability would be advantageous for several reasons. A higher chemical stability permits the conversion to alternative salt forms, it allows the incorporation of a wider variety of functional groups, and it gives prodrugs with a longer shelf-life. In addition, it may reduce hydrolysis during transport by iontophoresis across the human stratum corneum, the main barrier of the skin. A possible strategy to improve the chemical stability of prodrugs is the design of dipeptide esters. Therefore a series of dipeptide ester prodrugs of (S)-5-OH-DPAT based on glycine, L-valine and β-alanine were synthesized and the chemical stabilities were determined in citrate buffer pH 5 (donor phase) at 32 ^{0}C. All dipeptide ester prodrugs showed a higher chemical stability than their mono amino acid ester prodrug equivalents. These newly synthesized prodrugs are potential candidates for future studies on enzymatic stability and transdermal iontophoretic delivery.

6.1 INTRODUCTION

In vitro and *in vivo* studies show that the β-alanine ester of 5-OH-DPAT (**2.39**) is a promising prodrug, with a good balance between chemical stability, transport efficiency and enzymatic conversion (Chapter 3 and Chapter 5).[1] Nevertheless, the hygroscopicity, the difficulty to introduce some other interesting amino acids, a relatively short shelf-life and the partial hydrolysis during skin transport by iontophoresis, are reasons that demand an improved stability.

The mono amino acid ester prodrugs of 5-OH-DPAT were all highly hygroscopic which is probably caused by its dihydrochloride salt form (Chapter 2). Because the prodrugs were hydrolyzed very fast at higher pH, it was difficult to convert the prodrugs to the monohydrochloride salt or to other less hygroscopic salt forms. The hygroscopicity impeded easy handling and therefore it would be desirable to obtain chemically more stable prodrugs of 5-OH-DPAT which could be converted to the free amine without pronounced hydrolysis.

Unfortunately, amino acid prodrugs of 5-OH-DPAT with weakly basic (*L*-arginine and *L*-lysine) or alcoholic (*L*-serine) pro-moieties, showed insufficient chemical stability to be studied in iontophoretic experiments (Chapter 3). It would be eligible to incorporate these amino acids in a pro-moiety without losing chemical stability. Herewith, the influence of these weakly basic and alcoholic pro-moieties on transdermal iontophoretic delivery could be investigated.

The chemical hydrolysis of the *L*-valine (**2.31**, half life 53 hours) and β-alanine (**2.39**, half life 117 hours) 5-OH-DPAT prodrugs at pH 5 and 32 ºC showed sufficient stability for

iontophoresic experiments.[1] Nevertheless after 8 and 18 hours respectively, only 90% of the *L*-valine and β-alanine ester prodrugs would remain intact at this temperature and acidity. For practical use higher chemical stabilities are desired for a prolonged shelf-life.

The hydrolysis of the *L*-valine and β-alanine 5-OH-DPAT prodrugs during transport through human stratum corneum was 27% and 20%, respectively.[1] If the prodrug is prevented to hydrolyze during the transport across the human stratum corneum, the iontophoretic transport might be improved due to full availability of the additional charge on the pro-moiety and/or the lower lipophilicity of the prodrug. Therefore, an improved chemical and enzymatic stability would be advantageous.

A possible strategy to increase the chemical stability of 5-OH-DPAT prodrugs would be the design of dipeptide esters. According to Nashed and Mitra both geometrical isomerism and hydrogen bonding might enhance the stability of dipeptide ester prodrugs.[2] Dipeptide prodrugs of the aliphatic alcohols acyclovir and ganciclovir showed higher chemical stabilities than their respective mono amino acid ester prodrugs.[3-5] Dipeptide prodrugs of lopinavir did not show significant degradation in buffer solution.[6] Also dipeptide prodrugs of the phenolic drug paracetamol led to highly soluble and chemically stable prodrugs.[7] In contrast, dipeptide prodrugs of floxuridine generally showed lower chemical stabilities compared to the corresponding mono amino acid prodrugs.[8] Thus, the ability of the dipeptide prodrug strategy to significantly increase the chemical stability depends on both the nature of the pro-moieties and the parent drug.

In this chapter we describe the synthesis of a series of dipeptide prodrugs of 5-OH-DPAT. The hydrolysis rates of various combinations of glycine, *L*-valine and β-alanine were determined in order to gain insights in the influence of the position of amino acids in the dipeptide pro-moiety. These prodrugs could be used in further experiments for enzymatic stability and *in vitro* and *in vivo* transdermal iontophoretic delivery.

6.2 CHEMISTRY

From the glycine (**2.28**), *L*-valine (**2.31**) and β-alanine (**2.39**) esters of (S)-5-OH-DPAT a series of eight *N*-Boc-protected dipeptide (S)-5-OH-DPAT esters was synthesized. The coupling procedure was based on the carbodiimide method mentioned in Chapter 2, besides that *N*-methylmorpholine (NMM) was added to the reaction mixture in order to liberate the reacting amino group from its hydrochloride salt form. In this manner the Boc-protected dipeptide (S)-5-OH-DPAT esters **6.1-6.8** were prepared in yields between 28% and 82% (Scheme 6.1 to Scheme 6.3).
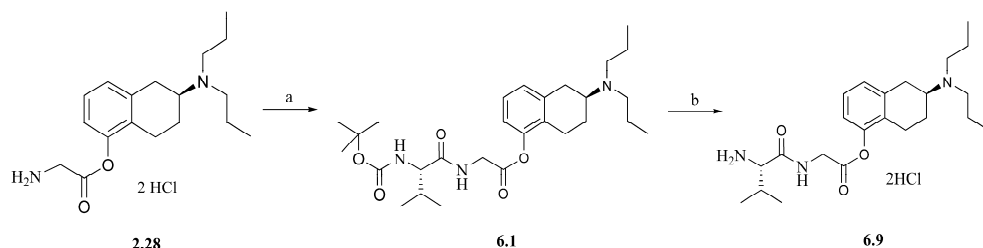
Scheme 6.1 Synthesis of *L*-valine-glycine (S)-2-(di-*n*-propyl-amino)tetralin-5-yl ester 2HCl salt (**6.9**). Reagents and conditions: a) EDC, *N-tert*-Boc-amino acid, NMM, HOBt hydrate, 0°C-RT; b) 4N HCl in dioxane, RT.

Although the *N*-Boc-*L*-valine-glycine (**6.1**) ester was obtained in a high yield, related compounds *N*-Boc-glycine-glycine and *N*-Boc-β-alanine-glycine (S)-5-OH-DPAT esters (not shown) were obtained in low yields and the synthesis of these compounds was abandoned. These low yields may be attributable to a very high aqueous solubility resulting in an increased uptake in the aqueous layer during extraction, and hydrolysis during column chromatography.

Table 6.1 Overall yields and purities of dipeptide prodrugs of 5-OH-DPAT **6.9-6.16**.

Compound	Prodrug Moiety	Yield (%)	HPLC Purity (%)
6.9	*L*-Valine-Glycine	19	98
6.10	Glycine-*L*-Valine	20	100
6.11	*L*-Valine-*L*-Valine	16	100
6.12	β-Alanine-*L*-Valine	13	100
6.13	Glycine-β-Alanine	14	95
6.14	*L*-Valine-β-Alanine	33	99
6.15	β-Alanine-β-Alanine	16	99
6.16	*L*-Lysine-β-Alanine	29	96

The deprotection procedure of the *N*-Boc-dipeptide (S)-5-OH-DPAT esters **6.1-6.8** was completed in a hydrogen chloride solution in dioxane. The reaction products precipitated as oils and were separated from the dioxane. Next, the oils were dissolved in dry methanol and precipitated with dry ether to yield the dipeptide (S)-5-OH-DPAT esters **6.9-6.16** as the dihydrochloride salts with overall yields of 13%-33% and with purities of ≥ 95% (Scheme 6.1 - Scheme 6.3 and Table 6.1).
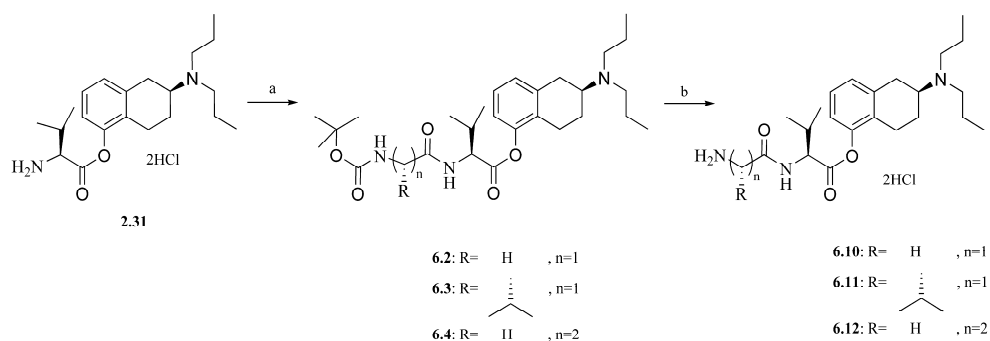
Scheme 6.2 Synthesis of glycine-*L*-valine (**6.10**), *L*-valine-*L*-valine (**6.11**) and β-alanine-*L*-valine (**6.12**) (S)-2-(N,N-di-*n*-propyl-amino)tetralin-5-yl esters as 2HCl salts. Reagents and conditions: a) EDC, *N-tert*-Boc-amino acid, NMM, HOBt hydrate, 0°C-RT; b) 4N HCl in dioxane, RT.
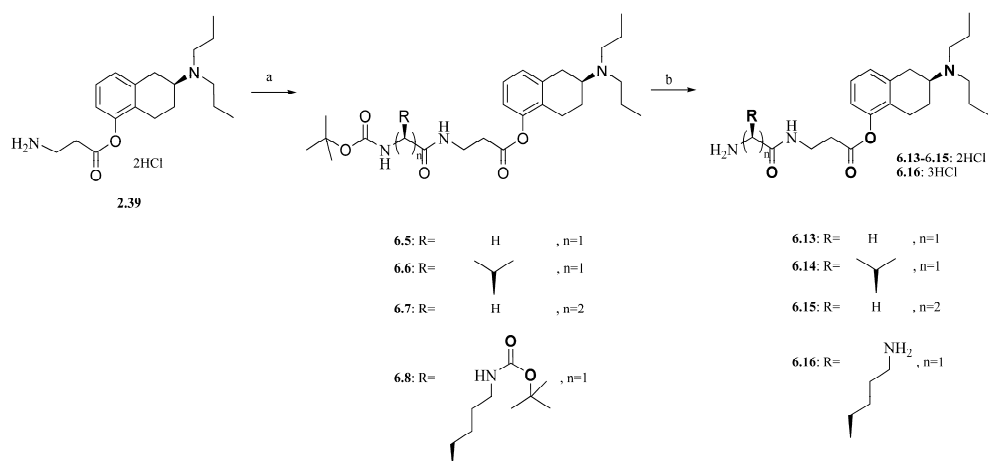
Scheme 6.3 Synthesis of glycine-β-alanine (**6.13**), *L*-valine-β-alanine (**6.14**), β-alanine-β-alanine (**6.15**) and *L*-lysine-β-alanine (**6.16**) (S)-2-(*N,N*-di-*n*-propyl-amino)tetralin-5-yl esters as HCl salts. Reagents and conditions: a) EDC, *N-tert*-Boc-amino acid, NMM, HOBt hydrate, 0°C-RT; b) 4N HCl in dioxane, RT.

6.3 RESULTS

6.3.1 Chemical Stability

The hydrolysis rate constants (k_{obs}) and half-lives ($t_{1/2}$) of compounds **2.28**, **2.31**, **2.39** and **6.9**-**6.16** were obtained by measuring the initial rate of 5-OH-DPAT formation during hydrolysis experiments in 5 mM citrate buffer pH 5 at 32 ºC which is the temperature of the skin *in vivo*. The hydrolysis rate plots of these experiments are presented in Figure 6.1.
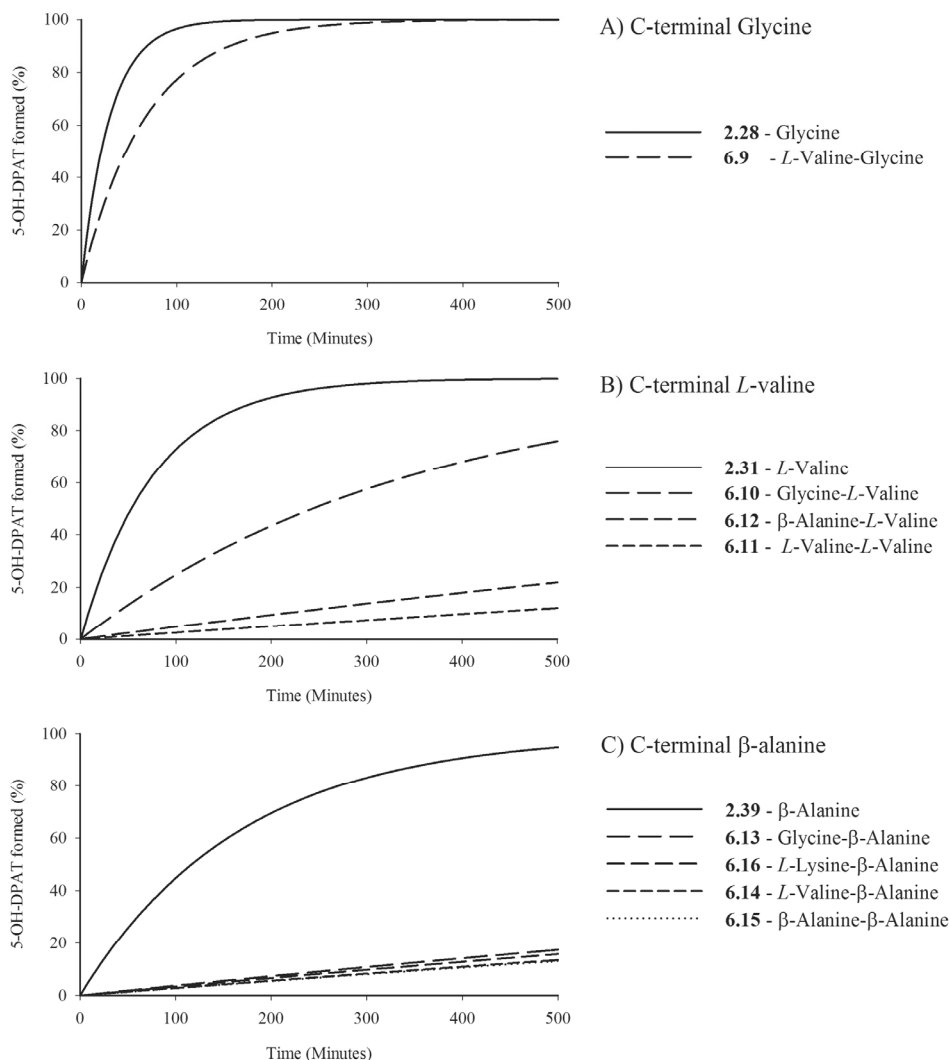
Figure 6.1 Pseudo first-order rate plots of 5-OH-DPAT formation during prodrug hydrolysis in citrate buffer pH 5 at 32°C, based on the estimated half-lives presented in Table 6.2. The prodrugs are listed per group in sequence of ascending half-life. The C-terminal is the carboxylic acid terminal end of the dipeptide.

The formation of 5-OH-DPAT during prodrug hydrolysis followed pseudo-first-order kinetics and is described by: $[5\text{-}OH\text{-}DPAT]_{formed} = [5\text{-}OH\text{-}DPAT]_{max}(1-e^{-kt})$. The observed first-order hydrolysis rate constants of the 5-OH-DPAT formation from the selected prodrugs were determined by plotting the logarithm $(1-\dfrac{[5\text{-}OH\text{-}DPAT]_{formed}}{[5\text{-}OH\text{-}DPAT]_{max}})$ as a function of time. The linear regression slopes of these plots ($r^2 \geq 0.95$) are related to the

observed rate constant, k_{obs}, and are given by: $k_{obs} = \dfrac{1}{\log e} \times \text{slope} \, (\log C \text{ vs time})$. The

half-lives $(t_{1/2})$ can be estimated by the equation: $t_{1/2} = \dfrac{\ln 2}{k}$ and are presented in Table

6.2.No mono amino acid ester prodrug degradation products were detected.

Table 6.2 Estimated hydrolysis half-lives $(t_{1/2})$ of 5-OH-DPAT prodrugs **2.28, 2.31, 2.39** and **6.9-6.16** in 0.005 M citrate buffer (pH 5) at 32 ºC (n=3, exceptions are **2.28** (n=9), **2.31** (n=6) and **2.39** (n=6)).

Compound	5-OH-DPAT ester	$t_{1/2} \pm$ SEM (hours)	k_{obs} x 10^3 (hours^{-1})	ratio $t_{1/2}$
2.28	Glycine	20.7±0.3	33.5	1
6.9	*L*-Valine-Glycine	46.8±3.2	14.9	2.3
2.31	*L*-Valine	53.1±1.6	13.1	2.6
6.10	Glycine-*L*-Valine	243±2.6	2.85	11.7
6.11	*L*-Valine-*L*-Valine	2690±135	0.259	130
6.12	β-Alanine-*L*-Valine	1399±54	0.497	68
2.39	β-Alanine	117.0±5.3	5.99	5.7
6.13	Glycine-β-Alanine	1824±52[b]	0.381	88
6.14	*L*-Valine-β-Alanine	2407±49[a]	0.288	116
6.15	β-Alanine-β-Alanine	2481±140[a]	0.281	120
6.16	*L*-Lysine-β-Alanine	2033±228[a, b]	0.351	98

[a,b] The mean $t_{1/2}$ values were not significantly different (one-way ANOVA with post-hoc Tukey's test for comparing means of **2.39** and **6.13-6.16** , $p < 0.05$).

The chemical stability trend among the dipeptide prodrugs is as following: *L*-valine-*L*-valine (**6.11**, 2690 hrs) ≥ β-alanine-β-alanine (**6.15**, 2481 hrs) ≈ *L*-valine-β-alanine (**6.14**, 2407 hrs) ≥ *L*-lysine-β-alanine (**6.16**, 2033 hrs) ≥ glycine-β-alanine (**6.13**, 1824 hrs) > β-alanine-*L*-valine (**6.12**, 1399 hrs) > glycine-*L*-valine (**6.10**, 243 hrs) > *L*-valine-glycine (**6.9**, 46.8 hrs). The dipeptide prodrugs all show higher chemical stabilities compared to the glycine reference prodrug **2.28** with factors between 2 and 130 times of increased stability.

A) Dipeptide prodrugs with a C-terminal glycine. From the comparison of the *L*-valine-glycine dipeptide prodrug **6.9** with the glycine amino acid ester **2.28**, an increased stability with a factor 2.3 was shown. The coupling of an *L*-valine amino acid to the amino group of an already esterified glycine, gave a higher chemical stability to the 5-OH-DPAT prodrug. Still, dipeptide prodrug **6.9** was the most labile prodrug to chemical hydrolysis of all investigated dipeptide prodrugs of 5-OH-DPAT.

B) Dipeptide prodrugs with a C-terminal *L*-valine. The dipeptide prodrugs **6.10-6.12** which were based on the *L*-valine ester of 5-OH-DPAT (**2.31**) all showed an increased chemical stability compared to **2.31**. The glycine-*L*-valine prodrug **6.10** gave the smallest increase in stability, whereas the *L*-valine-*L*-valine prodrug **6.11** gave the highest increase, i.e. a half-life which was a factor of 50 and 130 times larger than the half-life of the *L*-valine ester prodrug **2.31** and the glycine ester prodrug **2.28**, respectively. In fact, prodrug **6.11** showed the highest chemical stability of all the investigated dipeptide ester prodrugs.

The β-alanine-*L*-valine ester prodrug **6.12** showed an increase in stability of a factor 68 compared to the reference glycine prodrug **2.28** and a factor 26 when compared to the reference *L*-valine prodrug **2.31**.

C) Dipeptide prodrugs with a C-terminal β-alanine. In general, the dipeptide prodrugs based on the β-alanine ester of 5-OH-DPAT, namely **6.13**–**6.16**, all showed a greatly enhanced chemical stability compared to the reference glycine prodrug **2.28** with factors varying between 88 and 120 (Table 6.2). Compared to the β-alanine reference prodrug **2.39**, dipeptides **6.13**-**6.16** showed chemical stability increased ratios between 16 and 21. All four dipeptides showed half-lives around 2000 hours. The half-lives were not significantly different from each other, with the exception of the glycine-β-alanine prodrug of which the half-live differed significantly from the *L*-valine-β-alanine (**6.14**) and β-alanine-β-alanine (**6.15**) dipeptide prodrugs.

6.4 DISCUSSION

Santos *et al.* investigated the chemical hydrolysis of dipeptide esters of paracetamol in buffer at pH 7.4. During the degradation studies paracetamol and diketopiperazines were quantitatively released, which indicated cyclization-activation (Figure 6.2).[7, 9] Other hydrolysis pathways could be 1) stepwise removal of the amino acid residues and 2) direct cleavage of the dipeptide carrier. Since no mono amino acid ester prodrug degradation products were detected, it is expected that the dipeptide monoester prodrugs of 5-OH-DPAT degrade *via* cyclization activation and/or direct dipeptide cleavage pathways which are similar to those suggested for glycine-phenylalanine dipeptide alkyl ester prodrugs by Larsen *et al.*[10] Based on the previous results of the dipeptide prodrugs of the phenolic paracetamol, the release of 5-OH-DPAT from the dipeptide ester prodrugs could occur via cyclization-activation. However, the experiments were performed at pH 5 and it has been reported that the rate of intramolecular aminolysis is negligible at pH values below 6 because the N-terminal amino group is protonated at low pH therefore not available for cyclization.[10-12] Moreover, Tsume *et al.* reported that for dipeptide ester prodrugs of floxuridine no formation of diketopiperazine was observed in chemical stability studies at pH lower than 10.[8] Therefore, the dipeptide ester prodrugs of 5-OH-DPAT probably followed direct cleavage of the dipeptide carrier as main degradation mechanism, and therefore we did not investigate the generation of diketopiperazines.

In contrast to the influence of the amino acid pK_a (data not shown) on the hydrolysis of several amino acid ester prodrugs of 5-OH-DPAT (Chapter 3), intramolecular catalysis appears to play the bigger role in the hydrolysis of dipeptide esters of 5-OH-DPAT (Figure 6.3).

Dipeptide ester prodrug   Diketopiperazine
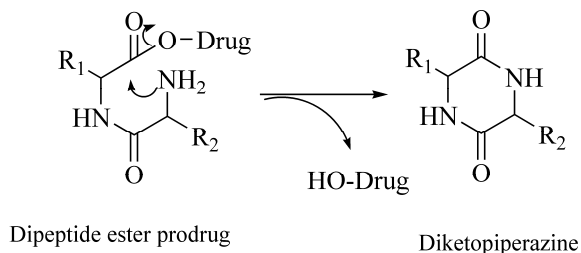
Figure 6.2 Release of the parent drug by intramolecular cyclization forming diketopiperazines.

A) Dipeptide prodrugs with a C-terminal glycine. Tsume *et al* showed that branched N-terminal residues (the primary amino terminal end of the dipeptide) like *L*-leucine and *L*-isoleucine next to a C-terminal residue (the carboxylic acid terminal end of the dipeptide) glycine, renders the prodrug of floxuridine more labile to chemical hydrolysis at 37 ºC in buffer pH 7.4. The degradation pathway was direct cleavage of the peptide.[8] The *L*-valine-glycine ester of paracetamol was relatively stable and showed a half-life similar to the glycine-*L*-valine ester prodrug of paracetamol at 37ºC in pH 7.4 buffer. In these experiments the degradation pathway was through diketopiperazine formation.[7] Peptide coupling of a branched *L*-valine amino acid to the glycine ester prodrug of 5-OH-DPAT at pH 5 increased the chemical stability, although not to the extent of the other dipeptide prodrugs of 5-OH-DPAT. As described in Chapter 3 differences in the hydrolysis rate are assumed to arise only from differences in pH, pK_a and intramolecular catalysis of the amino group of the pro-moiety through several possible mechanisms (Figure 6.3). Apparently steric hindrance of the *L*-valine residue slightly hindered the intramolecular catalysis of the amino group.

A   **B**   **C**
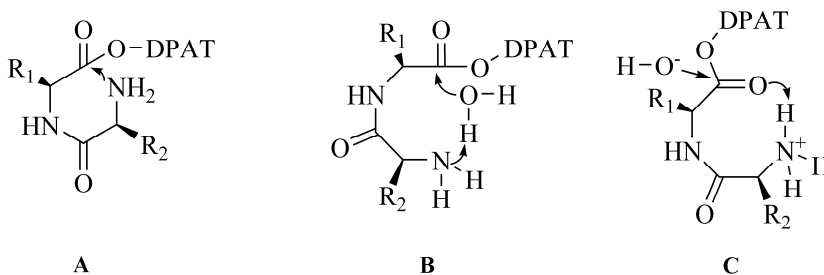
Figure 6.3 Possible mechanisms of intramolecular catalysis of dipeptide esters of 5-OH-DPAT: A A) nucleophilic catalysis; B) general-base catalysis; C) intramolecular general-acid specific base catalysis.

B) Dipeptide prodrugs with a C-terminal *L*-valine. Both Anand *et al.* and Majumdar *et al.* found that a C terminal *L*-valine residue of dipeptide esters stabilized the ester bond compared to prodrugs with only one *L*-valine moiety.[3, 4] Dipeptide prodrugs **6.10-6.12** which all contained *L*-valine as the C terminal residue also showed higher chemical

stabilities than the mono *L*-valine ester prodrug **2.31**. This stabilization could be explained by the steric hindrance introduced in the pro-moiety near the ester bond which could inhibit conformations which favour intramolecular catalysis. This is illustrated in Figure 6.3 where R1 is an isopropyl group. In contrast to an N-terminal *L*-valine residue as in prodrug **6.9**, a C-terminal *L*-valine residue increased the chemical stability of dipeptide esters considerably. This was also found by Santos *et al.* for the degradation of dipeptide prodrugs of AZT, acyclovir and paracetamol, although the degradation of these prodrugs followed cyclization-activation.[5, 7, 13] The *L*-valine-*L*-valine prodrug **6.11** showed one of the highest chemical stabilities of the dipeptide prodrugs of 5-OH-DPAT which could be explained by additional steric hindrance by the second *L*-valine residue. This high chemical stability induced by two *L*-valine residues was also found for dipeptide esters of acyclovir and AZT.[3, 5, 13] The β-alanine residue at the N-terminal of compound **6.12** stabilized the ester bond more than the N-terminal glycine residue of compound **6.10** possibly because the incorporation of the β-alanine led to seven- and nine-membered rings during intramolecular catalysis which may be less favourable for catalysis (Figure 6.3). Talluri *et al.* synthesized dipeptide ester prodrugs with combinations of *D*- and *L*-valine which were all chemically stable. An advantage of the incorporation of *D*-valine at the terminal position or esterification with a peptide of two *D*-valine residues gave prodrugs which were less susceptible to enzymatic hydrolysis.[14] This strategy could also be applied to dipeptide ester prodrugs of 5-OH-DPAT if higher enzymatic stability would be desired concerning hydrolysis during iontophoretic transport through the stratum corneum.

C) Dipeptide prodrugs with a C-terminal β-alanine. All prodrugs **6.13-6.16** with β-alanine at the C-terminal showed extremely high chemical stabilities. A reason for these high chemical stabilities might be the unfavourable seven- and nine membered ring conformations during intramolecular catalysis. Variations in the amino acids in the N-terminal position did not influence the chemical stability much, although a glycine residue at the N-terminus gave the lowest chemical stability in this group. Both *L*-arginine and *L*-lysine would be interesting amino acids to incorporate in a dipeptide prodrug to increase the number of protonatable groups. Schuetz *et al.* found that peptides with a lysine residue exhibited significantly higher iontophoretic fluxes than peptides with an arginine residue. Charge type appeared to play a significant role, with the primary amine in the lysine side-chain functioning as a more favourable positive charge centre than the more delocalized guanidinium group present in arginine.[15] Therefore, we synthesized prodrug **6.16**, a dipeptide with an N-terminus *L*-lysine residue.

First, more stable prodrugs could be converted to less hygroscopic salt forms. Second, these prodrugs allow the introduction of amino acids which may be advantageous for iontophoretic transdermal delivery, e.g. *L*-lysine for an additional chargeable group, while maintaining good chemical stability and aqueous solubility. The influence on iontophoretic flux of additional charges could be negative or positive, which depends on the interaction of the molecules with charged sites in the stratum corneum, hydrated molecular volume of the

ions and the charge/molecular weight ratio.[16-18] Third, the high chemical stability of these dipeptide ester prodrugs give a prolonged shelf-life. Fourth, the possible higher stabilities of these 5-OH-DPAT prodrugs may lead to iontophoretic transfer through the human stratum corneum without or with less hydrolysis. Therefore the advantageous properties of the prodrug stay intact until arrival in the epidermis, dermis or blood stream. Fifth, the hydrolysis rates of various combinations of glycine, *L*-valine and β-alanine were determined in order to gain insights in the influence of the position of amino acids in the dipeptide pro-moiety.

In conclusion, in this chapter the synthesis of a series of dipeptide ester prodrugs of 5-OH-DPAT is presented. These prodrugs all show improved chemical stabilities compared to the mono amino acid ester 5-OH-DPAT prodrugs which are discussed in Chapter 2 and Chapter 3. Especially the *L*-valine-*L*-valine ester prodrug **6.11** and the C-terminal β-alanine dipepeptide ester prodrugs **6.13-6.16** are extremely stable and can be used in future studies on the enzymatic stability and transdermal iontophoretic delivery.

6.5 EXPERIMENTAL

6.5.1 Chemistry

6.5.1.1 General

The materials and analysis methods are described in section 2.4.1

6.5.1.2 General procedure for preparation of protected dipeptide (S)-2–(*N,N*-di-*n*-propyl-amino)tetralin-5-yl esters 6.1-6.8.

The protected amino acid (0.33 mmol) and HOBt hydrate (0.33 mmol) were suspended in 1 mL anhydrous CH_2Cl_2 under nitrogen atmosphere and cooled to 0 ^{o}C. EDC (0.33 mmol) was added and the reaction mixture was stirred for 15 minutes. After all solid material dissolved, the appropriate amino acid (S)-5-OH-DPAT ester (0.30 mmol) in 1 mL anhydrous CH_2Cl_2 and NMM (0.90 mmol) were added to the solution. The yellow solution was allowed to attain room temperature and was shaken overnight at 32 ^{o}C in a closed vessel. CH_2Cl_2 (4 mL) was added and the reaction mixture was washed with aqueous 1 N HCl (0.5 mL) and 1 N NaOH (0.5 mL). The organic layer was dried over $MgSO_4$ and evaporated *in vacuo*; the resultant yellow oil was purified by column chromatography (SiO_2, CH_2Cl_2/MeOH = 30:1 to 15:1, gradient) to afford the pure compounds **6.1-6.8** as light yellow oils.

***N-tert*-Boc-*L*-valine-glycine (S)-2-(*N,N*-di-*n*-propyl-amino)tetralin-5-yl ester (6.1).** Prepared from compound **2.28** with *N*-tert-Boc-*L*-valine. Yield: 82%; IR (Na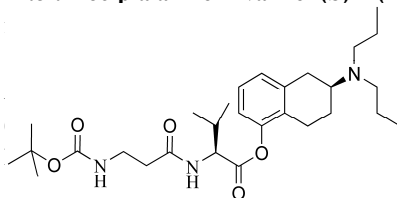Cl, cm^{-1}) ν_{max} 3325, 2960, 1774, 1662, 1532, 1457, 1366, 1236, 1158; ^{1}H NMR (400 MHz, CDCl$_3$): δ 7.10 (t, *J*=7.7 Hz, 1H, ArH), 6.99 (d, *J*=7.7 Hz, 1H, ArH), 6.90-6.77 (m, 2H, NH, ArH), 5.14 (d, *J*=8.8 Hz, 1H, NH), 4.38-4.17 (m, 2H, α-CH$_2$), 4.09-3.97 (m, 1H, α'-CH), 2.99-2.72 (m, 4H, H$_{1ax}$, H$_{1eq}$, H$_{2ax}$, H$_{4eq}$), 2.54-2.40 (m, 1H, H$_{4ax}$), 2.46 (t, *J*=7.3 Hz, N(*CH$_2$*CH$_2$CH$_3$)$_2$), 2.24-2.10 (m, 1H, β-CH), 2.06-1.96 (m, 1H, H$_{3eq}$), 1.62-1.31 (m,
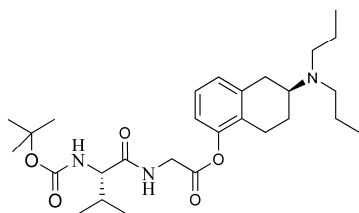
5H, H$_{3ax}$, N(CH$_2$CH$_2$CH$_3$)$_2$), 1.43 (s, 9H, OC(CH$_3$)$_3$), 0.98 (d, J=6.6 Hz, 3H, γ-CH$_3$), 0.93 (d, J=7.0 Hz, 3H, γ-CH$_3$), 0.87 (t, J=7.3 Hz, 6H, N(CH$_2$CH$_2$CH$_3$)$_2$); ^{13}C NMR (50 MHz, CDCl$_3$): δ 172.5, 168.6, 156.2, 148.6, 139.4, 129.0, 127.8, 126.6, 119.0, 80.3, 60.0, 56.4, 52.8, 41.4, 32.2, 31.1, 28.5, 25.3, 24.2, 22.2, 19.5, 17.9, 12.1; HR-MS m/z Calcd. for C$_{28}$H$_{45}$N$_3$O$_5$ 504.3432 (M+H)$^+$, found 504.3432 (M+H)$^+$.

N-*tert*-Boc-glycine-*L*-valine (S)-2-(*N,N*-di-*n*-propyl-amino)tetralin-5-yl ester (6.2). Prepared from compound **2.31** with N-*tert*-Boc-glycine. Yield: 65%; IR (NaCl, cm^{-1}) ν$_{max}$ 3313 (br), 2956, 1757, 1711, 1679, 1536, 1457, 1164; ^{1}H NMR (400 MHz, CDCl$_3$): δ 7.12 (t, J=7.7 Hz, 1H, ArH), 7.00 (d, J=7.7 Hz, 1H, ArH), 6.82 (d, J=8.1 Hz, 1H, ArH), 6.77-6.68 (m, 1H, NH), 5.18 (br s, 1H, NH), 4.87-4.77 (m, 1H, α-CH), 3.93-3.74 (m, 2H, α-CH$_2$), 3.05-2.74 (m, 4H, H$_{1ax}$, H$_{1eq}$, H$_{2ax}$, H$_{4eq}$), 2.60-2.35 (m, 5H, H$_{4ax}$, N(CH$_2$CH$_2$CH$_3$)$_2$), 2.13-2.03 (m, 1H, H$_{3eq}$), 1.67-1.37 (m, 6H, H$_{3ax}$, N(CH$_2$CH$_2$CH$_3$)$_2$, β-CH), 1.45 (s, 9H, OC(CH$_3$)$_3$), 1.08 (d, J=7.0 Hz, 3H, γ-CH$_3$), 1.03 (d, J=7.0 Hz, 3H, γ-CH$_3$), 0.89 (t, J=7.3 Hz, 6H, N(CH$_2$CH$_2$CH$_3$)$_2$); ^{13}C NMR (50 MHz, CDCl$_3$): δ 175.1, 170.5, 170.0, 148.7, 139.0, 128.8, 127.7, 126.6, 119.1, 80.8, 57.3, 56.6, 52.7, 44.9, 32.2, 31.4, 28.5, 25.2, 24.3, 21.9, 19.6, 17.7, 12.1; HR-MS m/z Calcd. for C$_{28}$H$_{46}$N$_3$O$_5$ 504.3432 (M+H)$^+$, found 504.34311 (M+H)$^+$.
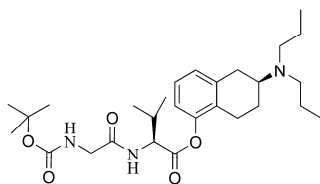
N-*tert*-Boc-*L*-valine-*L*-valine (S)-2-(*N,N*-di-*n*-propyl-amino)tetralin-5-yl ester (6.3). Prepared from compound **2.31** with N-*tert*-Boc-*L*-valine. Yield: 65%; IR (NaCl, cm^{-1}) ν$_{max}$ 3325 (br), 2960, 1761, 1687, 1655, 1524, 1175; ^{1}H NMR (400 MHz, CDCl$_3$): δ 7.11 (t, J=7.7 Hz, 1H, ArH), 6.99 (d, J=7.7 Hz, 1H, ArH), 6.80 (d, J=8.1 Hz, 1H, ArH), 6.49 (br d, J=8.4 Hz, 1H, NH), 5.11 (br d, J=8.1 Hz, 1H, NH), 4.83-4.75 (m, 1H, α'-CH), 3.94 (t, J=6.3 Hz, 1H, α-CH), 3.00-2.70 (m, 4H, H$_{1ax}$, H$_{1eq}$, H$_{2ax}$, H$_{4eq}$), 2.57-2.35 (m, 6H, H$_{4ax}$, β-CH, N(CH$_2$CH$_2$CH$_3$)$_2$), 2.21-2.08 (m, 1H, β'-CH), 2.07-1.99 (m, 1H, H$_{3eq}$), 1.82-1.37 (m, 5H, H$_{3ax}$, N(CH$_2$CH$_2$CH$_3$)$_2$), 1.43 (s, 9H, OC(CH$_3$)$_3$), 1.08 (d, J=7.0 Hz, 3H, γ-CH$_3$), 1.04 (d, J=7.0 Hz, 3H, γ-CH$_3$), 0.97 (d, J=7.0 Hz, 3H, γ-CH$_3$), 0.95 (d, J=7.0 Hz, 3H, γ-CH$_3$), 0.88 (t, J=7.3 Hz, 6H, N(CH$_2$CH$_2$CH$_3$)$_2$); ^{13}C NMR (50 MHz, CDCl$_3$): δ 172.1, 170.5, 156.1 148.8, 139.3, 128.9, 127.7, 126.6, 119.0, 60.5, 57.4, 56.4, 52.8, 32.3, 31.4, 30.8, 28.5, 25.3, 24.4, 22.2, 19.6, 18.2, 17.8, 12.1; HR-MS m/z Calcd. for C$_{31}$H$_{52}$N$_3$O$_5$ 546.39015 (M+H)$^+$, found 546.39001 (M+H)$^+$.
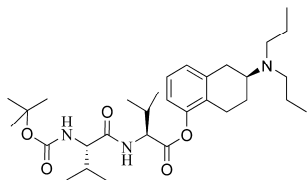
N-*tert*-Boc-β-alanine-*L*-valine (S)-2-(*N,N*-di-*n*-propyl-amino)tetralin-5-yl ester (6.4). Prepared alanine. Yield: 28%; IR (NaCl, cm^{-1}) ν$_{max}$ 3330 (br), 2960, 74; ^{1}H NMR (400 MHz, CDCl$_3$): δ 7.11 (t, J=7.9 Hz, 1H, (d, J=8.1 Hz, 1H, ArH), 6.24 (br d, J=8.1 Hz, 1H, NH), 5.19), 3.51-3.33 (m, 2H, β'-CH$_2$), 3.02-2.65 (m, 4H, H$_{1ax}$, H$_{1eq}$, I$_2$, β'-CH, N(CH$_2$CH$_2$CH$_3$)$_2$), 2.11-1.98 (m, 1H, H$_{3eq}$), 1.67-CH$_2$CH$_2$CH$_3$)$_2$), 1.41 (s, 9H, OC(CH$_3$)$_3$), 1.07 (d, J=6.6 Hz, 3H, γ-CH$_3$), 1.03 (d, J=7.0 Hz, 3H, γ-CH$_3$), 0.88 (t, J=7.3 Hz, 6H, N(CH$_2$CH$_2$CH$_3$)$_2$); ^{13}C NMR (50 MHz, CDCl$_3$): δ 172.0, 170.8, 156.3, 148.7, 139.3, 128.8, 127.8, 126.6, 119.0, 67.1, 57.4, 56.5, 55.6,

52.8, 36.5, 32.3, 31.3, 28.6, 25.3, 24.4, 22.2, 19.6, 17.9, 12.1; HR-MS *m/z* Calcd. for $C_{29}H_{48}N_3O_5$ 518.35885 (M+H)$^+$, found 518.35889 (M+H)$^+$.

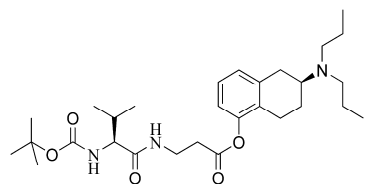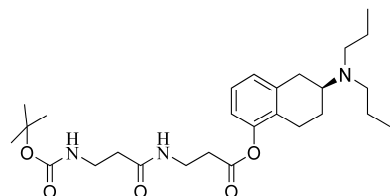***N*-tert-Boc-glycine-β-alanine (S)-2-(*N,N*-di-*n*-propyl-amino)tetralin-5-yl ester (6.5).** Prepared from compound **2.39** with *N-tert*-Boc-glycine. Yield: 27%; IR (NaCl, cm^{-1}) ν$_{max}$ 3309 (br), 2958, 1755, 1714, 1667, 1535, 1367, 1246, 1162; ^{1}H NMR (400 MHz, CDCl$_3$): δ 7.11 (t, *J*=7.7 Hz, 1H, ArH), 6.99 (d, *J*=7.3 Hz, 1H, ArH), 6.82 (d, *J*=7.7 Hz, 1H, ArH), 6.75-6.67 (m, 1H, NH), 5.16 (br s, 1H, NH), 3.77 (d, *J*=5.9 Hz, 2H, α'-CH$_2$), 3.64 (q, *J*=6.2 Hz, 2H, β-CH$_2$), 3.03-2.70 (m, 6H, H$_{1ax}$, H$_{1eq}$, H$_{2ax}$, H$_{4eq}$, α-CH$_2$), 2.56-2.42 (m, 5H, H$_{4ax}$, N(*CH$_2$*CH$_2$CH$_3$)$_2$), 2.10-1.99 (m, 1H, H$_{3eq}$), 1.65-1.51 (m, 1H, H$_{3ax}$), 1.50-1.35 (m, 4H, N(CH$_2$*CH$_2$*CH$_3$)$_2$), 1.42 (s, 9H, OC(CH$_3$)$_3$), 0.88 (t, *J*=7.7 Hz, 6H, N(CH$_2$CH$_2$*CH$_3$)$_2$); ^{13}C NMR (50 MHz, CDCl$_3$): δ 171.1, 169.8, 156.2, 148.8, 139.1, 128.8, 127.7, 126.6, 119.2, 80.6, 56.6, 52.8, 44.6, 35.1, 34.1, 32.1, 28.5, 25.3, 24.3, 22.1, 12.1; HR-MS *m/z* Calcd. for $C_{26}H_{42}N_3O_5$ 476.3119 (M+H)$^+$, found 476.31192 (M+H)$^+$.
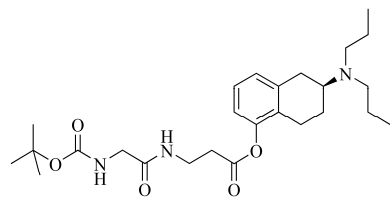
***N*-tert-Boc-*L*-valine-β-alanine (S)-2-(*N,N*-di-*n*-propyl-amino)tetralin-5-yl ester (6.6).** Prepared from compound **2.39** with *N-tert*-Boc-L-valine. Yield: 57%; IR (NaCl, cm^{-1}) ν$_{max}$ 3308 (br), 2956, 1756, 1714, 1693, 1650, 1536, 1365, 1161; ^{1}H NMR (400 MHz, CDCl$_3$): δ 7.12 (t, *J*=7.7 Hz, 1H, ArH), 7.00 (d, *J*=7.3 Hz, 1H, ArH), 6.81 (d, *J*=7.7 Hz, 1H, ArH), 6.58-6.50 (m, 1H, NH), 5.10-4.99 (m, 1H, NH), 3.92-3.84 (m, 1H, α'-CH), 3.72-3.54 (m, 2H, β-CH$_2$), 3.04-2.70 (m, 6H, H$_{1ax}$, H$_{1eq}$, H$_{2ax}$, H$_{4eq}$, α-CH$_2$), 2.59-2.42 (m, 5H, H$_{4ax}$, N(*CH$_2$*CH$_2$CH$_3$)$_2$), 2.19-2.08 (m, 1H, β'-CH), 2.07-1.98 (m, 1H, H$_{3eq}$), 1.65-1.35 (m, 5H, H$_{3ax}$, N(CH$_2$*CH$_2$*CH$_3$)$_2$), 1.42 (s, 9H, OC(CH$_3$)$_3$), 0.95 (d, *J*=6.6 Hz, 3H, γ-CH$_3$), 0.94-0.82 (m, 9H, γ-CH$_3$, N(CH$_2$CH$_2$*CH$_3$)$_2$); ^{13}C NMR (50 MHz, CDCl$_3$): δ 171.9, 171.1, 156.0, 148.8, 139.1, 128.8, 127.7, 126.6, 119.2, 80.2, 60.2, 56.5, 52.8, 35.1, 34.1, 32.2, 31.1, 28.5, 25.3, 24.3, 22.1, 19.5, 17.9, 12.1; HR-MS *m/z* Calcd. for $C_{29}H_{47}N_3O_5$ 518.35885 (M+H)$^+$, found 518.35889 (M+H)$^+$.

***N*-tert-Boc-β-alanine-β-alanine (S)-2-(*N,N*-di-*n*-propyl-amino)tetralin-5-yl ester (6.7).** Prepared from compound **2.39** with *N-tert*-Boc-β-alanine. Yield: 33%; IR (NaCl, cm^{-1}) ν$_{max}$ 3321, 2955, 1755, 1711, 1648, 1535, 1458, 1365, 1247, 1162; ^{1}H NMR (400 MHz, CDCl$_3$): δ 7.12 (t, *J*=7.7 Hz, 1H, ArH), 6.99 (d, *J*=7.7 Hz, 1H, ArH), 6.82 (d, *J*=8.1 Hz, 1H, ArH), 6.34 (br s, 1H, NH), 5.20 (br s, 1H, NH), 3.61 (q, *J*=6.2 Hz, 2H, β'-CH$_2$), 3.39 (q, *J*=5.9 Hz, 2H, β-CH$_2$), 3.03-2.70 (m, 6H, H$_{1ax}$, H$_{1eq}$, H$_{2ax}$, H$_{4eq}$, α-CH$_2$), 2.55-2.41 (m, 5H, H$_{4ax}$, N(*CH$_2$*CH$_2$CH$_3$)$_2$), 2.40-2.30 (m, 2H, α'-CH$_2$), 2.09-1.97 (m, 1H, H$_{3eq}$), 1.65-1.51 (m, 1H, H$_{3ax}$), 1.50-1.30 (m, 4H, N(CH$_2$*CH$_2$*CH$_3$)$_2$), 1.42 (s, 9H, OC(CH$_3$)$_3$), 0.88 (t, *J*=7.3 Hz, 6H, N(CH$_2$CH$_2$*CH$_3$)$_2$); ^{13}C NMR (50 MHz, CDCl$_3$): δ 171.8, 171.2, 156.3, 148.8, 139.2, 128.8, 127.7, 126.6, 119.1, 79.6, 56.5, 55.6, 52.8, 36.5, 35.1, 34.2, 32.2, 28.6, 25.3, 24.3, 22.2, 12.1; HR-MS *m/z* Calcd. for $C_{27}H_{44}N_3O_5$ 490.32755 (M+H)$^+$, found 490.32761 (M+H)$^+$.

***N*α,*N*ε-di-*tert*-Boc-*L*-lysine-β-alanine (S)-2-(*N,N*-di-*n*-propyl-amino)tetralin-5-yl ester (6.8).** Prepared from compound **2.39** with *N*α,*N*ε-di-*tert*-Boc-L-lysine. Yield: 58%; IR (NaCl, cm^{-1}) ν$_{max}$
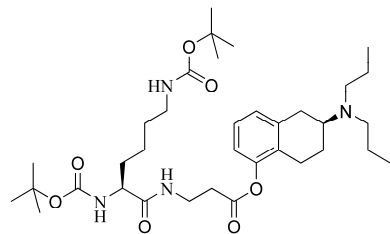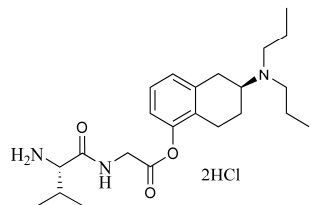
3352, 2955, 1755, 1711, 1689, 1667, 1518, 1365, 1248, 1165; ^{1}H NMR (400 MHz, CDCl$_3$): δ 7.11 (t, *J*=7.7 Hz, 1H, ArH), 6.99 (d, *J*=7.3 Hz, 1H, ArH), 6.83 (d, *J*=8.1 Hz, 1H, ArH), 6.71 (br s, 1H, NH), 5.20 (br s, 1H, NH), 4.69-4.58 (m, 1H, NH), 4.07-3.95 (m, 1H, α'-CH), 3.68-3.56 (m, 2H, β-CH$_2$), 3.16-3.02 (m, 2H, ε-CH$_2$), 3.01-2.71 (m, 6H, H$_{1ax}$, H$_{1eq}$, H$_{2ax}$, H$_{4eq}$, α-CH$_2$), 2.55-2.42 (m, 5H, H$_{4ax}$, N(*CH$_2$*CH$_2$CH$_3$)$_2$), 2.10-2.00 (m, 1H, H$_{3eq}$), 1.89-1.76 (m, 1H, H$_{β'}$), 1.67-1.54 (m, 2H, H$_{β'}$, H$_{3ax}$), 1.53-1.26 (m, 8H, δ-CH$_2$, γ-CH$_2$, N(CH$_2$*CH$_2$*CH$_3$)$_2$), 1.42 (s, 9H, OC(CH$_3$)$_3$), 1.41 (s, 9H, OC(CH$_3$)$_3$), 0.88 (t, *J*=7.3 Hz, 6H, N(CH$_2$CH$_2$*CH$_3$)$_2$); ^{13}C NMR (50 MHz, CDCl$_3$): δ 172.5, 171.0, 156.4, 156.0, 148.8, 139.0, 128.8, 127.6, 126.6, 119.2, 80.3, 79.4, 56.6, 54.8, 52.8, 40.0, 35.2, 34.1, 32.2, 32.1, 29.9, 28.7, 28.5, 25.3, 24.3, 22.0, 12.1; HR-MS *m/z* Calcd. for C$_{35}$H$_{59}$N$_4$O$_7$ 647.43783 (M+H)$^+$, found 647.43823 (M+H)$^+$.

6.5.1.3 General deprotection procedure for the preparation of the dipeptide (S)-2-(*N,N*-di-*n*-propyl-amino)tetralin-5-yl ester hydrochlorides 6.9-6.16.

The *N-tert*-Boc-amino acid 2-(di-*n*-propyl-amino)tetralin-5-yl ester was dissolved in 4 N HCl in dioxane (0.5 mL) under nitrogen atmosphere. The solution was stirred for 2 hours at r.t. until. The product was precipitated with dry Et$_2$O and the dioxane/ Et$_2$O was removed. The vessel was cooled in ice and the remaining oil was dissolved in dry MeOH (0.5 mL) under nitrogen atmosphere. The product was reprecipitated with dry Et$_2$O, the solvent was removed, the remaining oil was evaporated *in vacuo* and dried on the oil pump overnight to afford the hydrochloric acid salts of **6.9-6.16** as hygroscopic solid foams.

***L*-valine-glycine (S)-2-(*N,N*-di-*n*-propyl-amino)tetralin-5-yl ester 2HCl salt (6.9).** Yield: 46%; Purity: 98% (HPLC); IR (KBr, cm^{-1}) ν$_{max}$ 3399 (br), 3215 (br), 2967, 2649, 1772, 1686, 1561, 1461, 1154; ^{1}H NMR (400 MHz, CD$_3$OD): δ 7.22 (t, *J*=7.9 Hz, 1H, ArH), 7.14 (d, *J*=7.7 Hz, 1H, ArH), 6.96 (d, *J*=7.3 Hz, 1H, ArH), 4.42 (d, *J*=7.6 Hz, 1H, α-CH$_2$), 4.24 (d, *J*=8.0 Hz, 1H, α-CH$_2$), 3.82 (d, 1H, α'-CH), 3.78-3.68 (m, 1H, H$_{2ax}$), 3.35-3.07 (m, 6H, H$_{1ax}$, H$_{1eq}$, N(*CH$_2$*CH$_2$CH$_3$)$_2$), 3.05-2.95 (m, 1H, H$_{4eq}$), 2.76-2.63 (m, 1H, H$_{4ax}$), 2.44-2.33 (m, 1H, H$_{3eq}$), 2.30-2.19 (m, 1H, β-CH), 2.00-1.88 (m, 1H, H$_{3ax}$), 1.87-1.74 (m, 4H, N(CH$_2$*CH$_2$*CH$_3$)$_2$), 1.09 (t, *J*=6.8 Hz, 6H, γ-CH$_3$), 1.05 (td, *J*=7.3 Hz; 1.10 Hz, 6H, N(CH$_2$CH$_2$*CH$_3$)$_2$); ^{13}C NMR (50 MHz, CD$_3$OD): δ 169.1, 168.2, 148.8, 134.9, 127.7, 127.3, 127.1, 120.0, 59.9, 58.4, 52.9, 52.5, 40.8, 30.4, 29.2, 23.3, 22.7, 18.6, 18.4, 17.5, 16.8, 10.2; HR-MS *m/z* Calcd. for C$_{23}$H$_{38}$N$_3$O$_3$ 404.29077 (M+H)$^+$, found 404.29053 (M+H)$^+$.
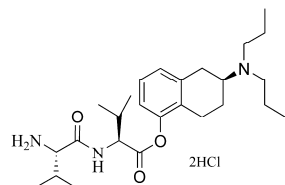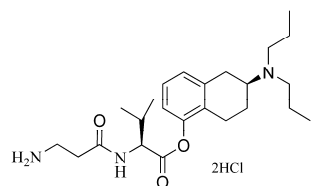
Glycine-*L*-valine (S)-2-(*N,N*-di-*n*-propyl-amino)tetralin-5-yl ester 2HCl salt (6.10). Yield: 51%; Purity: 100% (HPLC); IR (KBr, cm^{-1}) ν$_{max}$ 3400 (br), 3205 (br), 2966, 2622, 1760, 1687, 1461, 1119; ^{1}H NMR (400 MHz, CD$_3$OD): δ 7.22 (t, *J*=7.9 Hz, 1H, ArH), 7.14 (d, *J*=7.7 Hz, 1H, ArH), 6.93 (d, *J*=7.7 Hz, 1H, ArH), 4.65 (d, *J*=5.5 Hz, 1H, α-CH), 3.82 (d, *J*=3.7 Hz, 2H, α'-CH$_2$), 3.85-3.70 (m, 1H, H$_{2ax}$), 3.37-3.08 (m, 6H, H$_{1ax}$, H$_{1eq}$,
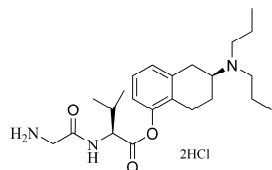
N(CH_2CH$_2$CH$_3$)$_2$), 3.04-2.96 (m, 1H, H$_{4eq}$), 2.76-2.63 (m, 1H, H$_{4ax}$), 2.48-2.33 (m, 2H, H$_{3eq}$, β-CH), 1.99-1.75 (m, 5H, H$_{3ax}$, N(CH$_2$CH_2CH$_3$)$_2$), 1.12 (d, *J*=6.6 Hz, 3H, γ-CH$_3$), 1.11 (d, *J*=6.6 Hz, 3H, γ-CH$_3$), 1.05 (t, *J*=7.3 Hz, 6H, N(CH$_2$CH$_2$CH_3)$_2$); ^{13}C NMR (50 MHz, CD$_3$OD): δ 170.1, 166.7, 148.9, 134.9, 127.5, 127.3, 127.1, 120.0, 59.9, 58.4, 52.5, 40.3, 30.4, 29.2, 23.3, 22.9, 18.6, 18.5, 17.1, 10.2, 10.1; HR-MS *m/z* Calcd. for C$_{23}$H$_{38}$N$_3$O$_3$ 404.29077 (M+H)$^+$, found 404.29034 (M+H)$^+$.

L-valine-L-valine (S)-2-(*N,N*-di-*n*-propyl-amino)tetralin-5-yl ester 2HCl salt (6.11). Yield: 42%; Purity: 100% (HPLC); IR (KBr, cm^{-1}) ν$_{max}$ 3420 (br), 3230 (br), 2968, 2628, 1761, 1680, 1461, 1133; ^{1}H NMR (400 MHz, CD$_3$OD): δ 7.22 (t, *J*=7.9 Hz, 1H, ArH), 7.14 (d, *J*=7.3 Hz, 1H, ArH), 6.92 (d, *J*=7.7 Hz, 1H, ArH), 4.60 (d, *J*=5.5 Hz, 1H, α-CH), 3.87 (d, *J*=5.5 Hz, 1H, α'-CH), 3.82-3.70 (m, 1H, H$_{2ax}$), 3.35-3.09 (m, 6H, H$_{1ax}$, H$_{1eq}$, N(CH_2CH$_2$CH$_3$)$_2$), 3.05-2.95 (m, 1H, H$_{4eq}$), 2.77-2.64 (m, 1H, H$_{4ax}$), 2.58-2.30 (m, 2H, H$_{3eq}$, β-CH), 2.27-2.19 (m, 1H, β'-CH), 1.99-1.76 (m, 5H, H$_{3ax}$, N(CH$_2$CH_2CH$_3$)$_2$), 1.16 (d, *J*=2.6 Hz, 3H, γ-CH$_3$), 1.15 (d, *J*=2.6 Hz, 3H, γ-CH$_3$), 1.09 (d, *J*=7.0 Hz, 3H, γ'-CH$_3$), 1.05 (d, *J*=6.6 Hz, 3H, γ'-CH$_3$), 1.05 (t, *J*=7.3 Hz, 6H, N(CH$_2$CH$_2$CH_3)$_2$); ^{13}C NMR (50 MHz, CD$_3$OD): δ 170.0, 169.1, 148.9, 134.9, 127.5, 127.3, 127.1, 119.9, 59.9, 58.7, 58.1, 52.8, 30.6, 30.2, 29.2, 23.2, 23.0, 18.6, 18.5, 17.7, 17.4, 16.6, 10.1; HR-MS *m/z* Calcd. for C$_{26}$H$_{44}$N$_3$O$_3$ 446.33772 (M+H)$^+$, found 446.33762 (M+H)$^+$.

β-alanine-L-valine (S)-2-(*N,N*-di-*n*-propyl-amino)tetralin-5-yl ester 2HCl salt (6.12). Yield: 76%; Purity: 100% (HPLC); IR (KBr, cm^{-1}) ν$_{max}$ 3428 (br), 3256 (br), 2967, 2641, 1759, 1656, 1461, 1135; ^{1}H NMR (400 MHz, CD$_3$OD): δ 7.22 (t, *J*=7.7 Hz, 1H, ArH), 7.13 (d, *J*=8.1 Hz, 1H, ArH), 6.93 (d, *J*=7.5 Hz, 1H, ArH), 4.58 (d, *J*=5.5 Hz, 1H, α-CH), 3.82-3.68 (m, 1H, H$_{2ax}$), 3.38-3.05 (m, 8H, β-CH$_2$, H$_{1ax}$, H$_{1eq}$, N(CH_2CH$_2$CH$_3$)$_2$), 3.04-2.96 (m, 1H, H$_{4eq}$), 2.81-2.63 (m, 3H, α'-CH$_2$, H$_{4ax}$), 2.44-2.30 (m, 2H, H$_{3eq}$, β-CH), 2.00-1.72 (m, 5H, H$_{3ax}$, N(CH$_2$CH_2CH$_3$)$_2$), 1.12 (d, *J*=2.9 Hz, 3H, γ-CH$_3$), 1.11 (d, *J*=2.9 Hz, 3H, γ-CH$_3$), 1.05 (t, *J*=7.3 Hz, 6H, N(CH$_2$CH$_2$CH_3)$_2$); ^{13}C NMR (50 MHz, CD$_3$OD): δ 171.6, 170.5, 148.9, 134.8, 127.5, 127.2, 127.1, 120.0, 59.9, 58.4, 52.5, 35.8, 31.2, 30.3, 29.2, 23.3, 22.9, 18.5, 17.3, 10.1; HR-MS *m/z* Calcd. for C$_{24}$H$_{40}$N$_3$O$_3$ 418.30642 (M+H)$^+$, found 418.30634 (M+H)$^+$.

Glycine-β-alanine (S)-2-(*N,N*-di-*n*-propyl-amino)tetralin-5-yl ester 2HCl salt (6.13). Yield: 66%; Purity: 95% (HPLC); IR (KBr, cm^{-1}) ν$_{max}$ 3391 (br), 3236 (br), 2965, 2643, 1753, 1686, 1460, 1151; ^{1}H NMR (400 MHz, CD$_3$OD): δ 7.21 (t, *J*=7.9 Hz, 1H, ArH), 7.12 (d, *J*=7.3 Hz, 1H, ArH), 6.97 (d, *J*=7.7 Hz, 1H, ArH), 3.70 (s, 2H, α'-CH$_2$), 3.62 (t, *J*=6.6 Hz, 2H, β-CH$_2$), 3.81-3.09 (m, 7H, H$_{2ax}$, H$_{1ax}$, H$_{1eq}$, N(CH_2CH$_2$CH$_3$)$_2$), 2.95 (dd, 1H, H$_{4eq}$), 2.89 (t, *J*=6.6 Hz, 2H, α-CH$_2$), 2.75-2.59 (m, 1H, H$_{4ax}$), 2.43-2.33 (m, 1H, H$_{3eq}$), 1.99-1.87 (m, 1H, H$_{3ax}$), 1.86-1.72 (m, 4H, N(CH$_2$CH_2CH$_3$)$_2$), 1.05 (t, *J*=7.0 Hz, 6H, N(CH$_2$CH$_2$CH_3)$_2$); ^{13}C NMR (50 MHz, CD$_3$OD): δ 170.3, 166.9, 149.0, 134.7, 127.6, 127.1, 127.0, 120.2, 60.0, 52.9, 52.5, 40.3, 35.2, 33.4, 29.2, 23.3, 22.7, 18.6, 18.4, 10.1; HR-MS *m/z* Calcd. for C$_{21}$H$_{34}$N$_3$O$_3$ 376.25947 (M+H)$^+$, found 376.25946 (M+H)$^+$.
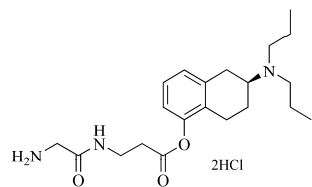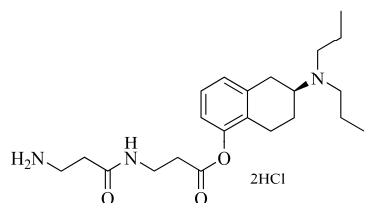
L-valine-β-alanine (S)-2-(*N,N*-di-*n*-propyl-amino)tetralin-5-yl ester 2HCl salt (6.14). Yield: 76%; Purity: 99% (HPLC); IR (KBr, cm^{-1}) ν$_{max}$ 3413 (br), 3226 (br), 2969, 2628, 1754, 1677, 1461, 1148;
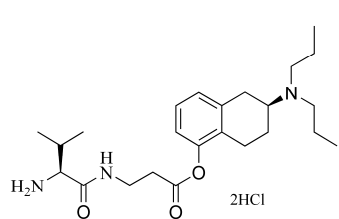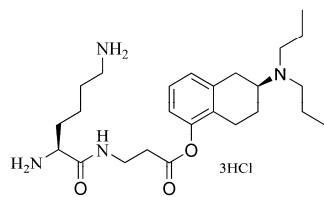
^{1}H NMR (400 MHz, CD$_3$OD): δ 7.21 (t, *J*=7.7 Hz, 1H, ArH), 7.12 (d, *J*=7.3 Hz, 1H, ArH), 6.96 (d, *J*=7.7 Hz, 1H, ArH), 3.79-3.61 (m, 3H, H$_{2ax}$, β-CH$_2$), 3.69 (d, *J*=5.9 Hz, 1H, α'-CH), 3.61-3.08 (m, 6H, H$_{1ax}$, H$_{1eq}$, N(*CH$_2$*CH$_2$CH$_3$)$_2$), 3.00-2.86 (m, 3H, H$_{4eq}$, α-CH$_2$), 2.73-2.61 (m, 1H, H$_{4ax}$), 2.44-2.33 (m, 1H, H$_{3eq}$), 2.22-2.12 (m, 1H, β'-CH), 1.98-1.75 (m, 5H, H$_{3ax}$, N(CH$_2$*CH$_2$*CH$_3$)$_2$), 1.13-0.93 (m, 12H, γ-CH$_3$, N(CH$_2$CH$_2$*CH$_3$)$_2$);

^{13}C NMR (50 MHz, CD$_3$OD): δ 170.2, 168.5, 149.0, 134.7, 127.6, 127.1, 127.0, 120.2, 59.9, 58.6, 52.9, 52.5, 35.3, 33.4, 30.3, 29.2, 23.3, 22.8, 18.6, 18.5, 17.7, 16.9, 10.2; HR-MS *m/z* Calcd. for C$_{24}$H$_{40}$N$_3$O$_3$ 418.30642 (M+H)$^+$, found 418.30634 (M+H)$^+$.

β-alanine-β-alanine (S)-2-(*N,N*-di-*n*-propyl-amino)tetralin-5-yl ester 2HCl salt (6.15). Yield: 65%; Purity: 99% (HPLC); IR (KBr, cm^{-1}) ν$_{max}$ 3414 (br), 3249 (br), 2961, 2636, 1752, 1656, 1460, 1149; ^{1}H NMR (400 MHz, CD$_3$OD): δ 7.21 (t, *J*=7.7 Hz, 1H, ArH), 7.12 (d, *J*=7.7 Hz, 1H, ArH), 6.96 (d, *J*=7.7 Hz, 1H, ArH), 3.84-3.73 (m, 1H, H$_{2ax}$), 3.58 (t, *J*=6.6 Hz, 2H, β-CH$_2$), 3.38-3.02 (m, 8H, H$_{1ax}$, H$_{1eq}$, β'-CH$_2$, N(*CH$_2$*CH$_2$CH$_3$)$_2$), 2.99-2.89 (m, 1H, H$_{4eq}$), 2.86 (t, *J*=6.6 Hz, 2H, α-CH$_2$), 2.63 (t, *J*=6.6 Hz, 2H, α'-CH$_2$), 2.73-2.57 (m, 1H, H$_{4ax}$), 2.46-2.30 (m, 1H, H$_{3eq}$), 2.00-1.73 (m, 5H, H$_{3ax}$, N(CH$_2$*CH$_2$*CH$_3$)$_2$), 1.05 (t, *J*=7.2 Hz, 6H, N(CH$_2$CH$_2$*CH$_3$)$_2$); ^{13}C NMR (50 MHz, CD$_3$OD): δ 171.1, 170.4, 149.0, 134.7, 127.6, 127.1, 127.0, 120.2, 60.0, 52.9, 52.5, 35.9, 35.1, 33.5, 31.6, 29.2, 23.3, 22.8, 18.7, 18.5, 10.1; HR-MS *m/z* Calcd. for C$_{22}$H$_{36}$N$_3$O$_3$ 390.27512 (M+H)$^+$, found 390.2742 (M+H)$^+$.

***L*-lysine-β-alanine (S)-2-(*N,N*-di-*n*-propyl-amino)tetralin-5-yl ester 3HCl salt (6.16).** Yield: 63%; Purity: 96% (HPLC); IR (KBr, cm^{-1}) ν$_{max}$ 3417 (br), 3225 (br), 2941, 2635, 1753, 1680, 1461, 1150; ^{1}H NMR (400 MHz, CD$_3$OD): δ 7.22 (t, *J*=7.7 Hz, 1H, ArH), 7.12 (d, *J*=7.7 Hz, 1H, ArH), 6.99 (d, *J*=7.7 Hz, 1H, ArH), 3.93 (t, *J*=6.6 Hz, 1H, α'-CH), 3.82-3.07 (m, 9H, β-CH$_2$, H$_{1ax}$, H$_{1eq}$, H$_{2ax}$, N(*CH$_2$*CH$_2$CH$_3$)$_2$), 3.00-2.83 (m, 5H, H$_{4eq}$, α-CH$_2$, ε-CH$_2$), 2.76-2.63 (m, 1H, H$_{4ax}$), 2.45-2.35 (m, 1H, H$_{3eq}$), 2.00-1.77 (m, 7H, H$_{3ax}$, β'-CH$_2$, N(CH$_2$*CH$_2$*CH$_3$)$_2$), 1.76-1.69 (m, 2H, δ-CH$_2$), 1.56-1.44 (m, 2H, γ-CH$_2$), 1.05 (td, *J*=7.3 Hz; 1.10 Hz, 6H, N(CH$_2$CH$_2$*CH$_3$)$_2$); ^{13}C NMR (50 MHz, CD$_3$OD): δ 170.3, 169.0, 149.0, 134.7, 127.6, 127.1, 127.0, 120.2, 60.0, 53.0, 52.9, 52.5, 39.1, 35.4, 33.5, 30.9, 29.2, 26.9, 23.3, 22.8, 21.7, 18.6, 18.4, 10.2; HR-MS *m/z* Calcd. for C$_{25}$H$_{43}$N$_4$O$_3$ 447.33297 (M+H)$^+$, found 447.33286 (M+H)$^+$.

6.5.2 Chemical hydrolysis experiments in 5 mM citrate buffer pH 5

The methods for the chemical hydrolysis experiments of compounds **2.28**, **2.31** and **2.39** were already described in Chapter 3.

6.5.2.1 Procedure

For the experiments with prodrugs **6.9-6.16** the chemical hydrolysis was initiated by adding 6 µl of a 25 mM stock solution in 5 mM citrate buffer (pH 5) to 2.994 mL 5 mM citrate buffer (pH 5) preheated at 32 °C. The final concentration of the resulting solutions was about 50 µM. The test

solutions of the compounds were vortexed and maintained in a Lab-Line Orbit Shaker at a constant temperature of 32±0.2 °C. At appropriate intervals samples of 100 μL were withdrawn and diluted with 100 μL H_2O/ACN/TFA (1.2/1/0.004) giving a concentration of 25 μM. The samples were stored in the freezer until they were analyzed by HPLC. The 5-OH-DPAT concentration was estimated by measuring the peak heights in relation to those of 5-OH-DPAT standards which were prepared by serial dilution of known concentrations (0.5, 5, 10 and 25 μM) and chromatographed under the same conditions.

6.5.2.2 HPLC analysis

Samples of prodrugs **6.9-6.16** were analyzed isocratically on a Hewlett Packard Series 1100 HPLC system connected to a Tray-Cooling Marathon Basic+ Autosampler and a Hewlett Packard HP3395 Integrator. The samples were injected onto a Supelco Discovery C18 reversed-phase column (5 μm, 250 x 4.6 mm I.D.). The mobile phase for the analysis of compounds **6.9** and **6.11-6.16** consisted of a mixture of 23% acetonitrile and 77% water with 0.1% trifluoroacetic acid added (eluent A). The mobile phase for the analysis of compounds **6.10** consisted of a mixture of 20% acetonitrile and 80% water with 0.1% trifluoroacetic acid added (eluent B). The flow was set at 1.0 mL/min and the analysis was performed at room temperature. The injection volume was 20 μL and the compounds were detected by UV at 217 nm. The runtime was 20 minutes. The retention times of 5-OH-DPAT and the amino acid 5-OH-DPAT esters were: 9.46 min (**2.12**, eluent A), 13.32 (**2.12**, eluent B), 6.94 min (**6.9**), 17.82 min (**6.10**, eluent B), 16.19 min (**6.11**), 10.40 min (**6.12**), 5.06 min (**6.13**), 6.83 min (**6.14**), 5.59 min (**6.15**), 4.42 min (**6.16**).

6.5.2.3 Data analysis

All hydrolysis experiments were carried out in triplicate. The pseudo-first-order hydrolysis rate constants and the pseudo-first-order chemical hydrolysis rate constants were calculated from the linear slopes of plots of the logarithm of the formed 5-OH-DPAT concentration against time. The slopes of these plots are related to the rate constant, k, and given by k = 2.303 x slope (log C vs time). The formation of 5-OH-DPAT during prodrug hydrolysis follows pseudo-first-order kinetics and is described by the following formula: $[5\text{-}OH\text{-}DPAT] = [5\text{-}OH\text{-}DPAT]_{max}(1-e^{-kt})$. The half-

lives ($t_{1/2}$) can be estimated by the equation: $t_{1/2} = \dfrac{\ln 2}{k}$.

6.6 ACKNOWLEDGMENTS.

6.7 REFERENCES

1.   Ackaert, O. W.; De Graan, J.; Capancioni, R.; Della Pasqua, O. E.; Dijkstra, D.; Westerink, B. H.; Danhof, M.; Bouwstra, J. A. The in vitro and in vivo evaluation of new synthesized prodrugs of 5-OH-DPAT for iontophoretic delivery. *J. Controlled Release* **2010**, *144,* 296-305.

2.   Nashed, Y. E.; Mitra, A. K. Synthesis and characterization of novel dipeptide ester prodrugs of acyclovir. *Spectrochim. Acta, Part A* **2003**, *59*, 2033-9.

3.   Anand, B.; Nashed, Y.; Mitra, A. Novel dipeptide prodrugs of acyclovir for ocular herpes infections: Bioreversion, antiviral activity and transport across rabbit cornea. *Curr. Eye Res.* **2003**, *26*, 151-63.

4.   Majumdar, S.; Nashed, Y. E.; Patel, K.; Jain, R.; Itahashi, M.; Neumann, D. M.; Hill, J. M.; Mitra, A. K. Dipeptide monoester ganciclovir prodrugs for treating HSV-1-induced corneal epithelial and stromal keratitis: in vitro and in vivo evaluations. *J. Ocul. Pharmacol. Therapeut.* **2005**, *21*, 463-74.

5.   Santos, C. R.; Capela, R.; Pereira, C. S.; Valente, E.; Gouveia, L.; Pannecouque, C.; De Clercq, E.; Moreira, R.; Gomes, P. Structure-activity relationships for dipeptide prodrugs of acyclovir: Implications for prodrug design. *Eur. J. Med. Chem.* **2008**, .

6.   Agarwal, S.; Boddu, S. H.; Jain, R.; Samanta, S.; Pal, D.; Mitra, A. K. Peptide prodrugs: improved oral absorption of lopinavir, a HIV protease inhibitor. *Int. J. Pharm.* **2008**, *359*, 7-14.

7.   Santos, C.; Mateus, M. L.; dos Santos, A. P.; Moreira, R.; de Oliveira, E.; Gomes, P. Cyclization-activated prodrugs. Synthesis, reactivity and toxicity of dipeptide esters of paracetamol. *Bioorg. Med. Chem. Lett.* **2005**, *15*, 1595-1598.

8.   Tsume, Y.; Hilfinger, J. M.; Amidon, G. L. Enhanced cancer cell growth inhibition by dipeptide prodrugs of floxuridine: increased transporter affinity and metabolic stability. *Mol. Pharmaceutics* **2008**, *5*, 717-27.

9.   Gomes, P.; Vale, N.; Moreira, R. Cyclization-activated prodrugs. *Molecules* **2007**, *12*, 2484-2506.

10.   Larsen, S. W.; Ankersen, M.; Larsen, C. Kinetics of degradation and oil solubility of ester prodrugs of a model dipeptide (Gly-Phe). *Eur. J. Pharm. Sci.* **2004**, *22*, 399-408.

11.   Goolcharran, C.; Borchardt, R. T. Kinetics of diketopiperazine formation using model peptides. *J. Pharm. Sci.* **1998**, *87*, 283-8.

12.   Jensen, E.; Bundgaard, H. Peptide esters as water-soluble prodrugs for hydroxyl containing agents: Chemical stability and enzymatic hydrolysis of benzyl esters of glycine, diglycine and triglycine. *Int. J. Pharm.* **1991**, *71*, 117-125.

13.   Santos, C.; Morais, J.; Gouveia, L.; de Clercq, E.; Pannecouque, C.; Nielsen, C. U.; Steffansen, B.; Moreira, R.; Gomes, P. Dipeptide derivatives of AZT: synthesis, chemical stability, activation in human plasma, hPEPT1 affinity, and antiviral activity. *ChemMedChem* **2008**, *3*, 970-8.

14.   Talluri, R. S.; Samanta, S. K.; Gaudana, R.; Mitra, A. K. Synthesis, metabolism and cellular permeability of enzymatically stable dipeptide prodrugs of acyclovir. *Int. J. Pharm.* **2008**, *361*, 118-24.

15.   Schuetz, Y. B.; Carrupt, P. A.; Naik, A.; Guy, R. H.; Kalia, Y. N. Structure-permeation relationships for the non-invasive transdermal delivery of cationic peptides by iontophoresis. *Eur. J. Pharm. Sci.* **2006**, *29*, 53-9.

16.   Abla, N.; Naik, A.; Guy, R. H.; Kalia, Y. N. Effect of charge and molecular weight on transdermal peptide delivery by iontophoresis. *Pharm. Res.* **2005**, *22*, 2069-78.

17.   Lai, P. M.; Roberts, M. S. An analysis of solute structure-human epidermal transport relationships in epidermal iontophoresis using the ionic mobility: pore model. *J. Controlled Release* **1999**, *58*, 323-33.

18.   Phipps, J. B.; Padmanabhan, R. V.; Lattin, G. A. Iontophoretic delivery of model inorganic and drug ions. *J. Pharm. Sci.* **1989**, *78*, 365-9.

7

# Structural analogs of 5-OH-DPAT: synthesis and their influence on *in vitro* transdermal iontophoretic delivery

Abstract

The transdermal iontophoretic flux of small molecules depends on the physicochemical properties of the transported molecule. In order to investigate the influence of the molecular structure of phenolic and catecholic dopamine (DA) agonists on the transdermal iontophoretic flux and solubility, we synthesized a series of analogs of 5-OH-DPAT with varying alkyl length, lipophilicity and molecular weight, i.e. 5-OH-EPAT, 5-OH-MPAT, 8-OH-DPAC 5,6-(OH)₂-MPAT and 5,6-(OH)₂-DPAT. 8-OH-DPAC showed the highest solubility. 5-OH-MPAT and 5-OH-EPAT showed the highest increase in total transdermal iontophoretic flux in vitro. The synthesized DA receptor agonists are valuable compounds for studies to improve the understanding of molecular structure on transdermal iontophoretic delivery.

7.1 INTRODUCTION

The iontophoretic flux of small molecules depends on several physicochemical properties of the transported molecule. Important properties are the molecular volume or molecular weight[1-3], the ratio of charge/molecular weight[4], and the degree of lipophilicity.[5, 6] In order to investigate the influence of the molecular structure of phenolic and catecholic DA agonists on the iontophoretic flux, we synthesized a series of analogs of 5-OH-DPAT with varying alkyl length, lipophilicity and molecular weight. Furthermore, the influence of the molecular structure and lipophilicity on aqueous solubility was investigated.

Besides 5-OH-DPAT which is the parent drug of the compounds discussed in Chapter 2 to Chapter 6, the phenolic derivatives 5-hydroxy-2-(*N*-*n*-propyl-amino)-tetralin (5-OH-MPAT) and 5-hydroxy-2-(*N*-ethyl-*N*-*n*-propyl-amino)tetralin (5-OH-EPAT) are found to be potent DA D_2 agonists. The trend of increasing *in vivo* biochemical potencies was 5-OH-MPAT < 5-OH-EPAT < 5-OH-DPAT.[7] Moreover, van Vliet *et al* showed that the receptor affinity of (S)-5-OH-DPAT for cloned human DA receptor subtypes D_{2L}, D_3 and D_4 was higher than the affinity of 5-OH-MPAT.[8] Also the catecholic tetralin analogs 5,6-dihydroxy-2-(*N*,*N*-di-*n*-propyl-amino)tetralin (5.6-(OH)₂-DPAT) and 5,6-dihydroxy-2-(*N*-*n*-propyl-amino)tetralin (5,6-(OH)₂-MPAT) showed high DAergic activity, whereas the monopropyl analogue showed a lower potency *in vivo*.[9-11] Additionally, 8-hydroxy-3,4-dihydro-3-(*N*,*N*-di-*n*-propylamino)-2*H*-1-benzopyran (8-OH-DPAC) exhibited high DAergic activity *in vivo* and good DAergic receptor binding and affinity *in vitro*.[12-16] The aminochroman was even found to displace the DAergic ligand [³H] 2-(*N*-propyl-*N*-2-thienylethylamino)-5-hydroxytetralin with a higher potency than apomorphine and 5-OH-DPAT.[17] The structures of the DA agonists are depicted in Figure 7.1.
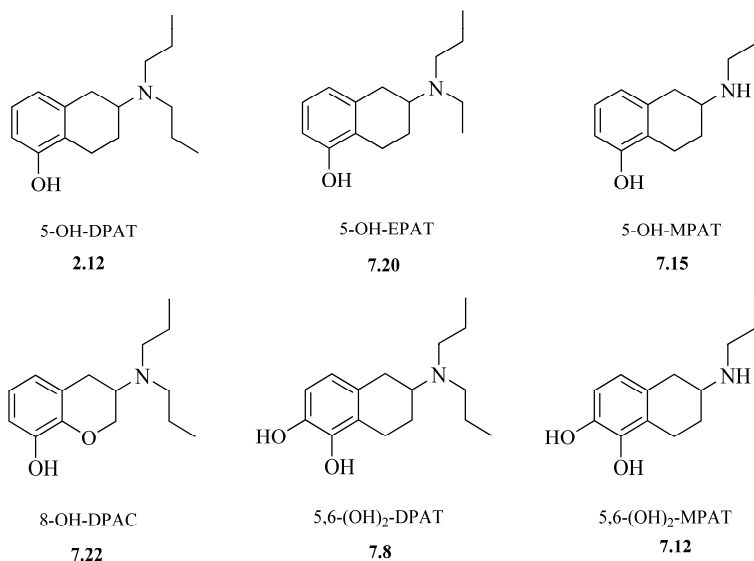
Figure 7.1 Molecular structures of the DA agonists 5-OH-DPAT (**2.12**), 5-OH-EPAT (**7.20**), 5-OH-MPAT (**7.15**), 8-OH-DPAC (**7.22**), 5,6-(OH)$_2$-DPAT (**7.8**) and 5,6-(OH)$_2$-MPAT (**7.12**).

Iontophoretic studies could give insight in the structure-transport relationships of DA agonists with a tetrahydronaphthalene core. Also information on structure-solubility relationships may aid the optimization of drugs for transdermal delivery by iontophoresis.

7.2 CHEMISTRY

7.2.1 Synthesis of 5,6-dihydroxy-2-(*N,N*-di-*n*-propyl-amino)tetralin (7.8) and 5,6-dihydroxy-2-(*N-n*-propyl-amino)tetralin (7.12)

In order to prepare compounds **7.8** (5,6-(OH)$_2$-DPAT) and **7.12** (5,6-(OH)$_2$-MPAT), first intermediate 5,6-dimethoxy-2-tetralone (**7.6**) was synthesized. The synthesis of **7.6** was described by Horn *et al.*, Taber *et al.*, McDermed *et al.* and Copinga *et al.*[11, 18-20] We started with the route according to Taber *et al.* which is a modification of the routes described by Horn *et al.* and McDermed *et al.* First, 1,6-dibromo-2-naphthol was methylated by a nucleophilic substitution reaction with iodomethane to give 1,6-dibromo-2-methoxy-naphthalene (**7.9**). Then, compound **7.9** was methoxylated using sodium methoxide in the presence of cuprous iodide and 2,4,6-collidine to form 1,2,6-trimethoxy-naphthalene (**7.10**) with a yield of 68%. This particular reaction only worked under very dry conditions and only with highly purified starting material. Via a Birch reduction the enol ether was prepared. Acid hydrolysis gave finally 5,6-dimethoxy-2-tetralone (**7.6**)(Scheme 7.1). Unfortunately, the reaction mixture solidified to a thick gel during the reduction and many side-products had been formed. For that reason, we decided to choose another route for the synthesis of the 2-tetralone **7.6**.
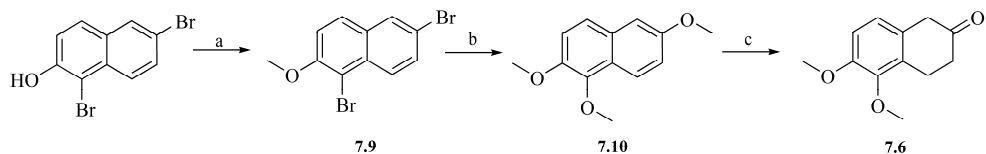
Scheme 7.1 Synthesis of 5,6-dimethoxy-2-tetralone (**7.6**) according to Taber *et al*. Reagents and conditions: a) iodomethane, K$_2$CO$_3$, DMF, beneath 30 °C, 3h; b) Na, MeOH, 2,4,6-collidine, copper(I)iodide, reflux, 5h; c) Na, EtOH, H$_2$O, 36% HCl.

The synthesis route according to Copinga *et al*. was chosen and the reactions are outlined in Scheme 7.2. Vanillin was methylated by a reaction with dimethylsulfate to afford 2,3-dimethoxy-benzaldehyde (**7.1**).[21] The methylated benzaldehyde was converted to (*E*)-3-(2,3-dimethoxyphenyl)-2-propenoic acid (**7.2**) via the Doebner modification of the Knoevenagel condensation.[22] Compound **7.2** was hydrogenated with palladium on carbon as catalyst into 2,3-dimethoxybenzenepropanoic acid (**7.3**) which was subsequently converted to the acid chloride **7.4** with thionyl chloride. The diazoketone **7.5** was prepared from the reaction of the acid chloride **7.4** with freshly prepared diazomethane. After a rhodium(II)-acetate-catalysed cyclization and a transformation under the influence of trifluoroacetic acid, crude 5,6-dimethoxy-2-tetralone (**7.6**) was synthesized.[18] In contrast to literature, we were unable to purify **7.6** by vacuum distillation. Therefore the product was purified by sodium bisulfite adduct formation to give pure tetralone with an overall yield of 11%.[10, 19, 23]
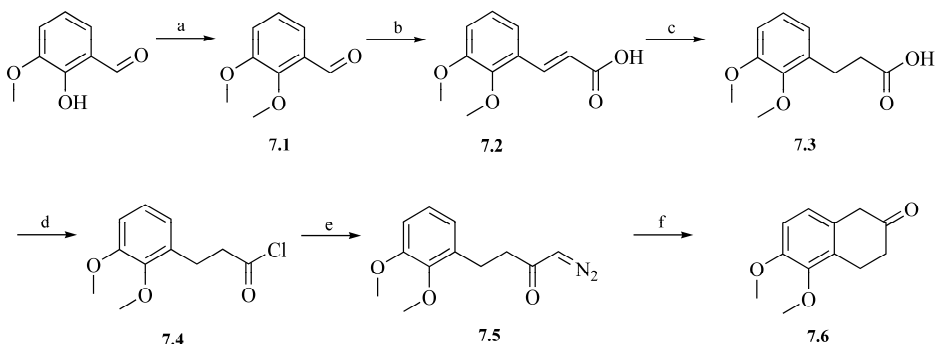
Scheme 7.2 Synthesis of 5,6-dimethoxy-2-tetralone (**7.6**) according to Copinga *et al*. Reagents and conditions: a) K$_2$CO$_3$, (CH$_3$)$_2$SO$_4$, MeOH, reflux, overnight; b) malonic acid, piperidine, pyridine, 75°C, 2h, reflux, overnight; c) 3.5 bar H$_2$, 10% Pd/C, 96% EtOH, RT; d) SOCl$_2$, toluene, reflux, 1h; e) diazomethane, Et$_2$O, 5°C, RT, overnight; f) [Rh(CH$_3$COO)$_2$]$_2$, CH$_2$Cl$_2$, reflux for 20 min, CF$_3$COOH, 15 min reflux.

Then, 5,6-dimethoxy-2-(*N,N*-di-*n*-propyl-amino)tetralin (**7.7**) and 5,6-dimethoxy-2-(*N-n*-propyl-amino)tetralin (**7.11**) were synthesized by condensation with dipropylamine and propylamine, respectively, followed by catalytic hydrogenation.[11] The final catechols **7.8** and **7.12** were obtained after refluxing in 48% aqueous hydrobromic acid. The two-step yields for **7.8** and **7.12** were 17% and 20%, respectively (Scheme 7.3).

7.7: R=Propyl
7.11: R=H

7.8: R=Propyl
7.12: R=H
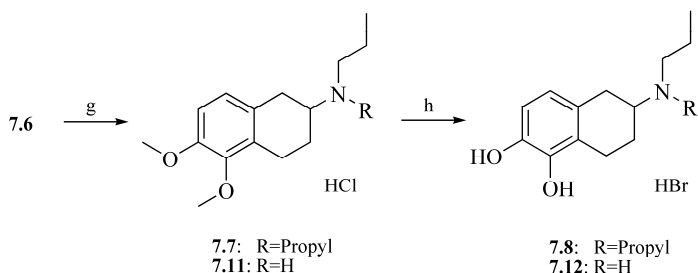
Scheme 7.3 Synthesis of 5,6-dihydroxy-2-(*N,N*-di-*n*-propyl-amino)tetralin HBr-salt (**7.8**) and 5,6-dihydroxy-2-(*N-n*-propyl-amino)tetralin HBr/HCl-salt (**7.12**). Reagents and conditions: g) step 1: dipropylamine (**7.7**) / propylamine (**7.11**), *p*-toluenesulfonic acid, toluene; step 2: 3 bar H$_2$, PtO$_2$, 100% EtOH, RT; h) 48% HBr, reflux.

7.2.2 Synthesis of 5-hydroxy-2-(*N-n*-propyl-amino)-tetralin (7.15) and 5-hydroxy-2-(*N*-ethyl-*N-n*-propyl-amino)tetralin (7.20)

2-(Benzylamino)-5-methoxytetralin (**2.9**) was propylated with 1-iodopropane to give 5-methoxy-2-(*N*-benzyl-*N-n*-propyl-amino)-tetralin (**7.13**). Subsequently, compound **7.13** was debenzylated by hydrogenolysis and demethylated by refluxing in 48% hydrobromic acid. Final compound 5-hydroxy-2-(*N-n*-propyl-amino)-tetralin (**7.15**) was obtained as the hydrobromide salt with a three-step yield of 14% (Scheme 7.4).

2.9   **7.13**   **7.14**   **7.15**
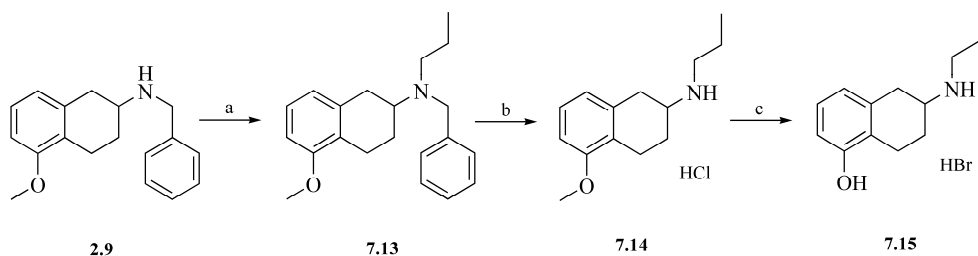
Scheme 7.4 Synthesis of 5-hydroxy-2-(*N-n*-propyl-amino)-tetralin HBr-salt (**7.15**). Reagents and conditions: a) K$_2$CO$_3$, 2-butanone, 1-iodopropane, reflux, overnight; b) 3 bar H$_2$, 10% Pd/C, 100% EtOH, 50°C; c) 48% HBr, reflux.

Because of limited amounts of compound **7.14** the synthesis of compound 5-hydroxy-2-(*N*-ethyl-*N*-propyl-amino)tetralin (**7.20**) was started from intermediate **2.9**. The benzylaminotetraline was amidated with acetylchloride and then reduced by lithium aluminium hydride to give 5-methoxy-2-(*N*-benzyl-*N*-ethyl-amino)tetralin (**7.17**). Compound **7.17** was then successively debenzylated, amidated with propionylchloride and reduced with lithium aluminium hydride to 5-methoxy-2-(*N*-ethyl-*N*-propyl-amino)tetralin (**7.19**). After demethylation in 48% hydrobromic acid the final compound 5-hydroxy-2-(*N*-ethyl-*N*-propyl-amino)tetralin (**7.20**) was obtained as the hydrobromide salt with a yield of 7% over five steps.
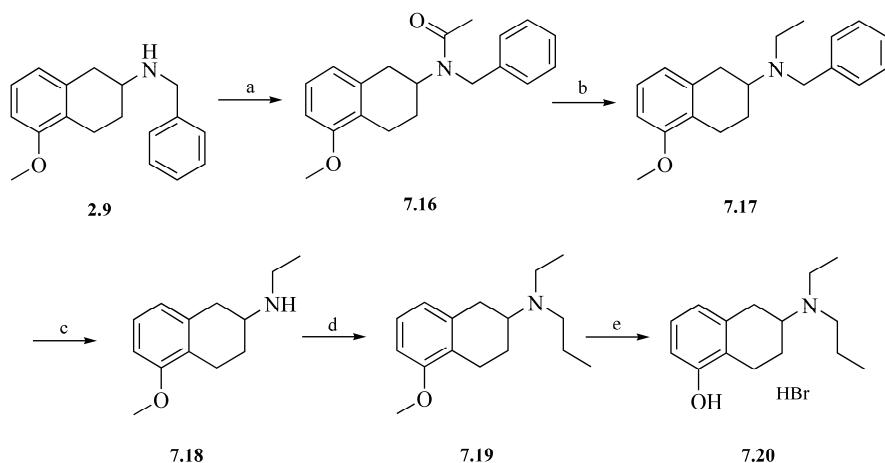
Scheme 7.5 Synthesis of 5-hydroxy-2-(*N*-ethyl-*N*-*n*-propyl-amino)tetralin HBr-salt (**7.20**). Reagents and conditions: a) TEA, toluene, acetylchloride, RT, 1.5 h; b) THF, LiAlH$_4$, RT, 40 min; c) 3.5 bar H$_2$, 10% Pd/C, 100% EtOH, 50°C; d) step 1: TEA, toluene, propionylchloride, RT, 30 min; step 2: THF, LiAlH$_4$, RT, 20 min; e) 48% HBr, reflux.

7.2.3 Synthesis of 8-hydroxy-3,4-dihydro-3-(*N,N*-di-*n*-propylamino)-2*H*-1-benzopyran (7.22)

The route for the synthesis of 8-hydroxy-3,4-dihydro-3-(*N,N*-di-*n*-propylamino)-2*H*-1-benzopyran (**7.22**) is outlined in Scheme 7.6. Benzopyranone **8.5** of which the synthesis was described in detail in Chapter 8, was condensated with dipropylamine in the presence of glacial acetic acid in pentan-1-ol, followed by catalytic hydrogenation to give 8-methoxy-3,4-dihydro-3-(*N,N*-di-*n*-propylamino)-2*H*-1-benzopyran (**7.21**). After the demethylation in 48% hydrobromic acid the final compound 8-hydroxy-3,4-dihydro-3-(*N,N*-di-*n*-propylamino)-2*H*-1-benzopyran (**7.22**) was obtained as the hydrobromide salt with a two-step yield of 4%.[12] Both reactions gave very low yields because of difficulties during the purification steps.

Boyé *et al.* observed an unexpected rearrangement after refluxing benzopyran **7.21** with boron tribromide in dichloromethane. Instead of the expected formation of compound **7.22** another product was obtained, i.e. 7-hydroxy-2,3-dihydro-2-(*N,N*-di-*n*-propylaminomethyl)-2*H*-1-benzofuran **7.23**.[14] In addition, we found that this rearrangement not only occurred after refluxing with boron tribromide, but also during the reaction when performed at -30 ºC. Wise *et al.* performed the reaction in chloroform at -30 ºC and did not observe any rearrangement.[12] Hence, the solvent could have influence on a possible rearrangement of the benzopyran to the benzofuran. Further investigations were not performed.
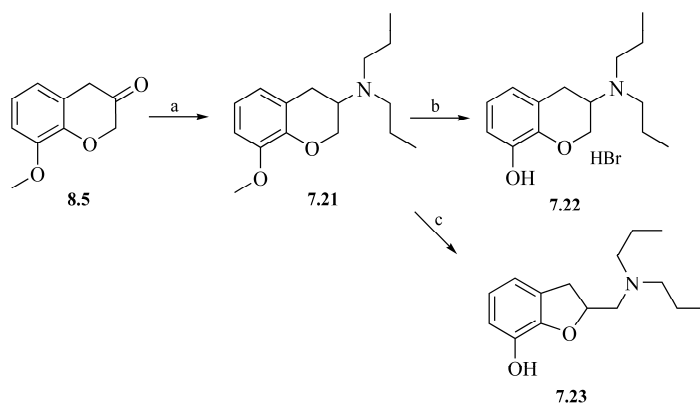
Scheme 7.6 Synthesis of 8-hydroxy-3,4-dihydro-3-(*N,N*-di-*n*-propylamino)-2*H*-1-benzopyran HBr-salt (**7.22**) and 7-hydroxy-2,3-dihydro-2-(*N,N*-di-*n*-propylaminomethyl)-2*H*-1-benzofuran (**7.23**). Reagents and conditions: a) step 1: dipropylamine, CH$_3$COOH, pentan-1-ol, reflux, 3 h; step 2: 3.5 bar H$_2$, PtO$_2$, MeOH, RT, overnight; b) 48% HBr, reflux; c) BBr$_3$, CH$_2$Cl$_2$, -30°C-RT, overnight.

Table 7.1 Overall yields and purities of the HBr salts of compounds **7.8**, **7.12**, **7.15**, **7.20**, **7.22**.

Compound	Name	Yield (%)	Purity (%)
7.8	5,6-(OH)$_2$-DPAT	1.8	>99[a]
7.12	5,6-(OH)$_2$-MPAT	2.3	>99[a]
7.15	5-OH-MPAT	3.8	>95[b]
7.20	5-OH-EPAT	5.8	99[c]
7.22	8-OH-DPAC	2.5	>95[b]

[a] Based on elemental analysis; [b] Based on HPLC; [c] Based on GCMS

7.3 RESULTS

The solubility data and *in vitro* iontophoretic transport results of the synthesized DA agonists that are presented in Section 7.3.1 and Section 7.3.2 were all adapted from studies by Ackaert *et al.*[24]

7.3.1 Aqueous solubility

The results of the solubilities of the HBr salts of compounds **7.8**, **7.12**, **7.15**, **7.20**, **7.22** in citric buffer 5mM pH 5.0, containing 4 g l^{-1} NaCl and 23.1 g l^{-1} D-mannitol can be found in Table 7.2. The solubility data of rotigotine.HCl and 5-OH-DPAT.HBr were added to the table for comparison. The DA agonists are ranked in order of increasing solubility as follows: rotigotine < 5,6-(OH)$_2$-DPAT < 5-OH-DPAT < 5-OH-MPAT < 5-OH-EPAT < 8-OH-DPAC. Also the calculated log P values are presented in Table 7.2.[24]

Table 7.2 The physicochemical properties and iontophoretic fluxes of compounds **7.8**, **7.12**, **7.15**, **7.20**, **7.22**.[24] The molecular weight (MW), calculated log P (cLogP), aqueous solubility, and the observed flux after 9h iontophoresis across HSC and DHS are presented. The MW, cLogP, and solubility of 5-OH-DPAT and rotigotine, obtained from literature, are added to the table for comparison.

Compound	Name	MW (g.mol^{-1})	cLogP^c	Solubility (mM)	HSC Flux$_{9h}$ (nmol.cm^{-2}.h^{-1})	DHS Flux$_{9h}$ (nmol.cm^{-2}.h^{-1})
7.8	5,6-(OH)$_2$-DPAT	263.38	3.74	44.2	175.0±15.9	175.2±25.9
7.12	5,6-(OH)$_2$-MPAT	221.30	2.50	n.d.	134.5±12.9	n.d.
7.15	5-OH-MPAT	205.30	2.93	93.1	219.7±31.4	241.8±11.2
7.20	5-OH-EPAT	233.36	3.71	111.7	247.7±12.1	199.8±8.0
7.22	8-OH-DPAC	249.36	3.40	282.5	175.9±18.9	168.2±13.2
2.12	5-OH-DPAT	247.38	4.15	56.7 ^{a}	207.7±38.0	193.0±19.9
	Rotigotine	315.48	4.82	7.1 ^{b}	-	-

a,b: value adapted from literature.[1, 25];c: Calculated using ALOGPS 2.1.[26-28]; n.d.: not determined

7.3.2 Iontophoretic transport across human stratum corneum and dermatomed human skin

We have found that at pH 5.0 5,6-(OH)$_2$-MPAT (**7.12**) and 5,6-(OH)$_2$-DPAT (**7.8**) were more stable against oxidation than at pH 6.0. Increasing the pH to 7.4 resulted even in a more pronounced degradation of the mono *N*-propyl derivative **7.12**.[24]

The flux of the different compounds at a concentration of 3.9 mM was evaluated statistically after 9 hours of iontophoresis across human stratum corneum (HSC) and dermatomed human skin (DHS) (current density 500 µA.cm^{-2}). Across HSC and DHS 1-way ANOVA analysis showed an overall significant difference in the flux of the different compounds ($p<0.0001$ and $p<0.05$, respectively). The observed flux over HSC after 9 hours increased in the following order: 5,6-(OH)$_2$-MPAT < 5,6-(OH)$_2$-DPAT < 8-OH-DPAC < 5-OH-DPAT < 5-OH-MPAT < 5-OH-EPAT. A similar trend was seen for iontophoretic transport studies across DHS: 8-OH-DPAC < 5,6-(OH)$_2$-DPAT < 5-OH-DPAT < 5-OH-EPAT < 5-OH-MPAT.[24]

A significantly higher electro-osmotic contribution was observed when 5,6-(OH)$_2$-DPAT (12.1 ± 3.4%) was transported through HSC, compared to the other compounds 5-OH-EPAT (4.5 ± 0.9%), 5-OH-MPAT (4.6 ± 1.4%) and 8-OH-DPAT (6.1 ± 0.4%) (1-way ANOVA, Bonferroni post test; $p<0.01$).[24]

7.4 DISCUSSION

7.4.1 Aqueous solubility

The calculated lipophilicity expressed as the logP (clogP) of 5-OH-DPAT (**2.12**) is higher than the clogP of 5,6-(OH)$_2$-DPAT (**7.8**). Nevertheless the aqueous solubility of both compounds are of the same order of magnitude. Apparently the catecholic structure abolishes the increased hydrophilicity which should have rendered the molecule more soluble. The reason of the absence of increased solubility may be intramolecular hydrogen bonding between the two alcohol groups which reduces the reactivity and solubility of catechols (Figure 7.2).[29] The aqueous solubility of 5-OH-MPAT (**7.15**) and 5-OH-EPAT (**7.20**) are approximately two-fold the solubility of 5-OH-DPAT. Thus, decreasing the alkyl chain length on the amino group from propyl to ethyl or hydrogen led to a significant increase of aqueous solubility. Even though aminochroman **7.22** possibly also forms intramolecular hydrogen bonds (Figure 7.2), this compound showed the highest aqueous solubility. The impact on solubility of changing a methylene group in the tetrahydronaphthalene for an ether group as in the aminochroman is apparently large. Perhaps a significant decrease of intermolecular hydrogen bonding compared to that of the catechols gives the increased solubility.
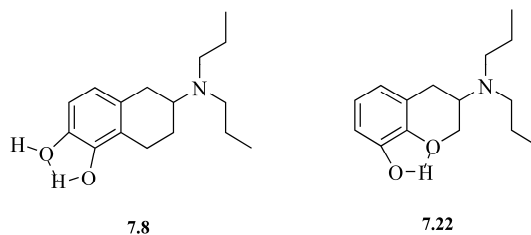
Figure 7.2 Possible intramolecular hydrogen bonding in the molecular structures of the DA agonists 5,6-(OH)$_2$-DPAT (**7.8**) 5-OH-DPA and 8-OH-DPAC (**7.22**).

7.4.2 Transdermal iontophoretic delivery *in vitro*

Although the catecholic compounds **7.8** and **7.12** have a lower calculated lipophilicity, these agonists showed lower iontophoretic fluxes than 5-OH-DAT, which may indicate that the additional ortho-subsituted phenol group interferes with the iontophoretic transport. A reason for this inhibition of iontophoretic delivery could be an increased molecular volume through intramolecular hydrogen bonds between the alcohol groups. It has been shown that an increased molecular volume leads to a decreased total iontophoretic flux.[2, 3] Also the significantly increased electro-osmotic contribution observed with 5,6-(OH)$_2$-DPAT compared to the mono-phenolic compounds may be explained by an increased molecular volume of the catechol.[24, 30]

A similar explanation can be given for the low iontophoretic flux found for 8-OH-DPAC (**7.22**). Intramolecular hydrogen bond formation could lead to an enlarged molecular volume and consequently can be the reason for a lower iontophoretic flux (Figure 7.2). Also the electro-osmotic contribution of **7.22** is higher than this contribution of the tetralin monophenolic analogues 5-OH-MPAT and 5-OH-EPAT which is also an indication for a higher molecular volume.[24] On the other hand, the high solubility found for aminochroman **7.22** contradicts the occurrence of strong hydrogen bonding. This may be explained by a difference between intra- and intermolecular hydrogen bonding. The intramolecular hydrogen bonding being important for the iontophoretic flux, and the intermolecular hydrogen bonding being important for the solubility of this compound.

The higher iontophoretic fluxes of 5-OH-MPAT as well as 5-OH-EPAT compared to 5-OH-DPAT can be explained by the lower lipophilicity originating from the decreased alkyl chain length. Del Terzo *et al*. found that iontophoretic enhancement values decreased linearly with increasing alkyl chain length.[6]

The influence of molecular structural features on transdermal iontophoretic delivery has been investigated in the literature, and molecular volume and molecular weight have been assigned as important physicochemical properties. Based on the results described in this chapter it is concluded that lipophilicity and molecular volume also play a significant role in the iontophoretic transdermal delivery of structurally related DA agonists. Possibly intramolecular hydrogen bonding within catecholic tetraline and alcoholic chroman structures leads to an increased molecular volume and decreased transdermal iontophoretic delivery.

In conclusion, compared to 5-OH-DPAT, 8-OH-DPAC shows the highest solubility, which could allow a smaller patch size, higher concentrations in the donor phase of the iontophoretic device, and a higher iontophoretic flux. Also considering its strong DAergic activity, this agonist can be an interesting candidate for further investigation on transdermal iontophoretic delivery. The synthesized DA receptor agonists proved valuable compounds for studies to improve the understanding of molecular structure on transdermal iontophoretic delivery.
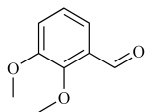
7.5 EXPERIMENTAL

7.5.1 General

The materials and analysis methods are described in section 2.4.1

### 7.5.2 Preparation of 5,6-dihydroxy-2-(*N,N*-di-*n*-propyl-amino)tetralin

2,3-Dimethoxy-benzaldehyde (7.1).[21] A mixture of *o*-vanillin (11 g, 1.19 mol), K_2CO_3 (269 g, 1.95 mol), dimethylsulfate (200 mL, 2.1 mol) and MeOH (950 mL) was refluxed overnight. The yellow

suspension was cooled to room temperature, diluted with H_2O (450 mL) and carefully acidified with 2.5 M H_2SO_4 (aq). Most of the MeOH was evaporated *in vacuo* and the remaining aqueous suspension was extracted with CH_2Cl_2 (4x400mL). The combined organic layers were washed with 2N NaOH (3x200 mL), H_2O (200 mL), brine (200 mL), dried on $MgSO_4$ and evaporated *in vacuo* to yield **7.1** as white solid material (178 g, 90%). Purity>98%; IR (KBr, cm[-1]) ν_{max} 1688, 1584, 1481, 1263, 1121; ^{1}H NMR (200 MHz, $CDCl_3$): δ 10.37 (s, 1H, CH=O), 7.41-7.30 (m, 1H, ArH), 7.17-7.02 (m, 2H, ArH), 3.93 (s, 3H, 2-OCH$_3$), 3.85 (s, 3H, 3-OCH$_3$); ^{13}C NMR (50 MHz, $CDCl_3$): δ 190.3, 153.2, 152.9, 129.9, 124.3, 119.3, 118.3, 62.5, 56.2; EI-MS *m/z* 166 (M)[+].

(*E*)-3-(2,3-Dimethoxyphenyl)-2-propenoic acid (7.2).[22] A stirred mixture of **7.1** (178 g, 1.07 mol), malonic acid (263 g, 2.53 mol), piperidine (19.3 mL, 0.20 mol) and pyridine (600 mL, 7.42 mol) was heated at 75 °C for 2 hours and then refluxed overnight. The reaction mixture was cooled to room temperature and was slowly neutralized with 37% HCl (aq) while cooling in ice until no precipitation occurred anymore. The white precipitation was collected by filtration and was suspended and stirred in H_2O for 1 hour. After filtration and drying *in vacuo* **7.2** was obtained as white solid material (192 g, 86%). Purity: 100%; EI-MS *m/z* 208 (M)[+].
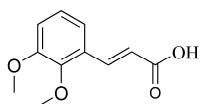
2,3-Dimethoxybenzenepropanoic acid (7.3).[18] To a solution of **7.2** (50 g, 0.24 mol) in 96% EtOH (240 mL) was added Pd/C 10% (3.5 g) under nitrogen atmosphere. The mixture was hydrogenated at room temperature under 3.5 bar H_2 atmosphere. After completion of the reaction the mixture was filtrated and evaporated *in vacuo* to yield **7.3** as a light yellow solid (39.4 g, 78%). Purity: 100%; IR (KBr, cm[-1]) ν_{max} 2939, 1705, 1598,1480, 1433, 1289, 1215, 1085, 1045, 1003; EI-MS *m/z* 210 (M)[+].
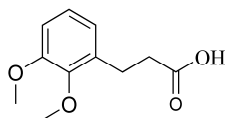
2,3-Dimethoxybenzenepropanoyl chloride (7.4).[18] $SOCl_2$ (8 mL, 0.11 mol) was added to a solution of **7.4** (16.5 g, 0.079 mol) in toluene (100 mL) under nitrogen atmosphere. The reaction mixture was refluxed for 1 hour and after cooling, the volatiles were removed *in vacuo*. The crude acid chloride was yielded as a dark yellow oil which was used without further purification in the next step. IR (NaCl, cm[-1]) ν_{max} 2941, 1794, 1585, 1481, 1271, 1223, 1082.
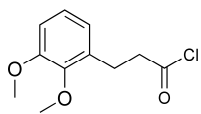
1-Diazo-4-(2,3-dimethoxyphenyl)-2-butanone (7.5).[18] A solution of crude acid chloride **7.4** was dissolved in dry Et_2O (100 mL) and slowly added to a cold dry yellow ethereal solution of diazomethane[31] (approx. 8.5 g) at 5 °C under an atmosphere of nitrogen. When all acid chloride was added, the orange reaction mixture was stirred overnight at room temperature to allow excess diazomethane to evaporate in the fume hood. The solution was evaporated *in vacuo* to yield the crude product of **7.5** as a thick yellow-brown oil (23.4 g). IR (NaCl, cm[-1]) ν_{max} 2911, 2102, 1643, 1480, 1389, 1269, 1077.
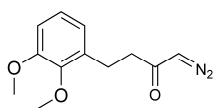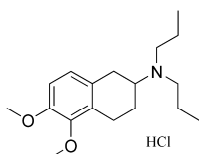
5,6-dimethoxy-2-tetralone (7.6).[18] The crude diazoketone **7.5** (23.4 g) was dissolved in CH_2Cl_2 (200 mL) and was slowly added to a stirring solution of rhodium diacetate dimer (200 mg) in CH_2Cl_2 (150 mL) under nitrogen atmosphere. The reaction mixture was refluxed for 20 minutes, 3 drops of CF_3COOH were added and refluxing was continued for 15 minutes. After cooling down, the reaction mixture was washed with $NaHCO_3$ (sat), brine and dried over $MgSO_4$. The solvent was evaporated *in*
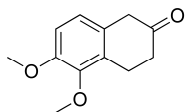
vacuo to yield a brown-orange oil (14.2 g). The oil was added to 50 mL of a solution of $Na_2S_2O_5$ (80 g in 140 mL H_2O and 70 mL EtOH) and the mixture was stirred vigorously until precipitation occurred. After filtration, the precipitated salt was washed with EtOH and Et_2O. The white precipitation was dissolved in H_2O, basified with Na_2CO_3, extracted with Et_2O, dried on $MgSO_4$ and evaporated *in vacuo* to give **7.5** as white solid material (3.0 g, 18.3% over 3 steps). Purity: 100%; IR (NaCl cm^{-1}) v_{max} 2935, 1715, 1493, 1273, 1088; ^{1}H NMR (400 MHz, CDCl$_3$): δ 6.82 (d, *J*=8.4 Hz, 1H, ArH), 6.79 (d, *J*=8.4 Hz, 1H, ArH), 3.85 (s, 3H, OCH$_3$), 3.81 (s, 3H, OCH$_3$), 3.50 (s, 2H, H$_1$), 3.10 (t, *J*=6.6 Hz, 2H, H$_4$), 2.48 (t, *J*=6.6 Hz, 2H, H$_3$); EI-MS *m/z* 206 (M)$^+$.

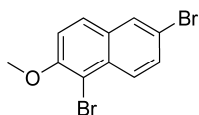**5,6-dimethoxy-2-(*N,N*-di-*n*-propyl-amino)tetralin HCl-salt (7.7)[11]** Under nitrogen atmosphere a solution of **7.6** (2.0 g, 9.7 mmol), dipropylamine (5.5 mL, 39.7 mmol) and *p*-toluenesulfonic acid monohydrate (0.19 g, 1 mmol) in toluene (55 mL) was refluxed with continuous removal of water. After completion of the reaction, 100% EtOH (60 mL) and PtO$_2$ (97 mg) were added and the reaction mixture was hydrogenated at room temperature under 3 bar H$_2$ atmosphere. The reaction mixture was filtrated and the solvent was evaporated *in vacuo* to yield the crude product as a brown-red oil which was converted to the HCl-salt. The salt was decolourized with active charcoal and recrystallized from MeOH/Et$_2$O to yield **7.7** as white solid material (2.0 g, 62%). IR (KBr, cm^{-1}) v_{max} 2968, 2419, 1491, 1457, 1280, 1089, 1051; ^{1}H NMR (200 MHz, CD$_3$OD): δ 6.87 (s, 2H, ArH), 3.81 (s, 3H, OCH$_3$), 3.76 (s, 3H, OCH$_3$), 3.72-3.58 (m, 1H, H$_{2ax}$), 3.33-2.91 (m, 7H, H$_{1ax}$, H$_{1eq}$, N(*CH$_2$*CH$_2$CH$_3$)$_2$, H$_{4eq}$), 2.84-2.60 (m, 1H, H$_{4ax}$), 2.42-2.27 (m, 1H, H$_{3eq}$), 1.99-1.71 (m, 5H, H$_{3ax}$, N(CH$_2$*CH$_2$*CH$_3$)$_2$), 1.04 (t, J=7.3 Hz, 6H, N(CH$_2$CH$_2$*CH$_3$)$_2$); ^{13}C NMR (50 MHz, CD$_3$OD): δ 151.2, 146.4, 128.9, 124.6, 111.2, 60.5, 59.2, 55.2, 52.7, 28.9, 23.5, 22.7, 18.5, 10.2; EI-MS *m/z* 291 (M)$^+$.
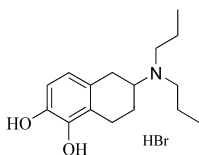
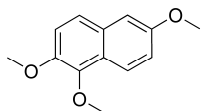**5,6-dihydroxy-2-(*N,N*-di-*n*-propyl-amino)tetralin HBr-salt (7.8).** A mixture of freshly distilled 48% HBr (11 mL) and **7.7** (0.93 g, 2.9 mmol) was refluxed for 2 hours under nitrogen atmosphere. The hot solution was cooled down overnight while stirring slowly to allow the HBr salt to crystallize from the solution. The white crystals were filtrated, washed with EtOH 100% and recrystallized from 100% EtOH/Et$_2$O to afford the HBr salt of **7.8** as white solid material (0.26 g, 27%). IR (KBr, cm^{-1}) v_{max} 3233, 2930, 2727, 1498, 1293; ^{1}H NMR (300 MHz, *d$_6$*-DMSO): δ 9.25 (br s, 1h, NH), 9.04 (d, *J*=4.8 Hz, 1H, OH), 8.25 (d, *J*=3.3 Hz, 1H, OH), 6.60 (d, *J*=8.1 Hz, 1H, ArH), 6.40 (d, *J*=8.1 Hz, 1H, ArH), 3.63-3.45 (m, 1H, H$_{2ax}$), 3.28-2.77 (m, 7H, H$_{1ax}$, H$_{1eq}$, N(*CH$_2$*CH$_2$CH$_3$)$_2$, H$_{4eq}$), 2.59-2.41 (m, 1H, H$_{4ax}$), 2.33-2.18 (m, 1H, H$_{3eq}$), 1.86-1.58 (m, 5H, H$_{3ax}$, N(CH$_2$*CH$_2$*CH$_3$)$_2$), 0.90 (t, J=7.3 Hz, 6H, N(CH$_2$CH$_2$*CH$_3$)$_2$); ^{13}C NMR (50 MHz, *d$_6$*-DMSO): δ 143.5, 143.0, 124.7, 123.2, 129.8, 114.2, 60.2, 52.3, 39.8, 29.4, 23.5, 18.6, 11.7; HR-MS *m/z* Calcd. for $C_{16}H_{26}NO_2$ 264.19581 (M+H)$^+$, found 264.19540 (M+H)$^+$; Anal. Calcd for $C_{16}H_{26}NO_2Br$: C, 55.82; H, 7.61; N, 4.07. Found: C, 55.73; H, 7.64; N, 4.07.

**1,6-Dibromo-2-methoxy-naphthalene (7.9).[20]** Iodomethane (41 mL, 0.66 mol) was added dropwise to a stirring suspension of 1,6-dibromo-2-naphthol (101 g, 0.33 mol) and K$_2$CO$_3$ (114 g, 0.83 mol) in anhydrous DMF (100 mL) while the temperature was kept beneath 30 °C. After stirring for 3 hours, the reaction mixture was partitioned between CH$_2$Cl$_2$/H$_2$O and extracted with CH$_2$Cl$_2$ (2x). The combined organic layers were dried on MgSO$_4$, evaporated *in vacuo* and recrystallized from Et$_2$O/Hexane to yield **7.9** as white crystals (93 g, 89%). Purity:100% (GCMS); EI-MS *m/z* 316 (M)$^+$.

198

1,2,6-Trimethoxy-naphthalene (7.10).[19, 20] Under nitrogen atmosphere slowly sodium cut in small pieces (43.5 g, 1.95 mol) was added to cold dry MeOH (690 mL) while cooling in ice. When almost all sodium was added, the mixture was heated slightly to dissolve the remaining sodium. Vacuum-dried **7.9** (90 g, 0.28 mol) and dry 2,4,6-collidine (280 mL, 2.10 mol) were added and the grey cloudy grey solution turned into a clear brown solution. Then, vacuum-dried copper(I)iodide (65 g, 0.34 mol) was added and the solution turned into a yellow-green suspension. The nitrogen-flushed reaction mixture was refluxed for 5 hours , was filtrated over celite and evaporated *in vacuo*. The resultant orange slurry was diluted with H_2O (1.4 L), neutralized with 37% HCl (aq, 240 mL) and extracted with EtOAc (3 x 1L). The combined organic layers were washed with 1N HCl (aq, 250 mL), H_2O (250 mL), brine (100 mL), dried on $MgSO_4$ and evaporated *in vacuo*. After purification by column chromatography (SiO_2, Hexane/EtOAc=32:1 to 16:1, gradient) crude **7.10** was afforded as white-green solid material (45.9 g, 68%). Purity: 90%; IR (KBr, cm^{-1}) ν_{max} 2960, 1602, 1448, 1358, 1271, 1241, 1161, 1095, 1021; EI-MS *m/z* 218 (M)$^+$.

7.5.3 Preparation of 5,6-dihydroxy-2-(*N-n*-propyl-amino)tetralin

5,6-dimethoxy-2-(*N-n*-propyl-amino)tetralin HCl-salt (7.11).[11] Under nitrogen atmosphere a solution of **7.6** (0.98 g, 4.7 mmol), propylamine (0.48 mL, 5.8 mmol) and a catalytic amount of *p*-toluenesulfonic acid monohydrate in toluene (16 mL) was refluxed with continuous removal of water. After completion of the reaction, the solvent was evaporated *in vacuo* and 100% EtOH (25 mL) and PtO_2 (19 mg) were added and the reaction mixture was hydrogenated at room temperature under 3 bar H_2 atmosphere. The reaction mixture was filtrated and the solvent was evaporated *in vacuo* to yield the crude product as a dark purple oil which was converted to the HCl-salt. The salt was decolourized with active charcoal and recrystallized from 100% EtOH/Et_2O to yield **7.11** as solid light-brown material (0.48 g, 36%). Purity: 93% (GCMS); ^{1}H NMR (400 MHz, CDCl$_3$): δ 6.79 (d, *J*=8.4 Hz, 1H, ArH), 6.72 (d, *J*=8.1 Hz, 1H, ArH), 3.82 (s, 3H, OCH$_3$), 3.79 (s, 3H, OCH$_3$), 3.04-2.79 (m, 3H, H$_2$, H$_4$), 2.72-2.57 (m, 3H, N(*CH$_2$*CH$_2$CH$_3$), H$_1$), 2.51 (dd, *J*=15.4 Hz, *J*=9.5 Hz, 1H, H$_1$), 2.10-1.97 (m, 1H, H$_{3eq}$), 1.59-1.45 (m, 3H, H$_{3ax}$, N(CH$_2$*CH$_2$*CH$_3$)), 1.38 (br s, NH, 1H), 0.93 (t, *J*=7.5 Hz, 3H, CH$_3$); ^{13}C NMR (50 MHz, CDCl$_3$): δ 150.7, 146.7, 130.9, 129.0, 124.6, 110.5, 60.1, 56.1, 52.7, 49.3, 36.5, 29.5, 23.8, 22.7, 12.1; EI-MS *m/z* 249 (M)$^+$.
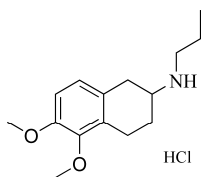
5,6-dihydroxy-2-(*N*-propyl-amino)tetralin HBr/HCl-salt (7.12). A mixture of freshly distilled 48% HBr (5 mL) and **7.11** (264 mg, 1.1 mmol) was refluxed for 3 hours under nitrogen atmosphere. The hot solution was allowed to attain room temperature and the HBr salt crystallized from the solution as white needles. The crystals were filtrated, washed with 100% EtOH and stirred in hot 2N HCl in MeOH for 2 hours to convert the HBr-salt to the HCl-salt. After recrystallization from MeOH/Et_2O compound **7.12** was afforded as the HBr/HCl (6:1) salt as white solid material (135 mg, 58%). IR (KBr cm^{-1}) ν_{max} 3486, 3096, 2972, 1498, 1464, 1299, 1015; ^{1}H NMR (400 MHz, CD$_3$OD): δ 6.63 (t, *J*=8.4 Hz, 1H, ArH), 6.48 (d, *J*=8.4 Hz, 1H, ArH), 3.46-3.36 (m, 1H, H$_{2ax}$), 3.14 (ddd, *J*=5.9 Hz, *J*= 3.7 Hz, *J*=1.8 Hz, 1H, H$_1$) 3.11-3.04 (m, 2H, N*CH$_2$*CH$_2$CH$_3$, H$_{4eq}$), 3.00 (ddd, *J*=17.6 Hz, *J*=5.9 Hz, *J*=3.3 Hz, 1H, H$_{4eq}$), 2.79 (dd, *J*=15.2 Hz, *J*=10.4 Hz, 1H, H$_1$), 2.66 (ddd, *J*=17.6 Hz, *J*=11.4 Hz, *J*=6.2 Hz, 1H, H$_{4ax}$), 2.37-2.25 (m, 1H, H$_{3eq}$), 21.85-1.65 (m, 5H,
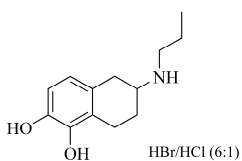
H$_{3ax}$, N(CH$_2$CH$_2$CH$_3$)$_2$), 1.05 (t, J=7.5 Hz, 6H, N(CH$_2$CH$_2$CH$_3$)$_2$); ^{13}C NMR (50 MHz, CD$_3$OD): δ 160.2, 147.0, 127.5, 126.2, 123.5, 117.3, 58.8, 50.6, 35.6, 29.6, 25.6, 23.7, 14.1; HR-MS m/z Calcd. for C$_{13}$H$_{20}$NO$_2$ 222.14886 (M+H)$^+$, found 222.14888 (M+H)$^+$; Anal. Calcd for C$_{13}$H$_{20}$NO$_2$Br/C$_{13}$H$_{20}$NO$_2$Cl (6:1): C, 52.78; H, 6.81; N, 4.73. Found: C, 52.75; H, 6.83; N, 4.72.

7.5.4 Preparation of 5-hydroxy-2-(*N*-*n*-propyl-amino)-tetralin

5-methoxy-2-(*N*-benzyl-*N*-*n*-propyl-amino)-tetralin (7.13). A mixture of **2.9** (which was recovered as free amine from the combined motherliquors of the resolution of **(±)-2.9**) (0.70 g, 2.4 mmol), K$_2$CO$_3$ (0.99 g, 7.2 mmol) were suspended in 6 mL 2-butanone. 1-Iodopropane (0.64 mL, 6.6 mmol) was added while the mixture was heated to reflux under nitrogen atmosphere. After refluxing overnight and evaporation of the solvent *in vacuo*, the reaction material was partitioned between CH$_2$Cl$_2$ and H$_2$O. The organic layer was separated, dried on MgSO$_4$ and evaporated *in vacuo* to give crude **7.13** as an oil (0.70 g, 63%). Purity: 67% (GCMS); IR (NaCl, cm^{-1}) ν$_{max}$ 2930, 1585, 1467, 1259, 1094; EI-MS m/z 309 (M)$^+$.
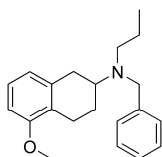
5-methoxy-2-(*N*-*n*-propyl-amino)-tetralin HCl salt (7.14). In a Parr flask, crude **7.13** (0.70 g, 2.3 mmol) was dissolved in 100% EtOH (100 mL) and Pd/C 10% (200 mg) was added under nitrogen atmosphere. The dark suspension was hydrogenolyzed at 50 °C under 3 bar H$_2$ atmosphere. After completion of the reaction the mixture was filtrated, evaporated *in vacuo*, converted to the HCl-salt and recrystallized from 100% EtOH/Et$_2$O to yield the HCl-salt of **7.14** as light pink crystals (0.27 g, 55%). IR (KBr, cm^{-1}) ν$_{max}$ 3435, 2958, 1589, 1471, 1261, 1094; ^{1}H NMR (400 MHz, CDCl$_3$): δ 7.09 (t, J=7.9 Hz, 1H, ArH), 6.71 (d, J=7.7 Hz, 1H, ArH), 6.66 (d, J=8.1 Hz, 1H, ArH), 3.81 (s, 3H, OCH$_3$), 3.07-2.81 (m, 3H, H$_1$, H$_2$), 2.69 (t, J=7.3 Hz, 2H, N(CH_2CH$_2$CH$_3$)$_2$), 2.65-2.48 (m, 2H, H$_4$), 2.12-2.01 (m, 1H, H$_{3eq}$), 1.64-1.43 (m, 4H, NH, H$_{3ax}$, N(CH$_2$CH_2CH$_3$), 0.95 (t, J=7.3 Hz, 3H, CH$_3$); ^{13}C NMR (50 MHz, CDCl$_3$): δ 157.4, 137.0, 126.4, 125.4, 121.8, 107.2, 55.4, 53.4, 49.3, 37.1, 29.5, 23.8, 22.4, 12.1; EI-MS m/z 219 (M)$^+$.
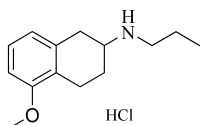
5-hydroxy-2-(*N*-*n*-propyl-amino)-tetralin HBr-salt (7.15). A mixture of freshly distilled 48% HBr (20 mL) and **7.14** (0.40 g, 1.6 mmol) was refluxed overnight under nitrogen atmosphere. After cooling down, the reaction mixture was evaporated *in vacuo* and the resultant orange-brown solid material was decolourized with active charcoal in MeOH. After recrystallization from MeOH/Et$_2$O the HBr-salt of **7.15** was obtained as light grey crystals (0.18 g, 40%); Purity>95% (HPLC); IR (KBr, cm^{-1}) ν$_{max}$ 3305, 2938, 2457, 2166, 1591, 1468, 1283; ^{1}H NMR (200 MHz, CD$_3$OD): δ 6.96 (t, J=7.8 Hz, 1H, ArH), 6.62 (d, J=7.6 Hz, 2H, ArH), 3.58-3.37 (m, 1H, H$_{2ax}$), 3.22-2.77 (m, 5H, H$_{1ax}$, H$_{1eq}$, N(CH_2CH$_2$CH$_3$), H$_{4eq}$), 2.76-2.45 (m, 1H, H$_{4ax}$), 2.44-2.21 (m, 1H, H$_{3eq}$), 1.94-1.61 (m, 3H, H$_{3ax}$, N(CH$_2$CH_2CH$_3$)), 1.0 (t, J=7.3 Hz, 3H, N(CH$_2$CH$_2$CH_3)); ^{13}C NMR (50 MHz, CD$_3$OD): δ 155.0, 133.2, 126.8, 121.9, 120.0, 112.3, 54.7, 46.7, 32.0, 25.6, 21.5, 19.8, 10.2; EI-MS m/z 205 (M)$^+$; Anal. Calcd for C$_{13}$H$_{19}$NO.HBr: C, 54.56; H, 7.04; N, 4.89; Found: C, 53.56; H, 7.03; N, 4.81.

7.5.5 Preparation of 5-hydroxy-2-(*N*-ethyl–*N*-*n*-propyl-amino)tetralin

5-methoxy-2-(*N*-benzylacetamido)-tetralin (7.16). TEA (1.8 mL, 12.9 mmol) was added to a cooled solution of **2.9** (which was recovered as free amine from the combined motherliquors of the resolution
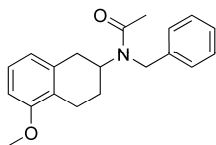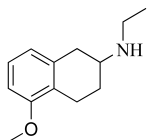
of (±)-2.9) (3.7 g, 12.5 mmol) in dry toluene (30 mL) under nitrogen atmosphere. Acetylchloride (1.0 mL, 14.0 mmol) was added and the reaction mixture was stirred for 1.5 hours. The TEA-HCl salt was removed by filtration and the solvent was evaporated *in vacuo*. The resultant oil was purified on column chromatography (Al$_2$O$_3$, EtOAc/Hexane=1:8 to 1:4, gradient) to yield **7.16** as a clear yellow oil (2.6 g, 68%). Purity: 88% (GCMS); IR (NaCl, cm^{-1}) ν_{max} 2947, 1642, 1585, 1467, 1413, 1261; EI-MS *m/z* 309 (M)$^+$.

5-methoxy-2-(*N*-benzyl-*N*-ethyl-amino)tetralin (7.17). Under nitrogen atmosphere a solution of **7.16** (2.2 g, 7.1 mmol) in dry THF (30 mL) was added to a suspension of LiAlH$_4$ (0.41 g, 10.8 mmol) in dry THF (30 mL) and the mixture was stirred for 40 minutes. After addition of EtOAc, diluted H$_2$SO$_4$ (8 mL) was added until precipitation at pH 2. The mixture was filtrated, basified with 2N NaOH (10 mL) and extracted with EtOAc (2x75 mL). The combined organic layers were washed with brine, dried on MgSO$_4$, evaporated *in vacuo* and purified on column chromatography (Al$_2$O$_3$, Hexane/EtOAc=3:1 to 1:1, gradient) to yield **7.17** as a colourless oil (1.19 g, 56%). Purity: 89% (GCMS); IR (NaCl, cm^{-1}) ν_{max} 2929, 1585, 1468, 1260, 1094; EI-MS *m/z* 295 (M)$^+$.
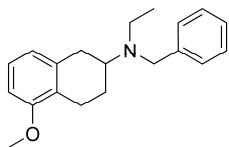
5-methoxy-2-(*N*-ethyl-amino)tetralin (7.18). In a Parr flask, **7.17** (1.14 g, 3.9 mmol) was dissolved in 100% EtOH (100 mL) and Pd/C 10% (0.66 g) was added under nitrogen atmosphere. The dark suspension was hydrogenolyzed at 50 °C under 3.5 bar H$_2$ atmosphere. After completion of the reaction the mixture was filtrated, evaporated *in vacuo* to yield **7.18** as a colourless oil (0.58 g, 74%). Purity: 93% (GCMS); IR (NaCl, cm^{-1}) ν_{max} 2933, 1585, 1469, 1258, 1095; EI-MS *m/z* 205 (M)$^+$.

5-methoxy-2-(*N*-ethyl-*N*-propyl-amino)tetralin (7.19). TEA (0.4 mL, 2.9 mmol) was added to a cooled solution of **7.18** (0.58 g, 2.8 mmol) in dry toluene (15 mL) under nitrogen atmosphere. Propionylchloride (0.25 mL, 2.9 mmol) was added and the reaction mixture was stirred for 30 minutes. The TEA-HCl salt was removed by filtration and the solvent was evaporated *in vacuo* to give the intermediate crude amide as a light yellow oil which solidified on standing (0.78 g). Under nitrogen atmosphere a solution of the amide in dry THF (10 mL) was added dropwise to a suspension of LiAlH$_4$ (0.16 g, 4.2 mmol) in dry THF (10 mL) and the mixture was stirred for 20 minutes. After addition of EtOAc, diluted H$_2$SO$_4$ was added until precipitation at pH 2. The mixture was filtrated, basified with 2N NaOH (10 mL) and extracted with EtOAc. The combined organic layers were washed with brine, dried on MgSO$_4$, evaporated *in vacuo* and purified by column chromatography (SiO$_2$ (NH$_3$), CH$_2$Cl$_2$/MeOH=20:1) to yield **7.19** as a clear yellow oil (0.43 g, 61%). Intermediate amide: EI-MS *m/z* 261 (M)$^+$. Final compound: Purity: 68% (GCMS); IR (NaCl, cm^{-1}) ν_{max} 2959, 2933, 1585, 1468, 1259, 1095; EI-MS *m/z* 247 (M)$^+$.
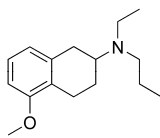
5-hydroxy-2-(*N*-ethyl-*N*-propyl-amino)tetralin HBr-salt (7.20). A mixture of freshly distilled 48% HBr (5 mL) and **7.19** (0.37 g, 1.5 mmol) was refluxed for 1 hour under nitrogen atmosphere. After cooling down, the reaction mixture was evaporated *in vacuo* and the resultant orange-brown solid material was recrystallized from 100% EtOH/Et$_2$O to yield the HBr-salt of **7.20** as white crystals (0.18 g, 40%). Purity: 99% (GCMS); IR (KBr, cm^{-1}) ν_{max} 3186, 2940, 2646, 1591, 1466, 1271, 1015; ^{1}H NMR (200 MHz, CD$_3$OD): δ 6.97 (t, *J*=7.8 Hz, 1H, ArH), 6.69-6.57 (m, 2H, ArH), 3.80-3.59 (m,
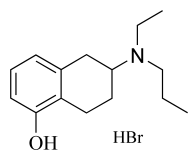
1H, H$_{2ax}$), 3.58-2.97 (m, 7H, H$_{1ax}$, H$_{1eq}$, N(CH$_2$CH$_2$CH$_3$), N(CH$_2$CH$_3$), H$_{4eq}$), 2.76-253 (m, 1H, H$_{4ax}$), 2.45-2.37 (m, 1H, H$_{3eq}$), 2.01-1.71 (m, 3H, H$_{3ax}$, N(CH$_2$CH$_2$CH$_3$)), 1.40 (t, J=7.2 Hz, 3H, N(CH$_2$CH$_2$CH$_3$)), 1.05 (t, J=7.4 Hz, 3H, N(CH$_2$CH$_3$)); ^{13}C NMR (50 MHz, CD$_3$OD): δ 155.0, 133.7, 126.8, 121.9, 120.0, 112.3, 60.0, 52.0, 46.6, 29.8, 23.7, 22.5, 18.7, 10.2, 9.4; EI-MS m/z 233 (M)$^{+}$; Anal. Calcd for C$_{15}$H$_{23}$NO.HBr: C, 57.33; H, 7.70; N, 4.46. Found: C, 57.50; H, 7.76; N, 4.50.

7.5.6 Preparation of 8-hydroxy-3,4-dihydro-3-(N,N-di-n-propylamino)-2H-1-benzopyran

8-methoxy-3,4-dihydro-3-(N,N-di-n-propylamino)-2H-1-benzopyran (7.21).[12] A mixture of benzopyranone **9.5** (1.2 g, 6.7 mmol), dipropylamine (1.3 mL, 9.5 mmol), and glacial acetic acid (0.06 mL, 1.0 mmol) in pentan-1-ol (10 mL) was refluxed for 3 hours with continuous removal of water via a Dean-Stark water trap. The solvent was evaporated in vacuo, the residue was dissolved in EtOAc and filtered through a bed of silica gel. After evaporation of the solvent, the resultant dark oil was dissolved in MeOH (25 mL) and PtO$_2$ (12 mg) was added under nitrogen atmosphere in a Parr flask. The mixture was hydrogenated overnight at room temperature under 3.5 bar H$_2$ atmosphere. The reaction mixture was filtrated, evaporated in vacuo and purified by column chromatography (SiO$_2$, Hexane/EtOAc=2:1, 0.1% TEA) to yield **7.21** as a yellow oil (0.25 g, 14.4%). Purity: 94% (GCMS); IR (NaCl, cm^{-1}) ν$_{max}$ 2958, 1585, 1485, 1262, 1212, 1083; ^{1}H NMR (200 MHz, d$_6$-DMSO): δ 6.77-6.57 (m, 3H, ArH), 4.26-4.13 (m, 1H, H$_2$), 3.80-3.71 (m, 1H, H$_2$), 3.68 (s, 3H, OCH$_3$), 3.09-2.88 (m, 1H, H$_3$), 2.74 (d, J=7.6 Hz, 2H, H$_4$), 2.44 (t, J=7.2 Hz, 4H, N(CH$_2$CH$_2$CH$_3$)$_2$), 1.45-1.24 (m, 4H, N(CH$_2$CH$_2$CH$_3$)$_2$), 0.81 (t, J=7.4 Hz, 6H, N(CH$_2$CH$_2$CH$_3$)$_2$); ^{13}C NMR (50 MHz, d$_6$-DMSO): δ 148.7, 123.2, 122.5, 120.5, 110.3, 67.9, 56.1, 53.4, 52.6, 28.4, 22.0, 12.3; EI-MS m/z 263 (M)$^{+}$.
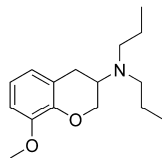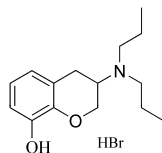
8-hydroxy-3,4-dihydro-3-(N,N-di-n-propylamino)-2H-1-benzopyran HBr-salt (7.22).[12] A mixture of freshly distilled 48% HBr (1.5 mL) and **7.21** (0.20 g, 0.76 mmol) was refluxed for 45 minutes under nitrogen atmosphere. After cooling down, the reaction mixture was evaporated in vacuo and the resultant brown solid material was recrystallized from 100% EtOH to yield the HBr-salt of **7.22** as white crystals (0.08 g, 24%). Purity>95% (HPLC); IR (KBr, cm^{-1}) ν$_{max}$ 3133 (br), 2937, 2647, 2519, 1586, 1501, 1474, 1340, 1273, 1218, 1185, 1001; ^{1}H NMR (300 MHz, CD$_3$OD): δ 6.80 (t, J=7.9 Hz, 1H, ArH), 6.69 (d, J=7.0 Hz, 2H, ArH), 4.63-4.48 (m, 1H, H$_2$), 4.47-4.38 (m, 1H, H$_2$), 4.08-3.95 (m, 1H, H$_3$), 3.45-3.13 (m, 6H, H$_4$, N(CH$_2$CH$_2$CH$_3$)$_2$), 1.95-1.70 (m, 4H, N(CH$_2$CH$_2$CH$_3$)$_2$), 1.02 (t, J=7.3 Hz, 6H, N(CH$_2$CH$_2$CH$_3$)$_2$); ^{13}C NMR (50 MHz, CD$_3$OD): δ 122.0, 120.1, 114.2, 64.1, 56.4, 53.0, 25.4, 17.8, 10.1; HR-MS m/z Calcd. for C$_{15}$H$_{24}$N$_1$O$_2$ 250.1802 (M+H)$^{+}$, found 250.18001 (M+H)$^{+}$; Anal. Calcd for C$_{15}$H$_{24}$NO$_2$Br: C, 54.55; H, 7.32; N, 4.24. Found: C, 54.42; H, 7.32; N, 4.22.

7-Hydroxy-2,3-dihydro-2-(N,N-di-n-propylaminomethyl)-2H-1-benzofuran (7.23).[14] Compound **7.21** (0.56 g, 1.9 mmol) was dissolved in CH$_2$Cl$_2$ and cooled to -30 °C. 1M BBr$_3$ in CH$_2$Cl$_2$ (2.5 mL, 2.2 mmol) was added and the reaction mixture was allowed to slowly attain room temperature and stirred overnight. The reaction mixture was poured on ice (200 mL) and 25% NH$_3$ (aq, 50 mL) was added. The basic water layer was extracted with CH$_2$Cl$_2$, filtrated and evaporated in vacuo. The crude brown oil was purified on column chromatography (SiO$_2$, EtOAc) and **7.11** was obtained as a light
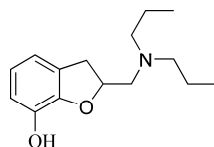
yellow oil (99 mg, 15%). Purity>98% (GCMS); IR (NaCl, cm^{-1}) ν_{max} 3145, 2965, 2751, 1762, 1616, 1469, 1239, 1215; ^{1}H NMR (300 MHz, CD$_3$OD): δ 6.78-6.62 (m, 3H, ArH), 5.35-5.15 (m, 1H, H$_2$), 3.55=3.35 (m, 3H, CH*CH$_2$*N), 3.34-3.12 (m, 4H, H$_3$, N(*CH$_2$*CH$_2$CH$_3$)), 2.94 (dd, *J*=15.9 Hz; 6.2 Hz, 1H, H$_3$), 1.92-1.63 (m, 4H, N(CH$_2$*CH$_2$*CH$_3$)$_2$), 1.03 (t, *J*=7.4 Hz, 6H, N(CH$_2$CH$_2$*CH$_3$*); ^{13}C NMR (50 MHz, CD$_3$OD): δ 122.2, 116.1, 116.0, 115.5, 76.9, 56.2, 33.9, 17.0, 10.0; EI-MS *m/z* 249 (M)$^+$.

7.6 ACKNOWLEDGMENTS

7.7 REFERENCES

1.   Ackaert, O. W.; Van Smeden, J.; De Graan, J.; Dijkstra, D.; Danhof, M.; Bouwstra, J. A. Mechanistic studies of the transdermal iontophoretic delivery of 5-OH-DPAT in vitro. *J. Pharm. Sci.* **2010**, *99,* 275-85.
2.   Roberts, M. S.; Lai, P. M.; Anissimov, Y. G. Epidermal iontophoresis: I. Development of the ionic mobility-pore model. *Pharm. Res.* **1998**, *15,* 1569-78.
3.   Lai, P. M.; Roberts, M. S. An analysis of solute structure-human epidermal transport relationships in epidermal iontophoresis using the ionic mobility: pore model. *J. Controlled Release* **1999**, *58,* 323-33.
4.   Abla, N.; Naik, A.; Guy, R. H.; Kalia, Y. N. Effect of charge and molecular weight on transdermal peptide delivery by iontophoresis. *Pharm. Res.* **2005**, *22,* 2069-78.
5.   Schuetz, Y. B.; Carrupt, P. A.; Naik, A.; Guy, R. H.; Kalia, Y. N. Structure-permeation relationships for the non-invasive transdermal delivery of cationic peptides by iontophoresis. *Eur. J. Pharm. Sci.* **2006**, *29,* 53-9.
6.   Del Terzo, S.; Behl, C. R.; Nash, R. A. Iontophoretic transport of a homologous series of ionized and nonionized model compounds: influence of hydrophobicity and mechanistic interpretation. *Pharm. Res.* **1989**, *6,* 85-90.
7.   Hacksell, U.; Svensson, U.; Nilsson, J. L. G.; Hjorth, S.; Carlsson, A.; Wikstrom, H.; Lindberg, P.; Sanchez, D. N-Alkylated 2-Aminotetralins - Central Dopamine-Receptor Stimulating Activity. *J. Med. Chem.* **1979**, *22,* 1469-1475.
8.   vanVliet, L. A.; Tepper, P. G.; Dijkstra, D.; Damsma, G.; Wikstrom, H.; Pugsley, T. A.; Akunne, H. C.; Heffner, T. G.; Glase, S. A.; Wise, L. D. Affinity for dopamine D-2, D-3, and D-4 receptors of 2-aminotetralins. Relevance of D-2 agonist binding for determination of receptor subtype selectivity. *J. Med. Chem.* **1996**, *39,* 4233-4237.
9.   Feenstra, M. G.; Rollema, H.; Mulder, T. B.; De Vries, J. B.; Horn, A. S. In vivo dopamine receptor agonist binding in rat brain: relation with pharmacological effects. *Eur. J. Pharmacol.* **1983**, *90,* 433-6.
10.   Cannon, J. G.; Lee, T.; Goldman, H. D.; Costall, B.; Naylor, R. J. Cerebral Dopamine Agonist Properties of Some 2-Aminotetralin Derivatives After Peripheral and Intracerebral Administration. *J. Med. Chem.* **1977**, *20,* 1111-1116.
11.   McDermed, J. D.; McKenzie, G. M.; Phillips, A. P. Synthesis and Pharmacology of Some 2-Aminotetralins - Dopamine Receptor Agonists. *J. Med. Chem.* **1975**, *18,* 362-367.
12.   Wise, L. D.; Dewald, H. A.; Hawkins, E. S.; Reynolds, D. M.; Heffner, T. G.; Meltzer, L. T.; Pugsley, T. A. 6-Hydroxy-3,4-Dihydro-3-(Dipropylamino)-2H-1-Benzopyrans and 8-Hydroxy-3,4-Dihydro-3-(Dipropylamino)-2H-1-Benzopyrans - Dopamine Agonists with Autoreceptor Selectivity. *J. Med. Chem.* **1988**, *31,* 688-691.

13.   Dijkstra, D.; Mulder, T. B.; Rollema, H.; Tepper, P. G.; Van der Weide, J.; Horn, A. S. Synthesis and pharmacology of trans-4-n-propyl-3,4,4a,10b-tetrahydro-2H,5H-1-benzopyrano[4,3-b]-1,4-oxazin-7- and -9-ols: the significance of nitrogen pKa values for central dopamine receptor activation. *J. Med. Chem.* **1988**, *31,* 2178-82.

14.   Boye, S.; Pfeiffer, B.; Renard, P.; Rettori, M. C.; Guillaumet, G.; Viaud, M. C. N,N-disubstituted aminomethyl benzofuran derivatives: synthesis and preliminary binding evaluation. *Bioorg. Med. Chem.* **1999**, *7,* 335-41.

15.   Alneirabeyeh, M.; Reynaud, D.; Podona, T.; Ou, L.; Perdicakis, C.; Coudert, G.; Guillaumet, G.; Pichat, L.; Gharib, A.; Sarda, N. Methoxy and Hydroxy Derivatives of 3,4-Dihydro-3-(Di-Normal-Propylamino)-2H-1-Benzopyrans - New Synthesis and Dopaminergic Activity. *Eur. J. Med. Chem.* **1991**, *26,* 497-504.

16.   Horn, A. S.; Kaptein, B.; Vermue, N. A.; Devries, J. B.; Mulder, T. B. A. Synthesis and Dopaminergic Activity of a New Oxygen Isostere of the 2-Aminotetralins - N,N-Dipropyl-8-Hydroxy-3-Chromanamine. *Eur. J. Med. Chem.* **1988**, *23,* 325-328.

17.   Vermue, N. A.; Kaptein, B.; Tepper, P. G.; de Vries, J. B.; Horn, A. S. Pharmacological profile of N,N dipropyl-8-hydroxy-3-chromanamine, an oxygen isostere of the dopamine agonist N,N dipropyl-5-hydroxy-2-aminotetralin with enhanced presynaptic selectivity. *Arch. Int. Pharmacodyn. Ther.* **1988**, *293,* 37-56.

18.   Copinga, S.; Dijkstra, D.; Devries, J. B.; Grol, C. J.; Horn, A. S. Synthesis and Pharmacological Evaluation of 5,6,7,8-Tetrahydro-6-[Propyl[2-(2-Thienyl)Ethyl]Amino]-1,2-Naphthalenediol - A Novel Nonselective Dopamine-Receptor Agonist. *Recl. Trav. Chim. Pays-Bas* **1993**, *112,* 137-142.

19.   Horn, A. S.; Grol, C. J.; Dijkstra, D.; Mulder, A. H. Facile Syntheses of Potent Dopaminergic Agonists and Their Effects on Neurotransmitter Release. *J. Med. Chem.* **1978**, *21,* 825-828.

20.   Taber, D. F.; Neubert, T. D.; Rheingold, A. L. Synthesis of (-)-morphine. *J. Am. Chem. Soc.* **2002**, *124,* 12416-12417.

21.   Moos, W. H.; Gless, R. D.; Rapoport, H. Codeine Analogs - Synthesis of Spiro[Benzofuran-3(2h),4'-Piperidines] and Octahydro-1h-Benzofuro[3,2-E]Isoquinolines. *J Org Chem J Org Chem; J. Org. Chem.* **1981**, *46,* 5064-5074.

22.   Copinga, S.; Tepper, P. G.; Grol, C. J.; Horn, A. S.; Dubocovich, M. L. 2-Amido-8-Methoxytetralins - A Series of Nonindolic Melatonin-Like Agents. *J. Med. Chem.* **1993**, *36,* 2891-2898.

23.   Cornforth, J. W.; Robinson, R. Experiments on the Synthesis of Substances Related to the Sterols .48. Synthesis of a Tricyclic Degradation Product of Cholesterol. *J. Chem. Soc.* **1949**, 1855-1865.

24.   Ackaert, O. W.; De Graan, J.; Capancioni, R.; Dijkstra, D.; Danhof, M.; Bouwstra, J. A. Transdermal iontophoretic delivery of a novel series of dopamine agonists in vitro: physicochemical considerations. *J. Pharm. Pharmacol.* **2010**, *62,* 709-20.

25.   Nugroho, A. K.; Li, G. L.; Danhof, M.; Bouwstra, J. A. Transdermal iontophoresis of rotigotine across human stratum corneum in vitro: Influence of pH and NaCl concentration. *Pharm. Res.* **2004**, *21,* 844-850.

26.   Anonymous *VCCLAB, Virtual Computational Chemistry Laboratory;* 2005; .

27.   Tetko, I. V.; Gasteiger, J.; Todeschini, R.; Mauri, A.; Livingstone, D.; Ertl, P.; Palyulin, V. A.; Radchenko, E. V.; Zefirov, N. S.; Makarenko, A. S.; Tanchuk, V. Y.; Prokopenko, V. V. Virtual computational chemistry laboratory - design and description. *J. Comput. -Aided Mol. Des.* **2005**, *19,* 453-463; 453.

28.   Tetko, I. V.; Bruneau, P. Application of ALOGPS to predict 1-octanol/water distribution coefficients, logP, and logD, of AstraZeneca in-house database. *J. Pharm. Sci.* **2004**, *93,* 3103-10.

29.   Vermerris, W.; Nicholson, R. *Phenolic compound biochemistry;* Springer Science: 2008; .

30.   Peck, K. D.; Srinivasan, V.; Li, S. K.; Higuchi, W. I.; Ghanem, A. H. Quantitative description of the effect of molecular size upon electroosmotic flux enhancement during iontophoresis for a synthetic membrane and human epidermal membrane. *J. Pharm. Sci.* **1996**, *85,* 781-8.

31.   Furniss, B. S. *Vogel's textbook of practical organic chemistry;* Longman: New York, 1989; , pp 1514.

8

# Synthesis and chemical stability studies of prodrugs of (-)-8-OH-DPAC, a potent dopamine D_2 agonist

Abstract

*Skin depot formation can be a disadvantage in the treatment of Parkinson's disease when rapid changes in a transdermal iontophoresis delivery scheme are required. When drugs are delivered by iontophoresis, the compounds with lower lipophilicity show a decreased skin depot formation. Moreover, drugs with improved physico-chemical properties like low lipophilicity and high aqueous solubility can be advantageous for transdermal iontophoretic delivery. In comparison to 5-OH-DPAT, 8-OH-DPAC shows a higher aqueous solubility and a lower lipophilicity. In order to further improve the physico-chemical properties we synthesized a series of less lipophilic, highly water-soluble mono amino acid prodrugs of (-)-8-OH-DPAC suitable for iontophoretic delivery. The chemical stability in citrate buffer pH 5 at 32 ^oC (donor phase) was determined. Especially, the 1-aminocyclopropane-1-carboxylic acid (**8.18**) and the β-alanine (**8.21**) prodrugs of 8-OH-DPAC showed suitable half-lives in combination with a decreased calculated lipophilicity compared to equivalent 5-OH-DPAT amino acid prodrugs. These candidates may be used for further in vitro and in vivo experiments on transdermal iontophoretic delivery.*

8.1 INTRODUCTION

In Chapter 2 the synthesis of mono amino acid esters of 5-OH-DPAT is described. These compounds were designed to decrease lipophilicity and therewith increase aqueous solubility and iontophoretic flux of the parent drug 5-OH-DPAT. The 1-aminocyclopropane-1-carboxylic acid (**2.30**), *L*-valine (**2.31**), *L*-isoleucine (**2.33**) and β-alanine (**2.39**) esters of (S)-5-OH-DPAT, the pharmacologically active enantiomer, showed chemical stabilities which were considered sufficient for *in vitro* and *in vivo* iontophoretic experiments (Chapter 3). After iontophoretic *in vitro* experiments the highly soluble β-alanine ester prodrug of (S)-5-OH-DPAT, which showed a lower calculated log P than the parent drug, was evaluated *in vivo*. Although this prodrug gave lower plasma concentrations than (S)-5-OH-DPAT, the prodrug showed post-iontophoretic higher plasma concentrations which could be explained by a delayed release due to skin depot formation. Nevertheless, despite a lower steady state plasma concentration the same maximum pharmacodynamic effect as iontophoretic administration of (S)-5-OH-DPAT was achieved.[1] A prolonged effect due to depot formation can be a drawback to initiate therapy to treat Parkinson's disease, since rapid changes in delivery schemes may be required. At the other hand, the prolonged effect of the prodrug can be beneficial for patients who suffer from nocturnal disturbances.[2, 3]
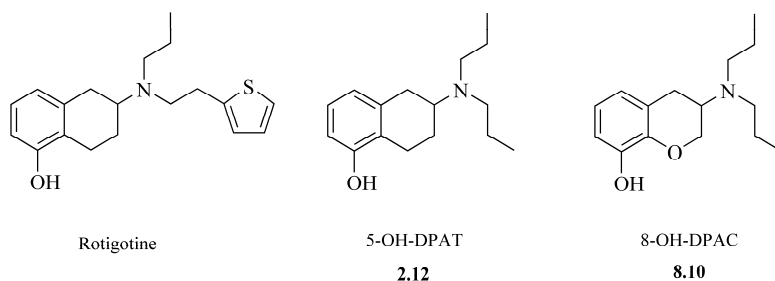
Figure 8.1 Structures of rotigotine, 5-OH-DPAT (**2.12**) and 8-OH-DPAC (**8.10**).

To study the effect of hydrophilicity on the iontophoresis and skin depot formation some less hydrophobic amino ester prodrugs of DA D_2 receptor agonists were synthesized. Compared to rotigotine (calculated log P = 4.67) the absence of the thienyl group makes 5-OH-DPAT (calculated log P = 3.99) (**2.12**) less lipophilic (Figure 8.1).[4-6] A lower lipophilicity could provide benefits for the delivery by iontophoresis, and accordingly the iontophoretic delivery of 5-OH-DPAT over human stratum corneum resulted in an increase of the transport rate relative to rotigotine.[7] A small selection of chemicals was studied on dermal permeation by Moody *et al.*, and the compounds with the higher lipophilicity showed higher skin depot formation.[8]

The aim of this study was to decrease skin depot formation and at the same time achieve high aqueous solubility. A structural modification to decrease lipophilicity of the mono amino acid esters of 5-OH-DPAT is the bioisosteric replacement of a methylene group by an oxygen atom in the parent molecule structure as in 8-hydroxy-3,4-dihydro-3-(*N*,*N*-di-*n*-propylamino)-2*H*-1-benzopyran (8-OH-DPAC, **8.10**, calculated log P = 3.20[4-6]) (Figure 8.1). 8-OH-DPAC is a potent DA agonist comparable to 5-OH-DPAT with selectivity for presynaptic D_2 DA receptors and only moderate affinity for 5-HT and NA receptors.[9-11] Although the aqueous solubility of 8-OH-DPAC was 5-fold higher than that of 5-OH-DPAT (Chapter 7), the *in vitro* iontophoretic transport of 8-OH-DPAC was lower.[12] Nevertheless, conversion to an amino acid prodrug could improve the iontophoretic transport rate and this would be interesting to examine.

In this chapter we describe the synthesis of mono amino acid prodrugs of (-)-8-OH-DPAC, the pharmacologically active enantiomer, and the evaluation of their chemical stability. The selection of coupled amino acid pro-moieties was based on the chemically most stable 5-OH-DPAT prodrugs (Chapter 3). The influence of the bioisosteric replacement of the methylene group (5-OH-DPAT) by an oxygen atom (8-OH-DPAC) on chemical hydrolysis was also studied. The most stable prodrug might be used in further *in vitro* and *in vivo* experiments to study the influence of a less lipophilic dopaminergic amino acid prodrug on transdermal iontophoretic delivery and skin depot formation.

8.2 CHEMISTRY

8.2.1 Synthesis of (-) and (+)-8-hydroxy-3,4-dihydro-3-(*N,N*-di-*n*-propylamino)-2*H*-1-benzopyran ((-)-8.10 and (+)-8.10).

Neirabeyeh *et al.* developed a route for the synthesis of the enantiomers of **8.10** including a resolution of an intermediate compound, i.e. (±)-8-methoxy-3,4-dihydro-3-diallyllamino-2*H*-1-benzopyran (**8.22**) using binaphthylphosphoric acid as the chiral resolving agent.[11] Moreover, Holmberg *et al.* presented a resolution of another suitable intermediate compound, namely (±)-8-methoxy-3,4-dihydro-3-(*N,N*-dibenzylamino)-2*H*-1-benzopyran (**8.23**). This compound was recrystallized as the *L*-dibenzoyltartrate salt from a mixture of water and dichloromethane.[13] Also Brisander *et al.* showed a resolution of an appropriate intermediate (±)-3,4-dihydro-3-(*N,N*-dibenzylamino)-2*H*-1-benzopyran (**8.24**) which was recrystallized from 95% ethanol as the mandelate salt (Figure 8.2).[14]


8.22   **8.23**   **8.24**
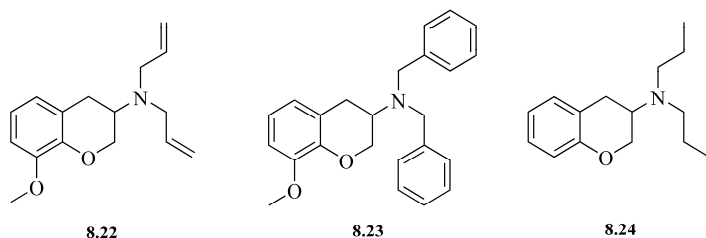
Figure 8.2 Structures of resolvable intermediates (±)-8-methoxy-3,4-dihydro-3-diallyllamino-2*H*-1-benzopyran (**8.22**), (±)-8-methoxy-3,4-dihydro-3-(*N,N*-dibenzylamino)-2*H*-1-benzopyran (**8.23**) and (±)-3,4-dihydro-3-(*N,N*-dibenzylamino)-2*H*-1-benzopyran (**8.24**).

However, we preferred the synthesis of the benzylamino intermediate **(±)-8.6** and the resolution thereof. Because of the successful resolution of 2-(benzylamino)-5-methoxytetralin (**2.9**) described in Chapter 2, a synthetic route was chosen which includes the oxygen isostere of **2.9**, i.e. (±)-8-methoxy-3,4-dihydro-3-(*N*-benzylamino)-2*H*-1-benzopyran (**(±)8.6**).[15] For that reason, the synthesis of (-) and (+)-8-hydroxy-3,4-dihydro-3-(*N,N*-di-*n*-propylamino)-2*H*-1-benzopyran (**(-)-8.10** and **(+)-8.10**) was performed based on the procedure described by Wise *et al.*[16] The absolute stereochemistry of the enantiomers of **8.6** and **8.10** were not found in literature, therefore the enantiomers are denoted by their optical rotation. The nitrile **8.3** was synthesized by the treatment of 2-hydroxy-3-methoxybenzaldehyde with acrylonitrile and 1,4-diazabicyclo[2.2.2]octane under reflux. Then, nitrile **8.3** was hydrolyzed to the carboxylic acid **8.4** under alkaline conditions, and was further converted to the ketone **8.5** by a Curtius rearrangement using diphenylphosphoryl azide followed by acidic hydrolysis. Subsequently, the racemic mixture of **8.6** was synthesized by reductive amination with sodium cyanoborohydride and benzylamine (Scheme 8.1).[13]
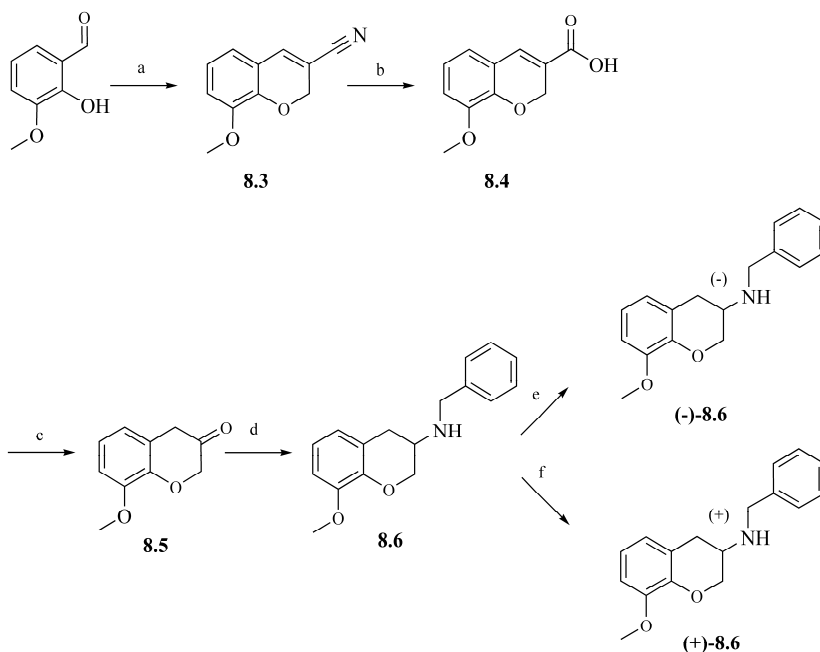
Scheme 8.1 Synthesis and resolution of 8-methoxy-3,4-dihydro-3-(*N*-benzylamino)-2*H*-1-benzopyran (**8.6**). Reagents and conditions: a) acrylonitrile, 1,4-diazabicyclo[2.2.2]octane, reflux overnight, recrystallization from MeOH; b) 10% NaOH, 6h reflux, 37% HCl (aq); c) step 1: diphenyl phosphoryl azide, toluene, TEA, CH$_2$Cl$_2$, RT-60°C, 1.5 h at 85°C, step 2: 6N HCl (aq), 2h reflux; d) CH$_3$COOH, benzylamine, THF, 30 min RT, NaCNBH$_3$; e) (+)-chlocyphos, recrystallization from 96% EtOH; f) (-)-chlocyphos, recrystallization from 96% EtOH.

First, the diastereomeric *D*-(-)-mandelate and (+)-di-*p*-toluoyl-tartrate salts were recrystallized from 95% ethanol, but unfortunately no crystal formation or resolution was observed for the two salt forms. In order to continue the investigation to a successful resolution of (±)-**8.6**, the enantiomers of the resolving agent 4-(2-chlorophenyl)-5,5-dimethyl-2-hydroxy-1,3,2-dioxaphosphorinane 2-oxide (**8.2**, chlocyphos) were synthesized by the method described by Ten Hoeve and Wynberg.[17] An aldol-Cannizaro reaction of 2-chloro-benzaldehyde with isobutyraldehyde in a solution of 6% potassium hydroxide in a mixture of water and ethanol gave 2,2-dimethyl-1-(2-chlorophenyl)-1,3-propanediol (**8.1**). Next, **8.1** was converted to the cyclic phosphoric acid chloride with phosphorus oxychloride, where after it was hydrolyzed with aqueous sodium hydroxide to form 4-(2-chlorophenyl)-5,5-dimethyl-2-hydroxy-1,3,2-dioxaphosphorinane 2-oxide (**8.2**). The (-)-(*p*-hydroxyphenyl)-glycinate salt of **8.2** was crystallized from a mixture of ethanol and water to yield after conversion to the free acid **(S)-8.2**. Ultimately, the motherliquor of the crystallization was collected, converted to the free acid and yielded pure **(R)-8.2**. The overall yield was 35%.
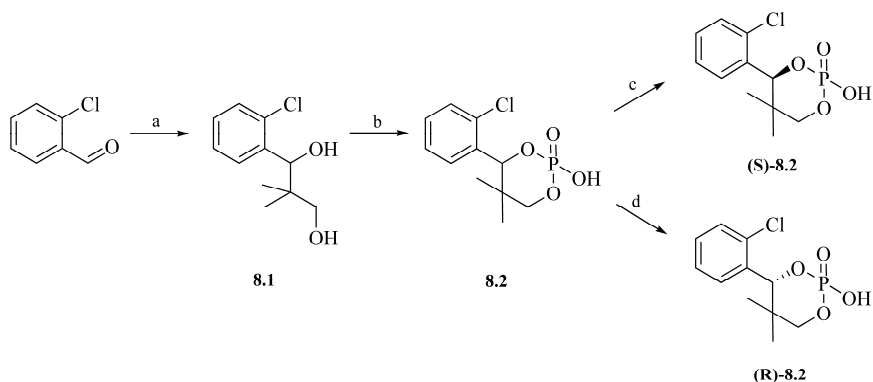
Scheme 8.2 Synthesis and resolution of 4-(2-chlorophenyl)-5,5-dimethyl-2-hydroxy-1,3,2-dioxaphosphorinane 2-oxide (**8.2**, chlocyphos). Reagents and conditions: a) isobutyraldehyde, KOH in H$_2$O/EtOH; b) step 1: POCl$_3$, CH$_2$Cl$_2$, 45°C, 1.5 h at reflux; step 2: 2.4 M NaOH at 95°C, 15 min at 60°C, 37% HCl; c) (-)-(*p*-hydroxyphenyl)-glycine, crystallization from 96% EtOH; d) conversion of mother liquor obtained from step c.

The resolution of **(±)-8.6** was achieved by recrystallization of the diastereomeric chlocyphos salts of **8.6** from 96% ethanol (Scheme 8.1).[18] By parallel synthesis the (-)- and (+)-enantiomers of **8.6** were alkylated with 1-iodopropane to give the enantiomeric 8-methoxy-3,4-dihydro-3-(*N*-benzyl-*N*-propyl-amino)-2*H*-1-benzopyrans (**8.7**) (Scheme 8.3). After deprotection by hydrogenolysis with palladium on carbon under hydrogen atmosphere, 8-methoxy-3,4-dihydro-3-(*N*-*n*-propylamino)-2*H*-1-benzopyran (**8.8**) was converted to the *N*-alkylated amide and immediately reduced to enantiomeric pure 8-methoxy-3,4-dihydro-3-(*N*,*N*-di-*n*-propylamino)-2*H*-1-benzopyran (**8.9**). Finally, (-) and (+)-8-hydroxy-3,4-dihydro-3-(*N*,*N*-di-*n*-propylamino)-2*H*-1-benzopyran (**(-)-8.10** and **(+)-8.10**) were obtained as the hydrobromide salts after demethylation in 48% hydrobromic acid with e.e. values of 98% and 93%, respectively. The nine-step yield for **(-)-8.10** was 3 % and for **(+)-8.10** this was 5 %.
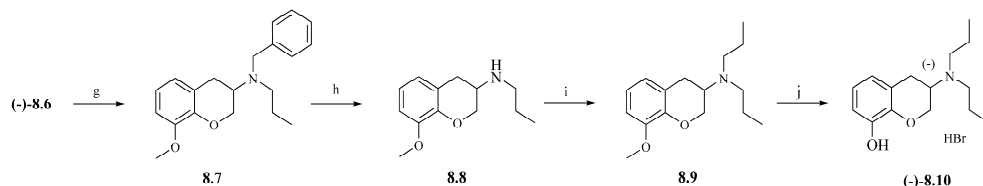
Scheme 8.3 Synthesis of (-)-8-hydroxy-3,4-dihydro-3-(*N*,*N*-di-*n*-propylamino)-2*H*-1-benzopyran (**(-)-8.10**). The synthesis of **(-)-8.10** followed the same reaction steps starting with **(+)-8.10**. Reagents and conditions: g) K$_2$CO$_3$, 2-butanone, 1-iodopropane, reflux, 3 days; h) 3.5 bar H$_2$, 10% Pd/C, RT; i) step 1: TEA, toluene, propionylchloride, RT, 30 min; step 2: THF, LiAlH$_4$, reflux, 1h. j) 48% HBr, reflux, 4h.

8.2.2 Synthesis of (-)-3,4-dihydro-3-(*N,N*-di-*n*-propylamino)-2*H*-1-benzopyran-8-yl esters (8.17-8.21)

The prodrugs of (-)-**8.10** were synthesized according to a procedure described in Chapter 2. The Boc-protected amino acid (-)-8-OH-DPAC esters **8.12-8.16** were synthesized from (-)-**8.10** by coupling the Boc-protected amino acid to (-)-8-OH-DPAC with EDC and HOBt in dichloromethane. The obtained yields of the coupling reaction varied between 62% and 79%. Compounds **8.12-8.16** were deprotected by a reaction in hydrogen chloride in dioxane to give the amino acid (-)-8-OH-DPAC esters **8.17-8.21** as hygroscopic dihydrochloride salts (Scheme 8.4). The yields of these final compounds varied between 49% and 79%. The glycine (-)-8-OH-DPAC ester (**8.17**) was obtained with a purity of 86%, while the other esters had purities over 95%. Although compound **8.17** showed a lower purity, this prodrug would still be useful for investigations on chemical stability, because the hydrolysis rate is independent of prodrug concentration. Concluding, as the concentrations are still measurable, 86% purity is sufficient for this particular research. All overall yields and purities are presented in Table 8.1.
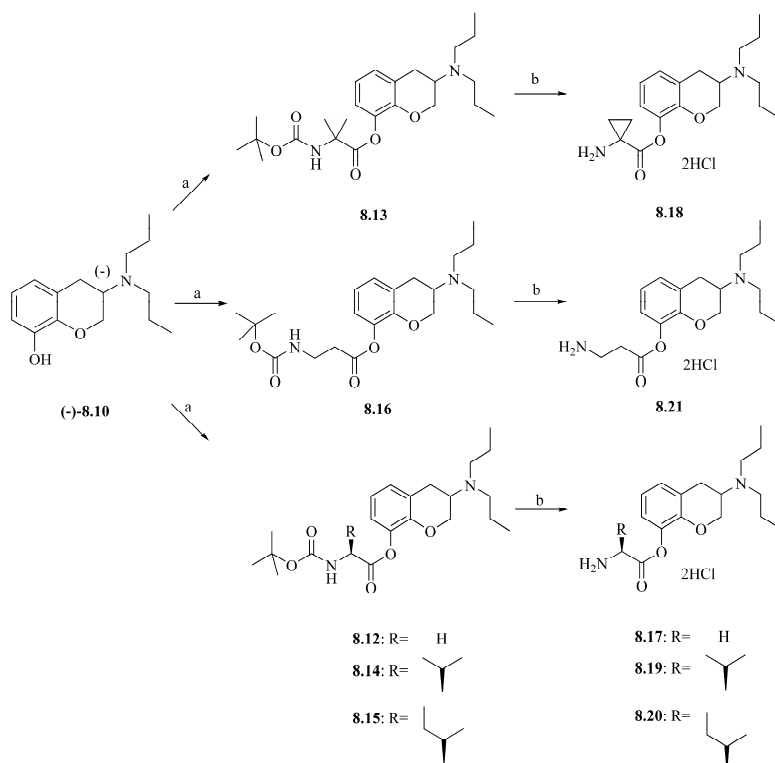
Scheme 8.4 Synthesis of glycine (**8.17**), 1-aminocyclopropane-1-carboxylic acid (**8.18**), L-valine (**8.19**), L-isoleucine (**8.20**) and β-alanine (**8.21**) (-)-3,4-dihydro-3-(N,N-di-*n*-propylamino)-2*H*-1-benzopyran-8-yl esters as 2HCl salts. Reagents and conditions: a) EDC, N-*tert*-Boc-amino acid, HOBt hydrate, 0°C-RT; b) 4N HCl in dioxane, RT.

Table 8.1 Overall yields and purities (HPLC) of 8-OH-DPAC (**8.10**) and the prodrugs **8.17-8**.**21**. The overall yields of the prodrugs were calculated with **8.10** as the starting material.

Compound	Prodrug Moiety	Yield (%)	Purity (%)
(-)-**8.10**	-	3.5	100[a]
(+)-**8.10**	-	4.4	100[a]
8.17	Glycine	48	86
8.18	1-Aminocyclopropane-1-carboxylic acid	38	98
8.19	L-Valine	38	98
8.20	L-Isoleucine	46	95
8.21	β-Alanine	62	97

[a] Purity determined on GCMS

## 8.3 RESULTS

8.3.1 Calculated log P and pK$_a$ values

The calculated log P vales of 5-OH-DPAT and 8-OH-DPAC are 3.99 and 4.67, respectively. The calculated log P values of the mono amino acids prodrugs of 5-OH-DPAT are shown in Table 8.2. All 8-OH-DPAC prodrugs have calculated log P values which are ±0.75 units lower than the log P values of the 5-OH-DPAT prodrugs.

Table 8.2 Calculated log P and of mono amino acid esters of 5-OH-DPAT and 8-OH-DPAC prodrugs.[4-6]

Prodrug Moiety	5-OH-DPAT Prodrug		8-OH-DPAC Prodrug	
	Compound	Cacluated Log P[a]	Compound	Cacluated Log P[a]
Glycine	**2.28**	2.90	**8.17**	2.15
1-Aminocyclopropane-1-carboxylic acid	**2.30**	3.37	**8.18**	2.66
L-Valine	**2.31**	4.04	**8.19**	3.25
L-Isoleucine	**2.33**	4.47	**8.20**	3.72
β-Alanine	**2.39**	3.16	**8.21**	2.40

8.3.2 Chemical Stability

The hydrolysis rate constants (k$_{obs}$) and half-lives (t$_{1/2}$) of compounds **8.17-8.21** were obtained by measuring the remaining prodrug concentration in time during hydrolysis experiments in 5 mM citrate buffer pH 5 at 32 ºC which is the temperature of the skin *in vivo*. The hydrolysis rate plots of these experiments are presented in Figure 8.3.
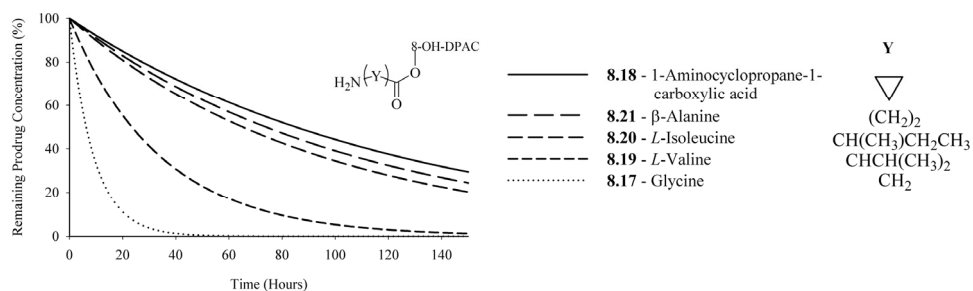
Figure 8.3 Pseudo first-order hydrolysis rate plots of 5-OH-DPAT prodrugs in citrate buffer pH 5 at 32 ºC, based on the estimated half-lives presented in Table 8.3. The prodrugs are listed per group in sequence of descending half-life.

Least-square equations, derived by correlating areas in HPLC chromatograms to known concentrations of prodrug were used for calculation of the residual prodrug concentration in the studied samples. The correlation coefficients of the standard curves were 0.99. The observed first-order hydrolysis rate constants of the 5-OH-DPAT prodrugs were determined by plotting the logarithm of the remaining prodrug concentration as a function of time. The linear regression slopes of these plots ($r^2 \geq 0.95$) are related to the observed rate constant, k_{obs}, and are given by: $k_{obs} = \dfrac{1}{\log e} \times \text{slope} \, (\log C \text{ vs time})$. The hydrolysis half-lives were then estimated by the equation: $t_{1/2} = \dfrac{\ln 2}{k_{obs}}$. The half-lives of (-)-8-OH-DPAC prodrugs **8.17**-**8.21** and reference (S)-5-OH-DPAT prodrugs **2.28**, **2.30**, **2.31**, **2.33**, **2.39** are presented in Table 8.3.

Table 8.3 Estimated hydrolysis half-lives ($t_{1/2}$) of prodrugs **2.28** (n=9), **2.30**, **2.31**, **2.33**, **2.39** (n=6) and **8.17**-**8.21** (n=3).

| | 0.005 M Citrate Buffer (pH 5) | | | | |
| | (S)-5-OH-DPAT Prodrug | | (-)-8-OH-DPAC Prodrug | | |
Prodrug Moiety	**Compound**	**Estimated $t_{1/2}$ ± SEM (hours)**	**Compound**	**Estimated $t_{1/2}$ ± SEM (hours)[a]**	**$t_{1/2}$ ratio 5-OH-DPAT /8-OH-DPAC**
Glycine	**2.28**	20.7±0.3	**8.17**	6.3±0.05	3.3
1-Aminocyclopropane-1-carboxylic acid	**2.30**	149.7±3.2	**8.18**	85.1±0.7	1.8
L-Valine	**2.31**	53.1±1.6	**8.19**	23.5±2.3	2.3
L-Isoleucine	**2.33**	72.7±2.8	**8.20**	65.1±2.6[a]	1.1
β-Alanine	**2.39**	117.0±5.3	**8.21**	73.8±4.0[a]	1.6

[a]The mean $t_{1/2}$ values of prodrugs **8.17**-**8.21** were significantly different, with exception of compound **8.20** vs **8.21** (one-way ANOVA with post-hoc Tukey's test for comparing means, $p < 0.05$).

The half-lives of the 8-OH-DPAC prodrugs were all lower than the half-lives of their corresponding 5-OH-DPAT reference prodrugs. The hydrolysis rate of the 8-OH-DPAC prodrugs was a factor 1.1 to 3.3 times faster than the hydrolysis rate of the 5-OH-DPAT prodrugs (Table 8.3). The effect of 8-OH-DPAC as the leaving group during hydrolysis instead of 5-OH-DPAT was the most significant for the glycine ester prodrug **8.17** and the least significant for the *L*-isoleucine ester prodrug **8.20**. The chemical stability trend for the 5-OH-DPAT prodrugs was as follows: 1-aminocyclopropane-1-carboxylic acid (**2.30**, 150 hrs) > β-alanine (**2.39**, 117 hrs) > *L*-isoleucine (**2.33**, 73 hrs) > *L*-valine (**2.31**, 53 hrs) > glycine (**2.28**, 21 hrs). The chemical stability trend for the 8-OH-DPAC prodrugs was as follows: 1-aminocyclopropane-1-carboxylic acid (**8.18**, 85 hrs) > β-alanine (**8.21**, 74 hrs) ≈ *L*-isoleucine (**8.20**, 65 hrs) > *L*-valine (**8.19**, 24 hrs) > glycine (**8.17**, 6 hrs). The difference between both trends was that the $t_{1/2}$ found for the β-alanine 8-OH-DPAC prodrug was not significantly different than the $t_{1/2}$ of the *L*-isoleucine 8-OH-DPAC prodrug. In contrast, the $t_{1/2}$ of the β-alanine 5-OH-DPAT prodrug significantly differed from the $t_{1/2}$ of the *L*-isoleucine 5-OH-DPAT prodrug.

8.4 DISCUSSION

The calculated pK_a values for the phenol group of 5-OH-DPAT and 8-OH-DPAC were 11.29 and 10.68, respectively, which indicate that the alcohol group of 8-OH-DPAC is more acidic than the alcohol group of 5-OH-DPAT.[19] Therefore 8-OH-DPAC may be the better leaving group in hydrolysis of ester prodrugs when compared to 5-OH-DPAT. Santos *et al*. showed for dipeptide ester prodrugs that a better leaving group led to faster hydrolysis of the ester bond.[20] This property of 8-OH-DPAC could explain the shorter half-lives of the mono amino acid esters of 8-OH-DPAC compared to the prodrugs of 5-OH-DPAT. Generally the ascending half-life sequence of the 8-OH-DPAC prodrugs is equal to this sequence of the 5-OH-DPAT prodrugs. Apparently there is no significant difference in structural influence of the various amino acid residues in combination with this structural modification in the parent drug ring system on hydrolysis. The glycine prodrug was the most sensitive to the change in leaving group, while the *L*-isoleucine prodrug did not change much in half-life. Possibly steric hindrance of the *s*-butyl group of the *L*-isoleucine 8-OH-DPAC prodrug makes the hydrolysis rate of the ester bond less susceptible to structural changes in the parent molecule. The glycine 8-OH-DPAC prodrug lacks a particular steric group, which may make the ester bond more liable to hydrolysis when varying to a better leaving group.

In conclusion, the calculated lipophilicity of all 8-OH-DPAC prodrugs was lower than the calculated lipophilicity of the corresponding 5-OH-DPAT prodrugs. The improved physico-chemical property of the prodrugs could be advantageous for the transdermal iontophoretic delivery. Especially, the 1-aminocyclopropane-1-carboxylic acid (**8.18**) and the β-alanine (**8.21**) prodrugs of 8-OH-DPAC showed suitable half-lives in combination with decreased

lipophilicity compared to the 5-OH-DPAT amino acid prodrugs. These candidates might be used for further *in vitro* and *in vivo* experiments to study the influence of the decreased lipophilicity on transdermal iontophoretic delivery and skin depot formation.

8.5.EXPERIMENTAL

8.5.1 Chemistry

8.5.1.1 General

The materials and analysis methods are described in section 2.4.1

The e.e. of compounds **(-)-8.6**, **(+)-8.6**, **(-)-8.10** and **(+)-8.10** were determined on a HPLC system, which consisted of an ISCO Model 2360 Gradient Programmer, a Waters 510 HPLC Pump, a Waters 486 Tunable Absorbance Detector and a HP 3396 Series II Integrator. The e.e. of compounds **(-)-8.6** and **(+)-8.6** were determined at λ =254 nm on a Chiralcel OD column (250 x 4.6 mm) with an eluent mixture of 60% hexane and 40% ethanol with 0.1% triethylamine added and at a flow rate of 0.5 ml/min. The e.e. of compounds **(-)-8.10** and **(+)-8.10** were determined at λ =275 nm on a Chiralcel OD column (250 x 10 mm) with an eluent mixture of 98.4% hexane and 1.6% ethanol with 0.1% triethylamine added and at a flow rate of 4.0 ml/min.

8.5.1.2 Preparation of (-) –and (+)-4-(2-Chlorophenyl)-5,5–dimethyl–2–hydroxy–1,3,2-dioxaphosphorinane 2-oxide (Chlocyphos).
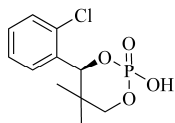
2,2-Dimethyl-1-(2-chlorophenyl)-1,3-propanediol (8.1).[17] To a mixture of 2-chloro-benzaldehyde (40 mL, 0.36 mol) and isobutyraldehyde (65 mL, 0.72 mol) was added slowly 300 mL of a 6% solution of KOH (20 g, 0.36 mol in 30 mL H_2O and 300 mL 95% ethanol). An exothermic reaction started and the solution turned yellow; when the temperature of the mixture had reached 50˚C, the flask was cooled by an ice bath. Usually the temperature rised to ca 70˚C and dropped again. When the temperature has fallen to ca. 55˚C, the remainer of the KOH solution was added rapidly (ca. 10 min). The reaction mixture was heated at 50-60˚C for 4 hours and then evaporated *in vacuo*. Water (500 mL) was added to the remaining residue, and this mixture was extracted with CH_2Cl_2 (3x100mL). The organic layer was washed with H_2O (180 mL), dried over Na_2SO_4 and evaporated *in vacuo* to obtain the crude product as a yellow oil (52 g, 68%). IR (KBr cm^{-1}) v_{max} 3366 (br), 2969, 1571, 1470, 1188, 1031; ^{1}H NMR (200 MHz, CDCl$_3$): δ 7.58-7.43 (m, 1H, ArH), 7.32-7.03 (m, 3H, ArH), 5.19 (s, 1H, CH), 3.52 and 3.47 (AB-system, J_{AB}= 10.9 Hz, 2H, CH$_2$OH), 3.03 (br s, 2H, OH), 0.85 (s, 3H, CH$_3$), 0.81 (s, 3H, CH$_3$); ^{13}C NMR (50 MHz, CDCl$_3$): δ 139.4, 133.5, 129.8, 129.5, 128.8, 126.8, 77.0, 73.7, 72.6, 22.6, 19.0.

4-(2-Chlorophenyl)-5,5-dimethyl-2-hydroxy-1,3,2-dioxaphosphorinane   2-Oxide   (8.2).[17]   A solution of POCl$_3$ (24.6 mL, 0.27 mol) in 50 mL CH_2Cl_2 was added slowly to a warm (45 °C) solution of **8.1** (51.7 g, 0.24 mol) in 100 mL CH_2Cl_2 over 60 minutes. The yellow mixture was heated under reflux for 1.5 hours and then evaporated to give a brown residue. The residue was added in 15-30 min to a 95˚C solution of NaOH (28.9 g, 0.72 mol) in 300 ml H_2O at such a rate that the strongly
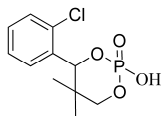
exothermic reaction is kept under control. After being stirred for 15 min the solution was cooled to ca. 60°C and then acidified with 60 mL 37% HCl (aq) to precipitate the phosphoric acid. After the solution had cooled to room temperature, the product was sucked off, washed with water, washed with Et$_2$O and dried *in vacuo* to obtain **8.2** as white solid material (47.7 g, 72%). A small amount was recrystallized from 96% EtOH for analytical purposes. IR (NaCl cm^{-1}) v_{max} 2977, 1473, 1441, 1313, 1037, 998; ^{1}H NMR (200 MHz, CDCl$_3$): δ 8.28 (br s, 1H, OH), 7.48-7.31 (m, 1H, ArH), 7.23-7.03 (m, 3H, ArH), 5.65 (d, *J*=1.8 Hz, 1H, CH), 4.18 (d, *J*=11.2 Hz, 1H, *CH$_2$*OPO$_3$H), 3.69 (dd, *J*=19.4 Hz, 11.2 Hz, 1H, *CH$_2$*OPO$_3$H), 0.94 (s, 3H, CH$_3$), 0.65 (s, 3H, CH$_3$); ^{13}C NMR (50 MHz, CDCl$_3$): δ 134.2, 132.8, 130.3, 129.7, 129.4, 126.6, 82.1, 78.3, 37.5, 20.7, 17.9.
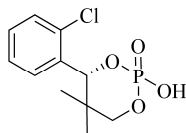
(S)-(-)-4-(2-Chlorophenyl)-5,5-dimethyl-2-hydroxy-1,3,2-dioxaphosphorinane 2-Oxide ((S)-8.2).[17] A mixture of racemic **8.2** (47.7 g, 0.17 mol), (-)-(*p*-hydroxyphenyl)-glycine (28.9 g, 0.17 mol), 290 ml of 96% EtOH, and 225 ml of H$_2$O was heated to solution. The clear solution was allowed to cool to the room temperature while stirring. After the solution was stirred overnight, the salt was sucked off, washed with 100 ml of H$_2$O and dried to give a white salt (48.6 g). This salt was stirred for 6 hours with 50 ml of 37% HCl (aq) and 235 ml H$_2$O, filtrated, washed with H$_2$O and dried *in vacuo* to give **(S)-(-)-8.2** as white solid material (17.7 g, 74%). m.p. 232 °C; $[\alpha]_D^{21} - 46.0°$ (c 1.0, MeOH).

(R)-(+)-4-(2-Chlorophenyl)-5,5-dimethyl-2-hydroxy-1,3,2-dioxaphosphorinane 2-Oxide ((R)-8.2).[17] The filtrate from the crystallization of **(S)-8.2** (including the water used for washing) was stirred overnight with 75 ml of 37% HCl (aq). The crystals were filtrated, washed with H$_2$O and dried *in vacuo* to give **(R)-(+)-8.2** as white solid material (16.9 g, 71%). m.p. 220-231 °C; $[\alpha]_D^{21} + 46.0°$ (c 1.0, MeOH).

8.5.1.3 Synthesis of (-)-8-OH-DPAC

3-Cyano-8-methoxy-2*H*-1-benzopyran (8.3).[16] A mixture of 2-hydroxy-3-methoxybenzaldehyde (25 g, 0.16 mol), acrylonitrile (54.5 mL, 0.82 mol) and 1,4-diazabicyclo[2.2.2]octane (5.2 g, 0.046 mol) was refluxed overnight. The reaction mixture was diluted with Et$_2$O, washed with 1N NaOH, 1N HCl (aq), brine and dried over Na$_2$SO$_4$. After evaporation *in vacuo*, the residue was recrystallized from MeOH to afford **8.3** as yellow crystals (30.6 g, 89%). Purity: 100% (GCMS); IR (KBr, cm^{-1}) v_{max} 2204, 1624, 1576, 1482, 1275, 1222, 1097; ^{1}H NMR (200 MHz, CDCl$_3$): δ 7.41 (s, 1H, H$_4$), 6.97-6.87 (m, 2H, ArH), 6.78-6.67 (m, 1H, ArH), 4.85 (s, 2H, OCH$_2$), 3.87 (s, 3H, OCH$_3$); ^{13}C NMR (50 MHz, CDCl$_3$): δ 148.3, 139.1, 122.5, 120.9, 120.5, 116.6, 115.5, 103.7, 64.8, 56.4; EI-MS *m/z* 187 (M)$^+$.
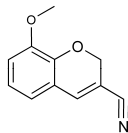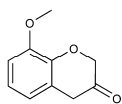
3-Carboxy-8-methoxy-2*H*-1-benzopyran (8.4).[16] A suspension of **8.3** (28 g, 0.15 mol) in 10% NaOH (450 mL) was heated to solution and refluxed for 6 hours. The reaction mixture was acidified with 37% HCl (aq) and the precipitate was filtrated and dried *in vacuo* for 3 days to yield **8.4** as yellow solid material (30.9 g, 100%). Purity: 100% (GCMS); IR (KBr, cm^{-1}) v_{max} 1671, 1483, 1342, 1271; ^{1}H NMR (200 MHz, *d$_6$*-DMSO): δ 7.41 (s, 1H, H$_4$), 7.11-6.84 (m, 3H, ArH), 4.87 (s, 2H,
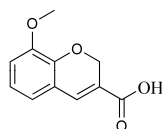
OCH$_2$), 3.75 (s, 3H, OCH$_3$); ^{13}C NMR (50 MHz, d_6-DMSO): δ 166.1, 148.2, 133.2, 124.2, 122.2, 122.1, 121.5, 115.7, 102.9, 64.7, 56.4; EI-MS m/z 206 (M)$^+$.

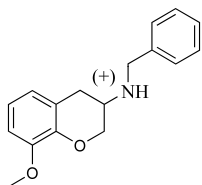**8-Methoxy-3,4-dihydro-2H-1-benzopyran-3-one (8.5).**[16] A solution of diphenyl phosphoryl azide (25 g, 0.09 mol) in 100 mL toluene was added dropwise to a mixture of **8.4** (18.7 g, 0.09 mol), TEA (14.5 mL, 0.10 mol) and CH$_2$Cl (180 mL) while heating slowly to distill the CH$_2$Cl$_2$. At 60 °C an additional 100 mL toluene was added and subsequently the reaction mixture was heated for 1.5 hours at 85 °C. Then, 145 mL of 6N HCl (aq) was added dropwise and the mixture was refluxed for 2 hours. After attaining room temperature, the organic layer was separated, washed with NaHCO$_3$ (sat), brine, dried over MgSO$_4$, evaporated *in vacuo* to afford **8.5** as a brown-yellow oil (13 g, 81%). A small sample was purified on column chromatography (SiO$_2$, Et$_2$O:Hexane) for analytical purposes. For synthetic uses, the crude product was used without purification in the subsequent step. Purity>95% (GCMS); IR (NaCl, cm^{-1}) v_{max} 3375 (br), 2927, 1728, 1662, 1581, 1484, 1264, 1088; ^{1}H NMR (200 MHz, CDCl$_3$): δ 6.90 (t, J=7.8 Hz, 1H, ArH), 6.73 (d, J=7.1 Hz, 1H, ArH), 6.62 (d, J=7.6 Hz, 1H, ArH), 4.36 (s, 2H, 2-OCH$_2$), 3.80 (s, 3H, OCH$_3$), 3.51 (s, 2H, 4-CH$_2$); ^{13}C NMR (50 MHz, CDCl$_3$): δ 207.8, 149.5, 143.8, 123.6, 122.9, 120.7, 111.0, 73.3, 56.2, 41.0; EI-MS m/z 178(M)$^+$.

8-methoxy-3,4-dihydro-3-(benzylamino)-2H-1-benzopyran (8.6).[13] Glacial acetic acid (25.5 mL, 0.42 mol) was added in portions to a mixture of **8.5** (13 g, 0.073 mol) and benzylamine (15.6 g, 0.15 mol) in 65 mL (THF). After stirring for 30 minutes at room temperature, NaBH$_3$CN (5.0 g, 0.08 mol) was added portionwise and the reaction mixture was stirred overnight. The solvent was evaporated *in vacuo* and the residue was dissolved in CH$_2$Cl$_2$ (50 mL), washed with brine (3x50 mL), dried over MgSO$_4$. After filtration, evaporation *in vacuo* and purification by column chromatography (SiO$_2$ (NH$_3$), Hexane/Et$_2$O=1:2 to 100% Et$_2$O, gradient) compound **8.6** was obtained as an orange-yellow oil (8.3 g, 42%). Purity: 100% (GCMS); IR (KBr, cm^{-1}) v_{max} 2930, 2833, 1584, 1485, 1265, 1212, 1083; ^{1}H NMR (200 MHz, CDCl$_3$): δ 7.37-7.21 (m, 5H, C$_6$H$_5$), 6.86-6.64 (m, 3H, ArH), 4.35-4.20 (m, 1H, H$_2$), 4.10-3.96 (m, 1H, H$_2$), 3.92 (s, 2H, CH_2C$_6$H$_5$), 3.86 (s, 3H, OCH3), 3.28-3.08 (m, 1H, H$_3$), 3.07-2.91 (m, 1H, H$_4$), 2.81-2.62 (m, 1H, H$_4$); ^{13}C NMR (50 MHz, CDCl$_3$): δ 148.4, 143.8, 140.3, 128.7, 128.3, 127.4, 122.3, 121.4, 120.5, 109.5, 69.2, 56.0, 51.3, 49.4, 32.2; EI-MS m/z 269 (M)$^+$.
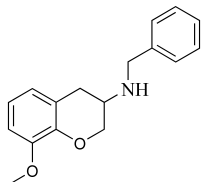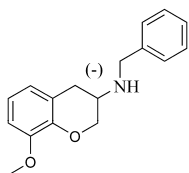
(+)-8-methoxy-3,4-dihydro-3-(benzylamino)-2H-1-benzopyran ((+)-8.6). (-)-Chlocphos (13.3 g, 0.048 mol) and racemic 8-methoxy-3,4-dihydro-3-(benzylamino)-2H-1-benzopyran (13.0 g, 0.048 mol) were added together and were recrystallized 3 times from 96% EtOH (150 mL, 90 mL, 68 mL) to give the chlocyphos-salt as white needles. The salt was converted to the free amine and **(+)-8.6** was afforded as a colourless oil (2.0 g, 31%). $[\alpha]_D^{27} + 8.47°$ (c 0.3, MeOH); e.e.=96.8% (HPLC).

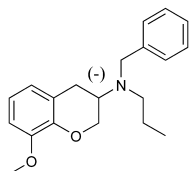**(-)-8-methoxy-3,4-dihydro-3-(benzylamino)-2H-1-benzopyran ((-)-8.6).** The motherliquors of the recrystallizations of compound **(+)-8.6** were collected, evaporated *in vacuo* and converted to the free amine. (+)-Chlocyphos (9.1 g, 0.033 mol) was added to the resultant oil (8.9 g, 0.033 mol) and the mixture was recrystallized 3 times from 96% EtOH (147 mL, 103 mL, 87 mL) and the chlocyphos-

salt was obtained as white needles. The salt was converted to the free amine and yielded **(-)-8.6** as a colourless oil (1.7 g, 26%). $[\alpha]_D^{27} - 8.27°$ (c 1.0, MeOH); e.e.=91.9% (HPLC).
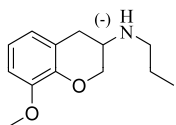
(-)-8-methoxy-3,4-dihydro-3-(*N*-benzyl-*N*-propyl-amino)-2*H*-1-benzopyran ((-)-8.7). A mixture of **(+)-8.6** (2.0 g, 7.4 mmol), K_2CO_3 (3.1 g, 22.3 mmol) were suspended in 25 mL 2-butanone. 1-Iodopropane (2.0 mL, 20.8 mmol) was added while the mixture was heated to reflux under nitrogen atmosphere. After refluxing for 3 days, the solvent was evaporated *in vacuo* and purified on column chromatography (SiO$_2$ (NH$_3$), Hexane/Et$_2$O=1:1) to yield **(-)-8.7** as a light yellow oil (1.7 g, 73%). Purity: 100% (GCMS); $[\alpha]_D^{26} - 18.1°$ (c 1.1, MeOH); IR (NaCl, cm^{-1}) ν_{max} 2958, 2932, 1584, 1485, 1262, 1213; ^{1}H NMR (200 MHz, CDCl$_3$): δ 7.42-7.15 (m, 5H, C$_6$H$_5$), 6.88-6.75 (m, 1H, ArH), 6.74-6.63 (m, 2H, ArH), 4.38-4.52 (m, 1H, H$_2$), 4.01-3.89 (m, 1H, H$_2$), 3.85 (s, 3H, OCH$_3$), 3.76 (s, 2H, *CH$_2$*C$_6$H$_5$), 3.35-3.15 (m, 1H, H$_3$), 2.98-2.80 (m, 2H, H$_4$), 2.65-2.47 (m, 2H, N(*CH$_2$*CH$_2$CH$_3$), 1.65-1.38 (m, 2H, N(CH$_2$*CH$_2$*CH$_3$), 0.88 (t, *J*=7.4 Hz, 3H, N(CH$_2$CH$_2$*CH$_3$*); ^{13}C NMR (50 MHz, CDCl$_3$): δ 148.5, 144.0, 140.7, 128.5, 127.1, 122.9, 122.2, 120.3, 109.2, 68.2, 56.0, 55.1, 52.5, 52.4, 28.1, 21.6, 11.9; EI-MS *m/z* 311 (M)$^+$.

(+)-8-methoxy-3,4-dihydro-3-(*N*-benzyl-*N*-propyl-amino)-2*H*-1-benzopyran ((+)-8.7). Similar to the procedure described for the synthesis of **(-)-8.7**. Compound **(+)-8.7** was obtained from **(-)-8.6** as a light yellow oil (1.6 g, 81%). Purity: 100% (GCMS); IR (NaCl, cm^{-1}) ν_{max} 2957, 2933, 1584, 1485, 1262, 1212, 1083; ^{1}H NMR (200 MHz, CDCl$_3$): δ 7.44-7.14 (m, 5H, C$_6$H$_5$), 6.89-6.75 (m, 1H, ArH), 6.89-6.63 (m, 2H, ArH), 4.52-4.36 (m, 1H, H$_2$), 4.01-3.89 (m, 1H, H$_2$), 3.85 (s, 3H, OCH$_3$), 3.76 (s, 2H, *CH$_2$*C$_6$H$_5$), 3.35-3.13 (m, 1H, H$_3$), 2.99-2.76 (m, 2H, H$_4$), 2.64-2.43 (m, 2H, N(*CH$_2$*CH$_2$CH$_3$), 1.60-1.38 (m, 2H, N(CH$_2$*CH$_2$*CH$_3$), 0.88 (t, *J*=7.2 Hz, 3H, N(CH$_2$CH$_2$*CH$_3$*); ^{13}C NMR (50 MHz, CDCl$_3$): δ 148.5, 143.9, 140.7, 128.5, 127.1, 122.9, 122.2, 120.2, 109.2, 68.2, 56.0, 55.1, 52.5, 52.4, 28.1, 21.6, 11.9; EI-MS *m/z* 311 (M)$^+$.
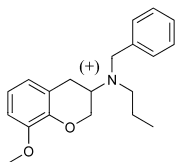
(-)-8-methoxy-3,4-dihydro-3-(*N*-*n*-propylamino)-2*H*-1-benzopyran ((-)-8.8). Compound **(+)-8.7** (1.6 g, 5.1 mmol) was dissolved in 100 mL EtOH 100% and Pd/C 10% (0.51 g) was added under nitrogen atmosphere. The solution was transferred to a Parr flask and hydrogenolyzed at room temperature under 3.5 bar H$_2$ atmosphere. After completion of the reaction the mixture was filtrated, evaporated *in vacuo* and purified by column chromatography (SiO$_2$, CH$_2$Cl$_2$/MeOH=10:1) to yield **(-)-8.8** as a light yellow oil (1.0 g, 90%). Purity: 100% (GCMS); $[\alpha]_D^{26} - 28.3°$ (c 1.0, MeOH); IR (NaCl, cm^{-1}) ν_{max} 2956, 2931, 1584, 1484, 1264, 1212, 1097, 1079; ^{1}H NMR (400 MHz, CDCl$_3$): δ 6.80 (t, *J*=8.0 Hz, 1H, ArH), 6.71 (d, *J*=7.3 Hz, 1H, ArH), 6.66 (d, *J*=7.7 Hz, 1H, ArH), 4.35-4.23 (m, 1H, H$_2$), 4.03-3.93 (m, 1H, H$_2$), 3.85 (s, 3H, OCH$_3$), 3.20-3.08 (m, 1H, H$_3$), 3.07-2.93 (m, 1H, H$_4$), 2.77-2.58 (m, 3H, H$_4$, N(*CH$_2$*CH$_2$CH$_3$), 1.60-1.40 (m, 3H, NH, N(CH$_2$*CH$_2$*CH$_3$), 0.92 (t, *J*=7.3 Hz, 3H, N(CH$_2$CH$_2$*CH$_3$*); ^{13}C NMR (50 MHz, CDCl$_3$): δ 148.4, 143.8, 122.2, 121.5, 120.5, 109.3, 69.4, 56.0, 50.3, 49.3, 32.3, 23.7, 12.0; EI-MS *m/z* 221 (M)$^+$.

(+)-8-methoxy-3,4-dihydro-3-(*N*-*n*-propylamino)-2*H*-1-benzopyran ((+)-8.8). Similar to the procedure described for the synthesis of **(-)-8.8**. Compound **(+)-8.8** was obtained from **(-)-8.7** as a light yellow oil (1.1 g, 91%). Purity>98% (GCMS); $[\alpha]_D^{26} + 27.0^{\circ}$ (c 1.1, MeOH); IR (NaCl, cm^{-1}) ν_{max} 2957, 2930, 1584, 1485, 1264, 1212, 1098, 1079; ^{1}H NMR (400 MHz, CDCl$_3$): δ 6.80 (t, *J*=7.9 Hz, 1H, ArH), 6.70 (d, *J*=8.1 Hz, 1H, ArH), 6.66 (d, *J*=7.7 Hz, 1H, ArH), 4.32-4.23 (m, 1H, H$_2$), 3.97 (dd, *J*=10.6 Hz; 7.3 Hz, 1H, H$_2$), 3.85 (s, 3H, OCH$_3$), 3.18-3.09 (m, 1H, H$_3$), 3.05-2.95 (m, 1H, H$_4$), 2.76-2.60 (m, 3H, H$_4$, N(*CH$_2$*CH$_2$CH$_3$)), 1.58-1.44 (m, 3H, NH, N(CH$_2$*CH$_2$*CH$_3$)), 0.92 (t, *J*=7.3 Hz, 3H, N(CH$_2$CH$_2$*CH$_3$)); ^{13}C NMR (50 MHz, CDCl$_3$): δ 148.4, 143.8, 122.2, 121.5, 120.5, 109.3, 69.4, 56.0, 50.3, 49.3, 32.3, 23.7, 12.0; EI-MS *m/z* 221 (M)$^+$.
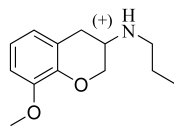
(-)-8-methoxy-3,4-dihydro-3-(*N,N*-di-*n*-propylamino)-2*H*-1-benzopyran ((-)-8.9). TEA (0.75 mL, 5.3 mmol) was added to a cooled solution of **(+)-8.8** (1.06 g, 4.8 mmol) in dry toluene (10 mL) under nitrogen atmosphere. Propionylchloride (0.5 mL, 5.3 mmol) was added and the reaction mixture was stirred for 30 minutes. The TEA-HCl salt was removed by filtration and the solvent was evaporated *in vacuo*. The resultant oil was dissolved in dry THF (8 mL) under nitrogen atmosphere and a suspension of LiAlH$_4$ (0.33 g, 7.2 mmol) in dry THF (8 mL) was added and the mixture was refluxed for 1 hour. After addition of EtOAc (5 mL), diluted H$_2$SO$_4$ was added until precipitation at pH 4. The mixture was filtrated, basified with 1N NaOH (20 mL) and extracted with EtOAc (3x50 mL). The combined organic layers were washed with brine, dried on MgSO$_4$, evaporated *in vacuo* and purified on column chromatography (SiO$_2$, CH$_2$Cl$_2$/MeOH=40:1, 1% TEA) to yield **(-)-8.9** as a colourless oil (1.09 g, 80%). Intermediate amide: EI-MS *m/z* 277 (M)$^+$. Final compound: Purity: 100% (GCMS); $[\alpha]_D^{26} - 5.8^{\circ}$ (c 1.0, MeOH); IR (NaCl, cm^{-1}) ν_{max} 2957, 1585, 1485, 1263, 1213, 1084; ^{1}H NMR (200 MHz, CDCl$_3$): δ 6.85-6.74 (m, 1H, ArH), 6.73-6.62 (m, 2H, ArH), 4.50-4.35 (m, 1H, H$_2$), 3.85 (s, 3H, OCH$_3$), 3.92-3.76 (m, 1H, H$_2$), 3.27-3.08 (m, 1H, H$_3$), 2.85 (d, *J*=8.5 Hz, 2H, H$_4$), 2.59-2.42 (m, 4H, N(*CH$_2$*CH$_2$CH$_3$)$_2$), 1.58-1.33 (m, 4H, N(CH$_2$*CH$_2$*CH$_3$)$_2$), 0.87 (t, *J*=7.4 Hz, 6H, N(CH$_2$CH$_2$*CH$_3$)$_2$); ^{13}C NMR (50 MHz, CDCl$_3$): δ 148.5, 144.0, 122.9, 122.2, 120.3, 109.2, 68.5, 56.0, 53.4, 52.9, 28.6, 21.9, 12.0; EI-MS *m/z* 263 (M)$^+$.
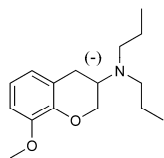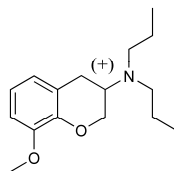
(+)-8-methoxy-3,4-dihydro-3-(*N,N*-di-*n*-propylamino)-2*H*-1-benzopyran ((+)-8.9). Similar to the procedure described for the synthesis of **(-)-8.9**. Compound **(+)-8.9** was obtained from **(-)-8.8** as a very light yellow oil (0.89 g, 76%). %). Intermediate amide: EI-MS *m/z* 277 (M)$^+$. Final compound: Purity: 100% (GCMS); $[\alpha]_D^{26} + 5.6^{\circ}$ (c 1.0, MeOH); IR (NaCl, cm^{-1}) ν_{max} 2955, 1585, 1485, 1263, 1213, 1084; ^{1}H NMR (200 MHz, CDCl$_3$): δ 6.87-6.75 (m, 1H, ArH), 6.74-6.62 (m, 2H, ArH), 4.43 (dd, *J*=10.3 Hz; 3.2 Hz, 1H, H$_2$), 3.85 (s, 3H, OCH$_3$), 3.92-3.75 (m, 1H, H$_2$), 3.28-3.08 (m, 1H, H$_3$), 2.85 (d, *J*=8.2 Hz, 2H, H$_4$), 2.59-2.43 (m, 4H, N(*CH$_2$*CH$_2$CH$_3$)$_2$), 1.46 (sextet, *J*=7.3 Hz, 4H, N(CH$_2$*CH$_2$*CH$_3$)$_2$), 0.87 (t, *J*=7.4 Hz, 6H, N(CH$_2$CH$_2$*CH$_3$)$_2$); ^{13}C NMR (50 MHz, CDCl$_3$): δ 148.5, 144.0, 122.9, 122.2, 120.3, 109.2, 68.5, 56.0, 53.4, 52.9, 28.6, 21.9, 12.0; EI-MS *m/z* 263 (M)$^+$.

(-)-8-hydroxy-3,4-dihydro-3-(*N,N*-di-*n*-propylamino)-2*H*-1-benzopyran HBr salt ((-)-8.10). A mixture of freshly distilled 48% HBr (5 mL) and **(+)-8.9** (1.0 g, 3.8 mmol) was refluxed for 4 hours under nitrogen atmosphere. After cooling down, the reaction mixture was evaporated *in vacuo* and the
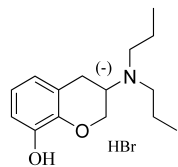
resultant orange solid material was recrystallized from 100% EtOH to afford the HBr salt of **(-)-8.10** as white crystals (1.0 g, 81%). Purity: 100% (GCMS). $[\alpha]_D^{27} - 74.5°$ $(c\, 0.6, CHCl_3)$; e.e.>98% (HPLC); IR (KBr, cm^{-1}) ν_{max} 3133 (br), 2934, 2647, 2525, 1586, 1502, 1474, 1338, 1274, 1217, 1187, 1000; ^{1}H NMR (400 MHz, CD$_3$OD): δ 6.80 (t, *J*=7.9 Hz, 1H, ArH), 6.68 (d, *J*=8.1 Hz, 2H, ArH), 4.55 (ddd, *J*=11.0 Hz; 5.5 Hz; 1.5 Hz, 1H, H$_2$), 4.48-4.37 (m, 1H, H$_2$), 4.05-3.94 (m, 1H, H$_3$), 3.36 (dd, *J*=7.6 Hz; 6.2 Hz, 1H, H$_4$), 3.32-3.08 (m, 5H, H$_4$, N(C*H$_2$*CH$_2$CH$_3$)$_2$), 1.91-1.69 (m, 4H, N(CH$_2$*CH$_2$*CH$_3$)$_2$), 1.02 (t, *J*=7.3 Hz, 6H, N(CH$_2$CH$_2$*CH$_3$*)$_2$); ^{13}C NMR (50 MHz, CD$_3$OD): δ 145.8, 142.2, 122.0, 120.1, 119.2, 114.2, 64.1, 56.4, 53.1, 25.4, 17.9, 10.1; EI-MS *m/z* 249 (M)$^+$; Anal. Calcd for C$_{15}$H$_{24}$NO$_2$Br: C, 54.55; H, 7.32; N, 4.24. Found: C, 54.54; H, 7.35; N, 4.27.
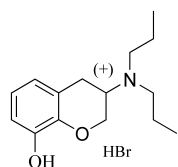
(+)-8-hydroxy-3,4-dihydro-3-(*N,N*-di-*n*-propylamino)-2*H*-1-benzopyran HBr salt ((+)-8.10).
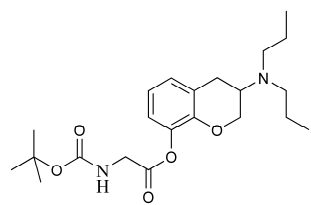Similar to the procedure described for the synthesis of **(-)-8.10**. The HBr salt of compound **(+)-8.10** was obtained from **(-)-8.9** as white crystals (0.98 g, 89%). Purity: 100% (GCMS). $[\alpha]_D^{27} + 74.6°$ $(c\, 0.6, CHCl_3)$; e.e.=93.0% (HPLC); IR (KBr, cm^{-1}) ν_{max} 3131 (br), 2934, 2648, 2525, 1586, 1502, 1474, 1338, 1274, 1217, 1187, 1000; ^{1}H NMR (400 MHz, CD$_3$OD): δ 6.79 (t, *J*=7.9 Hz, 1H, ArH), 6.68 (d, *J*=8.3 Hz, 2H, ArH), 4.55 (ddd, *J*=10.8 Hz; 5.3 Hz; 1.3 Hz, 1H, H$_2$), 4.43 (dd, *J*=12.1 Hz; 1.83 Hz, 1H, H$_2$), 4.05-3.95 (m, 1H, H$_3$), 3.36 (dd, *J*=7.6 Hz; 6.2 Hz, 1H, H$_4$), 3.32-3.09 (m, 5H, H$_4$, N(C*H$_2$*CH$_2$CH$_3$)$_2$), 1.91-1.66 (m, 4H, N(CH$_2$*CH$_2$*CH$_3$)$_2$), 1.02 (t, *J*=7.3 Hz, 6H, N(CH$_2$CH$_2$*CH$_3$*)$_2$); ^{13}C NMR (50 MHz, CD$_3$OD): δ 145.8, 142.2, 122.0, 120.1, 119.2, 114.2, 64.1, 56.4, 53.1, 25.4, 17.9, 10.1; EI-MS *m/z* 249 (M)$^+$; Anal. Calcd for C$_{15}$H$_{24}$NO$_2$Br: C, 54.55; H, 7.32; N, 4.24. Found: C, 54.52; H, 7.34; N, 4.28.

8.5.1.4 General procedure for preparation of protected amino acid (-)-3,4-dihydro-3-(N,N-di-n-propylamino)-2H-1-benzopyran-8-yl esters 8.12-8.16

The preparation of the protected amino acid (-)-3,4-dihydro-3-(di-*n*-propylamino)-2*H*-1-benzopyran-8-yl esters from **(-)-8.10** was similar to the preparation of the protected amino acid (S)-2-(di-*n*-propyl-amino)tetralin-5-yl esters from **(-)-2.12** described in section 2.5.5.

***N-tert*-Boc-glycine (-)-3,4-dihydro-3-(*N,N*-di-*n*-propylamino)-2*H*-1-benzopyran-8-yl ester (8.12).**
Yield: 71%; IR (NaCl, cm^{-1}) ν_{max} 3408 (br), 2957, 1778, 1719, 1481, 1366, 1254, 1152; ^{1}H NMR (400 MHz, CDCl$_3$): δ 6.97 (d, *J*=7.3 Hz, 1H, ArH), 6.90-6.78 (m, 2H, ArH), 5.13 (br s, 1H, NH), 4.31 (dd, *J*=10.3 Hz; 2.9 Hz, 1H, H$_2$), 4.20 (d, *J*=5.1 Hz, 2H, α-CH$_2$), 3.78 (t, *J*=10.3 Hz, 1H, H$_2$), 3.23-3.12 (m, 1H, H$_3$), 2.86 (d, *J*=8.1 Hz, 2H, H$_4$), 2.57-2.41 (m, 4H, N(C*H$_2$*CH$_2$CH$_3$)$_2$), 1.53-1.34 (m, 4H, N(CH$_2$*CH$_2$*CH$_3$)$_2$), 1.46 (s, 9H, OC(CH$_3$)$_3$), 0.87 (t, *J*=7.3 Hz, 6H, N(CH$_2$CH$_2$*CH$_3$*)$_2$); ^{13}C NMR (50 MHz, CDCl$_3$): δ 168.9, 155.8, 146.1, 138.7, 128.1, 124.2, 120.5, 120.3, 80.3, 68.4, 53.2, 52.9, 42.5, 28.5, 28.3, 22.0, 11.9; HR-MS *m/z* Calcd. for C$_{22}$H$_{35}$N$_2$O$_5$ 407.25405 (M+H)$^+$, found 407.25397 (M+H)$^+$.

***N-tert*-Boc-1-aminocyclopropane-1-carboxylic acid (-)-3,4-dihydro-3-(*N,N*-di-*n*-propylamino)-2*H*-1-benzopyran-8-yl ester (8.13).** Yield: 62%; IR (NaCl, cm^{-1}) ν_{max} 3358 (br), 2964, 1757, 1723,
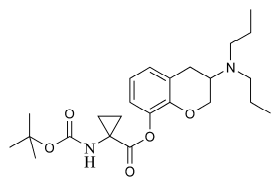
1481, 1253, 1133; ^{1}H NMR (400 MHz, CDCl$_3$): δ 6.97-6.88 (m, 1H, ArH), 6.87-6.74 (m, 2H, ArH), 5.31 (br s, 1H, NH), 4.34-4.25 (m, 1H, H$_2$), 3.76 (t, J=10.3 Hz, 1H, H$_2$), 3.23-3.10 (m, 1H, H$_3$), 2.84 (d, J=8.4 Hz, 2H, H$_4$), 2.57-2.37 (m, 4H, N(CH_2CH$_2$CH$_3$)$_2$), 1.80-1.65 (m, 2H, β-CH$_2$), 1.56-1.33 (m, 4H, N(CH$_2$$CH_2CH_3$)$_2$), 1.45 (s, 9H, OC(CH$_3$)$_3$), 1.32-1.18 (m, 2H, β-CH$_2$), 0.86 (t, J=7.3 Hz, 6H, N(CH$_2$CH$_2$$CH_3$)$_2$); ^{13}C NMR (50 MHz, CDCl$_3$): δ 171.6, 156.2, 146.3, 139.1, 127.8, 124.0, 120.7, 120.3, 80.3, 68.4, 53.2, 52.9, 34.7, 28.5, 28.2, 22.0, 18.3, 11.9; HR-MS m/z Calcd. for C$_{24}$H$_{37}$N$_2$O$_5$ 433.2697 (M+H)$^+$, found 433.26929 (M+H)$^+$.

N-tert-Boc-L-valine (-)-3,4-dihydro-3-(N,N-di-n-propylamino)-2H-1-benzopyran-8-yl ester (8.14). Yield: 78%; IR (NaCl, cm^{-1}) ν$_{max}$ 3442 (br), 2965, 1765, 1713, 1483, 1367, 1254, 1174, 1027; ^{1}H NMR (400 MHz, CDCl$_3$): δ 6.99-6.91 (m, 1H, ArH), 6.87-6.77 (m, 2H, ArH), 5.10 (d, J=9.2 Hz, 1H, NH), 4.50 (dd, J=9.2 Hz; 4.4 Hz, 1H, α-CH), 4.26 (dd, J=10.5 Hz; 3.5 Hz, 1H, H$_2$), 3.85-3.73 (m, 1H, H$_2$), 3.24-3.12 (m, 1H, H$_3$), 2.85 (d, J=7.3 Hz, 2H, H$_4$), 2.56-2.43 (m, 4H, N(CH_2CH$_2$CH$_3$)$_2$), 2.42-2.28 (m, 1H, β-CH), 1.54-1.32 (m, 4H, N(CH$_2$$CH_2CH_3$)$_2$), 1.46 (s, 9H, OC(CH$_3$)$_3$), 1.05 (d, J=3.9 Hz, 3H, γ-CH$_3$), 0.96 (d, J=6.6 Hz, 3H, γ-CH$_3$), 0.87 (t, J=7.3 Hz, 6H, N(CH$_2$CH$_2$$CH_3$)$_2$); ^{13}C NMR (50 MHz, CDCl$_3$): δ 170.7, 155.9, 146.2, 138.8, 128.0, 124.1, 120.3, 80.0, 68.2, 58.8, 53.2, 52.9, 31.7, 28.6, 28.1, 22.0, 19.3, 17.5, 11.9; HR-MS m/z Calcd. for C$_{25}$H$_{41}$N$_2$O$_5$ 449.301 (M+H)$^+$, found 449.30093 (M+H)$^+$.
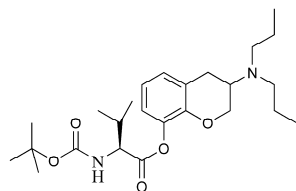
N-tert-Boc-L-isoleucine (-)-3,4-dihydro-3-(N,N-di-n-propylamino)-2H-1-benzopyran-8-yl ester (8.15). Yield: 72%; IR (NaCl, cm^{-1}) ν$_{max}$ 3445 (br), 2967, 1765, 1714, 1482, 1254, 1159; ^{1}H NMR (400 MHz, CDCl$_3$): δ 6.98-6.90 (m, 1H, ArH), 6.87-6.77 (m, 2H, ArH), 5.11 (d, J=9.2 Hz, 1H, NH), 4.54 (dd, J=9.2 Hz; 4.4 Hz, 1H, α-CH), 4.25 (dd, J=10.3 Hz; 3.3 Hz, 1H, H$_2$), 3.86-3.74 (m, 1H, H$_2$), 3.24-3.12 (m, 1H, H$_3$), 2.86 (d, J=7.7 Hz, 2H, H$_4$), 2.58-2.40 (m, 4H, N(CH_2CH$_2$CH$_3$)$_2$), 2.13-1.98 (m, 1H, β-CH), 1.70-1.56 (m, 1H, γ-CH$_2$), 1.52-1.34 (m, 4H, N(CH$_2$$CH_2CH_3$)$_2$), 1.33-1.18 (m, 1H, γ-CH$_2$), 1.46 (s, 9H, OC(CH$_3$)$_3$), 1.06 (d, J=7.0 Hz, 3H, γ'-CH$_3$), 0.98 (t, J=7.5 Hz, 3H, δ-CH$_3$), 0.87 (t, J=7.3 Hz, 6H, N(CH$_2$CH$_2$$CH_3$)$_2$); ^{13}C NMR (50 MHz, CDCl$_3$): δ 170.6, 155.8, 146.2, 138.7, 128.0, 124.1, 120.6, 120.3, 80.0, 68.2, 58.3, 53.2, 52.9, 38.4, 28.6, 28.1, 25.0, 22.0, 15.7, 12.1, 11.9; HR-MS m/z Calcd. for C$_{26}$H$_{43}$N$_2$O$_5$ 463.31665 (M+H)$^+$, found 463.31616 (M+H)$^+$.
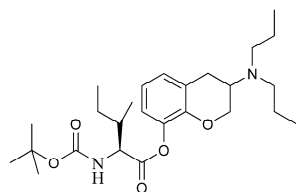
N-tert-Boc-β-alanine (-)-3,4-dihydro-3-(N,N-di-n-propylamino)-2H-1-benzopyran-8-yl ester (8.16). Yield: 79%; IR (NaCl, cm^{-1}) ν$_{max}$ 3384 (br), 2960, 1762, 1716, 1481, 1252, 1164; ^{1}H NMR (400 MHz, CDCl$_3$): δ 6.98-6.93 (m, 1H, ArH), 6.89-6.80 (m, 2H, ArH), 5.41 (br s, 1H, NH), 4.36 (dd, J=10.3 Hz; 3.3 Hz, 1H, H$_2$), 3.82 (t, J=10.3 Hz, 1H, H$_2$), 3.58-3.47 (m, 2H, β-CH$_2$), 3.25-3.13 (m, 1H, H$_3$), 2.86 (d, J=8.1 Hz, 2H, H$_4$), 2.76 (t, J=5.9 Hz, 2H, α-CH$_2$), 2.57-2.40 (m, 4H, N(CH_2CH$_2$CH$_3$)$_2$), 1.54-1.35 (m, 4H, N(CH$_2$$CH_2CH_3$)$_2$), 1.45 (s, 9H, OC(CH$_3$)$_3$), 0.87 (t, J=7.3 Hz, 6H, N(CH$_2$CH$_2$$CH_3$)$_2$); ^{13}C NMR
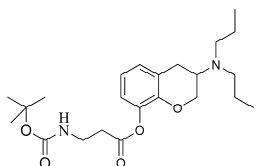
(50 MHz, CDCl$_3$): δ 170.6, 156.1, 145.9, 138.9, 128.0, 124.2, 120.7, 120.5, 79.5, 68.5, 53.1, 52.9, 36.6, 35.2, 28.7, 28.1, 22.1, 11.9; HR-MS *m/z* Calcd. for C$_{23}$H$_{37}$N$_2$O$_5$ 421.2697 (M+H)$^+$, found 421.26953 (M+H)$^+$.

8.5.1.5 General deprotection procedure for the preparation of the amino acid (–)-3,4-dihydro-3-(*N,N*-di-*n*-propylamino)-2*H*-1-benzopyran-8-yl ester hydrochlorides 8.17-8.21

The preparation of the amino acid (-)-3,4-dihydro-3-(di-*n*-propylamino)-2*H*-1-benzopyran-8-yl ester hydrochlorides was similar to the preparation of the amino acid (S)-2-(di-*n*-propyl-amino)tetralin-5-yl ester hydrochlorides described in section 2.5.6.

Glycine (-)-3,4-dihydro-3-(*N,N*-di-*n*-propylamino)-2*H*-1-benzopyran-8-yl ester 2HCl salt (8.17). Yield: 68%; Purity: 86% (HPLC); IR (KBr, cm^{-1}) ν$_{max}$ 3431 (br), 2970, 2883, 2631, 2520, 1778, 1484, 1257, 1188; ^{1}H NMR (400 MHz, CD$_3$OD): δ 7.19 (dd, *J*=7.3 Hz; 1.1 Hz, 1H, ArH), 7.10-6.97 (m, 2H, ArH), 4.61 (dd, *J*=12.1 Hz; 4.8 Hz, 1H, H$_2$), 4.45 (dd, *J*=12.2 Hz; 2.3 Hz, 1H, H$_2$), 4.18 (s, 2H, α-CH$_2$), 4.10-4.00 (m, 1H, H$_3$), 3.44 (dd, *J*=17.8 Hz; 6.8 Hz, 1H, H$_4$), 3.37-3.08 (m, 5H, H$_4$, N(*CH$_2$*CH$_2$CH$_3$)$_2$), 1.89-1.70 (m, 4H, N(CH$_2$*CH$_2$*CH$_3$)$_2$), 1.00 (t, *J*=7.3 Hz, 6H, N(CH$_2$CH$_2$*CH$_3$*)$_2$); ^{13}C NMR (50 MHz, CD$_3$OD): δ 165.7, 145.4, 138.5, 127.9, 121.7, 121.0, 120.9, 64.3, 55.6, 53.2, 52.9, 39.8, 24.6, 18.1, 18.0, 10.1; HR-MS *m/z* Calcd. for C$_{18}$H$_{29}$N$_2$O$_3$ 307.20162 (M+H)$^+$, found 307.20515 (M+H)$^+$.
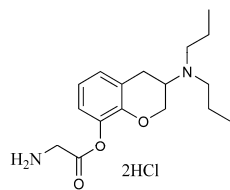
1-Aminocyclopropane-1-carboxylic acid (-)-3,4-dihydro-3-(*N,N*-di-*n*-propylamino)-2*H*-1-benzopyran-8-yl ester 2HCl salt (8.18). Yield: 62%; Purity (HPLC): 98%; IR (KBr, cm^{-1}) ν$_{max}$ 3424 (br), 2970, 2880, 2649, 1762, 1484, 1165; ^{1}H NMR (400 MHz, CD$_3$OD): δ 7.19 (dd, *J*=7.0 Hz; 2.2 Hz, 1H, ArH), 7.07-6.95 (m, 2H, ArH), 4.59 (dd, *J*=12.1 Hz; 4.4 Hz, 1H, H$_2$), 4.46 (dd, *J*=12.1 Hz; 2.2 Hz, 1H, H$_2$), 4.10-3.99 (m, 1H, H$_3$), 3.47-3.36 (m, 1H, H$_4$), 3.35-3.10 (m, 5H, H$_4$, N(*CH$_2$*CH$_2$CH$_3$)$_2$), 1.92-1.70 (m, 6H, β-CH$_2$, N(CH$_2$*CH$_2$*CH$_3$)$_2$), 1.64-1.54 (m, 2H, β-CH$_2$), 1.01 (t, *J*=7.2 Hz, 6H, N(CH$_2$CH$_2$*CH$_3$*)$_2$); ^{13}C NMR (50 MHz, CD$_3$OD): δ 167.9, 145.4, 138.4, 127.9, 121.7, 121.0, 120.9, 64.4, 55.6, 53.3, 34.2, 24.6, 18.1, 13.8, 10.1; HR-MS *m/z* Calcd. for C$_{19}$H$_{29}$N$_2$O$_3$ 333.21727 (M+H)$^+$, found 333.21725 (M+H)$^+$.
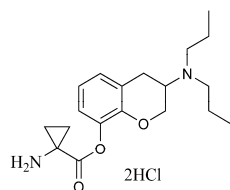
L-Valine (-)-3,4-dihydro-3-(*N,N*-di-*n*-propylamino)-2*H*-1-benzopyran-8-yl ester 2HCl salt (8.19). Yield: 49%; Purity: 98% (HPLC); IR (KBr, cm^{-1}) ν$_{max}$ 3412 (br), 2971, 2880, 2631, 1768, 1484, 1257, 1189, 1162; ^{1}H NMR (400 MHz, CD$_3$OD): δ 7.21 (dd, *J*=7.0 Hz; 2.2 Hz, 1H, ArH), 7.10-6.97 (m, 2H, ArH), 4.60 (dd, *J*=11.9 Hz; 5.0 Hz, 1H, H$_2$), 4.47 (dd, *J*=12.1 Hz; 2.2 Hz, 1H, H$_2$), 4.27 (d, *J*=4.8 Hz, 1H, α-CH), 4.13-4.02 (m, 1H, H$_3$), 3.45 (dd, *J*=17.6 Hz; 6.6 Hz, 1H, H$_4$), 3.38-3.10 (m, 5H, H$_4$, N(*CH$_2$*CH$_2$CH$_3$)$_2$), 2.57-2.43 (m, 1H, β-CH), 1.93-1.72 (m, 4H, N(CH$_2$*CH$_2$*CH$_3$)$_2$), 1.23 (d, *J*=4.8 Hz, 3H, γ-CH$_3$), 1.22 (d, *J*=4.8 Hz, 3H, γ-CH$_3$), 1.01 (td, *J*=7.3 Hz; 2.9 Hz, 6H, N(CH$_2$CH$_2$*CH$_3$*)$_2$); ^{13}C NMR (50 MHz, CD$_3$OD): δ 166.9, 145.3, 138.3, 128.1, 121.8, 121.1, 120.9, 64.3, 58.2, 55.6, 53.4, 52.9, 30.1, 24.6, 18.1, 17.2, 17.1, 10.1; HR-MS *m/z* Calcd. for C$_{20}$H$_{33}$N$_2$O$_3$ 349.24857 (M+H)$^+$, found 349.24854 (M+H)$^+$.
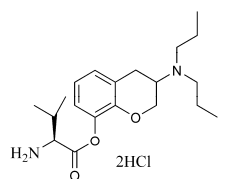
L-Isoleucine (-)-3,4-dihydro-3-(*N,N*-di-*n*-propylamino)-2*H*-1-benzopyran-8-yl ester 2HCl salt (8.20). Yield: 64%; Purity: 95% (HPLC); IR (KBr, cm^{-1}) ν$_{max}$ 3403 (br), 2970, 2877, 2629, 1769,
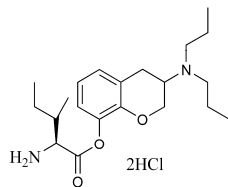
1484, 1258, 1184, 1164; ^{1}H NMR (400 MHz, CD$_3$OD): δ 7.21 (dd, J=6.6 Hz; 2.2 Hz, 1H, ArH), 7.10-6.99 (m, 2H, ArH), 4.61 (dd, J=12.3 Hz; 5.0 Hz, 1H, H$_2$), 4.46 (dd, J=12.3 Hz; 2.4 Hz, 1H, H$_2$), 4.35 (d, J=3.7 Hz, 1H, α-CH), 4.14-4.00 (m, 1H, H$_3$), 3.45 (dd, J=17.6 Hz; 6.2 Hz, 1H, H$_4$), 3.38-3.10 (m, 5H, H$_4$, N(CH$_2$CH$_2$CH$_3$)$_2$), 2.27-2.11 (m, 1H, γ-CH$_2$), 1.90-1.68 (m, 5H, N(CH$_2$CH$_2$CH$_3$)$_2$, γ-CH$_2$), 1.57-1.45 (m, 1H, β-CH), 1.20 (d, J=7.0 Hz, 3H, γ'-CH$_3$), 1.08 (t, J=7.3 Hz, 3H, δ-CH$_3$), 1.01 (t, J=7.3 Hz, 6H, N(CH$_2$CH$_2$CH$_3$)$_2$); ^{13}C NMR (50 MHz, CD$_3$OD): δ 166.8, 145.3, 138.3, 128.1, 121.8, 121.2, 120.9, 64.3, 57.2, 55.7, 53.5, 52.9, 36.9, 25.5, 24.6, 18.1, 13.7, 11.0, 10.1; HR-MS m/z Calcd. for C$_{21}$H$_{35}$N$_2$O$_3$ 363.26422 (M+H)[+], found 363.26416 (M+H)[+].

β-Alanine (-)-3,4-dihydro-3-(N,N-di-n-propylamino)-2H-1-benzopyran-8-yl ester 2HCl salt (8.21). Yield: 79%; Purity: 97% (HPLC); IR (KBr, cm[-1]) ν$_{max}$ 3433 (br), 2968, 2888, 2632, 2522, 1761, 1483, 1257, 1178; ^{1}H NMR (400 MHz, CD$_3$OD): δ 7.15 (dd, J=7.2 Hz; 2.0 Hz, 1H, ArH), 7.07-6.96 (m, 2H, ArH), 4.58 (dd, J=12.1 Hz; 5.1 Hz, 1H, H$_2$), 4.45 (dd, J=12.1 Hz; 2.2 Hz, 1H, H$_2$), 4.09-3.99 (m, 1H, H$_3$), 3.43 (dd, J=16.7 Hz; 5.7 Hz, 1H, H$_4$), 3.37-3.05 (m, 5H, H$_4$, N(CH$_2$CH$_2$CH$_3$)$_2$), 3.32 (t, J=6.8 Hz, 2H, β-CH$_2$), 3.07 (t, J=6.8 Hz, 2H, α-CH$_2$), 1.91-1.72 (m, 4H, N(CH$_2$CH$_2$CH$_3$)$_2$), 1.00 (t, J=7.3 Hz, 6H, N(CH$_2$CH$_2$CH$_3$)$_2$); ^{13}C NMR (50 MHz, CD$_3$OD): δ 168.9, 145.5, 139.0, 127.5, 121.6, 121.1, 120.8, 64.3, 55.7, 53.3, 52.8, 35.2, 30.9, 24.8, 18.1, 10.1; HR-MS m/z Calcd. for C$_{18}$H$_{29}$N$_2$O$_3$ 321.21727 (M+H)[+], found 321.21725 (M+H)[+].
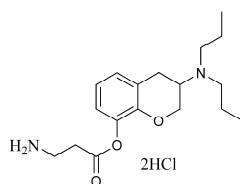
8.5.2 Chemical hydrolysis experiments in 5 mM citrate buffer pH 5

The methods for the chemical hydrolysis experiments of compounds **2.28**, **2.30**, **2.31**, **2.33** and **2.39** were already described in Chapter 3.

8.5.2.1 Procedure

For the experiments with prodrugs **8.17-8.21** the chemical hydrolysis was initiated by adding 6 μl of a 25 mM stock solution in 5 mM citrate buffer (pH 5) to 2.994 mL 5 mM citrate buffer (pH 5) preheated at 32 °C. The final concentration of the resulting solutions was about 50 μM. The test solutions of the compounds were vortexed and maintained in a Lab-Line Orbit Shaker at a constant temperature of 32±0.2 °C. At appropriate intervals samples of 100 μL were withdrawn and diluted with 100 μL H$_2$O/ACN/TFA (1.2/1/0.004) giving a concentration of 25 μM. The samples were stored in the freezer until they were analyzed by HPLC. The prodrug concentration was estimated by measuring the peak heights in relation to those of prodrug standards which were prepared by serial dilution of known concentrations (0.5, 5, 10 and 25 μM) and chromatographed under the same conditions.

8.5.2.2 HPLC analysis

Samples of prodrugs **8.17-8.21** were analyzed isocratically on a Hewlett Packard Series 1100 HPLC system connected to a Tray-Cooling Marathon Basic+ Autosampler and a Hewlett Packard HP3395 Integrator. The samples were injected onto a Supelco Discovery C18 reversed-phase column (5 μm,

250 x 4.6 mm I.D.). The mobile phase for compound **8.17** and **8.20** consisted of a mixture of 22% acetonitrile and 78% water with 0.1% trifluoroacetic acid added (eluent A). The mobile phase for compound **8.18** and **8.21** consisted of a mixture of 20% acetonitrile and 80% water with 0.1% trifluoroacetic acid added (eluent B). The mobile phase for compound **8.19** consisted of a mixture of 23% acetonitrile and 77% water with 0.1% trifluoroacetic acid added (eluent C). The flow was set at 1.0 mL/min and the analysis was performed at room temperature. The injection volume was 20 μL and the compounds were detected by UV at 217 nm. The runtime was 12 minutes. The retention times of 8-OH-DPAC and the amino acid 8-OH-DPAC esters were: 6.95 min (**8.10**, eluent A), 8.15 min (**8.10**, eluent B), 6.46 min (**8.10**, eluent C), 4.12 min (**8.17**, eluent A), 5.25 min (**8.18**, eluent B), 5.41 min (**8.19**, eluent C), 8.31 min (**8.20**, eluent A), 4.85 min (**8.21**, eluent B)

8.5.2.3 Data analysis

All hydrolysis experiments were carried out in triplicate. The pseudo-first-order chemical hydrolysis rate constants (k) from the experiments were calculated from the linear slopes of plots of the logarithm of the remaining prodrug concentration against time (t). The slopes of these plots are related to the rate constant, k, and given by k = 2.303 x slope (log C vs time). The hydrolysis of the prodrug follows pseudo-first-order kinetics described by the formula: $[\text{Prodrug}] = [\text{Prodrug}]_0 e^{-kt}$.

The half-lives ($t_{1/2}$) can be estimated by the equation: $t_{1/2} = \dfrac{\ln 2}{k}$.

8.6 ACKNOWLEDGMENTS

8.7 REFERENCES

1.   Ackaert, O. W.; De Graan, J.; Capancioni, R.; Della Pasqua, O. E.; Dijkstra, D.; Westerink, B. H.; Danhof, M.; Bouwstra, J. A. The in vitro and in vivo evaluation of new synthesized prodrugs of 5-OH-DPAT for iontophoretic delivery. *J. Controlled Release* **2010**, *144,* 296-305.

2.   Comella, C. L. Sleep disorders in Parkinson's disease: an overview. *Mov. Disorders* **2007**, *22 Suppl 17,* S367-73.

3.   Steiger, M. Constant dopaminergic stimulation by transdermal delivery of dopaminergic drugs: a new treatment paradigm in Parkinson's disease. *Eur. J. Neurol.* **2008**, *15,* 6-15.

4.   Anonymous *VCCLAB, Virtual Computational Chemistry Laboratory;* 2005; .

5.   Tetko, I. V.; Gasteiger, J.; Todeschini, R.; Mauri, A.; Livingstone, D.; Ertl, P.; Palyulin, V. A.; Radchenko, E. V.; Zefirov, N. S.; Makarenko, A. S.; Tanchuk, V. Y.; Prokopenko, V. V. Virtual computational chemistry laboratory - design and description. *J. Comput. -Aided Mol. Des.* **2005**, *19,* 453-463; 453.

6.   Tetko, I. V.; Bruneau, P. Application of ALOGPS to predict 1-octanol/water distribution coefficients, logP, and logD, of AstraZeneca in-house database. *J. Pharm. Sci.* **2004**, *93,* 3103-10.

7.   Nugroho, A. K.; Li, L.; Dijkstra, D.; Wikstrom, H.; Danhof, M.; Bouwstra, J. A. Transdermal iontophoresis of the dopamine agonist 5-OH-DPAT in human skin in vitro. *J. Controlled Release* **2005**, *103,* 393-403.

8.   Moody, R. P.; Akram, M.; Dickson, E.; Chu, I. In Vitro Dermal Absorption of Methyl Salicylate, Ethyl Parathion, and Malathion: First Responder Safety. *J. Toxicol. Environ. Health A* **2007**, *70,* 985-999; 985.

9.   Vermue, N. A.; Kaptein, B.; Tepper, P. G.; de Vries, J. B.; Horn, A. S. Pharmacological profile of N,N dipropyl-8-hydroxy-3-chromanamine, an oxygen isostere of the dopamine agonist N,N dipropyl-5-hydroxy-2-aminotetralin with enhanced presynaptic selectivity. *Arch. Int. Pharmacodyn. Ther.* **1988**, *293,* 37-56.

10.   Horn, A. S.; Kaptein, B.; Vermue, N. A.; Devries, J. B.; Mulder, T. B. A. Synthesis and Dopaminergic Activity of a New Oxygen Isostere of the 2-Aminotetralins - N,N-Dipropyl-8-Hydroxy-3-Chromanamine. *Eur. J. Med. Chem.* **1988**, *23,* 325-328.

11.   Alneirabeyeh, M.; Reynaud, D.; Podona, T.; Ou, L.; Perdicakis, C.; Coudert, G.; Guillaumet, G.; Pichat, L.; Gharib, A.; Sarda, N. Methoxy and Hydroxy Derivatives of 3,4-Dihydro-3-(Di-Normal-Propylamino)-2H-1-Benzopyrans - New Synthesis and Dopaminergic Activity. *Eur. J. Med. Chem.* **1991**, *26,* 497-504.

12.   Ackaert, O. W.; De Graan, J.; Capancioni, R.; Dijkstra, D.; Danhof, M.; Bouwstra, J. A. Transdermal iontophoretic delivery of a novel series of dopamine agonists in vitro: physicochemical considerations. *J. Pharm. Pharmacol.* **2010**, *62,* 709-20.

13.   Holmberg, P.; Sohn, D.; Leideborg, R.; Caldirola, P.; Zlatoidsky, P.; Hanson, S.; Mohell, N.; Rosqvist, S.; Nordvall, G.; Johansson, A. M.; Johansson, R. Novel 2-aminotetralin and 3-AminoChroman derivatives as selective serotonin 5-HT7 receptor agonists and antagonists. *J. Med. Chem.* **2004**, *47,* 3927-3930.

14.   Brisander, M.; Caldirola, P.; Johansson, A. M.; Hacksell, U. Alkylation of tricarbonylchromium-stabilized benzylic anions of 3-(dipropylamino)chroman. *J. Org. Chem.* **1998**, *63,* 5362-5367.

15.   Karlsson, A.; Bjork, L.; Pettersson, C.; Anden, N. E.; Hacksell, U. (R)-5-Hydroxy-2-(Dipropylamino)Tetralin and (S)-5-Hydroxy-2-(Dipropylamino)Tetralin (5-Oh Dpat) - Assessment of Optical Purities and Dopaminergic Activities. *Chirality* **1990**, *2,* 90-95.

16.   Wise, L. D.; Dewald, H. A.; Hawkins, E. S.; Reynolds, D. M.; Heffner, T. G.; Meltzer, L. T.; Pugsley, T. A. 6-Hydroxy-3,4-Dihydro-3-(Dipropylamino)-2H-1-Benzopyrans and 8-Hydroxy-3,4-Dihydro-3-(Dipropylamino)-2H-1-Benzopyrans - Dopamine Agonists with Autoreceptor Selectivity. *J. Med. Chem.* **1988**, *31,* 688-691.

17.   Tenhoeve, W.; Wynberg, H. The Design of Resolving Agents - Chiral Cyclic Phosphoric-Acids. *J. Org. Chem.* **1985**, *50,* 4508-4514.

18.   Sonesson, C.; Barf, T.; Nilsson, J.; Dijkstra, D.; Carlsson, A.; Svensson, K.; Smith, M. W.; Martin, I. J.; Duncan, J. N.; King, L. J.; Wikstrom, H. Synthesis and Evaluation of Pharmacological and Pharmacokinetic Properties of Monopropyl Analogs of 5-[[[(Trifluoromethyl)Sulfonyl]Oxy]-2-Aminotetralin, 7-[[[(Trifluoromethyl)Sulfonyl]Oxy]-2-Aminotetralin, and 8-[[[(Trifluoromethyl)Sulfonyl]Oxy]-2-Aminotetralin - Central Dopamine and Serotonin Receptor Activity. *J. Med. Chem.* **1995**, *38,* 1319-1329.

19.   AnonymousPallas 1.2. **1994**, .

20.   Santos, C. R.; Capela, R.; Pereira, C. S.; Valente, E.; Gouveia, L.; Pannecouque, C.; De Clercq, E.; Moreira, R.; Gomes, P. Structure-activity relationships for dipeptide prodrugs of acyclovir: Implications for prodrug design. *Eur. J. Med. Chem.* **2008**, .

9

Summary and general discussion

The neurotransmitter dopamine (DA) plays an important role in the central nervous system and is related to symptoms of Parkinson's disease. Parkinson's disease is a neurodegenerative disorder with the gradual loss of nigrostriatal DAergic neurons as its main feature. The best therapeutic strategy for treatment of Parkinson's disease is based on restoring the DA deficiency by increasing DA concentrations with *L*-DOPA, MAO-B inhibitors or COMT inhibitors. Another approach for treatment of Parkinson's disease is the replacement of the decreased DA levels with potent DA receptor agonists. Although not as efficacious as *L*-DOPA, their effect is significant and DA agonists are frequently given as monotherapy or as adjunctive therapy in combination with *L*-DOPA.

Unfortunately, in many cases disabling motor complications appear after a few years of *L*-DOPA treatment, i.e. motor fluctuations and dyskinesia. Continuous DAergic stimulation (CDS) might delay or prevent these motor complications and this strategy should be taken into consideration when designing new therapies for Parkinson's disease. An interesting development in the field of CDS is the application of Duodopa® which continuously delivers *L*-DOPA directly into the duodenum. Another promising method of CDS is the transdermal delivery of DA receptor agonists by iontophoresis. Transdermal iontophoresis is a non-invasive technique which transports molecules across the human skin under influence of an electrical current. Iontophoresis enables constant, programmed, and controlled delivery by manipulating the current to the needs of the patient. Moreover, the circumvention of the first-pass metabolism is advantageous for drugs which are sensitive to this.

Apomorphine, rotigotine and 5-OH-DPAT (**2.12**) are DA receptor agonists which have been evaluated for transdermal iontophoretic delivery. Iontophoresis is ideal for these drugs because they are sensitive to first-pass metabolism. Furthermore, they have a narrow therapeutic window and thus should be titrated accurately. In addition they represent relatively small molecules that are positively charged at low pH which enables electro-repulsion from the electrode. Drugs which lack a positive ionic group are unlikely to be transported by iontophoresis, but conversion to a prodrug and introduction of a cationic moiety can make them suitable for iontophoresis.

The transdermal iontophoretic delivery of 5-OH-DPAT has been investigated *in vitro* and *in vivo*. Important factors which influence the transdermal iontophoretic flux of 5-OH-DPAT are the drug concentration and electrical current density. Although a sufficient amount of drug was delivered *in vivo* to achieve a strong DAergic effect, the moderate lipophilicity and the relatively low aqueous solubility can cause a limitation for further development of its iontophoretic delivery into a clinical application. By increasing the aqueous solubility two major improvements can be accomplished, i.e. both the iontophoretic patch size as well as the necessary electrical current can be decreased. A possible strategy is conversion of 5-OH-DPAT into a prodrug with improved physicochemical properties for iontophoretic transport. By preparation of prodrugs with

naturally occurring amino acids, an additional positive charge is introduced in the molecule making the prodrugs more water soluble. It would also be of interest to determine the influence of these bivalent cationic prodrugs on iontophoresis. Overall, our aim was the development of highly soluble prodrugs which can be delivered efficiently by transdermal iontopheretic delivery.

In **Chapter 2** we describe the synthesis of a series of amino acid ester prodrugs of 5-OH-DPAT (**2.12**) with various amino acids in order to primarily obtain a chemically stable prodrug, and in addition to investigate the influence of the side chain groups on the hydrolysis rate. The prodrugs were obtained as the hydrochloride salts which were highly water soluble, but also hygroscopic. Hygroscopicity impedes easy handling and therefore investigation of other salt forms would be desired, e.g. dicarboxylic acids. However, the low chemical stability of the prodrugs under basic aqueous conditions interfered with conversion of the hydrochloride salt to the free amines to form alternative salt forms. It would thus be attractive to synthesize prodrugs with higher chemical stability. Besides the utilization of dipeptides described in **Chapter 6**, rigid promoieties as piperidine carboxylic acids or unsaturated derivatives of β-alanine or GABA may prevent hydrolysis by intramolecular catalysis. A disadvantage is the likely toxicity of these promoieties.

The determination of the chemical stabilities of the amino acid ester prodrugs of 5-OH-DPAT is presented in **Chapter 3**. Especially the 1-aminocyclopropane-1-carboxylic acid (**2.30**), *L*-valine (**2.31**), *D*-valine (**2.32**), *L*-isoleucine (**2.33**) and β-alanine (**2.39**) ester prodrugs of (S)-5-OH-DPAT (**S-2.12**), the active enantiomer of 5-OH-DPAT (**2.12**), show relatively high chemical stabilities. Steric hindrance by aliphatic side chains probably stabilizes the ester function against hydrolysis. The number of carbon atoms between the promoiety's amino group and the carbonyl group are crucial for chemical stability, with ethyl being the optimum in this series. A higher pK_a of the amino group in the promoiety can cause faster chemical hydrolysis, e.g. by increased intramolecular catalysis. The chemically stable prodrugs **2.30**, **2.31**, **2.32**, **2.33** and **2.39** were selected for enzymatic hydrolysis studies. Fortunately, all were shown to hydrolyze instantaneously in human blood plasma at 37 ºC which indicates the immediate release of the drug from its prodrug form after uptake in the blood stream.

First, in **Chapter 4** the relationship between the current density, the *in vivo* iontophoretic transport and the (S)-5-OH-DPAT (**(S)-2.12**) plasma profile has been described. The results show that the passage of the drug into the skin can be controlled accurately by modifying the current density. Second, the effect of transdermal iontophoresis on the striatal DA release was investigated in anesthetized rats. With this study a rat model was established which displayed stable DA release levels during anesthesia, which enabled us to investigate the DAergic effect of (S)-5-OH-DPAT following intravenous infusion and transdermal iontophoresis. Finally, the pharmacokinetic (PK) and pharmacodynamic (PD) relationship following transdermal iontophoresis of (S)-5-OH-DPAT was investigated. This study

demonstrated that the applied DA agonist induced a clear long lasting and reversible decrease in the release of DA. These results are crucial for designing a self-controlled delivery device, guided by a feedback system based on PK-PD modeling.
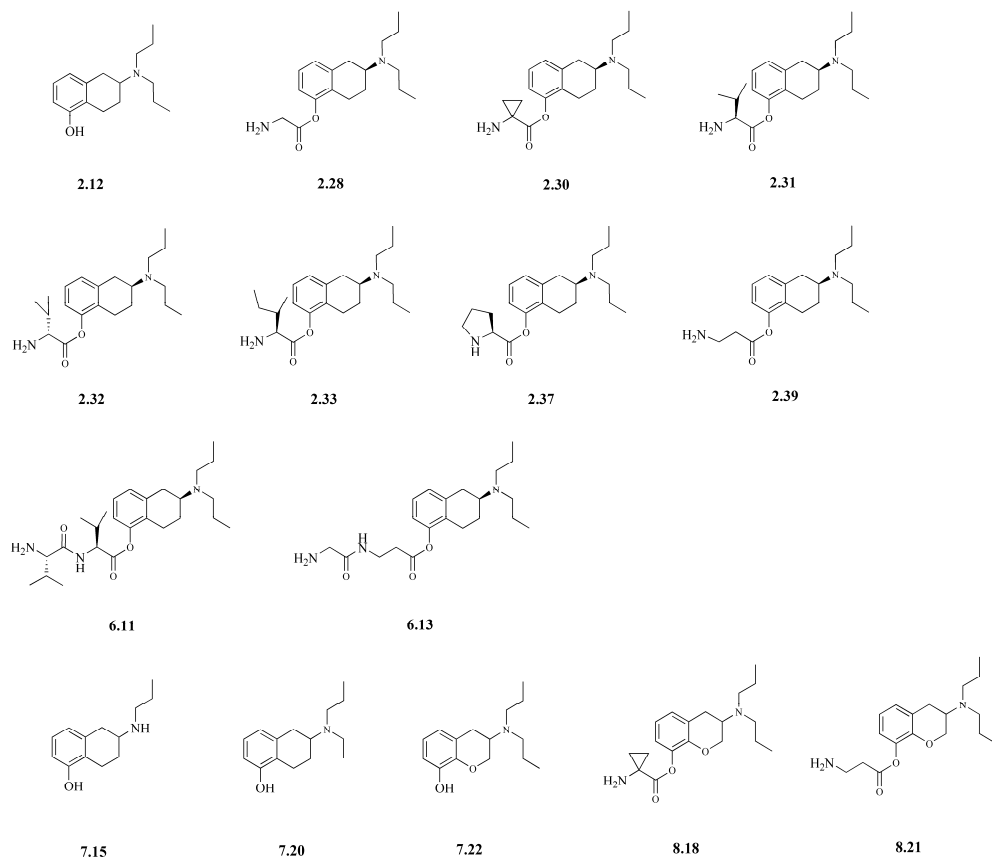
Scheme 9.1 Overview of analogs and prodrugs of 5-OH-DPAT.

Chapter 5 covers the *in vitro* and *in vivo* studies of a selection of the amino acid ester prodrugs of (S)-5-OH-DPAT for iontophoresis. The feasibility of the transdermal iontophoretic delivery of the highly aqueous soluble glycine (**2.28**), *L*-proline (**2.37**), *L*-valine (**2.31**) and β-alanine (**2.39**) prodrugs of (S)-5-OH-DPAT (**(S)-2.12**) was investigated *in vitro*. Subsequently, the PK and PD effect of the β-alanine prodrug, which showed the highest *in vitro* transport efficiency, was investigated *in vivo*. Despite a higher *in vitro* transport, lower plasma concentrations were observed following 1.5 h current application (250 μA/cm^2) of the β-alanine (S)-5-OH-DPAT ester in comparison to (S)-5-OH-DPAT. This resulted in a pharmacological effect with the same maximum as 5-OH-DPAT, but the effect lasted for a longer time. In conclusion, this study demonstrates the potential of improving solubility, iontophoretic transport and changing the plasma profile and the PD effect of the promising DA agonist 5-OH-DPAT by using a prodrug approach.

In **Chapter 6** the synthesis and evaluation of the chemical stability of a series of novel dipeptide esters of (S)-5-OH-DPAT (**(S)-2.12**) is described. The dipeptide promoiety esterified with (S)-5-OH-DPAT consisted of glycine, *L*-valine, β-alanine and *L*-lysine combinations. All dipeptide esters showed a higher chemical stability than their mono amino acid ester prodrug equivalents. In particular, the *L*-valine-*L*-valine (S)-5-OH-DPAT ester (**6.11**) and the dipeptide ester prodrugs with β-alanine at the C-terminal of the dipeptide (**6.13** to **6.16**) gave excellent chemical stabilities. The high chemical stability may be explained by the steric hindrance in the case of **6.11** and conformers which are unfavourable to hydrolysis in the case of **6.13** to **6.16**. These factors may diminish intramolecular catalysis during hydrolysis. The newly synthesized dipeptide prodrugs could be valuable candidates to improve iontophoretic transport by maintaining an intact prodrug structure during transport across the human stratum corneum. Moreover, extremely stable dipeptide prodrugs with multiple charges can be synthesized in order to further investigate the influence of drug valency on iontophoretic transport.

The synthesis of a series of 5-OH-DPAT analogs is described in **Chapter 7**. These compounds were used to study the influence of the molecular structure of phenolic and catecholic DA receptor agonists on their aqueous solubility and iontophoretic flux *in vitro*. The aminochroman 8-OH-DPAC (**7.22**) showed the highest solubility, and the aminotetralins 5-OH-MPAT (**7.15**) and 5-OH-EPAT (**7.20**) were delivered with higher fluxes than 5-OH-DPAT. Intra -and intermolecular hydrogen bonding may explain the different aqueous solubilities. The found iontophoretic fluxes are possibly dependent on molecular weight, molecular volume and lipophilicity.

Improved aqueous solubility and decreased lipophilicity are molecular properties which can benefit transdermal iontophoresis. Therefore in **Chapter 8** the synthesis of a series of amino acid ester prodrugs of the water-soluble potent DA agonist (-)-8-OH-DPAC is given. Chemical stability studies show that 1-aminocyclopropane-1-carboxylic acid (**8.18**) and β-alanine (**8.21**) (-)-8-OH-DPAC esters are suitable candidates for further *in vitro* and *in vivo* iontophoretic studies.

In conclusion, highly water-soluble prodrugs and several analogs of 5-OH-DPAT have been synthesized and developed specifically for transdermal iontophoresis. By investigation of these novel compounds we have gained more understanding of the influence of molecular structure on chemical stability, enzymatic stability, solubility and iontophoretic flux *in vitro* and *in vivo*. The extremely soluble β-alanine ester prodrug of (S)-5-OH-DPAT (**2.39**) is the most promising candidate for further research on transdermal iontophoretic delivery of DAergic prodrugs for the treatment of Parkinson's disease.

Appendix

List of Abbreviations

Samenvatting en algemene discussie

Samenvatting voor niet ingewijden

Dankwoord

List of publications

LIST OF ABBREVIATIONS

3-MT	3-Methoxytyramine
5-OH-DPAT	5-Hydroxy-2-(N,N-di-n-propylamino)tetralin
(S)-5-OH-DPAT	(S)-5-Hydroxy-2-(*N,N*-di-*n*-propylamino)tetralin
5,6-(OH)$_2$-DPAT	5,6-Dihydroxy-2-(*N,N*-di-*n*-propylamino)tetralin
5,6-(OH)$_2$-MPAT	5,6-Dihydroxy-2-(*N-n*-propylamino)tetralin
6-OH-DA	6-Hydroxydopamine
6-OH-DPAT	6-Hydroxy-2-(*N,N*-di-*n*-propylamino)tetralin
(R)-7-OH-DPAT	(R)-7-Hydroxy-2-(*N,N*-di-*n*-propylamino)tetralin
8-OH-DPAC	8-hydroxy-3,4-dihydro-3-(*N,N*-di-*n*-propylamino)-*2H*-1-benzopyran
AAAD	Aromatic-L-amino-acid decarboxylase
AC	Adenylate cyclase
ADEPT	Antibody-directed enzyme prodrug therapy
AIC	Aikaike Information Criterion
AZT	Zidovudine
BBB	Blood-brain barrier
BCSFB	Blood-cerebrospinal fluid barrier
BDCRB	2-Bromo-5,6-dichloro-1-(β-*D*-ribofuranosyl)benzimidazole
Boc	*N-tert*-butoxycarbonyl
cAMP	Cyclic adenosine monophosphate
Cbz	Carbobenzyloxy
C_{DA}	Baseline values of DA
CDS	Continuous dopaminergic stimulation
CL	Clearance
cLogP	Calculated log P
CNS	Central nervous system
COMT	Catechol-O-methyltransferase
C_p	Plasma concentration
C_s	Striatal concentration
CSF	Cerebrospinal fluid
D_1	Dopamine D_1 receptor
D_2	Dopamine D_2 receptor
d_2-5-OH-DPAT	5-Hydroxy-2-(N-n-propyl-N-α,α-dideutero-propylamino)-tetralin
DA	Dopamine
DAergic	Dopaminergic
DBS	Deep brain stimulation
DCC	*N,N'*-Dicyclohexylcarbodiimide
DHEA	Dehydroepiandrosteron
DHS	Dermatomed human skin
DOPAC	3,4-Dihydroxyphenylacetic acid
ECF	Extracellular fluid
EDC	*N*-(3-Dimethylaminopropyl)-*N'*-ethylcarbodiimide
EI	Electron ionization
Enk	Enkephalin
ESI	Electrospray ionization
FOCE	First order estimation method
GABA	γ-Aminobutyric acid

GCMS	Gas chromatography–mass spectrometry
Glu	Glutamate
GLUT1	Glucose transporter 1
GPCR	G protein-coupled receptor
GPe	External segment of globus pallidus
GPi	Internal segment of globus pallidus
GTP	Guanosine triphosphate
H	Hill-slope coefficient
HBP	Human blood plasma
HOBt	1-Hydroxybenzotriazole
HPLC	High-performance liquid chromatography
HPLC-MS/LC-MS	Liquid chromatography–mass spectrometry
HRMS	High-resolution mass spectrometry
HSA	Human serum albumin
HSC	Human stratum corneum
HVA	Homovanillic acid
IC_{50}	Half maximal inhibitory concentration
I_{max}	Maximum inhibition of the DA production
ITS	Iontophoresis transdermal system
IV	Intravenous
k	Hydrolysis rate constant
k_{obs}	Observed rate constant
LAT1	*L* Amino acid transporter 1
L-DOPA	3,4-Dihydroxy-L-phenylalanine
LOD	Limit of detection
LOQ	Limit of quantification
MAO-B	Monoamine oxidase B
MPP^{+}	1-Methyl-4-phenylpyridinium
MPTP	1-Methyl-4-phenyl-1,2,3,6-tetrahydropyridine
MRM	Multiple Reaction Monitoring
mRNA	Messenger ribonucleic acid
MS	Mass spectrometry
MVOF	The minimum value of the objective function
N-0437	5-Hydroxy-2-(*N*-propyl-*N*-2-thienylethylamino)tetralin
NMDA	*N*-Methyl-*D*-aspartate
NMR	Nuclear magnetic resonance
PBS	Phosphate buffered saline
PD	Pharmacodynamic
PEPT1	Peptide transporter 1
PK	Pharmacokinetic
PK-PD	Pharmacokinetic-pharmacodynamic
PMEA	9-[2-(Phosphonomethoxy)-ethyl] adenine
Q	Inter compartmental clearance
SC	Stratum corneum
SN	Substantia nigra
SNc	Substantia nigra pars compacta
SNr	Substantia nigra pars reticulata
STN	Subthalamic nucleus
Subst P	Substance P

$t_{1/2}$	Half-life
Thal	Thalamus
TLC	Thin-layer chromatography
V_2	Volume of central compartment
V_3	Volume of peripheral compartment
VPC	Visual predictive check

SAMENVATTING EN ALGEMENE DISCUSSIE

De neurotransmitter dopamine (DA) speelt een belangrijke rol in het centrale zenuwstelsel en is gerelateerd aan symptomen van de ziekte van Parkinson. De ziekte van Parkinson is een neurodegeneratieve ziekte waarbij het geleidelijke verlies van striatonigrale DAerge neurons het hoofdkenmerk is. De beste therapeutische strategie voor de behandeling van de ziekte van Parkinson is gebaseerd op het herstellen van het DA tekort door een verhoging van de DA concentraties met L-DOPA, MAO-B remmers en COMT remmers. Een andere benadering voor de behandeling van de ziekte van Parkinson is de vervanging van de verlaagde DA niveaus met potente DA receptor agonisten. Ook al zijn DA agonisten niet zo effectief als L-DOPA, toch is hun effect significant en worden DA agonisten gegeven als monotherapie of als adjunctieve therapie in combinatie met L-DOPA.

Helaas verschijnen er in veel gevallen invaliderende motor complicaties na een aantal jaar behandeling met L-DOPA, bijvoorbeeld motor fluctuaties en dyskinesie. Continue DAerge stimulatie (CDS) zou deze motor complicaties kunnen vertragen of voorkomen, en hier zou rekening mee moeten worden gehouden tijdens het ontwerpen van nieuwe therapieën voor de ziekte van Parkinson. Een interessante ontwikkeling op het gebied van CDS is de toepassing van Duodopa® welke L-DOPA op een continue wijze rechtstreeks in het duodenum afgeeft. Een andere veelbelovende methode van CDS is de transdermale afgifte van DA receptor agonisten met iontoforese. Transdermale iontoforese is een niet-invasieve techniek die moleculen over de menselijke huid transporteert onder invloed van een elektrische stroom. Iontoforese maakt constante, geprogrammeerde en gecontroleerde afgifte mogelijk door het instellen van de stroom naar de behoefte van de patient. Bovendien is de omzeiling van het first-pass metabolisme voordelig voor geneesmiddelen die hiervoor gevoelig zijn.

Apomorphine, rotigotine en 5-OH-DPAT (**2.12**) zijn DA receptor agonisten welke zijn geëvalueerd voor transdermale iontoforetische afgifte. Iontoforese is ideaal voor deze geneesmiddelen omdat ze gevoelig zijn voor het first-pass metabolisme, ze hebben een smal therapeutisch venster en moeten dus nauwkeurig worden getitreerd, en hun kleine moleculaire structuur is positief geladen bij lage pH wat elektro-repulsie vanaf de elektrode mogelijk maakt. Het is onwaarschijnlijk dat geneesmiddelen die een ionische groep missen, kunnen worden getransporteerd met iontoforese, maar de omzetting naar een prodrug en daarbij de introductie van een geïoniseerde deel zou ze geschikt kunnen maken voor iontoforese.

De transdermale iontoforetische afgifte van 5-OH-DPAT is *in vitro* en *in vivo* onderzocht. Belangrijke factoren die de transdermale iontoforetische flux van 5-OH-DPAT beïnvloeden zijn de geneesmiddel concentratie en de elektrische stroomdichtheid. Hoewel een voldoende hoeveelheid van het geneesmiddel *in vivo* was afgegeven om een sterk DAerg effect te bewerkstelligen, kunnen de matige lipofiliciteit en de relatief lage water

oplosbaarheid de verdere ontwikkeling van deze iontoforetische afgifte tot een klinische toepassing beperken. Door het verhogen van de water oplosbaarheid kan de grootte van de iontoforetische pleister worden verkleind en de benodigde elektrische stroom worden verlaagd. Een mogelijke strategie is de omzetting van 5-OH-DPAT in een prodrug met verbeterde fysisch-chemische eigenschappen voor het iontoforetische transport. Door de bereiding van prodrugs met natuurlijk voorkomende aminozuren, wordt een additionele positieve lading in het molecuul geïntroduceerd. Ook zou het interessant zijn om de invloed van bivalente kationische prodrugs op transdermale iontoforetische afgifte te onderzoeken.

In **Hoofdstuk 2** beschrijven we de synthese van een serie aminozuur ester prodrugs van 5-OH-DPAT (**2.12**) met verscheidene aminozuren vooral om een chemisch stabiele prodrug te verkrijgen, en daarbovenop te onderzoeken wat de invloed is van de zijketen groepen op de hydrolyse snelheid. De prodrugs werden verkregen als het hydrochloride zout welke bijzonder water oplobaar, maar tevens hygroscoop waren. Hygroscopiciteit verhindert gemakkelijke handelbaarheid, en daarom zou onderzoek naar andere zoutvormen zoals dicarbonzuren gewenst zijn. Alhoewel, de lage chemische stabiliteit van de prodrugs onder basische condities verhinderde de conversie van het zout naar de vrije amines om zodoende andere zoutvormen te vormen. Het zou daarom interessant zijn om prodrugs te synthesizeren met een hogere chemische stabiliteit. Mogelijke rigide prodrug deeltjes zoals piperidine carbonzuren of onverzadigde afgeleiden van β-alanine or GABA zouden de hydrolyse door intramoleculaire katalyse kunnen verhinderen. Echter een nadeel is de mogelijke toxiciteit van deze moleculen.

De bepaling van de chemische stabiliteit van de aminozuur ester prodrugs van 5-OH-DPAT wordt gepresenteerd in **Hoofdstuk 3**. Vooral de 1-aminocyclopropaan-1-carbonzurur (**2.30**), *L*-valine (**2.31**), *D*-valine (**2.32**), *L*-isoleucine (**2.33**) en β-alanine (**2.39**) ester prodrugs van (S)-5-OH-DPAT (**S-2.12**), de actieve enantiomeer van 5-OH-DPAT (**2.12**), vertonen een relatief hoge chemische stabiliteit. Sterische hinder door alifatische zijketens stabiliseren waarschijnlijk de ester functionele groep tegen hydrolyse. Het aantal koolstof atomen tussen de amino groep en de het carbonzuur op het prodrug gedeelte, zijn cruciaal voor de chemische stabiliteit, waarbij ethyleen de optimale lengte is in deze serie. Een hogere pK_a van de amino groep in het prodrug gedeelte kan zorgen voor een snellere chemische hydrolyse, bijvoorbeeld door een verhoogde intramoleculaire katalyse. De chemisch stabiele prodrugs **2.30**, **2.31**, **2.32**, **2.33** and **2.39** werden geselecteerd voor enzymatische hydrolyse studies en elke prodrug vertoonde hydrolyse in menselijk bloedplasma bij 37 ºC.
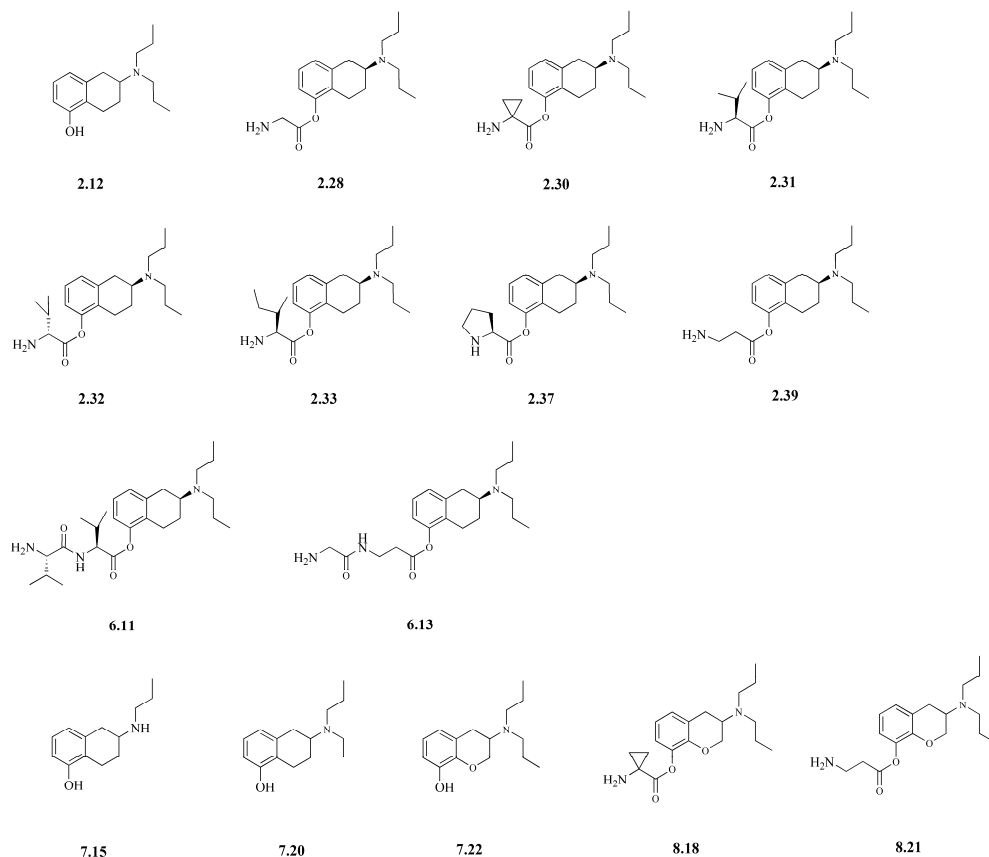
Schema Overzicht van analoga en prodrugs van 5-OH-DPAT.

Ten eerste is in **Hoofdstuk 4** de relatie tussen de stroomdichtheid, het *in vivo* iontoforetische transport en het (S)-5-OH-DPAT (**(S)-2.12**) plasma profiel beschreven. De resultaten laten zien dat de drug input in de huid nauwkeurig kan worden gecontroleerd door het veranderen van de stroomdichtheid. Ten tweede werd het effect van het anaesthesie mengsel, de transdermale iontoforese en het nemen van bloedmonsters op de striatale DA afgifte onderzocht. Met deze studie werd een proefdiermodel van de rat ontwikkeld met stabiele DA afgifte levels tijdens anesthesie. Dit maakte het voor ons mogelijk om het DAerge effect van (S)-5-OH-DPAT na intraveneuze infusie en transdermale iontoforese te volgen. Tot slot werd de pharmacokinetische (PK) en pharmacodynamische (PD) relatie na transdermale iontoforese onderzocht tijdens een gecontroleerde en reversibele farmacologische respons. Deze studie laat zien dat niet alleen een gecontroleerde DAerge reversibel effect kan worden behaald, maar ook dat een continue stimulatie van de DA receptoren mogelijk is. Samen met PK-PD modeling zullen deze resultaten cruciaal zijn voor de ontwerpen van een zelf-gecontroleerd afgifte apparaat, geleid door een feedback systeem.

Hoofdstuk 5 behandelt de *in vitro* en *in vivo* studie met een selectie van de aminozuur ester prodrugs van (S)-5-OH-DPAT voor iontoforese. De uitvoerbaarheid van de transdermale iontoforetische afgifte van de zeer water oplosbare glycine (**2.28**), *L*-proline (**2.37**), *L*-valine (**2.31**) en β-alanine (**2.39**) prodrugs van (S)-5-OH-DPAT (**(S)-2.12**) werden onderzocht *in vitro*. Vervolgens werd het PK en PD effect van de prodrug met de hoogste *in vitro* transport efficientie *in vivo* onderzocht. Ondanks het hogere *in vitro* transport, werden lagere plasma concentraties waargenomen na 1.5 uur stroom toepassing (250 μA/cm^2) van de β-alanine (S)-5-OH-DPAT ester in vergelijking met (S)-5-OH-DPAT. Dit resulteerde in een farmacologisch effect met hetzelfde maximum als 5-OH-DPAT, maar het effect duurde langer. In conclusie toonde deze studie de kracht van het gebruik van prodrugs aan voor het verbeteren van de oplosbaarheid, het iontoforetische transport en het veranderen van het plasma profiel en het PD effect van de veelbelovende DA agonist 5-OH-DPAT.

In **Hoofdstuk 6** wordt de synthese en evaluatie van de chemische stabiliteit van een serie dipeptide esters van (S)-5-OH-DPAT (**(S)-2.12**) behandeld. Het dipeptide deeltje dat werd veresterd met (S)-5-OH-DPAT bestond uit glycine, *L*-valine, β-alanine en *L*-lysine combinaties om de invloed van de aminozuur volgorde op chemische hydrolyse te onderzoeken. Alle dipeptide esters vertoonden een hogere chemische stabiliteit van hun mono aminozuur ester prodrug equivalenten. Met name, de *L*-valine-*L*-valine (S)-5-OH-DPAT ester (**6.11**) en de dipeptide ester prodrugs met β-alanine aan het C-uiteinde van de dipeptide (**6.13** tot en met **6.16**) vertoonden de hoogste chemische stabiliteit. De hoge chemische stabiliteit kan worden uitgelegd door de sterische hinder in het geval van **6.11** en door conformeren die nadelig zijn voor hydrolyse in het geval van **6.13** tot en met **6.16**. Deze factoren kunnen de intramoleculaire katalyse tijdens hydrolyse verminderen. De dipeptide prodrugs kunnen waardevolle kandidaten zijn die het iontoforetische transport kunnen verbeteren door het behouden van de intacte prodrug structuur tijdens het transport over het humane stratum corneum. Bovendien kunnen dipeptide prodrugs worden gesynthetiseerd met meerdere ladingen om de invloed van de valentie van een geneesmiddel op iontoforetisch transport te kunnen onderzoeken.

De synthese van een serie van 5-OH-DPAT analoga is beschreven in **Hoofdstuk 7**. Deze verbindingen werden gebruikt om de invloed van de molecuulstructuur van fenolische en catecholische DA receptor agonisten op hun wateroplosbaarheid en *in vitro* iontoforetische flux te bestuderen. De aminochromaan 8-OH-DPAC (**7.22**) vertoonde de hoogste oplosbaarheid, en de aminotetralines 5-OH-MPAT (**7.15**) en 5-OH-EPAT (**7.20**) werden afgegeven met een hogere flux dan 5-OH-DPAT. Intra- en intermoleculaire waterstofbruggen zouden de verschillende wateroplosbaarheden kunnen verklaren. De gevonden iontoforetische flux waarden zijn mogelijk afhankelijk van molecuul gewicht, moleculair volume en lipofiliteit.

Een verbeterde wateroplosbaarheid en verminderde lipofiliteit zijn moleculaire eigenschappen waar transdermale iontoforese van kan profiteren. Daarom wordt in

Hoofdstuk 8 de synthese van een serie aminozuur ester prodrugs van de wateroplosbare potente DA agonist (-)-8-OH-DPAC beschreven. Studies met betrekking tot de chemische stabiliteit laten zien dat 1-aminocyclopropaan-1-carbonzuur (**8.18**) en β-alanine (**8.21**) (-)-8-OH-DPAC esters geschikte kandidaten zijn voor verdere iontoforetische studies *in vitro* en *in vivo*.

Samenvattend, zeer wateroplosbare prodrugs en verscheidene analoga van 5-OH-DPAT werden gesynthetiseerd en specifiek ontwikkeld voor transdermale iontoforese. Door het onderzoeken van deze nieuwe verbindingen hebben we meer inzicht gekregen in de invloed van de molecuulstructuur op chemische stabiliteit, enzymatische stabiliteit, oplosbaarheid en iontoforetische flux *in vitro* en *in vivo*. De extreem wateroplosbare β-alanine ester prodrug van (S)-5-OH-DPAT (**2.39**) is de meest veelbelovende kandidaat voor verder onderzoek naar transdermale iontoforetische afgifte van DAerge prodrugs voor de behandeling van de ziekte van Parkinson.

SAMENVATTING VOOR NIET INGEWIJDEN

De substantia nigra en het striatum zijn twee hersengebieden die belangrijk zijn voor coördinatie en beweging. De zenuwcellen tussen deze twee gebieden communiceren via een signaalstof genaamd dopamine. Bij de ziekte van Parkinson zijn deze zenuwcellen sterk verminderd waardoor er minder dopamine wordt afgegeven en het bewegingsapparaat verstoord raakt. De meest voorkomende symptomen zijn trillen, spierstijfheid, bewegingsarmoede en een verstoorde houding. De geneesmiddelen die doorgaans worden gebruikt in de farmacotherapie hebben als doel de verlaagde dopamine afgifte in de hersenen te herstellen (levodopa), te verhogen (MAO-B remmers en COMT remmers) of na te bootsen (dopamine agonisten). In de loop van de tijd treden er echter vooral bij toediening van levodopa, het meest effectieve geneesmiddel tot nu toe, zeer ernstige bijwerkingen op. Deze bijwerkingen zijn dyskinesieën (onwillekeurige bewegingen) en motorfluctuaties. Motorfluctuaties kunnen worden samengevat als de (on)voorspelbare, afnemende of wisselende werking van levodopa op het bewegingsapparaat van de patiënt. Uit onderzoek blijkt dat een meer constante dopaminespiegel deze bijwerkingen zou kunnen beperken, iets wat bij orale toediening van levodopa niet gerealiseerd wordt. Een bekende methode om een geneesmiddel constant af te geven is via infusie, echter hierbij is kans op ontsteking. Een alternatief is het toedienen van een geneesmiddel vanuit een pleister met behulp van een lage elektrische stroom vanuit een batterij. Deze techniek heet transdermale iontoforese. Transdermale iontoforese geeft een constante afgifte van het geneesmiddel en maakt het mogelijk om de juiste dosis in te stellen door de stroomsterkte te variëren. Bovendien is de kans op ontsteking klein door de niet invasieve aard van deze techniek.

De chemische structuur van sommige dopamine agonisten maakt dat deze geneesmiddelen gevoelig zijn voor de grootschalige afbraak in de lever na orale inname, dit heet het first-pass-effect. Transdermale iontoforese zou deze afbraak in de lever kunnen omzeilen, omdat het geneesmiddel via de huid direct in de bloedbaan terechtkomt. Verscheidene dopamine agonisten werden al onderzocht op de mogelijkheid om deze via iontoforese toe te dienen. Het blijkt mogelijk te zijn, echter een hogere oplosbaarheid van de geneesmiddelen zou een tweetal voordelen kunnen bieden. Ten eerste zou een hogere oplosbaarheid de grootte van de pleister tot handbare proporties kunnen verkleinen, omdat dezelfde hoeveelheid geneesmiddel dan kan worden opgelost in een kleiner volume vloeistof. Ten tweede, de mate van afgifte met transdermale iontoforese kan afhankelijk zijn van de concentratie van het geneesmiddel. Een hogere oplosbaarheid geeft een hogere concentratie en wellicht dus ook een snellere afgifte. Hierdoor kan de benodigde stroomsterkte verkleind worden en wordt de kans op irritaties van de huid verminderd.

In dit proefschrift beschrijven we het chemisch bereiden en de evaluatie van zeer wateroplosbare varianten van de dopamine agonist 5-OH-DPAT. Deze varianten zijn

chemisch aan elkaar gekoppelde stoffen van de dopamine agonist 5-OH-DPAT met andere moleculen. In dit geval zijn dat aminozuren. In de farmacie noemt men deze stoffen prodrugs. Een prodrug is een niet werkzame stof die na omzetting in het lichaam het actieve geneesmiddel vrijgeeft. Ons onderzoek heeft geleid tot een aantal bevindingen. Ten eerste blijkt het mogelijk te zijn zeer wateroplosbare prodrugs te maken die voldoende stabiel zijn in de iontoforese pleister (voldoende houdbaarheid), maar eenmaal in de bloedbaan het geneesmiddel direct vrijgeven. Ten tweede, door het koppelen van 5-OH-DPAT aan dipeptiden (twee gecombineerde aminozuren), is het mogelijk de stabiliteit van de prodrug in de pleister nog groter te maken. Ten derde is het mogelijk om 5-OH-DPAT gecontroleerd toe te dienen aan het lichaam wat de ontwikkeling van een feedback systeem in principe mogelijk zou maken. En als laatste vonden we dat de iontoforetische toediening van een zeer wateroplosbare prodrug van 5-OH-DPAT een verlenging van het effect van het geneesmiddel geeft in vergelijking met 5-OH-DPAT zelf.

Al deze resultaten laten zien dat de toepassing van prodrugs voordelig kan zijn bij de toediening van dopamine agonisten of andere geneesmiddelen met behulp van transdermale iontoforese. Verder onderzoek naar deze farmaceutische toedieningsvorm zou uiteindelijk kunnen leiden tot een nieuwe farmacotherapie voor patiënten met de ziekte van Parkinson.

DANKWOORD

Verscheidene jaren van onderzoek en schrijven hebben uiteindelijk geleid tot het proefschrift dat nu voor u ligt. Echter, het tot stand komen van deze dissertatie was niet mogelijk geweest zonder de hulp en steun van verscheidene mensen die ik bij deze nog graag wil bedanken.

Oliver, het was heel fijn om met jou samen te werken. Als je weer naar Groningen kwam, betekende dat weer een leuke en leerzame afwisseling van de chemie om met jou onze microdialyse experimenten uit te voeren op de vijfde verdieping. In het begin hadden we zo nu en dan nog wat hulp nodig van Jan de Vries, maar uiteindelijk liep alles op rolletjes. Ook onze regelmatige telefonische en MSN updates naar elkaar toe hielden de afstand Leiden-Groningen kort. We hebben met ons beider enthousiasme en interesse een mooi project afgerond met mooie resultaten. Ook buiten het werk om was het altijd gezellig en ik hoop dat we elkaar in de toekomst nog vaak zullen gaan zien Heel veel geluk voor jou, Eveline en julie dochter Roseline. Bedankt.

Natuurlijk wil ik mijn begeleider Durk Dijkstra ook heel graag bedanken voor het zijn van mijn mentor, voor het zijn van mijn vraagbaak voor alles omtrent farmacochemie, voor het leveren van goede ideeën omtrent ons onderzoek, en natuurlijk voor het meerdere malen lezen van mijn manuscript. Ik vond het bijna dagelijkse contact met u erg prettig en ook de gezamenlijke bezoeken aan de congressen in Istanbul en Wenen waren niet alleen leerzaam maar ook gezellig. Ook bedankt voor de etentjes samen met Ali, ik heb ervan genoten. Ik hoop dat we contact blijven houden, en anders kom ik zo af en toe wel in Bedum langs om te genieten van het prachtige uitzicht achter jullie huis.

Ook professor Westerink hartelijk dank voor alle inbreng die u heeft gehad in het project. Bovendien zou het zonder uw hulp voor ons niet mogelijk zijn geweest om op efficiënte wijze onze microdialyse experimenten uit te voeren bij B&S en BOL. En bovendien was uw commentaar op mijn proefschrift zeer waardevol.

Professor Wikström, u bent korte tijd mijn professor geweest, en ik wilde u toch bedanken voor uw input en interesse voor het project. Ook ben ik u dankbaar voor het introduceren van een aantal handige praktische technieken op het gebied van organische chemie, die ik overigens nu nog steeds toepas.

Professor Bouwstra, Joke, en Professor Danhof, Meindert, mijn dank gaat ook uit naar jullie voor het opzetten van het project en de goede begeleiding. Ik geloof dat we een mooie samenwerking tussen onze universiteiten hebben volbracht.

Alexander, ik ken je al vanaf de eerste week dat ik in Groningen woon, dat was in '98. Ik ben blij dat we altijd contact hebben gehouden. Bedankt voor alle gezelligheid en goede adviezen de afgelopen jaren. Je hebt me, misschien zonder dat je het door had, toch telkens weer aangezet om het schrijven tot een einde te brengen. Ik hoop dat we elkaar nog heel

lang mogen zien onder het genot van een concert, in de Ekko of gewoon met een biertje op de bank. Natuurlijk ook mijn dank aan je vrouw Rozemarijn, jullie beiden zijn heel fijne vrienden. Veel geluk met jullie kindje Mirthe.

Gossen, als enigen van onze jaarclub wonen wij nog in Groningen. Toevallig dat we beide onze grote projecten nu eindelijk tot een einde gaan brengen. Al vanaf '99 hebben wij elke woensdag onze jaarclub avond. Zelfs toen al onze clubgenoten richting het westen vertrokken waren, hebben wij de traditie doorgezet, uiteindelijk zelfs met aanhang. Mijn dank voor al je adviezen, je luisterend oor en de introductie tot het vegetarische eten. Samen met Alena hebben jullie mij een fijne tijd in Groningen gegeven.

Mijn collega's van de vakgroep farmacochemie, Ulrike, Danyang, Andre, Pieter en Cor, zou ik ook graag willen bedanken voor het delen van jullie kennis en het geven van hulp en gezelligheid. Ook vond ik het fijn om nog een periode op hetzelfde lab te werken met Frank Dekker en zijn promovendi Massimo en Rosalina. Tijdens mijn project heb ik een aantal bijvakstudenten begeleid, namelijk Anette, Samuel en Willem. Jullie hebben een aantal waardevolle verbindingen voor mij gesynthetiseerd, dank jullie wel. Peter, Nico en Eveline ook al deden jullie geen bijvak bij mij, toch bedankt voor het brengen van een dynamische sfeer op zaal.

Ik wil ook Yi (en Durk) bedanken dat hij mij de kans heeft gegeven om bij Axon Medchem BV aan het werk te gaan. Bedankt voor de vrijheid die ik kreeg om het werk bij Axon te combineren met het schrijven van mijn proefschrift.

Mijn dank gaat ook uit naar technologiestichting STW voor alle financiën en coördinatie van het project, bedankt hiervoor Ellen. Ook mijn dank aan alle leden van de gebruikerscommissie, met name aan Ronald van der Geest voor zijn frequente aanwezigheid, betrokkenheid en input.

De afdeling massaspectrometrie, voornamelijk Andries Bruins, Annie en Margot, wil ik ook hartelijk bedanken voor alle hulp en uitleg. Ik heb bij jullie geleerd om toch extra schoon te werken bij het meten van zeer lage concentraties. Dergelijke concentraties kennen wij in de organische chemie niet zo goed. Dat was een wijze les.

De volgende personen hebben mij zeer goed geholpen met de zuiverheids analyse en de karakterisering van mijn verbindingen: Jan Visser en Meint Lukkien voor de hulp met HPLC, Hans van der Velde voor het uitvoeren van de element analyses, en Wim Kruizinga voor de ondersteuning bij NMR. Dank jullie wel.

De personen van de vakgroep biomonitoring and sensoring (B&S): Si, Marieke, Miranda, Jelle, Carlos, Wahono en van Brains On-Line (BOL): Thomas, Gunnar, Martin, Marius wil ik graag bedanken voor het gebruik mogen maken van jullie laboratorium voor onze *in vivo* experimenten. Jan, Karola, en Suzanne, aan jullie veel dank voor het voorbereidende werk en alle hulp bij het uitvoeren van onze experimenten, mede dankzij jullie is alles soepel en efficiënt verlopen.

Ook Janneke, Margriet en Janine bedankt voor de hulp bij alle administratieve zaken.

Bij deze wil ik ook graag Prof. Minnaard, Prof. Frijlink en Prof. Kruse hartelijk danken voor het lezen en goedkeuren van mijn manuscript.

Lieve Dianili, bedankt voor je steun bij de laatste fase van de vervaardiging van dit proefschrift. Ik geloof dat wij een mooie en liefdevolle toekomst tegemoet gaan.

Mijn lieve ouders en lieve zusje Amber, mijn familie. Ik ben heel blij met jullie. Jullie steun gedurende het hele project, maar natuurlijk ook gedurende mijn hele leven, betekent veel voor me, jullie zijn mijn basis. Osvaldo en mijn nichtje Serena, jullie ook bedankt, ik ben heel blij dat jullie nu bij onze familie horen.

Lieve Ivanka, jij bent de belangrijkste steun geweest tijdens het hele project. Vanaf mijn studie farmacie tot de laatste opgeschreven woorden van mijn manuscript. Van het mij vergezellen bij de vele HPLC analyses die ik uitvoerde tot het geven van allerlei goede adviezen. Ik heb aan jou zoveel te danken, voor alle liefde en support die je gaf. Ik wens je veel sterkte en alle geluk in de wereld toe. Bedankt voor alles.

LIST OF PUBLICATIONS

O.W. Ackaert, J. Van Smeden, J. De Graan, D. Dijkstra, M. Danhof, J.A. Bouwstra Mechanistic studies of the transdermal iontophoretic delivery of 5-OH-DPAT *in vitro*. *Journal of Pharmaceutical Sciences*. 2010 Jan;99(1):275-85.

O.W. Ackaert, J. De Graan, R. Capancioni, D. Dijkstra, M. Danhof, J.A. Bouwstra. Transdermal iontophoretic delivery of a novel series of dopamine agonists *in vitro*: physicochemical considerations. *Journal of Pharmacy and Pharmacology*. 2010 Jun;62(6):709-20.

J. De Graan*, O.W. Ackaert*, R. Capancioni, O.E. Della Pasqua, D. Dijkstra. B.H. Westerink, M. Danhof, J.A. Bouwstra. The *in vitro* and *in vivo* evaluation of new synthesized prodrugs of 5-OH-DPAT for iontophoretic delivery. *Journal of controlled release*. 2010 Jun 15;144(3):296-305.

J. De Graan*, O.W. Ackaert*, S. Shi, R. Vreeken, O.E. Della Pasqua, D. Dijkstra, B.H. Westerink, M. Danhof, J.A. Bouwstra. The pharmacokinetics and pharmacological effect of (S)-5-OH-DPAT following controlled delivery with transdermal iontophoresis. *Journal of Pharmaceutical Sciences*. 2011 Jul;100(7):2996-3009.

J. De Graan, O.W. Ackaert, A. Boltjes, J.A. Bouwstra, B.H. Westerink, D. Dijkstra. Synthesis and evaluation of the chemical and enzymatic stability of a series of novel amino acid prodrugs of the potent dopamine D_2 agonist (S)-5-OH-DPAT developed for transdermal iontophoresis. *Manuscript in preparation.*

*contributed equally as first author

"If music be the food of love, play on"

William Shakespeare, from "Twelfth Night"